Integrated Assessment of Black Carbon and Tropospheric Ozone

UNEP

World Meteorological Organization

UNEP

World
Meteorological
Organization

Integrated Assessment
of Black Carbon
and Tropospheric Ozone

Acknowledgements

Contents

Preface

There is growing evidence that a wide range of airborne pollutants are contributing significantly to climate change while harming human health, agricultural production and ecosystems, such as forests. This Assessment considers black carbon and tropospheric ozone, including the tropospheric ozone precursor methane, which affect climate and air quality and are also 'short-lived' in the atmosphere when compared with carbon dioxide which implies that benefits can be realized in the near-term if measures are implemented to reduce emissions now.

The *Integrated Assessment of Black Carbon and Tropospheric Ozone* addresses the short-lived climate forcers (SLCFs) that also have an impact on air quality. Its findings on both the state of scientific knowledge and existing policy options to cut emissions come from 50 authors convened by UNEP and WMO. Previous assessments have often studied either the impacts on climate from such pollutants or the direct effects of air pollution on human health and ecosystems, but not both in an integrated manner. This report gives a comprehensive assessment of the multiple benefits of practical measures to reduce emissions of black carbon – a key component of soot – and the gases leading to the formation of tropospheric ozone, especially methane.

The Assessment assembled an international team to review the scientific literature on all aspects of black carbon and tropospheric ozone to provide findings that are relevant to policy making. The Assessment team recognised that there was a gap in the existing literature to fully enable important multiple benefits of plausible policy options to be quantified. Therefore the team also undertook new modelling exercises to better identify the potential for co-benefits and to quantify them. Key to the Assessment was the identification of a small number of measures that are likely to provide both climate and air quality benefits. These are made up of existing technologies and measures, many of which are linked to actions to improving access to energy, sustainable transport and health initiatives.

The Assessment shows that, if rapidly and widely implemented, the identified measures will bring significant improvements in human health, the wider environment and the climate in the near term. Action under a range of international, regional and national treaties, laws and regulations may therefore help improve the chances of keeping the global temperature rise under 2ºC above the pre-industrial level while also meeting other challenges for human well-being, including achieving the Millennium Development Goals that relate to human health and food security.

The climate, health and crop-yield benefits are quantified using global climate-composition models. The benefits are shown to be considerable, significantly reducing the rate of warming over the next two to four decades, improving the chances of remaining below the 2ºC target, preventing millions of premature deaths from small particulate pollution and preventing the loss of millions of tonnes of crops from ozone pollution every year. It also shows that action on these substances is complementary to, but does not replace the challenge to dramatically reduce emissions of carbon dioxide from the burning of fossil fuels and deforestation.

Full implementation of the identified measures would also have substantial benefits close to the regions where action is taken, including in Asia where these short-lived pollutants are likely altering regional climate patterns such as the Asian Monsoon.

The science in this field is rapidly maturing: this report provides clear recommendations as to where the policy response can deliver strategies that directly improve the lives and the realization of a more sustainable future for billions of people.
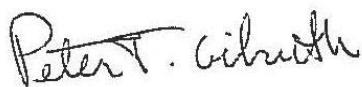
Peter Gilruth
Director
Division of Early Warning and Assessment
United Nations Environment Programme

Liisa Jalkanen
Chief
Atmospheric Environment Research Division
World Meteorological Organization

Reader's guide

Introduction

The *Integrated Assessment of Black Carbon and Tropospheric Ozone* looks into all aspects of anthropogenic emissions of black carbon and tropospheric ozone precursors, such as methane. It analyses the trends in emissions of these substances and the drivers of these emissions; summarizes the science of atmospheric processes where these substances are involved; discusses related impacts on the climatic system, human health and crops in vulnerable regions and ecosystems; and explores societal responses to the environmental changes caused by those impacts. The Assessment examines a large number of potential measures to reduce harmful emissions, identifying a small set of specific measures that would likely produce the greatest benefits, and which could be implemented with currently available technology. An outlook up to 2070 is developed illustrating the benefits of those emission mitigation policies and measures for human well-being and climate. The Assessment concludes that rapid mitigation of anthropogenic black carbon and tropospheric ozone precursor emissions would complement carbon dioxide reduction measures and would have immediate benefits for human well-being.

The *Integrated Assessment of Black Carbon and Tropospheric Ozone* is the result of a structured consultative process using an author team of more than 50 experts from across the globe. The author team was selected on the basis of their expertise in covering the scientific issues and were chosen from all regions of the World. An extensive review process was followed and over 40 external reviewers commented on the draft chapters. Eight review editors ensured that all of the review comments were adequately addressed.

The Assessment provides a comprehensive overview of the current state of knowledge in the scientific literature regarding the key substances emitted to the atmosphere that have a significant warming effect on climate and contribute to air quality degradation, especially black carbon, tropospheric ozone and its precursors (Chapters 2 and 3). This Assessment is also based on a dedicated study, integrating a range of models to evaluate the multiple benefits of implementing a carefully identified set of measures. Finally, the outcome of this dedicated study is merged with data and their uncertainties available in the literature in order to come to the final conclusions.

The dedicated study has been performed referring to the Driver-Pressure-State-Impact-Response (DPSIR, UNEP, 2007) framework. Hence, emission scenarios of long-lived greenhouse gases and short-lived climate forcers have been linked all the way to their impacts on climate, human health and ecosystems and options for policy responses. The following are the highlights of each chapter:

Chapter 1. Introducing the Assessment – introduces black carbon and tropospheric ozone and their influence on climate change. It also highlights the fact that multiple benefits will accrue for climate, human health and crop yields by reducing their concentrations in the atmosphere by addressing the emissions of black carbon and particular tropospheric ozone precursors, such as methane. Additionally, it summarises the approach taken in the Assessment.

Chapter 2. Black carbon and tropospheric ozone precursors: drivers, emissions and trends – highlights key drivers that give rise to emissions of black carbon and tropospheric ozone precursors. It then highlights their global emissions and also the emissions of pollutants and greenhouse gases that are co-emitted with them. As well as historical trends, it discusses uncertainties in emission estimates and observational support for the values estimated. It then develops emission progressions by region and sector for 1990, 2005 and 2030 according to the Reference Scenario used in the Assessment.

Chapter 3. Atmospheric processes, tropospheric ozone and black carbon concentrations, deposition, and radiative forcing – describes the chemical transformations and the physical processes that the substances undergo in the atmosphere once emitted. It describes the observed and modelled concentrations and composition of particles in the atmosphere, including their transport, transformation and removal. It describes the influence of black carbon, organic carbon and ozone on radiative forcing. It also shows the results from using models on the reference scenario emissions to estimate concentrations and radiative forcing. The models used are described in an Appendix.

Chapter 4. Impacts of black carbon and tropospheric ozone – are described on the climatic system in terms of global and regional temperatures, and impacts on regional rainfall patterns. Climate impact in key regions including the Himalayas and Arctic are highlighted. Modelled results of regional and global climatic changes under the reference scenario are shown. Impacts on health, crop yields and ecosystems are assessed, and modelled estimates of the changes in health and crop impacts according to the reference scenario are shown. The economic benefits of emission reductions are discussed and quantified. The vulnerability of certain regions and specific societal groups to black carbon and ozone impacts is explored.

Chapter 5. Options for policy responses and their impacts – assesses the potential for reductions in emissions and where possible quantifies the impact of these reductions on public health, ecosystems and climate. It describes the process by which seven methane measures and nine measures targeting black carbon emissions are identified. It also develops a scenario for CO_2 based on the emissions modelled using the assumptions of the IEA World Energy Outlook 2009 450 Scenario and the IIASA GAINS database. The impact of black carbon, methane and CO_2 measures on emissions of important substances (affecting climate and air quality impacts) are shown. These new emissions are then used in modelling to determine the climate, health and crop yield changes, highlighting regional benefits, and an economic analysis is also included. Finally, the chapter describes existing policy approaches for promoting the mitigation measures and provides examples where the different measures have been implemented around the world.

Chapter 6. Conclusions – explains the multiple reasons for controlling emissions of black carbon and precursors of tropospheric ozone, especially methane. It summarises the assessment of science and the findings relating to the impact of the black carbon and ozone precursors on climate and air quality impacts. It summarises the main findings from the modelling and the benefits from reducing emissions. It then highlights the policies and measures that already exist which could reduce the emissions of these short-lived climate forcers if implemented widely and rapidly.

Assessment conceptual framework

The Assessment uses the DPSIR as an organisational framework. The Assessment focuses on impacts of importance to human well-being that are affected by black carbon and tropospheric ozone, including its precursors, especially methane. The framework attempts to reflect the key components of the complex and multidimensional, spatial and temporal chain of cause-and-effect that characterizes the interactions between these substances, society and the environment. The approach was to identify measures that would give a benefit for both climate and air quality concerns (especially health and crop yields).

The *drivers* refer to processes in society that drive activities which give rise to emissions of black carbon or tropospheric ozone precursors. Key drivers include demographics, scientific and technological innovation and economic demand. The characteristics and importance of each driver affecting emissions differ substantially from one region to another, within regions and both between and within nations. For example, the use of biomass for cooking is a feature of poor people in Africa and parts of Asia, but not

necessarily of the more affluent people in those societies.

The *pressure* refers to the emissions of black carbon, tropospheric ozone precursors, and the emissions of other gases and particles that affect warming and/or have impacts on health, crops and ecosystems. These pressures on climate, human well-being and ecosystems vary regionally depending on the substance emitted, the distribution of relevant sources and the sensitivity of the receptors to impacts.

The *state* refers to the concentrations of the different pollutants in the atmosphere, deposition to different surfaces that leads to impacts or the change in radiative forcing caused by the substances in the atmosphere. The climate changes caused by changes in radiative forcing are also changes in the state of the environment that contributes to impacts on ecosystems and human well-being.

The *impacts* refer to how human well-being or the environment is directly or indirectly affected by the change in state of the atmosphere. The Assessment focuses on temperature changes caused by changes in relevant emissions as an indicator of climate impacts. The concentrations of $PM_{2.5}$ and ozone are

used to estimate health and crop yield impacts affected by a change in the concentrations of the relevant substances. The Assessment touches on some key impacts of climate change and the vulnerability of particular groups of people and particular regions to the changes in impacts.

The *responses* focus on the measures that will reduce warming and air quality impacts on health, crop yields and other ecosystem services. The responses are considered at different levels – in terms of the technical measures available, the policies that can be used to implement the measures and a number of case studies that show how the measures have been implemented in different parts of the world.

Regional breakdown

Emissions and impacts are disaggregated into five regional groupings based on UNEP's regional and sub-regional breakdown (UNEP, 2007) shown in Figure 2.12 in Chapter 2, below.

References

UNEP (2007). *Global Environment Outlook 4 (GEO-4): Environment for Development*. United Nations Environment Programme, Nairobi, Kenya.
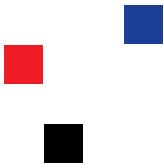
Chapter 1. Introducing the Assessment

Coordinating lead author: Frank Raes (Joint Research Centre, European Commission, Italy).

Lead authors: Drew Shindell (National Aeronautics and Space Administration Goddard Institute Space Studies, USA), Veerabhadran Ramanathan (Scripps Institution of Oceanography, USA), Johan C.I. Kuylenstierna (Stockholm Environment Institute, Environment Department, University of York, UK).

1.1 Scope

Limiting anthropogenic climate change and improving air quality are two of the most important environmental challenges facing humankind. It is increasingly recognized that, although changes in air quality and climate typically occur at different temporal and spatial scales, many aspects of these issues are closely linked. In particular, many of the emissions that lead to degraded air quality also contribute to climate change, while many potential measures to mitigate climate change affect emissions of air pollutants.

Strategies to deal with either challenge would improve human well-being directly through impacts on health, freshwater and food supply, with obvious impacts on the economy. They will also affect climate change in both the near term and the long term (e.g. Raes and Seinfeld, 2009). When considering strategies to avoid climate change and improve air quality there is a need to assess the impacts on both, and try to identify synergies (win-win) and avoid trade-offs (win-lose). In general, a single strategy that addresses a wider range of pollutants and a multitude of impacts is likely to be more cost-effective (e.g. Amann, 2001).

This Assessment focuses on measures to reduce emissions that lead to the formation of ozone in the lower part of the atmosphere (tropospheric ozone, O_3) and black carbon-containing aerosol particles (black carbon, BC) (Box 1.1). Tropospheric O_3 includes near-surface O_3. While only near-surface O_3 is relevant for health and agricultural impact studies, O_3's greenhouse warming effect is due to O_3 in the entire troposphere. Tropospheric O_3 and BC are known to impact negatively on people's well-being and on the sustainability of natural resources. They are also short-lived climate forcers (SLCFs), contributing to near-term global warming and changing local weather patterns (Chapter 4). Controls of tropospheric ozone and black carbon would therefore have multiple benefits. This assessment aims at turning these considerations into robust policy options for decision makers.

The control measures considered in this assessment are put in the context of climate policies leading to reductions in carbon dioxide (CO_2) and methane (CH_4). At the 16th Conference of the Parties to the United Nations Framework Convention on Climate Change (UNFCCC) in Cancun, Mexico, it was agreed that the global mean temperature increase should not exeed 2ºC above pre-industrial levels in order to avoid dangerous interference with the climate system. However, the current pledges by industrialized countries to reduce their long-lived greenhouse gas emissions fall short of the required effort (UNEP, 2010). The Assessment looks in particular at the extent to which controlling tropospheric O_3 and BC might enhance the chances of achieving this 2ºC target. In doing so, it takes into account the fact that BC and precursors to ozone are often emitted together with other substances (Chapter 2), so that the *net* effect of emissions reductions by a given measure might either reinforce or counter-act the effects aimed at from the reduction of ozone and BC alone.

Hydrofluorocarbons, which are potent greenhouse gases, do not influence air quality directly, and their treatment is therefore beyond the scope of this report. It has been proposed that HFCs be controlled under the Montreal Protocol (Molina *et al.*, 2009).

This Assessment responds to the increasing interest in SLCFs and the potential for SLCF measures to address near-term climate change, changes in local weather patterns and achieve co-benefits in terms of improved human health and ecosystem services. This interest has been particularly articulated in the Anchorage Declaration of 24 April 2009, adopted by the Indigenous Peoples' Global Summit on Climate Change; the Tromsø Declaration of 29 April 2009, adopted by the Sixth Ministerial Meeting of the Arctic Council; and the Eighth Session of the Permanent Forum on Indigenous Issues under the United Na-

tions Economic and Social Council (May 2009) which called on the United Nations Environment Programme (UNEP) to conduct a fast-track assessment of short-term drivers of climate change, specifically BC, with a view to initiating the negotiation of an international agreement to reduce its emissions. A need to take rapid action to address significant climate forcing agents other than CO_2, such as BC, was reflected in the 2009 declaration of the Group of Eight (G8) leaders, *Responsible Leadership for a Sustainable Future* (Group of Eight, 2009).

In what follows some background material is presented and definitions are given that will help to clarify the Assessment and its conclusions. It also presents the approach followed in the Assessment, which is not only based on the available scientific literature but also on a dedicated study undertaken for this Assessment.

Box 1.1: Denomination of aerosol particles

An **aerosol** is a suspension of solid particles or droplets in a gas. In principle, aerosol refers to both the particles or droplets *and* the gas.

Aerosol particles, sometimes referred to as just **particles**, refers to the particles or droplets of the aerosol.

Aerosol(s) is often used instead of aerosol particles when it is clear from the context that aerosol particles are meant: e.g. the aerosol mass concentration clearly means the mass concentration of aerosol particles.

Particulate matter is another way of referring to these particles. The climate-effects community tends to use aerosol particles, whereas the health-effects community prefers to use particulate matter or PM.

PM_X then means the particles with an aerodynamic diameter lower than x micrometer. $PM_{2.5}$ is often referred to as fine particulate matter, that is with a diameter of less than 2.5 micrometers which is the fraction commonly used to estimate health impacts associated with PM.

1.2 Tropospheric ozone

Ozone is a reactive gas that exists primarily in two layers of the atmosphere: the stratosphere (upper layer) and troposphere (ground level to ~10–15 km). In the stratosphere, O_3 is considered to be beneficial as its strong absorption of ultraviolet (UV-B) radiation protects life on Earth from this harmful solar radiation. Stratospheric ozone is however not the subject of this report.

In contrast, at ground level, ozone is an air pollutant harmful to human health and plants, and is the main air pollutant that reduces crop yields. It is also a major component of urban smog. Ozone also absorbs infrared (IR) radiation and consequently acts as a strong greenhouse gas.

In the troposphere, O_3 is produced from reactions of its precursors, which have both natural and man-made sources. These precursors are carbon monoxide (CO), methane (CH_4), other, non-methane volatile organic compounds (NMVOCs), and nitrogen oxides (NO_x). The relationship between precursor emissions and O_3 production is highly non-linear (Chapter 3). Methane is particularly important in the formation of tropospheric O_3 and is at the same time a potent greenhouse gas. Because of the increase in anthropogenic emissions of its precursors, tropospheric O_3 concentrations in the northern hemisphere have increased two to threefold during the past 100 years (Chapters 2 and 3).

1.3 Black carbon

Black carbon aerosol particles result from the incomplete combustion of fossil fuels, wood and other biomass. Complete combustion would turn all the carbon in the fuel into carbon dioxide (CO_2). In practice, combustion is never complete and together with CO_2 there is formation of carbon monoxide (CO), volatile organic compounds (VOCs), non-volatile organic compounds that condense and form organic carbon (OC), and BC aerosols. The complex mixture of particulate matter resulting from incomplete combustion is often referred to as soot, although a universally

accepted nomenclature is still lacking. The distinction between colourless OC and BC is operationally defined. In reality many organic substances, for example humic-like substances, do have a colour and will contribute to BC as measured with light absorption methods (Andreae and Gelencsér, 2006). It is also important to note that during their transport in the atmosphere, some of the VOCs emitted by incomplete combustion are transformed chemically into condensable products and lead to what are called secondary organic aerosols (SOA). SOA is most likely colourless.

During the past 100 years the global concentration of BC aerosols has undoubtedly increased, but it is uncertain by how much because biomass burning, and hence BC emissions, obviously occurred even in pre-industrial times (Chapter 2).

BC can constitute up to 10–15 per cent of fine particulate matter ($PM_{2.5}$) (Chapter 3). $PM_{2.5}$ is known to lead to adverse effects on human health (Chapter 4).

The black in black carbon obviously refers to the fact that these particles absorb visible light. This absorption leads to additions of solar energy to the atmosphere and a reduction at the Earth's surface referred to as surface dimming.

1.4 Impact of atmospheric-composition change on global and regional climate

Climate on Earth is determined by the planetary radiation balance, which is the balance between energy entering at the top of the atmosphere as sunlight (E_{in}) and that leaving the atmosphere as reflected light and heat back to space (E_{out}, Figure 1.1).

Apart from some natural disturbances by, for example, volcanoes, for about the last 10 000 years this balance, when averaged over decades, has remained roughly in equilibrium ($E_{in} \approx E_{out}$). In other words, no substantial amount of net energy (E_{in} - E_{out}) was added to the Earth system, and its global mean temperature therefore remained relatively constant ($\Delta T_{global} \approx 0$). Since the wide-
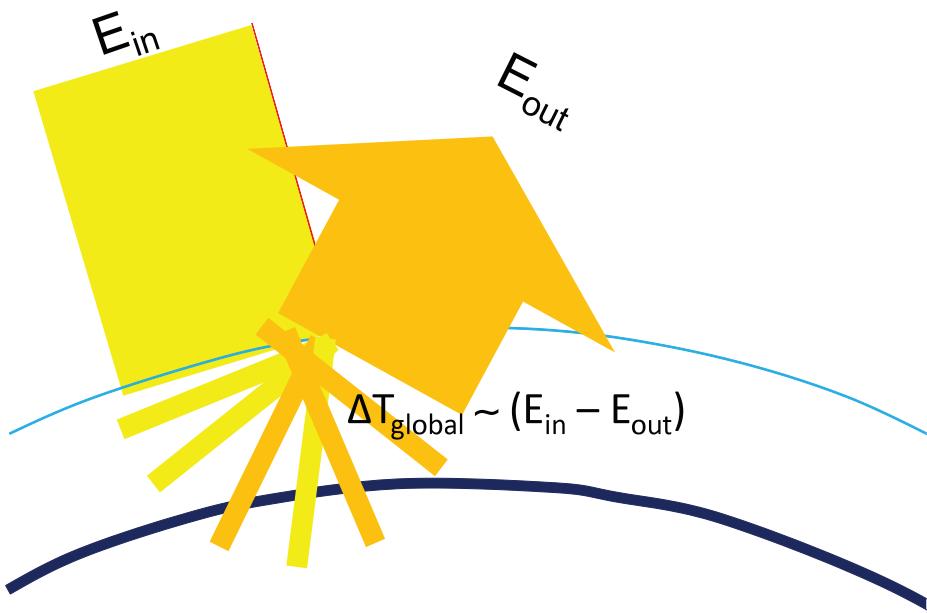
Figure 1.1. The planetary radiation balance at the top of the atmosphere. A change in global mean temperature (ΔT_{global}) results from a departure from the balance between incoming and outgoing fluxes of energy.

spread land clearing and the industrial revolution beginning in the 18th century, human-made emissions of greenhouse gases, aerosols and their precursors, have increasingly changed the composition of the atmosphere, leading to enhanced absorption and reflection of incoming light by aerosol particles and clouds, and enhanced absorption of outgoing IR radiation by greenhouse gases and, to a lesser extent, also by large aerosol particles and clouds. This has lead to a departure from the pre-industrial equilibrium, *which is referred to as radiative forcing*. As of today, less energy is leaving the Earth at the top of its atmosphere than is coming in ($E_{out} < E_{in}$). Hence, there is a positive radiative forcing which leads to the observed increase in the Earth's global mean temperature ($\Delta T_{global} > 0$).

The increase of tropospheric ozone in the past 100 years has made it one of the most important contributors to human-induced global warming, together with CO_2, CH_4 and BC. Even though its globally averaged tropospheric human-derived concentration is about 10 000 times smaller than that of CO_2, O_3's global radiative forcing is about one-sixth to one-third that of CO_2 (Chapter 3).

The radiative forcing of O_3 strongly depends on the altitude. Near-surface O_3 has a negligible forcing, whereas in the colder upper troposphere it has its largest forcing. This important fact has been known for a long time (e.g. Ramanathan *et al.*, 1987) and, recently confirmed by satellite measurements (e.g. Aghedo *et al.*, 2011). It has strong implications for O_3 mitigation actions. Reductions in CH_4 and CO will reduce O_3 throughout the troposphere at a global scale, whereas reductions of NO_x will mainly have impacts near the surface at local and regional scales, with secondary effects throughout the troposphere (Shindell *et al.*, 2005; West *et al.*, 2009). However, near-surface O_3 may substantially affect climate as a result of O_3 damage to plants reducing carbon uptake, though the magnitude of this effect is much less certain (Chapter 4).

Black carbon absorbs visible light at all wavelengths. That makes it absorb 1 000 000 times more energy per unit mass than CO_2, which absorbs only in specific IR wavelengths. Hence, even though the globally averaged ground-level concentration of BC is presently about 0.1 microgrammes/m³ (Chapter 3), compared to about 200 milligrammes/m³ of anthropogenic CO_2, its instantaneous radiative

4

forcing due to absorption alone may be about half that of anthropogenic CO_2. However, BC has other effects on climate. These include the absorption of light when deposited on ice and snow, leading to faster melting with further effects on local and global climate, ecology and livelihoods. Black carbon, like other aerosol particles, also interacts with clouds, changing their reflectivity and lifetime, again with effects on local and global climate. For these reasons there is uncertainty in determining the overall contribution of BC to radiative forcing (Chapter 3).

In addition, when calculating the climate effect of BC, it is important to realize that it is often mixed with OC which is also produced during combustion and which reflects sunlight much more strongly than it absorbs it. A low OC-to-BC ratio means a predominantly absorbing aerosol that will contribute to warming. A high OC-to-BC ratio means a predominantly reflecting (or scattering) aerosol that will contribute to cooling. The ratio depends on the emission source: it can be lower than 1 in the case of emissions from diesel engines, but will be much higher in the case of, for example, smouldering wood (Chapter 2).

A consideration of the global planetary radiation at the top of the atmosphere (TOA) is useful to describe global climate change in terms of global mean temperature. It does not, however, capture many other climate-related effects that occur more locally within the atmosphere or at the Earth's surface (Figure 1.2).

For instance, both absorbing and scattering aerosols lead to a reduction of solar radiation reaching the surface (also referred to as dimming), i.e. negative surface forcing, whereas absorbing aerosols lead to heating of the atmosphere, i.e. positive atmospheric forcing. The atmospheric and the surface forcings, i.e. changes in the net energy absorbed by the atmosphere or arriving at the Earth's surface, may be more useful indicators than TOA forcing in terms of influences on winds and precipitation (Ramanathan *et al.*, 2001; Andrews *et al.*, 2010). For BC, the magnitudes of the atmospheric and surface forcing are typically factors of 2 to 4 larger than TOA forcing (Satheesh and Ramanathan, 2000; Jacobson, 2001; Forster *et al.*, 2007), this has implications for evaporation, formation of clouds and precipitation, and hence the availability of water.
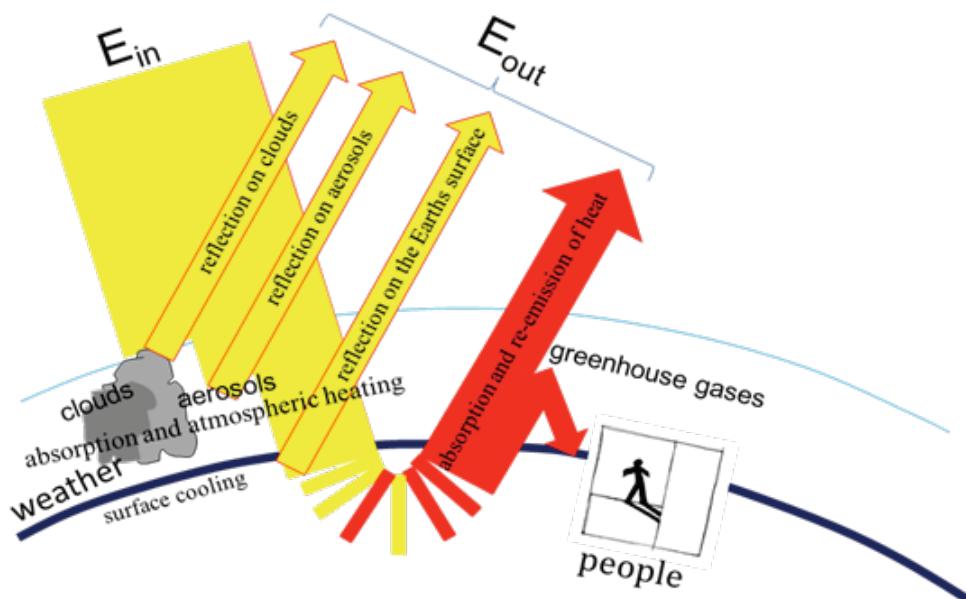
Figure 1.2. Radiation fluxes at the top of the atmosphere, within the atmosphere and at the Earth's surface. The latter two fluxes are particularly important for regional-scale processes relevant to people's lives.

These local issues are obviously of immediate relevance to people's lives. An assessment of atmospheric composition change must take in all effects, global and local, in order to reveal the true impacts.

1.5 Near-term and long-term climate effects of emission controls of gases and aerosols

Gases and aerosol particles that are emitted into or formed within the atmosphere remain there for longer or shorter times depending on their physical and chemical properties. For most gases and particles that are removed from the atmosphere by one major process, for example precipitation for aerosol particles, the concentrations would approximately follow an exponential decay as soon as their emissions or production are stopped. These lifetimes are shorter than the lifetime of carbon dioxide, for which the lifetime is of the order of 100 years or more. Their lifetime is defined as the "e-folding time", the time in which the original concentration drops to $1/e$ or about 37 per cent of the initial concentration.

Many air pollutants, including tropospheric O_3 and BC particles, have atmospheric lifetimes of the order of weeks. Methane, which is mainly removed through chemical reactions in the atmosphere, has a lifetime of about a decade. These lifetimes are shorter than that of CO_2. Accordingly, these substances are called short-lived climate forcers (SLCFs).

Carbon dioxide and other compounds that have lifetimes of the order of 100 years or more are called long-lived climate forcers (LLCF). They include nitrous oxide (N_2O, 114 years), sulphur hexafluoride (SF_6, 3 200 years), and chlorofluorocarbons (CFCs, 100+ years). The atmospheric lifetime of CO_2, the most important anthropogenic greenhouse gas, cannot be described by a single value. CO_2 molecules are distributed between the atmosphere, the ocean and the terrestrial biosphere, involving processes with time scales from decades to hundreds of years. Their permanent removal involves even slower processes such as chemical weathering

of rocks (Denman *et al.*, 2007, Archer *et al.*, 2009). If all anthropogenic CO_2 emissions were stopped today, the anthropogenic contribution to the CO_2 concentration in the atmosphere – about 110 ppm as of today – would drop by about 25 per cent of today's value in 50 years but by not more than 60 per cent over the following 1 000 years (Solomon *et al.*, 2009).

In discussing the climate response to a reduction in SLCF emissions, it is important to understand that the global mean temperature does not follow the concentration decrease of the SLCF, which can occur in a matter of weeks. Instead, the temperature response is governed by processes in the climate system, namely the uptake of heat by the surface layer of the ocean, which happens over a decade or so, and its subsequent transport into the deep ocean, which happens over hundreds of years.

In the case of an SLCF this means that, when its concentration and hence its radiative forcing is reduced by emission controls, the global mean temperature will achieve most of its decrease towards a new equilibrium value in about a decade. About 10 per cent of the full decrease will not be realized for hundreds of years, since the redistribution of heat stored in the deep ocean while the SLCF was active, and hence its upwards transport, will continue for hundreds of years (Solomon *et al.*, 2010). In the case of CO_2, more than 80 per cent of the expected decrease in global mean temperature after emission reductions will not be realized for hundreds of years. This is because the drawing down of atmospheric CO_2 into the deep ocean, and hence the decrease in its radiative forcing, is roughly offset by the upward transport of heat to the surface, since both phenomena are achieved by the same physics of deep-ocean mixing (Solomon *et al.*, 2009; Matthews and Weaver, 2010).

For the discussion in this Assessment, which looks at the near-term impacts of emission reductions of SLCFs, it is sufficient to consider what will happen in the next few decades. Thus the very long-term effects of emissions and emission controls are not addressed here.

6
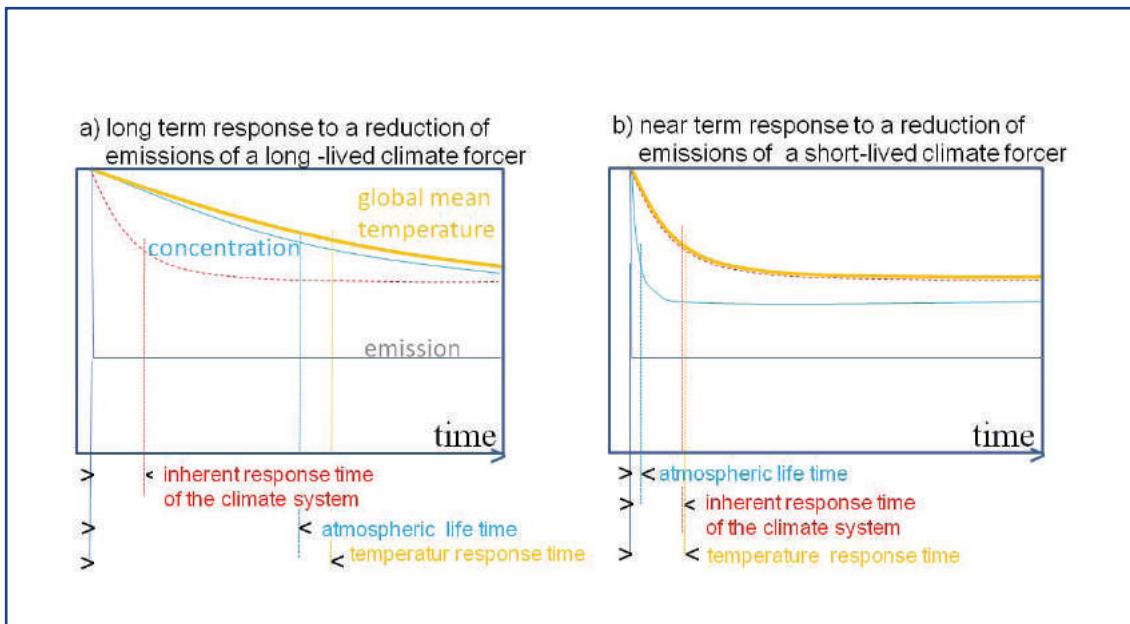
Figure 1.3. Schematic view of the response of global mean temperature to a sudden reduction in the emissions to the atmosphere of a climate forcer. Left: in the case of a long-lived climate forcer; right: in the case of a short-lived climate forcer. For simplicity, it is assumed that before the emission reduction takes place there is equilibrium between emission and removal of the climate forcer, and also between incoming and outgoing radiation ($E_{in} = E_{out}$). Both conditions are not always fulfilled in reality.

The short lifetime of SLCFs in the atmosphere also means that an equilibrium between their sources and sinks is quickly established. Hence, continuous and constant emissions will rapidly – within weeks to decades – result in constant levels of their concentrations in the atmosphere. Constant emissions of long-lived species, CO_2 for example, will result in growing concentrations during the first 100 years after emissions started. Therefore, constant emissions of short-lived air pollutants add a fixed amount of change to the evolving climate change provoked by the emissions of long-lived greenhouse gases. Reducing the emissions of short-lived pollutants will reduce their concentrations in a matter of weeks, with an effect on global temperature established during the following decade (Figure 1.3). Reducing emissions of long-lived greenhouse gases will have an effect only on longer time scales.

The schematic in Figure 1.4 illustrates the effects of reducing various short-lived air pollutants on the global mean temperature. The atmosphere contains, among many other compounds, CO_2, O_3 and BC aerosols, which all warm, and sulphate and OC aerosols that

cool. The present-day net effect is an observed warming, shown by the thick line. The reductions of CO_2 required today to stabilize climate in the long term will only have a small effect in the near term. Sulphate is likely to be reduced over the coming decades due to a focus on problems related to human health, acid rain and visibility, which will lead to accelerated warming (Ramanathan and Feng, 2008; Raes and Seinfeld, 2009). This Assessment evaluates the extent to which reducing BC and O_3 can help to reduce near-term warming.

1.6 Identifying emission control measures with multiple benefits

Many human activities lead to substantial emissions of either or both BC and tropospheric O_3 precursors (Chapter 2). Transportation is a large source of O_3 precursors and BC. Power generation by coal burning produces large amounts of nitrogen oxides (NO_x) and little BC, but a substantial amount of cooling particulate such as sulphate particles. Residential biofuel and open biomass burning is a major source of BC and OC, as well as CO emissions. The use of solvents in industrial and domestic sectors leads to substantial
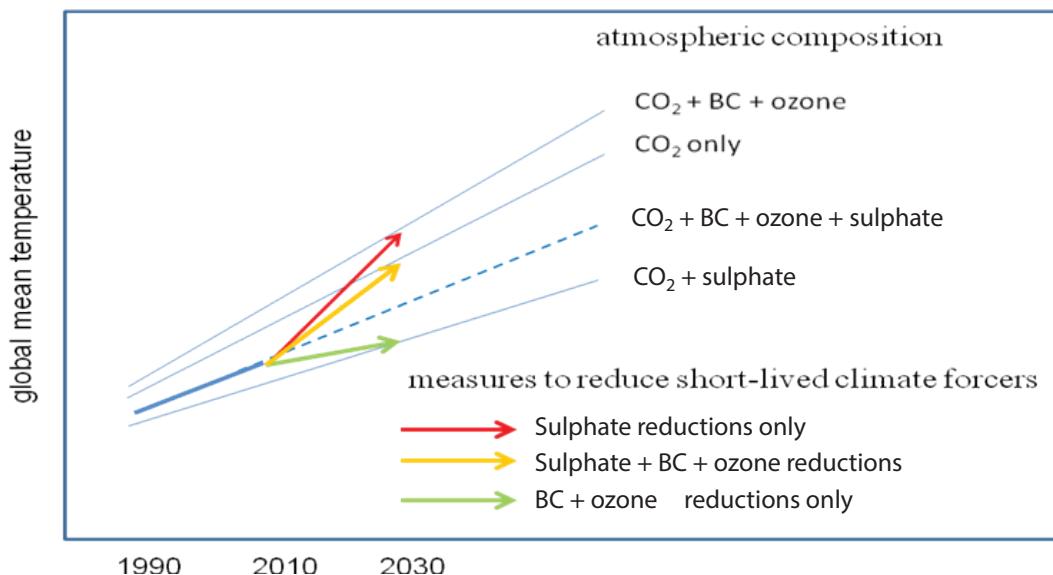
Figure 1.4. Schematic view of the effect of reducing various air pollutants on global mean temperature. The thick line represents the on-going warming. A reduction of cooling sulphate aerosols is expected to lead to an accelerated warming. A focus on reducing BC and O_3 is expected to reduce warming in the near term.

NMVOC emissions, while fossil fuel extraction, agricultural activities, including the rearing of livestock, and municipal waste lead to large emissions of CH_4.

Emissions are generally the result of an activity, for example a number of kilometres driven, multiplied by an emission factor, such as the number of grammes emitted per kilometre driven. Emissions can hence be controlled by technical measures to reduce the emission factor, for example fitting a filter or catalytic convertor, or by non-technical measures that reduce the activity, such as a reduction in fossil fuel use.

It is important to realize that one emission control measure seldom reduces either a single pollutant or all pollutants at once. For example, a particle filter on a diesel car will reduce the emission of BC particles, but not CO_2 which will pass unhindered. The Assessment looks for control measures in specific sectors that would lead primarily to the reduction of BC and O_3 precursors. It subsequently goes some way in quantifying the impact of these measures on regional and global climate, human health and crop yields and their associated economic impacts.

Successful air pollution policies in the developed world during the past few decades have focused mainly on the power and industrial sectors and led to the reduction of global sulphur and NO_x emissions. This has led to a partial unmasking of the greenhouse effect and accelerated warming (Figure 1.4).

Reductions of tropospheric O_3 and BC would help reduce warming in the near term. They would also contribute to a lower equilibrium global temperature in the long term (see Section 1.5). However, since multiple pollutants are affected by specific actions, including cooling pollutants, it has not always been clear which plausible emission reductions would achieve a net decrease in warming.

The vulnerability of natural or human systems to climate change is geographically dependent. Sometimes, vulnerable areas are close to or overlap with areas that have high levels of air pollution and expect rapid increases in temperature. In such regions, measures to control BC and O_3 could be particularly beneficial. The Arctic and Himalayan regions and monsoon-fed areas around the world are examples. Black carbon and O_3

8

reductions are expected to benefit the livelihoods of the populations in these areas, in particular the millions of people living in the highly polluted areas of, for example, South Asia. These high pollutant levels have severe effects on people's health and influence crop yields in regions where food security is an important issue.

1.7 The approach taken in the Assessment

This Assessment provides a comprehensive overview of the current state of knowledge in the scientific literature regarding the key substances emitted to the atmosphere that have a large warming effect on climate and contribute to air quality degradation, especially BC, tropospheric O_3 and its precursors (Chapters 2 and 3). This Assessment is furthermore based on a dedicated study, integrating a range of models to evaluate the joint benefits of implementing a carefully identified set of emission reduction measures. Finally, the outcome of this dedicated study is merged with existing data – including uncertainties – in the literature in order to come to conclusions.

The dedicated study was performed using the Driver-Pressure-State-Impact-Response (DPSIR, UNEP, 2007) framework. Hence, emission scenarios of long-lived greenhouse gases and SLCFs have been linked all the way to their impacts on climate, human health and ecosystems (Figure 1.5).

A reference emission scenario was developed by the International Institute for Applied Systems Analysis (IIASA), based on the Greenhouse Gas and Air Pollution Interactions and Synergies (GAINS) database (Chapter 2). This scenario describes emissions not only of O_3 precursors and BC, but of all substances that lead to the formation of $PM_{2.5}$ as well as long-lived greenhouse gases. It assumes that, between 2005 and 2030, all agreed air pollution policies would be fully implemented. Beyond 2030, until 2070, emissions of all SLCFs are assumed to remain constant.

The reference scenario was used as input for two global climate-composition models

(GCMs): GISS-PUCCINI (Shindell *et al.*, 2006) and ECHAM-HAMMOZ (Pozzoli *et al.*, 2008) (Chapter 3). These were the two models that, with the given level of resources, were available for the study. They were used to calculate global fields of all chemical substances – tropospheric O_3, all types of particulate matter including BC, and $PM_{2.5}$ – and their radiative forcing. It was considered good practice to use more than one model to calculate concentration fields and radiative forcing in order to increase confidence in the results, given the inherent complexity in the GCMs.

Chapter 4 assesses the effects of the change over time of the reference emissions. The effect of all gases and particles on temperature was calculated based on energy-balance equations that relate radiative forcing to temperature (Appendix A.4.1). The effect of all anthropogenically-derived $PM_{2.5}$ on health was calculated using appropriate concentration-response functions. Finally, the effects of ground-level O_3 on health and crop yields were calculated, again based on concentration-response functions from the literature.

A number of policy scenarios were developed that include the implementation of measures selected to produce benefits for climate and also for human health and crop yields (Chapter 5). The selection of those measures was based on their global warming potential (GWP), that is, maximizing the reduction in radiative forcing integrated over 100 years. The identified measures act on sectors with important O_3 precursor and BC emissions. Some of these measures, however, also reduce substances that are co-emitted, including OC and sulphur dioxide (SO_2), so that they not only reduce O_3 and BC but also other gases and constituents of $PM_{2.5}$. The policy scenarios were used in the two GCMs to calculate the effect of the measures on the global fields of all chemical substances and their radiative forcing. Subsequently, their effect on temperature, human health and crop yields was calculated (Chapter 4).

Chapter 5 further reviews policy options that could be used to facilitate the widespread

9
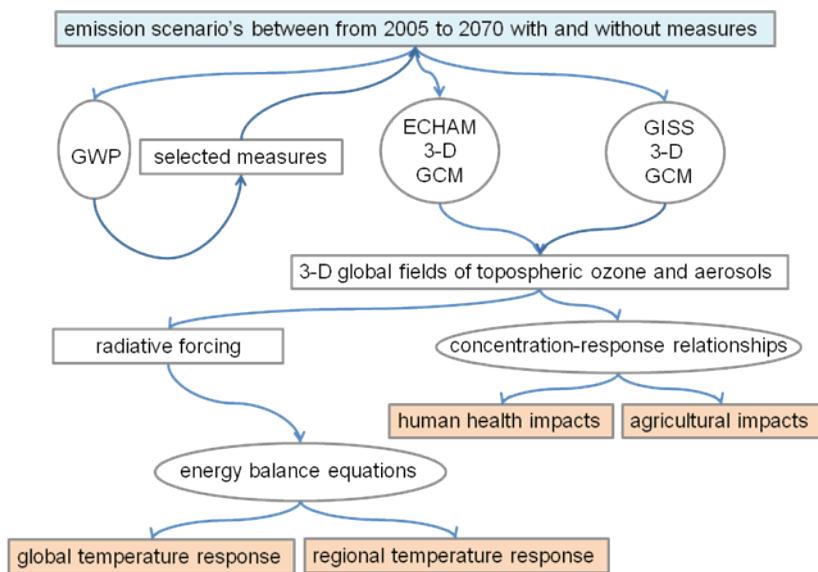
Figure 1.5. Chain of models used in the dedicated study of the Assessment.

implementation of the identified measures and illustrates this with case studies of their successful implementation in both developed and developing regions.

At each stage of the modelling undertaken in the Assessment (Figure 1.5), there are uncertainties in data and methods (uncertainty ranges are discussed in each chapter). The uncertainties in emissions and atmospheric composition were not considered when calculating the uncertainty of the modelled impacts. For the effect on warming, the results of the dedicated study were merged with the knowledge available from the literature reviewed, in particular to take account of the ranges of values that exist on the radiative forcing of BC and the range of climate responses to forcing. This was done so that the results would not be limited to the values produced by the two global climate-composition models used. In Chapter 4 the uncertainties concerning impacts are related to the uncertainties in concentration-response relationships. The resulting numbers are compared with other estimates in the literature.

References

Aghedo, A. M., Bowman, K. W., Worden, H. M.,
Kulawik, S. S., Shindell, D. T., Lamarque,
J. F., Faluvegi, G., Parrington, M., Jones,
D. B. A. and Rast, S. (2011). The vertical
distribution of ozone instantaneous radiative
forcing from satellite and chemistry climate
models. J. Geophys. Res., 116, D01305,
doi:10.1029/2010JD014243.

Amann, M. (2001). Emission inventories, emission
control options and control strategies: An
overview of recent developments. Water Air
Soil Poll., 130, 43–50.

Andreae, M. O. and Gelencsér, A. (2006). Black
carbon or brown carbon? The nature of light-
absorbing carbonaceous aerosols. Atmos.
Chem. Phys., 6, 3131–3148.

Andrews, T., Forster, P. M., Boucher, O., Bellouin,
N. and Jones, A. (2010). Precipitation,
radiative forcing and global temperature
change. Geophys. Res. Lett., 37, L14701,
doi:10.1029/2010GL043991.

Archer, D., Eby, M., Brovkin, V., Ridgwell, A.,
Cao, L., Mikolajewicz, U., Caldeira, K.,
Matsumoto, K., Munhoven, G., Montenegro,
A. and Tokos, K. (2009). Atmospheric lifetime
of fossil fuel carbon dioxide. Annu. Rev. Earth
Planet. Sci., 37, 117–124.

Denman, K. L., Brasseur, G., Chidthaisong,
A., Ciais, P., Cox, P. M., Dickinson, R. E.,
Hauglustaine, D., Heinze, C., Holland, E. and
Jacob, D. (2007). Couplings between changes
in the climate system and biogeochemistry. In:
Solomon, S., Qin, D., Manning, M., Chen,
Z., Marquis, M., Averyt, K. B., Tignor, M.
H. and Miller, L. (eds) Climate Change 2007:
The Physical Science Basis. Contribution of
Working Group I to the Fourth Assessment
Report of the Intergovernmental Panel on
Climate Change, 541–584.

Forster, P., Ramaswamy, V., Artaxo, P., Berntsen,
T., Betts, R., Fahey, D. W., Haywood, J., Lean,
J., Lowe, D. C., Myhre, G., Nganga, J., Prinn,
R., Raga, G., Schulz, M., and Van Dorland,
R. (2007). Changes in atmospheric constituents
and in radiative forcing. In: Solomon, S.,
Qin, D., Manning, M., Chen, Z., Marquis,
M., Averyt, K. B., Tignor, M. H. and Miller,
L. (eds) Climate Change 2007: The Physical
Science Basis. Contribution of Working Group
I to the Fourth Assessment Report of the
Intergovernmental Panel on Climate Change,
541–584.

Group of Eight (2009). Responsible Leadership
for a Sustainable Future. http://www.
g8italia2009.it/static/G8_Allegato/G8_
Declaration_08_07_09_final,0.pdf

Jacobson, M. Z. (2001). Global direct radiative
forcing due to multicomponent anthropogenic
and natural aerosols. J. Geophys. Res., 106,
1551–1568.

Matthews H.D. and A.J. Weaver, (2010).
Committed climate warming. Nature
Geoscience, 3, 142-143.

Molina, M., Zaelke, D., Madhava Sarma,
K., Andersen, S. O., Ramanathan, V. and
Kaniaru, D. (2009). Reducing abrupt climate
change risk using the Montreal Protocol and
other regulatory actions to complement cuts in
CO_2 emissions. PNAS, 106, 20616–20621.

Pozzoli, L., Bey, I., Rast, S., Schultz, M. G.,
Stier, P. and Feichter, J. (2008). Trace gas and
aerosol interactions in the fully coupled model
of aerosol-chemistry-climate ECHAM5-
HAMMOZ: 1. Model description and insights
from the spring 2001 TRACEP experiment.
J. Geophys. Res., 113, http://dx.doi.org/10.
1029/2007JD009007.

Ramanathan, V., Callis, L., Cess, R., Hansen, J.,
Isaksen, I., Kuhn, W., Lacis, A., Luther, F.,
Mahlman, J., Reck, R. and Schlesinger, M.
(1987). Climate-chemical interactions and
effects of changing atmospheric trace gases.
Rev. of Geophy., 25, 1441–1482.

Ramanathan, V., Crutzen, P. J., Lelieveld, J., Mitra, A. P., Althausen, D., Anderson, J. (2001). Indian Ocean Experiment: An integrated analysis of the climate forcing and effects of the great Indo-Asian haze. J. Geophys. Res., 106(D22), 28.

Ramanathan, V. and Feng, Y. (2008). On avoiding dangerous anthropogenic interference with the climate system: Formidable challenges ahead. PNAS, 105, 14245–14250.

Raes, F. and Seinfeld, J. (2009). New Directions: Climate change and air pollution abatement: A bumpy road. Atm. Env. 43, 5132–5133.

Satheesh, S. K. and Ramanathan, V. (2000). Large differences in tropical aerosol forcing at the top of the atmosphere and Earth's surface. Nature, 405, 60–63.

Shindell, D. T., Faluvegi, G., Bell, N. and Schmidt, G. A. (2005). An emissions-based view of climate forcing by methane and tropospheric ozone. Geophys. Res. Lett., 32, L04803, doi:10.1029/2004GL021900.

Shindell, D. T., Faluvegi, G., Unger, N., Aguilar, E., Schmidt, G. A., Koch, D., Bauer, S. E. and Miller, R. L. (2006). Simulations of preindustrial, present-day, and 2100 conditions in the NASA GISS composition and climate model G-PUCCINI. Atmos. Chem. Phys., 6, 4427–4459.

Solomon, S., Plattner, G.-K., Knutti, R. and Friedlingstein, P. (2009). Irreversible climate change due to carbon dioxide emissions. PNAS, 106, 1704–1709.

Solomon, S., Daniel, J. S., Sanford, T. J., Murphy, D. M., Plattner, G.-K., Knutti, R. and Friedlingstein, P. (2010). Persistence of climate changes due to a range of greenhouse gases. PNAS, 107, 18354–18359.

UNEP (2007) Global Envbironment Outlook 4 (GEO-4): Environment for Development. United Nations Environment Programme, Nairobi, Kenya.

UNEP (2010). The Emissions Gap Report http://www.unep.org/publications/ebooks/emissionsgapreport/pdfs/GAP_REPORT_SUNDAY_SINGLES_LOWRES.pdf

West, J. J., Naik, V., Horowitz, L. W. and Fiore, A. M. (2009). Effect of regional precursor emission controls on long-range ozone transport – Part 1: Short-term changes in ozone air quality. Atmos. Chem. Phys., 9, 6077–6093.

Chapter 2. Black carbon and tropospheric ozone precursors: drivers, emissions and trends

Coordinating lead author: David Streets (Argonne National Laboratory, USA).

Lead authors: Hajime Akimoto (Asia Center for Air Pollution Research, Japan), Paulo Artaxo (University of Sao Paulo, Brazil), Zbigniew Klimont (International Institute for Applied Systems Analysis, Austria), Kaarle Kupiainen (International Institute for Applied Systems Analysis, Austria), Greet Janssens-Maenhout (Joint Research Centre, European Commission, Italy), Harry Vallack (Stockholm Environment Institute, Environment Department, University of York, UK), Elisabetta Vignati (Joint Research Centre, European Commission, Italy).

Contributing authors: Gufran Beig (Indian Institute of Tropical Meteorology, India), Christopher Heyes (International Institute for Applied Systems Analysis, Austria), Lena Höglund Isaksson (International Institute for Applied Systems Analysis, Austria), Jean-François Lamarque (National Center for Atmospheric Research, USA), Zifeng Lu (Argonne National Laboratory, USA), N.T. Kim Oanh (Asian Institute of Technology, Thailand), Yuxuan Wang (Tsinghua University, China).

Key findings

Air pollution control policies will be effective. Up to the present time, emission reduction policies in North America and Europe have reduced emissions of sulphur dioxide (SO_2), nitrogen oxides (NO_x) and particulate matter (PM), including black carbon (BC), from many sectors. Current and planned regulations are expected to continue to drive down emissions in these two regions. In others, similar policies are expected to slow down their rate of growth in the future and, in the case of Northeast Asia, to bring about reduced emissions of BC, organic carbon (OC) and SO_2. Ensuring effective implementation of these policies is necessary to achieve the reductions. Sources emit a range of pollutants at the same time, and it is essential to consider co-emitted ones when designing abatement measures.

Without implementation of measures beyond current and planned regulations, methane (CH_4) emissions are expected to increase in the future. Increased coal mining and oil and gas production, coupled with growth in agricultural activities and municipal waste generation, are likely to lead to more than 25 per cent higher global anthropogenic CH_4 emissions by 2030 relative to 2005. The projected increase in fossil fuel production is the main driving force behind this growth.

Without implementation of measures beyond current and planned regulations, emissions of BC, OC and carbon monoxide (CO) are projected to remain relatively constant to 2030, as planned improvement in combustion technology will be offset by continued economic growth. The regional trends vary, however, with decreases in North America, Europe and Northeast Asia being balanced by increases in Africa and South Asia. Emission reductions in the transport sector will be the main cause of improvement. As the role of traditional biomass in residential combustion declines and improved technology comes into play, it is generally expected that primary OC/BC ratios will fall.

Emissions from residential biomass combustion are expected to become even more important in the future than they are today. Because efforts to curtail BC and OC emissions from transport and industrial sources are projected to be increasingly successful, the residential use of traditional biofuels in developing countries of Asia and Africa will dominate global emissions of anthropogenic carbonaceous aerosols in the future, contributing nearly half of BC emissions and about two-thirds of OC emissions by 2030.

Of those pollutants with a long history of control policies, NO_X emissions are expected to remain relatively constant in the future, while SO_2 emissions will decline between 2005 and 2030. Modest reductions in NO_x emissions in North America and Europe will be offset by increases everywhere else. Despite a strong increase, estimated at nearly 50 per cent, in South, West and Central Asia, global SO_2 emissions are projected to decline because of emissions reduction elsewhere, particularly in North America and Europe.

Open biomass burning is a large contributor to global emissions of carbonaceous aerosols and ozone (O_3) precursors. Recent estimates suggest that forest fires, savannah and grassland burning, etc., excluding agricultural burning, contribute about half of global BC and CO emissions and two-thirds of OC ones. It is not known how these emissions will change in the future and for this study they are assumed to remain constant at today's levels. Open biomass burning can be a key source contributor if it occurs close to a sensitive ecosystem such as the Arctic or the Himalayas, so the regional emissions distribution is important.

Confidence in emission estimates of primary aerosols and O_3 precursors varies by pollutant and world region. For NO_x, SO_2 and carbon dioxide (CO_2), knowledge of emission levels is relatively good. This derives from a history of emission measurements and consistent emissions from a given source type. However, despite an influx of new observational and measurement data in recent years, emissions of BC, OC, CO, CH_4 and non-methane volatile organic compounds (NMVOCs) remain quite uncertain for many source types. For CH_4 and NMVOCs, confidence is within a factor of three; and for the main products of incomplete combustion, BC, OC and CO, confidence at present is still only within a factor of roughly 2–5. Confidence is greater for the developed world than the developing regions because of a longer history of emission estimation, a wider dataset of source measurements, and more reliable statistical information on the number of sources and activity levels. As more sources are measured and more survey data gathered, confidence in emission estimates is expected to grow.

2.1 Introduction

This chapter discusses the current state of knowledge of primary emissions of carbonaceous aerosols, BC and OC, other fine particles and their precursors, SO_2 and ammonia (NH_3) and the precursors of tropospheric O_3, NO_x, CO, NMVOCs and CH_4. Emissions of CO_2 are also included in some presentations for comparison purposes. The chapter presents anthropogenic emissions of these species, as generated by the International Institute for Applied Systems Analysis Greenhouse Gas and Air Pollution Interactions and Synergies (IIASA GAINS) model for 1990, 2005 and 2030, the future reference scenario, as well as information on emissions from natural sources that are part of global climate modelling. It also shows results from some other global emission inventories by way of comparison and confirmation. Emissions of each species are disaggregated by major world region and emitting source category in order to highlight the most important contributors to global change and to direct the reader towards opportunities for mitigation action, which are discussed in detail in Chapter 5. To place present-day emissions in context, historical trends and likely future directions of emissions by considering socioeconomic and other drivers are also examined. The degree of confidence in these emission estimates is discussed,

with reference to available quantitative estimates of uncertainty. For some species the emission estimates are quite uncertain, and this carries over into uncertainty about their impacts and mitigation.

2.2 Socioeconomic and other drivers of emissions

Emissions of BC and tropospheric O_3 precursors are driven by basic societal forces that govern the production and consumption of energy, food and materials:

1. Population growth;

2. Economic development that drives, for example, the transition away from residential burning of solid fuels, the extent of private vehicle ownership, and dietary habits such as increased meat consumption that affects CH_4 emissions;

3. Consumption patterns, driven by population pressure, that include land-use changes involving deforestation and wetlands removal;

4. Technological change that can help in faster emission reductions through the spread of new, high-efficiency and low-emission technologies;

5. Environmental regulations driven by regional health and ecosystem concerns, resulting in, for example, reductions in PM, SO_2 and NO_x emissions; and

6. Other policy drivers such as global climate change mitigation agreements.

All these drivers interact with different sectors of human activity and have distinct time-frames for implementation and the achievement of objectives.

There are other driving forces that affect emissions but are not so directly linked to human activities. These include future climatological changes that may affect, for example, water availability and drought, which would in turn have an influence on food production and wild-fires, and consequently on emissions. Other examples might relate to the frequency and intensity of lightning and associated NO_x, soil NO_x and CH_4 released from warming tundra, increased tropospheric O_3 formation due to higher temperatures, etc. At the same time, previously unavailable areas may open up to enable some economic activities to shift or expand, such as drilling for oil and opening new shipping routes in the Arctic.

Before the start of the industrial revolution, emissions of BC and tropospheric O_3 precursors were essentially driven by natural episodic events – predominantly wildfires, volcanoes and other geogenic releases – and by the same kinds of continuous natural releases that are seen today, such as CH_4 emissions from wetlands, biogenic NMVOCs, and NO_x from lightning. Anthropogenic emissions at that time were limited to biomass burning for cooking and heating and represented only a small fraction of total emissions: for O_3 precursors and SO_2 less than 10 per cent, while for BC about a third of the total (Lamarque *et al.*, 2010). Some episodic releases, such as the large volcanic eruptions of El Chichon (1982) and Mount Pinatubo (1991), injected enormous amounts of ash, dust and gases into the atmosphere and had worldwide effects lasting two or three years (McCormick *et al.*, 1995).

The same is true of the large wildfires that periodically break out in Siberia and are often initiated by lightning strikes. Large boreal wildfires may also periodically inject smoke into the lower stratosphere (Fromm *et al.*, 2005). These episodic natural emissions can be of similar magnitude to anthropogenic emissions. Even some of the continuous natural emissions are on the same scale as present-day human-made emissions, examples of which include CH_4 from wetlands, bogs, swamps and tundra (200–400 Mt/yr, from Fung *et al.*, 1991); biogenic NMVOCs (500–750 Mt/yr, from Guenther *et al.*, 2006); volcanic SO_2 (13–15 Mt/yr, from Andres and Kasgnoc, 1998); lightning NO_x (about 5 Mt Nitrogen/year, from Schumann and Huntrieser, 2007) and NMVOCs from biomass burning (about 80 Mt/yr, from Lamarque *et al.*, 2010).

Though emissions from natural sources can show large inter-annual variability, they have not shown significant long-term trends (except for open biomass burning which has been growing strongly since the 1950s, largely from deforestation and land clearance, and hence is no longer exclusively natural). Anthropogenic emissions, on the other hand, have increased dramatically since pre-industrial times: for example, SO_2 and NO_x emissions had increased nearly 50-fold and emissions of BC and CO by factors of 5 and 10 respectively by the year 2000 (Lamarque *et al.*, 2010).

In the early to mid-19th century, widespread industrialization saw the advent of the use of fossil fuels, initially coal, to provide energy to power the production of goods and services. The development of the Haber-Bosch process for producing nitrogen fertilizer at the beginning of the 20th century led to an unprecedented growth in food production that supported strong population growth but at the same time caused a cascade of environmental changes, including increased air pollution and the perturbation of greenhouse-gas levels (Erisman *et al.*, 2008). At the same time, biofuels were being consumed in large amounts wherever human settlement occurred in timber-rich parts of the world (Fernandes *et al.*, 2007). At the beginning, the burning of wood and coal in factories and homes and on railways was an inefficient process that paid no regard to smoke emissions; large quantities of PM, rich in the carbonaceous products BC and OC, were therefore generated. Gaseous species including NO_x, CO, NMVOCs and SO_2 were produced at the same time in varying quantities.

Anthropogenic emissions began to grow rapidly, and it was not until the 1920s that attention began to be paid to limiting the emissions of PM through various add-on removal devices. The economic depression of the 1930s and installation of rudimentary emission controls led to a modest decline in most emissions. In many parts of the world, however, wartime production reversed this trend in the 1940s, and emissions began to increase rapidly in the post-war economic revival, beginning in about 1950. This trend spread quickly to most parts of the world, especially in the northern hemisphere, which until now has been responsible for the majority of human-caused pollution. As emissions grew and associated environmental and health impacts – acid rain, respiratory diseases, and heavy metals poisoning – became more evident, serious attention started to be paid to preventing atmospheric emissions in the early 1970s, at least in the developed world. The last few decades have seen a strong decline in emissions of PM and acidifying pollutants from industrial and transport sources in the developed world. However, since the late 1990s, a rapid increase in emissions in Asia has offset these reductions, often leading to continued growth at global level. Emissions of CO_2 have kept growing, and only the most recent economic crisis resulted in their temporary stabilization (Friedlingstein *et al.*, 2010).

For the future, it is generally expected that growth in emissions of air pollutants will be tempered by continuing pressure to achieve ever more ambitious environmental targets. In some cases emissions will be ameliorated simply by economic development, which will, for example, gradually replace residential solid fuel combustion with cleaner fuels and remove older vehicles from the road. This will go some way towards reducing emissions of PM, including BC and OC, as well as hydrocarbons and CO. For other species, primarily SO_2 and NO_x, where there is now a fairly long history of pollution control, the experience of developed countries can be expected to spread gradually throughout the world and hold down future emissions; recent emission inventories and assessments in Asia seem to confirm this assumption (for example, Zhang *et al.*, 2009a; Klimont *et al.*, 2009; Xu *et al.*, 2009). For some sources of all species, however, mitigation is either difficult or expensive and, without new policies, emissions will persist for the foreseeable future. This may lead to growth in total global emissions if the spread of cleaner technology cannot keep pace with economic and industrial growth. Emission projections are sensitive to the socioeconomic attributes of the scenarios, however, and it is not always clear which pathways will generate the

16

highest emissions. For example, while high economic growth is likely to result in high levels of emissions, it may also promote the transfer of high-performing technologies to less developed countries.

2.3 Global BC, OC and O$_3$ precursor emissions

This section reviews estimates of global emissions of BC, OC and tropospheric O$_3$ precursors, highlighting the important source types, economic sectors and geographical regions. It begins by describing the IIASA GAINS model used in this Assessment for emissions calculations, together with its assumptions about emission factors (Section 2.3.1). Section 2.3.2 presents emissions for the year 2005 from the IIASA GAINS model that were used to anchor the future reference scenario emissions to 2030. Though emphasis is on anthropogenic emissions, the major natural sources of relevant species are also introduced. Biomass-burning emissions are discussed in section 2.3.3, as they represent a large source of all relevant species. Uncertainties in present-day emissions are discussed in section 2.3.4, and key observational support for current emission trends is provided in section 2.3.5. How present-day emission levels were established is discussed in section 2.3.6, through examples of historical emission estimates since the beginning of industrialization. Section 2.4 describes the assumptions that were made for the construction of the reference scenario, and section 2.5 contains a detailed description of recent past, present and future emission estimates from the IIASA GAINS model used as the basis for the analysis of mitigation options (Chapter 5).

2.3.1 The IIASA GAINS model

Estimation of anthropogenic emissions in this chapter and the analysis of mitigation opportunities (Chapter 5) have been performed with the IIASA GAINS model (http://gains.iiasa.ac.at), an integrated assessment model that explores cost-effective emission control strategies to reduce greenhouse gases and/or improve local and regional air quality. The model has been applied to analyse strategies in a number of regions and countries and,

recently, for the whole world. The emission calculation in IIASA GAINS draws on the available measurement literature and has been reviewed by experts from academia, government and industry who work on source-specific issues and national aspects of emissions. The model applies emission factors that reflect country-specific conditions such as fuel quality, combustion technologies, fleet composition, maintenance levels and the application of control technologies.

Emission factors for BC and OC in the GAINS framework have been developed in parallel with the assessment of PM emissions to assure overall consistency (Kupiainen and Klimont, 2007). Detailed discussion of the calculation of BC and OC emissions in GAINS, including emission factors for the developed countries, is given in Kupiainen and Klimont (2007) and for Asia in Klimont et al. (2009). Emission factors for other world regions (see Cofala et al., 2007) are based on data from Bond et al. (2004, 2007). Methane emission factors have been derived following the guidelines (1997 and 2006 versions) of the Intergovernmental Panel on Climate Change (IPCC) as closely as data availability allows. Country-specific information has been included from the United Nations Framework Convention on Climate Change (UNFCCC) and other external sources. For some source categories (e.g., livestock and coal mines), country-specific implied emission factors have been used directly as reported to the UNFCCC, while for others (e.g., oil and gas production and transportation) emission factors have been derived from underlying data (e.g., fractions of heavy/conventional oil, current utilization of associated gas, pipeline lengths and amounts transported). For countries not reporting to the UNFCCC, emission factors have been derived based on underlying factors available from international statistics and national sources. For NO$_x$, the emission factors originate from the Regional Air Pollution Information and Simulation (RAINS) databases for Europe (Cofala and Syri, 1998a) and the GAINS model implementation for Asia (Klimont et al., 2009). For other regions, the default factors that distinguish the effects of applied emission control measures were used as a starting point, then adjusted to the values

17

implied by available national or international emission inventories (Cofala *et al.*, 2007). Similarly, for SO_2, information originating from Cofala and Syri (1998b), Cofala *et al.* (2007) and Klimont *et al.* (2009) was modified for other countries with coal quality parameters provided in the IEA Coal Research database (IEA, 1997). Emission factors for CO are based on the IPCC guidelines (Houghton *et al.*, 1997) and modified for country-specific conditions (e.g., for wood burning in the domestic sector and for transport) to the extent that appropriate information was available. For NMVOCs, sources include Klimont *et al.* (2000, 2002), Wei *et al.* (2008), and the EDGAR v4 database (EC-JRC/PBL, 2010). The CO_2 emission factors rely on IPCC recommended values and for NH_3 on Klimont and Brink (2004), Bouwman *et al.* (2002), Fischer *et al.* (2010) and EDGAR v4 (EC-JRC/PBL, 2010).

During 2010, for the purpose of this Assessment, emission factors for several priority sectors were revisited to include results from the most recent scientific literature. Emission factors for cook stoves and power generation now take into account measurements by Roden *et al.* (2006, 2009), Christian *et al.* (2010), and recent studies by Chen *et al.* (2009), Zhi *et al.* (2009) and Zhao *et al.* (2010). In the transport sector a major new feature is the estimation of emissions from high-emitting vehicles based on studies by Durbin *et al.* (1999), Yanowitz *et al.* (1999), Hsu and Mullen (2007), Ban-Weiss *et al.* (2009) and Subramanian *et al.* (2009). The update of input data to GAINS also included a revision of emission factors for diesel cars and trucks, for which emissions in real operating conditions differ from emission factors derived from test cycles. This revision was based on the results of research projects like ARTEMIS (http://ec.europa.eu/transport/road safety/projects/doc/artemis.pdf) and HBEFA (http://www.hbefa.net/e/index.html). Data used by IIASA were provided by the COPERT 4 (v7.1) model (http://lat.eng.auth.gr/copert/files/COPERT4_v7_1.pdf). Emission factors from brick manufacturing, coke production and garbage burning in the developing world were revised to take into account the recent source measurements conducted by Christian *et al.* (2010) and Bellprat (2009).

2.3.2 Emissions for the year 2005

Table 2.1 presents anthropogenic and natural emissions of each species for the year 2005, as used by the atmospheric models in this Assessment. The anthropogenic totals are taken from the GAINS model and are shown in Figure 2.1; other estimates of present-day emissions are presented in Appendix A.2. Anthropogenic contributions are discussed in detail in section 2.5. The transport sector in Table 2.1 includes emissions from international shipping and aviation that come from Representative Concentration Pathway 8.5 (Lamarque *et al.*, 2010). Aviation is a minor contributor to global anthropogenic emissions of these species, but international shipping contributes about 14 per cent and 23 per cent of global SO_2 and NO_x, respectively. As discussed in section 2.1, emissions from natural sources are significant for all pollutants and are essential inputs to the atmospheric and climate models. Table 2.1 includes the values of natural emissions that are used in the GISS and ECHAM models. With the exception of agricultural burning, open biomass burning is categorized as a natural source in Table 2.1. While it is clear that wildfires are under notable human influence (Achard *et al.*, 2008), it is not possible to quantify the human causation globally. Wildfires are also affected by local climatic factors (Bowman *et al.*, 2009) that may change over time. Policy measures to reduce wildfires and their emissions can only be of limited value, therefore, and are not a focus of this mitigation-oriented Assessment. Nevertheless, it must be remembered that wildfires in forested land and savannah are important sources of global carbonaceous aerosols and contribute substantially to O_3 precursors. Section 2.3.3 discusses biomass burning in greater detail.

2.3.3 Emissions from biomass burning

Emissions from fire are an important component of the Earth's system, controlling atmospheric composition at a global level (Bowman *et al.*, 2009). Biomass burning is the major source of BC, OC and O_3 precursors in the southern hemisphere and is an important contributor in the northern hemisphere. It is seasonal, with significant variability in

18

Table 2.1 Anthropogenic and natural emissions for the year 2005 used in this assessment (Mt/yr)

	BC	OC	$PM_{2.5}$	SO_2	NO_x[a]	CH_4	NMVOC	CO	NH_3[b]
Anthropogenic									
Large-scale combustion	0.10	0.15	8.1	71.6	34.1	0.36	1.2	29.9	0.07
Industrial processes	0.43	0.66	4.5	12.7	2.4	0	8.0	74.2	0.11
Residential-commercial combustion	2.7	9.6	17.8	5.8	5.0	8.8	37.9	195	0.34
Transport	1.6	1.4	3.4	15.9	71.5	2.3	38.5	266	0.36
Fossil-fuel extraction and distribution	0.28	0.06	0.51	2.4	1.4	101	36.4	2.0	0
Solvents	N/A	N/A	N/A	N/A	N/A	N/A	23.4	N/A	N/A
Waste/landfill	0.1	0.75	1.3	0.06	0.12	49.8	1.1	6.2	0.02
Agriculture[c]	0.31	1.2	3.4	0.16	0.26	126	4.0	25.5	39.5
Total anthropogenic	5.5	13.8	39.0	109	115	288	150	599	40.4
Natural[d]	3-3.7	33-38	6000[e]	28-31	54-60	210	470-549[f]	46-63	21
Global total	8.5-9.2	47-52	6039	137-140	169-175	498	620-699	645-662	61

a Reported as NO_2.

b NH_3 emissions are from EDGAR v4.1.

c Includes the burning of agricultural residues.

d Includes the open burning of all biomass other than agricultural residues.

e Includes total fluxes of sea salt and dust. According to IPCC (2007), the submicron shares of sea salt and dust are 15 per cent and 7–20 per cent, respectively.

f Isoprene.
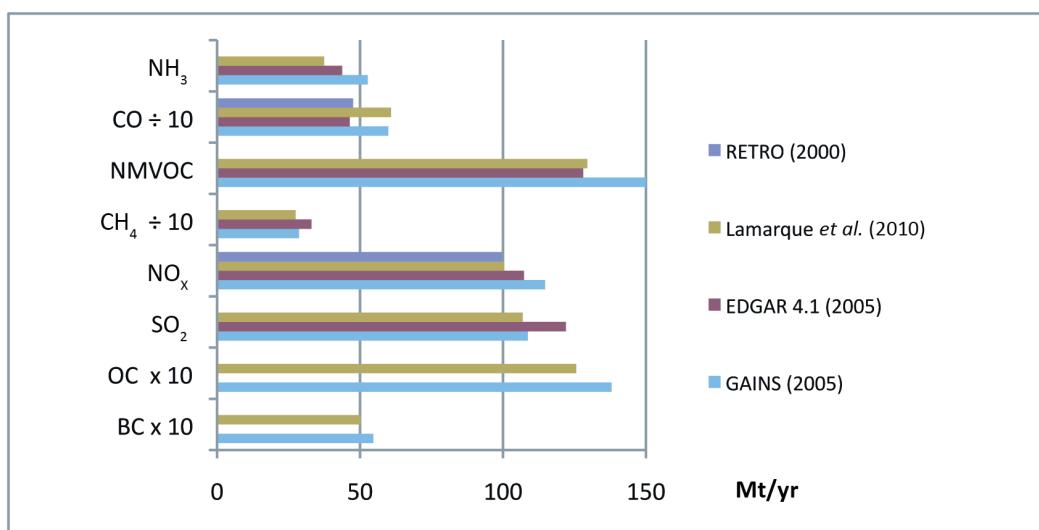
Figure 2.1. Comparison of GAINS 2005 emissions with other global inventories (not including open biomass burning).

emissions both temporally and geographically (Andreae and Merlet, 2001; Streets *et al.*, 2003b). Particles from biomass burning are the major anthropogenic aerosol component in South America, Africa and Southeast Asia during their respective dry seasons. Such emissions have been shown to significantly alter the radiation balance and cloud properties over large regions of the southern hemisphere (Reid *et al.*, 2005a, b; Andreae *et al.*, 2004; Artaxo *et al.*, 2002). Different approaches have been used to obtain emission factors for biomass-burning, such as direct measurements over fires in field experiments (Yamasoe *et al.*, 2000) and aircraft experiments (Yokelson *et al.*, 2007), as well as laboratory measurements (Christian *et al.*, 2003). Andreae and Merlet (2001) compiled emission factors for over 100 trace-gas species and aerosol components for tropical forests, extratropical forests and savannah and grassland emissions.

There are two main components to human-caused biomass burning: deforestation fires and management fires, for example of agricultural residue or as pasture maintenance. Although deforestation rates have been reduced since 2005, especially in the tropics, neither the incidence of fire nor the quantity of smoke in tropical regions has fallen commensurately (Artaxo and Andreae, 2007). Recent estimates of carbon emissions from open biomass burning range from 1 500 to 2 800 Mt C/yr (van der Werf *et al.*, 2010) over the period 1997–2009. In its Fourth Assessment Report (AR4) the IPCC estimated emissions from deforestation to be 1 600 Mt C/yr (IPCC, 2007). Efforts to provide online fire data worldwide through the Global Fire Monitoring Center show a very dynamic system that responds quickly to precipitation changes as well as policy measures.

Several detailed global inventories of biomass-burning emissions are available. These include EDGAR (Olivier *et al.*, 1996; EC-JRC/PBL, 2010), Bond *et al.* (2007) and Junker and Liousse (2008). A gridded historical (1850–2000) biomass-burning emissions product was recently made available in support of the IPCC's Fifth Assessment Report (AR5) (Lamarque *et al.*, 2010). However, only a few inventories include biomass-burning emissions for past decades (Ito and Penner, 2004; Schultz *et al.*, 2008). For the principal categories of biomass burning the main emission datasets are:

1. The RETRO inventory (Schultz *et al.*, 2008), which provides emissions from wildfires for each year during the 1960–2000 period, on a monthly basis;

2. The GICC inventory (Mieville *et al.*, 2010), which gives emissions from open biomass burning for the 20th century (1900–2000) on a decadal basis, based on Mouillot and Field (2005); and

3. The Global Fire Emissions Database (GFED) inventory (van der Werf *et al.*, 2006, 2010), which now covers emissions for the 1997–2009 period in GFED3.

Due to the efforts of several countries to reduce deforestation to avoid carbon emissions, several regions are observing important changes in deforestation rates and biomass-burning emissions (Artaxo, 2010). These efforts have been encouraged by the Reducing Emissions from Deforestation and Degradation (REDD) scheme, in which carbon credits can allow funding from developed nations to be used to protect forests in developing nations. Another important reason to reduce biomass burning is to lessen the effect of the smoke in suppressing cloud formation and precipitation, resulting in a slow-down of the hydrological cycle (Andreae *et al.*, 2004). Figure 2.2 gives deforestation rates in the Brazilian Amazonia from 1980 to 2009, showing a strong reduction in the last five years – from 27 000 km^2 deforested in 2004 to 7 000 km^2 in 2009 – through Brazil's implementation of national policies. Similar reductions are happening in other tropical areas including Indonesia, and if global policies to reduce deforestation come into place, these reductions can be even more significant and may change the future picture of emissions quite rapidly. On the other hand, a future climate with higher temperatures and reduced precipitation and soil moisture may increase the incidence of forest fires.

Even though progress is being made in reducing biomass burning in many parts of the world, it can still have an important influence on sensitive ecosystems nearby, for example, springtime fires in the boreal forests of Europe, Central Asia and Siberia have been shown to contribute significantly to pollution in the Arctic (Quinn *et al.*, 2008). Similarly, the Himalayas are vulnerable to biomass burning in nearby regions of South and Southeast Asia (Ramanathan and Carmichael, 2008). In both cases, enhanced environmental damage can arise from BC deposition on snow and ice and associated influences on the local albedo.

Emissions from biomass burning, which can be substantial percentages of total emissions (e.g., 34 per cent of total global BC, 65 per cent of OC and 43 per cent of CO), are included in the natural emissions category presented in Table 2.1. As mentioned earlier, the amount of biomass burning likely to occur in future is sensitive not only to socioeconomic forces but also to future climatological changes that may affect water availability and soil moisture, which will in turn influence the amount of open biomass burning. Emissions from burning of agricultural residues may increase in the developing countries of Asia, for example, as the living conditions of farmers

improve and pressure increases to have more crop cycles per year. For the purposes of this study, however, open biomass-burning emissions are assumed to remain constant between 2005 and 2030.

2.3.4 Uncertainties and issues in quantifying emission estimates

The degree of confidence in emission estimates varies widely depending on species, sector and region of the world. For some sources in some countries very little is known about activity levels and real-world emission factors, and choices for parameter values in such cases rely heavily on inferences of activity levels from quite limited and uncertain statistical information and extrapolations of emission factors from sources that have been measured in other parts of the world. Often, these are underestimated: many sources are uncounted in statistics and unmeasured sources tend to be poorer performers than tested ones. Additional factors influencing uncertainty in the estimation of emissions include fuel quality and the penetration and efficiency of abatement technology.

For global emissions of BC and OC, Bond *et al.* (2004) presented a formal uncertainty analysis with 95 per cent confidence intervals
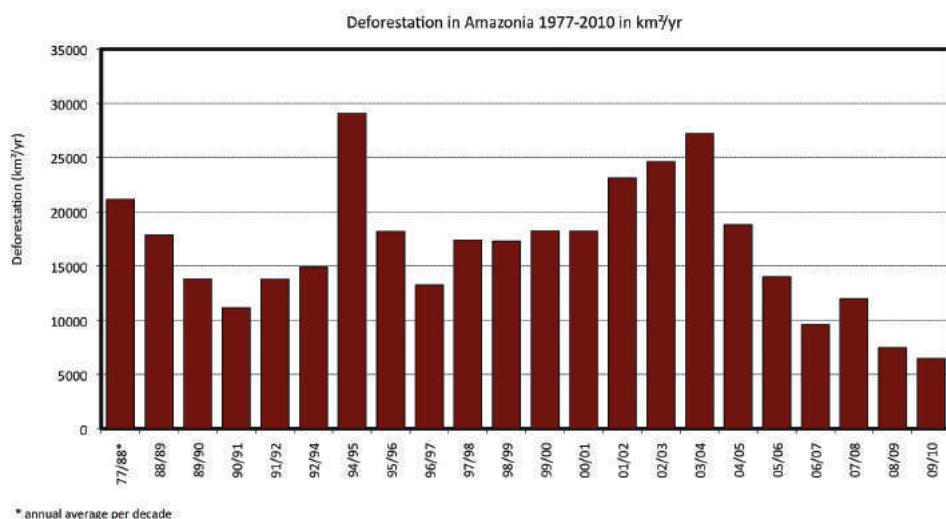
Figure 2.2. Annual deforestation rates in Brazil for the last 30 years, showing a strong reduction after 2004 (Artaxo, 2010).

Chapter 2. Black carbon and tropospheric ozone precursors: drivers, emissions and trends

for total global emissions. For BC emissions from contained combustion (essentially anthropogenic burning), the range was -30 per cent to +120 per cent. For BC from open biomass burning the range was -50 per cent to +200 per cent. For OC, the corresponding ranges were - 40 per cent to +100 per cent and -50 per cent to +130 per cent. The major source types contributing to uncertainty in anthropogenic BC emissions were identified as coke making, residential wood combustion, industrial coal combustion and on-road diesel vehicles. For anthropogenic OC, the largest contributors were residential wood combustion (by far), gasoline vehicles, and agricultural waste burning. Bond *et al.* (2004) showed that emissions are not predictable from overall stoichiometry (the amounts of fuel and air used in combustion). Rather they are determined by combustion kinetics and mixing. Moreover, carbonaceous aerosols are usually formed under poor combustion conditions, when insufficient oxygen is available for complete combustion. These conditions are generally associated with small, inefficient devices using poor-quality fuels, which are mostly, but by no means exclusively, to be found in developing countries. Residential cook stoves are a typical example of a combustion device that yields high emissions of carbonaceous aerosols; and if the extremely wide variation in stoves and their usage (stove type, fuel type and quality, fuel moisture content, oxygen availability, draft and ventilation conditions, temperature requirements, etc.) is taken into account, it should not be surprising that the uncertainty in emissions is high. The wide variation among emission factors reported from field and laboratory tests confirms this (e.g., Roden *et al.*, 2006, 2009).

Uncertainty in emissions of other species, including the precursors of tropospheric O_3 is generally not as high as for carbonaceous aerosols. As far as can be ascertained, there have been no formal estimates of uncertainty in global emissions of these species, such as are contained in the EDGAR inventory. Estimates for Asian gaseous emissions conducted for the NASA TRACE-P mission (Table 2.2) provide useful illustrations of the relative uncertainties in emissions by species and by level of economic development (Streets *et al.*,

2003a). The least uncertainty is associated with SO_2 (9–44 per cent) and CO_2 (7–91 per cent), both of which are to some extent constrained by the elemental concentrations in the fuels (sulphur and carbon). CO_2 can actually be an indicator of how well activity levels are known. Uncertainty in emissions of BC and OC were the highest by far (160–500 per cent for developing countries and 80–180 per cent for developed countries in Asia), mostly driven by high uncertainty in the emission factors of small sources like cook stoves, kilns and ovens, and some kinds of vehicles. NO_x, CO, CH_4 and NMVOCs are all subject to considerable uncertainty because of their sensitivity to combustion conditions, just like BC and OC; in addition, there are other, non-combustion contributions to CH_4 and NMVOC emissions that are hard to characterize. Emissions of NH_3 are largely associated with agricultural emissions, the sources of which are not easily quantified. Table 2.2 also shows the lower levels of uncertainty for developed countries like Japan (e.g., ±19 per cent for NO_x emissions), compared with the developing regions of South Asia (±63 per cent) and Southeast Asia (±92 per cent). This difference relates to variations in the availability and reliability of detailed activity statistics and the availability of measured emission factors (or lack of them). Discussion of uncertainties in Asian emissions was further developed by Zhang *et al.* (2009a) in the context of the updated TRACE-P emission inventory for the INTEX-B mission. They showed that incorporation of local knowledge for developed countries such as Japan and the Republic of Korea could reduce the uncertainties.

Uncertainties in the GAINS estimates of base-year emissions are similar to those reported in Table 2.2. Schöpp *et al.* (2005) discussed the uncertainties of emission estimates in the integrated assessment model RAINS, considering the uncertainties in the model parameters themselves. Overall, it was found that a typical range of uncertainties for modelled national emissions of SO_2, NO_x, and NH_3 in Europe lies between 10 and 30 per cent, which is consistent with the results presented in Table 2.2 for developed countries. In general, the uncertainties are strongly dependent on the potential for error

22

compensation. This compensation potential is larger (and uncertainties are smaller) if calculated emissions are composed of a larger number of equal-sized source categories, where the errors in input parameters are not correlated with each other. Thus, estimates of the national total emissions are generally more certain than estimates of sectoral emissions. While the analysis of Schöpp *et al.* (2005) showed that the actual uncertainties are critically influenced by the specific situation – including the pollutant, year and region – the emission factor is an important contributor to uncertainty in estimates of historical emissions, while uncertainty in the activity data dominates the uncertainty in future emission estimates.

A quantitative assessment of uncertainty for future-year emissions was not performed for this Assessment. As discussed in Nakicenovic *et al.* (2000) and Streets *et al.* (2004), uncertainties associated with long-term global projections are best treated within a scenario context. This helps in the assessment of future developments in complex systems that are either inherently unpredictable or that have high scientific uncertainties. In all stages of the scenario-building process, uncertainties of different kinds are encountered. A large uncertainty surrounds future emissions and the possible evolution of

their underlying driving forces, as reflected in a wide range of future emission paths in the literature. The uncertainty is further compounded in going from emission paths to formulating adaptation and mitigation measures and policies. In this Assessment a set of alternative scenarios was devised drawing on the two different developments of the energy system (reference and CO_2 measures scenarios from IEA, 2009) for which a number of control scenarios were prepared (Chapter 5). Hence, the alternative scenarios describe the range of possible future emissions.

2.3.5 Observational support for emission estimates

Present-day emission inventories of O_3 precursors can be verified by satellite and airborne and ground-based observational data. The estimation of emissions constrained by satellite observations is often called a top-down approach, as compared with the conventional bottom-up inventories based on activity data and emission factors. Further, *a priori* bottom-up emission estimates can now be assimilated with satellite data using inversion techniques to yield *a posteriori* estimates that are more consistent with observational data.

Table 2.2. TRACE-P uncertainty estimates (per cent) for Asian emissions (upper bound, +95 per cent confidence interval).

	SO_2	NO_X	BC	OC	CO_2	CO	CH_4	NMVOCs	NH_3
China	13	23	484	495	16	156	71	59	53
Japan	9	19	83	181	7	34	52	35	29
Other East Asia	12	24	160	233	13	84	101	49	31
Southeast Asia	27	92	257	345	91	214	95	218	87
India	26	48	359	544	33	238	67	149	101
Other South Asia	35	63	379	531	44	291	109	148	101
International shipping	44	56	402	402	40	72	72	204	–
All Asia	16	37	364	450	31	185	65	130	72

NO_X emissions

Much of the interest in verification of regional emissions of NO_X has focused on East China, where a rapid increase in emissions in recent decades is thought to have been a driver of the increase of O_3 in the northern hemisphere. From SCIAMACHY and OMI satellite data studies such as Ma *et al.* (2006), Akimoto *et al.* (2006), Zhang *et al.* (2007) and Lin *et al.* (2010), it can be concluded that, although emission inventories of fossil-fuel NO_X in China in the late 1990s to early 2000s could have been underestimated by more than 30 per cent due to errors in coal consumption statistics and other uncertainties, more recent bottom-up emission inventories of NO_X agree within 15 per cent with satellite-constrained estimates (Zhang *et al.*, 2009a). However, satellite data are able to provide more accurate spatial distributions of power plants and other anthropogenic and natural activities and therefore improve emission inventory mapping. For example, the OMI satellite products have been used to identify newly added NO_X emissions from new power plants in Inner Mongolia, China (Zhang *et al.*, 2009b).

CO emissions

Top-down approaches to constraining global CO emissions using satellite remote sensing data and surface observational data have long been pursued to validate inventory data and estimate their uncertainties. Several studies using inverse modelling techniques found that the earlier EDGAR inventory (Olivier *et al.*, 1996) appears to have underestimated sources for various regions (Kasibhatla *et al.*, 2002; Pétron *et al.*, 2004; Mueller and Stavrakou, 2005; Arellano *et al.*, 2006). Particularly, global inversion analyses using MOPITT satellite data found that sources in Asia and Africa are significantly underestimated by the ED-GAR inventory. The inter-comparison study of Shindell *et al.* (2006) showed that forward models underestimate CO in the northern extratropics. More specifically, analyses of aircraft data downwind of Asia obtained in the TRACE-P campaign imply that emissions of CO from China were too low in the original TRACE-P emission inventory (Carmichael *et al.*, 2003; Allen *et al.*, 2004). Motivated by these studies, Streets *et al.* (2006) developed a new bottom-up inventory of CO emissions for China that are 36 per cent higher than the earlier work and give much better agreement between modelled and observed CO concentrations.

NMVOC emissions

Among the key precursors of tropospheric O_3, NMVOC emissions are difficult to validate by observational data, since continuous measurement of each NMVOC component on the ground is very limited and satellite data are not available for non-methane hydrocarbons (NMHC). Recently, however, satellite data using GOME, SCIAMACHY and OMI sensors for column distribution of formaldehyde (HCHO) (e.g., De Smedt *et al.*, 2008) have been utilized to verify NMVOCs from biomass burning and to estimate emissions of isoprene, the most significant precursor of HCHO from the biosphere. For example, Fu *et al.* (2007) found that the biomass-burning source for East and South Asia is almost five times the TRACE-P inventory estimate, while an estimate of anthropogenic reactive NMVOC emissions from China is only 25 per cent higher based on wintertime GOME observations. Generally, NMVOC emissions from biomass burning in Asia are greatly underestimated in emission inventories. Dufour *et al.* (2009) studied HCHO tropospheric columns from SCIAMACHY with the CHIMERE chemical transport model for Europe, and reported that the agreement between measurements and model was within 20 per cent on average.

Decadal ozone trends

Consistency between trends of observed tropospheric O_3 abundance and precursor emissions in the last couple of decades is very important for assessing the relative importance of reducing O_3 compared to long-lived greenhouse gases for climate-change mitigation up to 2030. Emissions of O_3 precursors generally increased until the end of the 1980s in the northern hemisphere. After the 1990s, emissions in Europe and North America started to decrease due to successful control measures – including stringent regulations in the USA (Monks *et al.*, 2009) – and remained stable or slightly decreased through the 2000s,

24

consistent with long-term baseline O_3 measurements at Mace Head on the Atlantic coast of Ireland (Figure 2.3).

In contrast, emissions in Asia have been increasing rapidly since the 1980s, becoming comparable to emissions in Europe and North America in the 1990s, and have continued to increase in the 2000s, exceeding emissions from Europe and North America in the northern hemisphere (Akimoto, 2003). Figure 2.4, and similar data from other stations, confirms the increase in O_3 on the Asian continent.

Substantial amounts of surface O_3 trend data have been gathered in Europe, North America and Northeast Asia in the last couple of decades, and increasing trends are observed at most of the baseline sites in the northern hemisphere. Baseline observation sites in both Europe and North America typically show an increase of 0.3–0.4 parts per billion (ppb) per year of surface O_3 during the 1990s to early 2000s (Monks *et al.*, 2009). However, this rate of increase, which is more than 50 per cent of the rate observed in Northeast Asia, is too high to be ascribed to the precursor emission increase in Northeast Asia resulting from intercontinental transport. There is still significant uncertainty about the exact cause of these increases, which deserves further research.

2.3.6 Historical trends in emissions

BC emissions
There have been four studies to date that have attempted to reconstruct historical emission
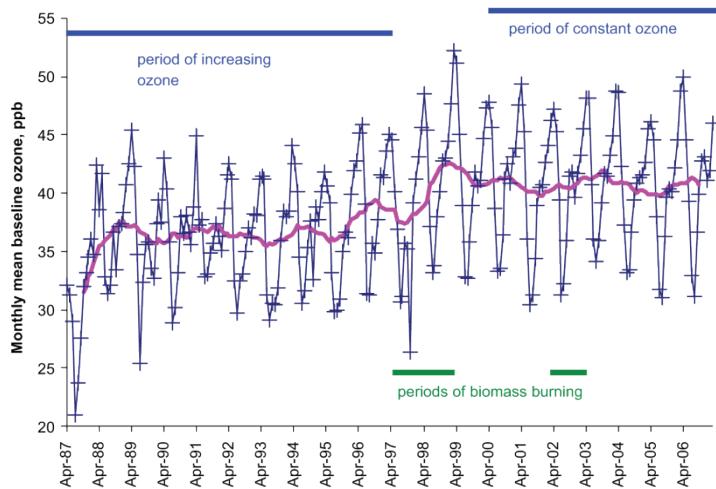
Figure 2.3. Time development of the monthly mean (+) and 12-month running mean (solid line) baseline O_3 mixing ratios from April 1987 at Mace Head (from Derwent *et al.*, 2007).
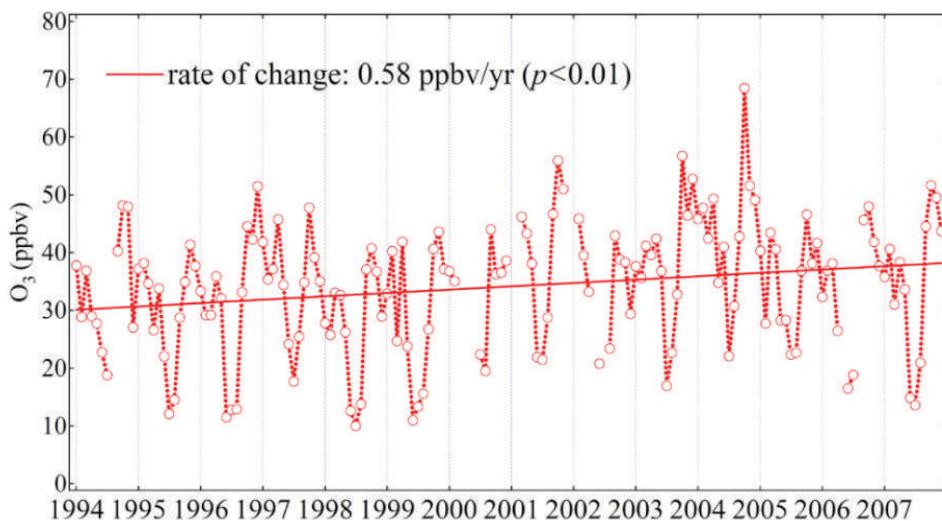
Figure 2.4. Monthly mean O_3 mixing ratios and the linear fit line at Hok Tsui, Hong Kong, during 1994–2007 (from Wang *et al.*, 2009).

Chapter 2. Black carbon and tropospheric ozone precursors: drivers, emissions and trends

inventories of carbonaceous aerosols. Bond *et al.* (2007) extended the earlier Bond *et al.* (2004) inventory for the year 1996 to the period 1850–2000 for biofuel and fossil-fuel combustion, building on a companion trend of global biofuel use for 1850–2000 (Fernandes *et al.*, 2007). Figure 2.5 compares the historical BC emission trends of Bond *et al.* (2007), Ito and Penner (2004) and Novakov *et al.* (2003). Qualitatively the trends of all three studies are similar. The major features are growth from the 19th century until about 1920, a period of little change from 1920 to about 1950, rapid increase from 1950 to about 1990, and then attenuation of the growth and perhaps a levelling off after 1990.

Quantitatively, however, the three studies show significant differences. The fossil-fuel trend of Novakov *et al.* tracks Bond *et al.* until 1950, after which it increases much more rapidly, ending up in 2000 at roughly double (~6 Mt/yr versus ~3 Mt/yr). This is attributed to the use by Novakov *et al.* of the emission factors of Cooke *et al.* (1999), which are now thought to be too high. On the other hand, the fossil-fuel BC trend of Ito and Penner agrees much better with Bond *et al.* in modern times, but is significantly lower in the early part of the 20th century. This might be due to the fact that Ito and Penner, for the most part, did not take into consideration the relatively poor technologies in the early time period, with much higher emission factors than today and no emission controls. The estimates of BC emissions from biofuel combustion of Bond *et al.* and Ito and Penner are quite similar. It should also be noted that Novakov *et al.* did not consider biofuel combustion.
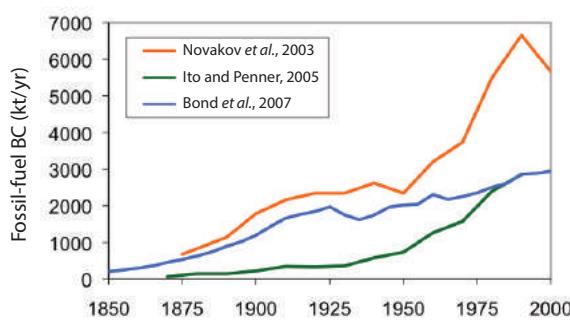
Ozone precursor emissions

The radiative forcing of tropospheric O_3 from the pre-industrial era to the present is very much dependent on the pre-industrial concentration of O_3. Estimates of surface O_3 concentrations at the end of the 19th century are of the order of 10 ppb, but are based on extremely limited quantitative data or more widespread data that are only qualitatively reliable (Pavelin *et al.*, 1999). Such low values cannot be explained by current models which, when anthropogenic emissions of NO_x, CO, NMVOCs and CH_4 are excluded, give around 20 ppb or more (Gauss *et al.*, 2006). A large reduction in natural-source emissions in the current inventories is required in order to reproduce the observed O_3 abundance (Mickley *et al.*, 2001). Although there remains uncertainty in the difference in tropospheric O_3 abundance between the pre-industrial and present day, current estimates of radiative forcing, which are comparable with that of methane, are generally based on the converging estimates of multi-model studies overestimating the pre-industrial level (IPCC, 2007). This apparent overestimation does not, however, imply a similar underestimation of the response to modern emission changes, as the uncertainty stems from poor knowledge of 19th century emissions rather than poor understanding of the atmospheric processes governing O_3. Consistency between trends of observed tropospheric O_3 abundance and precursor emissions in the last couple of decades is very important for assessing the relative importance of reducing O_3 emissions alongside other greenhouse gases for climate-change mitigation over the next few decades.
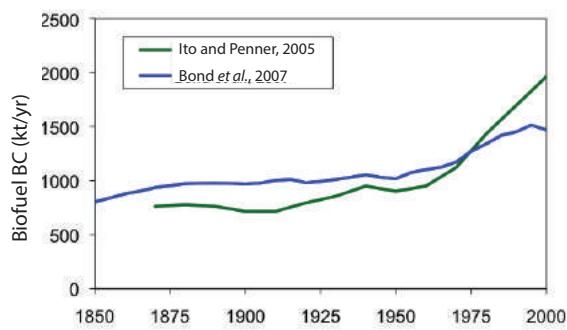
Figure 2.5. Historical BC emission trends from fossil-fuel (left) and biofuel (right) combustion from Novakov *et al.* (2003), Ito and Penner (2004) and Bond *et al.* (2007).

26

The most recent compilation of historical estimates of emissions of tropospheric O_3 precursors is the one developed for use in the chemistry model simulations that form part of the basis of the IPCC's fifth assessment report, as documented in Lamarque *et al.* (2010). This dataset is an historical reconstruction of global emissions back to 1850, normalized to year-2000 estimates. It does not develop new emission estimates from original data, but rather tries to take previously compiled trends and harmonize them. For BC and OC, the inventory of Bond *et al.* (2007) is used, and results are therefore identical to what was presented in the previous section. The historical trends for NO_x, CO, NMVOCs and CH_4 are developed from a combination of primary sources including the EDGAR-HYDE dataset (Olivier and Berdowski, 2001; van Aardenne *et al.*, 2001) and the RETRO dataset (Schultz *et al.*, 2008). Figure 2.6 shows the resulting trends for global anthropogenic emissions. Open biomass burning is not included. (The trends are rather smooth and do not contain the same level of temporal resolution as the Bond *et al.* inventory for BC). They all indicate growth in emissions from pre-industrial times until about 1990, when emission control measures in developed countries began to reverse the trend.

2.4 Development of emissions under the reference scenario

The GAINS reference scenario developed for this Assessment begins with the key macro-economic assumptions and energy demand presented in the *World Energy Outlook 2009* reference scenario (IEA, 2009), taking into account existing air quality and climate-related policies that imply implementation of emission control measures. Projections cover the period to 2030.
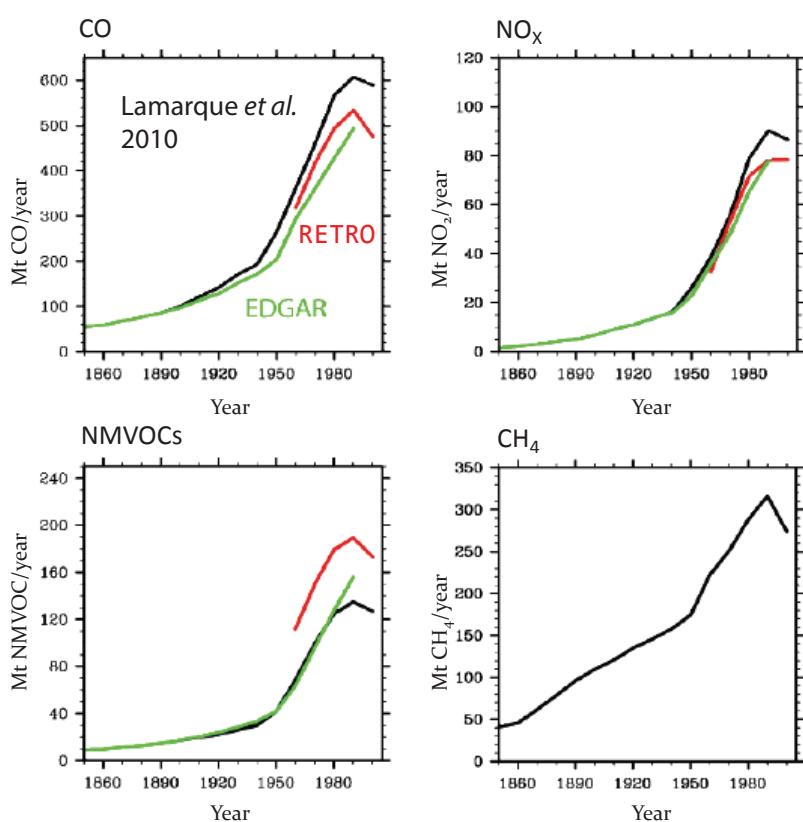
Figure 2.6. Historical trends in human-driven emissions of O_3 precursors from Lamarque *et al.* (2010), in black; RETRO (Schultz *et al.*, 2008; in red) and EDGAR-HYDE (Olivier and Berdowski, 2001; van Aardenne *et al.*, 2001) in green. Open biomass burning is not included.

2.4.1 Macroeconomic trends and energy demand

Figure 2.7 shows global development trends, differentiating regions that come under the Organisation for Economic Co-operation and Development (OECD) from those that do not. Global population is projected to grow by 1 per cent per year, from 6.6 billion in 2007 to 8.2 billion in 2030. Most of the increase will take place in Asia and Africa and will largely be in urban areas. Major drivers behind population projections are success in controlling the further spread of HIV, greater availability of treatment for AIDS and population aging.

Gross domestic product (GDP) projections consider the anticipated impacts of the global economic crisis of 2008–09. It is assumed that the rate of GDP growth recovers from its fall of 1.4 per cent in 2009 to reach 4.1 per cent in 2015, with an average of 3 per cent per year for the remaining period. The GDP of non-OECD countries grows significantly faster and is estimated to exceed that of the OECD region before 2020. Primary energy demand increases by 1.5 per cent per year on average between 2007 and 2030, with an overall increase of 40 per cent. The increase is driven mainly by development in China, India and the Middle East; overall, about 90 per cent of the increase occurs in non-OECD countries. However, their per capita energy consumption remains much lower than in the rest of the

world. Fossil fuels continue to be the dominant source of primary energy supply to the world economy, representing 80 per cent in 2030, with oil and coal shares of about 30 per cent each. Coal is one of the most important fuels in industry, although the picture is different across regions. Power plants and industrial boilers in Northeast and South Asia are major coal consumers and coal use is expected to grow in the future. Consequently, production, conversion and transportation of fossil fuels will remain a significant activity with associated fugitive emissions of CH_4.

Transport and industry are the sectors with the highest fossil-fuel consumption, representing 62 per cent of global demand in 2030. Figure 2.8 shows regional development in the road transport sector. (See section 2.5 for a full description of these regions.) Global fuel consumption is shown to rise by 46 per cent between 2005 and 2030, driven by growth in the developing world; however, fuel use continues to be high in North America and Europe, and is approximately equal to that of Asia in 2030. Growth in fuel use in the OECD region is expected to be marginal due to enforcement of new fuel economy standards, increased penetration of smaller vehicles, and new engine technologies such as hybrid cars, which are projected to account for about 6 per cent of the global car fleet. It is important to note that the share of diesel fuel (an important source of BC emissions) grows from 39 per cent in 2005 to 46 per cent in 2030.
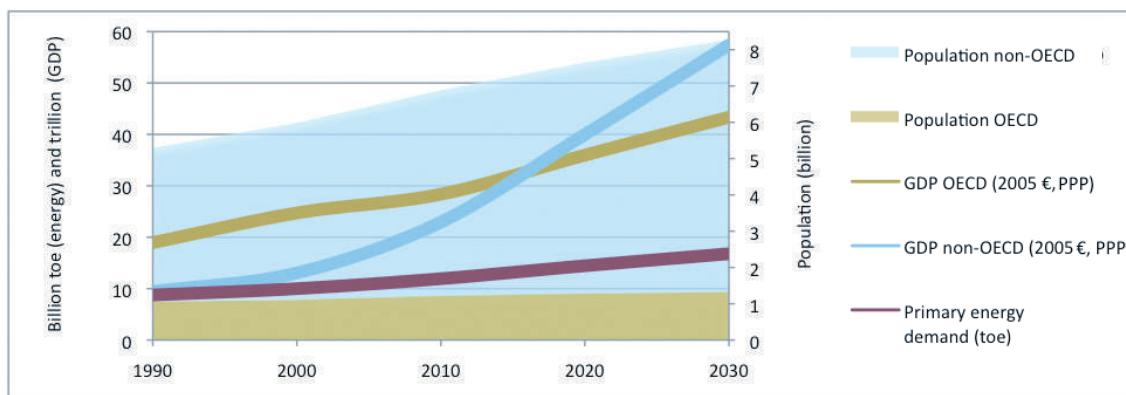
Figure 2.7. Key macroeconomic assumptions for the OECD and non-OECD regions and world primary energy demand (IEA, 2009).
Note: *PPP* = purchasing power parity; *toe* = tonnes of oil equivalent.

Solid fuel use (i.e., biofuel and coal) in the residential sector remains fairly constant during the period 2005–30, although there are differences between regions (Figure 2.9). Biomass, mostly used in the developing world in cooking and heating stoves, represents nearly 90 per cent of total domestic use of solid fuel, and is expected to grow slightly in all regions except Northeast Asia. Coal use in the residential sector is projected to decline by about 4 per cent, mostly in Northeast Asia and Europe.

Livestock breeding and crop production are associated with nearly half of CH_4 and over 80 per cent of NH_3 emissions. Growth in agricultural production is strongly linked with population and economic growth, the latter affecting lifestyles and leading to, for example, increased meat consumption. Most recently, greater demand for biofuels has resulted in additional growth in this sector. Agricultural data used in this study originate from global (Bruinsma, 2003; Alexandratos *et al.*, 2006; FAO, 2010; IFA, 2003; Döring *et al.*, 2010), regional (EFMA, 2010; Klimont, 2005) and national (Fischer *et al.*, 2010; Amann *et al.*, 2008) statistics, outlooks and projects. Figure 2.10 shows changes in selected key indicators in the reference scenario. All the activity growth is expected in non-OECD countries, as demonstrated

in the value added (VA) forecast. While growth is moderate for dairy cattle, demand for meat leads to strong growth in beef production.

2.4.2 Air pollution legislation in the reference scenario

The GAINS reference scenario assumes successful implementation of current air pollution control policies (i.e., policies that were in force or in the final stage of the legislative process as of mid-2010 in each country). The most influenced sectors are transport, power generation and industrial production. The degree and stringency of regulation varies across regions, however; strongly controlled sectors tend to converge in the longer time horizon to a comparable implied emission rate largely independent of the region. At the same time, it is assumed that there will be changes that are autonomous from legislation, such as the transition from traditional heating and cooking stoves to improved and clean stoves through turnover of the equipment, and the introduction of new vehicles with better fuel efficiency. However, the effects of such improvements are often only seen towards the end of the modelling horizon owing to the long lifetime of specific installations – such as heating stoves or off-road machinery – or other con-
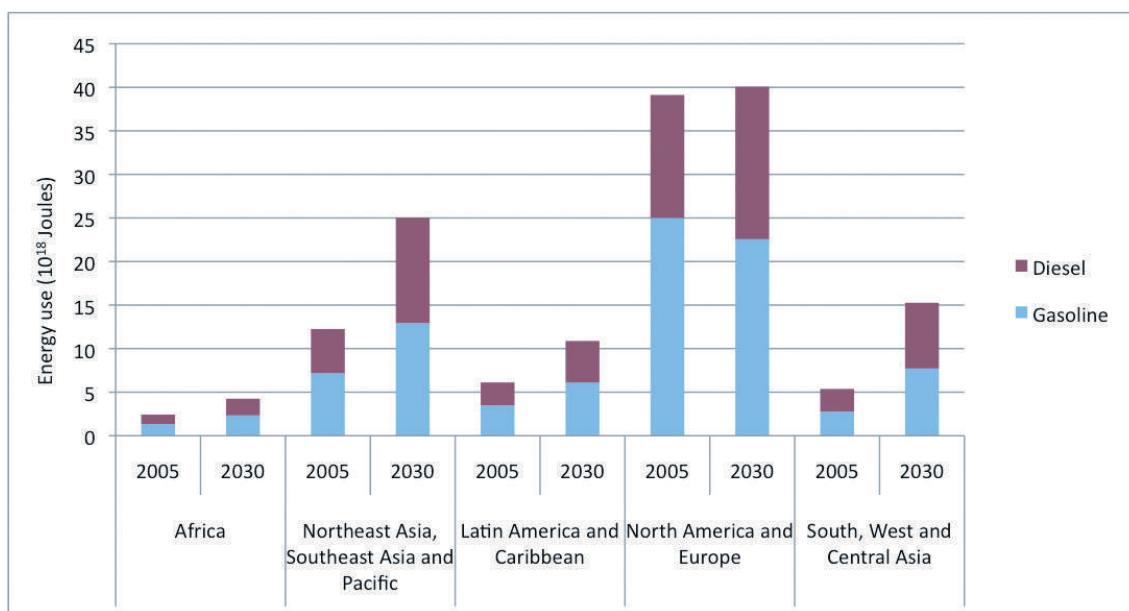
Figure 2.8. Use of diesel and gasoline fuel in the road transport sector in 2005 and 2030 in the reference scenario.

straints including a lack of infrastructure or economic stimulus in specific regions.

Implementation of national air pollution legislation, fuel efficiency standards, installation-specific emission limit values, and international laws and agreements such as the Convention on Long-range Transboundary Air Pollution (CLRTAP), implies changes in emission factors over time. These changes will vary across regions and sectors, reflecting the stringency of legislation. One additional aspect of environmental legislation is the actual level of

compliance, both in terms of the timely introduction of the laws (emission standards) and the actual performance of the control equipment. For projections in this study, it has been assumed that the technical abatement measures will be installed in a timely manner and will achieve the emission levels required to comply with the law. The only exception is the transport sector, where high-emitting vehicles (or super-emitters) are explicitly considered and assumptions are made about their region-specific shares and technology-specific deterioration factors. Figure 2.11 shows examples
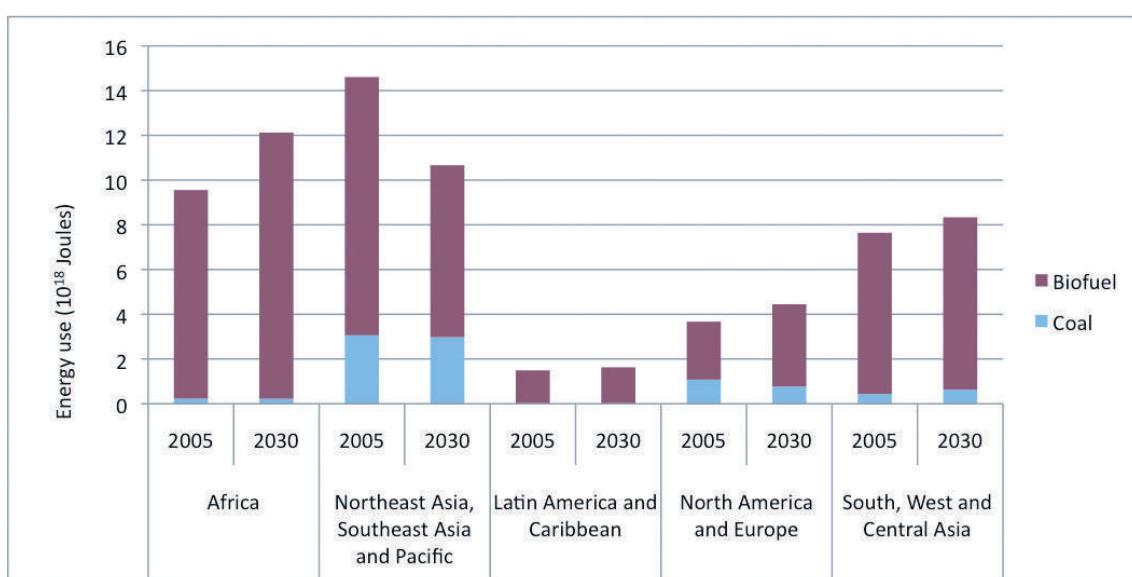
Figure 2.9. Use of solid fuels in the residential sector in 2005 and 2030 in the reference scenario.
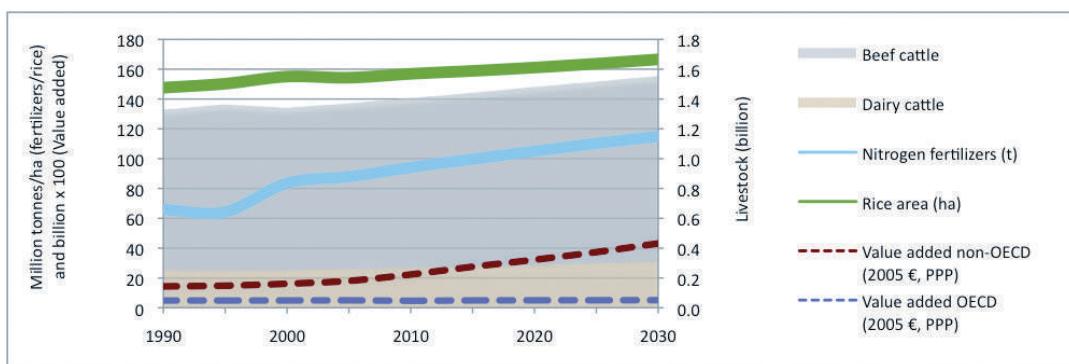
Figure 2.10. Key reference scenario developments for the agriculture sector.
Note: *PPP* = purchasing power parity.

of how implied emission factors change over time in China and India in selected sectors. The emission factors presented in this figure do not explicitly consider super-emitters.

For transport sources and non-road machinery, the reference scenario includes implementation of the Euro-standards, the US federal emission standards, the Japanese emission standards, and their fuel quality requirements. Other countries have adopted one or more of the above standards, mostly the European ones, with a somewhat delayed implementation stage (e.g., DieselNet, 2010; CAI, 2008). Assumptions about current and future emission controls in the power-plant sector have been cross-checked with detailed information from the database on world coal-fired power plants (IEA CCC, 2010) as well as collaboration with national expert teams, including from Asia (Klimont *et al.*, 2009), and various literature sources (e.g., Xu *et al.*, 2009; Zhang *et al.*, 2009a; Smith et al., 2011). Although several countries have emission standards for cooking and heating stoves and boilers, most of the solid fuels used in this sector are in the developing world where such legislation is lacking, and many of these traditional appliances are expected to remain in use until 2030.

2.5 Reference scenario emissions of BC, OC and O_3 precursors from key sectors and regions

The emissions described here are mainly derived from the GAINS model for the years 1990, 2005 and 2030 (see Sections 2.3.1 and 2.4). Global NH_3 and NMVOC emissions in developing countries originate from the CIRCE project, based on EDGAR v4.1, as documented in Döring et al. (2010). These global emissions are disaggregated into five regional groupings based on UNEP's sub-regional geographical breakdown (available at http://geodata.grid.unep.ch/extras/geosub-regions.php.) (Figure 2.12) plus an additional category concerning emissions from international shipping and aviation. Global emissions are also disaggregated into nine key anthropogenic emission source sectors:

1. Large-scale combustion (including power plants and industrial boilers);

2. Industrial processes (including cement, lime and brick kilns);

3. Residential-commercial combustion;
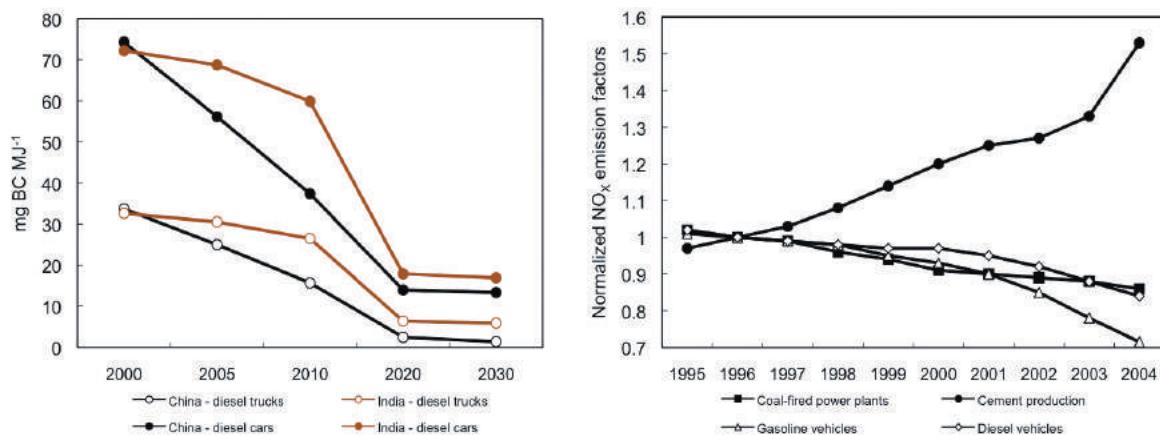
Figure 2.11. Examples of changes in emission factors over time. Left: transport-related BC in China and India (Klimont *et al.*, 2009). Right: NO_X (relative change to 1996) in several sectors in China (Zhang *et al.*, 2007).

Chapter 2. Black carbon and tropospheric ozone precursors: drivers, emissions and trends

4. Transport (excluding international shipping and aviation);

5. Fossil fuel extraction and distribution (including coal, oil, gas production, storage and distribution);

6. Waste/landfill (including open garbage burning);

7. Agriculture (including open burning of crop residues);

8. Solvent use; and

9. International shipping and aviation.

Emission densities vary regionally, depending on many factors such us structure of fuel use, population density, economic development and air quality legislation. Consequently, they are expected to change over the modelling time horizon. Figure 2.13 illustrates the spatial distributions of BC and NO_x emissions in 2005 and in the 2030 reference scenario, accordingly. In general, the regional trends for both pollutants are quite similar, with declining emissions in North America and Europe and increases projected in Asia. However, while BC emissions in Northeast Asia show a decline, this region becomes the largest emitter of NO_x. A more detailed analysis of regional and sectoral trends is included later

in this chapter. Shifts in the spatial distribution of emissions over time are important, because emissions from different locations cause different amounts of radiative forcing (Chapter 3). Figure 2.13 also includes international shipping emissions, which are not significant for BC emissions but represent a sizable part of NO_x and are expected to increase by 2030.

Emissions of NMVOCs, NH_3 and total $PM_{2.5}$ are discussed only in section 2.5.1. NMVOCs and NH_3 are presented in Figures 2.14 and 2.15, but because they are of lesser importance in the modelling and mitigation sections of this Assessment, they are not discussed thereafter. Total $PM_{2.5}$, which includes all primary emitted particles (BC, OC, sulphates, metals and minerals) but no secondary particles, is very relevant to human health and is further discussed in Chapter 4, while in this chapter emissions of the radiatively active components of primary particulate matter, BC and OC, are stressed. All 10 of the species presented in the following section are intimately connected and have their own unique suite of environmental effects. In addition, each source category emits a variety of species, and therefore a mitigation measure directed at a single one will simultaneously affect co-emissions. This may alter the benefit balance, as discussed at length in Chapter 5. Emissions from vegetation fires (including for-
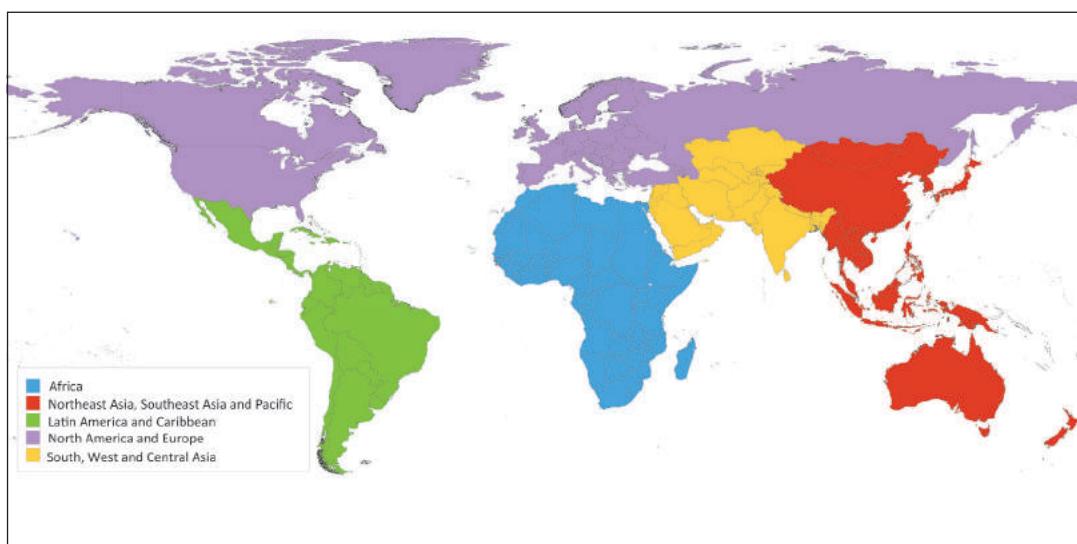
Figure 2.12. The regional groupings used in this analysis.

est and savannah burning) and natural sources are not covered in this section.

2.5.1 Sectoral/regional shares

The regional shares of global anthropogenic emissions for 2005 are shown in Figure 2.14. The Northeast Asia, Southeast Asia and Pacific region represents the largest source of emissions, the majority of which (60–80 per cent) originate in China (data not shown), except for NO_x and CO_2, where North America and Europe are responsible for the greatest share of global emissions. For BC, the next most important regions are North America and Europe, and South, West and Central Asia (of which 63 per cent is from India), each emitting almost a fifth of the global total. The second largest contribution for SO_2, CO and CH_4 comes from North America and Europe, while for OC it is Africa and for total $PM_{2.5}$ it is South, West and Central Asia (almost 70 per cent of both pollutants coming from India). Africa contributes only a small
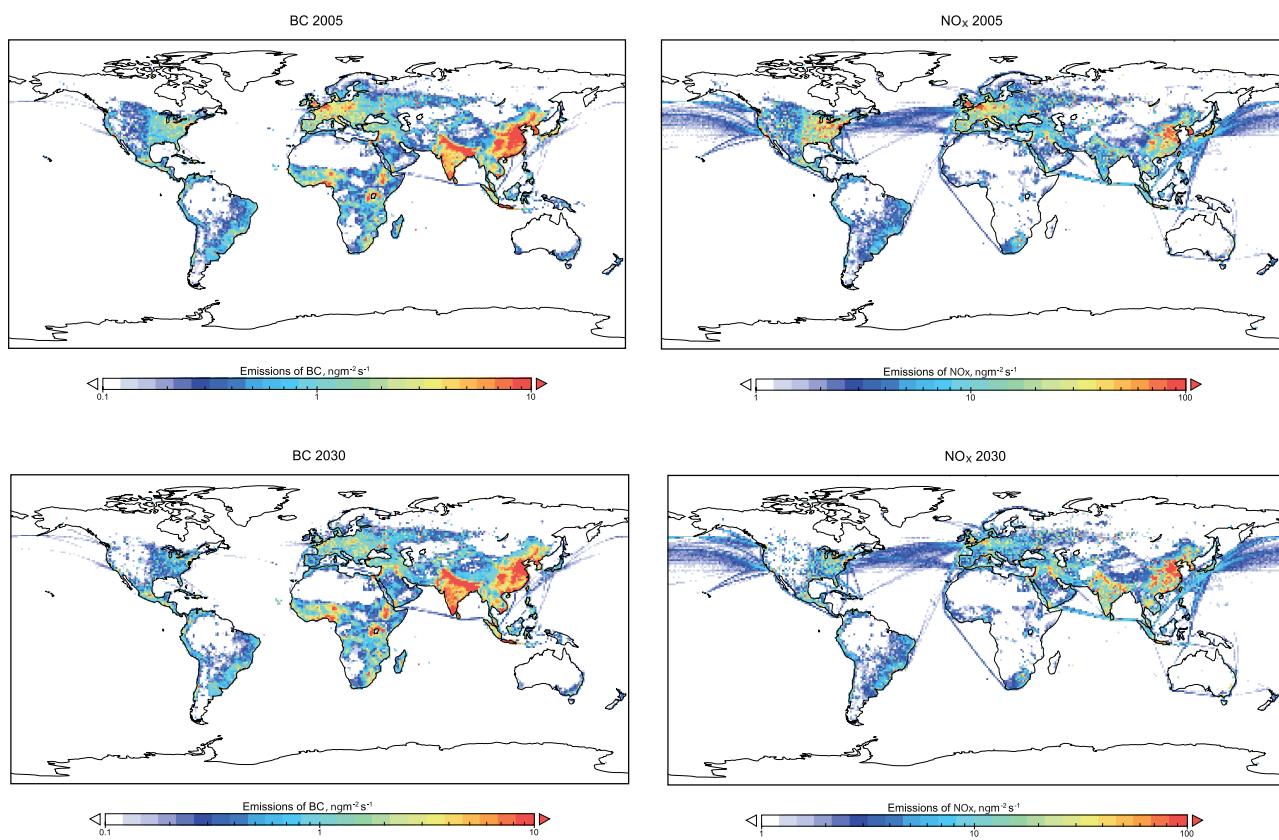
Figure 2.13. Spatial distribution of BC and NO_X (as N) emissions in 2005 and the 2030 reference scenario. Note the difference of scale between BC and NO_X emissions. The GAINS emissions were gridded on a 0.1° × 0.1° grid by the EDGAR team at the European Commission's Joint Research Centre, Ispra, Italy.
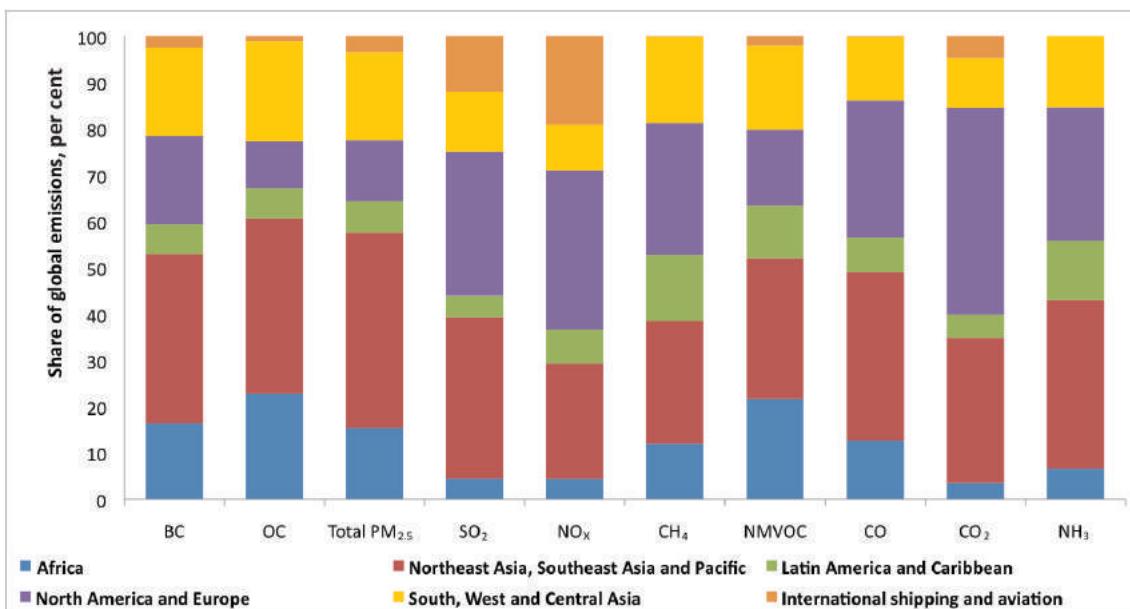
Figure 2.14. Regional shares of global anthropogenic emissions for 2005.

percentage of emissions associated with transportation and industrial activities, but ranks high for pollutants originating from incomplete combustion (traditional cook stoves), i.e., BC, OC, NMVOC, CO and total $PM_{2.5}$.

For each pollutant, the percentage shares of global emissions for 2005 represented by each of the nine key sectors are shown in

Figure 2.15; in this figure transport does not include emissions from international shipping and aviation, which are in a separate category. Primary carbonaceous aerosols (BC and OC) and total $PM_{2.5}$ emissions originate predominantly in the residential-commercial sector, which also contributes significant shares of NMVOCs and CO, consistent with the emission profiles of incomplete
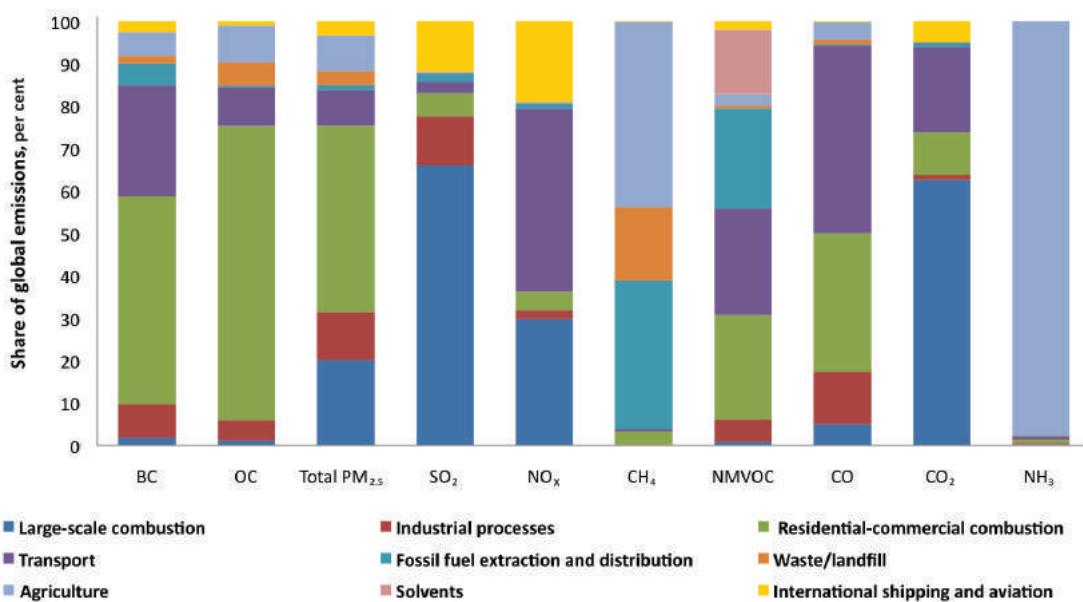
Figure 2.15. Sectoral shares of global anthropogenic emissions for 2005.

Integrated Assessment of Black Carbon and Tropospheric Ozone

combustion sources. The large-scale combustion sector is responsible for the majority of CO_2 and SO_2, as well as contributing nearly 30 per cent of NO_x and 20 per cent of total $PM_{2.5}$, while for other pollutants it does not play a significant role. Emissions from the transport and international shipping and aviation sectors taken together are key for NO_x and CO (45–60 per cent), and contribute about 25–30 per cent of CO_2, NMVOCs and BC. The agriculture sector accounts for the vast majority of NH_3 emissions and is the main source of CH_4; for other pollutants its contribution is linked with open burning of agricultural residues, which makes up almost 10 per cent of total OC. Fossil fuel extraction and distribution is a significant source of CH_4 and NMVOC emissions, also contributing about 5 per cent of BC, which is associated with oil and gas flaring. The waste/landfill sector represents about 15 per cent of CH_4 emissions, while solvents account for a similar share of NMVOCs.

2.5.2 Global trends

Figure 2.16 presents global emission trends by world region for the seven major pollutants that are of special relevance to modelling and mitigation analysis. Emissions of BC, OC, CO and NO_x declined in North America

and Europe due to implementation of strict air pollution control policies, especially in the transport, industry and power plant sectors, as well as the economic restructuring of Eastern Europe at the beginning of the 1990s. Emissions rose, however, between 1990 and 2005 in the other regions due to increasing activities and less ambitious implementation of emission controls. This resulted in slight net increases in global emissions of these four pollutants. Conversely, net global emissions of SO_2 declined between 1990 and 2005, mainly due to the large reduction in North America and Europe caused by end-of-pipe emission abatement and reductions in the sulphur content of fuels. These measures offset increased emissions from South, West and Central Asia. From 1990 to 2005, CO_2 emissions increased in all regions apart from North America and Europe where they remained relatively unchanged; this trend is projected to continue up to 2030. Emissions of BC, OC and CO, however, are projected to decrease between 2005 and 2030 in both Northeast Asia, Southeast Asia and Pacific and North America and Europe due to further air pollution legislation, resulting in slight net global decreases despite increases in most other regions. Emissions of CH_4 and NO_x are expected to grow between 2005 and 2030 in all regions apart from North America and Europe, resulting in a net
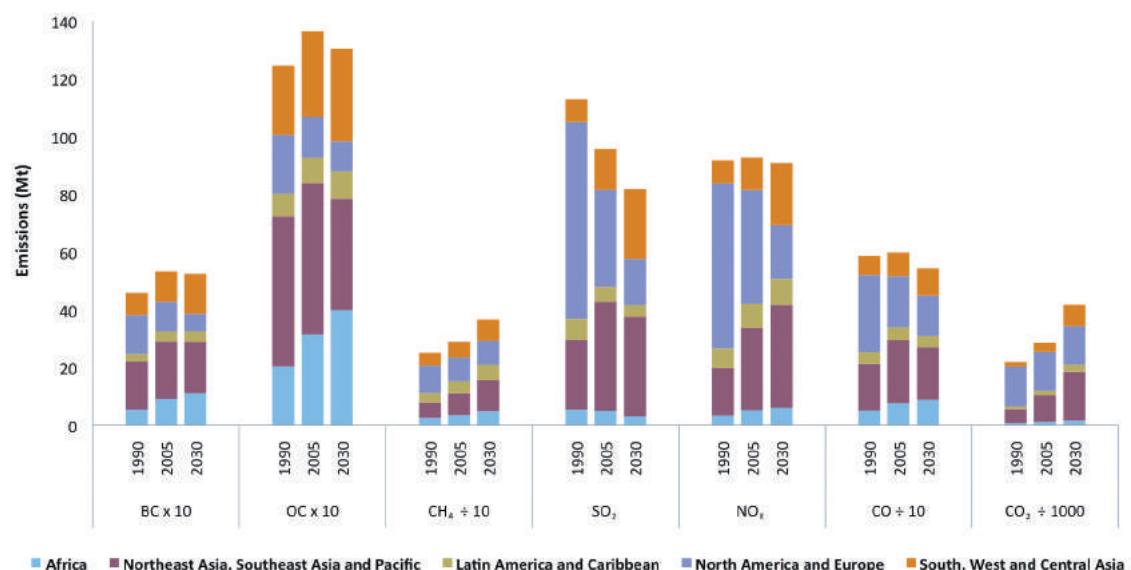
Figure 2.16. Regional splits of global emission trends for the major emitted pollutants.

Chapter 2. Black carbon and tropospheric ozone precursors: drivers, emissions and trends

global increase in the case of CH_4 and a slight decrease for NO_x.

For BC, OC and NO_x, Figure 2.17 does not show much change in the sectoral shares over time. For CO, however, there was a declining contribution from transport between 1990 and 2005, with this trend set to continue up to 2030. The transport sector has experienced a step-wise introduction of emission abatement technologies which will continue to reduce emissions as a result of equipment turnover. In some regions the emission benefits of further controls are offset by increases in activity levels. Over the same period, CO emissions from the residential-commercial sector remain static, whilst those from the other three sectors show a rising trend. For CH_4, the increased global emissions between 1990 and 2005 are largely due to fossil fuel extraction and distribution, and this trend is projected to continue up to 2030. The decline in total SO_2 emissions from 1990 to 2005 was mainly caused by reduced emissions from large-scale combustion and the residential-commercial sector, with a further decrease in emissions from large-scale combustion driving the ongoing reduction in global SO_2 emissions projected to 2030. The decline is a result of implementation of end-of-pipe control technologies, as well as fuel-related changes – mainly switches

to lower sulphur content and away from solid fuels. Large-scale combustion was also largely responsible for the increase in CO_2 emissions between 1990 and 2005, with the further increase projected to 2030 also driven by emissions from this sector.

2.5.3 Sectoral trends

Large-scale combustion (power plants and industrial boilers)
Carbon dioxide emissions from this sector (Figure 2.18) are a good illustration of expected growth in fossil-fuel use, especially in Asia where they increase nearly fourfold. At the same time, the trends for key air pollutants (SO_2 and NO_x) indicate increasing implementation of abatement technologies and fuel quality improvement. This figure also shows the relatively small emissions of BC, OC and CH_4 in comparison with other pollutants. SO_2 emissions from large-scale combustion declined from 1990 to 2005 due to large reductions in emissions from North America and Europe outweighing rising trends in Northeast Asia, Southeast Asia and Pacific (mainly China) and, to a lesser extent, in South, West and Central Asia (mainly India). The major drivers for SO_2 emission reductions in North America and Europe have been
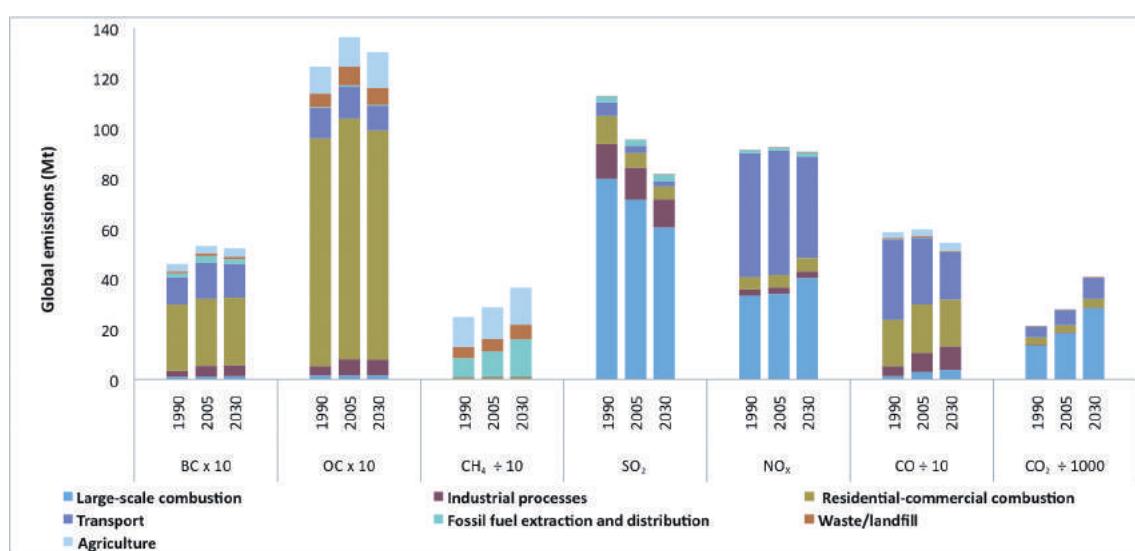
Figure 2.17. Sectoral splits of global emission trends for the major pollutants.
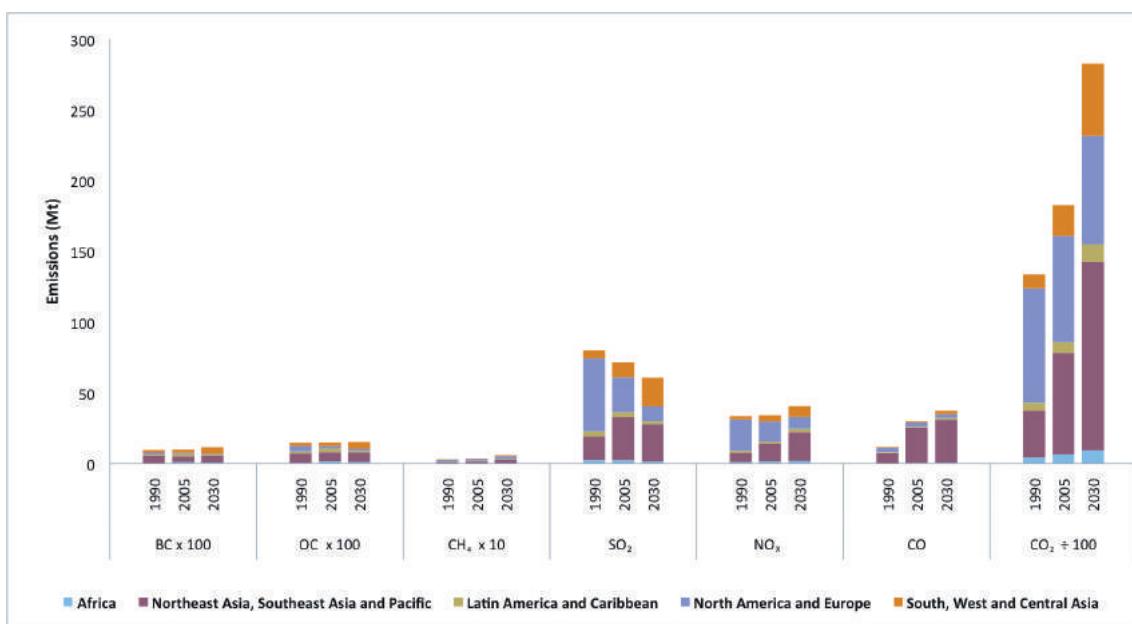
Figure 2.18. Trends in emissions from large-scale combustion.

efficient end-of-pipe measures accompanied by fuel switching and a reduced sulphur content in fuels. This overall declining trend in SO_2 emissions is set to continue to 2030 owing to sustained reductions in North America and Europe combined with more modest reductions in all other regions apart from South, West and Central Asia, where SO_2 emissions are actually projected to increase significantly due to expanded coal use without effective emission controls. For NO_X, overall emissions in 2005 were similar to those in 1990, with a marked decrease for North America and Europe being balanced by increases for all other regions. By 2030, the continued reduction in NO_X emissions projected for North America and Europe is more than offset by increases in all other regions, resulting in a net global increase for this sector. The increase is not, however, as large as in the case of CO_2, indicating that effective implementation of emission controls decouples emission rates from growth in fuel use. Global emissions of CO increased sharply between 1990 and 2005, largely due to rising emissions from coal combustion in Northeast Asia, Southeast Asia and Pacific. Emissions are projected to increase until 2030, but at a lower rate owing to better efficiency of new power plants.

Industrial processes
Globally, emissions from industrial processes are of relatively minor importance for the pollutants under discussion. Emissions of BC and OC in the study period are dominated by Northeast Asia, Southeast Asia and Pacific, and South, West and Central Asia; for CO, North America and Europe follows Northeast Asia, Southeast Asia and Pacific (Figure 2.19). Global emissions of these three pollutants almost doubled from 1990 to 2005. Major sources in these areas are brick- and coke-making (especially for BC and OC), which use rather primitive and low-cost production technologies without emission controls. Whereas BC and OC emissions are projected to stabilize (the reference scenario assumes partial replacement of the most inefficient technologies), the rising trend continues for CO to 2030 with increased emissions in all regions. Global SO_2 emissions declined slightly from 1990 to 2005 due to decreased emissions in regions other than Northeast Asia, Southeast Asia and Pacific (China represented 67 per cent of the regional total in 2005 and was responsible for most of the growth) and South, West and Central Asia. The gradual decline in SO_2 emissions globally is projected to continue to 2030, even though
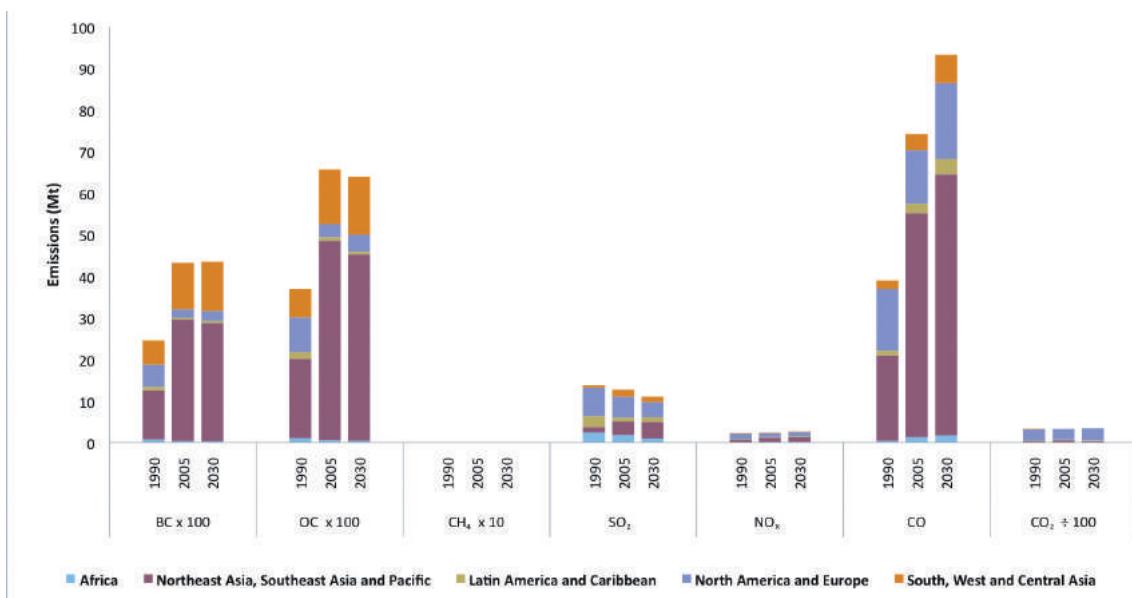
Figure 2.19. Trends in emissions from industrial processes.

emissions from Northeast Asia, Southeast Asia and Pacific (again, mostly from China) continue to increase due to high growth in activity. Emissions of CH_4, NO_x and CO_2 from this sector are relatively insignificant.

Residential-commercial combustion
This sector is the most important contributor to BC, OC and CO emissions. Emissions of all pollutants remain fairly constant over the whole modelling horizon (Figure 2.20), although regional shares change over time. The stability in emissions in this sector is explained by the rather constant global fuel use and, in the absence of regulation, only small switches towards improved and cleaner stoves. Patterns of variation in regional emissions of all species are strikingly similar owing to similarities in the emission profiles of key polluting installations, and consequently reflect fuel-use changes. Three regions – Africa, Northeast Asia, Southeast Asia and Pacific, and South, West and Central Asia – tend to dominate emissions of BC, OC, CO and CH_4, with decreases in Northeast Asia, Southeast Asia and Pacific and increases in Africa tending to cancel each other out, reflecting changing fuel-use patterns. Emissions of SO_2, NO_x and CO_2 from this sector are relatively insignificant. In the case of CO_2 this is because emissions from biomass combustion are regarded as carbon neutral, that is to say, do not lead to

a net increase in atmospheric CO_2 concentrations; it is acknowledged that this may not be true for every situation.

Transport
The study period covers a timeframe of strict air pollution control policies for on-road transport and to some extent also for off-road transport. This can be seen clearly in the development of emissions, especially in North America and Europe, where transport volumes remained rather constant or increased only slightly, while emissions of all pollutants, except BC, declined by 2005 (Figure 2.21). For BC, the increasing shares of diesel vehicles offset improvements in engine technology and reductions achieved in gasoline vehicles, as shown in Figure 2.8 and the accompanying text. Existing legislation for new vehicles results in a significant reduction in emissions from diesel vehicles, including BC and NO_x, and is expected to bring a substantial reduction in emissions by 2030, especially in North America and Europe. The other regions are adopting similar legislation to that of North America and Europe, but with delayed implementation timetables. This also applies to off-road transport, for which standards are not as strict as for the on-road sector. Increased emissions in other regions are mainly a result of dramatic increases in traffic volumes, particularly in Asia. Despite

38
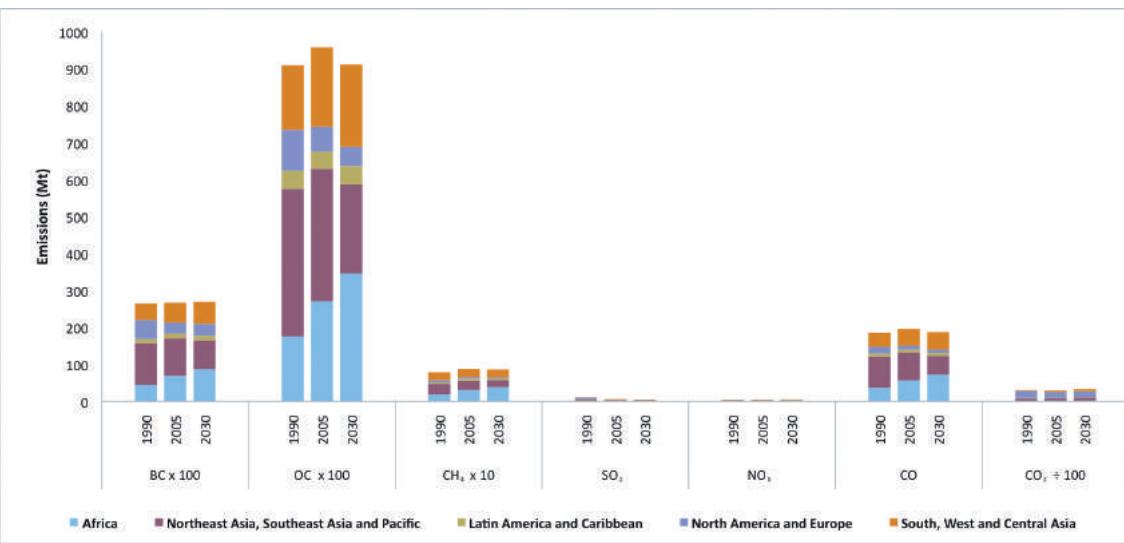
Figure 2.20. Trends in emissions from residential-commercial combustion.

some improvements in fuel economy, trends in transport activities can be seen in global emissions of CO_2, which increased from 1990 to 2005 and are projected to continue rising up to 2030. With the exception of international shipping, SO_2 is a relatively minor component of emissions from the transport sector because of fuel standards requiring the use of low-sulphur fuels.

International shipping emissions represent a relatively high share of global NO_x and SO_2 emissions, comprising 23 and 14 per cent of the anthropogenic and 15 and 11 per cent of total global emissions, respectively. The corresponding shares for BC are lower, at 3 per cent and 2 per cent respectively, and for the other pollutants are less than 1 per cent. Within the transport sector, international shipping contributed over 80 per cent of SO_2, 30 per cent of NO_x, 10 per cent of BC and 9 per cent of OC emissions in 2005. For CO the contribution is less than 1 per cent. About 80 per cent of the international shipping traffic occurs in the northern
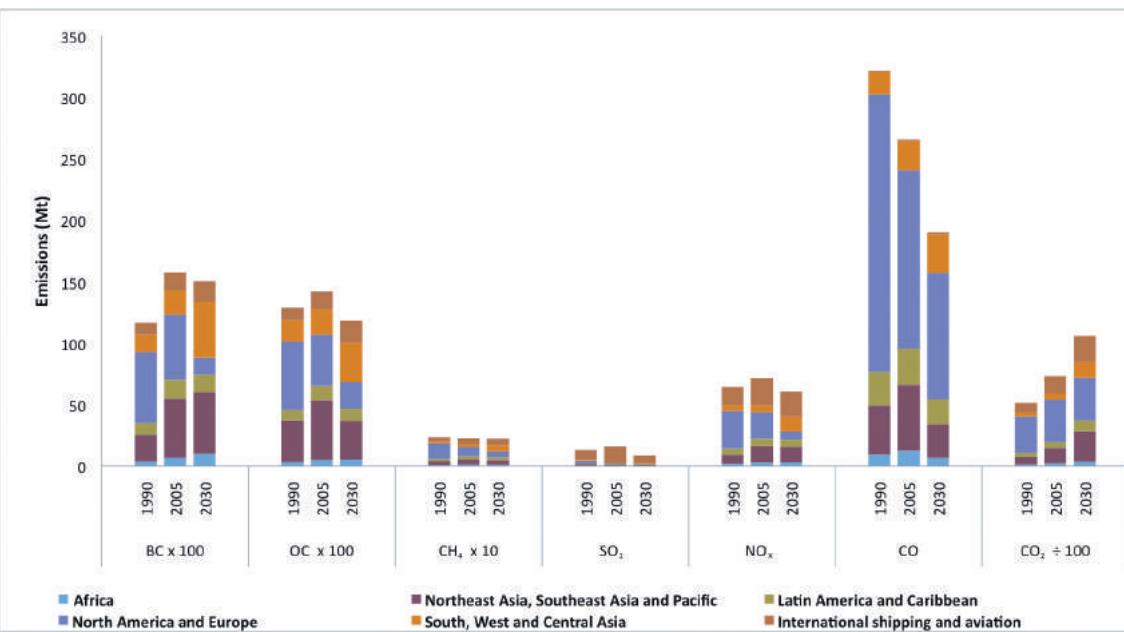
Figure 2.21. Trends in emissions from the transport sector.

Chapter 2. Black carbon and tropospheric ozone precursors: drivers, emissions and trends

hemisphere, with 32 per cent in the Atlantic, 29 per cent in the Pacific, 14 per cent in the Indian Ocean and 5 per cent in the Mediterranean (Eyring *et al.*, 2010). However, increasing Asian shipping activity may change the distribution in the future (Eyring *et al.*, 2010). At present, Arctic shipping contributes 1–3 per cent to global shipping emissions, depending on the pollutant, but its proximity to sensitive ecosystems might make it a much more important source locally in the future, especially when an extended period of ice-free Arctic waters is considered in future scenarios (Corbett *et al.*, 2010). Global annual growth of international ship traffic is estimated to be 2–3 per cent, depending on the scenario (Buhaug *et al.*, 2009), and annual growth in fuel use could be about 2 per cent (Eyring *et al.*, 2010). However, recent regulations of the International Maritime Organization (IMO) address emissions of SO_2 and NO_x, and some changes are expected for other pollutants as well. Since part of the fuel sulphur is emitted as particulate sulphate, the reductions may also affect primary PM emissions, including BC and OC (Buhaug *et al.*, 2009; Lack *et al.*, 2009). In the RCP 8.5 scenario, the average compound annual growth rates (CAGR) for global shipping emissions between 2005 and 2030 are 0.83–0.87 per cent for BC, OC, CH_4, CO and NMVOC. The NO_x annual growth rate is smaller at 0.44 per cent, and annual SO_2 emissions decline by 2.5 per cent on average; however, a significant decline is expected in the period between 2010 and 2020, following implementation of the IMO regulation.

Fossil fuel extraction and distribution

In 1990, North America and Europe accounted for more CH_4 emissions than any of the other four regions (Figure 2.22). By 2005, a fall in emissions from North America and Europe was more than offset by a rise in emissions from the other regions, producing an overall net increase; CH_4 emissions from Northeast Asia, Southeast Asia and Pacific (of which China accounted for over 80 per cent, mainly from coal mining) increased to equal those from North America and Europe. The projected global increase of almost 40 per cent by 2030 is mainly due to rapidly growing emissions from Northeast Asia, Southeast Asia and Pacific, driven strongly by growth of the Chinese coal-mining industry (see Figure 2.28), although increases also occur in the other four regions.

Waste/landfill

Emissions from this sector are dominated by CH_4. Global CH_4 emissions from waste/landfill increased by 10 per cent between 1990 and 2005 and are projected to increase by 20 per cent by 2030 (Figure 2.23). North America and Europe is the largest emitting region in all three years, although their CH_4 emissions actually decline over the period, the overall rising trend being driven by growth in emissions from the other four regions. For OC, global emissions increased from 1990 to 2005 and are projected to decrease slightly by 2030, although not back down to 1990 levels. For this
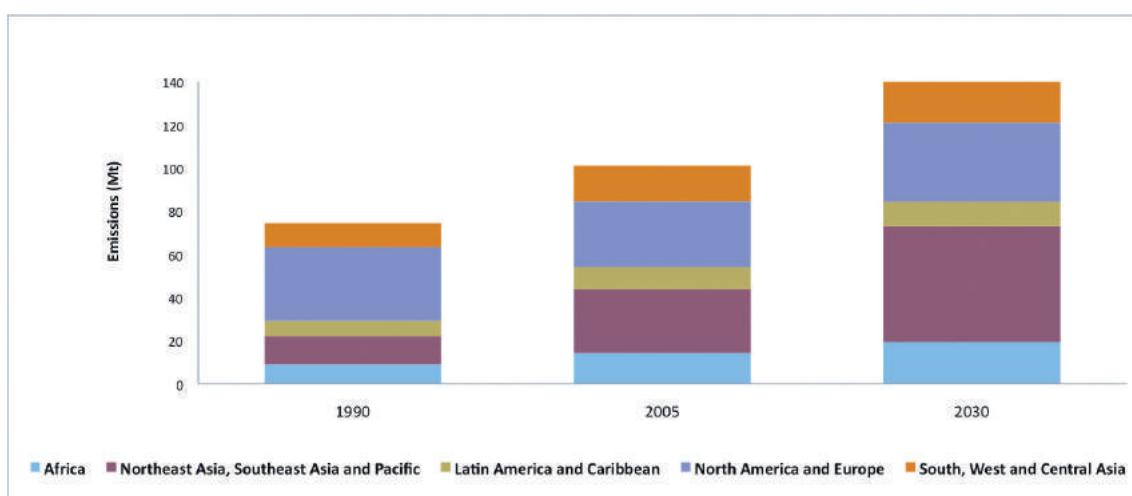
Figure 2.22. Trends in CH_4 emissions from fossil fuel extraction and distribution.
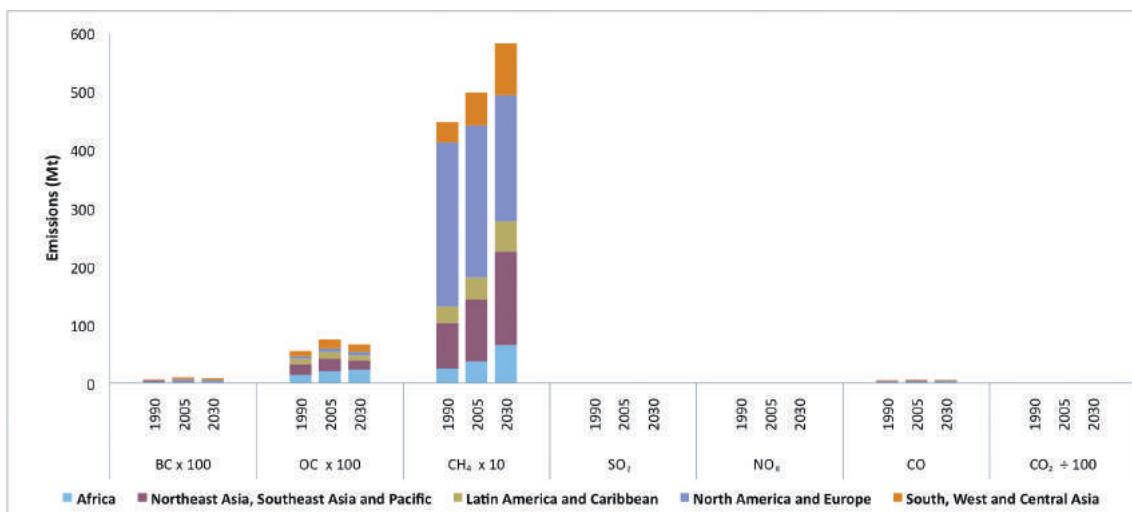
Figure 2.23. Trends in emissions from waste/landfill.

sector, emissions of BC, SO_2, NO_x, CO and CO_2 are relatively insignificant. In developing countries, where municipal waste collection and handling are not adequate, burning of solid waste (backyard and landfill fires) may contribute significantly to emissions of CO, NMVOCs, BC and OC. However, estimates and projections of emissions from such activities are almost completely lacking and further research is needed.

Agriculture
Global emissions of BC, OC, CH_4 and CO all increased between 1990 and 2005 and are projected to rise still further by 2030 (Figure 2.24). The BC, OC and CO emissions in this sector come mostly from open burning of crop residues, whilst CH_4 emissions are mainly due to enteric fermentation in livestock. Population and economic growth lead to changes in lifestyles and typically increased demand for meat and dairy products; consequently, agricultural activities increase sharply, leading to higher emissions of CH_4 and NH_3 (not shown). In all three years, the two regions with the greatest emissions of BC, OC and CO are Northeast Asia, Southeast Asia and Pacific (mainly China) and South, West and Central Asia (mainly India). Emissions of CH_4 tend to be more evenly distributed between regions. By 2030, Northeast Asia, Southeast Asia and Pacific, Latin America and Caribbean and South, West and Central Asia become the three regions with the largest CH_4 emissions.

Emissions of SO_2, NO_x and CO_2 from agriculture are relatively insignificant.

2.5.4 Sub-sector analysis for carbonaceous aerosols

Figure 2.15 showed that the residential-commercial sector is the predominant source of primary $PM_{2.5}$, this being particularly true for BC and OC. The transport sector is also an important emitter of BC and, to a lesser extent, OC. In developing countries, certain industrial processes, such as brick kilns and coke ovens, and the burning of crop residues within the agriculture sector are also notable contributors to primary aerosol emissions. In this section, therefore, these sectors are analysed at a greater level of disaggregation, focusing on those sub-sectors that are of most relevance to primary BC and OC emissions and where control measures (Chapter 5) have the greatest potential impact. Figures 2.25 and 2.26 (note the difference of scale between BC and OC emissions) show that for BC and OC emissions, residential biofuel use was a dominant and growing global source from 1990 to 2005, with Northeast Asia, Southeast Asia and Pacific being responsible for the greatest share (of which approximately two-thirds came from China) followed by Africa and then South, West and Central Asia. Despite a decline in solid fuel use and a resulting reduction in emissions from Northeast Asia, Southeast Asia and Pacific

41
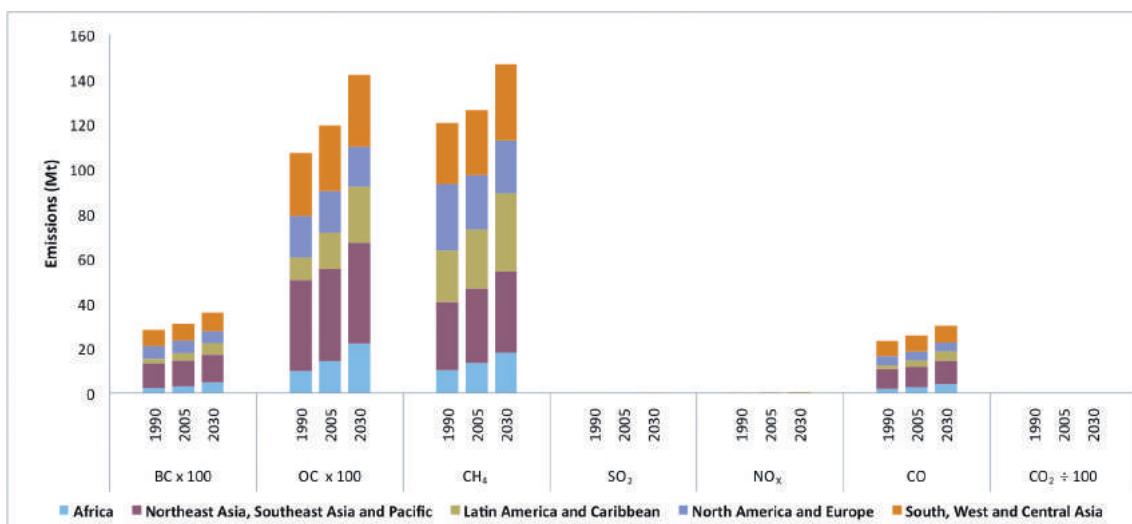
Figure 2.24. Trends in emissions from agriculture.

(almost entirely from China), global emissions from this sub-sector are projected to increase further by 2030. The development is largely driven by increases in biomass fuel use and consequent emissions from Africa. The main difference between BC and OC is that, while the BC trend is towards increasing emissions, global OC emissions are projected to decrease slightly by 2030, because improved combustion technologies are expected to reduce relatively more OC than BC.

Global emissions of BC and OC from residential coal use decreased between 1990 and 2005 and are projected to continue to decline up to 2030 as result of reduced emissions from North America and Europe and from Northeast Asia, Southeast Asia and Pacific (again almost entirely reductions in China due to improvements in combustion technologies). In 1990 and 2005, BC and OC emissions from brick and coke kilns were dominated by Northeast Asia, Southeast Asia and Pacific (China accounting for 85 per cent and 95 per cent of BC and OC, respectively) and South, West and Central Asia (India accounting for 50 per cent and 76 per cent, respectively). There was an increase in global emissions for this sector between 1990 and 2005, due mainly to an increase in Northeast Asia, Southeast Asia and Pacific (mainly China), with little subsequent change projected for 2030.

Road transport diesel combustion is also an important global source of BC and OC, with emissions having increased between 1990 and 2005, largely due to increases from Northeast Asia, Southeast Asia and Pacific, as well as South, West and Central Asia and Latin America and Caribbean, due to growth in transport activities. Reduced global BC and OC emissions from road transport diesel are projected by 2030. This is mainly a result of large reductions in emissions from North America and Europe resulting from strict emission controls and rather stable activity. Continued increases in emissions are projected for Northeast Asia, Southeast Asia and Pacific, and South, West and Central Asia, where the implementation of stricter air pollution policies is offset by growth in activity. The temporal trends and regional shares for off-road diesel closely follow those for road transport diesel, the main difference being a projected decrease for Northeast Asia, Southeast Asia and Pacific, and a projected increase for Latin America and Caribbean between 2005 and 2030. It is also worth noting that abatement technologies are penetrating the off-road transport sector more slowly than the on-road one. BC emissions from road transport powered by fuels other than diesel rose between 1990 and 2005, and this trend is projected to continue to 2030 as a result of a large increase in Northeast Asia, Southeast Asia and Pacific (entirely due to China). BC and OC emissions from agriculture, consist-
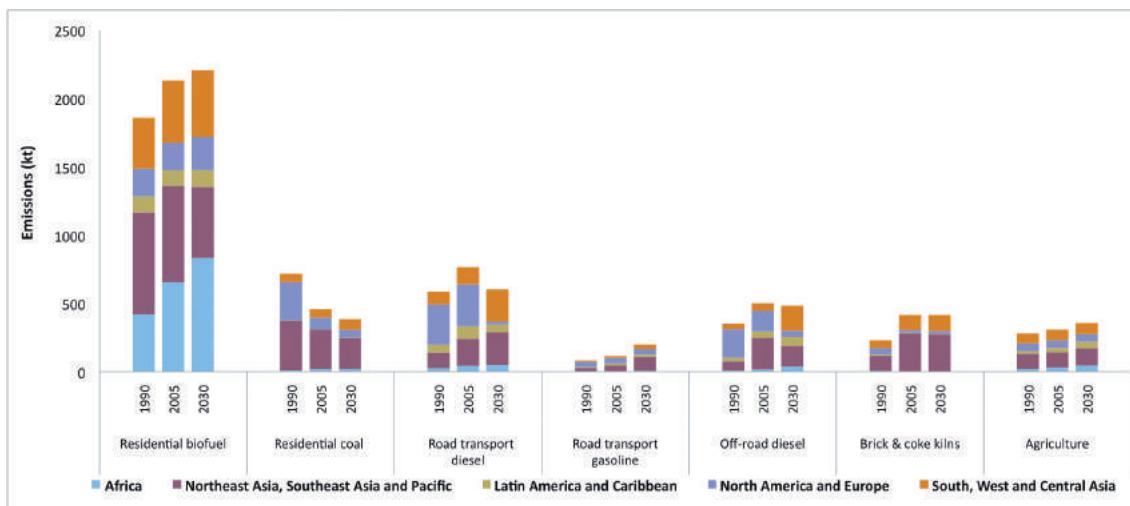
Figure 2.25. Trends in sub-sector BC emissions by region.
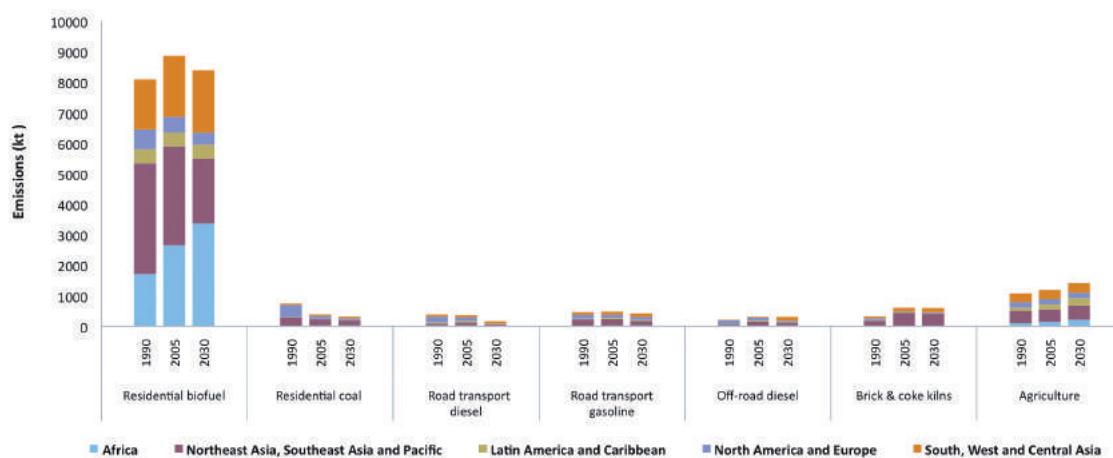
Figure 2.26. Trends in sub-sector OC emissions by region.

ing mainly of the burning of crop residues in the field, in 1990 and 2005 were also dominated by Northeast Asia, Southeast Asia and Pacific (China accounting for about 70 per cent) and South, West and Central Asia (India accounting for about 60 per cent). The climbing trend, which is projected to continue to 2030, is mainly due to increases in Africa and in Latin America and Caribbean. North America and Europe is the only region where a decline in emissions is expected.

OC/BC ratios

One significant aspect of carbonaceous aerosol emissions is the relative proportions of BC and OC. Because they have contrasting effects on radiative forcing, it is essential to know whether a particular type of source produces more BC than OC or vice versa. The OC/BC ratio is not the only factor determining sectoral contributions to a change in radiative forcing: other co-emitted aerosols and gases like SO_2 (especially from combustion of coal and high-sulphur oil), CO, NMVOCs, and NO_x, play a role too. However, for several sources, BC and OC are estimated to be the key determinants. Work assessing the magnitudes of direct and indirect effects, or even their sign, for BC and OC emissions and other aerosols is underway (Chapter 3).

43

It should be stressed that this section only addresses *primary* emissions of BC and OC and does not include secondary OC formed in the atmosphere after emission; this may appear to conflict with OC/BC ratios from modelling studies that include both primary and secondary OC combined.

Figure 2.27 shows the OC/BC mass ratios of the seven major source categories discussed above. The ratio of 1 (equal emissions) is highlighted as a reference level, but this does not imply equal effects on radiative forcing, because the forcing of BC per unit mass is greater than that of OC. In the case of emissions of a pure carbonaceous aerosol, an OC/BC mass ratio of more than about 10 would lead to cooling, since the global warming potential of OC and BC have been estimated to be about -70 and 700, respectively (Chapter 4). Because these source categories are relatively broad, they sometimes reflect mixtures of particular technologies and fuels, and they also reflect changing technologies and fuels into the future. This is an advantage, however, because it gives information on the overall proportions of BC and OC emitted from the sub-sector and how they are changing over time, and this gives insight into trends and opportunities for climate change mitigation. The different ratios in each of the five world regions are shown. A high OC/BC ratio represents a relatively unfavourable mitigation opportunity, because it reduces the cooling component more than the warming component. The three major source categories leading to high OC/BC ratios in 2005 are: residential biofuel use (OC/BC = 1.5–4.5), gasoline road transport (OC/BC = 3–6) and agriculture (OC/BC = 3–5). Residential coal use and brick and coke kilns have relatively similar emissions (OC/BC ≈ 1). Diesel road transport and off-road diesel have the lowest ratios (0.2–0.8) and are therefore good candidates for reducing net forcing.

Some ratios are likely to stay effectively constant until 2030, but others, mainly residential biofuel, diesel road transport and gasoline road transport, show a significant decline in their OC/BC ratio. In principle, the reductions in the OC/BC ratios reflect improvements in

combustion or the effects of exhaust after-treatment technologies. In the cases of residential biofuel and coal, the development of the ratio reflects the transition from traditional heating and cooking stoves to improved and cleaner stoves through turnover of the equipment. The improved stoves often reduce OC more than BC, which sometimes may remain at the level of traditional stoves (Roden *et al.*, 2006, 2009). The technologies in use are often different in different regions, which is reflected in the ratios. The development of the OC/BC ratio in the transport sector is the result of a mix of different stages of emission abatement technologies and the pace at which they are implemented in a given region. For both diesel and gasoline, the later stages tend to reduce more OC than BC, which is why the later year ratios are lower. However, these lower ratios are associated with small overall emissions and so there is very little reduction potential left.

For agriculture, the ratio does not change over time, as the only option included in this study is a ban that affects both compounds in the same way. Furthermore, we do not assume any changes over time in the shares of various crop residues burned. The regional differences visible in Figure 2.27 stem from different assumptions about emission factors for key crop residues, the shares of which vary from region to region.

2.5.5 Sub-sector analysis for methane

Figure 2.28 shows that enteric fermentation in domestic livestock was the predominant source of global anthropogenic CH_4 emissions between 1990 and 2005 and is projected to remain so to 2030. A slight decreasing trend in North America and Europe from 1990 to 2005 is more than offset by increasing emissions from all other regions, particularly Latin America and Caribbean (43 per cent from Brazil in both years), and this trend is set to continue to 2030. The next most important CH_4 source sector is oil and gas production and distribution, with a rising trend between 1990 and 2005 projected to continue to 2030. This growth is driven mainly by increasing emissions from South, West and Central Asia (almost half from the Middle East), although

there are also greater contributions projected for Africa and North America and Europe. In 1990, CH_4 emissions from landfill (dominated by North America and Europe) and rice production (dominated by Northeast Asia, Southeast Asia and Pacific, and South, West and Central Asia) were the next two most important source sectors. However, between 1990 and 2005, emissions from coal mining grew more rapidly than those from either rice production or landfill, due to a large increase in Northeast Asia, Southeast Asia and Pacific, and this trend is set to continue to 2030. Thus coal mining is projected to become the third most important CH_4 source sector by 2030, with Northeast Asia, Southeast Asia and Pacific the predominant emitting region (with 85 per cent from China). Combined, the two fossil-fuel related sectors would be the largest single source category. The treatment of waste water (municipal and industrial) is a minor contributor to global anthropogenic CH_4 production, although emissions increased in all regions between 1990 and 2005 and this trend is set to continue up to 2030.
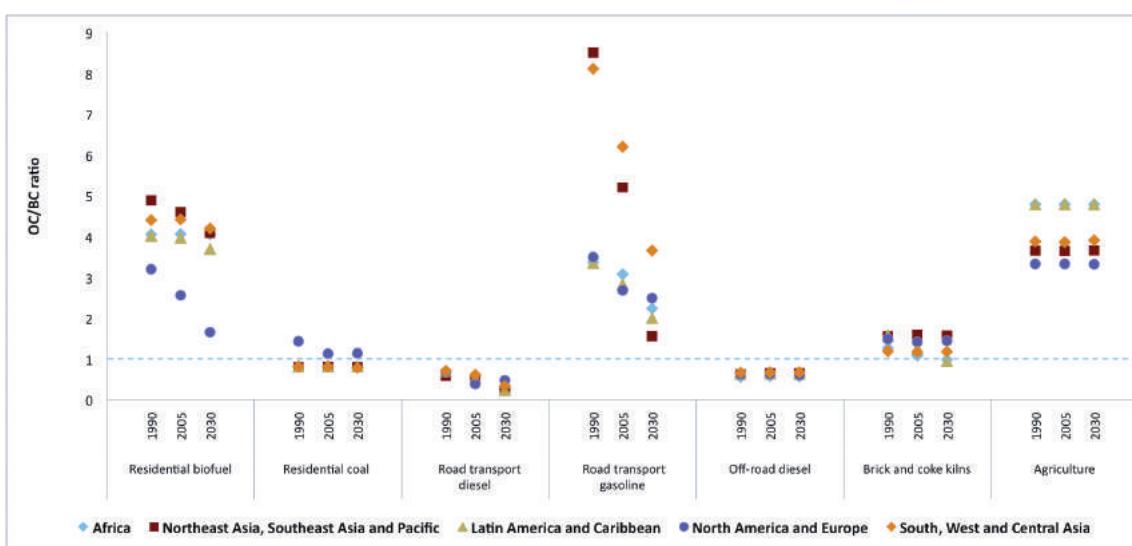
Figure 2.27. Trends in OC/BC mass ratios for important sub-sectors in each region.
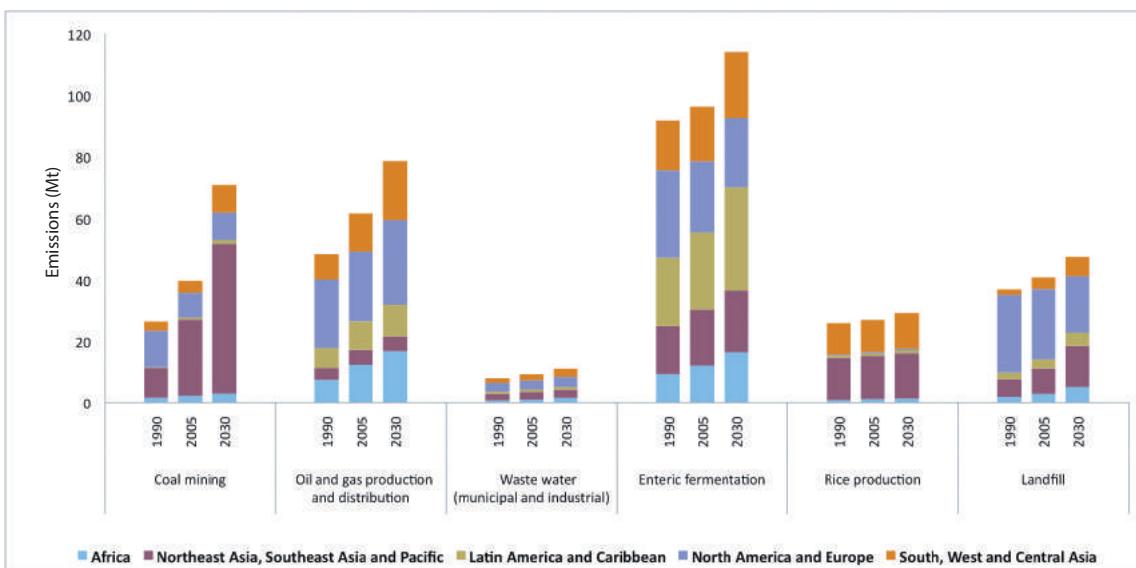
Figure 2.28. Trends in sub-sector CH_4 emissions by region.

Chapter 2. Black carbon and tropospheric ozone precursors: drivers, emissions and trends

Appendix A.2

There have been a number of attempts to compile estimates of present-day global emissions of pollutants relevant to this Assessment. These are not always consistent in their approaches to the three main categories of emission sources:

1. Fossil-fuel combustion, for which international statistics on fuel use are available;

2. Biofuel combustion, which is a large source in the developing world and for which international statistics are poor or non-existent; and

3. Open biomass burning, for which a variety of techniques, including national and regional surveys of burnt area and satellite observations, can be applied.

This section presents estimates of current emissions of BC, OC and tropospheric O_3 precursors developed in other works, against which the GAINS values can be compared. Although there are several of these inventories available, we present results from the two best known and most widely used inventories: Bond et al. (2004) for BC and OC and the EDGAR inventory for tropospheric O_3 precursors.

A.2.1 Present-day BC and OC emissions

A concise overview of global BC emissions can be obtained from Figures A.2.1 and A.2.2, based on data in Bond *et al.* (2004) for the year 1996. Although these data are somewhat old now, the distribution of emissions between regions and source types has not changed dramatically since then, and they are still informative. Total global BC emissions in 1996 were estimated at 8.0 Mt: 4.6 Mt from contained combustion – the burning of fossil fuels and biofuels for energy and other anthropogenic releases – and 3.3 Mt from open biomass burning. For contained combustion, Asia is the largest contributor, producing 2.5 Mt/yr or 55 per cent of the global total. China and India are the two largest emitting countries. With respect to open biomass burning – the accidental or intentional burning of forests, savannah/grassland and agricultural waste in fields – Africa produces the most BC: 1.9 Mt/yr or 44 per cent of the global total. Central/South America produces 0.91 Mt/yr or 27 per cent. The developed world (Europe, Former USSR, North America, Japan and the Pacific) is a relatively minor producer of BC of either kind. The global distributions of BC and OC are quite different, with over 70 per cent of BC emitted in the northern hemisphere and over 60 per cent of OC emitted in the southern hemisphere.
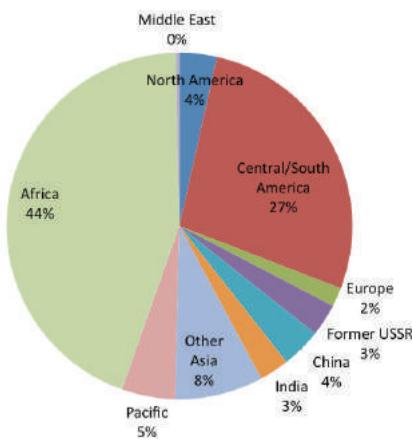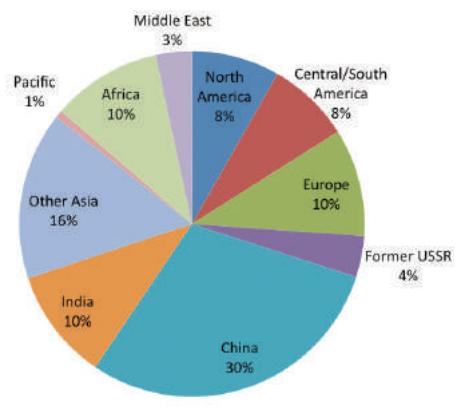
Figure A.2.1. Distribution of global BC emissions by world region for contained combustion (left) and open biomass burning (right) from Bond *et al.,* 2004.

Figure A.2.2 shows the relative contributions of all source types (both contained and open burning) to total global BC emissions. Open biomass burning is the largest individual contributor, with residential biofuel combustion the single largest anthropogenic source type at 1.5 Mt/yr or 19 per cent of the global total. On-road and off-road diesels produce a combined 1.4 Mt/yr or 17 per cent, while coal combustion in industry and the residential sector produces another 1.1 Mt/yr or 14 per cent. It should be noted that electric power generation, a major contributor to CO_2 emissions, does not appear on this chart because its contribution is so small. This is a powerful illustration of the very different nature of the sources of CO_2 and BC, and hence the different nature of the targets for mitigation. Although the spatial, temporal, sectoral and technological resolution of the inventory of Bond *et al.* and the GAINS model are different, the development of both has been closely coordinated between the groups, specifically with regard to the use of emission factors and principal assumptions on combustion technology in use. Therefore, the results are consistent between the two studies.

Global emissions of primary OC are about four times as large as global emissions of BC; note that secondary organic aerosols (SOA)
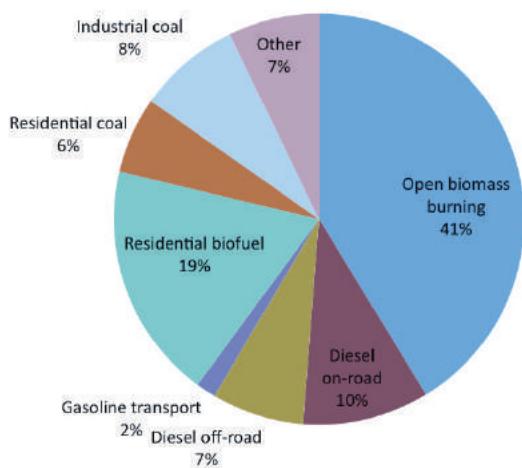
that are formed in the atmosphere through chemical reactions of gaseous species are not included. The total primary OC emissions reported by Bond *et al.* (2004) are 33.9 Mt for 1996. The underlying reason for differences in total BC and OC emissions lies in the fact that the OC/BC emission ratio for the burning of vegetation is much higher than the OC/BC ratio for fossil-fuel combustion. The regional distributions of global OC emissions from contained and open combustion are quite similar to those of BC, with the shares of regions that burn excessive amounts of biofuel and biomass being somewhat enhanced (e.g., India, Africa). China's share is lower because of its greater reliance on coal than biofuels. As regards the distribution of OC emissions by source type, we see a major difference from BC. Open biomass burning is by far the dominant source type (74 per cent versus 41 per cent for BC). Residential biofuel combustion comprises 17 per cent of the total, about the same as for BC. However, all other contributing source types are smaller for OC than for BC, showing the dominant role of vegetation burning in OC emissions.

A.2.2 Present-day emissions of tropospheric O_3 precursors

Levels of tropospheric O_3 at regional scale (as distinct from peak O_3 levels observed in urban areas) are determined primarily by the emissions of four major pollutants: NO_x, CO, NMVOCs and CH_4. Together, these four control the formation and destruction of tropospheric O_3 under prevailing atmospheric conditions of temperature, insolation, humidity, etc. NMVOCs encompass a wide range of compounds of very different reactivities and ozone formation potentials. In order to determine the role that NMVOCs plays in O_3 formation, the speciation profiles of the emissions in different sectors and regions of the world need to be known. And though we discuss below the anthropogenic emissions of NMVOCs, it should be remembered that emissions of biogenic NMVOCs are larger by a factor of 5–7 and highly relevant.

Figure A.2.2. Distribution of global BC emissions by major contributing source type from Bond *et al.,* 2004.

There are relatively few global emission inventories that are comprehensive in nature,

including all major species, source types and regions of the world. Perhaps the most well-known of them is the EDGAR (Emission Database for Global Atmospheric Research) (Olivier et al., 1996), presently hosted by the Joint Research Centre of the European Commission (EC-JRC/PBL, 2010). Results for the year 2005 from the recently released EDGAR v4.1 are shown below to illustrate the major sources of emissions of the four primary anthropogenic precursors of tropospheric O_3. Note that EDGAR only includes anthropogenic sources of emissions, following the UNFCCC convention. Open biomass burning is included but does not differentiate between wildfires and anthropogenic forest fires. The burning of forests and grassland for agriculture or habitation are included. As the EDGAR inventory is the most widely accepted global inventory of present-day emissions, it is desirable to compare its results with those that form the base case of the GAINS results for this study. Table A.2.1 summarizes the EDGAR v4.1 global emissions by species and major emitting sector.

NO_X emissions

In a similar way to the analysis followed above for BC, we can trace the major contributors to global NO_X emissions by world region, shown below in Figure A.2.3 (left) and by major emitting source type (right).

China is the largest contributor to global NO_X emissions, with 22 per cent of the total emission of 118.7 Mt. This reflects the large-scale use of fossil fuels, mainly coal, to power industrial and energy generation activities. In addition, China's NO_X emissions have grown very rapidly since 2000. North America (16 per cent), Europe (11 per cent), Africa (11 per cent) and Other Asia (11 per cent) are the other major emitting regions. Whereas industry and transport dominate the sources of NO_X in North America and Europe, it is biomass burning that largely accounts for the contributions of Africa and Other Asia. Sectoral emissions are dominated by industrial fuel combustion (including power generation) (43 per cent). On-road (22 per cent) and off-road (16 per cent) transport are also significant.

Table A.2.1. Global emissions of tropospheric O_3 precursors in 2005 by main source category from EDGAR v4.1 (Mt/yr).

	CO	NO_X	CH_4	NMVOCs
Industrial combustion	37.9	51.4	0.8	1.7
Fuel fugitive emissions	10.0	0.1	115.1	54.4
Domestic combustion	157.3	5.0	11.6	16.4
Transport on-road	147.0	25.9	0.7	21.9
Transport off-road	6.6	18.8	<0.1	1.4
Industrial processes	52.0	0.4	0.2	4.1
Solvent and other product use	0	0	0	21.9
Agriculture	248.4	12.9	150.5	14.5
Land-use change and forestry	188.3	3.9	11.7	14.2
Waste	<0.1	0.2	58.1	2.3
Other	2.5	<0.1	0.2	0.1
Global total	**850.2**	**118.7**	**349.0**	**152.9**
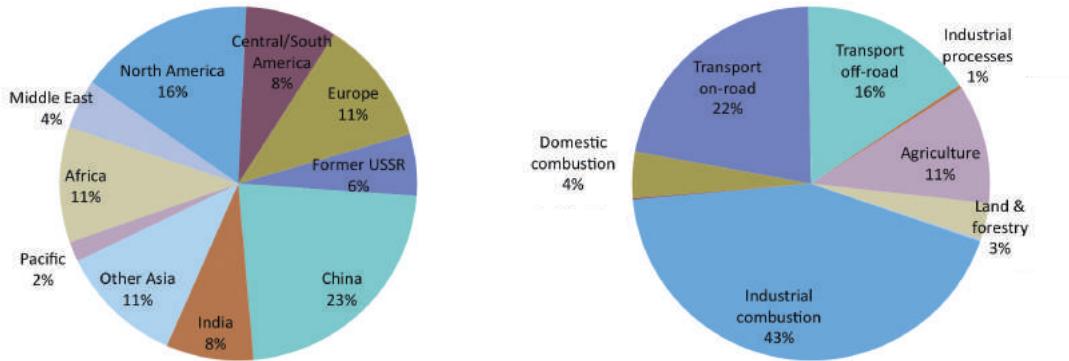
Figure A.2.3. Distribution of global NO$_X$ emissions in 2005 by world region (left) and by major source type (right), from EDGAR v4.1.

CO emissions

Because CO emissions (Figure A.2.4) are primarily caused by poor combustion, global emissions are dominated by the developing regions of the world, where biofuels and fossil fuels continue to be burned in small, inefficient devices for residential cooking and heating and small-scale industrial operations. The EDGAR v4.1 inventory shows that the total global CO emissions of 850 Mt in 2005 are dominated by Asia (34 per cent) and Africa (30 per cent), with relatively small contributions from North America (8 per cent) and Europe (4 per cent). The largest source categories are agriculture (29 per cent) and land use and forestry (22 per cent), mostly consisting

of various forms of vegetation burning for farming and human habitation. Residential combustion is also a large source of CO in the developing world (19 per cent) and transport (18 per cent) in all parts of the world.

NMVOC emissions

NMVOC emissions are more evenly distributed between the regions of the world (Figure A.2.5 (left)). The developed regions contribute significantly because of their large industrial sectors, handling substantial volumes of industrial chemicals, as well as their extensive transportation systems, processing and handling large quantities of oil products. On the other hand, NMVOC emissions are also
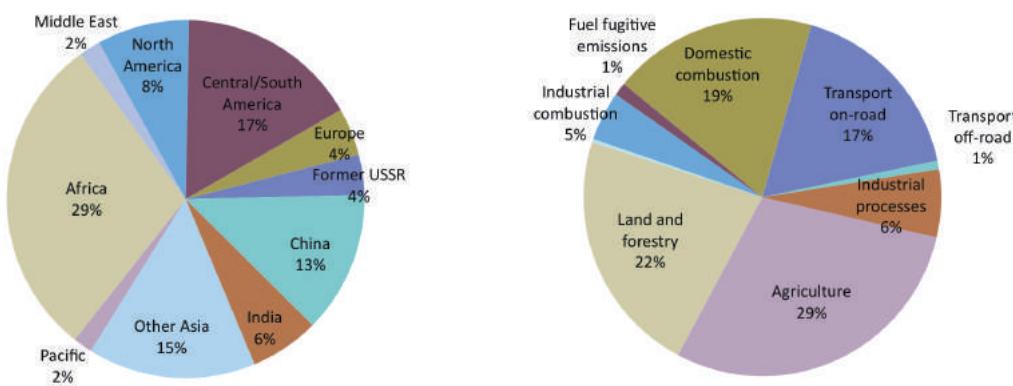
Figure A.2.4. Distribution of global CO emissions in 2005 by world region (left) and by major source type (right), from EDGAR v4.1.

a significant product of incomplete combustion, typically from traditional cooking and heating stoves, and therefore developing nations also contribute. On balance, Africa (20 per cent) and Other Asia (17 per cent) are the two largest emitting regions. North America (10 per cent) and Europe (10 per cent) contribute somewhat less. Fugitive emissions from oil, natural gas and solid fuels (36 per cent) is the largest contributing source category to global NMVOC emissions (Figure A.2.5 (right)), with transport (14 per cent) and solvent use (14 per cent) following. Several other source categories (residential fuel combustion, agriculture, and land use/forestry) are significant contributors to NMVOC emissions.
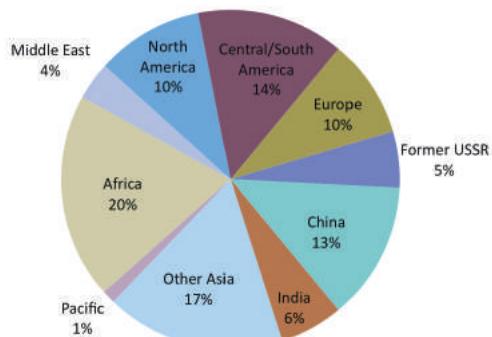
CH$_4$ emissions

Methane has rather a different sectoral profile to the other pollutants (Figure A.2.6 (right)). Distribution around world regions (Figure A.2.6 - left) is perhaps the most even of all, with the largest contributors being China (18 per cent), Central/South America (14 per cent), and Other Asia (13 per cent). Because of the contribution from coal mining, those regions that produce large quantities of coal are preferentially higher (like the former USSR). By source category (Figure A.2.6 - right), agriculture is the largest (43 per cent), reflecting the close association of CH$_4$ with rice growing and wetlands. Fugitive emissions from fuels generate 33 per cent of global CH$_4$, and waste disposal through landfills (17 per cent) is also a large source. All other sources of CH$_4$ are small.
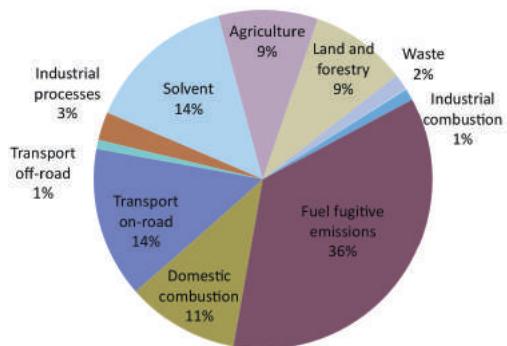
Figure A.2.5. Distribution of global NMVOC emissions in 2005 by world region (left) and by major source type (right), from EDGAR v4.1.
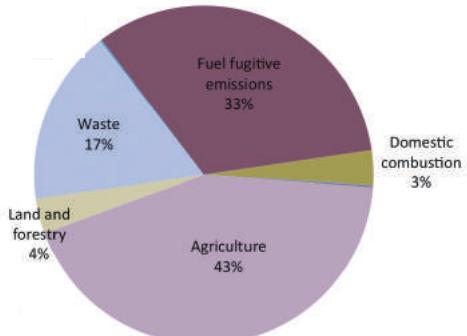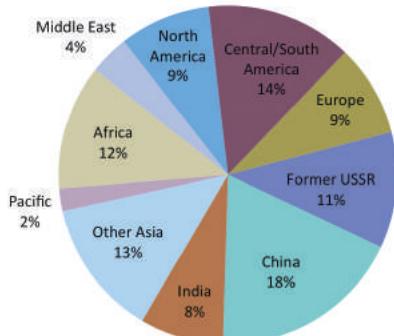
Figure A.2.6. Distribution of global CH$_4$ emissions in 2005 by world region (left) and by major source type (right), from EDGAR v4.1.

50

References

Achard, F., Eva, H. D., Mollicone, D. and Beuchle, R. (2008). The effect of climate anomalies and human ignition factor on wildfires in Russian boreal forests. *Philos. T. Roy. Soc. B*, 363, 2329–2337.

Akimoto, H. (2003). Global air quality and pollution. *Science*, 302, 1716–1719.

Akimoto, H., Ohara, T., Kurokawa, J. and Horii, N. (2006). Verification of energy consumption in China during 1996–2003 by using satellite observational data. *Atmos. Environ.*, 40, 7663–7667.

Alexandratos, N., Bruinsma, J., Boedeker, G., Schmidhuber, J., Broca, S., Shetty, P., and Ottaviani, M. G. (2006). *World agriculture: towards 2030/2050. Interim report. Prospects for food, nutrition, agriculture and major commodity groups.* FAO, Rome. http://www.fao.org/es/esd/AT2050web.pdf.

Allen, D., Pickering, K. and Fox-Rabinovitz, M. (2004). Evaluation of pollutant outflow and CO sources during TRACE-P using model-calculated, aircraft-based, and Measurements of Pollution in the Troposphere (MOPITT)-derived CO concentrations. *J. Geophys. Res.*, 109, D15S03, doi:10.1029/2003JD004250.

Amann, M., Kejun, J., Jiming, H., Wang, S., Xing, Z., Wei, W., Yi Xiang, D., Hong, L., Jia, X., Chuying, Z., Bertok, I., Borken, J., Cofala, J., Heyes, C., Höglund, L., Klimont, Z., Purohit, P., Rafaj, P., Schöpp, W., Toth, G., Wagner, F. and Winiwarter, W. (2008). *GAINS ASIA: Scenarios for Cost-effective Control of Air Pollution and Greenhouse Gases in China*. IIASA Policy Report. IIASA, Laxenburg, Austria.

Andreae, M. O. and Merlet, P. (2001). Emission of trace gases and aerosols from biomass burning. *Global Biogeochem. Cycles*, 15, 955–966.

Andreae, M. O., Rosenfeld, D., Artaxo, P., Costa, A. A., Frank, G. P., Longo, K. M. and Silva-Dias, M. A. F. (2004). Smoking rain clouds over the Amazon. *Science*, 303, 1337–1342.

Andres, R. J. and Kasgnoc, A. D. (1998). A time-averaged inventory of subaerial volcanic sulfur emissions. *J. Geophys. Res.,* 103, 25,251–25,261.

Arellano, A. F., Kasibhatla, P. S., Giglio, L., van der Werf, G. R., Randerson, J. T. and Collatz, G. J. (2006). Time-dependent inversion estimates of global biomass-burning CO emissions using Measurement of Pollution in the Troposphere (MOPITT) measurements. *J. Geophys. Res.*, 111, D09303, doi:10.1029/2005JD006613.

Artaxo, P., Martins, J. V., Yamasoe, M. A., Procopio, A. S., Pauliquevis, T. M., Andreae, M. O., Guyon, P., Gatti, L. V. and Leal, A. M. C. (2002). Physical and chemical properties of aerosols in the wet and dry seasons in Rondonia, Amazonia. *J. Geophys. Res.,* 107, 8081, doi:10.1029/2001JD000666.

Artaxo, P. and Andreae, M. O. (2007). Biomass burning as a driver for atmospheric composition and ecosystem changes. *iLEAPS Newsletter*, 4, 12–14.

Artaxo, P. (2010). Reductions in deforestation rates in Amazonia. *Global Atmospheric Pollution Forum Newsletter*, 8, 2–3.

Ban-Weiss, G. A., Lunden, M. M., Kirchstetter, T. W. and Harley, R.A. (2009). Measurement of black carbon and particle number emissions factors from individual heavy duty trucks. *Environ. Sci. Technol.*, 43, 1419–1424.

Bellprat, O. (2009). *Brick Kiln Evaluation Study in the Bajío Region GTO, México*. Instituto Nacional de Ecologia Mexico and Swiss Federal Institute of Technology, Zürich. September 2009.

Bond, T. C., Streets, D. G., Yarber, K. F., Nelson, S. M., Woo, J.-H. and Klimont, Z. (2004). A technology-based global inventory of black and organic carbon emissions from combustion. *J. Geophys. Res.*, 109, D14203, doi:10.1029/2003JD003697.

51

Bond, T. C., Bhardwaj, E., Dong, R., Jogani, R., Jung, S. K., Roden, C., Streets, D. G. and Trautmann, N. M. (2007). Historical emissions of black and organic carbon aerosol from energy-related combustion, 1850–2000. *Global Biogeochem. Cycles*, 21, GB2018, doi:10.1029/2006GB002840.

Bouwman, A. F., Boumans, L. J. M. and Batjes, N. H. (2002). Estimation of global NH$_3$ volatilization loss from synthetic fertilizers and animal manure applied to arable lands and grasslands. *Global Biogeochem. Cycles*, 16, 1024, doi:10.1029/2000GB001389.

Bowman, D. M. J. S., Balch, J. K., Artaxo, P., Bond, W. J., Carlson, J. M., Cochrane, M. A., D'Antonio, C. M., DeFries, R. S., Doyle, J. C., Harrison, S. P., Johnston, F. H., Keeley, J. E., Krawchuk, M. A., Kull, C. A., Marston, J. B., Moritz, M. A., Prentice, I. C., Roos, C. I., Scott, A. C., Swetnam, T. W., van der Werf, G. R. and Pyne, S. J. (2009). Fire in the Earth system. *Science*, 324, 481–484.

Bruinsma, J. (ed.) (2003). *World Agriculture: Towards 2015/2030, An FAO Perspective.* Earthscan, London and FAO, Rome. http://www.fao.org/DOCREP/005/Y4252E/Y4252E00.htm.

Buhaug, Ø., Corbett, J.J., Endresen, Ø., Eyring, V., Faber, J., Hanayama, S., Lee, D.S., Lee, D., Lindstad, H., Markowska, A.Z., Mjelde, A., Nelissen, D., Nilsen, J., Pålsson, C., Winebrake, J.J., Wu, W. and Yoshida, K. (2009). *Second IMO GHG Study 2009.* International Maritime Organization, London, UK.

CAI-Asia (2008). Emission standards for new vehicles (light duty). Clean Air Initiative for Asian Cities (CAI-Asia). http://www.cleanairnet.org/caiasia/1412/articles-58969_new.pdf.

Carmichael, G. R., Tang, Y., Kurata, G., Uno, I., Streets, D. G., Thongboonchoo, N., Woo, J. H., Guttikunda, S., White, A., Wang, T., Blake, D. R., Atlas, E., Fried, A., Potter, B., Avery, M. A., Sachse, G. W., Sandholm, S. T., Kondo, Y., Talbot, R. W., Bandy, A., Thornton, D. and Clarke, A. D. (2003). Evaluating regional emission estimates using the TRACE-P observations. *J. Geophys. Res.*, 108, 8810, doi:10.1029/2002JD003116.

Chen, Y., Zhi, G., Feng, Y., Liu, D., Zhang, G., Li, J., Sheng, G. and Fu, J. (2009). Measurements of black and organic carbon emission factors for household coal combustion in China: Implication for emission reduction. *Environ. Sci. Technol.*, 43, 9495–9500.

Christian, T. J., Kleiss, B., Yokelson, R. J., Holzinger, R., Crutzen, P. J., Hao, W. M., Saharjo, B. H. and Ward, D. E. (2003). Comprehensive laboratory measurements of biomass-burning emissions: 1. Emissions from Indonesian, African, and other fuels. *J. Geophys. Res.*, 108, 4719, doi:10.1029/2003JD003704.

Christian, T. J., Yokelson, R. J., Cárdenas, B., Molina, L. T., Engling, G. and Hsu, S.-C. (2010). Trace gas and particle emissions from domestic and industrial biofuel use and garbage burning in central Mexico. *Atmos. Chem. Phys.*, 10, 565–584.

Cofala, J. and Syri, S. (1998a). *Sulfur Emissions, Abatement Technologies and Related Costs for Europe in the RAINS Model Database.* International Institute for Applied Systems Analysis (IIASA), Laxenburg, Austria.

Cofala, J. and Syri, S., (1998b). *Nitrogen Oxides Emissions, Abatement Technologies and Related Costs for Europe in the RAINS Model Database.* International Institute for Applied Systems Analysis (IIASA), Laxenburg, Austria.

Cofala, J., Amann, M., Klimont, Z., Kupiainen, K. and Höglund-Isaksson, L. (2007). Scenarios of global anthropogenic emissions of air pollutants and methane until 2030. *Atmos. Environ.*, 41, 8486–8499.

Cooke, W., Liousse, C., Cachier, H. and Feichter, J. (1999). Construction of a 1° × 1° fossil fuel emission data set for carbonaceous aerosol and implementation and radiative impact in the ECHAM4 model. *J. Geophys. Res.,* 104, 22,137–162.

Corbett, J. J., Lack, D. A., Winebrake, J. J., Harder, S., Silberman, J. A. and Gold, M. (2010). Arctic shipping emissions inventories and future scenarios. *Atmos. Chem. Phys.*, 10, 9689–9704.

De Smedt, I., Müller, J.-F., Stavrakou, T., van der A, R., Eskes, H. and Van Roozendael, M. (2008). Twelve years of global observations of formaldehyde in the troposphere using GOME and SCIAMACHY sensors. *Atmos. Chem. Phys.*, 8, 4947–4963.

Derwent, R. G., Jenkin, M. E., Passant, N. R. and Pilling, M. J. (2007). Reactivity-based strategies for photochemical ozone control in Europe. *Environ. Sci. Policy,* 10, 445–453.

DieselNet (2010). Summary of worldwide diesel emission standards, http://www.dieselnet.com/standards.

Döring, U., Janssens-Maenhout, G., van Aardenne, J. and Pagliari, V. (2010). *Scenarios of Future Climate Change.* FP6 IP CIRCE del. 3.3.1, JRC technical note, Joint Research Centre (JRC).

Dufour, G., Wittrock, F., Camredon, M., Beekmann, M., Richter, A., Aumont, B. and Burrows, J. P. (2009). SCIAMACHY formaldehyde observations: constraint for isoprene emission estimates over Europe? *Atmos. Chem. Phys.,* 9, 1647–1664.

Durbin, T. D., Norbeck, J. M., Smith, M. R. and Truex, T. J. (1999). Particulate emission rates from light duty vehicles in the South Coast Air Quality Management District. *Environ. Sci. Technol.*, 33, 4401–4406.

EC-JRC/PBL (European Commission Joint Research Centre/Netherlands Environmental Assessment Agency) (2010). Emission Database for Global Atmospheric Research (EDGAR), http://edgar.jrc.ec.europa.eu.

EFMA (European Fertilizer Manufacturers Association) (2010). *Forecast of Food, Farming and Fertilizer Use in the European Union - 2009 to 2019.* Brussels, http://www.fertilizerseurope.com.

Erisman, J. W., Sutton, M. A., Galloway, J., Klimont, Z. and Winiwarter, W. (2008). How a century of ammonia synthesis changed the world. *Nat. Geosci.*, 1, 636-639.

Eyring, V., Isaksen, I. S. A., Berntsen, T., Collins, W. J., Corbett, J. J., Endresen, O., Grainger, R. G., Moldanova, J., Schlager, H. and Stevenson, D. S. (2010). Assessment of transport impacts on climate and ozone: Shipping. *Atmos. Environ.*, 44, 4735–4771.

FAO (2010). FAOSTAT: United Nations Food and Agriculture Organization (FAO) statistical databases, available at http://faostat.fao.org/site/339/default.aspx.

Fernandes, S. D., Trautmann, N. M., Streets, D. G., Roden, C. A. and Bond, T. C. (2007). Global biofuel use, 1850–2000. *Global Biogeochem. Cycles*, 21, GB2019, doi:10.1029/2006GB002836.

Fischer, G., Winiwarter, W., Ermolieva, T., Cao, G.-Y., Qui, H., Klimont, Z., Wiberg, D. and Wagner, F. (2010). Integrated modeling framework for assessment and mitigation of nitrogen pollution from agriculture: Concept and case study for China. *Agr., Ecosys. and Env.*, 136, 116–124.

Friedlingstein, P., Houghton, R. A., Marland, G., Hackler, J., Boden, T. A., Conway, T. J., Canadell, J. G., Raupach, M. R., Ciais, P. and Le Quéré, C. (2010). Update on CO_2 emissions. *Nat. Geosci.*, 3, 811–812.

Fromm, M., Bevilacqua, R., Servranckx, R., Rosen, J., Thayer, J. P., Herman, J. and Larko, D. (2005). Pyro-cumulonimbus injection of smoke to the stratosphere: Observations and impact of a super blowup in northwestern Canada on 3–4 August 1998. *J. Geophys. Res.*, 110, D08205, doi:10.1029/2004JD005350.

53

Fu, T.-M., Jacob, D. J., Palmer, P. I., Chance, K., Wang, Y. X., Barletta, B., Blake, D. R., Stanton, J. C. and Pilling, M. J. (2007). Space-based formaldehyde measurements as constraints on volatile organic compound emissions in east and south Asia and implications for ozone. *J. Geophys. Res.*, 112, D06312, doi:10.1029/2006JD007853.

Fung, I., John, J., Lerner, J., Matthews, E., Prather, M., Steele, L. P. and Fraser, P. J. (1991). Three-dimensional model synthesis of the global methane cycle. *J. Geophys. Res.*, 96, 13,033–13,065.

Gauss, M., Myhre, G., Isaksen, I. S. A., Grewe, V., Pitari, G., Wild, O., Collins, W. J., Dentener, F. J., Ellingsen, K., Gohar, L. K., Hauglustaine, D. A., Iachetti, D., Lamarque, J.-F., Mancini, E., Mickley, L. J., Prather, M. J., Pyle, J. A., Sanderson, M. G., Shine, K. P., Stevenson, D. S., Sudo, K., Szopa, S. and Zeng, G. (2006). Radiative forcing since preindustrial times due to ozone change in the troposphere and the lower stratosphere. *Atmos. Chem. Phys.*, 6, 575–599.

Granier, C., Bessagnet, B., Bond, T., D'Angiola, A., van der Gon, H. D., Frost, G. J., Heil, A., Kaiser, J. W., Kinne, S., Klimont, Z., Kloster, S., Lamarque, J.-F., Liousse, C., Masui, T., Meleux, F., Mieville, A., Ohara, T., Raut, J.-C., Riahi, K., Schultz, M. G., Smith, S. J., Thompson, A., van Aardenne, J., van der Werf, G. R. and van Vuuren, D. P. (2011). Evolution of anthropogenic and biomass burning emissions of air pollutants at global and regional scales during the 1980–2010 period. *Climatic Change* 109, 163-190. DOI 10.1007/s10584-011-0154-1

Guenther, A., Karl, T., Harley, P., Wiedinmyer, C., Palmer, P. I. and Geron, C. (2006). Estimates of global terrestrial isoprene emissions using MEGAN (Model of Emissions of Gases and Aerosols from Nature). *Atmos. Chem. Phys.*, 6, 3181–3210.

Houghton, J.T., Meira Filho, L.G., Lim, B., Tre'anton, K., Mamaty, I., Bonduki, Y., Griggs, D.J., and Callander, B.A., (eds.). (1997). *Revised 1996 IPCC Guidelines for National Greenhouse Gas Inventories*. Vol.1–3. Hadley Centre Meteorological Office, Bracknell, United Kingdom.

Hsu, Y. and Mullen, M. (2007). *Compilation of Diesel Emissions Speciation Data. Final Report.* CRC contract No. E-75.

IEA (1997). *Coal Power 2: World Coal-Fired Power Stations and Their Pollution Control Systems*. International Energy Agency, London, U.K.

IEA (2009). *World Energy Outlook 2009*. OECD/IEA, Paris, France.

IEA CCC (International Energy Agency Clean Coal Centre) (2010). Coal Power Database. IEA, available at http://www.iea-coal.org.uk.

IFA (International Fertilizer Industry Association) (2003). World Fertilizer Consumption Statistics, available from http://www.fertilizer.org/ifa/Home-Page/STATISTICS.

IPCC (2006). *2006 IPCC Guidelines for National Greenhouse Gas Inventories*. Report prepared by the National Greenhouse Gas Inventories Programme. Eggleston, H. S., Buendia, L., Miwa, K., Ngara, T. and Tanabe, K. (eds). IGES, Japan.

IPCC (2007). *Climate Change 2007: Synthesis Report. Contribution of Working Groups I, II and III to the Fourth Assessment Report of the Intergovernmental Panel on Climate Change*. Geneva, Switzerland.

Ito, A. and Penner, J. E. (2004). Global estimates of biomass burning emissions based on satellite imagery for the year 2000. *J. Geophys. Res.,* 109, D14S05, doi:10.1029/2003JD004423.

Junker, C. and Liousse, C. (2008). A global emission inventory of carbonaceous aerosol from historic records of fossil fuel and biofuel consumption for the period 1860–1997. *Atmos. Chem. Phys.*, 8, 1195–1207.

Kasibhatla, P., Arellano, A., Logan, J. A., Palmer, P. I. and Novelli, P. (2002). Top-down estimate of a large source of atmospheric carbon monoxide associated with fuel combustion in Asia. *Geophys. Res. Lett.,* 29, 1900, doi:10.1029/2002GL015581.

Klimont, Z., Amann, M. and Cofala, J. (2000). *Estimating Costs for Controlling Emissions of Volatile Organic Compounds from Stationary Sources in Europe.* Interim Report IR-00-51, International Institute for Applied Systems Analysis, Laxenburg, Austria.

Klimont, Z., Streets, D., Gupta, S., Cofala, J., Lixin, F. and Ichikawa, Y. (2002). Anthropogenic emissions of non-methane volatile organic compounds (NMVOC) in China. *Atmos. Environ.*, 36, 1309–1322.

Klimont, Z. and Brink, C. (2004). *Modeling of Emissions of Air Pollutants and Greenhouse Gases from Agricultural Sources in Europe.* Interim Report IR-04-048, International Institute for Applied Systems Analysis, Laxenburg, Austria.

Klimont, Z. (2005). Projections of agricultural emissions of ammonia in the European Union. In: Kuczynski, T. *et al.* (eds.) *Emissions from European Agriculture*. Wageningen Academic Publishers, Wageningen, Netherlands, pp. 227–246.

Klimont, Z., Cofala, J., Xing, J., Wei, W., Zhang, C., Wang, S., Kejun, J., Bhandari, P., Mathur, R., Purohit, P., Rafaj, P., Chambers, A. and Amann, M. (2009). Projections of SO_2, NO_x and carbonaceous aerosols emissions in Asia. *Tellus B,* 61, 602–617.

Kupiainen, K. and Klimont, Z. (2007). Primary emissions of fine carbonaceous particles in Europe. *Atmos. Environ.*, 41, 2156–2170.

Lack, D. A. *et al.* (2009). Particulate emissions from commercial shipping: Chemical, physical, and optical properties. *J. Geophys. Res.*, 114, D00F04, doi:10.1029/2008JD011300.

Lamarque, J.-F., Bond, T. C., Eyring, V., Granier, C., Heil, A., Klimont, Z., Lee, D., Liousse, C., Mieville, A., Owen, B., Schultz, M. G., Shindell, D., Smith, S. J., Stehfest, E., Van Aardenne, J., Cooper, O. R., Kainuma, M., Mahowald, N., McConnell, J. R., Naik, V., Riahi, K. and van Vuuren, D. P. (2010). Historical (1850–2000) gridded anthropogenic and biomass burning emissions of reactive gases and aerosols: methodology and application. *Atmos. Chem. Phys.,* 10, 7017–7039.

Lin, J. T., McElroy, M. B. and Boersma, K. F. (2010). Constraint of anthropogenic NO_x emissions in China from different sectors: a new methodology using multiple satellite retrievals. *Atmos. Chem. Phys.,* 10, 63–78.

Ma, J., Richter, A., Burrows, J. P., Nüss, H. and van Aardenne, J. A. (2006). Comparison of model-simulated tropospheric NO_2 over China with GOME-satellite data. *Atmos. Environ.,* 40, 593–604.

McCormick, M. P., Thomason, L. W. and Trepte, C. R. (1995). Atmospheric effects of the Mt Pinatubo eruption. *Nature*, 373, 399–404.

Mickley, L. J., Jacob, D. J. and Rind, D. (2001). Uncertainty in preindustrial abundance of tropospheric ozone: Implications for radiative forcing calculations. *J. Geophys. Res.,* 106, 3389–3399.

Mieville, A., Granier, C., Liousse, C., Guillaume, B., Mouillot, F., Lamarque, J.-F., Grégoire, J.-M. and Pétron, G. (2010). Emissions of gases and particles from biomass burning during the 20th century using satellite data and an historical reconstruction. *Atmos. Environ.,* 44, 1469–1477.

55

Monks, P.S., Granier, C., Fuzzi, S., Stohl, A., Williams, M.L., Akimoto, H., Amman, M., Baklanov, A., Baltensperger, U., Bey, I., Blake, N., Blake, R. S., Carslaw, K., Cooper, O. R., Dentener, F., Fowler, D., Fragkou, E., Frost, G. J., Generoso, S., Ginoux, P., Grewe, V., Guenther, A., Hansson, H.C., Henne, S., Hjorth, J., Hofzumahaus, A., Huntrieser, H., Isaksen, I.S.A., Jenkin, M.E., Kaiser, J., Kanakidou, M., Klimont, Z., Kulmala, M., Laj, P., Lawrence, M.G., Lee, J.D., Liousse, C., Maione, M., McFiggans, G., Metzger, A., Mieville, A., Moussiopoulos, N., Orlando, J.J., O'Dowd, C.D., Palmer, P.I., Parrish, D. D., Petzold, A., Platt, U., Pöschl, U., Prévôt, A.S.H., Reeves, C.E., Reimann, S., Rudich, Y., Sellegri, K., Steinbrecher, R., Simpson, D., t. Brink, H., Theloke, J., v. d. Werf, G., Vautard, R., Vestreng, V., Vlachokostas, C. and v. Glasow, R. (2009). Atmospheric composition change – global and regional air quality. *Atmos. Environ.*, 43, 5268–5350.

Mouillot, F. and Field, C. B. (2005). Fire history and the global carbon budget: a 1° × 1° fire history reconstruction for the 20th century. *Glob. Change Biol.*, 11, 398–420.

Mueller, J. F. and Stavrakou, T. (2005). Inversion of CO and NO_x emissions using the adjoint of the IMAGES model. *Atmos. Chem. Phys.*, 5, 1157–1186.

Nakicenovic, N. et al. (2000). Emissions Scenarios: A Special Report of Working Group III of the Intergovernmental Panel on Climate Change. Cambridge University Press, Cambridge, UK.

Novakov, T., Ramanathan, V., Hansen, J. E., Kirchstetter, T. W., Sato, M., Sinton, J. E. and Sathaye, J. A. (2003). Large historical changes of fossil-fuel black carbon aerosols. *Geophys. Res. Lett.*, 30, 1324, doi:10.1029/2002GL016345.

Olivier, J. G. J., Bouwman, A. F., Van der Maas, C. W. M., Berdowski, J. J. M., Veldt, C., Bloos, J. P. J., Visschedijk, A. J. H., Zandveld, P. Y. J. and Haverlag, J. L. (1996). Description of EDGAR Version 2.0, a set of global emission inventories of greenhouse gases and ozone-depleting substances for all anthropogenic and most natural sources on a per country basis and on 1×1 degree grid, RIVM/TNO report, Bilthoven, The Netherlands.

Olivier, J. G. J. and Berdowski, J. J. M. (2001). Global emissions sources and sinks. In: Berdowski, J. J. M., Guicherit, R. and Heij, B. J. (eds.), *The Climate System*. A. A. Balkema Publishers/Swets & Zeitlinger Publishers, Lisse, The Netherlands.

Pavelin, E. G., Johnson, C. E., Rughooputh, S. and Toumi, R. (1999). Evaluation of pre-industrial surface ozone measurements made using Schönbein's method. *Atmos. Environ.,* 33, 919–929.

Pétron, G., Granier, C., Khattatov, B., Yudin, V., Lamarque, J.-F., Emmons, L., Gille, J. and Edwards, D. P. (2004). Monthly CO surface sources inventory based on the 2000–2001 MOPITT satellite data. *Geophys. Res. Lett.,* 31, L21107, doi:10.1029/2004GL020560.

Quinn, P. K., Bates, T. S., Baum, E., Doubleday, N., Fiore, A. M., Flanner, M., Fridland, A., Garrett, T. J., Koch, D., Menon, S., Shindell, D., Stohl, A. and Warren, S. G. (2008). Short-lived pollutants in the Arctic: their climate impact and possible mitigation strategies. *Atmos. Chem. Phys.*, 8, 1723–1735.

Ramanathan, V. and Carmichael, G. (2008). Global and regional climate changes due to black carbon. *Nat. Geosci.*, 1, 221–227.

Reid, J. S., Koppmann, R., Eck, T. F. and Eleuterio, D. P. (2005a). A review of biomass burning emissions part II: intensive physical properties of biomass burning particles. *Atmos. Chem. Phys.*, 5, 799–825.

Reid, J. S., Eck, T. F., Christopher, S. A., Koppmann, R., Dubovik, O., Eleuterio, D. P., Holben, B. N., Reid, E. A. and Zhang, J. (2005b). A review of biomass burning emissions part III: intensive optical properties of biomass burning particles. *Atmos. Chem. Phys.*, 5, 827–849.

Roden, C. A., Bond, T. C., Conway, S., Benjamin, A. and Pinel, O. (2006). Emission factors and real-time optical properties of particles emitted from traditional wood burning cookstoves. *Environ. Sci. Technol.*, 40, 6750–6757.

Roden, C. A., Bond, T. C., Conway, S., Pinel, A. B. S., MacCarty, N. and Still, D. (2009). Laboratory and field investigations of particulate and carbon monoxide emissions from traditional and improved cookstoves. *Atmos. Environ.*, 43, 1170–1181.

Schöpp, W., Klimont, Z., Suutari, R. and Cofala, J. (2005). Uncertainty analysis of emission estimates in the RAINS integrated assessment model. *Environ. Sci. Policy*, 8, 601–613.

Schultz, M. G., Heil, A., Hoelzemann, J. J., Spessa, A., Thonicke, K., Goldammer, J. G., Held, A. C., Pereira, J. M. C. and van het Bolscher, M. (2008). Global wildland fire emissions from 1960 to 2000. *Global Biogeochem. Cycles*, 22, GB2002, doi:10.1029/2007GB003031.

Schumann, U. and Huntrieser, H. (2007). The global lightning-induced nitrogen oxides source. *Atmos. Chem. Phys.*, 7, 3823–3907.

Shindell, D. T. *et al.* (2006). Multimodel simulations of carbon monoxide: Comparison with observations and projected near-future changes. *J. Geophys. Res.*, 111, D19306, doi:10.1029/2006JD007100.

Smith, S. J., van Aardenne, J., Klimont, Z., Andres, R. J., Volke, A. and Delgado Arias, S. (2011). Anthropogenic sulfur dioxide emissions: 1850–2005. *Atmos. Chem Phys.*, 11, 1101-1116.

Streets, D. G., Bond, T. C., Carmichael, G. R., Fernandes, S. D., Fu, Q., He, D., Klimont, Z., Nelson, S. M., Tsai, N. Y., Wang, M. Q., Woo, J.-H. and Yarber, K. F. (2003a). An inventory of gaseous and primary aerosol emissions in Asia in the year 2000., *J. Geophys. Res.*, 108, 8809, doi:10.1029/2002JD003093.

Streets, D. G., Yarber, K. F., Woo, J.-H. and Carmichael, G. R. (2003b). Biomass burning in Asia: Annual and seasonal estimates and atmospheric emissions. *Global Biogeochem. Cycles*, 17, 1099, doi:10.1029/2003GB002040.

Streets, D. G., Bond, T. C., Lee, T. and Jang, C. (2004). On the future of carbonaceous aerosol emissions, *J. Geophys. Res.*, 109, D24212, doi:10.1029/2004JD004902.

Streets, D. G., Zhang, Q., Wang, L. T., He, K. B., Hao, J. M., Wu, Y., Tang, Y. H. and Carmichael, G. R. (2006). Revisiting China's CO emissions after the Transport and Chemical Evolution over the Pacific (TRACE-P) mission: Synthesis of inventories, atmospheric modeling, and observations. *J. Geophys. Res.*, 111, D14306, doi:10.1029/2006JD007118.

Subramanian, R., Winijkul, E., Bond, T. C., Thiansathit, W., Oanh, N. T. K., Paw-Armart, I. and Duleep, K. G. (2009). Climate-relevant properties of diesel particulate emissions: results from a piggyback study in Bangkok, Thailand. *Environ. Sci. Technol.*, 43, 4213–4218.

van Aardenne, J. A., Dentener, F. J., Olivier, J. G. J., Goldewijk, C. G. M. K. and Lelieveld, J. (2001). A 1° × 1° resolution data set of historical anthropogenic trace gas emissions for the period 1890–1990. *Global Biogeochem. Cycles*, 15, 909–928.

van der Werf, G. R., Randerson, J. T., Giglio, L., Collatz, G. J., Kasibhatla, P. S. and Arellano, A. F. (2006). Interannual variability in global biomass burning emissions from 1997 to 2004. *Atmos. Chem. Phys.*, 6, 3423–3441.

van der Werf, G. R., Randerson, J. T., Giglio, L., Collatz, G. J., Mu, M., Kasibhatla, P. S., Morton, D. C., DeFries, R. S., Jin, Y. and van Leeuwen, T. T. (2010). Global fire emissions and the contribution of deforestation, savanna, forest, agricultural, and peat fires (1997–2009). *Atmos. Chem. Phys.*, 10, 11707–11735.

Wang, T., Wei, X. L., Ding, A. J., Poon, C. N., Lam, K. S., Li, Y. S., Chan, L. Y. and Anson, M. (2009). Increasing surface ozone concentrations in the background atmosphere of Southern China, 1994–2007. *Atmos. Chem. Phys.,* 9, 6216–6226.

Wei, W., Wang, S., Chatani, S., Klimont, Z., Cofala, J. and Hao, J. (2008). Emission and speciation of non-methane volatile organic compounds from anthropogenic sources in China. *Atmos. Environ.,* 42, 4976–4988.

Xu, Y., Williams, R. H. and Socolow, R. H. (2009). China's rapid deployment of SO_2 scrubbers. *Energy Environ. Sci.,* 2, 459–465.

Yamasoe, M. A., Artaxo, P., Miguel, A. H. and Allen, A. G. (2000). Chemical composition of aerosol particles from direct emissions of vegetation fires in the Amazon Basin: water-soluble species and trace elements. *Atmos. Environ.,* 34, 1641–1653.

Yanowitz, J., McCormick, R. L. and Graboski, M. S. (1999). In-use emissions from heavy-duty diesel vehicles. *Environ. Sci. Technol.*, 34, 729–740.

Yokelson, R. J., Karl, T., Artaxo, P., Blake, D. R., Christian, T. J., Griffith, D. W. T., Guenther, A. and Hao, W. M. (2007). The Tropical Forest and Fire Emissions Experiment: overview and airborne fire emission factor measurements. *Atmos. Chem. Phys.,* 7, 5175–5196.

Zhang, Q., Streets, D. G., He, K., Wang, Y., Richter, A., Burrows, J. P., Uno, I., Jang, C. J., Chen, D., Yao, Z. and Lei, Y. (2007). NO_x emission trends for China, 1995–2004: The view from the ground and the view from space. *J. Geophys. Res.,* 112, D22306, doi:10.1029/2007JD008684.

Zhang, Q., Streets, D. G., Carmichael, G. R., He, K. B., Huo, H., Kannari, A., Klimont, Z., Park, I. S., Reddy, S., Fu, J. S., Chen, D., Duan, L., Lei, Y., Wang, I. T. and Yao, Z. L. (2009a). Asian emissions in 2006 for the NASA INTEX-B mission. *Atmos. Chem. Phys.,* 9, 5131–5153.

Zhang, Q., Streets, D. G. and He, K. B. (2009b). Satellite observations of recent power plant construction in Inner Mongolia, China. *Geophys. Res. Lett.,* 36, L15809, doi:10.1029/2009GL038984.

Zhao, Y., Wang, S., Nielsen, C. P., Li, X. and Hao, J. (2010). Establishment of a database of emissions factors for atmospheric pollutants from Chinese coal-fired power plants. *Atmos. Environ.,* 44, 1515–1523.

Zhi, G., Peng, C., Chen, Y., Liu, D., Sheng, G. and Fu, J. (2009). Deployment of coal briquettes and improved stoves: possibly an option for both environment and climate. *Environ. Sci. Technol.*, 43, 5586–5591.

Chapter 3. Atmospheric processes, tropospheric ozone and black carbon concentrations, deposition and radiative forcing

Coordinating lead author: David Fowler (Centre for Ecology and Hydrology, UK).

Lead authors: Greg Carmichael (University of Iowa, USA), William Collins (UK Meteorological Office, UK), Johan C.I. Kuylenstierna (Stockholm Environment Institute, University of York, UK), N. T. Kim Oanh (Asian Institute of Technology, Thailand), Frank Raes (Joint Research Centre, European Commission, Italy), Veerabhadran Ramanathan (Scripps Institution of Oceanography, USA), Michael Schulz (Meteorological Institute, Norway), Drew Shindell (National Aeronautics and Space Administration), Goddard Institute for Space Studies, USA), Elisabetta Vignati (Joint Research Centre, European Commission, Italy).

Contributing authors: Gufran Beig (Indian Institute of Tropical Meteorology, India), Sarath Guttikunda (Urban Emissions, India/Desert Research Institute, USA), Hong Liao (Institute of Atmospheric Physics, Chinese Academy of Sciences, China), Maheswar Rupakheti (Asian Institute of Technology-UNEP Regional Resource Center for Asia and the Pacific, Thailand).

Key findings

Black carbon
Black carbon (BC) causes radiative forcing through direct absorption of solar radiation, and indirectly through induced changes in cloud properties, and also due to changes in snow/ice albedo. The overall uncertainty of the net radiative forcing by BC is largely due to physical complexity and the changes in cloud properties that may offset the positive forcing.

Globally averaged net forcing is likely to be positive and in the range 0.0 to 1.0 W/m^2, with a best estimate of 0.6 W/m^2 (values include the enhanced efficacy of BC forcing due to snow and ice darkening).

Ozone
The globally averaged net radiative forcing from tropospheric ozone (O_3) has been estimated to be in the range 0.25 to 0.65 W/m^2 (the range within which 95 per cent of values occur) with a median value of 0.35 W/m^2. Ozone is not an emitted pollutant and thus for control purposes it is appropriate to attribute the radiative forcing for O_3 to the precursor emissions of methane (CH_4), carbon monoxide (CO), non-methane volatile organic compounds (NMVOCs) and nitrogen oxides (NO_x).

Two-thirds of the O_3 radiative forcing to date may be attributed to the increase in atmospheric CH_4 over the last century, and hence CH_4 emissions are responsible for a large part of the increase. The emissions of NO_x contributed a small fraction of the O_3 radiative forcing, but other effects of NO_x emissions have had a greater negative radiative forcing effect, in particular the atmospheric destruction of CH_4 and the direct and indirect aerosol effects. Thus the net radiative effect of NO_x has been negative. Non-methane volatile organic compounds and CO emissions make small positive contributions to radiative forcing through effects on (O_3).

59

3.1 Introduction

Black carbon particles and tropospheric O_3 precursors, once emitted, are transported and subject to chemical transformations in the atmosphere and are subsequently removed by deposition to terrestrial and marine surfaces. This chapter examines the different atmospheric processes that regulate the concentrations, properties and fate of tropospheric O_3 and BC. Current understanding of these pollutants is formalized within global chemistry-transport models, which are used to assess effects on climate, health and ecosystems in Chapter 4.

This chapter presents concentrations of particulate matter (PM) and O_3 in the atmosphere and shows the degree to which they are captured by the models used for the Assessment. The direct warming effect of O_3 is fairly straightforward, but complexity is introduced by the fact that O_3 is created within the atmosphere from emitted precursor gases, so the warming needs to be associated with these precursors. This is important for the emission reduction strategies highlighted in Chapter 5. For BC, the effects on climate are complex due to the wide range of interactions between PM and the Earth's radiation balance.

This chapter also outlines the main processes, with a focus on BC, and provides links to the wider academic literature on the subject. Black carbon and O_3 precursors are often co-emitted with other gases and particles. Understanding the effect of these co-emitted substances on warming, climate change and the composition and concentrations of air pollutants is important when evaluating measures to reduce emissions of BC and O_3. Values for important parameters taken from the peer-reviewed literature and used in modelling or assessment of impacts are discussed.

3.2 Aerosol transport in the atmosphere, concentrations, deposition and radiative forcing with a focus on black carbon and organic carbon

3.2.1 Aerosol concentrations and chemical composition

Aerosol particles in the atmosphere exist at sizes from nanometres to tens of micrometres in diameter, and consist of different chemical species, including sulphate (SO_4^{2-}), nitrate (NO_3^-), ammonium (NH_4^+), BC, organic carbon (OC), sea salt, mineral dust and other components such as fly ash. Primary aerosol species – BC, primary organic carbon (POC), sea salt, mineral dust and ash – are directly emitted as particles by natural or anthropogenic sources, while secondary aerosol species – SO_4^{2-}, NO_3^-, NH_4^+ and secondary organic aerosols (SOA) – are produced in the atmosphere by chemical and physical processes.

Aerosols, once emitted or formed in the atmosphere, are subject to further changes in their properties during transport. Such changes include condensation or evaporation of gaseous species, mixing with other aerosol particles through coagulation, and cloud processing before being removed from the air by dry and wet deposition. Generally speaking, an aerosol is externally mixed – with individual particles consisting of a pure chemical species – close to its source, and then develops into an internally mixed aerosol, with individual particles consisting of a mixture of species – during transport in the atmosphere (Raes *et al.*, 2000; Jacobson 2001). This processing defines the physical, chemical and optical properties of the aerosol, the efficiency by which it is removed from the atmosphere by wet and dry deposition, and hence the lifetime and concentrations of particles in the air. In studies of their effect on human health, a distinction is commonly made between PM_{10} and $PM_{2.5}$, i.e. the mass of aerosols with a diameter of less than 10 and 2.5 μm (micrometres), respectively. Figures 3.1 and 3.2 show the concentrations of $PM_{2.5}$ at a range of locations in Europe and Asia.
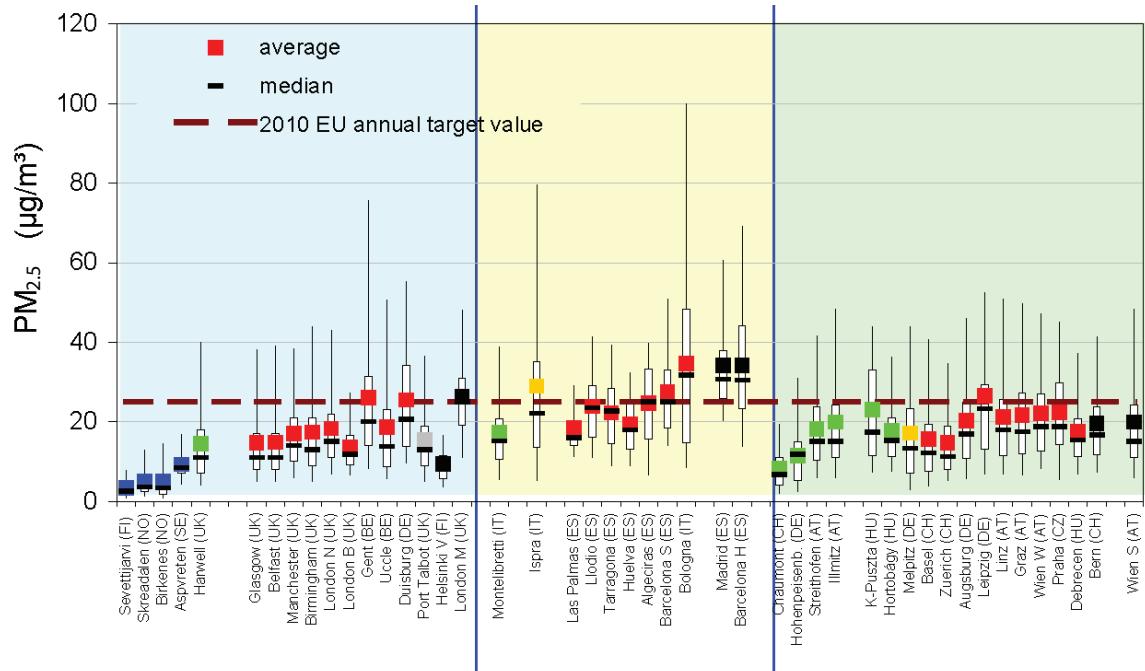
Figure 3.1. Annual averages of PM$_{2.5}$ mass concentrations, including the 5, 25, 50 (median), 75 and 95 per cent percentile of their 24-hour integrated concentrations from recent years in Europe. Symbol colours indicate the type of site (blue: natural background, green: rural background, yellow: near city, red: urban background, grey: industrial, black: roadside). Pastel backround colours make the distinction between sites in Northeastern (blue), Southern (yellow) and Central Europe (green) (Putaud *et al.*, 2010).
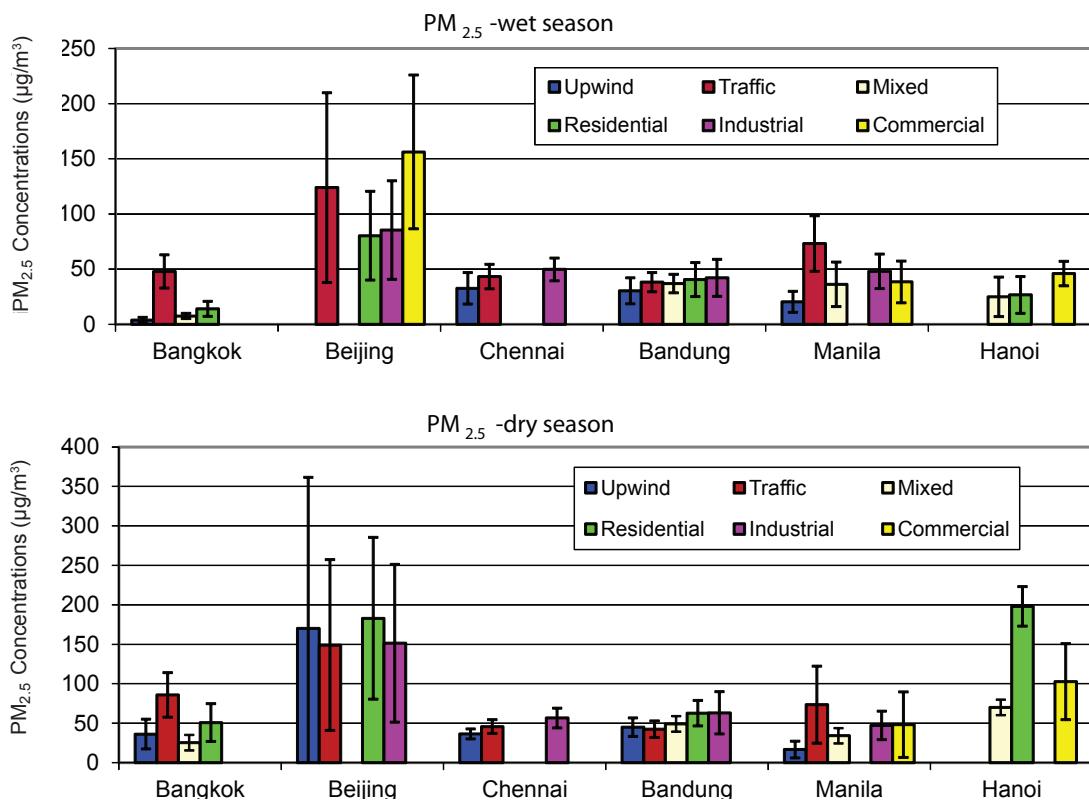
Figure 3.2. Average concentration of PM$_{2.5}$ in the dry and wet season in six Asian cities (2001–2004). Error bars represent one standard deviation (SD) from the average mass concentration (Oanh *et al.*, 2006)

Chapter 3. Atmospheric processes, tropospheric ozone and black carbon concentrations, deposition and radiative forcing
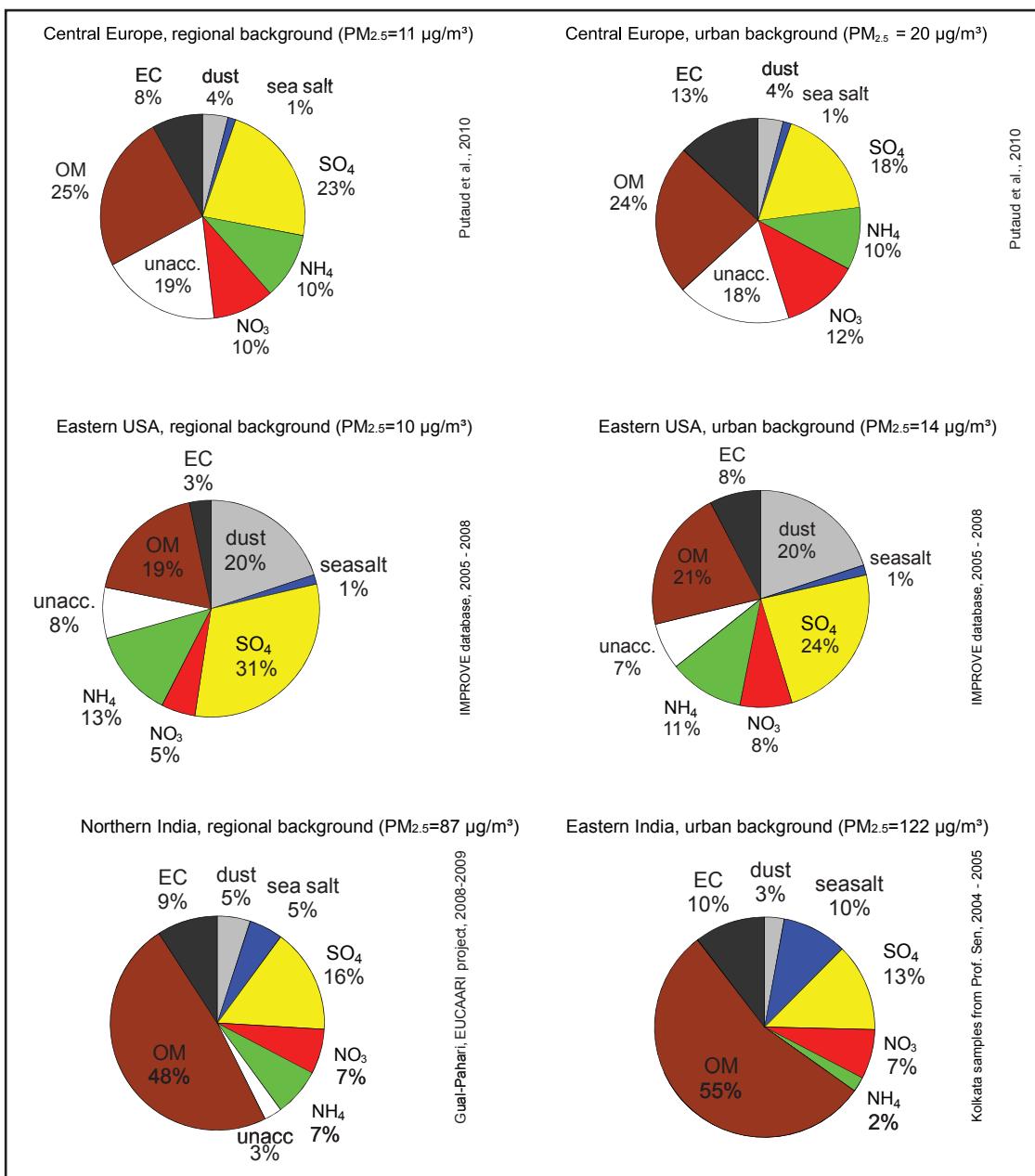
Figure 3.3. Chemical composition of PM$_{2.5}$ at various sites across the world. "OM" stands for organic matter, and is calculated as OC×1.4 at all sites. "EC" stands for Elemental Carbon. "Dust" consists of non carbonaceous and non water soluble species, and can be estimated differently at the various sites.

Concentrations of PM$_{2.5}$ are generally substantially larger in Asian cities than in European ones. Furthermore, the elevated concentrations are not confined to urban areas but are found over extensive tracts of polluted regions as a result of long-range transport of fine aerosols in the absence of rain. Concentrations of PM$_{2.5}$ in polluted areas can be orders of magnitude larger than those at remote locations on mountain tops or in polar regions.

In addition to the mass concentrations of PM, the chemical composition is important in determining the physical and optical properties and the effects both within the atmosphere and on the health of humans and ecosystems. Examples of the chemical composition of aerosols are provided in Figure 3.3 for India, North America and Europe, revealing large differences between regions, reflecting the different source characteristics and climate

of the three regions. Chemical complexity is further revealed by the differences between urban and rural locations.

The contributions by the dominant fractions by mass show important regional differences. The BC contribution sometimes measured and reported as elemental carbon (EC) represents up to 20 per cent of aerosol mass in some Central European cities. In India, dust and organic matter (OM) collectively contribute 50 to 60 per cent of the $PM_{2.5}$ mass, whereas in Europe and North America, sulphate (SO_4^{2-}), nitrate (NO_3^-), and OM contribute 50 to 60 per cent, showing the much greater contribution to aerosol composition made by combustion emissions in Europe and North America.

Organic carbon in the atmosphere refers to the carbonaceous fraction of aerosol particles. They are also called OM or particulate OM (POM) when the non-carbonanceous fraction – H, O and other atoms – is included. This component is frequently emitted along with BC during incomplete combustion processes, and is found as an internal mixture with BC.

Among natural sources, vegetation is a major source of VOCs which, following oxidation, contribute substantially to Secondary Organic Aerosols (SOAs). Over oceans, emissions of primary organic particles and precursors contribute directly to the burden of organic matter in the atmosphere (Vignati et al., 2010a). The anthropogenic emissions of VOCs, from transport, industry and others, are generally coupled with high NO_x emissions favouring production of SOAs and influencing the O_3 cycle.

In developing countries, and also in Central Europe, OM is often the dominant component in aerosol mass (15 to 35 per cent in $PM_{2.5}$), while BC accounts in general for up to 15 per cent (Ramanathan et al., 2001; Putaud et al., 2010). Organic matter is the major component of secondary aerosols, and present in aerosols of both anthropogenic and natural origin. The gaseous organic compounds can condense on cloud droplets – and also on to fine particles – and when the cloud evaporates they can reside in the aerosol phase.

3.2.2 Aerosol transport and global concentration fields

The mean residence time in the atmosphere for BC varies regionally and with season; based on an international evaluation of 16 models, the residence time of BC emitted in various regions ranges from about three to eight days (Shindell et al., 2008a).

Because of their relatively short lifetime, BC and other co-emitted aerosols such as OC, are generally concentrated in regional hotspots close to the sources. They can however contaminate entire geographical basins such as the Po Valley and Ganges Plain, and in the absence of precipitation may accumulate on a large regional scale and be transported over considerable distances, producing transcontinental and transoceanic plumes of brown clouds.

Recent observations have provided new insights into the concentrations and transport of BC aerosols. Figure 3.4 shows the annual average of measured BC concentrations at the surface (Koch et al., 2009a). The BC concentrations of 0.1 to 0.5 $\mu g/m^3$ over the United States were from the IMPROVE network for the years of 1995 to 2001, 0.5 to 5 $\mu g/m^3$ over Europe were from the EMEP network for 2002 to 2003, and those of 1 to14 $\mu g/m^3$ over Asia were from the late 1990s (Koch et al., 2007). Concentrations of BC were in the range of 0.01 to 0.1 $\mu g/m^3$ in the high northern latitudes and in general the values are much larger in areas with large emissions than in remote locations, especially at high northern latitudes (Figure 3.4) and as reported by Sharma et al. (2004, 2006).

The aerosol absorption optical depth (AAOD), or the non-scattering part of the aerosol optical depth, provides an indication of the atmospheric column abundance of absorbing aerosols. Figure 3.5 shows seasonal mean clear-sky AAOD ($\times100$) from AERONET (1996 to 2006) sunphotometer at 550 nanometres (nm) (e.g. Dubovik et al., 2000; Dubovik and King, 2000), satellite retrievals at 500 nm (2005 to 2007, from OMAERUV product; Torres et al., 2007), and

63
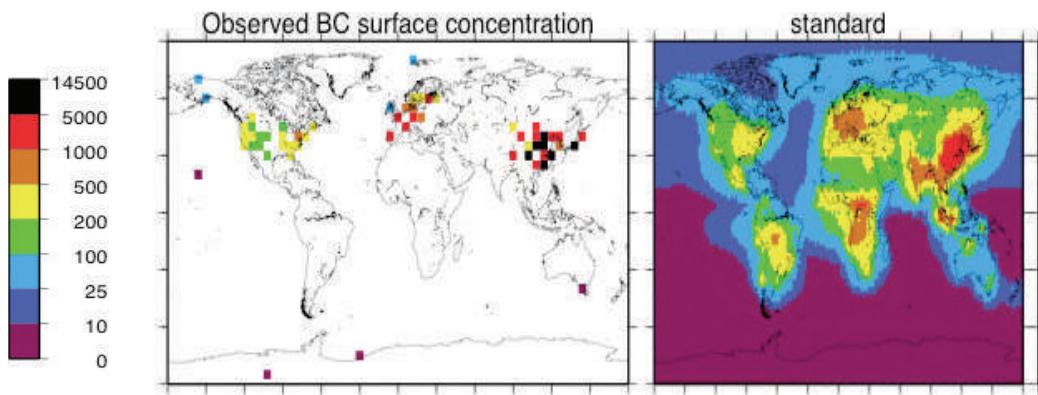
Figure: 3.4. Observed (left) and modelled (right) surface BC concentrations showing rather sparse measurements but reasonable correlation between model and measurement (ng/m³) (Koch *et al.*, 2009a).

the IPPC's Fourth Assessment Report (AR4) version of the GISS model at 550 nm (IPCC, 2007). Both BC and dust absorb radiation, so AAOD is most useful for testing BC in regions where its absorption is more significant than that of dust. The AERONET and OMI retrievals broadly agree with one another. Biomass burning seasonality, with peaks in June, July and August for Central Africa (OMI) and in September, October and November for South America, is simulated in the GISS model. In Asia, both retrievals have maximum AAOD in March, April and May as a result of the large amount of biomass burning in South Asia. BC in other industrial regions does not show seasonal variations. Summertime pollution outflow from North America is found in both OMI and the model results. Globally, as summarized by Koch *et al.* (2009a) the simulated AAODs in many models are about 50 per cent smaller than the observational values. (Additional discussion of the ability of models to capture observed aerosol distributions is presented in Appendix A.3).
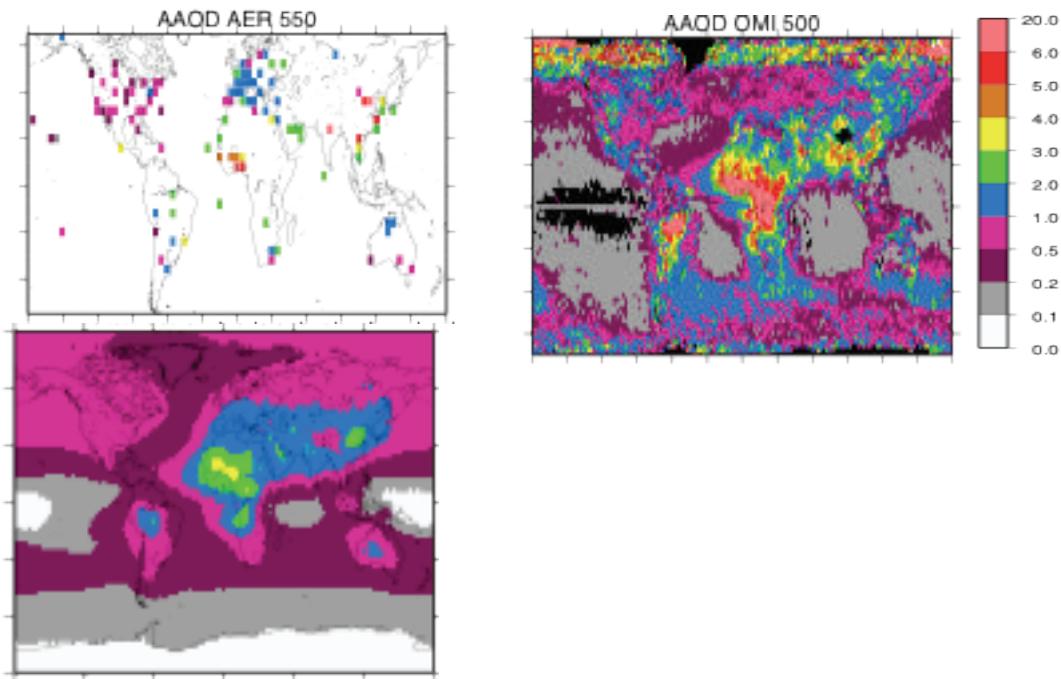
Figure 3.5. Aerosol absorption optical depth, AAOD, (x100) from AERONET (at 550 nm; upper left), OMI (at 500 nm; upper right); and from the GISS model (AR4 version; lower left) (Koch *et al.,* 2009a) showing rather sparse measurements but reasonable correlation between model and measurement.

64
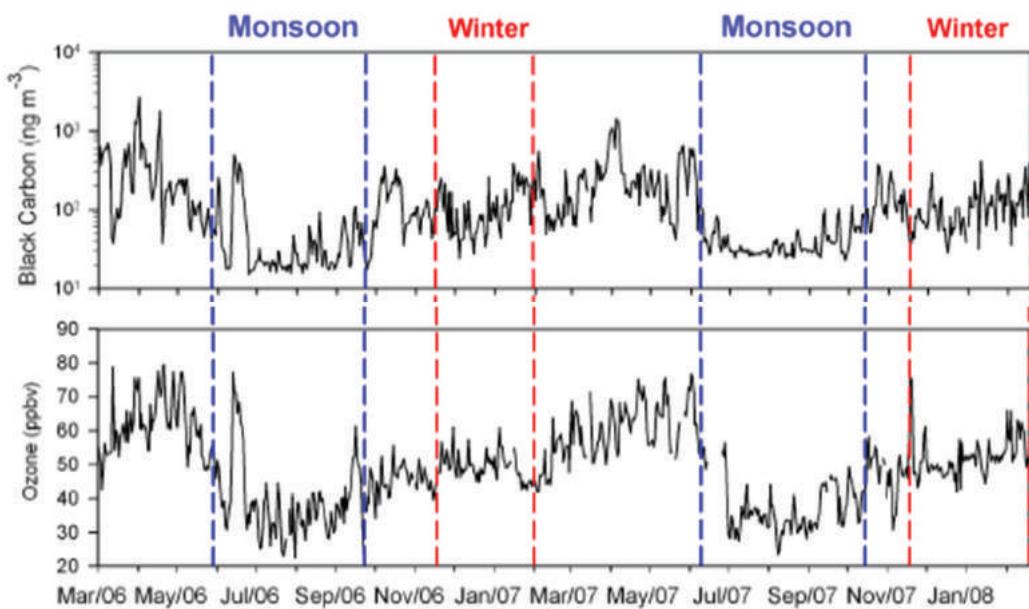
Figure 3.6. Black carbon and ozone concentrations (daily averages) measured from March 2006 to February 2008 at the GAW-WMO Global station "Nepal Climate Observatory - Pyramid" at 5 097 m above mean sea level near Mt. Everest, showing values comparable with polluted areas during several pre-monsoon days (Bonasoni *et al.*, 2010).

The transport, transformation, removal and hence the concentration of BC are also influenced by the special meteorological features and especially the precipitation patterns of any region. Monsoon circulations and rainfall in Asia, for example, govern the seasonal and inter-annual variations of aerosols (Corrigan *et al.*, 2006; Cao *et al.*, 2007), and pollution export. In South Asia, the dry period of November to March favours the accumulation of air pollutants. The BC and other pollutants are then transported, with some forced aloft to form elevated layers, over much of South Asia and the Indian Ocean by northeasterly flows (Ramanathan *et al.*, 2001; Lawrence and Lelieveld, 2010; Gustafsson *et al.*, 2009). On the other hand, the heavy rains during the summer monsoon generally reduce the local build-up and long-range transport of aerosol particles through enhanced removal by wet deposition. Figure 3.6 shows the variation of BC concentration at a high-elevation WMO GAW Global station[1] close to Mt. Everest caused by regional meteorology and, especially, the monsoon circulation and precipitation seasonality. Figure 3.6 also shows systematic differences in PM$_{2.5}$

concentration in the dry and wet seasons in the Asian cities, resulting from the above-mentioned meteorological processes.

Deep convective updrafts in the tropical region can also efficiently transport insoluble pollutants, such as CO, and possibly selected aerosol components, including BC, to the upper troposphere (Fu *et al.*, 2006). The tropical jet stream can then very effectively transport these pollutants over a long distance. Transport to and deposition at high northern latitudes differs greatly from tropical regions, as the stability of the column at high latitudes substantially restricts vertical transport through the atmosphere (Sharma *et al.*, 2006).

Since aerosols can move across international borders through long-range transport, local air quality and climate are influenced by emissions from other countries, and it is important to understand the source-receptor (S-R) relationships of the intercontinental transport of air pollutants (Grennfelt and Hov, 2005). A number of studies have quantified the S-R relationships for aerosols using atmospheric chemistry transport models (Shindell *et al.*, 2008b; Park and Kim 2005; Saikawa *et al.*, 2009).

---

[1] www.wmo.int/gaw/

The recent Task Force on Hemispheric Transport of Air Pollution (HTAP) report (Dentener *et al.*, 2010) introduced the Relative Annual Intercontinental Response (RAIR) metric, which is the sum of the changes in the annual average, regionally-averaged concentration due to a 20 per cent decrease in emissions in the other regions included in the HTAP report, divided by the sum of the changes in concentration within a region due to a 20 per cent decrease in emissions in all regions (with 0 per cent reflecting no contribution by intercontinental transport and 100 per cent indicating the total dominance of intercontinental transport). The HTAP report focused on four regions, North America, Europe, East Asia and South Asia. RAIR values for surface aerosols range from 1 to 12 per cent for Europe (low), North America, East Asia and South Asia (high).

In general, for the column loadings of BC, which are important for estimating climate forcing, the contribution from intercontinental transport increases from 15 to 24 per cent for these regions, reflecting the long-range transport of aerosols in the free troposphere above a receptor. For the Arctic, and other regions with low emissions, the RAIR values are large. Aerosol concentrations from primary sources generally respond linearly to changing emissions from both local and upwind source regions, while aerosols formed within the atmosphere show marked non-linearities with emissions of their gaseous precursor species (Fowler *et al.*, 2007).

Numerical models play a critical role in the HTAP report of the global transport and extent of BC and aerosols in general. They also link emissions to global concentration fields and their climate and environmental impacts. They therefore enable the study of changes in impacts of interest with respect to changes in emissions in particular sectors. The treatment of BC and other aerosol properties and processes in regional and global models is becoming increasingly complex; detailed representations of key aerosol properties such as size distributions, chemical composition (e.g., internal or external mixtures), hygroscopicity, optical properties, and cloud activation have been incorporated into global climate models (Binkowski and Shankar, 1995; Binkowski and Roselle, 2003; Adams and Seinfeld, 2003; Gong, 2003; Jacobson, 2001; Stier *et al.*, 2005; Jacobson, 2006; Kim *et al.*, 2008; Pierce and Adams, 2009). Current global models are able to capture the distributions of BC (Figure 3.4), with simulated ground-level BC concentrations generally within a factor of two of measurements (Koch *et al.*, 2009b), but challenges remain in capturing strong regional gradients in surface concentrations due to urban and industrial hotspots (Penner *et al.*, 2009) and estimating total column absorption, vertical distributions and microphysical properties.

3.2.3 Removal of BC from the atmosphere

The sizes of aerosols containing BC show great variability between regions, and in time, but the majority of BC is contained in aerosols in the 0.01 to 1.0 μm size fraction (Clark *et al.*, 2006). In this size range, deposition velocities to forest canopies are in the range 0.1 to 2.0 mm per second and for other terrestrial surfaces deposition velocities are substantially smaller and have been discussed in recent reviews (Nemitz *et al.*, 2002; Pryor *et al.*, 2008). By contrast with dry deposition, removal of BC from the atmosphere through wet scavenging processes is relatively efficient, especially for internally mixed BC with soluble species such as SO_4^{2-} and NO_3^-. Wet deposition is the main removal process for atmospheric BC (Jacobson, 2010). The high Arctic during the peaks in seasonal aerosol concentrations (autumn and spring) is very dry, and while deposition velocities are very small, dry deposition is the main loss process in these conditions.

Granat *et al.* (2010) found that BC wet removal during the monsoon season in sub-tropical marine air was similar to that of SO_4^{2-} and other fine-mode aerosol components, indicating that soot-containing particles in these situations were as efficient as cloud condensation nuclei. During the polluted winter days, on the other hand, the wet removal of soot was three times smaller than that of SO_4^{2-}.

66

This indicates that, even after a travel time of several days, the soot containing particles can retain much of their hydrophobic properties.

The deposition of BC on snow or ice reduces the surface albedo and enhances snow-melt, leading to radiative forcing of the climate at global and regional scales (Hansen and Nazarenko, 2004; Jacobson, 2004; Flanner *et al.*, 2007). Deposition of BC in Arctic snow has been reported by a number of studies (Clarke and Noone, 1985; Borys, 1989), and deposition over the Himalayas has been measured by Ming *et al.* (2008). A multi-model assessment of pollution transport to the Arctic has been presented by Shindell *et al.* (2008b). Based on the sensitivity simulations of 17 global models that participated in the HTAP report, the deposition of BC on Greenland is found to be most sensitive to North American and European emissions, with North America, Europe and East Asia contributing 40 per cent, 40 per cent and 20 per cent, respectively. Elsewhere in the Arctic, the total BC deposition is dominated by European emissions, although the HTAP report did not include emissions from Russia east of the Urals. Large differences between models have been found in the simulations of aerosols over the Arctic (Shindell *et al.*, 2008b), resulting primarily from differences in the physical and chemical processing of aerosols.

The deposition rate to snow surfaces is of particular importance as the optical properties of the snowpack are strongly influenced by the presence of BC, with substantial reductions in the albedo with increasing BC concentrations, as shown in Figure 3.7 from the work of Ming *et al.* (2009).

3.3 Radiative forcing by BC and OC

The global mean forcing at the top-of-the-atmosphere (TOA), or the tropopause, typically provides a good indication of the global mean surface temperature response (see Box 1.1). Forcing at the surface may be quite different, however, and the difference between the surface forcing and the forcing aloft provides an indication of the heating of the atmosphere. Both absorbing and scattering aerosols lead
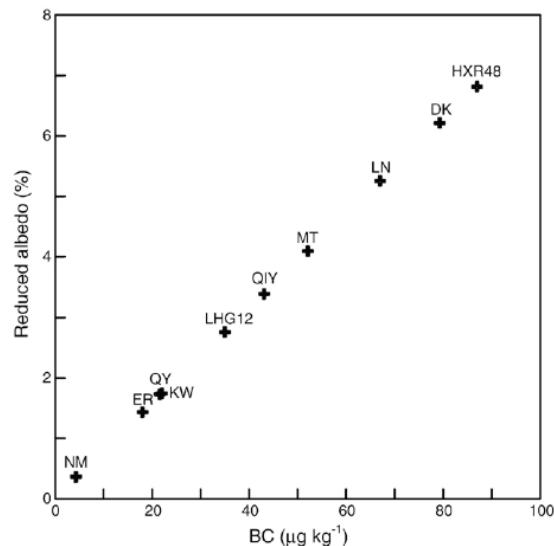
Figure 3.7. The effect of BC on the albedo of Asian glaciers (Ming *et al.*, 2009).

to a reduction of solar radiation at the surface known as negative surface forcing (also referred to as dimming), whereas only absorbing aerosols lead to heating of the atmosphere or positive atmospheric forcing. The atmospheric and the surface forcing may be more useful indicators of changes in winds and precipitation (Ramanathan *et al.*, 2001). Focus here is on TOA forcing, as the link between this and surface temperature response has been most clearly established. For BC, the magnitudes of the atmospheric and surface forcing are typically factors of 2 to 4 larger than the TOA forcing (Ramanathan *et al.*, 2001; Forster *et al.*, 2007) which has implications for regional climate changes due to BC. Furthermore, it is noted that, particularly in the case of BC, the relationship between forcing and response is not as simple as it is for well-mixed compounds such as CO_2. In particular, the direct and indirect response per unit forcing (efficacy) appears to be smaller than for CO_2, and is strongly dependent on the altitude at which the BC is located (Highwood and Kinnersley, 2006; Hansen *et al.*, 2005). These issues are discussed further in Chapter 4.

The direct effects of aerosols on solar and terrestrial radiation depends strongly on their chemical composition, as BC and a portion of the SOA called brown carbon (BrC) absorb radiation and heat the atmo-

sphere, while the remaining components scatter radiation and cool the atmosphere. The scattering components of aerosols on a mass basis contribute the largest fraction. The degree of internal or external mixing of BC with scattering components eventually determines aerosol absorption (Jacobson, 2000; Seland *et al.*, 2008; Moffet and Prather, 2009). Figure 3.8 shows the contribution of various aerosol species to the aerosol optical depth (AOD) over India, i.e. the extinction of sunlight due to absorption and scattering by aerosols in a vertical column of the atmosphere.

The indirect effects of aerosol particles on climate through their effects on clouds are also influenced by their chemical composition, as that determines the solubility of the particles and their ability to act as cloud condensation nuclei (Isaksen *et al.*, 2009; Granat *et al.*, 2010). Observations have shown that the size of a particle is more important than its chemical composition (Dusek *et al.*, 2006; Chen *et al.*, 2010a).

3.3.1 Anthropogenic fraction of forcing

The pre-industrial level of BC and OC forcing is not well known but relates directly to the evolution of different source categories.

Contribution to Aerosol Optical Depth
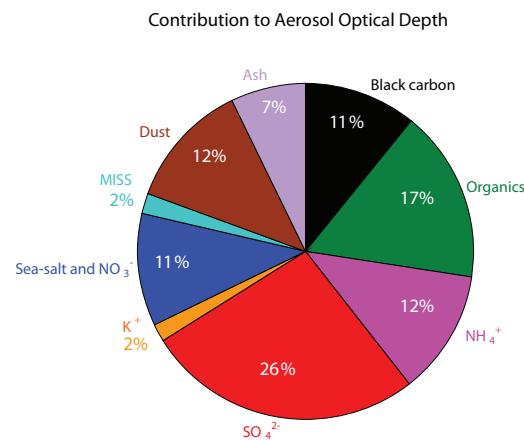
Figure 3.8. Contributions of different chemical species to aerosol optical depth over the North Indian Ocean based on data collected during the Indian Ocean Experiment from January to March 1999. At this time of year the North Indian Ocean is subject to northeasterly flow from South Asia, so the pie chart reflects aged aerosols transported from South Asia (Ramanathan *et al.*, 2001).

Recent emission inventories as summarized in Chapter 2 report a three- to sixfold increase in BC emissions between 1875 and 2000, indicating that pre-industrial (1875) emissions were ~10 to 25 per cent of present-day emissions.

3.3.2 Direct radiative forcing at TOA of BC

Black carbon is a strongly absorbing aerosol component (which is why it is black). The forcing it exerts by absorbing sunlight is referred to as direct radiative forcing, and is positive (i.e. warming). Global-scale studies, with a few exceptions that are noted below, are largely from models that use emissions as input and then include the physical, chemical and transport processes described above (for a recent review of such model studies, see Schulz *et al.*, 2006, and Forster *et al.*, 2007). Models include limited representations of the full complexity of aerosol properties and processing in the atmosphere, especially as regards mixing between different types of aerosols and interactions between aerosols and clouds (Vignati *et al.*, 2010b).

Models are evaluated against observations, but observations of radiative forcing do not exist on global scales. Field experiments such as the Indian Ocean Experiment (INDOEX) (Ramanathan *et al.*, 2001) and measurements with multiple unmanned aircraft vehicles have directly measured the surface, atmospheric and TOA forcing (using CERES satellite data) for BC and other aerosols from South Asia and East Asian aerosols over the Yellow Sea. Field measurements and models have also been used to quantify radiative impacts of aerosols in the Arctic (Stone *et al.*, 2008). An independent approach to that of the bottom-up approaches of global climate models (GCMs) is the semi-empirical approach which constrains as well as nudges the simulated values of column-integrated AODs and other aerosol optical properties with observations on local to global scales (Chung *et al.*, 2005a). Such an approach is made plausible by the availability of numerous datasets for aerosols, both scattering and absorbing.

The semi-empirical approaches (Sato *et al.*, 2003; Chung *et al.*, 2005b; Ramanathan and Carmichael, 2008) estimate the present-day total forcing, but are not able to estimate the pre-industrial forcing due to lack of observations. Furthermore, the semi-empirical approach implicitly includes the now well known positive forcing by BrC (Andreae and Gelencsér, 2006).

Typically, the GCM anthropogenic forcing (of fossil fuel + biofuel + biomass-burning sources of BC) ranges from 0.2 to 0.6 W/m^2 (e.g. see Schulz *et al.*, 2006, Forster *et al.*, 2007 for summaries). The two semi-empirical studies report just the total present-day forcing, which ranges from 0.9 W/m^2 (Ramanathan and Carmichael, 2008) to 1 W/m^2 (Sato *et al.*, 2003). There is considerable uncertainty in the pre-industrial forcing, ranging from 0.05 to 0.08 W/m^2 (Chen *et al.*, 2010a; Lamarque *et al.*, 2010) to as high as 0.35 W/m^2 (Hansen *et al.*, 2005). Using the 0.05 to 0.4 W/m^2 range of pre-industrial forcing, which is fairly consistent with the ~10 to 25 per cent fraction of present-day emissions during the pre-industrial era, the range of semi-empirical estimates for the BC anthropogenic direct forcing is 0.5 to 0.9 W/m^2, overlapping the GCM range of 0.2 to 0.6 W/m^2. In summary, present studies support a range of 0.2 to 0.9 W/m^2 for the BC direct anthropogenic forcing. The central value is more difficult to estimate, given the large uncertainty in BC emissions (Bond, 2007; also see Chapter 2), aerosol mixing and the large uncertainties in semi-empirical approaches. This Assessment assumes that the direct forcing is most likely to be within the range 0.3 to 0.6 W/m^2.

3.3.3 Semi-direct radiative forcing at TOA of BC

Black carbon has additional effects that other aerosols do not. Due to its strong absorption of incoming sunlight, BC's presence in the atmosphere causes the region where it is located to warm. This affects the vertical temperature profile and therefore stability, which in turn modifies cloud formation, both at that altitude and elsewhere in the column. The warming and increased stability of the bound-ary layer can decrease the relative humidity of the boundary layer and evaporate low clouds (Ackerman *et al.*, 2000). These cloud responses to heating induced by aerosols are commonly referred to as the semi-direct effect (Hansen *et al.*, 1997). Depending on the vertical location of aerosols with respect to clouds, in some cases cloud cover can increase rather than decrease. Absorption by BC inclusions within cloud drops increases cloud heating significantly when BC is treated as distributed inclusions as shown by Jacobson (2006). A recent review finds that the semi-direct effect is probably a substantial negative forcing (Koch and Del Genio, 2010). Consistent with this, several studies find that the efficacy (the surface temperature response to a given amount of radiative forcing) of BC is reduced relative to that of CO_2 by ~20 to 30 per cent, suggesting that the semi-direct forcing offsets the direct forcing by 20 to 30 per cent (Hansen *et al.*, 2005; Roberts and Jones 2004; Jones *et al.*, 2007; Chung and Seinfeld 2005), though one study finds an efficacy that is ~30 per cent greater (Sokolov, 2006). Another recent review (Isaksen *et al.*, 2009) reports a range of -0.25 to 0.50 W/m^2 for the semi-direct forcing, with no best estimate provided.

3.3.4 Indirect forcing at TOA of BC

Aerosols also affect the formation of clouds as they contribute to the concentrations of cloud condensation nuclei, which affect both cloud cover and lifetime (Oshima *et al.*, 2009; Chen *et al.*, 2010a; Jacobson 2010). They may also act as ice nuclei and therefore change ice or mixed-phase clouds (Liu *et al.*, 2007, 2009). These so-called 'indirect radiative forcing' effects are more difficult to quantify. Chen *et al.* (2010b) examined the net effect (direct and indirect) of co-emitted BC and OC and reported a net cooling (-0.31±0.33 W/m^2 for 50 per cent reduction in all BC and OC emissions). The Chen *et al.* (2010b) study did not include the semi-direct effects of BC. Bauer *et al.*, (2010) calculated the sum of indirect and semi-direct effects, and also reported a cooling effect for BC emissions (-0.12 W/m^2 for a 50 per cent emissions reduction), in their case ~80 per cent as large as the direct forcing. Their model includes changes in other

69

aerosols that mix with BC. Jacobson's (2010) model study on the other hand did not show such large offsetting of the direct forcing by BC indirect and semi-direct effects, although forcing was not diagnosed.

Studies of the effect of BC aerosols on mixed-phase or ice clouds are even fewer. One study suggested a strong negative forcing for ice clouds of -0.3 to -0.4 W/m^2 (Penner *et al.*, 2009), while another study found a positive forcing of about 0.2 to 0.4 W/m^2 (Liu *et al.*, 2007). A study of ice nucleation in mixed-phase clouds finds a forcing of 0.12 to 0.20 W/m^2 (Lohmann and Hoose 2009). Indeed a recent review found the effect of all aerosols on mixed-phase clouds to be from -0.5 to +0.5 W/m^2, with no best estimate (Isaksen *et al.*, 2009).

Observational data have been used to examine the relative impacts of semi-direct and indirect effects (Kaufman and Koren, 2006). These studies mainly focus on the Amazon, where aerosols from biomass-burning are the predominant species. Most GCMs conclude that such aerosols exert a large cooling effect (due to both the direct and the indirect forcing). Many of the observational studies, however, indicate otherwise. For example, for AODs larger than 0.2 (typical of Amazonian and other polluted regions such as South and East Asia, Africa, Europe and North and South America), the positive forcing from the semi-direct forcing exceeds the indirect forcing. This finding is also supported by studies examining the long-term (30 to 50 years) dimming trends in China and Europe (Ruckstuhl and Norris, 2009; Qian *et al.*, 2006; Norris and Wild, 2007; Ruckstuhl *et al.*, 2010). Both Europe and China witnessed decreases in surface solar radiation of about 5 per cent to more than 10 per cent during the period when their emissions of BC and sulphates increased by factors ranging from 2 to 5, but the decreases in surface solar radiation were mostly explained by corresponding decreases in clear sky solar radiation with very little change in the cloudy sky solar radiation. These studies (e.g. Ruckstuhl *et al.*, 2010) concluded that

the indirect effect had a negligible role in governing the dimming. Brioude *et al.* (2009), however, found a cooling semi-direct effect using satellite data in their analysis. Globally, however, it is very difficult to attribute cloud changes to aerosols in the complex real-world atmosphere with limited observations. Based on extant studies, this Assessment adopts a range for combined semi-direct and indirect effects of -0.4 to +0.4 W/m^2 as encompassing many of the estimates discussed above (assuming the semi-direct effect, warm cloud indirect effects and ice/mixed-phase cloud effects are independent sources of uncertainty).

3.3.5 Forcing from BC deposition

When BC falls on snow or ice surfaces, it can reduce their reflectivity, leading to a positive forcing often referred to as the BC-albedo forcing as described by Jacobson (2001). The estimated range is 0.01 to 0.08 W/m^2, with a mean value of 0.03 W/m^2. Studies examining the climate response to BC forcing by altered snow or ice albedo have found that the forcing is not, however, a good indicator of the eventual temperature changes. Instead, temperature changes tend to be substantially larger than the forcings might suggest (see Chapter 4). Hence this Assessment has adopted an effective forcing that is indicative of the climate response reported in model simulations (Koch *et al.*, 2009a; Flanner *et al.*, 2007, 2009) by increasing the forcing by an efficacy of five to provide a value of 0.15±0.10 W/m^2 as the effective forcing.

3.3.6 Radiative forcing at TOA of OC

OC has important optical properties respon-sible for a significant scattering of solar radia-tion, but can also have a small absorption (Andreae and Gelencsér, 2006; Chakrabarty *et al.*, 2010). This is sometimes called BrC – a light-absorbing carbon which is not black. Anthropogenic OC radiative forcings (pres-ent day – pre-industrial) at TOA estimated by global models is -0.19 ±0.20 W/m^2 (Schulz *et al.*, 2006; Forster *et al.*, 2007). The cen-tral values are encompassed by a range of -0.19 ±0.11 W/m^2, which is roughly the

standard deviation of the results and which encompasses all but the single highest and two (equal) lowest forcing values of the 18 assessed by Schulz *et al.* (2006). Many models may be overestimating the organic cooling, since they ignore absorption by BrC (Andreae and Gelencsér, 2006). OC may also exert a radiative forcing via indirect effects on clouds, but such effects have not been quantified. Climate forcing seems to be very sensitive to SOA, both natural and anthropogenic (Kanakidou *et al.*, 2005). The coating of BC by SOA can change the aerosol optical properties through changes in the single scattering albedo and the absorption cross-section of the soot particles.

3.3.7 Total anthropogenic forcing from BC and OC

The total forcing is the sum of the above components, and is the driver of changes in climate. While climate responses are discussed primarily in Chapter 4, it is noted that some models do not specifically diagnose radiative forcing but evaluate climate response. For example, Jacobson (2010), in one of the few model studies that include the direct, semi-direct and indirect effects as well as the solar absorption by BrC, the absorption by inclusion of BC in ice-clouds and the greenhouse effects of EC and OC, reported a temperature change from fossil fuel BC plus OC of 0.3 to 0.5°C at equilibrium, implying an imposed forcing of ~0.4 to 0.6 W/m². The result is consistent with a mean value of 0.4 W/m^{-2}, the sum of BC mean value (0.6 W/m^{-2}) and that of OC (-0.19 W/m^{-2}) as recommended in this study (Table 3.1). Obtaining values for the pre-industrial to present-day total aerosol forcing from all aerosols are available from several sources. Analyses of the Earth's radiation budget provide an estimate of -1.1 ±0.4 W/m² for the total forcing (direct and indirect) of present-day aerosols (Murphy *et al.*, 2009). Analysis of the spatial and temporal patterns of observed temperature changes and attribution of the regional forcing attributable to well-mixed greenhouse gases has led to an estimate of total aerosol forcing of -1.3±0.5 W/m² (Shindell and Faluvegi, 2009). These estimates include all aerosol effects (direct, indirect and semi-direct). Analyses of satellite data in conjunction with models has led to an estimate of the total direct forcing from aerosols of -0.35 W/m² (90 per cent range of 0.1 to 0.6 W/m²) by Chung *et al.* (2005b). More recent estimates, again using satellite data, have similar or larger negative direct aerosol forcing, including -0.3±0.2 W/m² (Myhre, 2009), -0.65 W/m² (Bellouin *et al.*, 2008) and -0.9±0.4 W/m² (Quaas *et al.*, 2008). Estimates of the total indirect effect of aerosols on clouds are from -0.3 to -2.9 W/m², centred at about -1.25 W/m² from a variety of modelling and observational studies (e.g. Isaksen *et al.*, 2009).

A summary of the BC forcings discussed is are presented in Table 3.1, which provides the range of values discussed as well as a smaller, more plausible range of central values based on the expert judgement of the assessment authors. Given the constraints on the total aerosol impact to be a strong negative forcing, it is difficult to reconcile a very large positive forcing from BC with this total negative forcing. Not all processes have been included, as some are very poorly known and/or have not been quantified. Additionally, aerosol-cloud interactions, which contribute the bulk of the uncertainty, have recently been suggested by several studies using satellite data to be smaller than many earlier estimates (see, for example, Isaksen *et al.*, 2009). This Assessment concluded that even though the sum of the effective forcing using the central values in the preceding sections is 0.0 to 1.3 W/m², the total effective forcing from all BC effects is unlikely to be greater than 1 W/m².

3.3.8 Regional present-day BC forcing at TOA, at the surface and in the atmosphere

BC radiative forcing is concentrated regionally (Figure 3.9). Semi-empirical approaches to estimate regional radiative forcing (see Appendix A.3), have provided observationally constrained direct radiative forcing estimates for BC. By absorbing solar radiation, BC keeps energy within the atmosphere that would otherwise have reached the surface. While the TOA forcing is a small difference between the positive atmospheric and the neg-

Table 3.1. Summary of anthropogenic BC forcings (see text for details).

Forcing	Range (W/m²)	Central values (W/m²)	Mean value (W/m²)
Direct	0.2 to 0.9	0.3 to 0.6	0.45
Semi-direct and indirect	-0.6 to 0.5	-0.4 to 0.4	0.0
Deposition	(0.01 to 0.08) corrected for efficacy (x5) 0.05 to 0.4	(0.01 to 0.05) 0.05 to 0.25	0.03 0.15
Total BC	-0.3 to 1.8	0.0 to 1.3 0.0 to 1.0 with constraints on total aerosol forcing	0.5 0.6 including efficacy of deposition
OC direct	0.01 to -0.39	-0.08 to -0.30	-0.19

Note: The mean value and central values are used in calculations of temperature response (Chapters 4 and 5).

ative surface forcing, it influences global mean changes in temperature and circulation, and regional changes in precipitation and climate. Elevated regions such as the Himalayas, are more influenced by the magnitudes and spatial gradients of the atmospheric and surface forcing. Hence, we show the atmospheric and surface forcing of BC separately (Figure 3.9). The sum of the two is the TOA forcing.

Over the Amazon region, the savannah-burning regions of Africa (south of the Equator), South Asia and East Asia, BC adds more than 10 to 20 W/m² (atmospheric forcing) and reduces surface solar absorption (dimming) by a comparable magnitude. The two forcing terms are factors of 10 to 50 larger than the global averaged TOA BC forcing range of 0.2 to 0.9 W/m².

BC also introduces significant north-south asymmetry in radiative forcing over the tropical Atlantic and Indian Oceans and over Asia, Africa and South America. Several model studies (e.g, Ramanathan *et al.* (2005), Wang (2004) and others discussed in Chapter 4) have shown that such asymmetric heating patterns by BC and other aerosols have a large impact on regional circulation and precipitation patterns.

3.4 Ozone formation and transport in the atmosphere: concentrations and deposition

Unlike many other air pollutants, O_3 is not directly emitted. It is a secondary pollut-

Figure 3.9. Annual average present-day BC forcing. The top panel is the atmospheric forcing and the bottom panel is the surface forcing, alternately known as surface dimming. The sum of the two panels yields the TOA radiative forcing discussed in IPCC reports and elsewhere in this Assessment (Ramanathan and Carmichael, 2008).

ant that is formed in the troposphere by sunlight-driven chemical reactions involving CO, VOCs (including CH_4), and NO_x as shown schematically in Figure 3.10. These precursors arise from both natural sources and a broad range of human activities. The breadth of sources of O_3 precursors, the role of natural and physical processes in O_3 distribution, production and destruction, and complex chemistry, mean that control of O_3 is not straightforward. The only practical management strategy is to control the emissions from human activities that lead to O_3 formation.
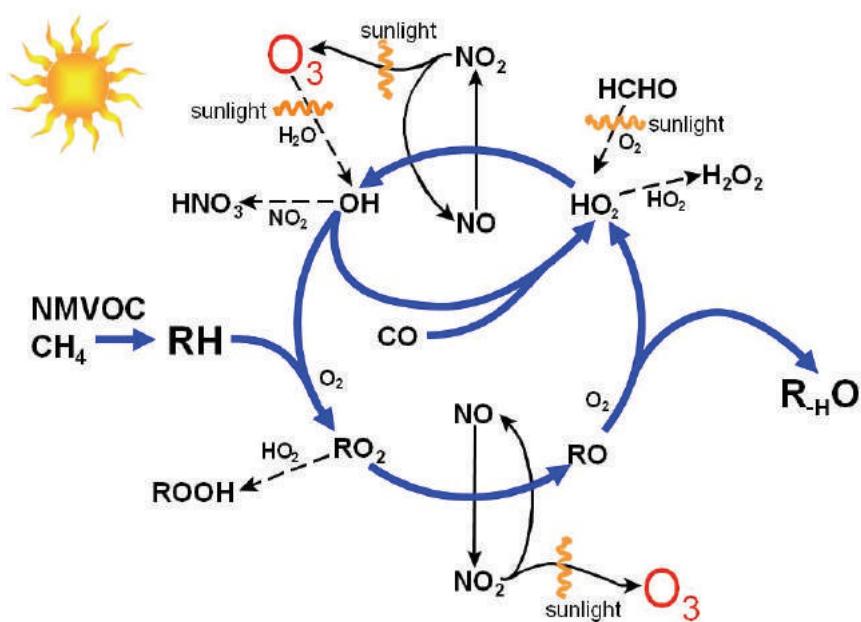
Figure 3.10. Ozone production through the photochemical degradation of methane (CH_4) and non-methane volatile organic compounds (NMVOCs) and carbon monoxide (CO) in the presence of nitrogen oxides (NO_X). (Source: courtesy of David Fowler).

Sources of tropospheric O_3 are (1) influx from the stratosphere and (2) generation by photochemical reactions in the troposphere. Removal of O_3 is by chemical processes in the atmosphere and by deposition at the surface.

The influx of O_3 from the stratosphere takes place mainly at middle and high latitudes and is most active in early spring. The precursors of tropospheric O_3 are emitted by major anthropogenic sources such as industry, motor vehicle exhausts, gasoline vapours, and chemical solvents, and also by natural sources with NMVOC emissions from vegetation (including isoprene and a wide range of terpenoids) and nitric oxide (NO) from soil, as discussed in Chapter 2.

The residence time of O_3 in the atmosphere varies from approximately a day in the boundary layer to a few weeks in the upper troposphere. High O_3 days (>60 ppb) are characterized by more intense solar radiation, higher temperature and lighter surface wind, all of which are favourable for photochemical production and the build up of O_3 (e.g. Permadi and Oanh, 2008).

The relationship between O_3 and precursor concentration is not linear. For example, in one situation O_3 increases if VOC increases, and in another the opposite is observed. The VOC-sensitive regime refers to situations in which a given percentage reduction in VOC emissions would result in a significantly greater O_3 decrease than that caused by the same reduction in NO_x (regime III in Figure 3.11). The NO_x-sensitive regime (II in Figure 3.11) refers to the opposite situation. This greatly complicates the formulation of policies to mitigate ground-level O_3 pollution. Chemistry-transport models provide the tools to investigate the relationships between O_3 precursor emissions and spatial and temporal concentrations and O_3 doses that are potentially damaging to the human population and ecosystems.

In the industrialized countries, emission controls have been reasonably effective at reducing the magnitude of peak O_3 concentrations and reflect decades of efforts aimed at identifying and managing the main polluting sectors and adopting technologies to reduce emissions. Such controls have reduced the magnitude and frequency of O_3 episodes in these countries with substantial benefits for local and regional populations and ecosystems. However, these regional policies have not

73
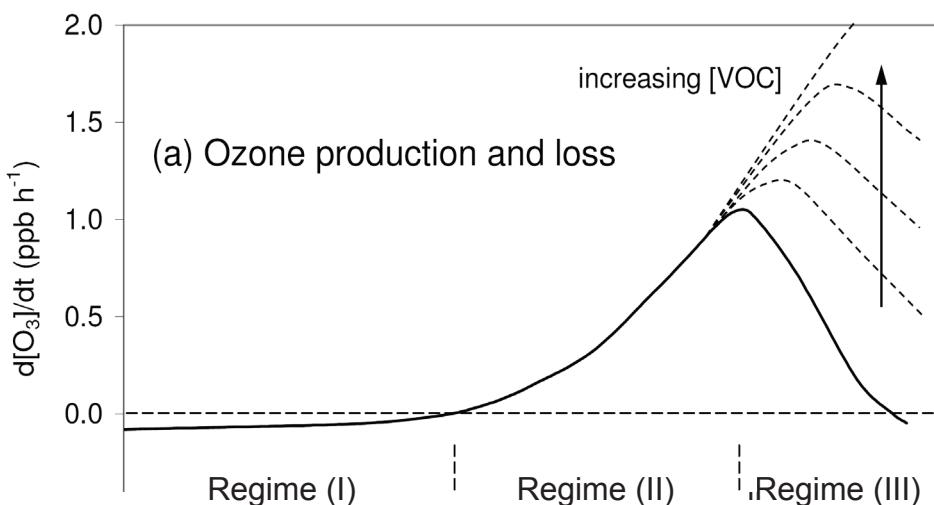
Figure 3.11. The dependence of ozone production rates on ambient NO_x concentrations (Royal Society, 2008).

been effective at controlling the background concentration of O_3, which has increased at about 2 ppb per decade in the mid-latitude northern hemisphere. This is because O_3 and its precursors can travel long distances. Ozone is therefore a hemispheric-scale problem.

The largest concentrations of tropospheric O_3 are found in the mid-latitude northern hemisphere, where O_3 precursor emissions are also largest. The present-day distribution of O_3 is shown in Figure 3.12. High levels of near-surface O_3 are not restricted to the high population centres, rather O_3 is seen to be enhanced throughout the northern hemisphere. Tropical areas where biomass-burning emissions are a major source of NO_x and tropical forests are a major source of NMVOCs also experience large O_3 concentrations, as shown in Figure 3.12. The increase in O_3 concentrations since the Industrial Revolution are also clear in these global maps, which show that in large areas of the world O_3 concentrations have more than doubled since pre-industrial times. Also shown is the percentage of surface O_3 due to anthropogenic activity (bottom right panel), which for the majority of the land area and especially in the northern hemisphere is between 30 and 50 per cent.

The pre-industrial to present-day differences do not reveal much more about recent trends in O_3 exposure. In North America and Europe, control measures on NMVOCs

and NO_x emissions have reduced peak O_3 concentrations. The magnitude and timing of the control measures vary regionally, but the majority of the control has been in the last 20 years, and as a result peak O_3 concentrations have declined by between 20 and 40 per cent in large areas (Jenkin, 2008). However, during the same period, background O_3 concentrations have increased at rates in the range 0.1 to 0.3 ppb per year (Jenkin, 2008).

Measured trends in surface O_3 show increases over Europe that are observed most clearly at remote Global Atmosphere Watch (GAW) Global stations on mountain-top locations such as Zugspitze in southern Germany (Figure 3.13) and at coastal locations such as Mace Head on the west coast of Ireland (Jenkin, 2008). Even in remote GAW marine sites such as Mauna Loa on Hawaii, an increase in background O_3 has been observed. Models capture observed behaviour relatively well, but underestimate increases over Europe. Ozone present throughout the free troposphere is transported over long distances due to its relatively long atmospheric lifetime in the mid-troposphere, remote from the efficient removal by dry deposition to the surface for O_3 in the boundary layer. Thus the O_3 advected from polluted regions contributes to the hemispheric background and is the cause of the steady rise in background O_3. In polluted regions, photochemical production readily generates concentrations in
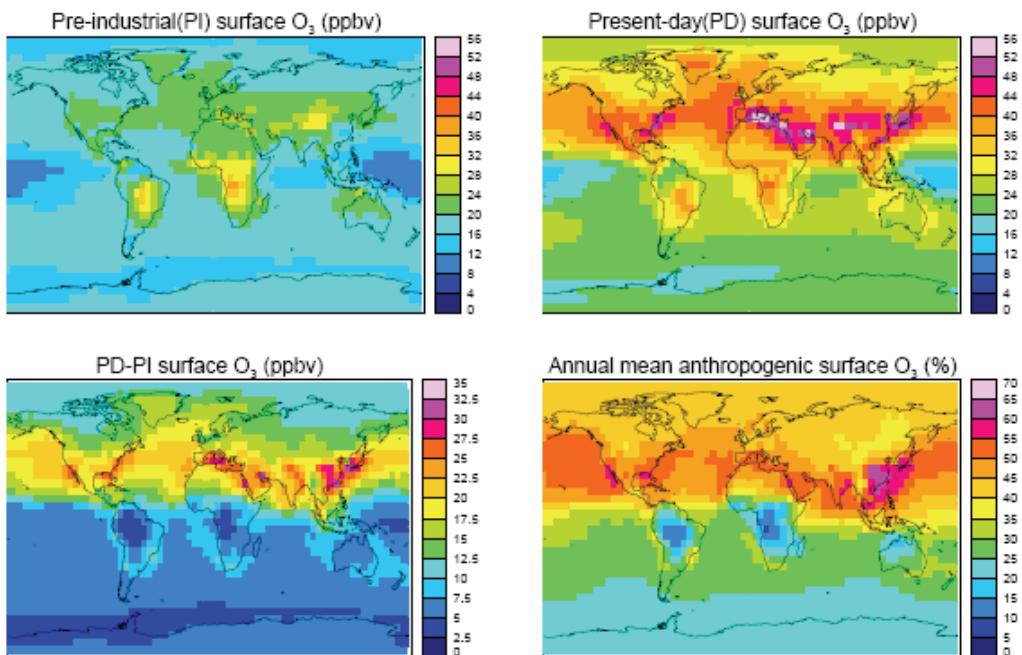
Figure 3.12. Multi-model annual mean surface ozone (ppb) from five models (TM4, FRSGC, UMCam, STOCHEM-HadGEM and STOCHEM-HadAM3). Top panels show ozone in the pre-industrial (PI) (left) and year 2000 (PD) (right). Lower left panel shows the change in ozone (PD-PI). Lower right panel shows the percentage of present-day ozone that is anthropogenic. NB In these simulations biomass burning emissions are not considered anthropogenic, and present-day values are used in both PI and PD. Full details of the simulations are given in Royal Society (2008). (Source : Royal Society (2008) with data courtesy of Twan van Noije, Oliver Wild, Guang Zeng, Michael Sanderson and David Stevenson).

the range 60 to 150 ppb in the boundary layer, but these large concentrations decline rapidly at night as photochemical production stops and the deposition and dispersion processes continue.

The multi-model HTAP study found that the effect of intercontinental transport of O_3 on local O_3 pollution is important. The RAIR values for O_3 varied from 30 to 40 per cent for the continents of the northern hemisphere. The RAIR values for the column amounts (important from the climate-forcing perspective) of O_3 are larger and varied from 40 to 60 per cent (HTAP). Furthermore, the intercontinental contributions to annual O_3 concentrations were found to be most strongly influenced by changes in CH_4, followed by NO_x, VOCs, and CO. A drop in anthropogenic CH_4 emissions in a given region was shown to produce roughly the same decrease in intercontinental transport of O_3 to other regions as a similar percentage decrease in NO_x, VOCs, and CO emissions combined. The O_3 response to changes in CH_4 emissions, however, re-

quires several decades to be fully realized, given the 12-year average lifetime of CH_4. The contribution to increases in background O_3 are therefore dominated by CH_4 (~50 per cent), with smaller contributions from the other VOC species and CO.

3.5 Radiative forcing from ozone and its precursor emissions

The radiative forcing resulting from changes in tropospheric O_3 between 1750 and 2000 due to anthropogenic emissions of precursors is assessed as contributing 0.25 to 0.65 W/m² (5 to 95 per cent), with a median value of 0.35 W/m², in the IPCC's Fourth Assessment Report (Forster *et al.*, 2007). This is an entirely model-based result (Gauss *et al.*, 2006), since only a few measurements of pre-industrial O_3 are available. The uncertainty in most model estimates is largely driven by the different sensitivities of the different models to changes in O_3 precursors, though the high-end modelled forcing values (~0.45 to 0.65 W/m²) are based on different estimates of pre-industrial emissions, and on only a single study (Mickley *et al.*, 2001).

75
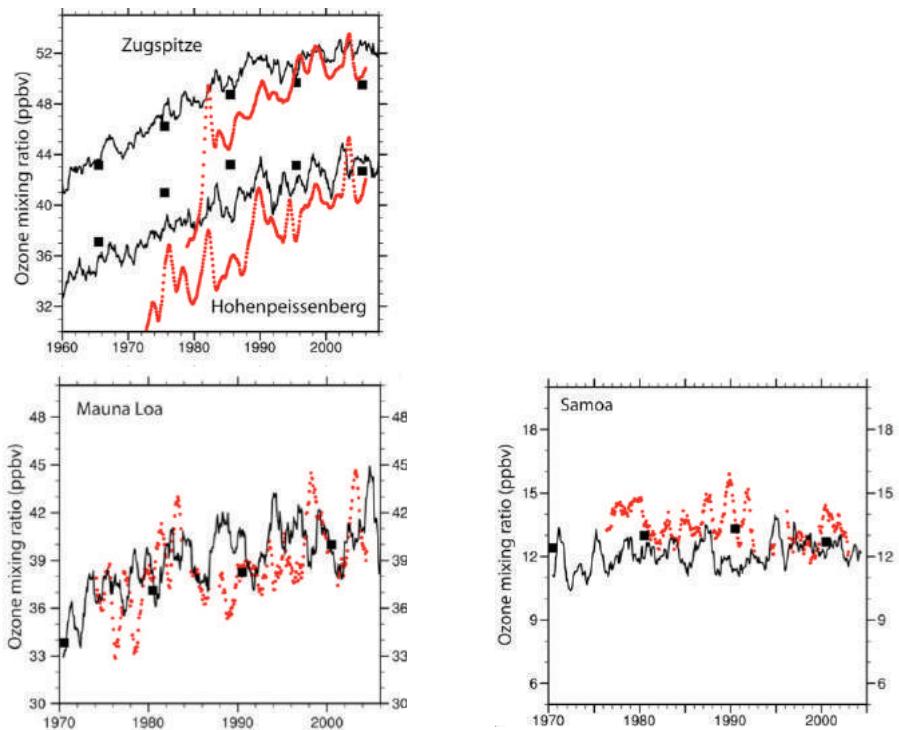
Figure 3.13. Ozone trends in observations (red) and in two global chemical models (black lines and boxes) (Lamarque *et al.*, 2010).

A global network of surface monitoring stations is available for comparison with global chemistry transport model concentration fields. In general these data show good agreement with modelled fields (Stevenson *et al.*, 2006). However, the very limited observational data available for the pre-industrial era suggest that, if anything, the models underestimate changes between pre-industrial and present times. Recently, satellite data have become available to constrain the total forcing from tropospheric O_3 (it is not possible to isolate the anthropogenic component), and indicate that models capture this forcing relatively well. Those results suggest that the total present-day O_3 forcing is in the 0.4 to 0.5 W/m² range, inconsistent with the larger anthropogenic values. Hence this Assessment adopts a central estimate of 0.35±0.10 W/m². It is also important to note that O_3 forcing is much larger in the northern hemisphere (Fishman *et al.*, 1979).

Ozone also has an indirect warming effect on climate by inhibiting the natural uptake of CO_2 by ecosystems (Sitch *et al.*, 2007; Collins *et al.*, 2010). This effect is very uncertain,

but may have led to a doubling of the climate forcing attributable to O_3 since pre-industrial times. This is explored in more detail in Section 4.6. By considering the O_3 damage, and making a crude estimate of the nitrogen fertilization, Collins *et al.* (2010) found that NO_x emissions could slightly warm climate on timescales of 20-year or less.

As O_3 is not directly emitted but formed by chemical reactions of its precursor species (NO_x, CO, VOCs and CH_4), O_3 forcing can in theory be attributed to these precursor emissions. This introduces additional considerations since these precursors do not simply affect the concentration of tropospheric O_3, but also the concentrations of other climate-forcing species. The species most affected are CH_4, and SO_4^{2-} and NO_3^- aerosols. Carbon monoxide, VOC and CH_4 emissions decrease the oxidizing capacity of the atmosphere, hence increasing the CH_4 lifetime and decreasing the rate of SO_4^{2-} formation. Conversely, NO_x emissions increase the oxidizing capacity, hence decreasing the CH_4 lifetime and increasing the rate of SO_4^{2-} formation. An additional effect of NO_x is to increase the

formation of NO_3^- aerosol; CH_4 also increases the concentration of water in the lower stratosphere (Forster *et al.*, 2007) and produces CO_2. The non-O_3 effects offset the O_3 warming for NO_x emissions and add to the warming for the other emissions. Shindell *et al.* (2009) calculated the impact of all these terms on the radiative forcing from pre-industrial times to 2000 (Figure 3.14).

The largest driver of O_3 forcing comes from CH_4 emissions, since CH_4 is an O_3 precursor. Methane emissions also affect the lifetime of methane itself over many years, inducing additional ozone changes. This effect is smaller than the direct production of O_3, but since CH_4 has a much longer lifetime than O_3 (~12 years), the impacts are longer lasting and are often termed the 'long-term ozone response'. For the other O_3 precursors their strongest climate forcing does not come from increasing O_3, but from their effects on CH_4 or aerosols. Shindell *et al.* (2009) found that although NO_x emissions produce O_3, their climate impact is a strong net cooling. It should be noted that the aerosol impacts are particularly uncertain and are only presented from one model.

The values presented so far have been for globally and annually averaged emissions. The forcing from O_3 precursors is expected to vary significantly with season and with emission region (Naik *et al.*, 2005). Typically, NO_x emissions have less O_3 production efficiency in high NO_x (polluted) conditions, and higher efficiency in low NO_x (clean) conditions as described above. The converse is true for CO and VOCs. The impact on CH_4 lifetime is strongest for O_3 precursor emissions in the tropical boundary layer. The O_3 response is largest for emissions at the time of highest photochemical activity (in the summer).

The strict definition of a radiative forcing is the change in forcing between pre-industrial conditions and a specified time horizon. This is not therefore a measure of the future impact of an increase or reduction in emissions. The different O_3 forcings act on different timescales. The direct O_3 response and aerosol responses act rapidly (order of weeks), the effects via CH_4 act on decadal timescales, and effects via the carbon cycle act on the timescale of the response of the terrestrial ecosystems (typically a few decades) (Collins *et al.*, 2010).
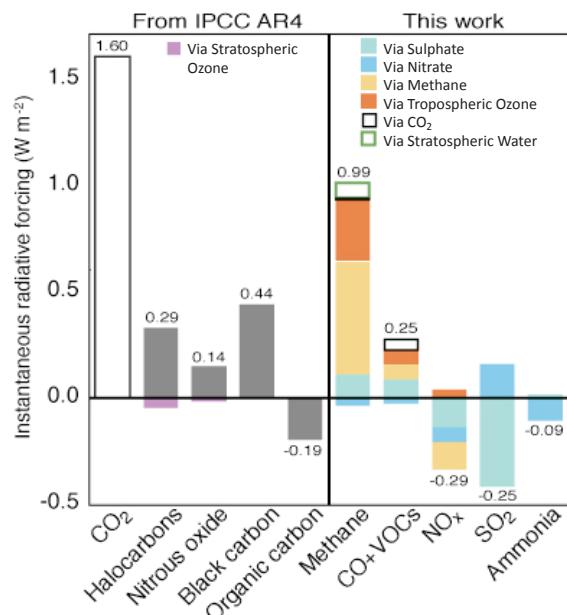
Figure 3.14. Global mean pre-industrial to present-day RF by emitted species from AR4 and Shindell *et al.*, 2009. Numerical values next to each bar give total forcing summed over all the effects included in the calculations. Aerosol indirect effects are not included, nor are interactions with ecosystems.

3.6 Reference trends over the coming decades

Due to variations in atmospheric conditions that regulate many processes such as residence times, background composition and available sunlight, emissions from different locations cause different amounts of radiative forcing. The timing of emissions can also affect the impact of BC and tropospheric O_3. This is unlike the situation for CO_2, which has such a long lifetime that it becomes well mixed in the atmosphere, so emissions from any location are basically equivalent in their impacts. As an example, the relative impact on global mean radiative forcing of BC emissions from different areas have been calculated in Rypdal *et al.* (2009), and other results have been summarized in Fuglestvedt *et al.* (2010). The studies generally show higher forcing per unit emission for emissions from South Asia and to a lesser extent South America, somewhat higher values for emissions from Africa in many models, and typically lesser values for emissions from East Asia, Europe and North America. Variations are roughly a factor of two from highest to lowest. For SO_4^{2-}, the response to a change in emissions in North America was roughly twice the magnitude of the response to emissions from South and East Asia (Shindell *et al.*, 2008a), indicating that regional variations again appear to be substantial. NO_x emissions generally have a larger effect on global mean forcing when they are closer to the equator than further away, or at higher altitudes. One study (Berntsen *et al.*, 2005), for example, showed that NO_x emissions from Asia had substantially larger impacts on global mean radiative forcing than emissions from Europe (and opposing sign). This is due to higher photolysis rates at lower latitudes leading to more hydroxide (OH^-) and, along with warmer temperatures, greater CH_4 oxidation so that the indirect CH_4 response is much larger at lower latitudes. In another study (Derwent *et al.*, 2001), a threefold greater impact of NO_x emissions was found for the southern hemisphere than the northern hemisphere. This is probably because most southern hemisphere emissions are at lower latitudes than northern hemisphere

emissions. For CH_4, and to a lesser extent CO, the location of emissions is less important in determining the resulting forcing.

It is also important to realize that the forcing due to a particular compound alone is often not useful. For example, BC is produced by incomplete combustion that nearly always also produces OC, whose climate impact can offset a portion of or even outweigh the effects of the BC. The exception is CH_4, whose sources are often distinct. Several studies have examined the net impact of the full range of pollutants emitted by particular activities (e.g. Fuglestvedt *et al.*, 2008; Shindell *et al.*, 2008c; Unger *et al.*, 2010). Such work has usually examined the impact of all current emissions, thus providing some indication of the impact of efficiency improvements to reduce overall usage. Prior work has not, however, quantified the impact of any plausible emissions changes, as this requires detailed analysis of the potential for emissions mitigation across regions and across the activities that lead to emissions. Hence the net impact of practical measures that could be taken to reduce the emissions of short-lived climate forcing agents during the next decades has not been available to policy makers.

To provide such information, new studies were carried out in support of this Assessment. The framework for these studies consists of several parts:

1. Reference emission projections and emission mitigation options were created for all climate forcing agents or precursors by activity and region around the world.

2. Global atmospheric composition-climate models (GISS-PUCCINI and ECHAM5-HAMMOZ) incorporating those emissions were used to calculate the resulting concentrations in the atmosphere, the climate forcing, and the surface pollutant concentrations.

3. Impact analyses then looked at the consequences of the climate and air quality changes.

Results for the reference emission projections are presented here for composition and forcing, and in Chapter 4 for impacts. Results for emissions mitigation scenarios are presented in Chapter 5.

Changes in surface $PM_{2.5}$ in 2030 under the reference scenario relative to 2005 show substantial decreases in concentrations over North America, Europe and East Asia (Figure 3.15a). In contrast, concentrations increase substantially over South Asia and parts of Central Africa. The two models used in this Assessment display spatial patterns of $PM_{2.5}$ changes in good agreement with one another in the broad sense. There are differences in the location of the maximum decrease over Europe between the two models (Northern Europe in GISS, Southern Europe in ECHAM) which may reflect the inclusion of nitrate (NO_3^-) aerosols in one model (GISS) but not the other. There are also differences in the magnitude of the reduction seen over East Asia in the models, and to a lesser extent in the magnitude of the increase over South Asia, with generally larger values in the ECHAM model. The two models thus help to characterize the range of uncertainty in the physical processes leading from emission changes to concentration changes.

The net radiative forcing at 2030 under the reference scenario relative to 2005 (Figure 3.15b) results from multiple, sometimes competing, effects. The broad spatial patterns of forcing are quite similar in the two models, with large positive forcings over North America and Europe and negative values over South Asia. In these regions, the forcing is predominantly driven by changes in SO_4^{2-} aerosols, which lead to strong positive forcing in eastern North America and western Europe and strong negative forcing over South Asia (there is also positive forcing over Europe, in particular from decreases in nitrate aerosols in the GISS model). Hence these forcings are something of a mirror image of the $PM_{2.5}$ changes.

Increases in BC over India are more than offset by increased SO_4^{2-} in both models. Over East Asia, the models exhibit larger differences, with a negative forcing in the GISS model, where decreases in BC outweigh decreases in SO_4^{2-} and other reflective aerosols and increases in O_3 and CH_4, and near neutral changes in the ECHAM model where these balance more closely. In the GISS model, the net forcing is the sum of offsetting influences of positive forcing caused by increased CH_4 (78 mW/m²) and O_3 (5 mW/m²) and decreased SO_4^{2-} (3 mW/m²) and weakly negative forcing caused by increased OC (-1 mW/m²) and NO_3^- (-2 mW/m²) and decreased BC (-1 mW/m²) (all values are global means). Radiative forcings in the ECHAM model are similar, with positive forcings from CH_4 (80 mW/m²) and O_3 (3 mW/m²) and a small net contribution from SO_4^{2-}+BC+OC (6 mW/m²; the GISS model has 2 mW/m² for this sum). Hence CH_4 is the largest component, with forcing from changes in O_3 and aerosols less than 10 per cent of the magnitude of the CH_4 forcing.

Changes in the deposition of BC at 2030 under the reference scenario relative to 2005 show patterns similar to those for surface $PM_{2.5}$ (Figure 3.16). In percentage terms, the largest decreases are seen over Europe and the Arctic in both models (25 to 50 per cent) while large increases are seen over South Asia and into the Tibetan Plateau (10 to 30 per cent). Again, the two models are generally consistent in the spatial pattern and magnitudes of BC deposition changes.

Atmospheric forcing, the difference between TOA or tropopause forcing and forcing at the surface, also shows strong regional patterns. Under the reference scenario, atmospheric forcing increases dramatically over South Asia and mildly over Africa, while decreasing over North America, Europe and East Asia in both models (Figure 3.17).
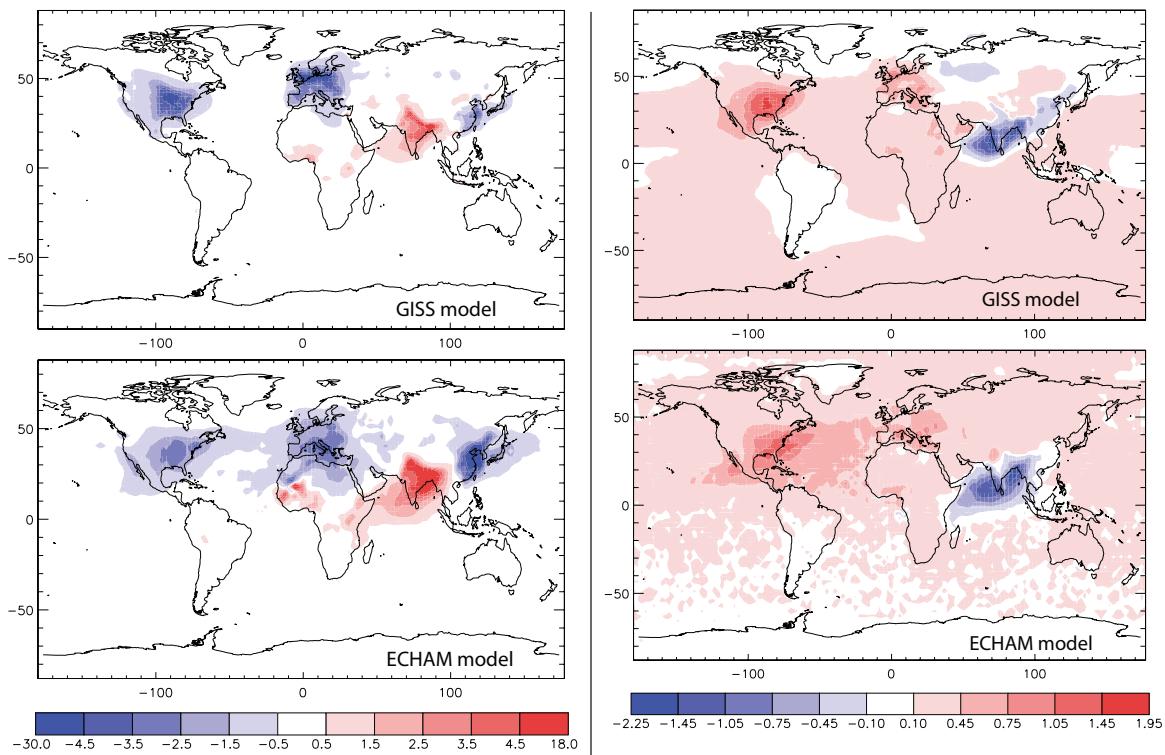
Figure 3.15a. Change in annual average PM$_{2.5}$ (µg/m^3), 2030 reference change relative to 2005.

Figure 3.15b. Radiative forcing (W/m^2) due to CH$_4$, O$_3$, and the direct effects of aerosols, 2030 reference change relative to 2005. Values are instantaneous at the tropopause (GISS) or TOA (ECHAM).
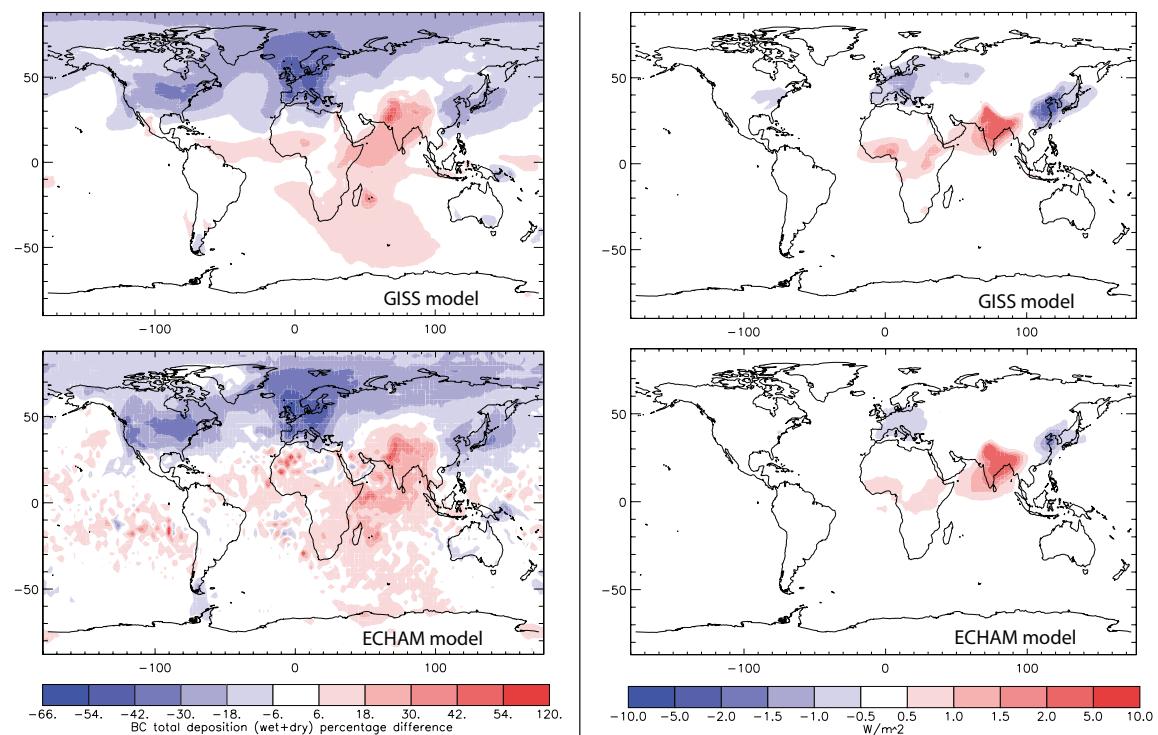
Figure 3.16. Change in annual average BC deposition (per cent), 2030 reference change relative to 2005.

Figure 3.17. Change in atmospheric forcing (TOA-surface forcing) due to aerosols, 2030 reference change relative to 2005.

80

Appendix A.3

A.3.1 Models used in this Assessment

Full three-dimensional modelling of processes going from emissions to concentrations and radiative forcing was carried out with two state-of-the-art composition-climate models. These models, one developed in Europe and one in the United States, have a long history of use in assessments such as those undertaken by the IPCC or national/regional bodies.

The GISS model for Physical Understanding of Composition-Climate INteractions and Impacts (GISS-PUCCINI) incorporates gas-phase (Shindell *et al.*, 2006), SO_4^{2-} (Koch *et al.*, 2006), BC (Koch and Hansen, 2005), NO_3^- (Bauer *et al.*, 2007) and secondary organic aerosol (Tsigaridis and Kanakidou, 2007) chemistry within the GISS ModelE general circulation model (Schmidt *et al.*, 2006). The chemistry scheme is quite similar to that documented previously, with the most notable additions being that acetone has been added to the hydrocarbons included in the model and a reaction pathway for $HO_2 + NO$ to yield HNO_3 has been added (Butkovskaya *et al.*, 2007). The scheme now includes 156 chemical reactions among 50 species. Evaluations of the present-day composition in the model against observations are generally quite reasonable (as documented in the references given above as well as in, for example, Koch *et al.*, 2009a and Aghedo *et al.*, 2011). The AOD and radiative forcing per unit burden change in this model have been discussed and compared with other models and available satellite observations previously (Shindell *et al.*, 2008a and b; Schulz *et al.*, 2006; Koch *et al.*, 2009a), with some additional evaluation for the current configuration in this Appendix.

For these simulations, the development version of the model near its 'frozen' state for IPPC's Fifth Assessment Report (AR5) simulations have been used. The model has a horizontal resolution of 2° latitude by 2.5° longitude, with increased effective resolution for tracers due to carrying higher order moments at each grid box. This configuration had 40 vertical hybrid sigma layers from the surface to 0.1 hectopascal (hPa). Tracer transport uses a non-diffusive quadratic upstream scheme (Prather, 1986). Prescribed ocean simulations were performed using observed 2000-era sea-surface temperatures (Rayner *et al.*, 2003), with most runs extended for 20 years.

ECHAM5-HAMMOZ is a fully coupled photochemistry-aerosol-climate model, composed of the general circulation model (GCM) ECHAM5, the tropospheric chemistry module MOZ, and the aerosol module HAM. The ECHAM5-HAMMOZ model is described in detail in Pozzoli *et al.* (2008a). ECHAM5 is a GCM developed at the Max Planck Institute for Meteorology (Roeckner *et al.*, 2003 and 2006; Hagemann *et al.*, 2006). In this study, a T42 resolution was used, corresponding to an Eulerian resolution of ca. 2.8° x 2.8° degrees, with 31 vertical levels from the surface up to 10 hPa and a time resolution for dynamics and chemistry of 20 minutes. The transport scheme is from Lin and Rood (1996). The radiative transfer calculation considers vertical profiles of the greenhouse gases (e.g., CO_2, O_3, CH_4) and aerosols, as well as the cloud water and ice.

The chemical scheme has been adopted from the MOZART-2 model (Horowitz *et al.*, 2003), and includes 63 transported tracers and 168 reactions to represent the NO_x-HO_X-hydrocarbons chemistry. The sulphur chemistry described by Feichter *et al.* (1996) includes oxidation of SO_2 by OH^- and dimethyl sulphide (DMS) oxidation by OH^- and NO_3^-. The aerosols are described by log-normal modes and are composed of SO_4^{2-}, OC and BC, mineral dust and sea salt (Vignati *et al.* 2004; Stier *et al.*, 2005). The biogenic monoterpene ($C_{10}H_{16}$) emissions of Guenther *et al.* (1995) are scaled by the factor 0.15 to estimate the production of secondary organic aerosol (SOA) from biogenic sources following Dentener *et al.* (2006). SOA is then injected into the atmosphere as primary organic aerosol.

The models have been extensively evaluated in previous studies (Stier *et al.*, 2005; Pozzoli

et al., 2008a and b; Isaksen et al., 2009) with comparisons to several measurements and to other model results. The large-scale meteorology is constrained to the year 2000, nudging the temperature, surface pressure, vorticity and divergence to the ECMWF (European Centre for Medium Weather Forecast) ERA40 reanalysis data.

A.3.2 Model simulations of present-day conditions

Many aspects of the models have been compared with observations in prior studies. Of primary interest here are those factors that contribute substantially to concentration and radiative forcing. For CH_4, one of the key metrics for evaluation is constraints on the CH_4 residence time in the atmosphere provided by measurements of the lifetime of methyl chloroform. These indirect constraints lead to a best estimate of the CH_4 chemical lifetime of 9.6 years (range 6.5 to 13.8) (Prather et al., 2001). The respective values for the GISS and ECHAM models are 10.2 (8.9 total residence time) and 12.3 (10.4 total) years. Ozone is generally simulated reasonably well in both models (e.g. Stevenson et al., 2006).

For aerosols, one of the best-observed quantities relevant to radiative forcing is total AOD. Figure A.3.1 shows an example of the AOD in both models compared with observations from two satellite instruments. The two models reproduce many patterns of the satellite AOD: plumes from Asia into the Pacific or from Northern Africa into the Atlantic, the gradients over North America and Europe. In a quantitative sense, ECHAM underestimates AOD over Africa and overestimates over the ocean accordingly to direct measurements (Multi-angle Imaging Spectro Radiometer (MISR)) Lower AODs over land from both models are found over the Middle East and in northern South America. The discrepancy over North Africa and the Middle East from ECHAM is most likely caused by dust AOD underestimation.

The global mean AOD values for GISS and ECHAM are 0.12 and 0.15, respectively. These agree quite well with estimates from AERONET surface observations of 0.135 and from a composite of multiple satellite datasets of 0.151 (Kinne et al., 2006) given the uncertainties in those datasets (i.e. limited coverage of AERONET, variations between different satellite measurements).

Of particular interest for measures emphasizing BC is the AAOD. Observations are much more limited and typically relatively unreliable in comparison with those for AOD as AAOD. Ground-based measurements are generally more accurate than satellite data, but are of course more limited in spatial coverage. This Assessment campares them with measurements from the AERONET network of ground-based aerosol Lidars (light detection and ranging) and from the OMI instrument on the NASA Aura satellite (Table A.3.1).

In comparison with AERONET, the GISS model shows a low bias virtually everywhere, by 30 to 60 per cent, the exception being North Africa/Middle East, where mineral dust dominates the AAOD. The ECHAM model shows low biases as well, with especially low values for Northern mid-latitude areas (North America, Europe, East Asia). The GISS model shows better agreement with OMI satellite observations than with AERONET, with a bias of 15 per cent or less over most regions, except North America with a 30 per cent low bias and South America with a 55 per cent low bias. ECHAM is also closer to OMI than AERONET, but still substantially too low over Northern mid-latitude areas. ECHAM also shows a large low bias (52 per cent) over South America, similar to GISS. This suggests that emissions from biomass burning, a dominant emission source in that region, may be underestimated in the inventory used in the modelling. For southern hemisphere Africa, the GISS AAOD is only about 40 per cent of that seen in AERONET, while ECHAM has about 60 per cent of the AERONET AAOD, again suggesting that biomass-burning emissions are too low. Consistent with this, a recent detailed emissions

82
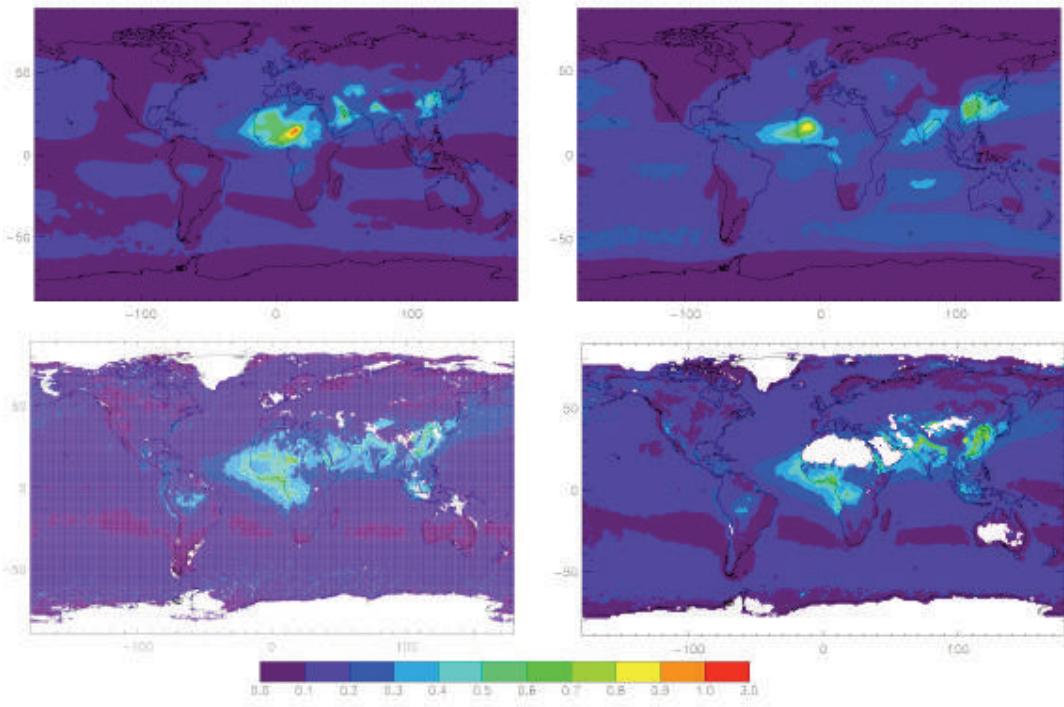
Figure A.3.1. Annual average clear-sky AOD at 550 nm in the models and in satellite observations. Model results are shown for GISS (upper left) and ECHAM (upper right) for average 2005 conditions, while measurements are from the MISR (lower left) and MODIS (lower right) instruments for 2004–2006. The ECHAM model includes contributions from SO_4^{2-}, BC, OC, sea salt and mineral dust. The GISS model includes those as well as NO_3^- and other secondary organic aerosols.

Table A.3.1. Average ratio of model to retrieved AERONET and OMI clear-sky AAOD at 550 nm within regions for the average of 14 AeroCom models and the two models used in this Assessment. Number of measurement sites is given for AERONET. Regions defined as North America (130W to 70W; 20N to 55N), Europe (15W to 45E; 30N to 70N), East Asia (100E to 160E; 30N to 70N), South America (85W to 40W; 34S to 2S), southern hemisphere Africa (20W to 45E; 34S to 2S), South and Southeast Asia (60E to 110E; 10N to 30N) and northern hemisphere Afrrica (20W to 60E; 0 to 30N). AeroCom results and the older results (marked 09) are from the analysis of Koch *et al*. (2009a).

	AeroCom	GISS (09)	MPIHAM (09) [ECHAM]	GISS (this study)	ECHAM-HAMMOZ (this study)
AER, North America #44	0.86	1.00	0.39	0.67	0.46
AER, Europe #41	0.81	0.83	0.21	0.67	0.28
AER, East Asia #11	0.67	0.49	0.29	0.50	0.31
AER, South America #7	0.68	0.59	0.43	0.55	0.53
AER, Southern hemisphere Africa #5	0.53	0.35	0.35	0.39	0.61
AER, South and Southeast Asia #4	NA	NA	NA	0.43	0.47
AER, Northern hemisphere Africa #15	NA	NA	NA	1.22	0.45
OMI, North America	0.52	0.73	0.21	0.70	0.49
OMI, Europe	1.60	1.40	0.29	0.91	0.41
OMI, East Asia	0.71	0.74	0.32	0.85	0.34
OMI, South America	0.35	0.29	0.22	0.45	0.48
OMI, Southern hemisphere Africa	0.47	0.40	0.35	0.92	1.25
OMI, South and Southeast Asia	NA	NA	NA	0.85	1.07
OMI, Northern hemisphere Africa	NA	NA	NA	1.06	0.69

The AERONET data are for 1996 to 2006, v2 level 2, annual averages for each year were used if more than eight months were present, and monthly averages for more than 10 days of measurements. The values at 550 nm were determined using the 0.44 and 0.87 µm Angstrom parameters. The OMI retrieval is based on OMAERUVd.003 daily products from 2005 to 2007 that were obtained through and averaged using GIOVANNI (Acker and Leptoukh, 2007).

Chapter 3. Atmospheric processes, tropospheric ozone and black carbon concentrations, deposition and radiative forcing
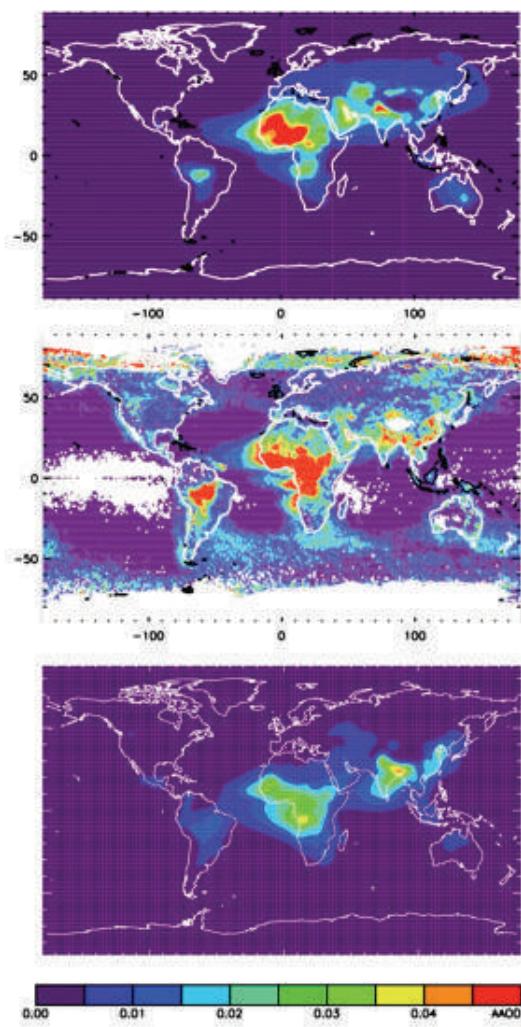
Figure A.3.2. Annual average clear-sky AAOD at 550 nm in the GISS model 2005 run (top), retrieved from the OMI satellite instrument for 2005-2007 (centre), and in the ECHAM model 2005 run (bottom). White areas in the satellite retrieval indicate no data.

inventory analysis concluded that biomass-burning emissions in Africa are roughly a factor of 2.4 higher than those in the GFED inventory used in the models (Liousse *et al.*, 2010). The two models differ most strongly over northern hemisphere Africa, where the ECHAM model's AAOD is too low. This result is at least partially due to the ECHAM model not including the super-coarse mode of mineral dust aerosols.

Differences between the AAOD observational datasets are substantial as well (see Figure A.3.2). For example, this version of the GISS model shows a much larger underestimate for Europe with respect to AERONET than the previous version (33 per cent versus 17 per cent), but a substantial improvement in the comparison with the OMI measurements over Europe (9 per cent underestimate versus 40 per cent overestimate). The improvement is also present for ECHAM-HAMMOZ in comparison to the version of the model containing only the aerosol scheme HAM. Issues include cloud-screening, spatial sampling and limited geographic coverage for AERONET. The comparison over South and Southeast Asia, for example, suggests a large low bias in the model with respect to AERONET. There are only four AERONET stations in that region, however, and comparison with the satellite data – with nearly complete coverage in that area, shows only a small low bias in the model (15 per cent).

As discussed in the main body of the Assessment, atmospheric forcing is highly relevant to driving changes in atmospheric circulation and in precipitation. Figure A.3.3 shows the present-day atmospheric forcing (tropopause-surface forcing) due to BC in the GISS model, for comparison with published estimates derived from observations.
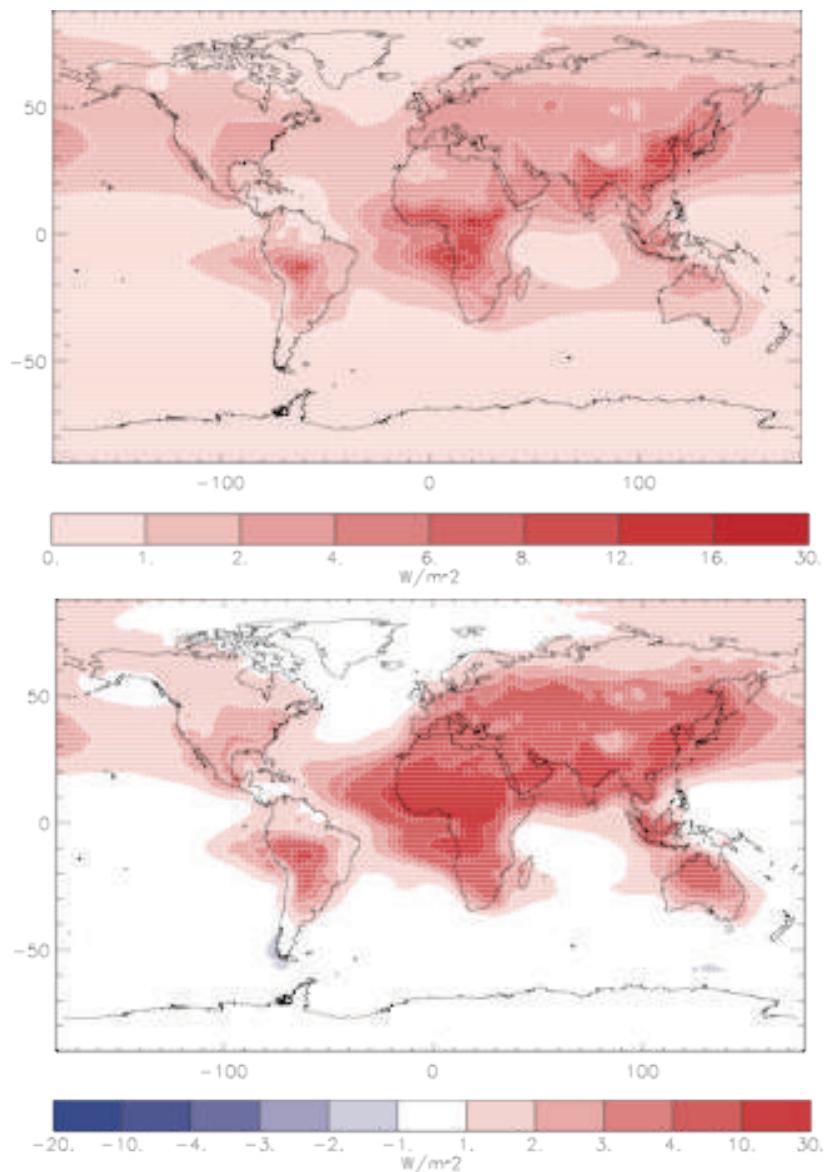
Figure A.3.3. Annual average atmospheric forcing (tropopause-surface) in the GISS model due to BC (top) and due to all absorbing aerosols (bottom). Note difference in scales.

References

Acker, J. G. and Leptoukh, G. (2007). Online Analysis Enhances Use of NASA Earth Science Data. *Transactions American Geophysical Union*, 88, 14.

Ackerman, A. S., Toon, O. B., Taylor, J. P., Johnson, D. W., Hobbs, P. V. and Ferek, R. J. (2000). Effects of aerosols on cloud albedo: Evaluation of Twomey's parameterization of cloud susceptibility using measurements of ship tracks. *J. Atmos. Sci.*, 57, 2684–2695.

Adams, P.J. and Seinfeld, J.H. (2003). Disproportionate impact of particulate emissions on global cloud condensation nuclei concentrations. *Geophys. Res. Lett.*, 30, 1239.

Aghedo, A. M., Bowman, K. W., Worden, H. M., Kulawik, S. S., Shindell, D. T., Lamarque, J. F., Faluvegi, G., Parrington, M., Jones, D. B. A. and Rast, S. (2011). The vertical distribution of ozone instantaneous radiative forcing from satellite and chemistry climate models. *J. Geophys. Res.*, 116, D01305.

Andreae, M. O. and Gelencsér, A. (2006). Black carbon or brown carbon? The nature of light-absorbing carbonaceous aerosols, *Atmos. Chem. Phys.*, 6, 3131–3148.

Bauer, S. E., Koch, D., Unger, N., Metzger, S. M., Shindell, D. T. and Streets, D. G. (2007). Nitrate aerosols today and in 2030: importance relative to other aerosol species and tropospheric ozone. *Atmos. Chem. Phys.*, 7, 5043–5059.

Bauer, S. E., Menon, S., Koch, D., Bond, T. C., and Tsigaridis, K. (2010). A global modeling study on carbonaceous aerosol microphysical characteristics and radiative effects, *Atmos. Chem. Phys.*, 10, 7439–7456.

Bellouin, N., Jones, A., Haywood, J. and Christopher, S. A. (2008). Updated estimate of aerosol direct radiative forcing from satellite observations and comparison against the Hadley Centre climate model, *Journal of Geophysical Research*, **113**, doi: 10.1029/2007JD009385.

Berntsen, T. K., Fuglestvedt, J. S., Joshi, M. M., Shine, K. P., Stuber, N., Ponater, M., Sausen, R., Hauglustaine, D. A. and Li, L. (2005). Response of climate to regional emissions of ozone precursors: sensitivities and warming potentials. *Tellus*, 57B, 283–304.

Binkowski, F. S. and Shankar, U. (1995). The Regional Particulate Matter Model 1. Model description and preliminary results. *J. Geophys. Res.*, 100, 26191–26209.

Binkowski, F. S. and Roselle, S. J. (2003). Models-3 Community Multiscale Air Quality (CMAQ) model aerosol component, 1. Model description. *J. Geophys. Res.*, 108, 4183.

Bonasoni, P., Laj, P., Angelini, F., Arduini, J., Bonafé, U., Calzolari, F., Cristofanelli, P., Decesari, S., Facchini, M. C., Fuzzi, S., Gobbi, G. P., Maione, M., Marinoni, A., Petzold, A., Roccato, F., Roger, J. C., Sellegri, K., Sprenger, M., Venzac, H., Verza, G. P., Villani, P. and Vuillermoz, E. (2008). The ABC-Pyramid Atmospheric Research Observatory in Himalaya for aerosol, ozone and halocarbon measurements. *Sci. Total Environ.*, 391, 252–261.

Bond, T. C. (2007). Can warming particles enter global climate discussions? *Environ. Res. Lett.*, 2, Issue: 4, Article Number: 04503, doi: 10.1088/1748-9326/2/4/045030

Borys, R. D. (1989). Studies of ice nucleation by Arctic aerosol on AGASP-II. *J. Atmos. Chem.*, 9, 169–185.

Brioude, J., Cooper, O. R., Feingold, G., Trainer, M., Freitas, S. R., Kowal, D., Ayers, J. K., Prins, E., Minnis, P., McKeen, S. A., Frost, G. J. and Hsie, E.-Y. (2009). Effect of biomass burning on marine stratocumulus clouds off the California coast. *Atmos. Chem. Phys.*, 9, 8841–8856.

Butkovskaya, N., Kukui, A. and Le Bras, G. (2007). HNO_3 Forming Channel of the HO_2 + NO Reaction as a function of pressure and temperature in the ranges of 72–600 Torr and 223–323 K. *J. Phys. Chem. A*, 111, 9047–9053.

Cao, J. J., Lee, S. C., Chow, J. C., Watson, J. G., Ho, K. F., Zhang, R. J., Jin, Z. D., Shen, Z. X., Chen, G. C., Kang, Y. M., Zou, S. C., Zhang, L. Z., Qi, S. H., Dai, M. H., Cheng, Y. and Hu, K. (2007). Spatial and seasonal distributions of carbonaceous aerosols over China. *J. Geophys. Res.*, 112, D22S11.

Chakrabarty, R. K., Moosmüller, H., Chen, L.-W. A., Lewis, K., Arnott, W. P., Mazzoleni, C., Dubey, M. K., Wold, C. E., Hao, W. M. and Kreidenweis, S. M. (2010). Brown carbon in tar balls from smoldering biomass combustion. *Atmos. Chem. Phys.*, 10, 6363–6370.

Chen W.-T., Nenes, A., Liao, H., Adams, P. J., Li, J.-L. F. and Seinfeld, J. H. (2010a). Global climate response to anthropogenic aerosol indirect effects: Present day and year 2100. *J. Geophys. Res.-Atmos.*, 115, D12207

Chen, W.-T., Lee, Y. H., Adams, P. J., Nenes, A., and Seinfeld, J. H. (2010b). Will black carbon mitigation dampen aerosol indirect forcing? *Geophys. Res. Lett.*, 37, L09801.

Chung, S. H. and Seinfeld, J.H. (2005a). Climate response of direct radiative forcing of anthropogenic black carbon, *J. Geophys. Res.*, 110, D11102.

Chung, C. E., Ramanathan, V., Kim, D. and Podgorny, I. A. (2005b). Global anthropogenic aerosol direct forcing derived from satellite and ground-based observations. *J. Geophys. Res.-Atmos.*, 110, D24, D24207.

Clarke, A. D., Owens, S. R. and Zhou, J. (2006). An ultrafine sea salt flux from breaking waves: Implications for cloud condensation nuclei in the remote marine atmosphere. *J. Geophys. Res.*, 111, D06202.

Clarke, A. D. and Noone, K. J. (1985). Soot in the Arctic snowpack: a cause for perturbations in radiative transfer. *Atmos. Env.*, 19, 2045–2053.

Collins, W.J., Sitch, S. and Boucher, O. (2010). How vegetation impacts affect climate metrics for ozone precursors. *J. Geophys. Res.*, 115, doi:10.1029/2010JD014187

Corrigan, C. E., Ramanathan, V. and Schauer, J. J. (2006). Impact of monsoon transitions on the physical and optical properties of aerosols. *J. Geophys. Res.*, 111, D18208.

Dentener, F., Kinne, S., Bond, T., Boucher, O., Cofala, J., Generoso, S., Ginoux, P., Gong, S., Hoelzemann, J. J., Ito, A., Marelli, L., Penner, J. E., Putaud, J.-P., Textor, C., Schulz, M., van der Werf, G. R. and Wilson, J. (2006). Emissions of primary aerosol and precursor gases in the years 2000 and 1750, prescribed data-sets for AeroCom. *Atmos. Chem. Phys. Discuss.*, 6, 2703–2763.

Dentener, F., Keating, T. and Akimoto H. (2010). *Hemispheric Transport of Air Pollution 2010, Part A: Ozone and Particulate Matter. Air Pollution Studies No. 17*. Prepared by the Task Force on Hemispheric Transport of Air Pollution acting within the framework of the Convention on Long-range Transboundary Air Pollution. United Nations, New York and Geneva. www.htap.org/activities/2010_Final_Report/HTAP 2010 Part A 110407.pdf

Derwent, R. G., Collins, W. J., Johnson, C. E. and Stevenson, D. S. (2001). Transient behaviour of tropospheric ozone precursors in a global 3-D CTM and their indirect greenhouse effects. *Clim. Change*, 49, 463–487.

Dubovik, O. and King, M. D. (2000). A flexible inversion algorithm for retrieval of aerosol optical properties from Sun and sky radiance measurements. *J. Geophys. Res.*, 105, 20673–20696.

Dubovik, O., Smirnov, A., Holben, B. N., King, M. D., Kaufman, Y. J., Eck, T. F. and Slutsker, I. (2000). Accuracy assessment of aerosol optical properties retrieved from Aerosol Robotic Network (AERONET) Sun and sky radiance measurements. *J. Geophys. Res.*, 105, 9791–9806.

Dusek, U., Frank, G. P., Hildebrandt, L., Curtius, J., Schneider, J., Walter, S., Chand, D., Drewnick, F., Hings, S., Jung, D., Borrman, S. and Andreae, M. O. (2006). Size matters more than chemistry for cloud-nucleating ability of aerosol particles. *Science*, 312, 1375–1378.

Feichter, J., Kjellstrom, E., Rodhe, H., Dentener, F., Lelieveld, J. and Roelofs, G. (1996). Simulation of the tropospheric sulfur cycle in a global climate model. *Atmos. Env.*, 30, 1693–1707.

Fishman, J., Ramanathan, V., Crutzen, P. J. and Liu, S. C. (1979). Tropospheric ozone and climate. *Nature*, 282, 818–820.

Flanner, M. G., Zender, C. S., Randerson, J. T. and Rasch, P. J. (2007). Present-day climate forcing and response from black carbon in snow. *J. Geophys. Res.*, 112, D11202.

Flanner, M. G., Zender, C. S., Hess, P. G., Mahowald, N. M., Painter, T. H., Ramanathan, V. and Rasch, P. J. (2009). Springtime warming and reduced snow cover from carbonaceous particles. *Atmos. Chem. Phys.*, 9, 2481–2497.

Forster, P., Ramaswamy, V., Artaxo, P., Berntsen, T., Betts, R., Fahey, D. W., Haywood, J., Lean, J., Lowe, D. C., Myhre, G., Nganga, J., Prinn, R., Raga, G., Schulz, M. and Van Dorland, R. (2007). Changes in atmospheric constituents and in radiative forcing. *In:* Solomon, S., Qin, D., Manning, M., Chen, Z., Marquis, M., Averyt, K. B., Tignor, M. and Miller, H.L. (eds). *Climate Change 2007: The Physical Science Basis. Contribution of Working Group I to the Fourth Assessment Report of the Intergovernmental Panel on Climate Change.* Cambridge University Press, Cambridge, United Kingdom and New York, NY, USA.

Fowler, D., Smith, R., Muller, J., Cape, J. N., Sutton, M., Erisman, J. W. and Fagerli, H. (2007). Long term trends in sulphur and nitrogen deposition in Europe and the cause of non-linearities. *Water Air Soil Pollut.: Focus*, 7, 41–47.

Fu, Q., Johanson, C. M., Wallace, J. M. and Reichler, T. (2006). Enhanced mid-latitude tropospheric warming in satellite measurements. *Science*, 312, 1179.

Fuglestvedt, J., Berntsen, T., Myhre, G., Rypdal, K. and Skeie, R. B. (2008). Climate forcing from the transport sectors. *Proc. Natl. Acad. Sci.*, 105, 454–458.

Fuglestvedt, J. S., Shine, K. P., Berntsen, T., Cook, J., Lee, D. S., Stenke, A., Skeie, R. B., Velders, G. J. M. and Waitz, I. A. (2010). Transport impacts on atmosphere and climate: Metrics. *Atmos. Env.*, 44, 4648–4677.

Gauss, M., Myhre, G., Isaksen, I. S. A., Grewe, V., Pitari, G., Wild, O., Collins, W. J., Dentener, F. J., Ellingsen, K., Gohar, L. K., Hauglustaine, D. A., Iachetti, D., Lamarque, J.-F., Mancini, E., Mickley, L. J., Prather, M. J., Pyle, J. A., Sanderson, M. G., Shine, K. P., Stevenson, D. S., Sudo, K., Szopa, S. and Zeng, G. (2006). Radiative forcing since preindustrial times due to ozone change in the troposphere and the lower stratosphere. *Atmos. Chem. Phys.*, 6, 575–599.

Gong, S. L. (2003). A parameterization of sea-salt aerosol source function for sub- and super-micron particles. *Global Biochemical Cycles*, 17, 1097.

Granat, L., Engstöm, J. E., Praveen, S. and Rodhe, H. (2010). Light absorbing material (soot) in rainwater and in aerosol particles in the Maldives. *J. Geophys. Res.*, 115, D16307.

Grennfelt, P. and Hov, Ø. (2005). Regional air pollution at a turning point. *Ambio*, 34, 2–10.

Guenther, A., Hewitt, C., Erickson, D., Fall, R., Geron, C., Graedel, T., Harley, P., Klinger, L., Lerdau, M., McKay, W. A., Pierce, T., Scholes, B., Steinbrecher, R., Tallamraju, R., Taylor, J. and Zimmerman, P. (1995). A global model of natural volatile organic-compound emissions, *J. Geophys. Res.*, 100, 8873–8892.

Gustafsson, Ö., Kruså, M., Zencak, Z., Sheesley, R. J., Granat, L., Engström, E., Praveen, P. S., Rao, P. S. P., Leck, C. and Rodhe, H. (2009). Brown clouds over South Asia: Biomass or fossil fuel combustion? *Science*, 323, 495–498.

Hagemann, S., Arpe, K. and Roeckner, E. (2006). Evaluation of the hydrological cycle in the ECHAM5Model. *J. Clim.*, 19, 3810–3827.

Hansen, J., Sato, M. and Reudy, R. (1997). Radiative forcing and climate response. *J. Geophys. Res.*, 102, 6831–6864.

Hansen, J. and Nazarenko, L. (2004). Soot climate forcing via snow and ice albedos. *Proc. Natl. Acad. Sci.*, 101, 423–428.

Hansen, J., Sato, M., Ruedy, R., Nazarenko, L., Lacis, A., Schmidt, G. A., Russell, G., Aleinov, I., Bauer, M., Bauer, S., Bell, N., Cairns, B., Canuto, V., Chandler, M., Cheng, Y., Del Genio, A., Faluvegi, G., Fleming, E., Friend, A., Hall, T., Jackman, C., Kelley, M., Kiang, N., Koch, D., Lean, J., Lerner, J., Lo, K., Menon, S., Miller, R., Minnis, P., Novakov, T., Oinas, V., Perlwitz, Ja., Perlwitz, Ju., Rind, D., Romanou, A., Shindell, D., Stone, P., Sun, S., Tausnev, N., Thresher, D., Wielicki, B., Wong, T., Yao, M. and Zhang, S. (2005). Efficacy of climate forcings. *J. Geophys. Res.*, 110, D18104.

Highwood, E. J. and Kinnersley, R. P. (2006). When smoke gets in our eyes: The multiple impacts of atmospheric black carbon on climate, air quality and health. *Environ. Int.*, 32, 560–566.

Horowitz, L. W., Walters, S., Mauzerall, D., Emmons, L., Rasch, P. J., Granier, C., Tie, X., Lamarque, J. F., Schultz, M. G., Tyndall, G. S., Orlando, J. J. and Brasseur, G. P. (2003). A global simulation of tropospheric ozone and related tracers: Description and evaluation of MOZART, version 2. *J. Geophys Res.*, 108, 4784.

Isaksen, I. S. A., Granier, C., Myhre, G., Berntsen, T. K., Dalsøren, S. B., Gauss, M., Klimont, Z., Benestad, R., Bousquet, P., Collins, W., Cox, T., Eyring, V., Fowler, D., Fuzzi, S., Jöckel, P., Laj, P., Lohmann, U., Maione, M., Monks, P., Prevot, A. S. H., Raes, F., Richter, A., Rognerud, B., Schulz, M., Shindell, D., Stevenson, D. S., Storelvmo, T., Wang, W.-C., van Weele, M., Wild, M. and Wuebbles, D. (2009). Atmospheric composition change: Climate-chemistry interactions. *Atmos. Env.*, 43, 5138–5192.

IPCC (2007). Climate Change 2007: Synthesis Report. Contribution of Working Groups I, II and III to the Fourth Assessment Report of the Intergovernmental Panel on Climate Change [Core Writing Team, Pachauri, R.K and Reisinger, A. (eds.)]. IPCC, Geneva, Switzerland, 104 pp.

Jacobson, M. Z. (2000). A physically based treatment of elemental carbon optics: Implications for global direct forcing aerosols. *Geophys. Res. Lett.*, 27, 217–220.

Jacobson, M. Z. (2001). Strong radiative heating due to the mixing state of black carbon in atmospheric aerosols. Nature, 409, 695–697.

Jacobson, M. Z. (2004). Climate response of fossil fuel and biofuel soot, accounting for soot's feedback to snow and sea ice albedo and emissivity. *J. Geophys. Res.*, 109, D21201.

Jacobson, M. Z. (2006). Effects of externally-through-internally-mixed soot inclusions within clouds and precipitation on global climate. *J. Phys. Chem. A.*, 110, 6860–6873.

Jacobson, M. Z. (2010). Short-term effects of controlling fossil-fuel soot, biofuel soot and gases, and methane on climate, Arctic ice, and air pollution health. *J. Geophys. Res.*, 115, D14209.

Jenkin, M. E. (2008). Trends in ozone concentration distributions in the UK since 1990: Local, regional and global influences. *Atmos. Env.*, 42(21), 5434–5445.

Jones, A., Haywood, J. M. and Boucher, O. (2007). Aerosol forcing, climate response and climate sensitivity in the Hadley Centre climate model. *J. Geophys. Res.*, 112, D20211.

Kanakidou M., Seinfeld, J. H., Pandis, S. N. *et al.* (2005). Organic aerosol and global climate modelling: A review. *Atmos. Chem. Phys.*, 5, 1053–1123.

Kaufman, Y. and Koren, I. (2006). Smoke and pollution aerosol effect on cloud cover. *Science*, 313. 5787, 655–658.

Kim, D., Wang, C., Ekman, A. M. L., Barth, M. C. and Rasch, P. (2008). Distribution and direct radiative forcing of carbonaceous and sulfate aerosols in an interactive size-resolving aerosol-climate model. *J. Geophys. Res.*, 113, D16309.

Kinne, S., Schulz, M. Textor, C., Guibert, S., Balkanski, Y., Bauer, S. E., Berntsen, T., Berglen, T. F., Boucher, O., Chin, M., Collins, W., Dentener, F., Diehl, T., Easter, R., Feichter, J., Fillmore, D., Ghan, S., Ginoux, P., Gong, S., Grini, A., Hendricks, J., Herzog, M., Horowitz, L., Isaksen, I., Iversen, T., Kirkevåg, A., Kloster, S., Koch, D., Kristjansson, J. E., Krol, M., Lauer, A., Lamarque, J. F., Lesins, G., Liu, X., Lohmann, U., Montanaro, V., Myhre, G., Penner, J., Pitari, G., Reddy, S., Seland, O., Stier, P., Takemura, T. and Tie, X. (2006). An AeroCom initial assessment – optical properties in aerosol component modules of global models. *Atmos. Chem. Phys.*, 6, 1815–1834.

Koch, D. and Hansen, J. (2005). Distant origins of Arctic black carbon: A Goddard Institute for Space Studies ModelE experiment. *J. Geophys. Res.*, 110, D04204.

Koch, D., Schmidt, G. and Field, C. (2006). Sulfur, sea salt and radionuclide aerosols in GISS ModelE. *J. Geophys. Res.*, 111, D06206.

Koch, D., Bond, T. C., Streets, D., Unger, N. and van der Werf, G. R. (2007). Global impacts of aerosols from particular regions and sectors. *J. Geophys. Res.-Atmos.*, 112, D2, D02205.

Koch, D., Schulz, M., Kinne, S., McNaughton, C., Spackman, J. R., Balkanski, Y., Bauer, S., Berntsen, T., Bond, T. C., Boucher, O., Chin, M., Clarke, A., De Luca, N., Dentener, F., Diehl, T., Dubovik, O., Easter, R., Fahey, D. W., Feichter, J., Fillmore, D., Freitag, S., Ghan, S., Ginoux, P., Gong, S., Horowitz, L., Iversen, T., Kirkevåg, A., Klimont, Z., Kondo, Y., Krol, M., Liu, X., Miller, R., Montanaro, V., Moteki, N., Myhre, G., Penner, J. E., Perlwitz, J., Pitari, G., Reddy, S., Sahum L., Sakamoto, H., Schuster, G., Schwarz, J. P., Seland, Ø., Stier, P., Takegawa, N., Takemura, T., Textor, C., van Aardenne, J. A. and Zhao, Y. (2009a). Evaluation of black carbon estimations in global aerosol models. *Atmos. Chem. Phys.*, 9, 9001–9026.

Koch, D., Menon, S., Del Genio, A., Ruedy, R., Aleinov, I. and Schmidt, G. A. (2009b). Distinguishing aerosol impacts on climate over the past century. *J. Climate*, 22, 2659–2677.

Koch, D. and Del Genio, A. (2010). Black carbon semi-direct effects on cloud cover: Review and synthesis. *Atmos. Chem. Phys.*, 10, 7685–7696.

Lamarque, J. F., Bond, T. C., Eyring, V., Granier, C., Heil, A., Klimont, Z., Lee, D., Liousse, C., Mieville, A., Owen, B., Schultz, M. G., Shindell, D., Smith, S. J., Stehfest, E., Van Aardenne, J., Cooper, O. R., Kainuma, M., Mahowald, N., McConnell, J. R., Naik, V., Riahi, K. and van Vuuren, D. P. (2010). Historical (1850–2000) gridded anthropogenic and biomass burning emissions of reactive gases and aerosols: Methodology and application. *Atmos. Chem. Phys.*, 10, 7017–7039.

Lawrence, M. G. and Lelieveld, J. (2010). Atmospheric pollutant outflow from southern Asia: a review. *Atmos. Chem. Phys. Discuss.*, 10, 9463–9646.

Lin, S.-J. and Rood, R. B. (1996). Multidimensional flux-form semi-Lagrangian transport schemes. *Monthly Weather Review*, 124, 2046–2070.

Liousse, C., Guillaume, B., Grégoire, J. M., Mallet, M., Galy, C., Pont, V., Akpo, A., Bedou, M., Castéra, P., Dungall, L., Gardrat, E., Granier, C., Konaré, A., Malavelle, F., Mariscal, A., Mieville, A., Rosset, R., Serça, D., Solmon, F., Tummon, F., Assamoi, E., Yoboué, V. and Van Velthoven, P. (2010). Western African aerosols modeling with updated biomass burning emission inventories in the frame of the AMMA-IDAF program. *Atmos. Chem. Phys. Discuss.*, 10, 7347–7382.

Liu, X., Penner, J. E., Ghan, S. J. and Wang, M. (2007) Inclusion of ice microphysics in the NCAR Community Atmospheric Model Version 3 (CAM3). *J. Climate*, 20, 4526–4547.

Liu, X., Penner, J. E. and Wang, M. (2009). Influence of anthropogenic sulfate and black carbon on upper tropospheric clouds in the NCAR CAM3 model coupled to the IMPACT global aerosol model. *J. Geophys. Res.*, 114, D03204, 19 PP., doi:10.1029/2008JD010492

Lohmann, U. and Hoose, C. (2009). Sensitivity studies of different aerosol indirect effects in mixed-phase clouds. *Atmospheric Chemistry and Physics*, 9, 8917–8934.

90

Mickley, L. J., Jacob, D. J. and Rind, D. (2001). Uncertainty in preindustrial abundance of tropospheric ozone: Implications for radiative forcing calculations. *J. Geophys. Res.*, 106, 3389–3399.

Ming, J., Cachier, H., Xiao, C., Qin, D., Kang, S., Hou, S. and Xu, J. (2008). Black carbon record based on a shallow Himalayan ice core and its climatic implications. *Atmos. Chem. Phys.*, 8, 1343–1352.

Ming, J., Xiao, C. D., Cachier, H., Qin, D. H., Qin, X., Li, Z. Q. and Pu, J. C. (2009). Black Carbon (BC) in the snow of glaciers in west China and its potential effects on albedos. *Atmospheric Research*, 92(1), 114–123.

Moffet, R. C. and Prather, K. (2009). In-situ measurements of the mixing state and optical properties of soot with implications for radiative forcing estimates. *Proc. Natl. Acad. Sci.*, 106, 11872–11877.

Murphy, D. M., Solomon, S., Portmann, R. W., Rosenlof, K. H., Forster, P. M. and Wong T. (2009). An observationally based energy balance for the Earth since 1950. *J. Geophys. Res.*, 114, D17107, doi:10.1029/2009JD012105.

Myhre, G. (2009). Consistency between satellite-derived and modeled estimates of the direct aerosol effect. *Science*, 325(5937), 187–190, doi:10.1126/science.1174461.

Naik, V., Mauzerall, D., Horowitz, L., Schwarzkopf, M. D., Ramaswamy, V. and Oppenheimer, M. (2005). Net radiative forcing due to changes in regional emissions of tropospheric ozone precursors. *J. Geophys. Res.*, 110, D24306.

Nemitz, E., Gallagher, M. W., Duyzer, J. H. and Fowler, D. (2002). Micrometeorological measurements of particle deposition velocities to moorland vegetation. *Quarterly Journal of the Royal Meteorological Society*, 128(585), 2281–2300.

Norris, J. R. and Wild, M. (2007). Trends in aerosol radiative effects over Europe inferred from observed cloud cover, solar "dimming", and solar "brightening". *J. Geophys. Res.*, 112, D08214.

Kim Oanh, N. T., Upadhyay, N., Zhuang, Y.-H., Hao, Z.-P., Murthy, D. V. S., Lestari, P., Villarin, J. T., Chengchua, K., Co, H. X., Dung, N. T. and Lindgren, E. S. (2006). Particulate air pollution in six Asian cities: Spatial and temporal distributions, and associated sources. *Atmos. Env.*, 40, 3367–3380.

Oshima, N., Koike, M., Zhang, Y. and Kondo, Y. (2009). Aging of black carbon in outflow from anthropogenic sources using a mixing state resolved model: 2. Aerosol optical properties and cloud condensation nuclei activities. *J. Geophys. Res.*, 114, D18202.

Park, S. S. and Kim, Y. J. (2005). Source contributions to fine particulate matter in an urban atmosphere. *Chemosphere*, 59(2), 217–226.

Penner, J. E., Chen. Y., Wang, M. and Liu, X. (2009). Possible influence of anthropogenic aerosols on cirrus clouds and anthropogenic forcing. *Atmos. Chem. Phys.*, 9, 879–896.

Permadi, D. A. and Oanh, N. T. K. (2008). Episodic ozone air quality in Jakarta in relation to meteorological conditions. *Atmos. Env.*, 42, 6806–6815.

Pierce, J. R. and Adams, P. J. (2009). A computationally efficient aerosol nucleation/condensation method: Pseudo-steady-state sulfuric acid. *Aerosol Sci. Tech.*, 43, 216–226.

Pozzoli, L., Bey, I., Rast, S., Schultz, M. G., Stier, P. and Feichter, J. (2008a). Trace gas and aerosol interactions in the fully coupled model of aerosol-chemistry-climate ECHAM5-HAMMOZ: 1. Model description and insights from the spring 2001 TRACE-P experiment. *J. Geophys. Res.*, 113, D07308.

Pozzoli, L., Bey, I., Rast, S., Schultz, M. G., Stier, P. and Feichter, J. (2008b). Trace gas and aerosol interactions in the fully coupled model of aerosol-chemistry-climate ECHAM5-HAMMOZ: 2. Impact of heterogeneous chemistry on the global aerosol distributions, *J. Geophys. Res.*, 113, D07309.

Prather, M. J. (1986). Numerical advection by conservation of second-order moments. *J. Geophys. Res.*, 91, 6671–6681.

Prather, M. J., Ehhalt, D., Dentener, F., Derwent, R. G., Dlugokencky, E. J., Holland, E. A., Isaksen, I. S., Katima, J., Kirchhoff, V., Matson, P., Midgley, P. and Wang, M. (2001). Atmospheric chemistry and greenhouse Gases. In: Houghton, J. T., Ding, Y., Griggs, D. J., Nogeur, M., van der Linden, P. J., Dai, X., Maskell, K. and Johnson, C. A. (eds). *Climate Change 2001.* Cambridge University Press, Cambridge.

Pryor, S. C., Gallagher, M., Sievering, H., Larsen, S. E., Barthelmie, R. J., Birsan, F., Nemitz, E., Kulmala, M., Taipale, R. and Vesala, T. (2008). A review of measurement and modelling results of particle atmosphere–surface exchange. *Tellus B*, 60(1), 42–75.

Putaud, J. P., Van Dingenen, R., Alastuey, A., Bauer, H., Birmili, W., Cyrys, J., Flentje, H., Fuzzi, S., Gehrig, R., Hansson, H. C., Harrison, R. M., Herrmann, H., Hitzenberger, R., Huglin, C., Jones, A. M., Kasper-Giebl, A., Kiss, G., Kousa, A., Kuhlbusch, T. A. J., Loeschau, G., Maenhaut, W., Molnar, A., Moreno, T., Pekkanen, J., Perrino, C., Pitz, M., Puxbaum, H., Querol, X., Rodriguez, S., Salma, I, Schwarz, J., Smolik, J., Schneider, J., Spindler, G., ten Brink, H., Tursic, J., Viana, M., Wiedensohler, A. and Raes, F. (2010). A European aerosol phenomenology-3: Physical and chemical characteristics of particulate matter from 60 rural, urban, and kerbside sites across Europe. *Atmospheric Environment*, 44(10), 1308–1320.

Qian, Y., Kaiser, D. P., Leung, L. R. and Xu, M. (2006). More frequent cloud-free sky and less surface solar radiation in China from 1955 to 2000. *Geophys. Res. Lett.*, 33, L01812.

Quaas, J., Boucher, O., Bellouin, N. and Kinne, S. (2008). Satellite-based estimate of the direct and indirect aerosol climate forcing. *J. Geophys. Res.*, 113, D05204.

Raes, F., Van Dingenen, R., Vignati, E., Wilson, J., Putaud, J.-P., Seinfeld, J. H. and Adams, P. (2000). Formation and cycling of aerosols in the global troposphere. *Atmos. Env.*, 34, 4215–4240.

Ramanathan, V., Crutzen, P. J., Kiehl, J. T. and Rosenfeld, D. (2001). Aerosols, climate, and the hydrological cycle. *Science*, 294, 2119–2124.

Ramanathan, V., Chung, C., Kim, D., Bettge, T., Buja, L., Kiehl, J. T., Washington, W. M., Fu, Q., Sikka, D. R. and Wild, M. (2005). Atmospheric brown clouds: Impacts on South Asian climate and hydrological cycle. *Proc. Natl. Acad. Sci.*, 102, 5326–5333.

Ramanathan, V. and Carmichael, G. (2008). Global and regional climate changes due to black carbon. *Nature Geoscience*, 1, 221–227.

Rayner, N. A., Parker, D. E., Horton, E. B., Folland, C. K., Alexander, L. V., Rowell, D. P., Kent, E. C. and Kaplan, A. (2003). Global analyses of sea surface temperature, sea ice, and night marine air temperature since the late nineteenth century. *J. Geophys. Res.*, 108, 4407.

Roberts, D. L. and Jones A. (2004). Climate sensitivity to black carbon aerosol from fossil fuel combustion. *J. Geophys. Res.*, 109, D16202.

Roeckner, E., Bauml, G., Bonaventura, L., Brokopf, R., Esch, M., Giorgetta, M., Hagemann, S., Kirchner, I., Kornblueh, L., Manzini, E., Rhodin, A., Schlese, U., Schulzweida, U. and Tompkins, A. (2003). The atmospheric general circulation model ECHAM5: Part 1. Tech. Rep. 349. Max Planck Institute for Meteorology, Hamburg.

Roeckner, E., Brokopf, R., Esch, M., Giorgetta, M., Hagemann, S., Kornblueh, L., Manzini, E., Schlese, U. and Schulzweida, U. (2006). Sensitivity of simulated climate to horizontal and vertical resolution in the ECHAM5 atmosphere model. *J. Clim.*, 19, 3771–3791.

Royal Society (2008). *Ground-level ozone in the 21st Century: future trends, impacts and policy implications.* Science Policy, Report 15/08. The Royal Society, London, UK.

Ruckstuhl, C., and Norris, J. R. (2009). How do aerosol histories affect solar "dimming" and "brightening" over Europe?: IPCC-AR4 models versus observations. *J. Geophys. Res.*, 114, D00D04.

Ruckstuhl, C., Norris, J. R. and Philipona, R. (2010). Is there evidence for an aerosol indirect effect during the recent aerosol optical depth decline in Europe? *J. Geophys. Res.*, 115, D04204.

Rypdal, K., Rive, N., Berntsen, T., Fagerli, H., Klimont, Z., Mideksa, T. K. and Fuglestvedt, J. S. (2009). Climate and air quality-driven scenarios of ozone and aerosol precursor abatement. *Environ. Sci. & Policy*, 12, 855–869.

Saikawa, E., Naik, V., Horowitz, L. W., Liu, J. and Mauzerall, D. L. (2009). Present and potential future contributions of sulfate, black and organic carbon aerosols from China to global air quality, premature mortality and radiative forcing. *Atmos. Env.*, 43, 2814–2822.

Sato, M., Hansen, J., Koch, D., Lacis, A., Ruedy, R., Dubovik, O., Holben, B., Chin, M., and Novakov, T. (2003). Global atmospheric black carbon inferred from AERONET. *Proc. Natl. Acad. Sci.*, 100, 6319–6324.

Schmidt, G. A., Ruedy, R., Hansen, J. E., Aleinov, I., Bell, N., Bauer, M., Bauer, S., Cairns, B., Canuto, V., Cheng, Y., Del Genio, A., Faluvegi, G., Friend, A. D., Hall, T. M., Hu, Y., Kelley, M., Kiang, N. Y., Koch, D., Lacis, A. A., Lerner, J., Lo, K. K., Miller, R. L., Nazarenko, L., Oinas, V., Perlwitz, J., Perlwitz, J., Rind, D., Romanou, A., Russell, G.L., Sato, M., Shindell, D. T., Stone, P. H., Sun, S., Tausnev, N., Thresher, D. and Yao, M.-S. (2006). Present day atmospheric simulations using GISS ModelE: Comparison to in-situ, satellite and reanalysis data. *J. Clim.*, 19, 153–192.

Schulz, M., Textor, C., Kinne, S., Balkanski, Y., Bauer, S., Berntsen, T., Berglen, T., Boucher, O., Dentener, F., Guibert, S., Isaksen, I.S.A., Iversen, T., Koch, D., Kirkevåg, A., Liu, X., Montanaro, V., Myhre, G., Penner, J. E., Pitari, G., Reddy, S., Seland, Ø., Stier, P. and Takemura, T. (2006). Radiative forcing by aerosols as derived from the AeroCom present-day and pre-industrial simulations. *Atmos. Chem. Phys.*, 6, 5225–5246.

Seland, Ø., Iversen, T., Kirkevåg, A. and Storelvmo, T. (2008). Aerosol-climate interactions in the CAM-Oslo atmospheric GCM and investigation of associated basic shortcomings. *Tellus A*, 60, 459–491.

Sharma, S., Lavoue, D., Cachier, H,. Barrie, L. A., Gong, S. L. (2004). Long-term trends of the black carbon concentrations in the Canadian Arctic. *J. Geophys. Res.-Atmos*, 109(D15), D15203.

Sharma, S., Andrews, E., Barrie, L. A., Ogren, J. A., Lavoue, D. (2006). Variations and sources of the equivalent black carbon in the high Arctic revealed by long-term observations at Alert and Barrow: 1989–2003. *J. Geophys. Res.-Atmos*, 111(D14), D14208.

Shindell, D. T., Faluvegi, G., Unger, N., Aguilar, E., Schmidt, G. A., Koch, D. M., Bauer, S. E. and Miller, R. L. (2006). Simulations of preindustrial, present-day, and 2100 conditions in the NASA GISS composition and climate model G-PUCCINI. *Atmos. Chem. Phys.*, 6, 4427–4459.

Shindell, D. T., Levy II, H., Schwarzkopf, M. D., Horowitz, L. W., Lamrque, J.-F. and Faluvegi, G. (2008a). Multimodel projections of climate change from short-lived emissions due to human activities. *J. Geophys. Res.*, 113, D11109.

Shindell, D. T., Chin, M., Dentener, F., Doherty, R. M., Faluvegi, G., Fiore, A. M., Hess, P., Koch, D. M., MacKenzie, I. A., Sanderson, M. G., Schultz, M. G., Schulz, M., Stevenson, D. S., Teich, H., Textor, C., Wild, O., Bergmann, D. J., Bey, I., Bian, H., Cuvelier, C., Duncan, B. N., Folberth, G., Horowitz, L. W., Jonson, J., Kaminski, J. W., Marmer, E., Park, R., Pringle, K. J., Schroeder, S., Szopa, S., Takemura, T., Zeng, G., Keating, T. J. and Zuber, A. (2008b). A multi-model assessment of pollution transport to the Arctic. *Atmos. Chem. Phys.*, 8, 5353–5372.

Shindell, D., Lamarque, J.-F., Unger, N., Koch, D., Faluvegi, G., Bauer, S., Ammann, M., Cofala, J. and Teich, H. (2008c). Climate forcing and air quality change due to regional emissions reductions by economic sector. *Atmos. Chem. Phys.*, 8, 7101–7113.

Shindell, D. and Faluvegi, G. (2009) Climate response to regional radiative forcing during the twentieth century. *Nature Geoscience*, 2, 294–300.

Shindell, D. T., Faluvegi, G., Koch, D. M., Schmidt, G. A., Unger, N. and Bauer, S. E. (2009). Improved attribution of climate forcing to emissions. *Science*, 326, 716–718.

Sokolov, A. P. (2006). Does model sensitivity to changes in CO_2 provide a measure of sensitivity to other forcings? *Journal of Climate*, 19(13), 3294–3306.

Sitch, S., Cox, P. M., Collins, W. J. and Huntingford, C. (2007). Indirect radiative forcing of climate change through ozone effects on the land-carbon sink. *Nature*, 448, 791–794.

Stevenson, D. S., Dentener, F. J., Schultz, M. G., Ellingsen, K., van Noije, T. P. C., Wild, O., Zeng, G., Amann, M., Atherton, C. S., Bell, N., Bergmann, D. J., Bey, I., Butler, T., Cofala, J., Collins, W. J., Derwent, R. G., Doherty, R. M., Drevet, J., Eskes, H. J., Fiore, A. M., Gauss, M., Hauglustaine, D. A., Horowitz, L. W., Isaksen, I. S. A., Krol, M. C., Lamarque, J.-F, Lawrence, M. G., Montanaro, V., Müller, J.-F, Pitari, G., Prather, M. J., Pyle, J. A., Rast, S., Rodriguez, J. M., Sanderson, M. G., Savage, N. H., Shindell, D. T., Strahen, S. E., Sudo, K. and Szopa, S. (2006). Multi-model ensemble simulations of present-day and near-future tropospheric ozone. *J. Geophys. Res.*, 111, D08301.

Stier, P., Feichter, J., Kinne, S., Kloster, S., Vignati, E., Wilson, J., Ganzeveld, L., Tegen, I., Werner, M., Balkanski, Y., Schulz, M., Boucher, O., Minikin, A. and Petzold, A. (2005). The aerosol-climate model ECHAM5-HAM. *Atmos. Chem. Phys.*, 5, 1125–1156.

Stone, R. S., Anderson, G. P., Shettle, E. P., Andrews, E., Loukachine, K., Dutton, E. G. and Schaaf, C., Roman, M. O., III. (2008). Radiative impact of boreal smoke in the Arctic: Observed and modeled. *J. Geophys. Res.-Atmos*, 113, D14: D14S16.

Torres, O., Tanskanen, A., Veihelmann, B., Ahn, C., Braak, R., Bhartia, P. K., Veefkind, P. and Levelt, P. (2007). Aerosols and surface UV products from Ozone Monitoring Instrument observations: An overview. *J. Geophys. Res.*, 112, D24S47.

Tsigaridis, K. and Kanakidou, M. (2007). Secondary organic aerosol importance in the future atmosphere. *Atmos. Env.*, 41, 4682–4692.

Unger, N., Bond, T. C., Wang, J. S., Koch, D. M., Menon, S., Shindell, D. T. and Bauer, S. (2010). Attribution of climate forcing to economic sectors. *Proc. Natl. Acad. Sci.*, 107, 3382–3387.

Vignati, E., Wilson, J. and Stier, P. (2004). M7: An efficient size-resolved aerosol microphysics module for large-scale aerosol transport models. *J. Geophys. Res.*, 109, D22202.

Vignati, E., Facchini, M. C., Rinaldi, M., Scannell, C., Ceburnis, D., Sciare, J., Kanakidou, M., Myriokefalitakis, S., Dentener, F, O'Dowd, C. D. (2010a). Global scale emission and distribution of sea-spray aerosol: Sea-salt and organic enrichment. *Atmospheric Environment*, 44(5), 670–677.

Vignati, E., Karl, M., Krol, M., Wilson, J., Stier, P. and Cavalli, F. (2010b). Sources of uncertainties in modelling black carbon at the global scale. *Atmos. Chem. Phys.*, 10, 2595–2611.

Wang, C. (2004). A modeling study on the climate impacts of black carbon aerosols. *J. Geophys. Res.*, 109, D03106.

Chapter 4. Impacts of black carbon and tropospheric ozone

Coordinating lead author:
Lisa D. Emberson (Stockholm Environment Institute, Environment Department, University of York, UK).

Lead authors: Susan Anenberg, (US Environmental Protection Agency), William Collins (UK Meteorological Office, UK), Mark Flanner (University of Michigan, USA), Kevin Hicks (Stockholm Environment Institute, Environment Department, University of York, UK), Johan C. I. Kuylenstierna (Stockholm Environment Institute, Environment Department, University of York, UK), Nicholas Muller (Middlebury College, USA), V. Ramanathan (Scripps Institution of Oceanography, USA), Joel Schwartz (Harvard University, USA), Drew T. Shindell (NASA Goddard Institute for Space Studies, USA), Rita Van Dingenen (Joint Research Centre, European Commission, Italy), Chien Wang (Massachusetts Institute of Technology, USA).

Contributing authors: Madhoolika Agrawal (Banares Hindu University, India), Devaraj de Condappa (Stockholm Environment Institute, USA), Frank Raes (Joint Research Centre, European Commission, Italy), Syed. I. Hasnain (Calicut University, India), Vishal Mehta (Stockholm Environment Institute, USA), Lina Mercado (Centre for Ecology and Hydrology, UK), Pam Pearson (International Cryosphere Climate Initiative, USA), David Purkey (Stockholm Environment Institute, USA), Stephen Sitch (University of Leeds, UK), Jason West (University of North Carolina, USA).

Key findings

The equilibrium warming that would result from changes in burdens of black carbon (BC) and tropospheric ozone (O_3) from pre-industrial to 2005 is estimated at 0.0 to 0.8°C for BC and 0.1 to 0.4°C for O_3 as a global average, with larger contributions in the northern hemisphere mid-latitudes. For comparison, the equilibrium warming for the observed increase in carbon dioxide (CO_2) over the same time period is about 1.3°C. These estimated values of warming use the central value of climate sensitivity in the Fourth Assessment Report of the Intergovernmental Panel on Climate Change (AR4). Warming due to BC and O_3 may be greatest in the Arctic.

There are strong regional variations in both concentrations and the climatic influence of BC and O_3 and such variations can lead to substantial regional climate impacts. The warming effect of these pollutants is greater in the northern hemisphere mid-latitudes. This asymmetry may affect tropical rainfall patterns. Large regional heating of the atmosphere caused by absorbing particles can also affect regional circulation patterns such as the Asian Monsoon. This may also have direct consequences for infrastructure as changes in precipitation can cause flooding, affecting human health, agriculture and forestry. The warming effect is larger in elevated regions such as the Himalayas, Tibet and other heavily glaciated regions. In part this is due to atmospheric heating from solar absorption by BC, and in part due to deposited BC darkening snow and ice surfaces, increasing their absorption of sunlight and leading to melting of snow and ice with subsequent effects on water supplies.

In the reference scenario, temperature changes occurring between 2010 and 2030 vary quite substantially between regions. The lowest increases of 0.5°C (0.3 to 0.7) occur in the southern hemisphere extratropics, whilst the largest increases of 0.7°C (0.5 to 1.1) occur in the Arctic. In both cases these changes are driven predominantly by historic and future changes in CO_2. In contrast to the large impact of CO_2, the compensating warming and cooling impacts of changes in short-lived climate forcers (SLCFs) and methane (CH_4) over the next 20 years under the reference scenario only lead to a small net impact of additional warming of less than 0.1°C globally; reductions in SLCFs, including BC emissions from North America and Europe, reduce the Arctic warming by about 5 per cent. Hence current policies are unlikely to produce substantial climate benefits via SLCFs.

Because of their high reflectance, snow and ice-covered regions exposed to sunlight are uniquely prone to large positive radiative forcing by BC which resides both within the atmosphere and the near-surface snow and ice. Essentially, any mixture of BC and co-emitted particulate matter (PM) exerts positive radiative forcing over pure snow. Furthermore, these regions are sensitive to radiative perturbations through snow and ice-albedo feedback.

Mid- and high-latitude BC very probably induces a net warming effect in the Arctic. This is caused by the darkening of snow and ice, atmospheric heating and increased cloud emissivity, but uncertainty persists in the impacts of indirect cloud effects and changes in meridional energy transport, both of which may reduce the equilibrium warming. Measurements indicate that BC amounts in the western Arctic near-surface atmosphere and snowpack have declined during the last two decades. Arctic forcing by SLCFs must, however, be considered in combination with long-lived greenhouse gas forcing. The incremental addition of forcing by short-lived agents is likely to induce a greater response in an Arctic environment with greater spatial and temporal coverage of area near the melting temperature.

Glaciers and seasonal snowpacks in the Himalaya, Tibetan Plateau, Hindu Kush and Karakoram region provide water to a large number of people and are proximal to, though not always downwind of, large BC sources in South and East Asia. Cryosphere vulnerability in this region is enhanced because of large surface insolation owing to low latitude, high altitude, and low vegetation cover. A small body of peer-reviewed literature suggests that BC is driving significant warming and melt in this region.

In the reference scenario, changes in outdoor concentrations of fine particulate matter ($PM_{2.5}$) and O_3 in 2030 relative to 2005 have substantial effects on air pollution-related mortality. Expected particle controls in North America and Europe are estimated to avoid 0.1 and 0.8 million annual deaths and in East Asia, Southeast Asia and the Pacific to avoid 0.1-1.1 million annual deaths. However, projected rapid emissions growth in South, West and Central Asia increases annual mortality by an estimated 0.1-1.8 million deaths. Globally, the reduction in premature deaths associated with $PM_{2.5}$ exposure is valued at US$1.7 trillion. In contrast, deaths associated with O_3 exposure increase and are valued at US$400 billion.

Reducing emissions from indoor cooking will produce direct health benefits to the approximately 50 per cent of the world's population that depend on solid fuel. These emissions are currently estimated to produce 1.6 million premature deaths (in 2000) from respiratory diseases alone, though this estimate is subject to large (and to date unquantified) uncertainties.

In the reference scenario, changes in O_3 in 2030 relative to 2005 have substantial regional impacts on the annual agricultural productivity of four staple crops, decreasing production by 7 to 120 million tonnes across Asia, with associated economic losses of US\$1 to 20 billion. Conversely, improvements in air quality in North America and Europe see improvements in crop yield leading to production and economic gains of 11 to 96 million tonnes and US\$1 to 11 billion, respectively. Ozone is also likely to affect the productivity of forests, grasslands and other semi-natural ecosystems, with implications for a number of important ecosystem services.

Limited evidence suggests that crop yields will be significantly affected by changes in regional climate that are likely to be enhanced in areas with high BC and O_3 pollution. Surface warming due to O_3 acting as a greenhouse gas and BC will affect temperatures, cloudiness, rainfall amounts and patterns, and river flow, the latter through BC impacts on glacier melting and evaporation; all of these factors will impact agricultural production. Additionally, changes in the amount and quality of photosynthetically active radiation caused by BC and aerosols may also affect crop yields. However, quantified attribution of these effects to regional burdens of O_3 and BC is not yet possible.

Changes in global ecosystem net primary productivity caused by an increase in O_3 damage will have a substantial impact on carbon sequestration in ecosystems and hence on radiative forcing. A global modelling study has shown that reduction in carbon sequestration caused by O_3 impacts on vegetation could double the effective radiative forcing attributable to tropospheric O_3 under a future 2100 SRES A2 scenario.

4.1 Introduction

This chapter focuses on the current knowledge of the links between emissions, deposition and the impacts of black carbon (BC) and tropospheric ozone (O_3) and its precursors that affect both air quality and climate, highlighting those relationships where the mechanisms are sufficiently understood to underpin policy development. This chapter also uses modelling approaches unique to this Assessment (see Chapter 1 and Appendix A.4), to assess the impacts that are likely to develop under the reference scenario projections of emission changes from 2005 to 2030 described in Chapter 2, and associated atmospheric concentration and deposition estimates developed in Chapter 3. Black carbon and O_3 affect global and regional climate and have important regional impacts on temperature and precipitation, in particular on the Arctic and other heavily glaciated regions of the world. Black carbon and O_3 also affect the health, food, water and economic security of large populations, both indirectly through the effects of climate change and directly through their impacts on human health, agriculture and ecosystems.

All the results of this Assessment's modelling study are presented within the context of published literature describing the influence of O_3 and BC on radiative forcing, climate, human health and ecosystems; both published observational data and modelling studies are included in this context setting. Black carbon is often discussed in combination with other aerosols or particulate matter (PM), especially for the assessment of health effects. This is due to difficulties in distinguishing impacts associated only with the BC fraction of PM; the text clearly indicates where assumptions are made in this regard. The focus is on impacts associated with radiative forcing and subsequent changes to global, regional and local climate; and on human health and agriculture. Within this Assessment we also provide qualitative discussion of BC and O_3 impacts that cannot be adequately represented by current modelling approaches due to large uncertainties in physical processes. Specifically these include processes describing perturbations to

97

precipitation and cloud cover as well as impacts on human health and agriculture associated with changes in temperature and precipitation. These effects are often concentrated in regions where climate sensitivity, population vulnerability and agricultural importance make the magnitude of the impacts large.

Estimating uncertainty

It is important to be clear which aspects of uncertainty are addressed in this chapter. Uncertainties in defining the global and regional temperature responses are quantified by ranges in radiative forcing estimates derived from the GISS-PUCCINI and ECHAM-HAM-MOZ models as well as from radiative forcing ranges described in the published literature. The health and agricultural impact assessment uncertainties are calculated based only on the stochastic uncertainties associated with the dose-response functions used to estimate either mortality for human health or yield loss for crops. As such, these impact assessments do not deal with uncertainties in emissions or estimates of atmospheric concentrations of pollutant species. For the health effects and economic valuation, the variance of the estimates (i.e. the slopes of the concentration-response function (CRF) and the value of risk reduction) have been used, and combined to calculate a confidence interval around our central estimates. This gives the uncertainty associated with these parameters. A similar approach was used to estimate uncertainty in crop yields. Further details of the uncertainty estimates for the entire Assessment are provided in Chapter 1, and those specific to the impacts considered in this Chapter are provided in the Appendix A.4.

4.2 Impacts on the climatic system

The concentrations of BC and O_3 and its precursors have various impacts on the climatic system. These are caused by changes in radiative forcing (see Chapters 1 and 3) affecting global temperatures and also regional effects such as changes in storminess, heatwaves and other extreme events and the impact of BC particles on cloud formation and rainfall patterns. By reducing the solar flux reaching the surface, aerosols including BC can directly affect surface evaporation and hence runoff and river flows. Direct and indirect effects of O_3 and aerosols on vegetation can also affect atmosphere-surface interactions such as evapotranspiration, CO_2 uptake and albedo. The focus in this section will be on the changes in surface temperature and precipitation, since these have been the subject of most research.

4.2.1 Impact on global temperatures

As discussed in Chapter 1, radiative forcing is a measure of the net change in the Earth's energy balance with space (i.e. incoming radiation from the sun minus outgoing radiation from the Earth). Ozone, its precursors, especially methane (CH_4), and BC all cause radiative forcing, and hence the Earth's temperature will respond until the outgoing radiation matches the incoming solar flux. In addition to increasing the radiative forcing at the top of atmosphere (TOA), BC redistributes the solar energy between the atmosphere and the surface, causing a large solar heating of the atmosphere and a correspondingly large solar dimming at the surface.

Annual average global mean temperature change is often discussed in the scientific literature and in the formulation of policy goals. Its long-term equilibrium response to a given radiative forcing can often be estimated reasonably well using the global mean radiative forcing imposed on the planet and knowledge of the climate sensitivity to such forcing. Climate sensitivity describes how much the temperature changes per unit of radiative forcing, given adequate time for the climate to fully adjust, and has been estimated from paleoclimate observations, modern instrumental data and models to likely be within the range of 0.5 to 1.2°C per W/m² radiative forcing from CO_2 (Hegerl *et al.*, 2007; IPCC, 2007). However, the climate impact of radiative forcing due to BC has been shown to vary substantially depending on the altitude at which the BC is located (Podgorny and Ramanathan, 2001; Hansen *et al.*, 2005; Cook and Highwood, 2004). In general, for some forcing agents that are not homogenously distributed (e.g. O_3 and BC),

Box 4.1: Metrics of climate impacts

Radiative forcing: a measure of the net change in the energy balance of the Earth with space, that is, the change in net radiation (i.e., incoming solar radiation minus outgoing terrestrial radiation) at the tropopause. At the global scale, the annual average radiative forcing at the top of the atmosphere (TOA), or tropopause, is generally a good indicator of global mean temperature change – though for BC in particular, forcing corresponds less closely to temperature change than for other agents (see also Chapter 1).

Climate sensitivity: a measure of the responsiveness of equilibrated global mean surface temperature to a change in radiative forcing equivalent to a doubling of the atmospheric CO_2 concentration. Climate sensitivity is hard to quantify since it needs to incorporate various couplings, feedbacks (particularly those related to clouds, sea ice and water vapour) and interactions that occur within the climate system in response to any changes within the system. Paleoclimate data provide useful constraints to quantify this term.

Temperature response: an estimate of temperature response to radiative forcing based on observational and modelling constraints on climate sensitivity. Peer-reviewed literature has established methods for simple estimates at the global scale and over large latitude bands, but not at more localized scales without the use of computationally expensive climate models.

Efficacy: a measure of how effective a forcing species is at causing a temperature response. It is defined as the ratio of the equilibrium temperature response from a 1 W/m² increase in forcing due to the species to that of a 1 W/m² forcing from CO_2.

Atmospheric forcing: the difference in the radiative forcing at the TOA and at the the Earth's surface, representing heat absorbed in the lower atmosphere. Gradients in heating from one place to another drive winds, and so regional differences in atmospheric forcing are closely connected to changes in regional circulation and precipitation.

the equilibrated temperature rise from a sustained 1 W/m² forcing can differ substantially from that due to a sustained 1 W/m² forcing from CO_2. The ratio of the responses is termed the efficacy of a species (Forster *et al.*, 2007). A value for the global mean equilibrium temperature change due to aerosol or O_3 forcing can be obtained by multiplying the radiative forcing by the climate sensitivity and the efficacy. The time scales for the climate to respond are determined by the rate of heat uptake of the oceans, which can take centuries. Over shorter periods the climate system will not be in equilibrium, and the temperature response will depend on the history of the radiative forcing. However, much of the reason the response to BC differs from the response to CO_2 is due to the semi-direct effect of BC on clouds. This effect is already incorporated into our forcing estimates. For O_3, the efficacy is subject to large uncertainty, even as to whether it is larger or smaller

than that of CO_2. Therefore, in this Assessment we assume that both O_3 and aerosols will produce the same temperature response per W/m² of forcing (including semi-direct components) as CO_2.

Using the BC forcing numbers from Section 3.3 (0.0 to 1.0 W/m²) would imply an equilibrium warming comparing present day and pre-industrial concentrations of 0.0 to 0.8°C. Similarly, the equilibrium warming from O_3 (forcing 0.3±0.15 W/m²) would be 0.1 to 0.4°C due to changes since pre-industrial times. The O_3 warming can be attributed to its precursor emissions. Applying a similar process to the O_3 precursor forcings from Figure 3.14 in Section 3.5 leads to an equilibrium warming of 0.1 to 0.3°C due to the O_3 change from methane (CH_4) (0.5 to 1.2°C total from CH_4 emissions), and much smaller contributions from the other O_3 precursors. All responses will be somewhat less due to the

extent that the climate system has not fully adjusted to the forcings (i.e. the ocean can take decades to centuries to equilibrate with forcings), though as the global mean levels of several of these compounds appears to have levelled off during recent decades, unlike CO_2, a substantial portion of the adjustment has already taken place. Hence the global temperature response to current concentrations of BC and O_3 is likely to be much nearer to equilibrium than the response to CO_2.

Other methods of estimating the impact on global temperatures include detection and attribution studies and analyses of historical temperature patterns against the spatial responses induced by aerosols. For BC, most studies find fairly consistent results. Jones *et al.* (2010) detect a global BC signal that accounts for a global warming of about 0.2±0.1°C from 1950 to 1999 (covering roughly half the emissions increase since pre-industrial times). Nagashima *et al.* (2006) also detect the influence of carbonaceous aerosols in their statistical analysis of historical temperatures, though they examine the sum of BC + organic carbon (OC). Shindell and Faluvegi (2009), using the regional patterns in observations and the regional responses to aerosol forcing, find a global impact of BC of ~0.35±0.25°C during the 20th century. Modelling studies using coupled ocean models in long integrations suggest a change in global mean surface temperature of 0.1 to 0.4°C resulting from current BC levels, depending on whether the BC is assumed to mix with other types of aerosol or not (Wang, 2004; Chung and Seinfeld, 2005). Jacobson's (2010) model, however, finds that just fossil fuel BC and OC contribute 0.3 to 0.5°C, while BC+OC from both fossil fuel and residential biomass combustion (cooking and home heating) contribute 0.4 to 0.7°C. The higher temperature response in this study is partially due to the treatment of absorption by BC inclusions in cloud drops and interstitially between cloud drops, which had large effects but were either not included in other studies or had a much smaller influence. Hence observational detection and attribution techniques seem to provide a tighter constraint on the climate effect of BC than the forward modelling (modelling from emissions

to atmospheric concentrations to climate impacts using basic physical equations) described in the previous paragraph. In particular they exclude both zero and the higher estimates of the uncertainty range.

It is much more difficult to detect an O_3 contribution to the global temperature rise because the pattern of the O_3 temperature response is much more homogeneous than for BC. Shindell and Faluvegi (2009) have attributed an O_3 contribution to the Arctic temperature rise, while Shindell *et al.* (2006) report results from a general circulation model (GCM) showing a contribution to 20th century global warming of just over 0.1°C, at the low end of the estimates above as would be expected for a transient rather than equilibrium result.

The climate responses to inhomogeneous forcings will depend on where the forcings are located. The dependence holds even for global mean temperature responses. Studies find an enhancement of around 45 per cent in the global mean temperature response to extra-tropical forcings relative to tropical ones, and 75 per cent enhancement for northern hemisphere forcing compared to southern hemisphere forcing (Shindell and Faluvegi, 2009; Hansen *et al.*, 1997). This reflects the influence of strong climate feedbacks, particularly snow and ice albedo feedbacks in the higher latitudes, and the greater land area in the northern hemisphere. The temperature change, and hence the efficacy, could be further enhanced when the snow albedo effect of BC is considered (Flanner *et al.*, 2009).

For climate purposes, the effectiveness of different mitigation strategies depends on the time scale under discussion. Ozone and BC have much shorter lifetimes (typically weeks) than CO_2, which persists for over a century. Consequently the impacts of reductions in emissions of short-lived species will be felt more quickly than reductions of CO_2 emissions (see Chapter 1). However, changes in CO_2 emissions lead to a long-term cumulative change in concentrations that will ultimately dominate the climate forcing. For the purposes of this Assessment it is necessary to define

100

the most appropriate metric to identify the most beneficial BC and O_3 precursor mitigation measures. Two metrics commonly used to compare the future impacts of climate forcing agents at different time scales are the global warming potential (GWP) and the global temperature-change potential (GTP). The GWP is the ratio of the radiative forcing produced by emitting 1 kg of the species integrated over the time period considered, to that of emitting 1 kg of CO_2. The GTP is the ratio of the temperature change at the end of the period considered caused by emitting 1 kg of the species at the end of the period considered compared to that caused by emitting 1 kg of CO_2. The GTP can therefore be used to predict future temperature changes from the emission of a species. There is substantial uncertainty in the values provided by these metrics, which is partly related to the uncertainty in the radiative forcings of the individual compounds (see Chapter 3 for a discussion on the uncertainties for BC radiative forcing). Bond and Sun (2005) quote 20- and 100-year GWPs for BC of 690 to 4 700 and 210 to 1 500 respectively. Jacobson (2010) calculates a different metric, surface temperature response per unit continuous emissions (STRE) which for BC has 20- and 100-years values of 1 230 to 1 960 and 790 to 1 250 respectively (having converted the STRE, reported relative to tonnes of carbon (C) rather than tonnes of CO_2, which must therefore be multiplied by 12/44 to obtain the STRE relative to CO_2 for appropriate comparison with GWP). Boucher and Reddy (2008) find that for BC the GTPs

at 20 and 100 years are reduced compared to the GWPs by factors of 3.5 and 7 since most of the temperature change occurs at the beginning of the period, although these factors are expected to be strongly dependent on the time scales for temperature response in the climate system. There is substantial controversy about the applicability of these metrics to very short-lived substances which is discussed further in Chapter 5.

It is not possible to calculate GWPs or GTPs for O_3 since it is not emitted directly. Instead these metrics can be calculated for emissions of O_3 precursor species. These species often have an impact on radiative forcing agents other than O_3 and their climate metrics need to take these into account (e.g. Collins *et al.*, 2002; Shindell *et al.*, 2009).

The 100-year GWP metric was chosen as the selection criterion for the measures investigated in this Assessment (see Chapter 5); their mean values and associated range of uncertainty are described in Table 4.1. As CO_2 emissions were largely unaffected, and hence all compounds were comparatively short-lived, using another time horizon such as 20 or 50 years would have little impact as all GWP values would change similarly.

Short-lived species may also induce longer-term climate changes through impacts on the carbon cycle. Collins *et al.* (2010) found that the ground-level O_3 formed from NO_x emissions damaged plants sufficiently for the

Table 4.1. Contribution to long-term climate objective (GWP100) chosen as selection criterion for measures based on literature ranges of GWP100.

	Mean value	Reference	Range	Reference
CO$_2$	1	IPCC (2007)		
CH$_4$	25	IPCC (2007)	16–34	IPCC (2007)
CO	1.9	IPCC (2007)	1–3	Range from AR3, cited in IPCC (2007)
VOC	3.4	IPCC (2007)	2–7	IPCC (2007)
BC	680	Bond and Sun (2005)	210–1 500	Bond and Sun (2005)
SO$_2$	-40	Fuglestvedt *et al.* (2009)	-24 – -56	Schulz *et al.* (2006)
OC	-69	Schulz *et al.* (2006)	-25 – -129	Bond *et al.* (2011)
NO$_x$	~0			

Note: The GWPs for CO and CH$_4$ include the indirect effects of O_3.

reduction in CO_2 uptake to compensate in global temperature change terms for the CH_4 destroyed by the NO_x. Mercado *et al.* (2009), however, suggest that aerosols contribute an additional climate cooling by increasing the efficiency of vegetation photosynthesis, thus removing CO_2 from the atmosphere (see also Section 4.5.4). A better understanding of these processes is crucial to inform the net direction of the effect on warming.

The importance of near-term climate mitigation becomes more significant when trying to reduce not just the magnitude, but also the rate of climate change, which is expected to peak in the next few decades (Raes and Seinfeld, 2009). The peak in the rate of climate change is due to the reduction of climate cooling pollutants (such as sulphate – SO_4^{2-}) that are being controlled directly or indirectly through air quality improvement measures. In order to counteract this short-term issue, policy measures would need to focus on controlling the short-lived warming species BC, O_3 and CH_4.

Future projections of the forcing from the changes in O_3, BC and other aerosols according to the 2030 reference scenario were discussed in Section 3.5. The temperature response to those changes, as well as to past and projected future CO_2 emissions, has been calculated through 2070 using global and regional temperature potentials (Shine *et al.*, 2005; Shindell and Faluvegi, 2010; see Appendix A.4). The results in Figure 4.1 and Table 4.2 show that under the reference scenario emissions, the Earth is projected to continue the rapid warming of the past several decades, with global mean temperatures rising another 1.9°C over the next 60 years. Most of this rise is due to CO_2 emissions, both future and past (committed change).
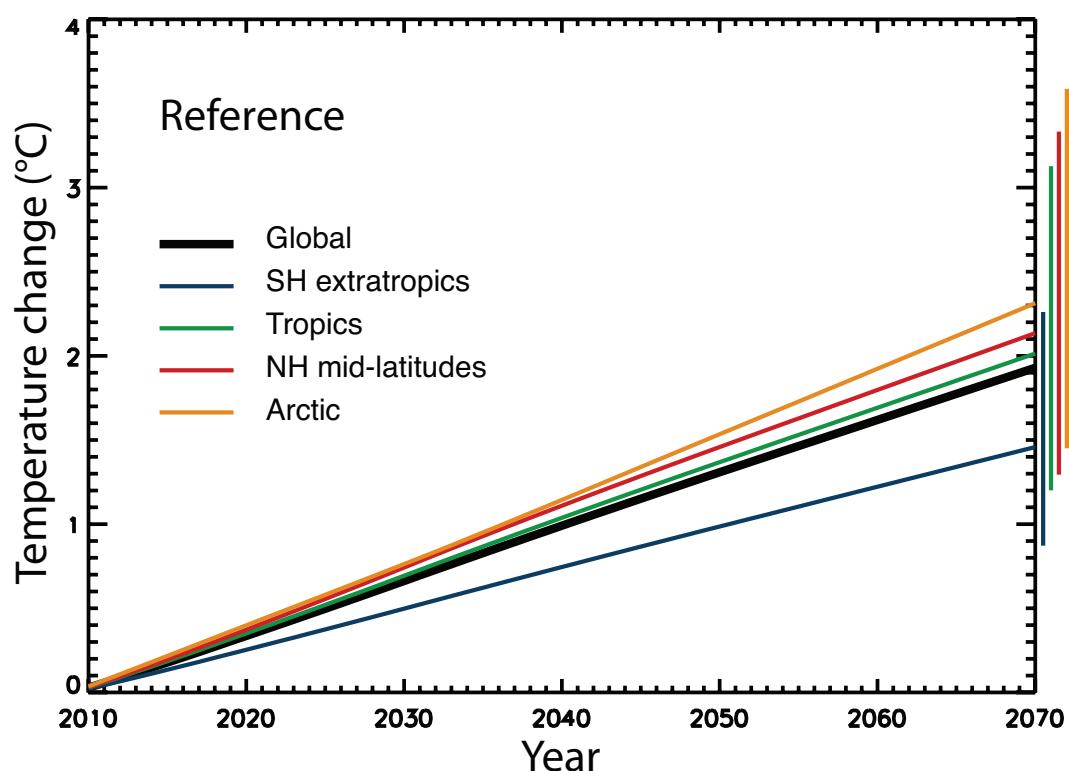
Figure 4.1. Global and regional temperature changes relative to 2009 projected under the reference scenario for different global regions (defined by latitude bands; see Table 4.2). Values are based on O_3, aerosol and CH_4 radiative forcings and responses in the GISS and ECHAM global climate models and also include forcings from both past and projected CO_2 increases. Bars on the right side of each plot give the range in temperature change at 2070 based on uncertainty in radiative forcing and climate sensitivity. Uncertainties for the period prior to 2009 are not shown for clarity, but have roughly the same proportion between regions to the temperature change ranges shown for the 2070 uncertainties. Most of the warming is due to CO_2; the contribution of SLCFs to this warming is shown in Figure 4.2. (SH=southern hemisphere, NH=northern hemisphere.)

Table 4.2. The change in temperature in °C due to SLCFs, O_3 and aerosols, CH_4 and LLGHGs from 2005 to 2030 for different latitude bands. The warming due to LLGHGs includes committed warming from CO_2 emissions prior to 2005. Emissions follow the reference scenario.

Forcing agents	Global	Southern hemisphere extra-tropics (28° to 90°S)	Tropics (28°S–28°N)	Northern hemisphere mid-latitudes (28°–60°N)	Arctic (60°–90°N)
SLCF	0.03	0.01	0.03	0.05	-0.04
SLCF+CH_4	0.06	0.03	0.06	0.08	-0.01
SLCF+CH_4+LLGHG	0.72	0.48	0.66	0.71	0.73

Changes in SLCFs involve both warming and cooling agents, with increases in some regions and decreases in others. Therefore, the central estimate of the net effect is small, although the uncertainties are large (see Figure 4.2 compared to Figure 4.1).

4.2.2 Impact on regional temperatures

While global mean temperatures provide some indication of climate impacts and their simplicity makes them widely used indicators, temperature changes can vary dramatically from place to place, even in response to forcing from long-lived greenhouse gases (LLGHGs) whose forcing is relatively uniform. This is because of differing regional response times (e.g. between land and ocean), differing feedbacks (e.g. retreating snow and clouds) and the influence of changes in atmospheric winds and ocean currents in response to forcing at the regional level. In the case of the short-lived climate forcing by aerosols and O_3, the forcing itself is also very unevenly distributed, and hence can cause even greater regional contrasts in the temperature response.

The global mean annual average temperature is useful, but often not sufficient for assessing impacts. While sea-level rise due to thermal expansion closely follows the time-evolution of this, most other impacts do not correlate so well. For forcing from CO_2, the regional effects and the effects on aspects of climate other than temperature can be related fairly well to the global mean temperature response. This is because the spatial patterns of the response of temperature, precipitation, etc., have been well-studied and these generally scale with the magnitude of the forcing. For example, the Arctic responds more strongly to CO_2 forcing than most other areas – the so-called polar amplification.

Early studies of the impact of regionally inhomogeneous radiative forcing found that at small scales of hundreds to thousands of kilometres responses are typically not closely correlated with the location of the radiative forcing (Taylor and Penner, 1994; Mitchell *et al.*, 1995). A substantial body of more recent work supports that conclusion, but also indicates that regional forcing from O_3 and aerosols can have an important impact on regional climate change (e.g. greater warming of the northern hemisphere than the southern hemisphere), distinct from that of quasi-uniform forcings (Hansen *et al.*, 2005; Shindell and Faluvegi, 2009; Stier *et al.*, 2006; Feichter *et al.*, 2004; Shindell *et al.*, 2008; Shindell, 2007; Levy *et al.*, 2008; Berntsen *et al.*, 2005; Boer and Yu, 2003; Chung and Seinfeld, 2005; Roberts and Jones, 2004; Jacobson, 2002; Kloster *et al.*, 2009). These studies, however, show that at larger scales the location of radiative forcing does influence the response. For example, the northern hemisphere response exceeds the southern hemisphere response when the northern hemispheric radiative forcing is greater.

More specific quantification of the influence of regional aerosol forcings indicates that they have a fairly strong impact on surface temperatures out to more than 10 000 km in an east-west direction, while in a north-south direction their influence is largely confined to areas within a few thousand kilometres (roughly 30° latitude) (Shindell *et al.*, 2010). These characterizations of the spatial rela-

tionship between forcing and response are robust across several independent climate models examined in that study.

In general, results suggest substantial temperature responses to SLCFs over northern hemisphere mid-latitude continents and also in the Arctic (see Section 4.2), based on both forward-looking model results and also results from detection/pattern-matching studies that use observations and models to assess historical conditions. Local responses to O_3 and aerosol forcing in polluted areas are generally larger relative to the global mean radiative forcing than the equivalent responses relative to the global mean radiative forcing from CO_2. Anthropogenic BC and tropospheric O_3 have made larger contributions to Arctic surface temperatures (estimated to be around 0.5 to 1.4°C and around 0.2 to 0.4°C respectively, according to Shindell and Faluvegi, 2009) since 1890 than they have to the global average (see also Section 4.2.1).The strong influence of meridional heat transport to the Arctic leads to substantial climate sensitivity there to forcing outside the Arctic (Boer and Yu, 2003; Shindell and Faluvegi, 2009).

Additionally, both O_3 and BC aerosols absorb solar radiation and thus heat the atmosphere, altering meridional circulation in ways that forcing from greenhouse gases or SO_4^{2-} does not. Thus for forcing in the Arctic, the climate response per unit TOA or surface radiative forcing for short-lived species can be quite different from the global mean response. Surface temperatures in the Arctic are strongly influenced by both local forcing and forcing at northern hemisphere mid-latitudes. As the latter is typically much greater, it can often play a more important role in driving Arctic climate changes for regionally uneven forcing (Shindell and Faluvegi, 2009). One climate forcing that is clearly local is the effect of BC on snow and ice albedo (darkening). This may have contributed around 0.1 to 0.2°C to 20th century warming in the Arctic (Flanner et al., 2007; Koch et al., 2009). Studies generally show a locally enhanced response to BC in the Arctic (Chung and Seinfeld, 2005; Roberts and Jones, 2004) though Jacobson's 2002 study does not. However, Jacobson's 2004 and 2010 studies both show strong surface warming over the Arctic due to BC.
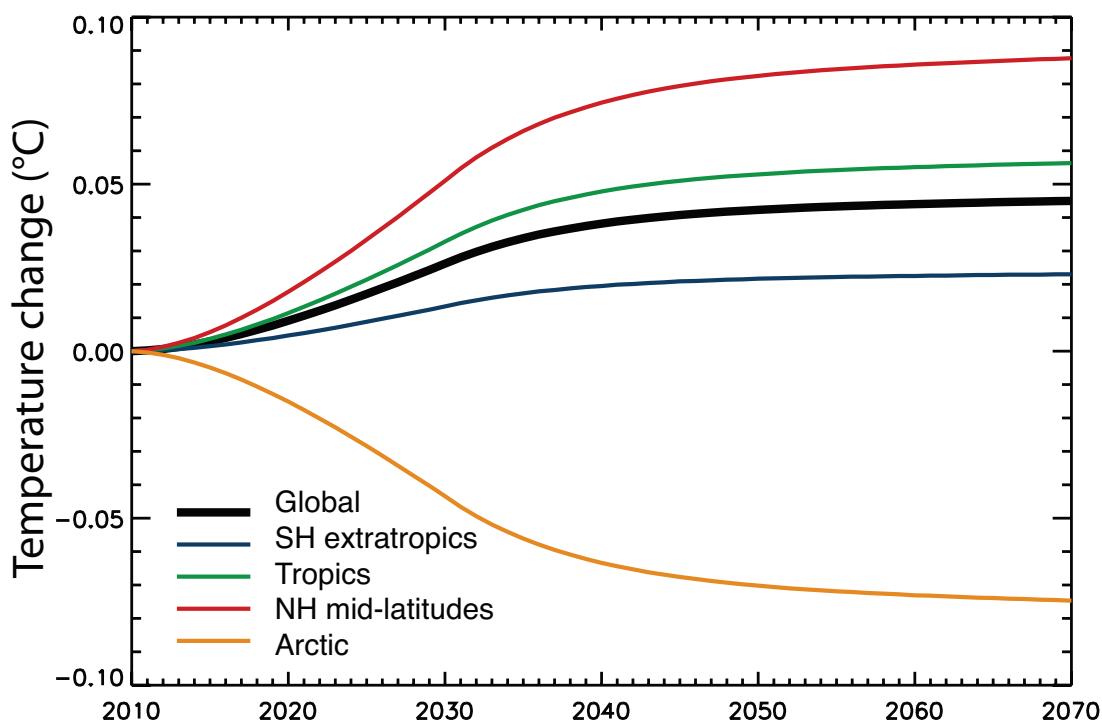
Figure 4.2. Warming in different latitude bands (see Table 4.2) due to O_3 and aerosols only following the reference scenario for emission projections from 2010 to 2030 and then assuming constant emissions at 2030 levels thereafter. (SH=southern hemisphere, NH=northern hemisphere).

Integrated Assessment of Black Carbon and Tropospheric Ozone

Box 4.2: Surface dimming and atmospheric BC heating over China and India

Field observations and semi-empirical (partially based on observations and partially on theory or models) studies (Ramanathan *et al*., 2001; also see Chapter 3, Section 3.3 of this Assessment) have revealed that present-day BC induces large dimming (10 to 20 W/m^2) at the surface over certain parts of the globe (Figure 3.9). This surface dimming, however, is smaller than the atmospheric solar absorption by BC, such that BC has a net positive radiative forcing at the TOA and has a net warming effect on the surface-atmosphere column. Observational studies conducted by scientists in China (see Ramanathan *et al*., 2008) and India (e.g. Babu and Moorthy, 2002; Satheesh, 2002) have also confirmed such large magnitudes of dimming. The annual mean surface dimming is of the order of 20 W/m^2. Since BC emissions over India and China have increased significantly over the last several decades, field studies imply that China and India should have witnessed large dimming trends, which indeed have been observed (Figures a and b below). The most direct consequence of the dimming is to reduce surface evaporation of moisture as shown by pan-evaporation data (Figure b).

a) Annual solar radiation over India reaching the surface (Kumari *et al*., 2007)
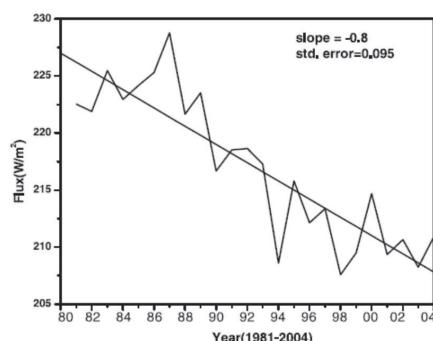
b) Annual departures of pan evaporation and solar irradiance for 1995-2000 for stations across China (Qian *et al*., 2006)
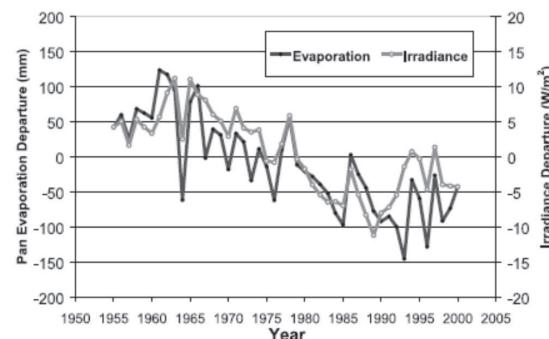
Atmospheric forcing by BC solar absorption has also been observed using unmanned aerial vehicles (Ramanathan *et al*., 2007; Ramana *et al*., 2010). These direct aircraft observations of BC over the Indian Ocean (caused by pollution from India) and the Western Pacific Ocean (caused by pollution from China) demonstrate enhanced background atmospheric solar heating by as much as 25 per cent. The dimming and atmospheric heating have important consequences for the monsoon rainfall and Himalayan glacier retreat, which are discussed later in this chapter.

The future radiative forcing changes between 2005 and 2030 from the reference scenario (Section 3.6) showed large heterogeneity with a positive forcing over the northern hemisphere mid-latitudes (particularly the USA and Europe), largely due to reductions in scattering aerosols, and a negative forcing over the tropics (particularly South Asia) due to increases in scattering aerosols. The forcings from CH$_4$ and O$_3$ changes are more homogeneous. The pattern of radiative forcing will manifest itself in an uneven surface temperature change. The resulting temperature changes are shown in Figure 4.2. These show a significantly larger warming in the northern hemisphere mid-latitudes (28 to 60°N) than the southern hemisphere extra tropics (28 to 90°S), with the tropics and the global mean lying between the two.

Changes in emissions of SLCFs or their precursors are expected to cool the Arctic through already legislated control measures for PM that have been implemented in North America and Europe. These should be important in controlling BC, especially for emission

sources such as diesel where BC makes up a substantial fraction of PM. The controls on SO_4^{2-} aerosol precursors on these two continents lead to increased warming in the northern hemisphere mid-latitudes, whereas growth in scattering aerosols over the Indian subcontinent reduces tropical warming. The homogenous forcing agents (CH_4 and LL-GHGs) are expected to warm the Arctic most. Hence overall, the dominance of CH_4 and the LLGHGs is expected to lead to a greater warming of the Arctic and lesser warming in the southern hemisphere extratropics. The fact that the Arctic cools in the SLCF+CH_4 case, despite the impacts of LLGHGs, emphasizes the sensitivity of the Arctic to changes in SLCFs. The more rapid warming of the northern hemisphere mid-latitudes than the southern hemisphere extratropics and the greatest warming in the Arctic are consistent with the historical record over recent decades. A more detailed discussion of climate effects in the Arctic is given in Section 4.3.1

The relatively low warming over the next 20 years from SLCFs and CH_4 compared to the LLGHGs seen in Table 4.2 is mainly due to counteracting effects. Emission controls in North America and Europe are expected to reduce both warming and cooling species, even while these are both expected to rise in comparison to the rest of the world. However, the control measures outlined in Chapter 5 would target only the warming species, giving scope for significant reductions in warming. In contrast, the warming from LLGHGs includes considerable committed warming which cannot be mitigated.

4.2.3 Impact on cloud cover and precipitation

Ozone and aerosols can influence many of the processes that lead to the formation of clouds and precipitation. They can alter overall surface temperature through radiative forcing, or directly change the radiation striking the surface, hence induce surface heating and affect evaporation. By absorbing sunlight in the atmosphere, they can change the vertical temperature structure of the air, altering convection and cloud formation. Aerosols can

also act as cloud condensation nuclei and ice nuclei, affecting the formation and concentration of cloud particles in both liquid and solid phases. They can change wind patterns by altering the regional temperature contrasts that drive the winds, influencing where rain and snow fall. Finally, the persistent existence of these rather locally-defined effects, when coupled with the large-scale circulation, can affect temperature, cloudiness and precipitation far away from the regions where the forcing was concentrated.

The impact of CO_2 forcing on water cycles has been studied (e.g., Held and Soden, 2006). Methane would induce precipitation responses similar to those caused by other well-mixed greenhouse gases. At the largest scales, these consist of enhancement near the equator, decreases in the subtropics, and enhancement at higher latitudes of both hemispheres. Short-lived climate forcers (e.g. O_3, and BC) are concentrated over source regions, mostly northern hemispheric land, and thus form a gradient in their radiative forcing distribution. It has been suggested in some studies (Rotstayn and Lohmann, 2002; Wang, 2004; Roberts and Jones, 2004; Ming and Ramaswamy, 2009; Chung and Seinfeld, 2005) that such a distribution causes shifts in tropical rainfall bands. This is consistent with modelling outcomes from idealized hemispheric forcing (Broccoli *et al.*, 2006; Kang *et al.*, 2008). Several detailed studies of the Asian monsoon suggest that regional forcing by absorbing aerosols substantially alters precipitation patterns (e.g. Meehl *et al.*, 2008; Ramanathan and Carmichael, 2008; Chung and Seinfeld, 2005; Wang *et al.*, 2009; Zhang *et al.*, 2009; see Box 4.3). Besides precipitation, these short-lived species could induce other regional changes, including to cloudiness and temperature. Such changes may be numerous, but are currently not well quantified.

South Asia has been studied relatively extensively in relation to impacts from BC. There is a suggestion that BC alters the timing and amount of monsoon precipitation, but results differ between models with and without a coupled ocean. Furthermore, models do not generally capture the intra-seasonal variability of monsoon systems well, so generally

106

perform rather poorly at simulating observed trends, making attribution to BC challenging. Recent theoretical advances suggest that convective energy is the most important process affecting the monsoon (Boos and Kuang, 2009). This supports model studies such as Wang *et al.* (2009) that find BC-caused changes in convective energy strongly linked to shifts in monsoon rainfall. The current modelling studies using a coupled atmosphere and ocean model suggest that BC forcing can cause an increase in pre-monsoonal rainfall followed by a decrease in monsoonal rainfall (Wang *et al.*, 2009; Meehl *et al.*, 2008; Ramanathan *et al.*, 2005). The studies conducted to date also suggest that the monsoon system response to BC forcing can occur over both the shorter (months to seasons) and longer term (years to decades); see Box 4.3. Therefore, the results from models using fixed sea-surface temperatures that tend to eliminate the latter long-term response must be interpreted very cautiously.

Evidence for an impact of BC on climate in China is even less robust. Menon *et al.* (2002) reported strong changes in precipitation over China (the southwest shift of precipitation in that model appears consistent with observations), but Liu *et al.* (2009a) found the opposite, and Meehl *et al.* (2008) found precipitation over China depended more on North Pacific conditions than Asian aerosols.

Black carbon can affect the formation and optical property of cloud through semi-direct and indirect effects. These concepts were introduced in Chapter 3 with discussion of contributions to radiative forcing. BC coated with inorganic acids or certain organic matters could have the same indirect effects as hygroscopic aerosols, that is to enhance cloud albedo or extend cloud lifetime, whereas the semi-direct effects can increase or decrease clouds depending on altitude (e.g., Johnson *et al.*, 2004). The overall impacts of aerosol and clouds on surface radiation global dimming and the consequences for agriculture are discussed by Stanhill and Cohen (2001) and Wild *et al.* (2005). Contributions of BC to this dimming are shown in Ramanathan and Carmichael, 2008 (see also Chapter 3, Sec-

tion 3.2 of this Assessment for further details of BC-induced surface dimming). In contrast, there has been little detailed analysis in the literature of the effects of O_3 on clouds and precipitation.

In conclusion, this Assessment has not yet been able to quantify changes in precipitation or clouds due to O_3 or aerosols, although there is confidence that changes in O_3 precursor and especially BC emissions will alter precipitation and clouds through changing large-scale heating patterns. Whilst there is also confidence that BC can affect cloud microphysics, the overall impact on local cloudiness and precipitation is not known. One major uncertainty regarding this issue is the impact of BC emissions on the number of cloud condensation nuclei (e.g., Chen *et al.*, 2010).

The global modelling studies performed for this Assessment (Appendix to Chapter 3) were run with fixed sea-surface temperatures and so cannot be used to diagnose changes in precipitation or clouds for the reference scenario or the suggested control measures discussed in Chapter 5 of this Assessment. In contrast to assessments of changes in surface temperature due to radiative forcing, there is no simple method of converting radiative forcing changes into precipitation or cloud changes (e.g., Wang, 2009).

4.2.4 Economic valuation of changes in global and regional climate

The economic costs of emissions of SLCFs can be roughly calculated by multiplying their emissions, expressed as GWP_{100} in CO_2 equivalents (CO_2e), by the social cost of carbon (SCC, see Tol, 2008). The implicit assumption is that a unit temperature change due to CO_2 emissions is equivalent to a unit change due to emissions of SLCFs. The shortcomings associated with this assumption include the fact that the warming effects from O_3 and BC have been much more in the northern than the southern hemisphere. Hence, these emissions will have a larger effect on crops, for example, because there is more land area in the northern hemisphere.

107

Box 4.3: BC and the Indian monsoon – a case study

The South Asian region has witnessed statistically significant trends in atmospheric and sea-surface temperatures, monsoonal circulation and rainfall since the 1950s. Over India, analyses based on rainfall data since early 1950 suggest that, in the last half-century, the frequencies of moderate and low rain days over the entire country have significantly decreased while the frequency and magnitude of extreme rain events have significantly increased (Goswami *et al.*, 2006; Dash *et al.*, 2009). Decreasing trends were also found in both early and late monsoon rainfall and the number of rainy days, implying a shorter monsoon over India (Ramesh and Goswami, 2007), accompanied by a fall in total rainfall of 5–7 per cent (Ramanathan *et al.*, 2005; Dash *et al.*, 2009). AR4 also shows that the drought severity index has increased over India. Another major trend is that the north-south gradients in the sea-surface temperature (SST) have weakened since the 1950s (Chung and Ramanathan, 2006). This is because the southern hemisphere tropical SST is warming at a faster rate than the northern hemisphere tropical Indian Ocean SSTs. Models with just the greenhouse forcing appear to be unable to account for many of these trends, except for the increase in intense rainfall.

Numerous modeling studies have explored the impact of BC and other man-made aerosols on the Indian monsoon system (Ramanathan *et al.*, 2001; Chung *et al.*, 2002; Ramanathan *et al.*, 2005; Lau *et al.*, 2006 and 2008; Meehl *et al.*, 2008; Randles and Ramaswamy, 2008; Collier and Zhang, 2009; Wang *et al.*, 2009; Krishnamurti *et al.*, 2009; Kumari and Goswami, 2010; Manoj *et al.*, 2010). While the qualitative and quantitative details may differ among them, these modeling studies conclude that BC radiative forcing is large enough to disturb or disrupt the Indian monsoon system and alter the precipitation patterns and amounts in a statistically significant manner. Though results from a single model should not be considered a reliable projection, they do illustrate the type of changes that can be expected due to strong regional aerosol forcing (Figure a). The model studies have also identified various mechanisms by which BC radiative forcing (solar heating of the atmosphere and the surface dimming) modifies the monsoon circulation and rainfall. These include altering the latitudinal gradient of the moist-static energy (sum of internal and thermodynamic energy) (Wang *et al.*, 2009), heating the elevated layers of the atmosphere (Lau *et al.*, 2006), change in the monsoonal circulation (Ramesh and Goswami, 2007; Krishnamurti *et al.*, 2009), decrease in surface evaporation (due to the dimming; Ramanathan *et al.*, 2005) and decrease in north-south SST gradient (Ramanathan *et al.*, 2005). The BC forcing is also attributed to an increase in pre-monsoonal rainfall followed by a decrease in monsoonal rainfall (Wang *et al.*, 2009; Meehl *et al.*, 2008; Ramanathan *et al.*, 2005). Another important impact identified by Wang *et al* (2009) is the northward extension of the monsoonal circulation due to the increase in moist static energy by BC solar heating of the boundary layer air. The relative importance of these various mechanisms requires further research (Lau *et al.*, 2008), but the studies to date suggest that the monsoon system response to BC forcing can be classified under a shorter-term (months to seasons) and a longer-term (years to decades) response. The shorter-term response involves the response of the atmosphere and the land surface to the BC solar heating of the air and surface dimming. The longer term involves the response of the coupled ocean-atmosphere system to the forcing by BC and other aerosols.
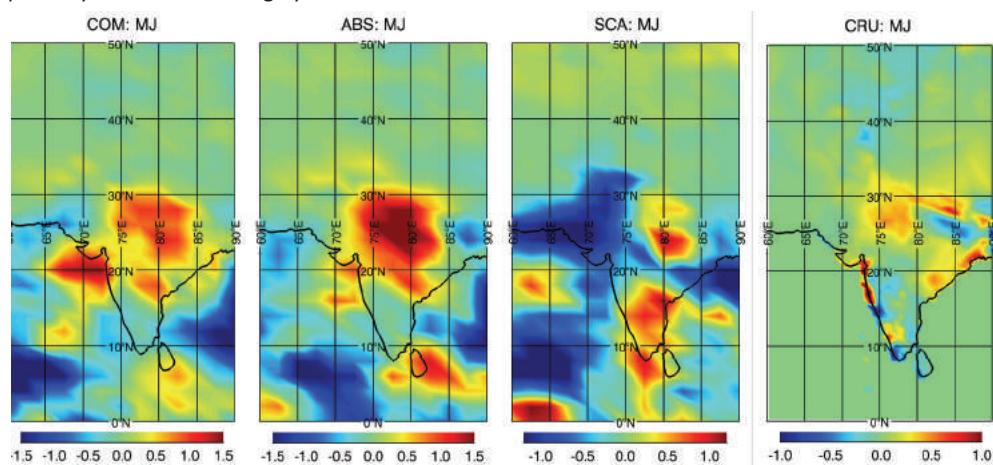
Figure a. May-June (MJ) average changes in convective precipitation (dm/season) derived from the model runs with: (1) both scattering and absorbing aerosols (COM); (2) only absorbing aerosols (ABS); and (3) only scattering aerosols (SCA) for India and surrounding regions. Also shown is the observed precipitation change (land-only; dm/season) derived from the data of the Climate Research Unit (CRU) at the University of East Anglia. Model results shown are based on 41-60 year mean differences with a reference run that excludes all aerosol effects. CRU results are derived from differences between 20-year means of 1981–2000 and 1946–1965, and based on the version 2.1 dataset with 0.5 degree. Aerosol levels were derived based on present-day emission estimations. (From Wang *et al.*, 2009).

For precipitation, effects are likely to be more spatially heterogeneous for BC than for well-mixed gases such as CO_2 or CH_4 because of strong local temperature gradients induced by BC and inter-hemispheric gradients induced by O_3 and aerosols. Highly regional effects in the Arctic or glaciated areas are also not captured using a global mean metric based on radiative forcing, which in addition does not encompass effects such as carbon fertilization, ocean acidification, etc. The application of existing Social Cost of Carbon (SCC) values for BC and O_3 emissions should be interpreted as conditional on the acknowledged analytical shortcomings of this approach. The intent, by using a range of values for the SCC, is to bracket the value of climate-related impacts of emissions (abatement) of BC and O_3 so as to inform potential abatement initiatives.

Table 4.3 estimates the valuation of global climate impacts associated with emission changes for different radiative forcing agents between 2005 and the 2030 projected according to the reference scenarios. For each pollutant, the GWP_{100} parameter is used (see Table 4.1 and Section 4.2.1) along with two values for the SCC. The first, US$265 per tonne of carbon (tC), represents the median of nearly 200 studies that employ a near-zero per cent discount rate. The alternative value of US$21/tC reflects the median for studies that employ a higher discount rate (3 per cent pure rate of time preference). Emission reductions in BC between 2005 and 2030 generate benefits that range between US$0.3 billion and US$4 billion in 2030. Abatement of carbon monoxide (CO) yields

climate benefits of between US$1.6 billion and US$20 billion. Methane emissions are projected to increase over the period 2005 to 2030. As such, greater climate impacts associated with CH_4 occur; damage increases to between US$184 billion and US$14.6 billion (shown as negative benefits in Table 4.3). NO_x emissions are projected to decrease between 2005 and 2030; because NO_x has a cooling effect, this emission decrease leads to a warming which yields decreased benefits valued between US$-22 billion and US$-1.7 billion. Benefits from emission changes of sulphur dioxide (SO_2) are valued at between US$3.2 billion and US$40 billion, while abatement of OC generates benefits of between of US$0.2 billion and US$3 billion. CO_2 emissions increase substantially generating negative benefits of between US$-75.6 billion and US$ -954 billion. In summary, the monetary value attributed to the reference scenario emissions changes is a substantial fraction of the economic valuation associated with improved human health (Section 4.3.3). When employing the lower SCC value of US$21/tC, the absolute value of emission changes declines by slightly more than one order of magnitude. Hence, the overall range produced by the application of the SCC values for GWP_{100} is between US$-1 090 billion and US$ -86.6 billion. For the case where GWP20 is applied (data not shown) the range is US$-1 377 billion to US$-109 billion. In summary, the monetary value attributed to the reference scenario emissions changes is a substantial fraction of the economic valuation associated with improved human health (Section 4.3.3).

Table 4.3. Valuation (in US$ billions) of BC, CO, NO_x, OC, SO_2, CO_2, and CH_4 emission changes between the Reference Scenario in 2030 compared to 2005.

SCC	Pollutant/GWP	BC	CH_4	CO	NO_x	OC	SO_2	CO_2	Total
US$265/tC	GWP_{100}	4	-184	20	-22	3	40	-954	-1 090
US$21/tC	GWP_{100}	0.3	-14.6	1.6	-1.7	0.2	3.2	-75.6	-86.6

All values expressed in (US$ billions for the year 2006).

Positive values reflect benefits of avoided climate impacts.

Estimates rely on GWP values reported in Boucher and Reddy (2008) for BC and OC and in Shindell *et al.* (2009) for gases.

109

4.3 Impacts in the Arctic, the Himalayas and other heavily glaciated areas

Regions with cryospheric cover are uniquely involved with climate change because of their capacity for large changes in surface reflectance in response to small changes in temperature, which in turn further influences temperature due to the snow/ice albedo feedback. Changes in the cryosphere may have important consequences for the availability of freshwater resources and subsequently human health as well as for ecosystems whose functionality requires ice or melted water. The sensitivity of cryosphere-covered regions to energy perturbations, combined in some cases with their proximity to anthropogenic emissions, facilitates a unique role for SLCFs. For example, snow and ice surfaces absorb more sunlight when darkened by BC deposition. Combined with atmospheric heating, this can increase snow and ice melt in regions such as the Arctic, Himalaya, Andes, Alps and Rockies. Additionally, the impact of BC sources is more powerful in these regions than elsewhere due to reduced cooling from co-emitted substances and more radiative forcing from deposited BC on reflective surfaces. These and other processes are explored further in the following sections.

4.3.1 Impacts of black carbon and tropospheric ozone in the Arctic

The Arctic has exhibited rapid environmental change in the last 30 years, including sea-ice loss (Serreze *et al.*, 2007). Warming in this region has been double the global rate, and has resulted in an accelerating loss of ice from the Greenland Ice Sheet (Velicogna, 2009; Rignot *et al.*, 2011). As discussed in Section 4.2.2, the Arctic is projected to warm more rapidly than the global mean under the reference scenario, and to be more strongly affected by changes in SLCFs. Arctic warming is of concern because:

i   Loss of sea-ice and seasonal snow cover reduces the planetary albedo because underlying surfaces (e.g., open water) are generally much darker. This constitutes a positive feedback process that amplifies warming.

ii   Melting of land-based glaciers and the Greenland Ice Sheet contribute to sea-level rise. Furthermore, retreating ice cover around Greenland leads to greater warming of shoreline ocean waters, which may contribute to increasing melt rates of glaciers that extend into them (Holland *et al.*, 2008). Surface meltwater on Greenland can also flow to the sub-glacial bedrock through moulins, lubricating ice flow and accelerating sea-level rise (e.g., Zwally *et al.*, 2002).

Short-lived climate forcing agents influence Arctic climate through several mechanism, as depicted in Figure 4.3 (Quinn *et al.*, 2008).

Aerosol impacts on the Arctic are complex and vary seasonally. Aerosol direct radiative forcing is important in summer when insolation is substantial, and tends to be more positive in the Arctic than elsewhere because of the pervasiveness of reflective clouds and ice. Any mixture of BC and OC exerts a positive radiative forcing over snow (Flanner *et al.*, 2009), even though OC likely exerts negative forcing globally. Aerosol-induced increases in cloud lifetime and optical thickness likely lead to cooling in summer, but warming in winter, through absorption of outgoing long-wave radiation when no incoming solar radiation is present. Furthermore, thin clouds have higher longwave emissivity when polluted (Garrett and Zhao, 2006; Lubin and Vogelmann, 2006), increasing net long-wave energy at the surface during all seasons. BC darkening of snow and sea-ice is also important when sunlight is present (Hansen and Nazarenko, 2004; Jacobson, 2004; Flanner *et al.*, 2007), and triggers greater equilibrium climate warming per unit of forcing than greenhouse gases or atmospheric BC. Although several studies have assessed the impacts of BC within snow on sea-ice, the influence of absorbing particles located within sea-ice is likely to be quite different and remains highly uncertain. Ozone concentrations are spatially heterogeneous and determined by numerous chemical and photochemical pathways. Ozone lifetime is sufficiently long for Arctic O_3 levels and subsequent radiative forcing to be strongly
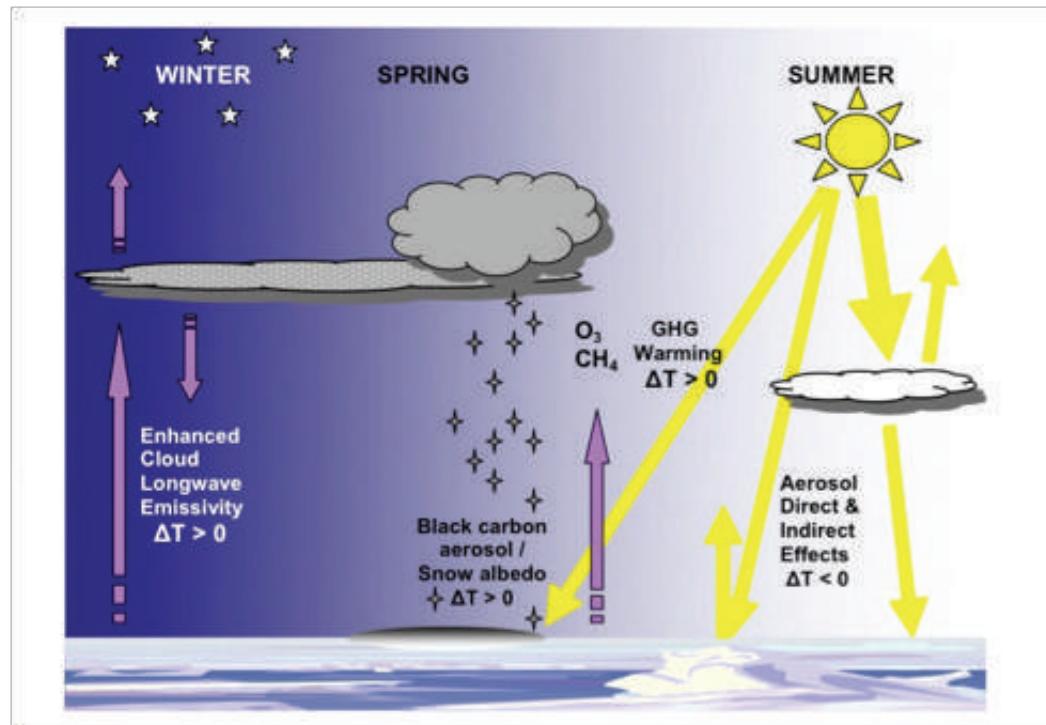
Figure 4.3. Arctic forcing by various processes (from Quinn *et al.*, 2008).

influenced by mid-latitude industrial O_3 pre-cursor emissions (Shindell *et al.*, 2006; Shindell, 2007).

Emission sources that are most likely to lead to transport of pollutants into the central Arctic include Northern European emissions (especially those during winter), and North American and Asian emissions that are uplifted outside the Arctic and descend within the Arctic (Koch and Hansen, 2005; Stohl, 2006). Source apportionment determined from positive matrix factorization (PMF) analyses of light absorbing carbon and co-emitted species measured in the Arctic snowpack indicate a dominant biomass contribution at most of the Arctic sites analyzed (Hegg *et al.*, 2009, 2010). Ice cores retrieved from central Greenland indicate that BC deposition peaked around 1910, and declined until 2000 (McConnell *et al.*, 2007), with the northeastern USA and Canada likely to have been the dominant source regions. Continuous measurements of BC in the near-surface atmosphere have been made since 1989 at Alert (Gong *et al.*, 2010) and Barrow (Sharma *et al.*, 2006), and since 1998 at the Zeppelin station above Ny-Ålesund (Eleftheriadis *et al.*, 2009). At all

three locations, the annual winter peak in BC has declined since the measurements began. Doherty *et al.* (2010) present more than 1 000 measurements of BC in Arctic snow collected in 2005 to 2009, showing systematically higher BC concentrations in eastern Arctic snow than in the western Arctic. Relative to a western Arctic survey conducted in 1983 to 984 (Clarke and Noone, 1985), the modern measurements show generally less BC, but the differences may not be statistically significant.

Observations of declining Arctic BC may challenge the notion that BC has driven recent Arctic warming. However, BC forcing must be considered in combination with greenhouse forcing. As more of the Arctic region approaches temperatures where melt can occur for longer periods of time during the year, more geographical area becomes vulnerable to incremental additions of forcing by short-lived pollutants. Although the magnitude of Arctic climate impacts from short-lived forcing agents remains unclear, pollutant sources that create proportionately large amounts of BC are very likely to induce warming, indicating that targeted BC reduction actions have the potential to slow the current rapid Arctic warming and

albedo feedback. Recently, Jacobson (2010), applying a model that includes numerous cloud-aerosol-gas microphysical processes, reported that eliminating all fossil BC/OC and biomass fuel BC+OC+GHG emissions would reduce Arctic warming by 1.7°C. Eliminating fossil BC+OC emissions alone would reduce Arctic warming by 1.2°C. However, climate feedback associated with aerosol heating in the Arctic is complex, and includes decreased meridional energy transport into the Arctic that offsets direct warming (Shindell, 2007); see also Section 4.2.1 of this Assessment. Mid-latitude forcing by BC can effectively warm the Arctic, and combined changes in BC and SO_2 precursor emissions were found to contribute substantially to Arctic warming from 1890 to 2007 (Shindell and Faluvegi, 2009). In an earlier study, the combined influence of O_3, CH_4 and BC on Arctic warming was found to be similar to the influence of CO_2 (Figure 4.4, Quinn *et al.*, 2008), although reflective aerosols produced a substantial cooling effect, again reinforcing the importance of considering co-emitted agents.

Although this section has focussed on the Arctic it is worth considering how these processes may manifest themselves in other parts of the globe. For example, the Antarctic Ice Sheet is experiencing growth in some high-altitude inner regions, but accelerated rates of loss in other regions, especially in western Antarctica, including the Peninsula (Bamber *et al.*, 2009). This is similar to the situation found in Greenland (Tedesco *et al.*, 2011; Chen *et al.*, 2006). Although Antarctica was once considered relatively pristine, sampling for aerosols has indicated some contribution of BC from human activity (Graf *et al.*, 2010).

4.3.2 Impacts on mountain glaciers

Annual changes in glacier mass depend on the balance between accumulation and loss. Mass sources include precipitation on the glacier in the form of snow or rain that subsequently freezes and deposition of frost from atmospheric water vapour. Loss includes the melting of ice and subsequent runoff, sublimation, and ice discharge from the glacier. The amount of ice melt is determined directly by

net energy balance, and indirectly by glacial dynamics that transport ice and liquid water. Most of the ice melt occurs at the glacier surface, and hence surface energy balance is critical for glacier mass balance. Net surface energy is determined by sensible heat exchange with the atmosphere, which is strongly influenced by surface temperature, latent heat flux determined by evaporation, condensation, sublimation, and deposition fluxes, net longwave radiative flux and net shortwave radiative flux. The two surface radiative flux terms are strongly influenced by cloudiness. Another key determinant of net shortwave flux is glacial albedo, which is controlled by several factors including snow grain size, the area and depth of melt ponds, debris cover, exposure of blue ice, and presence of absorbing constituents like black carbon, mineral dust, and biologically-active cryoconite (derived from wind-blown dust, algae and bacteria).

Most glaciers throughout the world are receding (e.g., Kaser *et al.*, 2006), with the exceptions of Himalayan glaciers that have heavy debris cover and those in some regions experiencing increased precipitation. Mountain glaciers in the western hemisphere are currently experiencing the greatest normalized loss rates (Figure 4.5). The Hindu Kush, Karakoram, Himalaya and Tibetan Plateau comprise the
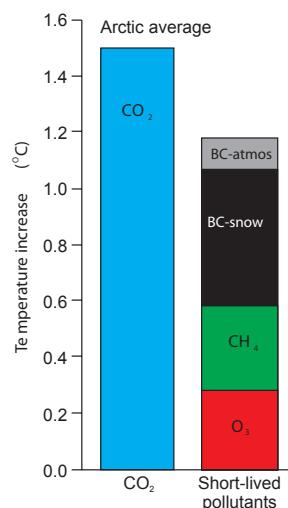
Figure 4.4. Estimated historic contributions to Arctic warming from CO_2 and from SLCFs. Reflective aerosols produced a substantial cooling effect (based on data in Quinn *et al.,* 2008).

112
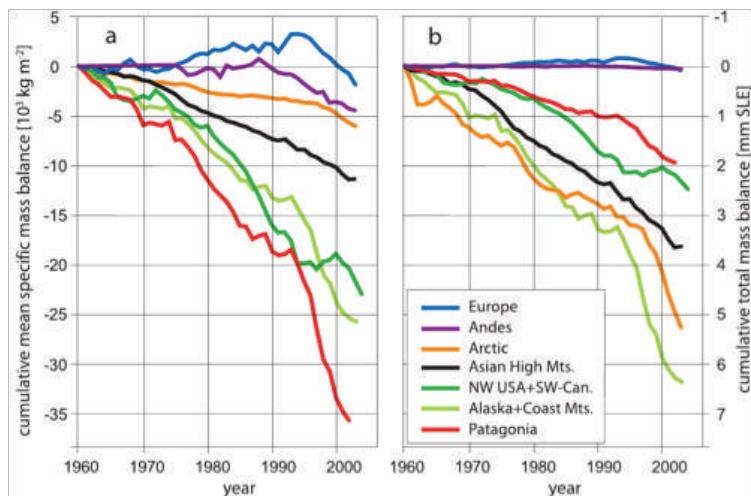
Figure 4.5. Time series estimates of glacier mass balance in different regions of the world (from Kaser *et al.*, 2006). Panel a shows mass balance normalized to the glacierized area in each region (specific mass balance), a measure of the relative response of each region, while Panel b shows change in total mass balance, reported in millimetres of sea-level equivalent (SLE).

Third Pole, holding the largest ice mass outside of the Arctic and Antarctic. A focus on this region is presented because of its importance as a source of freshwater to large populations, particularly in Pakistan, and because of its relative proximity to large emissions of BC. The total mass balance of these glaciers shows a substantial downward trend (Figure 4.5), although observations indicate faster decay rates in other parts of the world for 1961 to 2004 (Figure 4.5, Kaser *et al.*, 2006). Measurements of beta radioactivity in the Naimona'nyi Glacier in Tibet indicate that it has not experienced net accumulation of mass since at least 1950 (Kehrwald *et al.*, 2008). Remote sensing and GIS analyses of more than 5 000 glaciers in western China determined that more than 80 per cent of them retreated during the second half of the 20th century, with glaciers in the mountainous regions surrounding the Tibetan Plateau experiencing the greatest losses (Ding *et al.*, 2006). Measurements from the GRACE satellite instrument suggest the Asian high mountains lost about 47 Gt/yr of ice in 2003 to 2009 (Matsuo and Heki, 2010), higher than other estimates, but the analysis is complicated by uncertainty surrounding groundwater removal in northern India and tectonic uplift. Several studies attribute the retreat of Himalayan glaciers to rising air temperatures (e.g. Thompson *et al.*, 2003). Surface air warming has been greater in elevated levels of the Hindu Kush-Himalaya re-

gion (Liu *et al.*, 2009a; Ramanathan *et al.*, 2005; Gautam *et al.*, 2009b) and warming has been about 1.8 °C in the last 50 years on the Tibetan plateau (Wang *et al.*, 2008). Models are unable to capture the extent of observed warming in the Himalayan region without the inclusion of additional atmospheric warming resulting from BC concentrations (see Box 4.4).

Model simulations indicate that BC may be responsible for approximately 0.6°C warming in the Himalayan-Tibetan Plateau since the 1950s (Chung and Seinfeld, 2005; Ramanathan *et al.*, 2007; Ramanathan and Carmichael, 2008). Flanner *et al.* (2009), using a model that includes the effect of BC deposition as well as atmospheric heating, estimate that BC and co-emitted OC contribute to as much spring warming and snow melt in Eurasia as anthropogenic CO_2. As discussed in Section 4.2.3, modeling studies also suggest that absorbing aerosols could cause a shift of the Indian summer monsoon precipitation towards the foothills of the Himalaya (e.g., Lau *et al.*, 2006; Meehl *et al.*, 2008; Randles and Ramaswamy, 2008; Collier and Zhang, 2009; Wang *et al.*, 2009). However, due to the well-known limitation of current GCMs in simulating monsoon variability and detailed aerosol-cloud interactions, changes in monsoon precipitation, which also influence the glacial mass balance, cannot yet be

113

Box 4.4: Anomalously large warming over the Himalayas

Surface observations as well as microwave satellite data reveal that the elevated regions over South Asia and East Asia, particularly the Himalayan-Tibetan region, have warmed much more than the surrounding land areas (at sea level) over the last four decades (Figure a).

a) Elevation dependency of surface temperature trends over Tibet from 1961 to 2006. Liu *et al.* (2009b)
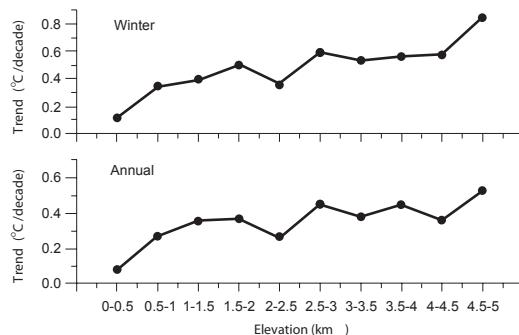
b) Differential temperature trends between the troposphere (T_t) and the surface (T_s) temperature for India: blue: microwave observations; green: simulated (with the NCAR Community Climate Model 3) with just CO_2 and SO_4^{2-}; red: same as green but with BC and OC. (Ramanathan *et al.*, 2005.)
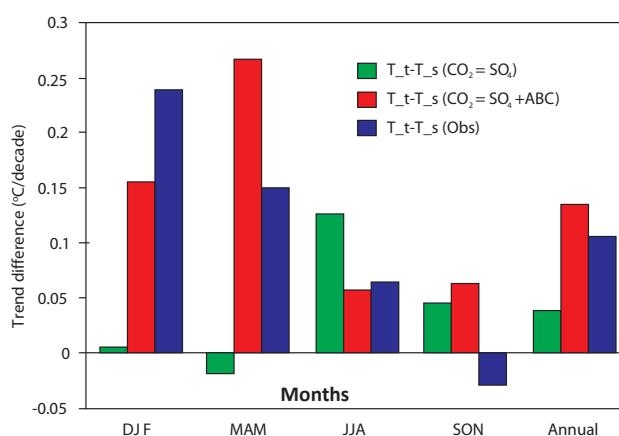
N.B. Positive values for T_t and T_s show that the atmophere is warming more than the surface, hence Figure (b) shows that the much larger warming of the atmosphere compared with the surface warming over India can not be explained by just the increase in CO_2 and SO_4^{2-}; inclusion of BC and OC in the model improves the simulated trends thus suggesting that BC and OC plays a significant role in warming the elevated atmospheric layers.

Surface temperature data over Tibet (Figure a) show warming trends of 0.4°C or more per decade above 3 km in elevation. While microwave data have limited vertical resolution, it also reveals that the tropospheric warming trend (averaged over India) is larger than the surface warming trend by 0.1 °C/decade (see annual mean bars in (Figure b); also see Gautam *et al.*, 2009) and the differential warming trend is particularly large during the dry season (December to May), when atmospheric concentrations of BC and OC reach peak levels. GCM studies with just greenhouse gases and sulphate aerosols (green bar, Figure b) are unable to simulate the observed warming (blue bar) of the elevated regions. Satellite Lidar data (CALIPSO instrument) (Ramanathan *et al.*, 2007) show that the Himalayas are covered by a 3 km-thick dense layer of aerosols. Direct measurements of solar heating of this layer by BC (and some dust) have been made with unmanned aircraft, and when these data are included in a general circulation model, the model simulates (red bar) large differential warming trends (Ramanathan *et al.*, 2007).

Box 4.5: Estimation of BC deposition from data collected at the Nepal Climate Observatory-Pyramid (NCO-P) and possible snow albedo changes over Himalayan glaciers during the pre-monsoon season (Yasunari *et al.*, 2010)

Nepal Climate Observatory-Pyramid (NCO-P) is located at 5 079 m above sea level in the Everest Region, Nepal. The study applied atmospheric aerosol measurements to estimate a BC deposition rate at NCO-P of 2.89 µg/m^2 per day during the pre-monsoon season (March-May). Assuming this BC deposition is distributed uniformly within a pure 2 cm surface snow layer, this deposition would produce a snow concentration of 26.0 to 68.2 µg BC per kilogram of ice (depending on a range of snow densities measured at Yala glacier, central Nepal). This range of BC concentrations could induce snow albedo reductions of 2.0 to 5.2 per cent. Assuming these albedo reductions persisted throughout the year, glacier mass balance modelling indicates that annual melt runoff could increase by 70 to 204 mm (equivalent to 11 to 34 per cent of the annual discharge of typical glaciers in this region). Although this analysis applies only to certain conditions (e.g. debris-free glaciers), it does indicate that BC could influence glacier melt, and also highlights the need to study BC-induced albedo reduction in combination with dust and other absorbing impurities.

reliably attributed to BC aerosols or BC-dust mixtures. Yasunari *et al.* (2010) applied observations of atmospheric BC concentrations from the NCO-Pyramid station in Nepal to determine potential pre-monsoon snow albedo changes (see Box 4.5). Extending these estimates to potential glacier impacts, they concluded that runoff could be increased by $11 - 34$ per cent because of local BC deposition.

Observational data from ice-cores shows the history of BC deposition onto the Himalaya-Hindu-Kush during recent decades

Box 4.6: Glacial lake outburst floods

In large parts of the Hindu Kush – Himalaya (HKH) region, glaciers are thinning and retreating as a result of climate warming, leading to the creation of many glacial lakes (Mool *et al.*, 2001). Glacial lakes are potentially unstable because their end moraines are composed of unsorted and unconsolidated boulders, gravel, sand and clay. Furthermore, they are frequently reinforced by frozen cores (permafrost) that, like the glaciers themselves, are now beginning to melt. As the volume of a lake that accumulates behind an end moraine increases, hydrostatic pressure builds up to put additional stress on the moraine dam causing it to become more unstable. Due to several causes, it may fail and release much or all of the lake water. Depending on the manner in which the dam fails, the ensuing outbreak can be sudden and highly dangerous to people and infrastructure located downstream. The surging flood water, a glacial lake outburst flood (GLOF), will often have the energy to entrain large masses of loose material (boulders, gravel, sand, and clay, as well as any broken masonry or torn out trees) as it is propelled down-valley.
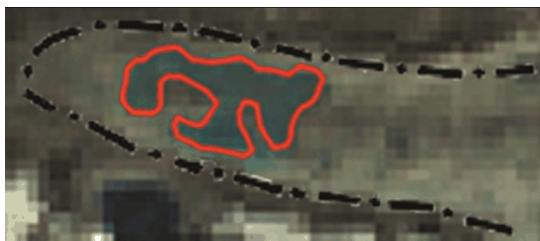
Land Sat MSS of 1975: development of a glacial lake at the tongue of Imja glacier in Dudh Koshi basin of Nepal
Source: (Ives *et al.*, 2010; ICIMOD, 2011)
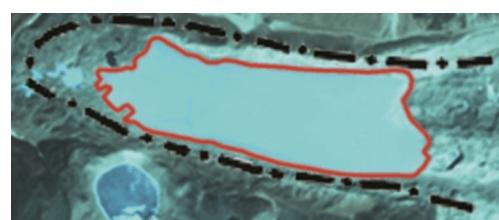
ALOS, AVNIR-2 March 2009: growing Imja glacial lake in Dudh Koshi basin of Nepal

115

(Xu *et al.,* 2009) (see Figure 4.6). BC deposition decreased in northern areas (downwind from Europe) from the 1970s to 1990s, but increased post-1980s in southern areas (downwind from South Asia). The latter change is coincident with increased glacial melt, but needs to be considered together with other agents causing melt (e.g. GHGs) and increased melt rates that have also been seen in other parts of the world not subject to strong BC deposition. For example, Asian glaciers have seen a 33 to 38 per cent increase in glacier melt runoff over the past few decades (Singh and Kumar, 1997). However, these changes are extremely similar to stream-flow changes in the western USA (Barnett *et al.,* 2005). Additionally, it is difficult to reliably gauge the effect of BC on albedo for debris-covered glaciers, which make up the majority of glaciers in this region (pers. comm. J. Srinivasan, 2010). Ming *et al.* (2008), analyzing an ice core from Mt. Everest, found increasing BC deposition since 1990.

Observations also indicate that glacier lakes are forming and expanding in the entire Third Pole region. They are being formed in front of the retreating glaciers and dammed by potentially unstable glacial moraines. In the case of moraine dam failure, a glacier lake outburst flood (GLOF) would result, posing danger to lives, livelihoods and infrastructure, including hydropower plants constructed recently on Himalayan rivers (see Box 4.6).

4.4 Uncertainties in climate impacts of BC sources due to co-emitted OC

Efforts to mitigate BC will reduce concentrations of BC as well as OC. The warming effect of BC and the compensating cooling effect of OC introduce large uncertainty in the net effect of any BC mitigation of global warming (see Appendix A.4). This uncertainty is particularly large for mitigation options that focus on biomass cookstoves and open biomass burning and smaller for those that focus on fossil fuels (i.e. diesel) because biomass combustion emits significantly more OC compared with fossil fuel burning.

On the other hand, the regional impacts, such as the impacts on the tropical rainfall, monsoon and snow-ice melting, of BC mitigation options are largely independent of their impact on global warming. In fact, biomass cookstoves and open biomass burning can have much larger effects than fossil fuels regionally. This is because BC directly increases atmospheric heating by intercepting sunlight, while OC reflects sunlight and contributes to dimming at the surface – a reduction of sunlight at the ground. It is this simultaneous atmospheric heating and surface dimming that leads to the impacts on the monsoon and tropical rainfall estimated by numerous published studies. The same conclusion applies to the impact of BC mitigation on snow and ice though for a slightly different reason; here BC, because it is much darker than snow and sea ice, significantly increases absorption of sunlight when it is deposited on these bright surfaces. OC that is deposited along with BC has very little effect on sunlight reflected by snow and sea ice since these surfaces are already very white.

4.5 Impacts on human health

Over the last two decades a substantial body of evidence has developed demonstrating that exposure to fine particles in the air is associated with early death. BC can form a substantial fraction, up to 15 per cent of the PM burden (see Chapter 3). More recently, health effects resulting from O_3 exposure have also been documented. This section briefly reviews this evidence describing PM (including BC) and O_3 impacts on human health, focussing on mortality but also considering morbidity. A methodology to assess mortality related to PM and O_3 is described with reference to supporting published literature. This methodology is applied within this Assessment to estimate changes in impacts on health from 2005 to 2030 according to PM and O_3 concentrations attributable to changes in emission under the Assessments reference scenario. Health impacts are quantified according to two different indices that describe the change in annual deaths and the years of life lost. The results are placed in the context of other published studies on consideration of variations in
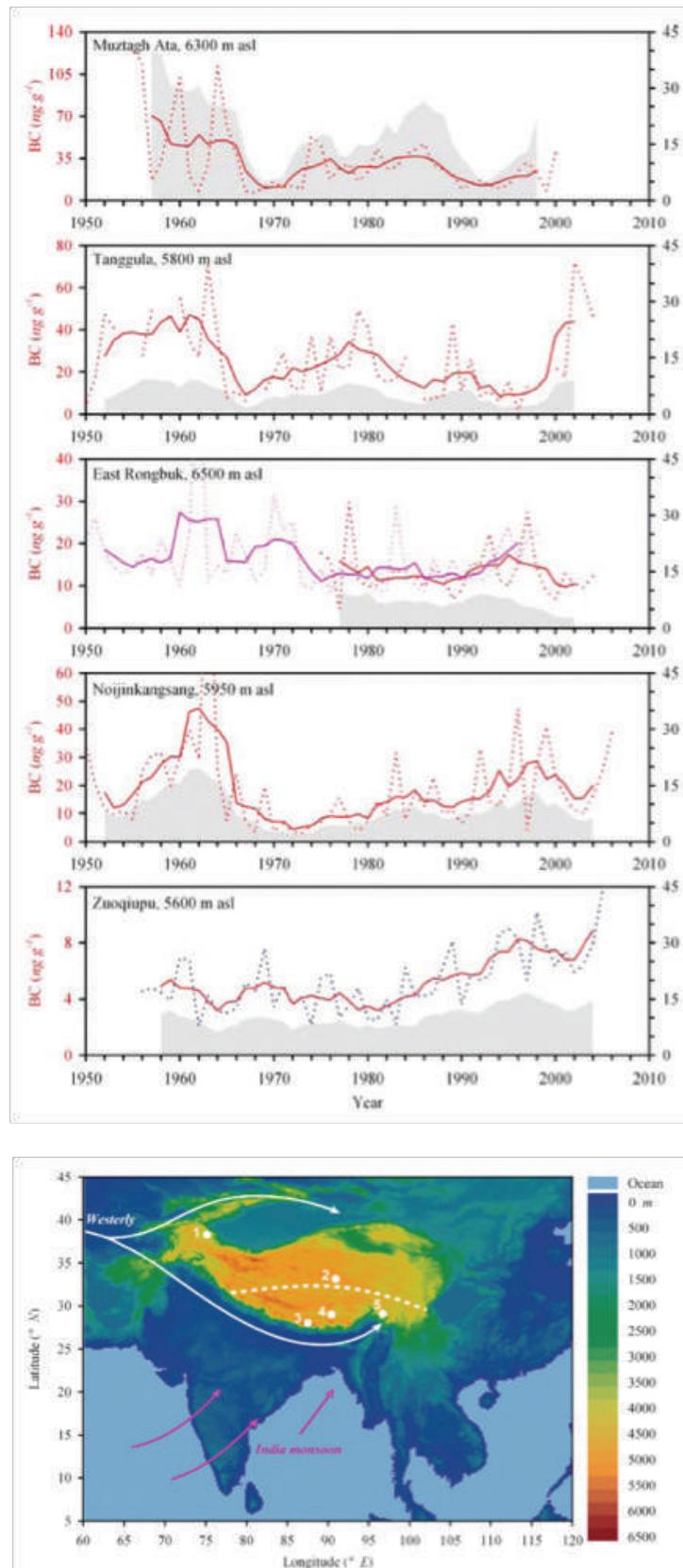
Figure 4.6. Observational data from ice-cores shows the history of BC deposition to the Hindu Kush – Himalaya region during recent decades (top). Ice core locations and atmospheric transport pathways are shown in the bottom figure (Xu *et al.*, 2009). The dotted line indicates a rough boundary between areas where transport is predominantly from the north (poleward of the line) or south (equatorward of the line).

117

methodological approach and associated uncertainties. The impacts on human health are also considered in economic terms based on valuation of measures that reduce the risk of early death (assuming both a single value and a GDP varied value of risk). These estimates are then placed in the context of other valuation methods and published studies; in this qualitative assessment the effects of morbidity are also considered.

It is also acknowledged that BC and O_3 will have indirect effects on human health through climate change. Numerous studies have demonstrated that both cold and hot weather are associated with increased deaths. However, these studies have demonstrated substantial heterogeneity in health effects by location. For example, Braga *et al.* (2001) showed no heat related mortality in Houston, Texas. Rather, they found that the amount of air conditioning and variability of summer time temperature, among other factors, appeared to explain much of the heterogeneity in health impacts. Given this heterogeneity, the uncertainty as to the factors that determine the response to changes in temperature, and the relative paucity of studies in the developing world, this Assessment has not tried to quantify these indirect effects of temperature change. Instead it discusses what we believe are the most important issues that might affect climate induced vulnerability related to human health.

There is clear, convincing evidence that PM is not merely a nuisance darkening the skies. It kills people. These conclusions are not due to failure to exclude other possible explanations. Similar PM associations are seen when other pollutants and weather are considered as well as pre-existing disease, smoking, etc. Moreover, animal and toxicological studies show changes in intermediary endpoints (e.g. electrocardiogram patterns, measures of inflammation, blood pressure) that are consistent with the changes seen in the epidemiologic studies (Baja *et al.*, 2010; Madrigano *et al.*, 2009; Kleinman *et al.*, 2008; Tamagawa *et al.*, 2008; Delfino *et al.* 2008; Puett *et al.* 2008; Maynard *et al.* 2007; Pope *et al.* 2007; Hoek *et al.* 2002; Katsouyanni *et al.* 1996). The conclusion that PM kills people has

been endorsed by World Health Organization (WHO), the US EPA and the European Union in separate scientific reviews.

Recent studies have examined the relation of changes in PM levels to change*s* in mortality (Pope *et al.*, 2009; Schindler *et al.*, 2009; Schwartz *et al.*, 2008; Zanobetti *et al.*, 2008; Pope *et al.*, 2007; Zanobetti and Schwartz, 2007). They have demonstrated that reducing PM levels prolongs lives, and the more recent studies have shown those benefits occur within a few years of the reductions. This is quite important for benefit analysis, since it indicates little need for discounting benefits because of time lags. Two important studies resulting from natural experiments, where labour strikes at a copper smelter in the Southwestern states of the USA and a steel mill in Utah resulted in sudden drops in PM concentrations, which were restored when the strikes ended, demonstrated those drops were associated with lower mortality rates, which went back up when the industrial pollution resumed (Pope *et al.*, 1992; Pope *et al.*, 2007). Finally, another two studies found that year-to-year changes in particle levels within cities related to year-to-year changes in mortality rates (Zanobetti *et al.*, 2008; Zanobetti and Schwartz, 2007). This is important because such findings cannot be due to differences between cities in other unmeasured risk factors.

4.5.1 The impact of outdoor particulate matter on human health

The measures proposed in Chapter 5 will lower PM, but are targeted at particularly lowering BC. There are two major issues in doing a human health risk assessment to assess the benefits of these PM reductions. First, most of the literature reports concentration-response functions (CRFs) between $PM_{2.5}$ and all cause mortality, not BC. Second, most of the literature describes human health impacts of PM (and by association BC) at concentrations prevalent in developed countries while exposures in developing countries are much higher. This raises questions about the extrapolation of the CRFs.

The first issue has more data on which to assess its importance. In developed countries, BC

primarily arises from diesel particles, and secondarily from four-stroke motorcycle engines although there are local variations in sources of BC (e.g. wild fires can contribute significantly at certain locations). As such, BC tends to be traffic derived and there is an extensive amount of literature on the health effects of particles generated by traffic. There is a modest, but growing, volume of literature on the effects of BC itself on mortality. For example, Maynard *et al.,* (2007) looked at the acute effects of exposure to BC in homes (based on a validated land use regression model) to mortality. They reported an effect size for BC that was roughly twice that reported for the acute effects of $PM_{2.5}$ in 112 US cities (Zanobetti and Schwartz, 2009). This suggests that, at least for acute responses, a 1μg/m³ increment in BC is worse than a similar increment in all fine particles.

Regarding long-term exposure, a recent case-control study looked at exposure to BC at homes and the incidence of heart attacks, and reported an association (Tonne *et al.,* 2009). Another study looked at survival of patients after being discharged alive following a heart attack, and again reported a strong association with BC exposure at home (von Klot *et al.,* 2009). In contrast, a recent re-analysis of the American Cancer Society (ACS) study found that there was an effect of BC, generally measured at a single monitor in the metropolitan area, and survival, but this was very sensitive to covariate selection (Smith *et al.,* 2009). However, BC shows much greater spatial heterogeneity than $PM_{2.5}$, and so the measurement error due to the use of only a single monitor for an entire metropolitan area is very high; this problem was also observed by Park *et al.,* (2008). In contrast, the two previous studies used BC concentrations estimated at each subject's home, based on a validated model. How much measurement error matters can be seen from a recent paper using the California Teachers' cohort (Ostro *et al.,* 2010). When Ostro restricted his analysis to subjects living within 8 km of the monitor, the reported effects of PM on all causes of mortality were significant. When the analysis was repeated using subjects living within 30 km of the monitors, differences were not significant, and slope of the CRF was attenuated ten-fold.

The ACS study includes subjects living much farther from the monitors. This suggests that measurement error is a major issue in the ACS BC study, and Ostro *et al.* (2010) provides a better estimate of the CRF.

Traffic has been used as a surrogate of exposure to traffic particles in numerous studies. For example, a study of acute exposures recently reported that being in traffic in the last two hours substantially increased the risk of a heart attack (Peters *et al.,* 2004). A study of survival of congestive heart failure patients found independent effects of traffic within 100 m of the home and distance to bus routes on life expectancy (Medina-Ramon *et al.,* 2008). Black carbon has also been associated with shortened survival in a Dutch study (Hoek *et al.,* 2002).

Indirect support for the view that BC has worse than average toxicity than other fine particles comes from studies that looked at other health outcomes. For example, in relation to $PM_{2.5}$, BC was more strongly associated with blood pressure (Lundback *et al.,* 2009; Mordukhovich *et al.,* 2009; Zanobetti *et al.,* 2004), more strongly associated with markers of the thickening of artery walls (atherosclerosis) (Madrigano *et al.,* 2009; Park *et al.,* 2008; Hansen *et al.,* 2007), more strongly associated with electrocardiogram changes that are risk factors for arrhythmia (abnormal electrical activity of the heart) (Zanobetti *et al.,* 2009), more strongly associated with electrocardiogram changes that are risk factors for ischemia (restriction in blood supply) (Chuang *et al.,* 2008; Gold *et al.,* 2005), and finally more strongly associated with changes in DNA methylation (Baccarelli *et al.,* 2009).

Based on the above, it is reasonable to conclude that traffic derived BC is, if anything, more toxic than might be expected for $PM_{2.5}$ as a whole. However, it is important to realize that BC is a surrogate for all of the particle mass that comes from diesel in one instance, and the particle mass that comes from household combustion in the other, and the fellow traveller particles are different in these cases. So it is important to ask separately about the evidence for household derived BC. Here the evidence is weaker,

although it is clear that biomass combustion increases the risk of respiratory disease (Samuelsen *et al.*, 2008; Dherani *et al.*, 2008; Smith *et al.*, 2000; Lipsett *et al.*, 1997). Recently, a randomized trial of a chimney stove intervention in Guatemala was shown to reduce blood pressure (McCracken *et al.*, 2007). Since blood pressure is a major risk factor for cardiovascular mortality, this provides support for the association of BC from such combustion and mortality.

Given the evidence that traffic-related BC is more toxic than average, and the weaker evidence on the relative toxicity of biomass particles, this Assessment has chosen to assume that BC particles are associated with average risks. Combined with the substantial fraction of the $PM_{2.5}$ reductions from the proposed interventions that are not BC, it is justifiable to use the literature on $PM_{2.5}$ to derive a concentration-response relationship between changes in long-term exposure to all types of $PM_{2.5}$ and mortality. Again, this is the scientific consensus. The US EPA's Scientific Advisory Board recently recommended that the agency treat all particles as equally toxic, as the evidence for using differential toxicity in risk assessment was not strong enough. This is consistent with prior findings by WHO and the findings of the long-term studies that that looked at BC (von Klot *et al.*, 2009; Smith *et al.*, 2009).

4.5.2 The impact of ozone on human health

While studies have reported adverse health responses to O_3, a highly oxidizing gas, for decades, reports that O_3 exposure might hasten deaths have been more recent. The first large-scale report came from Europe, where seven cities were studied using identical methods and the O_3-mortality concentration response results combined (Touloumi *et al.*, 1997). A significant association was found. Since then a number of other studies have reported similar results in both the USA and Europe, including three large meta-analyses commissioned by the US EPA (Bell *et al.*, 2005; Levy *et al.*, 2005; Ito *et al.*, 2005). Moreover, a large multi-city study has found no evidence of a threshold for O_3-mortality; effects were found to occur

down to 24 h mean concentration of 20 ppb (Bell *et al.*, 2006). In addition, some studies indicate that the effects of O_3 might interact with the effects of heatwaves (Filleul *et al.*, 2006; Ren *et al.*, 2008).

Further evidence has demonstrated that these associations are not confounded by temperature (Schwartz, 2004) or secondary particles (Franklin and Schwartz, 2008), and are not due to harvesting (the bringing forward of deaths by just a week or two) (Zanobetti and Schwartz, 2008). More recently an analysis of the ACS study has also demonstrated an association between long-term O_3 exposure and life expectancy in a cohort. A related econometric study looked at year-to-year deviations of O_3 concentrations from their trend and year-to-year deviations in mortality rates in all municipalities in England, and found a significant association (Janke *et al.*, 2009). Not only does this support the ACS finding that long-term exposure matters, it suggests, as with particles, that there is no long delay.

Other related studies have reported that O_3 was associated with oxidative stress in the lung (Romieu *et al.*, 2008), with growth of lung function in children (Rojas-Martinez *et al.*, 2007), systemic inflammation (Chuang *et al.*, 2007), and with arrhythmia (Sarnat *et al.*, 2006).

Since the ACS study is the only published investigation of the effects of longer-term O_3 exposure on mortality, and the effects of longer-term exposure are greater than those of short-term exposures this Assessment has taken that study for our effect estimates. This is consistent with other recent assessments (Smith *et al.*, 2009; Anenberg *et al.*, 2010). In addition, modelled estimates of longer-term O_3 concentrations have lower uncertainty than estimates of daily concentrations.

4.5.3 The impact of indoor particulate matter on human health

Acute lower respiratory infections (ALRI), mainly in the form of pneumonia, remains the most important cause of death among children under five years (Bryce *et al.*, 2005).

Epidemiological evidence from observational studies suggests that indoor air pollution (IAP) exposure from solid fuel use is an important risk factor for pneumonia (Dherani *et al.*, 2008; Smith *et al.*, 2000; Bruce *et al.*, 2000; Smith *et al.*, 2004). A recent WHO risk assessment (WHO, 2009) estimated 1.6 million premature deaths in 2000 due to respiratory diseases associated with indoor exposure to smoke from solid fuel use (both biomass and coal). Although increased cardiovascular disease (CVD) is the most important health effect of both ambient air pollution and second-hand tobacco smoke exposures, the WHO burden of disease estimates for biomass fuel smoke did not include cardiovascular disease because of a lack of epidemiologic studies. Hence these estimates are likely to be low.

As a component of the WHO Comparative Quantification of Health Risks project (Chapter 18), Smith *et al.* (2004) combined data from a total of 93 countries based on demographic and health surveys, the WHO World Health Survey, national censuses, and other sources. For 36 countries with no household solid fuel use data, the proportions of households using solid fuels were predicted based on gross national income, percentage of the population that is rural, and whether the country was located in the Eastern Mediterranean region. According to this assessment, 52 per cent of the world's population (over 3 billion people) depend on solid fuels (such as fuel wood, coal, cow dung, etc.), ranging from 77 per cent in Sub-Saharan Africa and 74 per cent in both Southeast Asia and the Western Pacific, to 36 per cent in the Eastern Mediterranean region and 16 per cent in both Latin American and the Caribbean and in Central and Eastern Europe. This suggests that reducing emissions from indoor cooking will produce direct health benefits for this approximately 50 per cent of the world's population that depend on solid fuel.

Recently McCracken and Schwartz (2009), in a report to the US EPA, have used the effects of biomass smoke on blood pressure to estimate the premature adult mortality due to cardiovascular disease. Their estimates are of 237 000 deaths per year, worldwide, which are in addition to the respiratory deaths estimated above.

4.5.4 Estimating the impact of indoor particulate matter on human health for the reference scenario

Because the selected measures evaluated in this Assessment reduce indoor air quality as well as outdoor air quality and SLCFs, it is also possible to estimate reductions in mortality from the indoor air quality improvements. To be conservative, we have limited this to respiratory mortality.

One of the major strategies to lower emissions of BC and CO is to replace current biomass combustion with improved stoves that have better combustion efficiency or to focus on LPG or non-solid fuel stoves. This would both reduce exposure indoors and reduce emissions, influencing outdoor exposures (e.g. see the global cookstove initiative of the UN Foundation; India's National Biomass Cookstoves Initiative; Project Surya at projectsurya.org) (Ramanathan and Balakrishnan, 2007).

Work by IIASA for the new Global Burden of Disease report contains estimates of exposure for 2030 under the reference scenario. These have been used to estimate the difference in health burden presented as deaths per year avoided, and years of life lost (YLL) (see Box 4.7). Mortality rates are held constant in this analysis, which may be conservative. Due to data limitations, we have only estimated benefits for India and China. We have taken data from the Global Burden of Disease report of 2004 for the burden of solid fuel use in the domestic sector in those countries in 2000 (Ezzati *et al.* 2004). This report provides a summary of the health effects and the dose-response relation.

4.5.5 Estimating the impact of changes in particulate matter and ozone on human health for the reference scenario

Changes in annual deaths due to changes in outdoor air pollution are estimated using a health impact function, taking into account the exposed population (Pop), baseline mortality rates (Y_0), the CRF (β) defined by the epidemiology literature, and the change in $PM_{2.5}$ and O_3 (ΔX), which are examined separately; this analyses is based on a data integration methods similar to that used by Anenberg *et al.* (2010):

$$\Delta \text{ Deaths} = \text{Pop} * Y_0 * (1-e^{-\beta \Delta X})$$

A number of recent risk assessments have chosen the CRF (β) from the ACS study (Cohen *et al.*, 2004; Liu *et al.*, 2009c; Anenberg *et al.*, 2010) as that to use in quantitatively estimating the effect of particle reductions. The primary argument has been that this is a large study. This Assessment has rejected that approach for a more integrative one for a number of reasons. First, to choose one study is to implicitly claim that the other studies have no information to offer on the size of the effect, they only help justify the plausibility. This is believed to be untenable. Some of the other studies (e.g. the Nurses' Health Study (Puett *et al.*, 2009)) were also quite large, others, such as the Six City Study (Ferris *et al.*, 1983) had advantages in random selection of subjects and less exposure error, and there are many studies whose cumulative impact on a judgment of the best CRF can hardly be zero. Moreover, the ACS study found effect modi-

fication by education (lower effects in college graduates) but substantially oversampled college graduates. Secondly, the main ACS analyses assign subjects to air pollution monitors in the same metropolitan area, even if they are in a different county. Some of the counties are very large, so that distances of more than 150 km between subject and monitor can occur. This induces error in the exposure, which, as discussed previously, also biases the results.

Of course, integrating the literature on air pollution and mortality, and incorporating supporting literature on effects on intermediary biomarkers is a daunting task; fortunately this had already been done by the US EPA. They recruited a panel of 12 experts to review the literature with the aim of estimating the CRF for all-cause mortality, and the uncertainty around it. Interestingly, the overselection of college-educated participants and higher than average measurement errors were cited by many experts as the reason that all but one expert (including two authors of the ACS papers) had mean estimates greater than the ACS slope. The average of the 12 estimates reported as part of the expert elicitation gives a mean function of 1.06 per cent decrease in deaths per 1 $\mu g/m^3$ decrease in $PM_{2.5}$, about 1.8 times higher than the estimate from the ACS study.

Studies of the acute effects of particles at high dose have shown a logarithmic CRF, with lower marginal impacts at higher concentrations. This suggests the concentration-response estimate above is likely too high for developing countries, where

---

BOX 4.7: Metrics of health impacts

Concentration-response function (CRF) – the relationship between ambient concentration and a health outcome.

Premature deaths – the number of deaths occurring earlier due to a risk factor than in the absence of that risk factor.

Years of life lost (YLL) – the average number of additional years a person would have lived if he or she would not have died prematurely.

Value of a statistical life (VSL) – The maximum amount an individual would be willing to pay to reduce his or her chance of dying by a small amount in a specified time period.

exposure is higher. However, due to emission reduction measures to which developing countries are already committed, this Assessment's baseline projections for $PM_{2.5}$ concentrations in these regions for 2030 are much lower. For example, projections show anthropogenic concentrations (which exclude dust and sea salt) in the 30's and 40's of $\mu g/m^3$ for China and India. This is within the range where the CRF was found to be linear by Schwartz *et al.* (2008), and so this Assessment has assumed a linear relationship with the 1.06% per $\mu g/m^3$ of $PM_{2.5}$ slope above.

The methodology used in this Assessment has previously been used by the WHO in 2004 to estimate the then current global burden of outdoor air pollution on human mortality (Cohen *et al.*, 2004). This WHO comparative risk assessment estimated that urban $PM_{2.5}$ was associated with about 800 000 annual deaths globally (Cohen *et al.*, 2004). A more recent study, again for current conditions, used a global chemical transport model to estimate the burden of outdoor anthropogenic $PM_{2.5}$ and O_3 in both urban and rural areas, finding about 3.7 million annual premature deaths due to $PM_{2.5}$ and about 700 000 due to O_3 (Anenberg *et al.*, 2010), with about 75 per cent of these occurring in Asia. These estimates will be revised again by the ongoing Global Burden of Disease 2010 Study (http://www.globalburden.org/). No study to date has examined the burden of outdoor air pollution on mortality in 2030, which would be influenced in opposite directions by several factors. Expected population growth, the epidemiological shift in developing countries from infectious disease to chronic disease, and increased emissions associated with economic development would lead to a larger burden; however, air pollution mitigation policies planned in North America and Europe along with expected future programmes in Asia would reduce the overall burden.

This Assessment examines the health impacts in 2030 due to the change in $PM_{2.5}$ and O_3 concentrations projected in 2030 relative to 2005 concentrations based on the reference scenario. Because the PM studies primarily show effects of exposure on deaths from cardiopulmonary disease and lung cancer, and the O_3 study effects on respiratory mortality, the estimates in this Assessment are restricted to changes in those specific causes of deaths. The equation above produces estimates of how many fewer deaths per year in 2030 would occur were the air pollutants lowered. In addition, YLL have been calculated, based on current life expectancies.

Regional changes in mortality for the 2030 population are estimated using the change in surface $PM_{2.5}$ and O_3 concentrations between 2005 and 2030 simulated by the two models, GISS-PUCCINI and ECHAM-HAMMOZ (see Appendix A.4). Globally, emission changes in 2030 relative to 2005 substantially impact air pollution-related mortality. For each region, changes in health impacts from $PM_{2.5}$ are larger than those from O_3, an effect of both the relative changes in concentration of the two pollutants and the stronger relationship of $PM_{2.5}$ with mortality (Figure 4.7). ECHAM-HAMMOZ simulates much larger $PM_{2.5}$ concentration changes and smaller O_3 changes compared with GISS-PUCCINI, though both models show the same directional change for each region (Figure 4.7). Both models also show similar spatial patterns, except for small areas in northern China where surface $PM_{2.5}$ increases in GISS-PUCCINI but decreases in ECHAM-HAMMOZ (Figure 4.8).

The impact of ambient PM is significant compared to other causes of death. Implementation of tight emission regulations in North America and Europe lead to 0.1-0.8 million avoided $PM_{2.5}$-related deaths annually (primarily in Europe), corresponding to 0.5-4.8 million avoided YLL. These ranges include estimates from both models and the associated 95 per cent confidence intervals. Expected regulations in East Asia, Southeast Asia and the Pacific are estimated to avoid 0.1-1.1 million annual $PM_{2.5}$-related deaths (0.4-7.7 million YLL), but O_3-related mortality is estimated to increase by 0-0.2 million (0.1-1.4 million YLL). Continued rapid emissions

123

growth in South, West and Central Asia is estimated to increase $PM_{2.5}$- and O_3- related deaths by 0.1-1.8 million (1.2-15.9 million YLL) and 0-0.2 million (0.1-2.4 million YLL), respectively. Only modest changes in air pollution-related mortality are expected in Africa and Latin America and the Caribbean.

The 95 per cent confidence intervals shown by the error bars in Figure 4.7 only represent the uncertainty in the CRF and exclude additional uncertainties that are more difficult to quantify. Some uncertainties, such as in emissions and the representation of atmospheric processes in the models used to simulate concentrations, occur upstream of the health impact calculation – the comparison between the two models gives some indication of the importance of the latter of these two factors. Uncertainties are also associated with extrapolating CRFs found in the developed world to the rest of the world. $PM_{2.5}$ concentrations simulated by ECHAM-HAMMOZ approach 95 μg/m^3 in East and Southeast Asia and the Pacific, which is larger than the maximum of 60 μg/m^3 simulated by GISS-PUCCINI. The true CRF at these high concentrations is unknown since no long-term epidemiology studies have yet included such high exposure

levels. The CRFs used in this Assessment are assumed to be linear; if the marginal impact of $PM_{2.5}$ is smaller at high concentrations, these results would be overestimates, particularly for results based on concentrations simulated by ECHAM-HAMMOZ.

These estimates are also based on a conservative population projection to 2030 and are limited to a population aged 30 and older, consistent with the ACS study. The substantial respiratory mortality in developing countries is likely to be impacted by air pollution (Carbajal-Arroyo *et al.*, 2011) in ways our model does not capture. These results also focus only on mortality and do not account for substantial changes in morbidity that would result from these changes in air pollution. The estimated changes in mortality may therefore be underestimates of the true health impacts of the projected changes in concentrations.

Indoor health estimate result
Using the CRF from Ezzati *et al.* (2004) and the exposure changes estimated by IIASA, we estimate 220 000 deaths and 6 million disability-adjusted years of life lost could be avoided in India in 2030 due to reduced indoor air pollution if the portfolio were implemented.
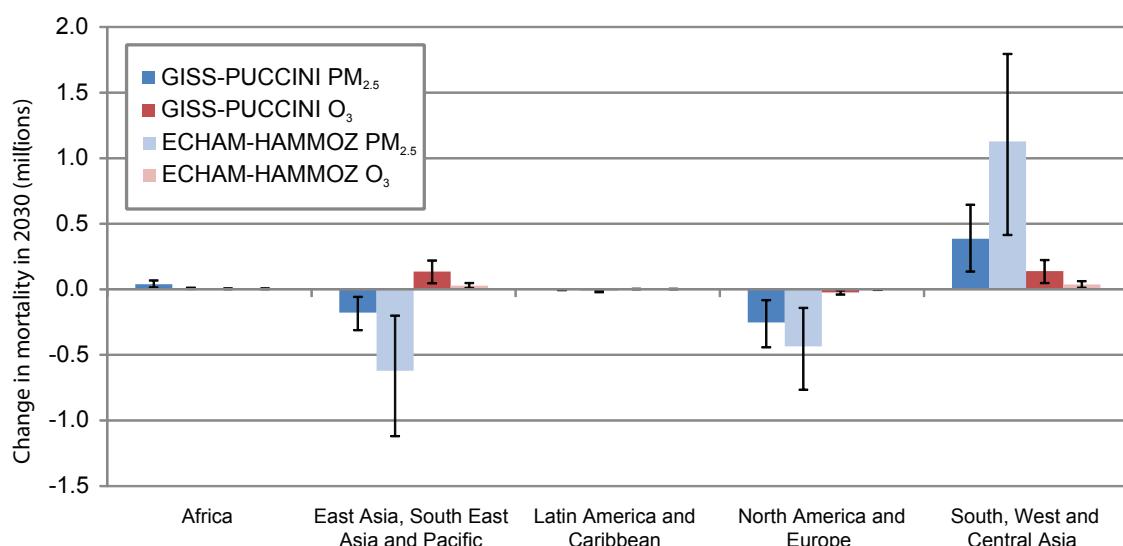
Figure 4.7. Regional change in annual $PM_{2.5}$ cardiopulmonary and lung cancer and O_3 respiratory mortality (in millions of lives) in 2030 relative to 2005 for the reference scenario, using simulated concentrations from the two models. Confidence intervals of 95 per cent are based on uncertainty in the CRF only.
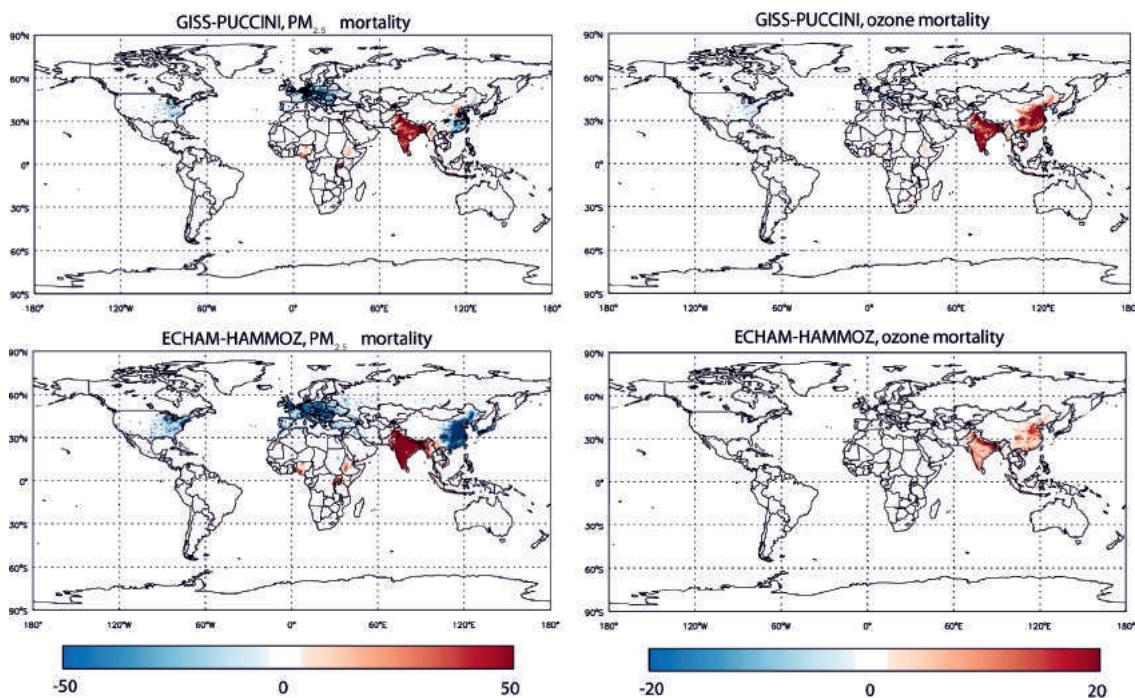
Figure 4.8. Change in annual PM$_{2.5}$ cardiopulmonary and lung cancer and O$_3$ respiratory mortality (lives per 1 000 km²) in 2030 relative to 2005 for the reference scenario.

In China, a reduction of 153 000 deaths in 2030 and 1.9 million disability-adjusted years of life lost is estimated.

4.5.6 Economic valuation of health impacts

The standard measure of the monetary value to an individual of a small change in the risk of mortality is described as the value per statistical life (VSL) (e.g. Jones-Lee, 1974; Viscusi, 1978; Hammitt, 2000; Alberini, 2005). The VSL is defined as the maximum rate at which an individual would pay to reduce his or her chance of dying by a small amount in a specified time period (e.g. the current year). This value should not be interpreted as the value of a life; this value reflects the trade-off that populations make between empirically measured mortality risks and money.

It is important to note that the VSL is not a constant but may vary with a number of factors including wealth and income, age, anticipated health status and total mortality risk. Since the Assessment spans regions in which income varies considerably the Assessment models the impact of income on VSL.

The rate at which VSL varies with income is typically described by the income elasticity, defined as the proportional change in VSL that corresponds to a proportional change in income. Adjustment for income is important for estimating VSL in lower-income populations for which direct estimates do not exist. Additionally, the application of different VSLs to populations with different incomes reflects differences in willingness and ability to pay for mortality risk reductions that have been documented empirically. This approach does not imply that lives are worth more or less as a function of income levels. Rather, income constrains an individual's ability to pay for risk reductions.

In this Assessment, the VSL approach is applied in two ways; both approaches rely on the US EPA's preferred VSL (which is equal to US$9 500 000 for the model year of the analysis: 2030) and are based on both a meta-analysis and a Science Advisory Board review. The first approach adjusts the US EPA VSL to each country based on the relationship between country-specific income per capita and income per capita in the USA, using an elasticity of 0.40 between income and VSL

(US EPA, 1999). This elasticity reflects the relationship between percentage changes in two variables. So in the current context, an elasticity of 0.40 implies that a 10 per cent increase in per capita income corresponds to a 4 per cent increase in the willingness to pay (WTP) to avoid mortality risks. The second approach applies the US EPA VSL uniformly across all countries, regardless of individual nations' income levels.

Although both $PM_{2.5}$ and O_3 impact the incidence rates of a wide range of morbidity states, the most economically important of which is chronic illness, this Assessment does not measure the impact of air pollution on morbidity due to a lack of necessary data in many countries.

Table 4.4 shows the results from the mortality valuation exercises conducted in this Assessment (based on the values provided in Figures 4.7 and 4.8) for the comparison of mortality incidence in 2030 and 2005.

Table 4.4 indicates that the value of mortality reductions between 2030 and 2005 is considerable in magnitude; the value of aggregate avoided global mortality is US$1.28 trillion using GISS concentration changes. The value of avoided mortality is considerably larger when the ECHAM model is used; the value increases to just over US$2.7 trillion. Table 4.4 also shows the regional split of these mortality impacts. Much of the difference between the two models centres on the change in East Asia, Southeast Asia and the Pacific, North America and Europe, and South, West and Central Asia. Specifically, the (absolute) value of avoided mortalities increases in East Asia, Southeast Asia and the Pacific by nearly US$1.5 trillion when the ECHAM model is used relative to the GISS model. In South, West and Central Asia, mortality damages are

Table 4.4. Valuation of Premature Deaths: 2030 versus 2005 according to emissions and concentrations resulting from the reference scenario. All values expressed in 2006 US$ billions. 95 per cent confidence intervals in parenthesis derived from confidence intervals reported for mortality CRF. Values reflect change in mortality damage; negative values imply improvement in welfare. The first column (left) indicates the geographical region (either global or each of five regions), and the second and third columns display the results when using country-specific VSLs for the mortality calculations based on the GISS (2nd column) and ECHAM (3rd column) modeled concentration changes. The fourth and fifth columns break down the results by exposure to $PM_{2.5}$ and O_3 individually.

Spatial Unit	Gross mortality value (2006 US$ billions)		Gross mortality value (GISS) (2006 US$ billions)	
	GISS	ECHAM	$PM_{2.5}$-related deaths	O_3-related deaths
Global	-1 280 (-399 , -2 360)	-2 710 (-797, -5 200)	-1 680 (-537, -2 990)	400 (139, 623)
Africa	73 (25, 124)	-25 (-8, 50)	66 (23, 112)	7 (2, 11)
East Asia, Southeast Asia and the Pacific	-237 (-76, -462)	-1 720 (-550, 3 090)	-564 (-186, -986)	327 (111, 523)
Latin America and the Caribbean	-3 (-1, -6)	-38 (-13, -67)	-11 (-4, -18)	7 (2, 12)
North America and Europe	-2 040 (-669, -3 560)	-2 960 (-964 -5 210)	-1 850 (-608, -3 240)	-189 (61, -320)
South, West and Central Asia	931 (322, 1 540)	2 030 (742, 3 220)	683 (238, 1 140)	248 (84, 397)

US$1 trillion larger when using the ECHAM model than when GISS is employed. In North America and Europe, the reduction in mortality damages is nearly US$1 trillion larger with ECHAM than when GISS is employed.

In Africa the GISS model predicts an increase in mortality damages, while the ECHAM model indicates that mortality damages will be smaller in 2030 than in 2005. A much smaller difference in mortality damages is seen between the two models for Latin America and the Caribbean.

Table 4.4 also expresses the country-specific VSL results according to whether the predicted deaths are due to $PM_{2.5}$ or O_3 exposure. These results are based on the GISS model. The greatest share of mortality damage is due to exposures to $PM_{2.5}$. Globally, the reduction in premature deaths associated with $PM_{2.5}$ exposure is valued at US$1.7 trillion. In contrast, O_3 exposure deaths increase and are valued at US$400 billion. In East Asia, South East Asia and the Pacific and in Latin America and the Caribbean this pattern of reduced $PM_{2.5}$-exposure deaths and increasing O_3-exposure deaths holds. And in each of these two regions the (absolute) value of $PM_{2.5}$-exposure deaths is in excess of that associated with O_3. In North America and Europe, both $PM_{2.5}$- and O_3-exposure deaths decrease relative to 2005 for the reference scenario. In Africa and South, West and Central Asia, premature deaths associated with both pollution species increase.

4.6 Impacts of black carbon and ozone on agriculture and ecosystems

Observational, experimental and modelling studies have demonstrated the effects of aerosols, of which BC is an important fraction, and O_3 on a variety of different ecosystems. Much of the current research has concentrated on agriculture, however, since these pollutants do not discriminate in their impacts on ecosystems, a wide variety of ecosystem services may be affected. Important services affected include the provisioning and supporting services associated with the productivity and biodiversity of forests, grasslands and wetlands as well as the regulating services related to the carbon sequestration potential of ecosystems. In this section the role that both O_3 and aerosols play in impairing these particular ecosystem services is discussed through references to published studies. For agriculture, results from this Assessment's modelling study are also used to quantify O_3 impacts on crop yield, production and subsequent economic losses.

Ozone is a strongly phytotoxic atmospheric pollutant and a vast body of literature describing experimental and observational studies have shown substantial effects of elevated O_3 levels – those exceeding pre-industrial O_3 concentration by upwards of 10 to 20 ppb – on visible leaf injury, growth, productivity, and nutrient composition for a large number of important agricultural, forest and grassland species and ecosystems (Ashmore, 2005).

The atmospheric brown cloud (ABC) (Ramanathan *et al.*, 2008) is a name given to the haze in the sky consisting of anthropogenic aerosols (BC, OC, SO_4^{2-} and nitrates (NO_3^-) among others) and pollutant gases such as CO and O_3. The ABC has been identified as a particular problem across much of Asia where high atmospheric aerosol loads alter the amount and quality of solar radiation reaching the Earth's surface with implications for agricultural productivity through influence on photosynthesis.

Finally, it is also acknowledged that BC and O_3 will affect agriculture and ecosystems indirectly through changes in climate. The IPCC AR4 assessment reports (IPCC, 2007) provide the most comprehensive reviews of the potential impacts to ecosystems associated with such changes in climate and these will not be repeated here. However, the conclusions of Section 4.2.2, that BC and O_3 are likely to produce greater regional enhancements to climate change than would occur from radiative forcing due to LLGHGs, should be emphasized. This is especially important due to the implications for the magnitude of the effect on ecosystems that are likely to suffer most because of their geographical location in particularly polluted regions and the subsequent influence

127

of regional radiative forcing. The implications of such climate-induced effects for vulnerability are considered further in this section.

4.6.1 Impacts on agriculture caused by ozone and black carbon

Ozone has been shown to cause a wide variety of impacts to important and staple agricultural crop species; these include visible injury to leafy crops (e.g. spinach, lettuce) (Emberson et al., 2003), reductions in crops yields and effects on crop quality (e.g. nitrogen content of grains, tubers etc. and nutritive quality of forage crops) (see review of Fuhrer and Booker, 2003). Ozone also affects grasslands, which is an important though often overlooked effect on agricultural systems with potentially significant impacts on fodder production for livestock.

Since O_3 is a secondary pollutant it tends to reach high concentrations some distance downwind of the industrial and urban sources of its primary precursors, meaning that it can cause particular problems in rural agricultural regions. This becomes particularly important in regions where agriculture is located close to large industrial and urban centres as is common in the rapidly industrializing economies of some South and East Asian countries.

Free air concentration enrichment (FACE) studies arguably provide the best estimate of real-world effects of O_3 on crops since they give estimates of yield losses under commercial growing conditions. However, they are limited in number with only two FACE sites investigating O_3 effects on crops; one that has been established for almost 10 years in Illinois, USA, and the second, which was only established in 2007, in Jiangdu, China. Both studies suggest substantial yield losses at concentrations representative of O_3 episodes that can occur in each region.

For example, the USA study found that seed yield of a commercial soybean cultivar, Pioneer 93B15, was reduced by 20 per cent when O_3 was increased from an 8-hour growing season average of 50 ppb to 63 ppb (Morgan et al., 2006). The first year results from China showed rice yield to be reduced by 6 per cent in a

japonica-type inbred variety and 21 per cent in an indica-type hybrid by the elevation of O_3 concentrations from 43 ppb to 53 ppb (mean 7-hour O_3 concentration across the three months centred on the flowering time) (Pang et al., 2009). This latter study indicates the importance of varietal differences in determining O_3 sensitivity.

Chamber experimental studies have been used far more widely than FACE studies, both in terms of geographical distribution and number of studies, due largely to their being less resource intensive. Such financial savings have meant that standardized pan-regional chamber study programmes have been performed both in the USA (the National Crop Loss Assessment Programme; NCLAN; Heck et al., 1983) and in Europe (the European Open Top Chamber Project; Jäger et al., 1992). The crop yield losses found in many of these studies are corroborated by FACE studies which used similar increases in O_3 concentration (Long et al., 2005 and Box 4.8). Importantly, these chamber studies have led to the development of CRFs for arable crops that can be used to assess the risk of crop yield losses across entire regions in modelling-based studies. When combined with O_3 photochemical modelling and agricultural production statistics (Emberson et al., 2003), this allows results from site-specific experimental studies to be extrapolated to larger regions providing an estimate of the spatial extent and magnitude of crop specific yield losses for whole regions (e.g. Europe, North America and more recently, parts of Asia).

The CRFs that have been developed during these pan-regional campaigns have used different indices to characterise O_3 exposure. These have evolved from average mean growing season indices (e.g. M_7 and M_{12} indices; where the 7 or 12 refers to the daylight hourly averaging period) to indices that give greater weight to higher or peak O_3 concentrations deemed more biologically relevant to the induction of damage (e.g. AOT40 in Europe, SUM06 and W126 in North America). The profile of the CRF should also be considered; for example the curve-linearity of the M_7/M_{12} indices essentially results in lower average O_3 concentrations contributing less to damage thereby

having a similar effect in terms of weighting the relative importance of higher end O_3 concentrations albeit as growing-season values rather than hourly averages. The importance of this effect varies according to the species-specific relationship. It should also be noted that CRFs are only now being derived for Asian conditions. This is especially important as a recent meta-analysis of chamber-derived data expressing O_3 impacts on yields of wheat, rice and soybean suggested that Asian cultivars, grown under Asian conditions may be more sensitive to O_3 than would have been suggested by North America derived concentration-response relationships (Emberson et al., 2009).

A recent global study by Van Dingenen et al. (2009) used the AOT40 and M_7/M_{12} indices to assess the current (2000) and future (2030) impact of O_3 on the yield and associated production and economic losses of four staple agricultural crops. Emission projections from which O_3 concentrations were modelled for the year 2030 were based on a current legislation scenario. Present day global relative yield losses are estimated to range between 7 per cent and 12 per cent for wheat, between 6 per cent and 16 per cent for soybean, between 3 per cent and 4 per cent for rice, and between 3 per cent and 5 per cent for maize (the ranges resulting from the use of two different indices [AOT40 and M_7/M_{12}] to express dose in the CRFs). These global yield losses represent an economic loss, assuming 2000 world market prices, of US\$14 to US\$26 billion annually. They are based on figures for wheat production losses due to O_3 estimated by Van Dingenen et al. (2009). About 40 per cent of this damage was found to occur in parts of China and India. For those Asian countries with an economy largely based on agriculture, O_3 induced damage was suggested as a real threat to economic growth, with losses estimated to offset 20 to 80 per cent of the increase in GDP in the year 2000.

The ABCs found across the Indian sub-continent and the northern Indian Ocean have been studied extensively since the Indo-US-European collaborative field study known as the Indian Ocean Experiment conducted during 1997 to 1999 (see summary in Ramanathan et al., 2008). Only a few studies have examined the impacts of ABCs on agriculture and have tended to focus just on the impact of solar radiation on yield. Such studies have estimated that the dimming effect of ABCs reduced rice yield by 6 to 17 per cent (Ramanathan et al., 2008). These studies have been criticized for using process-based crop-response simulation models, which might not accurately reflect crop growth under actual field conditions.

Black carbon can also impact agriculture through its effect on temperatures, cloudiness, rainfall and river flow via its impact on glacier melting. A study by Auffhammer et al., (2006) aimed to overcome limitations associated with the use of process-based crop growth models by examining the multiple impacts of ABCs on agriculture using multivariate regression methods and historical data from nine major rice-growing states of India. Surface warming due to greenhouse gases and BC decreased rice productivity, these reductions were amplified by further reductions in rice yield due to dimming and a decrease in monsoon rainfall attributed to ABCs. Although their study included the effects of all man-made aerosols (with SO_4^{2-}, OC and BC being dominant), BC and OC were found to contribute at least 70 per cent to their estimated ABC effects on agriculture. They estimated the losses of just ABCs on mean wet-season rice harvest to be 4 per cent during 1966 to 1984 and 11 per cent during 1985 to 1998; simultaneous reduction of ABCs and greenhouse gases would have increased mean wet-season rice harvest by 6 per cent for 1966 to 1984 and 14 per cent for 1985 to 1998.

4.6.2 Estimating the impact of changes in ozone on agriculture for the reference scenario

This Assessment uses the same methodology employed in the Van Dingenen et al. (2009) paper to assess changes in yield, production and economic value of the same four staple crops between 2005 and 2030.

For this study, the M_7 and M_{12}[1] O_3 concentration indices were applied, rather than AOT40 because of their higher robustness compared to the threshold-based AOT40 metric (Tuovinen *et al.*, 2007; Van Dingenen *et al.*, 2009). The methodology calculates O_3 indices from global modelled hourly O_3 fields from the global circulation ECHAM-HAMMOZ and GISS–PUCCINI models over a crop- and location-specific growing season; this produces gridded estimates of relative yield loss (*RYL*) for each relevant crop. The *RYL* field was overlaid with a higher resolution 1° x 1° crop production grid derived from national or regional agricultural production numbers. For each grid cell, the crop production loss (*CPLi*) is calculated from the *RYLi* and the actual crop production for the year 2005 within the grid cell (*CPi*):

$$CPL_i = \frac{RYL_i}{1 - RYL_i} . CP_i$$

The national *CPL* is then obtained by summing all grid cells belonging to each country. The economic loss (*EL*) is estimated by multiplying the crop production loss (*CPL*) with the producer prices for the year 2005 (*PP_{2005}*) as given by FAOSTAT (http://faostat.fao.org, accessed December 2007). The producer prices are used as a proxy for the domestic market price, due to the lack of information on actual crop market prices.

$$EL = CPL.PP_{2005}$$

PP_{2005} are not always available for some minor producing countries. In that case, the median crop price for the year 2005 was applied. By using this simple cost calculation, the Assessment neglects possible feedbacks of changes in supply and the demand on the price evolution. Adams *et al.* (1982) estimated that the simple multiplication approach overestimates

the damage by 20 per cent by not accounting for economic adjustments and compensating price effects. The error bars assigned to yield loss estimates in the present study reflect the uncertainty in the CRF. They result from the 95 per cent confidence interval on the Weibull function parameters, as reported in the literature (Lesser *et al.*, 1990).

The differences in *RYL, CPL* and *EL* between 2005 and 2030 under the reference scenario are shown in Figures 4.9. The estimated changes in CP in million tonnes between 2005 and 2030 are provided as absolute values and as a fraction of total global production in 2005 in Table 4.5. Positive *RYL* values indicate an increase in crop yield loss in 2030 compared with 2005. For the whole Asian region, all four crops show an increase in yield loss. Soybean and corn yields are the most affected, with losses increasing by 7 per cent (+8 per cent, -5 per cent) for soybean and by 8 per cent (±7 per cent) for corn in East Asia, Southeast Asia and the Pacific. The change in yield losses for wheat and rice are less than 3 per cent everywhere. However, corresponding changes in production losses (Figure 4.9b) for Asia are relatively large reflecting the importance of wheat-rice cropping systems in this region, in particular in the Indo-Gangetic plain region. It should be noted that the change in absolute production numbers for rice are highly uncertain due to the ill-defined CRF for that crop (see Appendix A.4.3). For all four crops nearly 40 million tonnes of production is lost across the entire Asian region reflecting the substantial area under cultivation that is exposed to elevated O_3 concentrations.

In contrast, the European and North American regional analysis suggests that all crops will see an improvement in yields, with soybean yields benefiting the most (in terms of relative yield). This is likely due to the relatively high sensitivity of soybean to O_3 meaning this crop will benefit to a greater extent compared to others. This highlights the benefits for arable production of the reference scenario emission reduction strategies that will reduce O_3 concentrations in these parts of the world.

---

[1] M_7 = 3-monthly growing season mean of hourly O_3 concentrations during the 7 hour period [09:00 – 15:59] local time (M_{12}: idem, but for the 12 hour period [08:00 – 19:59] local time).

130
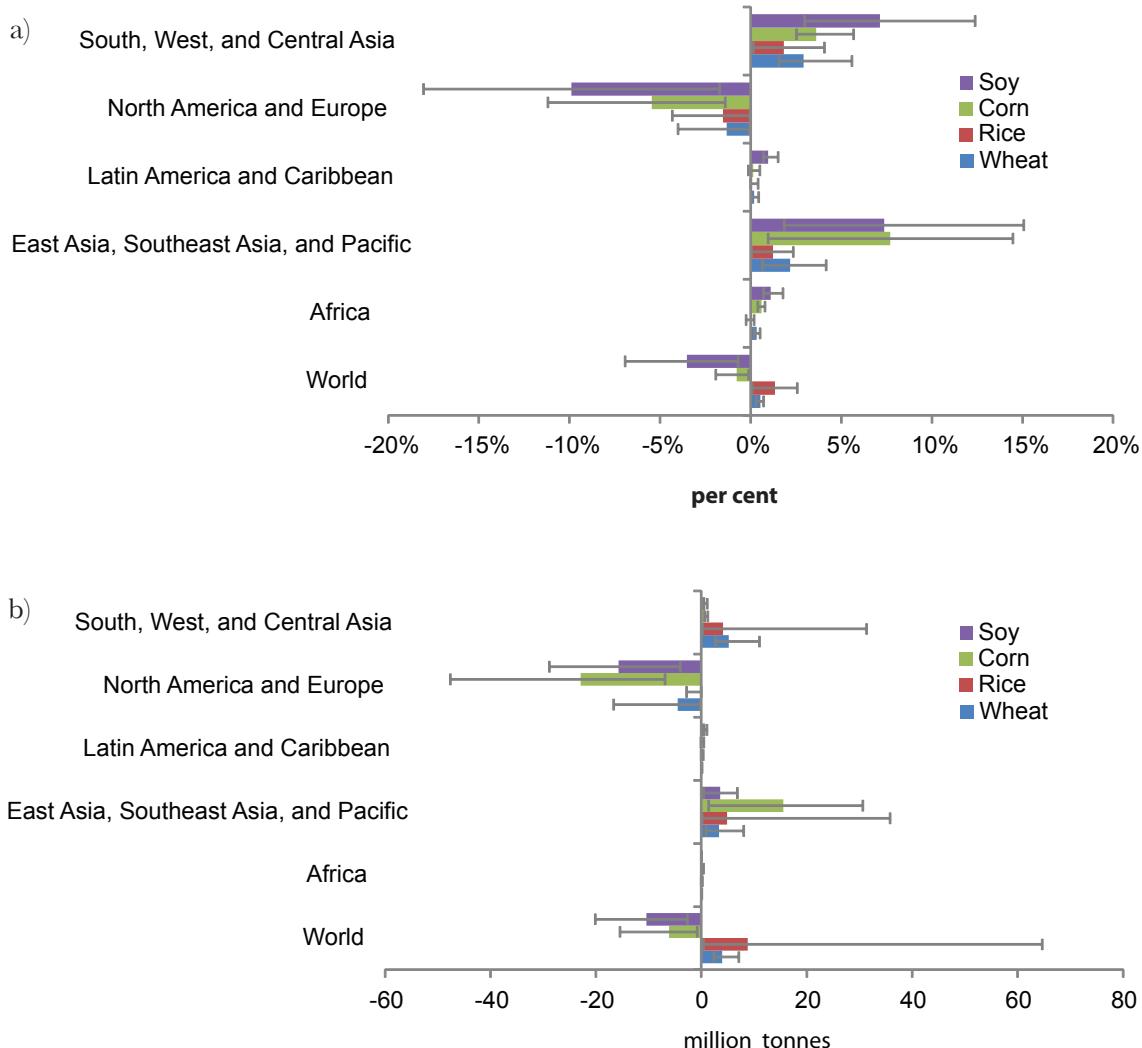
Figure 4.9. The differences in a) relative yield loss (%) and b) crop production loss (millions of tonnes) between 2005 and 2030 according to the reference scenario. Results are based on the average of the results using O_3 concentrations from the GISS PUCCINI and ECHAM-HAMMOZ models. Error bars represent resulting range in model output from the uncertainty associated with the CRFs at a 95 per cent confidence interval.

Figure 4.10 expresses these losses in economic terms to provide an insight as to the financial cost of O_3 damage assuming current world market commodity prices. The greatest losses for a single crop and commodity occur in East and South East Asia for maize with a central estimate of US\$3 ($\pm$ 3) billion being lost due to changes in O_3 exposure from 2005 to 2030 according to projections in emissions and concentrations according of the reference scenario. The economic losses for the whole of Asia are estimated at US\$ 1-20 billion. Conversely, the improvements in air quality in North America and Europe see increases in crop yield leading to production and economic gains of 11-96 million tonnes and US\$ 1-11 billion respectively.

It should be noted that this Assessment, though providing important information regarding the scale of the impacts associated with current and future changes in tropospheric O_3, has a number of associated uncertainties. These can most usefully be grouped into:

i   Those associated with estimating the crop yield losses: these include uncertainties with which estimates of global O_3 concentration fields can be expected to represent conditions at plant canopy height; uncertainties in relying upon chamber studies for the derivation of CRFs (see Box 4.8); uncertainties associated with

Table 4.5. The change in crop production between 2005 and 2030 under the reference scenario as millions of tonnes and a percentageof total global production in 2005 (FAO). The ranges cover the central value obtained from both the GISS-PUCCINI and ECHAM-HAMMOZ models.

Crop	Global production in 2005 (million tonnes)	Change in production 2005 to 2030 (million tonnes)	Change in production as a percentage of 2005 production (%)
Wheat	626	-3 to -5	-0.5 to -0.8
Rice	634	-4 to -14	-0.6 to -2.2
Corn	722	+5 to +8	+0.7 to +1.1
Soybean	214	+2 to +19	+1.2 to +8.7
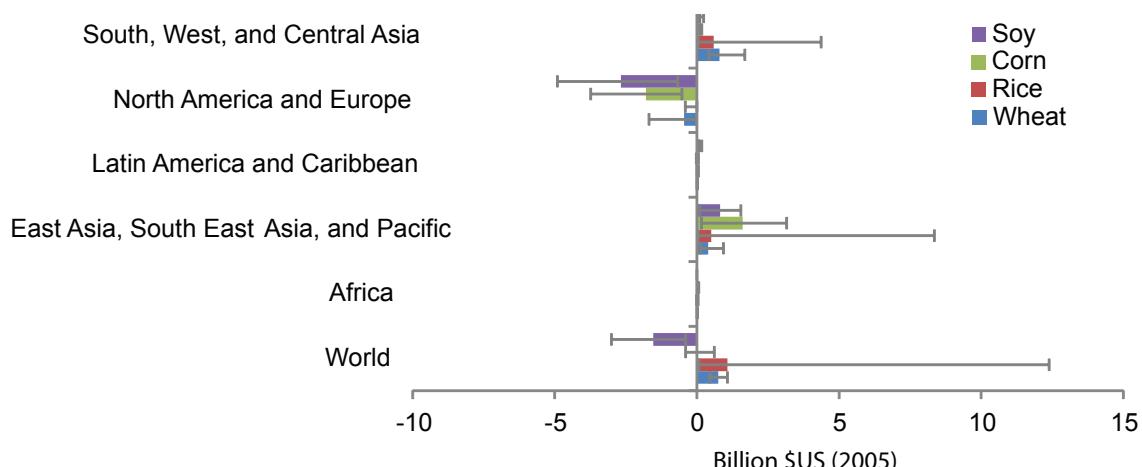
Figure 4.10. Change in economic losses in US$ billions from 2005 to 2030 (positive values are losses, negative values are gains). The ranges cover the central value obtained from both the GISS-PUCCINI and ECHAM-HAMMOZ models.

accurately defining the crop growing season and crop distribution; varietal differences in sensitivity to O_3; variability in results dependent upon selection of an O_3 dose metric (i.e. AOT40 versus M7/M12); suitability of O_3 dose metrics for global application (Emberson *et al.*, 2009); the influence of modifying factors which may decouple O_3 concentrations from O_3 uptake and hence damage. These uncertainties could to some extent be overcome through the use of flux-based exposure-response functions rather than the concentration based CRFs used here. For example, the UNECE Convention on Long-range Transboundary Air Pollution (CLRTAP) recommends that only flux-based indices be used for economic loss assessment (UNECE, 2010). Although theoretically feasible to perform flux-based yield-loss assessments, this method is currently limited both by the ability to estimate fluxes at the global scale – the methods have to date been developed and, more importantly, parameterized in Europe – and the existence of flux-response relationships for only a limited number of crop species (wheat, potato and tomato).

ii Those associated with capturing the entire impact of O_3 on agricultural productivity. Here it is important to stress that the Assessment investigates only four crops for a single year in an attempt to assess the benefits of changes in O_3 precursor emissions on agriculture. In actuality, a large number of other important crops are known to be sensitive to O_3 (Mills *et al.*, 2007) but have not been included since M7/M12 concentration-response relationships do not exist. In

132

Box 4.8: Chamber versus FACE studies

Unfortunately, the numbers of FACE studies that have investigated the influence of crops grown under elevated O_3 are limited. Only two sites (one in the USA and the other in China) have investigated three crops (soybean in the USA; wheat and rice in China). As such the CRFs (M7/M12 and AOT40 yield relationships) that are necessary to perform regional estimates of yield, production and economic loss due to O_3 are all primarily based on data from field chamber experiments. Concern has been raised that the chamber environment will modify plant response to O_3 (Elagöz and Manning, 2005), with environmental differences between the chamber and the open air either ameliorating or exacerbating the effects of elevated O_3 (Long *et al.* 2005).

In an attempt to estimate the potential under- or over-estimation of yield losses, the figure below compares the yield losses found for soybean in the USA FACE site (Morgan *et al.*, 2006) and for rice from the Chinese FACE experiments (Pang *et al.*, 2009), with predicted yield losses using the CRFs from the global modelling study presented here and in Van Dingenen *et al.* (2009). The results would suggest that, if anything, the chamber studies would tend to under-estimate the yield losses found in the FACE experiments though the importance of differential varietal sensitivity and year to year variability in sensitivity to O_3 are apparent.
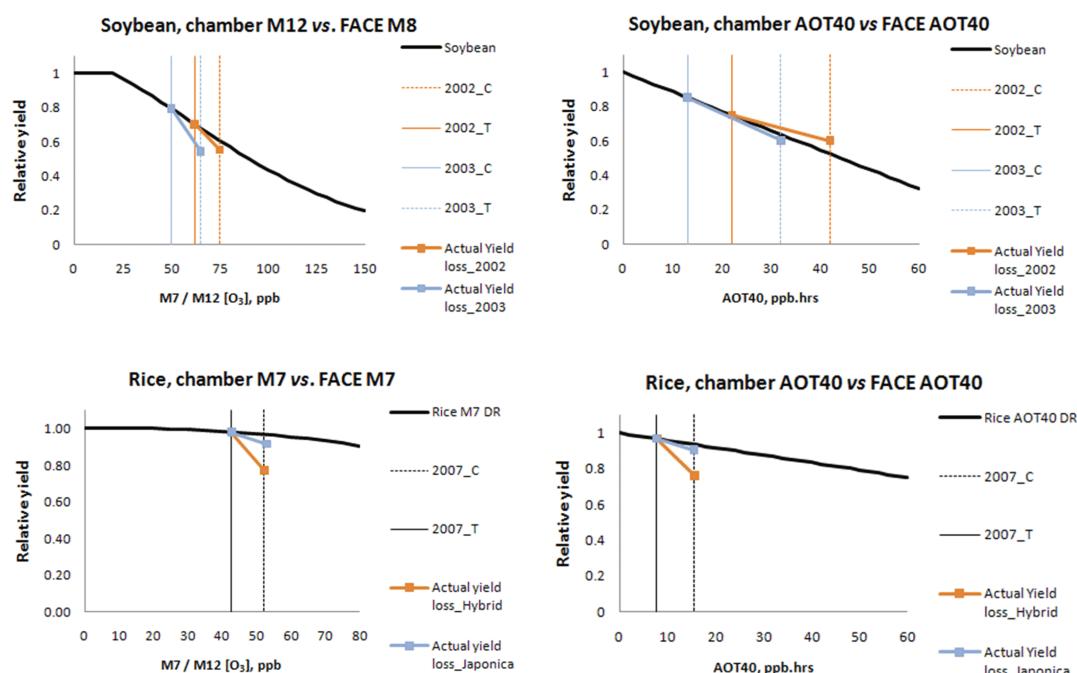
Ultimately, such comparisons show that there is an urgent need for more FACE experiments to reduce the uncertainty in future estimates of loss in crop productivity. Ideally these need to be conducted in a range of locations and to cover different cropping and management systems (see also Royal Society, 2008).

addition, for many crops, especially those grown in the tropics, the sensitivity to O_3 is unknown. Ozone is known to reduce the productivity and forage quality of productive pastures (Krupa *et al.*, 2004), with potentially important implications for livestock (Holland *et al.*, 2006).

iii   Those associated with putting a price on the agricultural impacts resulting from elevated O_3 exposures. These include the fact that the economic assessment has used global median producer prices for 2005 (from FAO) where country-specific prices are lacking, and it is important to recognize that there is heterogeneity between countries. There is also uncertainty in that prices will have changed by 2030 although this is not accounted for in the modelling. These estimates also do not reflect adaptive behaviors by producers in response to changing O_3 levels, but perhaps, even more importantly, the economic assessments provide only a macro-scale analyses of the situation, the influence of yield losses to, for example, subsistence farmers and hence impacts on farmers livelihoods are not captured.

The results from this exercise are similar in terms of the scale of yield, production and economic losses predicted by a number of other modelling studies conducted for particular global regions. For example, in the USA as a whole, agronomic crop loss to O_3 is estimated to range from 5 to 15 per cent, with an approximate cost of US$3 to US$5 billion annually (US EPA, 2006; Fiscus *et al.*, 2005). In Europe, similar studies have identified substantial economic losses due to O_3, for example, Holland *et al.*, estimated losses for 23 crops in 47 countries in Europe of €4.4 to 9.3 billion/year, around a best estimate of €6.7 billion for year 2000 emissions (Holland *et al.*, 2006). Studies performed for East Asia estimate annual losses of US$5 billion based on four key crops: wheat, rice, soybean and maize (Wang and Mauzerall, 2004).

However, all these methods use the same empirical approach derived from chamber studies to estimate yield losses and subsequent production and economic losses. Alternative, epide-

miologic methods are available and have been applied for crop loss assessments (Fishman *et al.*, 2010, Kaliakatsou *et al.*, 2010). Those studies have found that the influence of O_3 can be detected in regional production statistics and field-trial data although damage estimates have been found to differ from those obtained from risk assessments performed using empirically-derived CRFs (Kaliakatsou *et al.*, 2010). This may be due to these methods being most effective in those regions characterized by higher average O_3 concentrations (Fishman *et al.*, 2010) where the O_3 signal is strong enough to overcome the influence of confounding variables affecting yield. Here it is important to note that O_3 stress does not act independently but rather as one of many stresses or environmental modifications that will affect growth and productivity of crops (e.g. nutrient availability, drought stress, temperature stress, and in the future, CO_2 fertilization). Ideally, risk assessments would incorporate the interactions that occur between these different stresses; new flux-based risk assessment methods should go some way towards addressing these issues (Ashmore *et al.*, 2004) but, as discussed earlier, are not yet available for application at the global scale.

Despite the overwhelming evidence that current O_3 concentrations are causing yield losses, there has been little, if any, effort within crop breeding programmes to develop O_3 tolerant crop cultivars for a future higher-O_3 worl0 (Ainsworth *et al.*, 2008; Booker *et al.*, 2009) even though successes in identifying genetic elements associated with O_3 tolerance in rice indicate that breeding for O_3 tolerance in food crops is possible (Frei *et al.*, 2008; Frei *et al.*, 2010).

4.6.3 Impacts on ecosystems caused by ozone and black carbon

Ozone has been shown to have substantial impacts on forest trees including visible foliar injury, accelerated leaf senescence, reduced photosynthesis, altered carbon allocation and reduced growth and productivity (Karnosky *et al.*, 2007; Skarby *et al.*, 1998). These effects vary by forest tree species and genotype (Karnosky and Steiner, 1981). Ozone also

appears to weaken trees' resilience to a range of biotic (e.g. pest and pathogen attack) and abiotic (e.g. drought, frost hardiness) stresses. Much of our knowledge of forest species sensitivity to O_3 comes from experiments conducted on seedlings and saplings. The extent to such results obtained from tree seedlings/saplings can be extrapolated to mature trees under real forest conditions has been severely challenged (Kolb and Matyssek, 2001) and studies such as that conducted at Kranzberg Forest, Germany, on naturally growing and late-successional adult forest trees are being developed to clarify these issues.

The consequence of such O_3 impacts on forests will adversely impact timber yields (Reich, 1987). Much like the case of agriculture, the standard approach to valuing such O_3-induced damage relies on using current market stumpage prices. However, since yield losses will not be incurred until the timber is felled and brought to market, time, and therefore discounting, plays an important role in valuing timber losses. The yield loss multiplied by the market price for timber represents the gross timber damage. Karlsson et al. (2005) estimate yield losses at 2.2 per cent in Sweden over the period 1993 to 2003. The resulting economic loss was estimated to be a 2.6 per cent decline, which is equivalent to €56 million. Additionally, Muller and Mendelsohn (2007) estimate annual yield losses equivalent to US$80 million in the USA. Given the complexities in making such calculations, it is outside the scope of the present Assessment to try to quantify such O_3 effects on forest timber production (as has been done for agriculture in Section 4.6.2), though it should be noted that forest productivity will also be likely to be substantially affected by this pollutant.

Ozone can affect the diversity of plants in semi-natural habitats. For example, semi-natural grasslands are genetically highly diverse multi-species communities ranging from low to high productivity depending on the site conditions and management. Component species differ strongly in their sensitivity to O_3 (Bungener et al., 1999; Hayes et al., 2007; Timonen et al., 2004) and thus plant community composition may alter under the influence of O_3. However, changes in productivity and species composition in established temperate (Volk et al., 2006), calcareous (Thwaites et al., 2006) or alpine grassland (Bassin et al., 2007) are difficult to detect against a background of considerable natural spatial and temporal variability. Existing experimental evidence would tend to suggest that, in the longer run, grassland productivity may decline and species dominance may change in response to elevated O_3. In contrast, observations in Mediterranean therophytic grasslands of short-term O_3 effects on reproductive traits of annuals have been clearly identified (Gimeno et al., 2004). Similar to its impacts of on agriculture, BC also affects other ecosystems' carbon uptake through changes in radiation levels reaching vegetation, by causing changes to its amount and quality, and changes in surface air temperature and air-vapour deficit. Because BC absorbs light, it decreases the amount of solar radiation reaching the surface but also changes the direct-to-diffuse radiation ratio. The latter depends on concentrations of BC (non-scattering aerosols), their source (fossil fuel or biomass burning) (Ramana et al., 2010), and the concentration of scattering aerosols (i.e SO_4^{2-}) (Liepert and Tegen, 2002, Ramana et al., 2010). Increasing amounts of scattering aerosols enhance the diffuse component of the radiation reaching the surface, whereas increasing concentrations of absorbing aerosols such as BC can have the opposite effect. There is observational evidence that plants are overall more efficient under diffuse radiation conditions (Gu et al., 2002; Niyogi et al., 2004; Knohl and Baldocci, 2008; Oliveira et al., 2007). Therefore the overall effect of BC via radiation changes on plant carbon uptake is likely to be negative. However, the presence of BC contributes to a decrease in total radiation and, depending on the concentration of other aerosol types, possibly decreases diffuse radiation. Overall effects of BC on vegetation carbon uptake through the reduction of radiation and through corresponding changes in surface temperatures and water vapor pressure deficit can be assessed using process-based models.

4.6.4 Impacts on the carbon cycle and other potential feedbacks

Vegetation plays an important role in determining surface O_3 levels, through flux of O_3 to the interior of leaves through stomata. As atmospheric CO_2 levels rise, the stomata will not need to open as widely to allow sufficient CO_2 to enter for photosynthesis. This may reduce O_3 uptake, decreasing plant sensitivity (Sitch *et al.*, 2007). For example, Klingberg *et al.* (2011) found that despite substantially increased modelled future O_3 concentrations in central and southern Europe, the flux-based risk for O_3 damage to vegetation, which is based on estimates of stomatal conductance, was predicted to remain unchanged or decrease at most sites, mainly as a result of projected reductions in stomatal conductance under rising CO_2 concentrations. However, soil moisture and temperature were also found to play an important role in determining stomatal O_3 flux. Such reductions in O_3 uptake would also lead to increased O_3 concentrations in the boundary layer. Sanderson *et al.* (2007) found that surface O_3 levels over parts of Europe, Asia and the Americas were 4-8 ppb larger under CO_2 fertilization conditions during April, May and June (the approximate growing season for crops in northern Europe). However, the relationship between stomatal conductance and CO_2 concentration may prove to be more complex and depend on O_3-CO_2 interactions (Uddling *et al.*, 2010). In addition, recent research has found that effective regulation of stomatal conductance under drought conditions was disrupted by increasing background O_3 concentration (Mills *et al.*, 2010; Wilkinson and Davies, 2009, 2010). Further details of the potential climate change effects on O_3 fluxes can be found in Fowler et al. (2009) and Fuhrer (2009).

The mechanistic-based modelling study investigating plant-O_3 interactions under SRES A2 emission scenarios by Sitch *et al.* (2007) also found a significant suppression of the global land carbon sink due to O_3 induced damage to vegetation leading to reduced net primary productivity, with estimates of the reduction in land carbon sequestration being up to 260 gigatonnes of carbon (GtC) by 2100. This re-duced carbon sequestration leads to a higher atmospheric CO_2 concentration which was estimated to constitute an indirect radiative forcing that could exceed warming due to the direct radiative effect of tropospheric O_3 increases. However, as discussed above, elevated CO_2 concentrations may provide a degree of protection against O_3 damage, though there is uncertainty as to the magnitude and temporal longevity of this protection as well as which species groups would be affected.

The results from the Sitch *et al.* (2007) study and a similar investigation conducted by Sanderson *et al.* (2003) have been used to identify eco-regions where a significant effect on global primary productivity (GPP) might be expected to occur (Royal Society, 2008). The results in Figure 4.11 are based on the low sensitivity simulation of Sitch *et al.* (2007) which is overlain with the World Wildlife Fund (WWF) Global 200 priority conservation areas and used to assess threats of O_3 deposition to biodiversity. This identifies eco-regions of South and East Asia, Central Africa and Latin America as being at risk from elevated O_3 levels during this century, in addition to areas of North America and Europe where the effects of O_3 are better documented. However, there is almost no information available on whether the plant communities in regions outside of North America and Europe are as sensitive to O_3, and hence the real significance of these areas of potential risk to biodiversity is completely unknown.

As atmospheric CO_2 concentrations alter in the future, so too will climate, and particularly temperature and precipitation; both these factors are also important in determining stomatal conductance and hence crop productivity and uptake of pollutants such as O_3. As such, reduced stomatal conductance that might occur in response to elevated CO_2 may enhance water use efficiency of plants, which could help to partly alleviate the effects of reduced rainfall. The projected increase in temperatures in many parts of the world mean that yields from crops may also be reduced (Lobell and Field, 2007). Increased water stress in a warmer climate may also be expected to

136

decrease sensitivity to O_3 through reduced uptake; however O_3 induced damage to stomatal functioning (Mills *et al.*, 2010; Wilkinson and Davies, 2009, 2010) might confound this effect. The exact impacts of pollutants on vegetation in the future will be complicated by the differential response of plants to climate change and rising CO_2 levels, whereby the latter will increase growth and might offset some of the projected yield losses from crops by the former.

There is an impact of BC on the carbon cycle through the created dimming effect and its concomitant effects on surface temperature and air-vapour deficit changes. Only recently have global models been able to account for effects of PM on vegetation. This is done by accounting separately for direct and diffuse radiation and by dividing photosynthesis between sunlit and shaded leaves. A first attempt to quantify the effects of all types of PM (scattering and absorbing, including BC) and clouds on the regional and global carbon sinks (Mercado *et al.*, 2009) has estimated changes in the diffuse fraction of -5 per cent to 30 per cent during the global dimming period (1950-1980) which correspond to a contribution to the regional carbon sink of up to 30 g $C/m^2/yr$ across Europe, the eastern USA, East Asia and some tropical regions in Asia (Figure 4.12). Con-

versely, during the brightening period (1980-2000), a reduction in the diffuse fraction over Europe, eastern USA, western Australia, and some regions of Russia and China, led to a lower regional contribution to the land carbon sink from diffuse radiation. Globally, over the 1960-2000 period, diffuse radiation effects associated with changes in PM and clouds in the atmosphere enhanced the land carbon sink by about 25 per cent. This more than offsets the negative effect of reduced surface radiation on the land carbon sink, giving a net effect of changes in radiation on the land carbon sink of 10 per cent (Mercado *et al.*, 2009). The framework used in Mercado *et al.* (2009) could be used to evaluate the impacts of BC alone on land carbon uptake through the combination of reductions on surface radiation and concomitant changes in temperature and atmospheric vapor pressure deficits.

4.7 Vulnerability to changes in climate, black carbon and ozone concentrations

Vulnerability analysis is a form of risk analysis concerned with answering the question 'who is vulnerable to what, when and where'. To answer this in the context of possible impacts associated with BC and O_3 this Assessment attempts to provide specific examples of the ex-
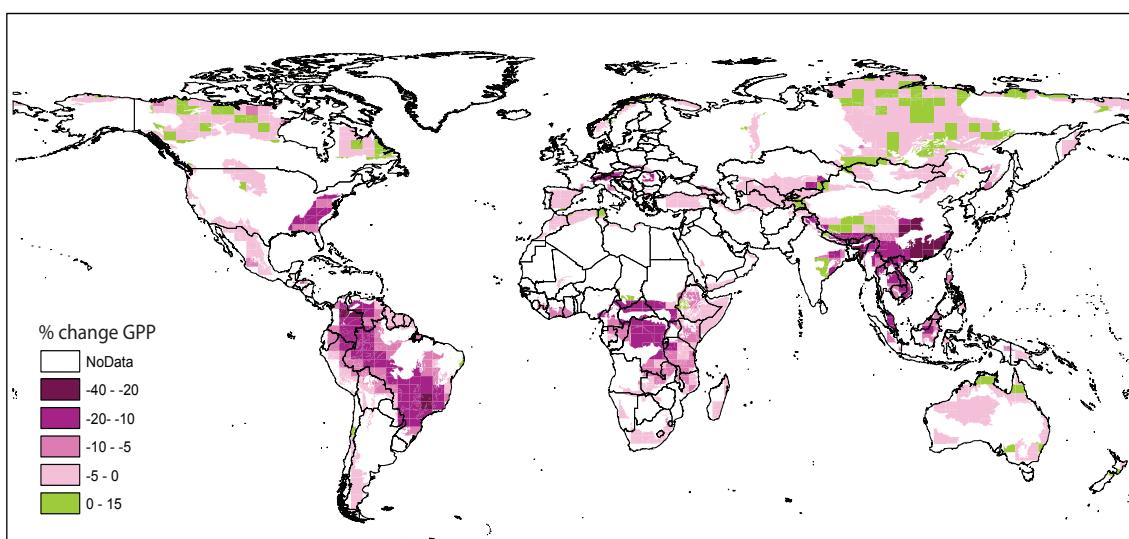
Figure 4.11. Global assessment of the key biodiversity areas at high risk from O_3 impacts; the figure shows the projected per cent decrease in gross primary productivity (GPP) due to O_3 within the Global 200 priority conservation areas. For further details see the Royal Society (2008).

137

posures/stressors that can be either environmental or non-environmental, the sensitivity of the system and its potential to cope or to adapt to the resulting change. Such examples need to be considered for each specific (place-based) situation that is understood within the context of the influencing factors outside the place (hence the need to look multi-scale). An analytical framework for vulnerability assessment is presented in Figure 4.13.

Ideally, this Assessment would be able to attribute vulnerability to a variety of environmental responses that occur as a result of BC and O_3 pollution, either indirectly through changes in radiative forcing leading to regional climate change, or directly through toxicological impacts on human health, agriculture and ecosystems, leading to the changes in the provision of ecosystems services. However, such accurate attributions are not possible due to uncertainties associated with the magnitude, geographical extent and even sometimes the direction of the response. As such this Assessment concentrates on assessing more generic vulnerability, identifying key environmental (regional climate), human health and ecosystem responses to BC and O_3 pollution in those regions, or under those human conditions where impacts are most likely to increase people's vulnerability to hazards. This section sets the scene, identifying the core vulnerabilities that might be expected as a consequence of environmental changes that could be attributed to BC and O_3.

4.7.1 Vulnerability to changes in regional climate

As discussed in the previous sections, the regional temperature, precipitation and cloud-cover environmental responses to BC and O_3 concentrations layered over large-scale changes in the global climate system, will have many implications for the human condition and may increase risks in regions where populations have particularly low resilience in the face of change. This section focuses on two regions of the world, South Asia and the Arctic, which have been identified as being particularly susceptible to environmental change resulting from BC and O_3 and whose communities' are particularly vulnerable to such change.

South Asia
One region of the world where the links between BC and O_3, regional climate, and hydrologic change are particularly acute is South Asia. In this region, high levels of BC and O_3 are likely to change regional weather patterns (see Section 4.2.2) affecting the availability and distribution of reliable water supplies. The link between regional climate and hydrology is further complicated in South Asia by the important role that snow and glacier ice play in the Himalayan Range, defining the regional hydrology and the links between BC, albedo and energy balances. At some level, changes in the regional hydrology would have implications for the management of installed
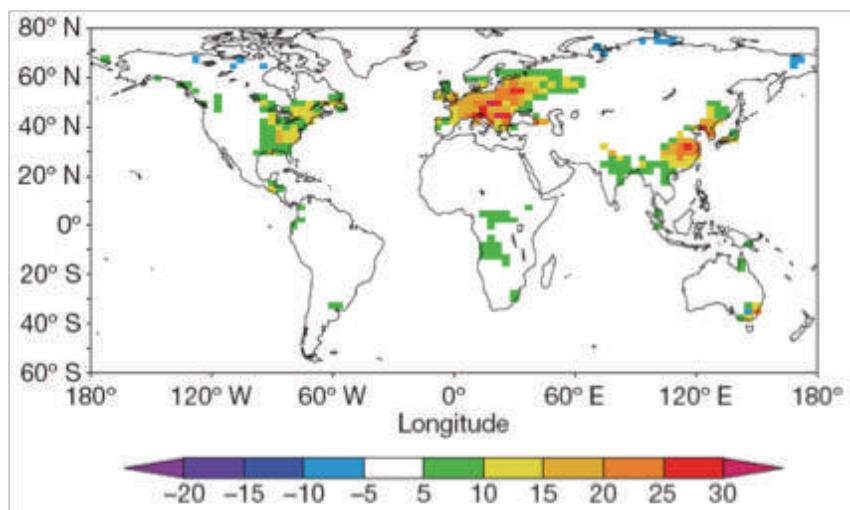
Figure 4.12. Simulated change (colour scale, g C/m²/yr) in diffuse fraction contribution to land carbon accumulation between 1950 and 1980 (Mercado *et al.*, 2009).

hydraulic infrastructure that is operated to meet multiple objectives, including the generation of hydropower and the provision of water to urban, industrial, and agricultural users. South Asia is a region which is industrializing rapidly, yet still a large number of people live in poverty, and are vulnerable to changes in climate and water supply. While this is true for the large number of rural poor reliant on agriculture, these people also lack infrastructure and resources to withstand natural disasters. People living in Himalayan valleys below rapidly developing glacial lakes (Box 4.6) are vulnerable to flooding of large areas that would result from these lakes bursting.

Whilst there is no evidence to link the recent floods in Pakistan to climate change, their impact illustrates the vulnerability of large numbers of people. The floods that hit Pakistan during the summer of 2010 came about through an unprecedented meteorological event caused by unusual holding patterns in the jet stream that coincided with the summer monsoon rains. The result was a series of sustained, extremely heavy precipitation events, the worst seen in the country for the past 80 years, leading to floods of unprecedented ferocity and duration that overwhelmed the infrastructure and management systems of the country. What the situation in Pakistan does indicate is how vulnerable countries can be to known hydrologic variability. Large investments in physical infrastructure, including large dams, are needed, e.g. Pakistan can store only 30 days of the average flow of the Indus.

This challenge is made more serious by uncertainties about climate change and its effect on rainfall and snowmelt in the Himalayas. Forty-five per cent of the normal flow of the Indus comes from glacial and snowmelt and, as has been shown in previous sections, BC and O_3 are potentially very important in determining the state of these Himalayan glaciers. While the Ganges basin is less dependent on glacier meltwater as a source of river flow, water users on the Gangetic Plain still benefit from mountain snow and ice, particularly in dry seasons, and are involved in livelihood activities that leave them vulnerable to change. The geo-political situation between nations in the Himalayas adds yet another level of complexity to this vulnerable system.
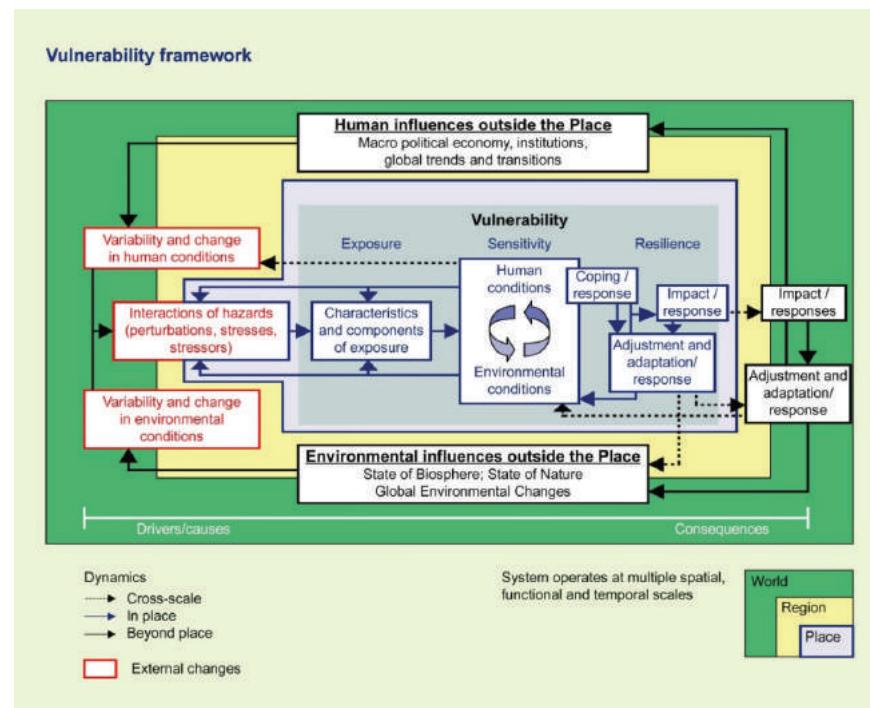
Figure 4.13. A framework to understand vulnerability and how it is affected by multiple factors (from Turner *et al.,* 2003) depicting how the different dimensions and characteristics of vulnerability are related.

139

The Arctic

The Arctic, which has experienced temperature rises twice that of the global mean over recent decades, is a region in which changes are already resulting in increased impacts in vulnerable ecosystems and human populations. In particular, the traditional economic and cultural activities of Arctic indigenous communities have already suffered.

Many indigenous communities rely on fishing, hunting, herding and linked activities. Already under cultural stress for several centuries, environmental changes in Arctic flora and fauna have placed these traditional activities at even greater risk. Recession of sea-ice around Greenland has, for example, made travel and hunting by dogsled or snowmobile dangerous or impossible during increasingly long periods of the year.

Patterns in fish populations have also changed, threatening Arctic livelihoods. New research, conducted under the auspices of the International Polar Year (2007-09), suggests that already-declining Arctic fish and sea mammal populations are at extreme near-term risk from the recession of sea-ice because of the dependence and specialization of the Arctic food chain on ice cover. Total collapse may occur within the space of two to three years after the disappearance of summer sea-ice, projected to occur around 2030 if current rates are not somehow slowed (Søreide *et al.*, 2010).

The combination of permafrost melt and sea-level rise has proven too much for many Arctic communities, with flooding, collapse of roads and buildings causing several communities to abandon traditional sites and move inland. Such damage is anticipated to accelerate and move further south should present rates of warming not be slowed. Norway and Sweden are among the nations that have already committed significant resources to managing these changes, including plans for wholesale movement of populations in anticipation of damage from permafrost melt and more frequent and severe weather events (O'Brien *et al.*, 2006; SOU, 2007).

Large industry has also experienced the impact of these changes. Reports from Russia, Canada and the USA indicate that repairs to oil and gas pipelines cannot keep pace with collapse from permafrost melt, leading to extensive leakage of CH_4 which will exacerbate global warming in addition to presenting increased risk from oil spills and explosions (Acclimatise, 2009; USGCRP, 2009; Lesikhina *et al.*, 2007, Williams and Wallis, 2009).

4.7.2 Increased vulnerability from black carbon and ozone affects on human health

Human health can be directly affected by regional climate change. Impacts can occur through a number of different means which include changes in temperature leading to increased occurrences of heat-stress – though these may, to some extent, be off-set by milder winters leading to reduced cold-stress. Changes in hydrology, mediated by precipitation and glacial melt, leading to riverine flooding. In the worst case this can lead to death but also to other flood-related health problems including both mental and physical effects through water-borne diseases. These diseases may be caused by increases in water temperature and increases in wash-off reducing water quality leading to poor sanitation; by increases in vector-borne diseases such as malaria and tick fever and by increases in incidences of food poisoning as a result of food contamination. Physical effects can also be caused by increased frequencies of storms and high winds, leading to an increase in injuries from flying debris.

Human health impacts, including mortality and morbidity, directly arising from BC (considered here as $PM_{2.5}$) and O_3 can manifest themselves as differential responses at an individual level resulting from exacerbations of the effect of exposure by underlying disease status, by psychosocial factors such as stress, or by socio-material factors including poverty. Examples include: people with diabetes have twice the risk of cardiovascular mortality following exposure to PM air pollution (Bateson and Schwartz, 2004), race and educational level strongly modify the mortality risk on very hot days (O'Neill *et al.*, 2003), and genes related to oxidative

140

stress defenses modify the risk of air pollution (Madrigano *et al.*, 2009; Curjuric *et al.*, 2009; Chahine *et al.*, 2007). Overall, there is some evidence of gender differences in the health effects of air pollutants, and clear evidence of susceptibility being modified by obesity and diabetes, the prevalence of which is rapidly increasing in the developing world especially in China and India.

Of particular importance, the health effects of O_3 have been shown to be higher when temperature is higher, suggesting the pattern of increased temperature and O_3 will be particularly toxic, especially in populations unable to afford or use air conditioning. The health effects of BC on birth weight were found to be worse in people with a poor standard of living (Zeka *et al.*, 2008). These issues can be addressed through attempts to define sub-populations with two or three times the risk, providing evidence that exposure contributes to health disparities as well as ill health. This can then be coupled with differential exposure, where the wealthier people have cleaner cooking fuels, live in less polluted areas, etc, which also contribute to health disparities. For example, exposure to BC is highest in less developed countries that depend on biomass fuels but within these countries, this is more prevalent amongst poorest people. Using such covariation of exposures with susceptibility factors, a recent risk assessment showed a considerable disparity in the impact of air pollution on mortality in Mexico (Stevens *et al.*, 2008), and, relevant to cumulative risk assessment, showed the same disparity gradient for poor water quality and cooking fuel use.

These countries, and many of their inhabitants, often lack the resilience to deal successfully with challenges. Most studies of air pollution and mortality have reported CRF slopes that increase with age. The age pyramid is changing in the developing world and an increased age of the population, as well as increased prevalence of diabetes is expected by 2030. This will exacerbate the effects of pollution. Finally, these differential impacts, both within and between countries, generally result in a greater additional burden to the people who have the worst health in the first place.

4.7.3 Increased vulnerability of agriculture and ecosystems to black carbon and ozone

Agricultural production will be affected by changes in regional climate especially through alterations in precipitation reliability and timing. Such changes may lead to increases in the frequency and severity of flooding or droughts, warmer temperatures may increase demand for irrigation, and can also reduce yields.

The study of O_3 impacts on agriculture performed in this Assessment uses national production and world market prices to estimate economic losses. It ignores subsistence farming – where products tend to be produced and consumed within households or local communities. The study is also unable to capture the importance of changes in supply affecting food prices that, in turn, will affect access to food; for low-income households, where a large fraction of income goes for food provision, such price increases can substantially affect food security of the poor and the most vulnerable.

Finally, vulnerability to O_3 impacts on agriculture vary, in the same way as discussed previously for human health, according to the co-variation of a number of different factors such as O_3 exposure, agricultural management practices, geographical location and growing-season distribution of sensitive crops and crop varieties. Other stressors to agricultural production that may interact with O_3 impacts include the ability of farming systems to adapt to such stresses and the capacity of consumers to cope with increased prices of key commodities; these factors will vary regionally and with socioeconomic demographics. All these combine to determine vulnerability and need to be understood to provide an accurate assessment of which individuals, communities and farming practices are most at risk from impacts resulting from BC and O_3.

Appendix A.4

The impact assessment methodology used in Chapter 4, describing the Assessments reference scenario, is further described within this Appendix A.4. This methodology is the same as that is used in Chapter 5 to evaluate the impacts of the emission reductions measures identified in this Assessment.

A.4.1. Methodology for the composition-climate modeling

A methodology was developed to place the results of the new modelling performed specifically for this Assessment into context with the wider assessment of the literature. As such, use is made of the radiative forcing calculated by the two models used (GISS-PUCCINI and ECHAM-HAMMOZ), but those results are scaled according to the best estimates of total anthropogenic forcing described in Chapter 3. Hence the values from the specific models are used as initial inputs to the temperature projections, but the results are unlikely to be sensitive to potential systematic biases in the models (e.g. the direct forcing from BC being on the low end of the range) due to the scaling to the literature range. Furthermore, the scaling provides an uncertainty range on the temperature projections that is far more representative of the current state of knowledge than would be the results from only the two models. Note that the results presented in this appendix are based upon the reference scenario described in Chapter 4 and the emissions control measures described in Chapter 5.

Ozone forcing and direct forcings for aerosols were calculated internally within the climate models. The two models produced very similar values for aerosols (within 10 per cent), but somewhat larger differences of 30 to 50 per cent for O_3 (Table A.4.1). Forcing from NO_3^- aerosols is based only on the GISS model as ECHAM did not simulate them, but this is a very small component of aerosol forcing (global mean 0.01 W/m^2 or less for the 2030 reference versus 2005 or for any of the 2030 measures versus reference).

As aerosol indirect effects (AIE) have very high uncertainties (Chapter 3) and are difficult to diagnose in climate models, using results from the pair of models run for this Assessment has been avoided. Instead it includes an estimate of AIE based on the range of values given in the literature. For scattering aerosols, the assumption that they are equal to the direct effect from SO_4^{2-} aerosols is used. Calculations based on detailed modeling and observations suggest that the ratio of AIE to direct SO_4^{2-} radiative forcing (RF) is 1.5 to 2.0 (Kvalevåg and Myhre, 2007), but a lower value of 1.0 is used as recent analyses based on satellite data suggest that at least a portion of the AIE may in fact be fairly weak (Quaas et al., 2008) and that adjustments to cloud liquid water path may offset changes in particle size, and models that now include aerosol effects on mixed-phase clouds tend to show smaller indirect forcings than earlier models (Isaksen et al., 2009). While there are many studies showing substantial AIE for sulfate aerosols (as many early simulations included only sulfate aerosols), we were unable to find any publications isolating AIE attributable to other scattering aerosol species. In the absence of any quantification of AIE due to OC or nitrate, we assigned the full scattering aerosol AIE to sulfate. Dominance of sulfate in AIE is consistent with its greater solubility and mass relative to carbonaceous or nitrate aerosols, but we caution that apportionment of AIE to individual aerosol species is not well constrained and requires further study. An uncertainty of 66 per cent on the reflective aerosols NO_3^- and SO_4^{2-} is included, based on a recent assessment (Isaksen et al., 2009); for NO_3^- assuming their impact is only through direct effects while for the SO_4^{2-} it is included for both the direct and indirect effects.

As discussed, there is a wide range of results in the literature for both the direct forcing by BC and its many indirect effects. Following the discussion in Chapter 3, all the forcing results are scaled to a range of 0.3 to 0.6 W/m^2 as the most probable range for the pre-industrial to present-day direct forcing, with the central value simply the mid-point of this range. Hence the effect of measures are the direct BC forcings cal-

Table A.4.1. GISS-PUCCINI and ECHAM-HAMMOZ 2030 forcing relative to the reference due to the measures (W/m²).

	CH₄ measures	CH₄+BC Group 1 measures	All measures
ECHAM O$_3$	-0.09	-0.10	-0.10
GISS O$_3$	-0.10	-0.17	-0.19
ECHAM aerosols*	-0.01	-0.06	-0.15
GISS aerosols* (BC, OC, SO$_4^{2-}$, NO$_3^-$)	-0.01 (0.00, 0.00, -0.02, 0.00)	-0.06 (-0.10, 0.06, -0.02, 0.01)	-0.17 (-0.22, 0.07, -0.02, 0.01)
ECHAM CH$_4$	-0.22	-0.22	-0.20
GISS CH$_4$	-0.20	-0.20	-0.18

*For aerosols, the value for ECHAM is the sum of the direct BC+OC+SO$_4^{2-}$ forcing, while for GISS the same sum is presented first with individual components listed afterwards (the ECHAM model has more realistic internally mixed aerosols, so components are not separable). Note that methane forcing at 2030 is roughly 70–75 per cent of the forcing that is eventually realized from methane emission changes through 2030.

culated in the GISS model (see Table A.4.2), for example, scaled by 0.45/0.32 to get the central estimate of direct forcing from BC and by 0.3/0.32 and 0.6/0.32 to get the lower and upper bounds where 0.32 is the preindustrial to present-day forcing in the GISS model. Note that the positive scaling for even the central estimate is consistent with the underestimate of Absorbing Aerosol Optical Depth (AAOD) in the model in some regions discussed in the Appendix to Chapter 3. Again based on the studies dis-

cussed in 3.A, the assumed combined effect of the semi-direct and indirect effects of BC is from -0.4 to +0.4 W/m² from preindustrial time to the present day, and hence add an uncertainty of ±0.4/0.32 times the direct forcing calculated in this Assessment's models. Black carbon's effect on snow and ice albedo (Warren and Wiscombe, 1980) is included as an effective forcing equal to 0.05 to 0.25 W/m² from pre-industrial time to the present day (see Chapter 3), but rather

Table A.4.2. Derivation of forcing values used in the temperature response calculations (W/m²).

	Average forcing from GISS and ECHAM models	Forcing as a percentage of total anthropogenic forcing	Assessment range for anthropogenic forcing from literature	Resulting forcing used in temperature response calculation
CH$_4$ measures	O$_3$: -.10	-37%	O$_3$: .35 (.25 to .45)	O$_3$: -.13 (-.09 to -.17)
	CH$_4$: -.21	-44%	CH$_4$: .48 (.43 to .53)	CH$_4$: -.21 (-.19 to -.23)
	BC direct: .00	0%	BC direct: .45 (.30 to .60)	BC direct: .00 (.00 to .00)
	BC semi-direct +indirect: .00	N/A	BC semi-direct +indirect: .00 (-.40 to .40)	BC semi-direct +indirect: .00 (.00 to .00)
	BC dep: N/A	0%	BC dep: .15 (.05 to .25)	BC dep: .00 (.00 to .00)
	OC: .00	0%	OC: -.20 (-.09 to -.31)	OC: .00 (.00 to .00)
	SO$_4^{2-}$: -.02	7%	SO$_4^{2-}$: -.29 (-.10 to -.48)	SO$_4^{2-}$: -.02 (-.01 to -.03)
	SO$_4^{2-}$ indirect: -.02	7%	SO$_4^{2-}$ indirect: -.29 (-.10 to -.48)	SO$_4^{2-}$ indirect: -.02 (-.01 to -.03)
	NO$_3^-$: .00	0%	NO$_3^-$: -.10 (-.03 to -.17)	NO$_3^-$: .00 (.00 to .00) Sum: -.38 (-.30 to -.46)

	Average forcing from GISS and ECHAM models	Forcing as a percentage of total anthropogenic forcing	Assessment range for anthropogenic forcing from literature	Resulting forcing used in temperature response calculation
CH_4 + BC Group 1 measures	O_3: -.14 CH_4: -.21 BC direct: -.10 BC semi-direct +indirect: .00 BC dep: N/A OC: .06 SO_4^{2-}: -.02 SO_4^{2-} indirect: -.02 NO_3^-: .01	-52% -44% -31% N/A -38% -63% 7% 7% -10%		O_3: -.18 (-.13 to .23) CH_4: -.21 (-.19 to -.23) BC direct: -.14 (-.09 to -.19) BC semi-direct +indirect: .00 (-.13 to .13) BC dep: -.06 (-.02 to -.10) OC: .13 (.06 to .20) SO_4^{2-}: -.02 (-.01 to -.03) SO_4^{2-} indirect: -.02 (-.01 to -.03) NO_3^-: .01 (.00 to .02) Sum: -.49 (-.32 to -.66)
CH_4 + All BC measures	O_3: -.15 CH_4: -.19 BC direct: -.21 BC semi-direct +indirect: .00 BC dep: N/A OC: .07 SO_4^{2-}: -.02 SO_4^{2-} indirect: -.02 NO_3^-: .01	-56% -40% -66% N/A -66% -74% 7% 7% 10%		O_3: -.20 (-.14 to -.25) CH_4: -.19 (-.17 to -.21) BC direct: -.30 (-.20 to -.40) BC semi-direct +indirect: .00 (-.26 to .26) BC dep: -.10 (-.03 to -.17) OC: .15 (.07 to .23) SO_4^{2-}: -.02 (-.01 to -.03) SO_4^{2-} indirect: -.02 (-.01 to -.03) NO_3^-: .01 (.00 to .02) Sum: -.67 (-.23 to -1.10)

Notes: Radiative forcing due to BC deposition (called BC dep) was not calculated, rather BC deposition itself was used to derive the fractional change, which was multiplied by the assessed value of the effective forcing from BC deposition. The ECHAM model has more realistic internally mixed aerosols, so components are not separable, hence the relative contribution to aerosol forcing from individual species is based on the GISS model. The assessment range for anthropogenic forcing is not repeated for each measure as it is independent of measure.

than base this on the direct forcing the Assessment uses the change in BC deposition calculated in the GISS simulations relative to the pre-industrial time to present-day BC deposition change – the latter was not available for ECHAM, but the deposition changes appear to be quite similar in the two models (Chapter 3). Finally, given that there are constraints on the total aerosol forcing, the scalings applied to BC's direct forcing are limited so that the total value cannot exceed 1 W/m² (see Chapter 3).

For consistency in the treatment of different pollutants, a similar methodology was adopted for organic carbon, scaling GISS results, for example, by -0.20/-0.095 for the central estimate, and -0.09/-0.095 and -0.31/-0.095 for the bounds. For O_3, the central estimate was scaled by 0.35/0.27, and 0.25/0.27 and

0.45/0.27 for the bounds. These ranges are again based on the evaluations in Chapter 3. This provides a consistent framework for evaluation of the key species involved in the recommended measures other than CH_4 (see below). No adjustments were applied to SO_4^{2-} or NO_3^- forcings, as these were very similar to the central range from the IPCC AR4 at -0.29 W/m^2 and -0.10 W/m^2 respectively (GISS model). Aerosol forcings were assumed not to be independent given constraints on their total, and hence were summed, based on their absolute value, to obtain upper and lower bounds. The total aerosol forcing and all other forcing uncertainties were assumed to be independent, so the larger values and the smaller values were summed separately to derive upper and lower bounds (the study did not sum in quadrature as it did not know the probability distribution within the ranges and it was believed that summation in quadrature would produce unrealistically small uncertainties).

The response to CO_2 emissions was calculated using impulse response functions derived from the Bern Carbon Cycle Model (Siegenthaler and Joos, 1992) based on the version used in the IPCC TAR. Exponential fits to those functions are used to calculate the CO_2 concentration at a given year resulting from all emissions in prior years. This approach is limited compared with a more sophisticated carbon cycle model, especially in the latter part of the 21st century when CO_2 levels become substantially larger in some scenarios and could induce additional feedbacks. Historical emissions of CO_2 are taken from the Carbon Dioxide Information Analysis Center database (Marland *et al.*, 2008). Carbon dioxide emissions for both the reference and the 450 scenario, the latter corresponding to the long-term stabilisation of the atmospheric concentration of greenhouse gases at 450 ppm CO_2e, are from the International Energy Agency World Energy Outlook 2009 report (IEA, 2009). In the period from 2030 to 2050 the CO_2 emissions increase by ~12 Gt in the reference scenario but decrease by ~16 Gt in the IEA 450 scenario.

The Assessment also performed an offline calculation of the CH_4 response to changes in emissions over time using an analogous model but with a single impulse-response function that uses the CH_4 lifetime. Emissions under the reference or IEA 450 scenarios were used along with the lifetime calculated for those scenarios in the full global composition model (emissions after 2030 are assumed to be constant). For other scenarios, the difference between the average year 15 to 19 methane abundance simulated in the full composition model and the baseline model was linearly imposed upon the baseline concentration trends between 2005 and 2040, as the bulk of the response to emissions changes through 2030 would have been realized given a decade or more response time. Radiative forcing from CO_2 and CH_4 are calculated using the standard IPCC TAR formulation (Ramaswamy *et al.*, 2001), with an uncertainty of 10 per cent for the radiative effect of each as in previous studies (e.g. Forster *et al.*, 2007) plus additional uncertainties of 1 per cent for the CH_4 response to hydroxide (OH) changes (Prather *et al.*, 2001) and 5 per cent for CO_2 to account for carbon-cycle feedbacks. All values are instantaneous forcings at the tropopause.

The surface temperature response to the calculated radiative forcings is estimated following the methodology used in calculation of global temperature potentials (Shine *et al.*, 2005). This is further extended to regional temperatures following the method described in Shindell and Faluvegi (2010). In essence, a rough approximation of global and regional responses was obtained by multiplying the calculated RF by the global or regional transient sensitivity and accounting for ocean inertia by including a tapering influence of forcing during the prior 20 years (based on a fit to the prior model runs). While many simple global energy balance models exist, the calculations that allow estimation of regional responses which include the influence of both local and remote forcings using the results of Shindell and Faluvegi (2009) and the spatial patterns of forcing calculated here.

In the calculations, the surface temperature change in area *a* between time 0 and time *t* is given by:

145

$$dT_a(t) = \int_0^t ((k_{SHext,a}*F_{SHext}(t') + k_{Tropics,a}*F_{Tropics}(t') +$$

$$k_{NHml,a}*F_{NHml}(t') + k_{Arctic,a}*F_{Arctic}(t')K\ Gk_{Global,a})*f(t-t')\ dt'$$

where F_{area} is the radiative forcing in the particular area (where NHml is northern hemisphere mid-latitudes, SHext is southern hemisphere extratropics), and the $k_{x,y}$s are the response coefficients giving temperature response in the area y to forcing in area x (Shindell and Faluvegi, 2009) (Table A.4.3). The first term in the integral represents the RF weighted by regional sensitivities while the second term, $f(t)$, describes the climate system's inertial response. The latter is defined as:

$$f(t) = 0.541/8.4\ \exp(-t/8.4) +$$

$$0.368/409.5\ \exp(-t/409.5)$$

where t is the time in years and the two exponentials represent the relatively rapid response of the land and upper ocean, and the slower response of the deep ocean as reported for simulations with the Hadley Centre climate model (Boucher *et al.*, 2009), with absolute responses scaled by 0.857 to match the transient climate sensitivity of the GISS model (0.53°C per W/m² for increasing greenhouse gases) for consistency with the other model results used in this Assessment and as the sensitivity in the simulations used to derive the responses was high even compared with standard Hadley Centre simulations.

Historical forcing is based solely on CO_2 emissions as forcing from CO_2 alone is approximately equal to the net forcing to date (Forster *et al.*, 2007), so that the inertial response to historical CO_2 forcing provides a good estimate for the total inertial climate response. Forcings for aerosols and O_3 were linearly interpolated between 2010 and 2030. We assumed that these forcings remained constant after 2030 in these temperature response calculations. Methane emissions also remained constant after 2030, though methane concentration continued to evolve. Carbon dioxide emissions were linearly extrapolated past 2030, increasing at 1.53 per cent per year in the reference scenario and decreasing by 0.84 per cent per year under the low-carbon scenario. Calculations were performed for each latitude band and for the global mean. Uncertainties were derived by adding the forcing uncertainty in quadrature with the uncertainty in climate sensitivity, where for the latter we use the 2 to 4.5 °C range about a central estimate of 3 °C for a doubling of CO_2 given in Hegerl *et al.* (2007) and deemed there to represent the 67 per cent confidence interval for climate sensitivity (corresponding to a transient climate response of 1.3 to 3 °C for a doubling of CO_2). In cases with large forcing from BC, uncertainties may be even larger as the surface temperature response per unit radiative forcing can vary substantially depending on the vertical profile of the BC (Hansen *et al.*, 2005).

Regional estimates of temperature change from climate models are not reliable in many cases. Hence the estimates of the regional temperature response to the measures analyzed in this Assessment are based on the regional temperature changes calculated for each latitude band. The temperature changes were multiplied by the ratio of land area versus the total latitude band change seen in observations (Hansen *et al.*, 2005) to account for the more rapid response of land to forcing. For each region, the temperature changes were then averaged by latitude band weighting the result by the land area of that region within each band.

A.4.2. Methodology for the health impact assessment

Health impacts of changes in outdoor air pollution from 2005 to 2030 according to the reference scenario are based on $PM_{2.5}$ and O_3 concentrations simulated by the GISS and ECHAM global chemical transport models (see Chapter 1). For assessment of the impacts related to PM, a scaling methodology has been used to allow for the within-grid variation in PM concentrations resulting from proximity to urban centers and hence emissions sources.

Methodology for urban increment

A parameterization of the urban increment for non-reactive primary emitted anthropogenic BC and organic matter has

146

Table A.4.3. Regional response coefficients (°C per W/m² local forcing)

Forcing region	SHext	Tropics	NHml	Arctic	Global
Response region					
SHext	0.19	0.05	0.02	0.00	0.39
Tropics	0.09	0.24	0.10	0.02	0.47
NHml	0.07	0.17	0.24	0.06	0.53
Arctic	0.06	0.16	0.17	0.31	0.64

Regional responses per unit forcing are the mean of responses to CO_2 and SO_4^{2-} taken from Figure 1 of (Shindell and Faluvegi, 2009).

been developed and tested with a global air quality model with 1°x1° resolution (TM5, Krol *et al.*, 2005). The correction is applied off-line after the mean grid cell $PM_{2.5}$ values have been calculated with the air quality model. The correction takes into account that within a single model grid cell, $PM_{2.5}$ concentration gradients may occur, in particular if part of the grid cell is more densely populated than the remainder of the grid cell. This is accomplished using a high-resolution (2.5'x2.5') population dataset (CIESIN, university of Columbia) which subdivides the 1°x1° "native" grid in (in this case) 24x24 subgrids. A subgrid is labelled as 'urban' if the population density exceeds 600/km², and 'rural' otherwise. The same methodology can be applied to any model resolution larger or smaller than 1°x1° as long as it contains at least 4 population sub-grid cells.

Let f_{UP} be the urban population fraction, defined as the fraction of the population within the native grid cell which resides in the urban-flagged sub-grids, and f_{UA} the urban area fraction, being the fraction of the native grid area occupied by the urban-flagged sub-grids (the number of urban sub-grids divided by the total number of sub-grids).

Let E_{BC} be the emission strength of the anthropogenic BC of the whole native grid cell. The assumption is made that the fraction $f_{UP} \cdot E_{BC}$ is emitted from area $f_{UA} \cdot A$ (A being the grid cell area) and $(1- f_{UP}) \cdot E_{BC}$ from area $(1- f_{UA}) \cdot A$.

Under steady-state conditions, neglecting the incoming concentration of BC from neighbouring grid cells, the native grid-average BC concentration can be written as:

$$C_{BC,av} = \frac{E_{BC}}{\lambda} \qquad \text{with } \lambda = \text{ventilation factor.}$$

Assuming the ventilation factor λ is also valid for the urban and rural part of the grid cell (equivalent with the assumption that mixing layer height and wind speed are the same), the steady-state concentration in the urban and rural sub-areas can be written as:

$$C_{BC,URB} = \frac{f_{UP}}{f_{UA}} \frac{E_{BC}}{\lambda} \qquad \text{and}$$

$$C_{BC,RUR} = \frac{(1 - f_{UP})}{(1 - f_{UA})} \frac{E_{BC}}{\lambda}$$

The ventilation factor l, including an implicit correction factor for the non-zero background concentration in neighbouring cells, is obtained by taking advantage of the explicitly modelled grid cell concentration with the air quality model:

$$\lambda = \frac{E_{BC}}{C_{BC,av}}$$

Hence,

$$C_{BC,URB} = \frac{f_{UP}}{f_{UA}} C_{BC,av} \qquad \text{and}$$

$$C_{BC,RUR} = \frac{(1 - f_{UP})}{(1 - f_{UA})} C_{BC,av}$$

In order to avoid artificial spikes in urban concentrations when occasionally a very small fraction of the native grid cell contains a very

Chapter 4. Impacts of black carbon and tropospheric ozone

large fraction of the population, empirical bounds are applied on the adjustment factors:

1) Rural Primary BC and POM $(C_{eq,RUR})$ should not be lower than 0.5 times the native grid average;

2) Urban primary BC and POM should not exceed the rural concentration by a factor of five.

In any case, the urban and rural adjustments for each of the primary components must fulfill the condition:

$$f_{UA}C_{URB} + \left(1 - f_{UA}\right)C_{RUR} = C_{av}$$

The adjusted urban and rural concentrations of the primary emitted components can be cast in one native grid population-weighted average value:

$$C_{BC,av}^{pop} = f_{UP} \cdot C_{BC,URB} + \left(1 - f_{UP}\right) \cdot C_{BC,RUR}$$

After substituting $C_{BC,URB}$ and $C_{BC,RUR}$, the population-weighted concentration is expressed as a function of the original grid-averaged concentration at the native resolution:

$$C_{BC,av}^{pop} = \left[\frac{(f_{UP})^2}{f_{UA}} + \frac{(1 - f_{UP})^2}{1 - f_{UA}}\right] \cdot C_{BC,av}$$

And similar for primary anthropogenic organic carbon.

All secondary components (SO_4^{2-}, NO_3^-) and primary natural PM (mineral dust, sea salt) are assumed to be distributed uniformly over the native grid cell and hence are not incremented.

Validation of the urban increment methodology

Use is made of a consolidated database of urban measurements established in the frame of the Global Burden of Disease project (Brauer et al., 2011). Because the database contains exclusively urban measurements, the adjusted urban $PM_{2.5}$ is extracted from the model, rather than the population-weighted average for the whole grid cell. The scatter plots (Figure A.4.1.) show that, on average, the applied parameterization significantly improves the performance of the model compared to the non-adjusted $PM_{2.5}$ concentration, although the scatter remains high. Reproducing the high variability of primary $PM_{2.5}$ levels in the vicinity of its sources is beyond the scope and possibilities of the current global models, however it is believed that that region-wide exposure estimates are improved by applying the methodology described above.

Defining the human health dose-response relationships for $PM_{2.5}$ and ozone

Global chemical transport models have been used previously to estimate the global burden of anthropogenic air pollution on mortality (Anenberg et al., 2010) and mortality impacts due to future changes in emissions (West et al., 2006, 2007), changes in one sector's emissions (Corbett et al., 2007), and long-range transport of air pollution (Anenberg et al., 2009, Liu et al., 2009c, West et al., 2009). These studies have varied have used acute or chronic CRFs and assumed health effect thresholds at low and high concentrations.

This Assessment uses logarithmic $PM_{2.5}$ CRFs from the American Cancer Society Study (Pope et al., 2002), scaled by the substantially higher mean of the US EPA Expert Elicitation (Roman et al., 2008). The methodology used here is supported by recent advice from the US EPA Science Advisory Board to use the mean of the American Cancer Society and Harvard Six Cities Studies, which is generally consistent with the mean of the US EPA Expert Elicitation. This assessment does not apply health effect thresholds at low or high concentrations for $PM_{2.5}$; however, the logarithmic CRF results in a smaller marginal impact of $PM_{2.5}$ at high concentrations than at low concentrations.

For O_3, this Assessment uses long-term relative risk estimates from the American Cancer Society Study (Jerrett *et al.,* 2009). A large body of literature from around the world finds a significant relationship between daily mortality and acute O_3 exposure (e.g. Bell *et al.,* 2005, Bell *et al.,* 2006, Ito *et al.,* 2005, Levy *et al.,* 2005, Anderson *et al.,* 2004). Jerrett *et al.* (2009) is the first major study to find a relationship between chronic O_3 exposure and mortality. While European and US EPA health impact assessments continue to use short-term CRFs, the long-term relationships include both short-term and long-term effects of O_3, and are thus more comprehensive than the short-term impacts alone. Following recommendations from the National Academy of Sciences (2008), this Assessment does not apply health effect thresholds at low or high concentrations.

Because major causes of death differ around the world, the Assessment focuses on cause-specific mortality, rather than all-cause mortality. Since the US EPA Expert Elicitation focused only on all-cause mortality, logarithmic CRFs are used for cause-specific mortality based on the American Cancer Society Study (pers. comm. Burnett; Cohen *et al.,* (2004) which included the log relationships in a sensitivity analysis), which is then scaled up by a factor of 1.8, the ratio of all-cause mortality CRFs from the mean of the US EPA Expert Elicitation to that from the American Cancer Society study.
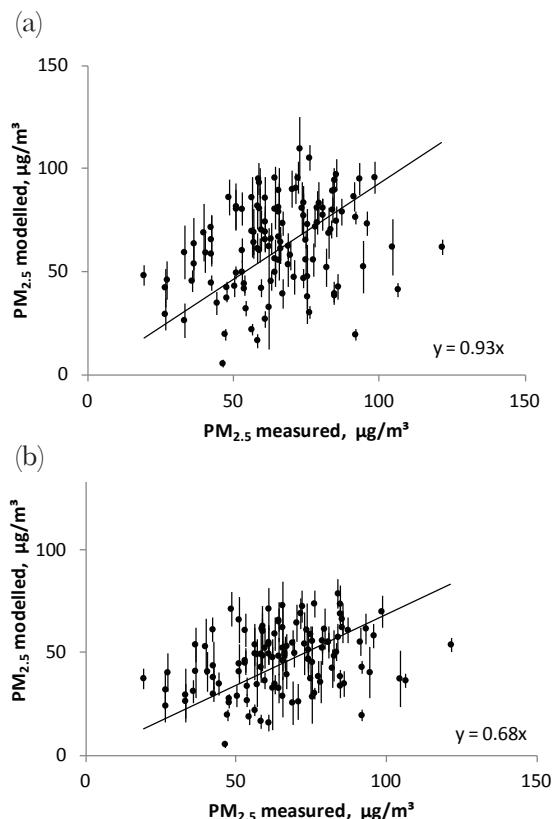
Health impacts resulting from the change in concentration from 2005 to 2030 according to the reference scenario and of the policy measures relative to the 2030 reference scenario are calculated for the 2030 population, projected using the conservative B2 growth scenario (global population increases to 8.4 billion in 2030) from the Intergovernmental Panel on Climate Change (IPCC) Special Report on Emissions Scenarios (SRES). Health impacts are calculated only for the population aged 30 and older, consistent with the American Cancer Society study. Baseline mortality rates are from the World Health Organization, following Anenberg *et al.* (2010), and are held constant to 2030, though continued development in many parts of the world will likely shift the disease burden from infectious disease to chronic and degenerative diseases, which are linked more closely to air pollution.

Several uncertainties are associated with using global chemical transport models to estimate the impacts of outdoor air pollution on mortality. These include:

- CRF;

- Extrapolating to high concentrations;

- Extrapolating to global populations;

- Assumption that all $PM_{2.5}$ components are equally toxic;

- Assumption that baseline mortality rates are unchanged from the present to 2030;

Figure A.4.1. Validation of modelled Chinese urban $PM_{2.5}$ data versus measured values. (a) unadjusted $PM_{2.5}$ model concentrations from grid-average, and (b) urban increment algorithm applied.

- Population projection to 2030;

- Large grid cells may not accurately capture exposure;

- Summation of O_3 and $PM_{2.5}$ mortalities assumes no interaction between the two.

A.4.3. Methodology for the crop impact assessment

The crop-yield loss estimates presented in this study use dose-response relationships that relate average mean growing season indices (termed M_7 and M_{12} indices relating to the 7 or 12 hours over which O_3 concentrations are averaged for the full growing season period). The indices used in the analysis were derived from a pan-US experimental campaign commonly referred to as the North American Crop Loss Assessment Network (NCLAN; Heck *et al.*, 1988). The indices and associated Weibull parameterization used for the four crops (wheat, rice, maize and soybean) investigated are provided in Table A.4.4 along with their estimated approximate standard errors that were used in the uncertainty analysis.

The Weibull dose-response model expresses

$$\gamma = \alpha.\exp\left[-\left(\frac{O_3}{\omega}\right)^{\lambda}\right]$$

Where α is the theoretical yield at zero O_3, ω is a scale parameter on O_3 dose and reflects the dose at which expected response is

reduced to 0.37 α, and λ is a shape parameter affected the change in the rate of loss in expected response.

Crop yield uncertainty analysis

Figure A.4.2 shows the 95 per cent point-wise uncertainty bounds around the median for wheat estimated in 1 ppb (0.001 ppm) O_3 increments up to 100 ppb (0.1 ppm). The uncertainties for the other crops were estimated using the same method. These uncertainty estimates assume no covariance of the Weibull parameters between exposures. Note the large uncertainty associated with rice, compared with the other crops, that has a standard error of 0.05 and 1.1 for ω and λ respectively. The uncertainty estimates are applied to provide uncertainty of crop yield losses between 2005 and the reference scenario 2030 according to:

Var(Y2 –Y1)=Var(Y2) + Var(Y1), and so the

standard deviation (sd) of the difference is:

$$sd = \sqrt{sd_1{}^2 + sd_2{}^2}$$

Where Y1 is the yield in 2005 and Y2 is the yield in 2030.

Since the 95 per cent confidence interval has a standard deviation of 3.92, the 95 per cent confidence interval of the difference is estimated by dividing the two confidence intervals by 3.92, squaring them, adding them, taking the square root, and finally multiplying by ± 1.96 to get the amounts to add and subtract from the difference.

Table A.4.4. Parameter estimates for the Weibull average response to O_3 in each crop species (wheat, rice, maize and soybean).

Crop	ω	λ	Reference
Wheat	0.136 (0.006)	2.56 (0.41)	Adams *et al.*, 1989
Rice	0.202 (0.05)	2.47 (1.1)	Adams *et al.*, 1989
Maize	0.124 (0.002)	2.83 (0.23)	Lesser *et al.*, 1990
Soybean	0.107 (0.003)	1.58 (0.16)	Lesser *et al.*, 1990

N.B. Estimated approximate standard errors are shown in parenthesis

Wheat Relative Yield by Ozone

Figure A.4.2. The 95 per cent point wise uncertainty bounds around the median for wheat estimated in 1 ppb (0.001 ppm) O_3 increments up to 100 ppb (0.1 ppm).

References

Acclimatise (2009). *Building Business Resilience to Inevitable Climate Change*. Carbon Disclosure Project Report 2008. Global Oil and Gas, Oxford, UK.

Adams, R. M., Crocker, T. D. and Thanvaibulchai, N. (1982). An economic assessment of air pollution damages to selected annual crops in southern California. *Journal of Environmental Economics and Management* 9, 42–58.

Adams, R. M., Glyer, J. D., Johnson, S. L. and McCarl, B. A. (1989). A reassessment of the economic effects of ozone on United States agriculture. *Journal of the Air Pollution Control Association* 39(7), 960–968.

Ainsworth, E. A., Rogers, A. and Leakey, A. D. B. (2008). Targets for crop biotechnology in a future high-CO_2 and high-O_3 world. *Plant Physiology* 147, 7.

Alberini, A. (2005). What is a life worth? Robustness of VSL values from contingent valuation surveys. *Risk Analysis* 25, 783-800.

Anenberg, S. C., West, J. J., Fiore, A. M., Jaffe, D. A., Prather, M. J., Bergmann D., Cuvelier, K., Dentener, F. J., Duncan, B. N., Gauss, M., Hess, P., Jonson, J. E., Lupu, A., MacKenzie, I. A., Marmer, E., Park R. J., Sanderson, M. G., Schultz, M., Shindell, D. T., Szopa, S., Vivanco, M. G., Wild, O. and Zang, G. (2009). Intercontinental impacts of ozone pollution on human mortality. *Environ. Sci. and Technol.* 43(17), 6482–6487.

Anenberg, S. C., Horowitz, L. W., Tong, D. Q. and West, J. J. (2010). An estimate of the global burden of anthropogenic ozone and fine particulate matter on premature human mortality using atmospheric modeling. *Environ. Health Perspect.* 118(9), 1189–1195.

Anderson, H. R., Atkinson, W. A., Peacock, J. L., Marston, L. and Konstantinou, K. (2004). *Meta-analysis of Time-Series Studies and Panel Studies of Particulate Matter (PM) and Ozone (O3)*. Report of a WHO Task Group. World Health Organization, Copenhagen.

Ashmore, M., Emberson, L., Karlsson, P. E. and Pleijel, H. (2004). New directions, a new generation of ozone critical levels for the protection of vegetation in Europe. *Atmospheric Environment* 38 (15), 2213–2214.

Ashmore, M. R. (2005). Assessing the future global impacts of ozone on vegetation. *Plant, Cell and Environment* 28, 949–964.

Auffhammer, M., Ramanathan, V. and Vincent, J. R. (2006). Integrated model shows that atmospheric brown clouds and greenhouse gases have reduced rice harvests in India. *PNAS* 10.1073/pnas.0609584104.

Babu, S. S. and Moorthy, K. K. (2002). Aerosol black carbon over a tropical coastal station in India. *Geophys. Res. Lett.* 29(23), 1880.

Baccarelli, A., Wright, R. O., Bollati, V., Tarantini, L., Litonjua, A. A., Suh, H. H., Zanobetti, A., Sparrow, D., Vokonas, P. S. and Schwartz, J. (2009). Rapid DNA methylation changes after exposure to traffic particles. *Am. J. Respir. Crit. Care Med.* 179(7), 572–578.

Baja, E. S., Schwartz, J. D., Wellenius, G. A., Coull, B. A., Zanobetti, A., Vokonas, P. S. and Suh, H. H. (2010). Traffic-related air pollution and QT interval, modification by diabetes, obesity, and oxidative stress gene polymorphisms in the Normative Aging Study (NAS). *Environ. Health Perspect.* 118, 840–846.

Bamber, J. L., Gomez-Dans, J. L. and Griggs, J. A. (2009). A new 1 km digital elevation model of the Antarctic derived from combined satellite radar and laser data. *The Cryosphere* 3, 101–111.

Barnett, T. P., Adam, J. C. and Lettenmaier, D. P. (2005). Potential impacts of a warming climate on water availability in snow-dominated regions. *Nature* 438, 303–309, doi,10.1038/nature04141.

152

Bassin, S., Volk, M., Suter, M., Buchmann, N. and Fuhrer, J. (2007). Nitrogen deposition but not ozone affects productivity and community composition of sub-alpine grassland after three years of treatment. *New Phytologist* 175, 523–534.

Bateson, T. F. and Schwartz, J. (2004). Who is sensitive to the effects of particulate air pollution on mortality? A case-crossover analysis of effect modifiers. *Epidemiology* 15(2), 143–149.

Bell, M. L., Dominici, F. and Samet, J. M. (2005). A meta-analysis of time-series studies of ozone and mortality with comparison to the national morbidity, mortality, and air pollution study. *Epidemiology* 16(4), 436–445.

Bell, M. L., Peng, R. D. and Dominici, F. (2006). The exposure-response curve for ozone and risk of mortality and the adequacy of current ozone regulations. *Environ. Health Perspect.* 114(4), 532–536.

Berntsen, T. K., Fuglestvedt, J. S., Joshi, M. M., Shine, K. P., Stuber, N., Ponater, M., Sausen, R., Hauglustaine, D. A. and Li, L. (2005). Response of climate to regional emissions of ozone precursors, sensitivities and warming potentials. *Tellus B* 57(4), 283–304.

Boer, G. and Yu, B. (2003). Climate sensitivity and response. *Climate Dynamics* 20, 415–429.

Bond, T. C. and Sun, H. (2005). Can reducing black carbon emissions counteract global warming? *Environ. Sci. Technol.* 39, 5921–5926.

Bond, T. C., Zarzycki, C., Flanner, M. G. and Koch, D. M. (2011). Quantifying immediate radiative forcing by black carbon and organic matter with the Specific Forcing Pulse. *Atmos. Chem. Phys*. 11, 1505–1525, doi,10.5194/acp-11-1505-2011.

Booker, F., Muntifering, R., McGrath, J. M., Burkey, K., Decoteau, D., Fiscus, E., Manning. W., Krupa, S., Chappelka, A. and Grantz, D. (2009). The ozone component of global change, Potential effects on agricultural and horticultural plant yield, product quality and interactions with invasive species. *Journal of Integrative Plant Biology* 51, 337–351.

Boos, W. R. and Kuang, Z. (2009). Dominant control of the South Asian monsoon by orographic insulation versus plateau heating. *Nature* 463, 218–223.

Boucher, O. and Reddy, M. S. (2008). Climate trade-off between black carbon and carbon dioxide emissions. *Energy Policy* 36(1), 193–200.

Boucher, O., P. Friedlingstein, B. Collins, and K. P. Shine (2009), The indirect global warming potential and global temperature change potential due to methane oxidation, *Environ. Res. Lett.*, *4*, doi,10.1088/1748-9326/1084/1084/044007.

Braga, A. L. F., Zanobetti, A. and Schwartz, J. (2001). The time course of weather-related deaths. *Epidemiology* 12, 662–667.

Brauer, M., Amman, M., Burnett, R., Cohen, A., Dentener, F., Ezzati, M., Henderson, S., Krzyzanowski, M., Martin, R., Pandey, K.D., Van Dingenen, R., van Donkelaar, A., Thurston, G. (2011). Exposure assessment for the estimation of the global burden of disease attributable to outdoor air pollution. Environ. Sci. Technol., doi, 10.1021/es2025752 Broccoli, A. J., Dahl, K. A. and Stouffer, R. J. (2006). Response of the ITCZ to northern hemisphere cooling. *Geophys. Res. Lett.* 33(1).

Bruce, N., Perez-Padilla, R. and Albalak, R. (2000). Indoor air pollution in developing countries, a major environmental and public health challenge. *Bull. World Health Organ.* 78(9), 1078–1092.

Bryce, J., Boschi-Pinto, C., Shibuya, K. and Black, R. E. (2005). WHO estimates of the causes of death in children. *The Lancet* 365(9465), 1147–1152.

Bungener, P., Nussbaum, S. and Grub, A. (1999). Growth response of grassland species to ozone in relation to soil moisture condition and plant strategy. *New Phytologist* 142, 283–293.

Carbajal-Arroyo, L., Miranda-Soberanis, V., Medina-Ramon, M., Rojas-Bracho, L., Tzintzun, G., Solis-Gutierrez, P., Mendez-Ramirez, I., Hurtado-Diaz, M., Schwartz, J. and Romieu, I. (2011). Effect of PM_{10} and O_3 on infant mortality among residents in the Mexico City Metropolitan Area, a case-crossover analysis, 1997–2005. *J. Epidemiol. Commun. Health*, 65,715-721. doi,10.1136/jech.2009.101212

Chahine, T., Baccarelli, A., Litonjua, A., Wright, R. O., Suh, H., Gold, D. R., Sparrow, D., Vokonas, P. and Schwartz, J. (2007). Particulate air pollution, oxidative stress genes, and heart rate variability in an elderly cohort. *Environ. Health Perspect.* 115(11), 1617–1622.

Chen, J. L., Wilson, C. R. and Tapley, B. D. (2006). Satellite gravity measurements confirm accelerated melting of Greenland ice sheet. *Science* 313, 1958–1960.

Chen, W.T., Lee, Y. H., Adams, P. J., Nenes, A., and Seinfeld, J. H. (2010) Will black carbon mitigation dampen aerosol indirect forcing? *Geophys. Res. Lett.*, 37, L09801, doi,10.1029/2010GL042886.

Chuang, K. J., Chan, C. C., Su, T. C., Lee, C. T. and Tang, C.S. (2007). The effect of urban air pollution on inflammation, oxidative stress, coagulation, and autonomic dysfunction in young adults. *Am. J. Respir. Crit. Care Med.* 176(4), 370–376.

Chuang, K. J., Coull, B. A., Zanobetti, A., Suh, H., Schwartz, J., Stone, P. H., Litonjua, A.; Speizer, F. E. and Gold, D. R. (2008). Particulate air pollution as a risk factor for ST-segment depression in patients with coronary artery disease. *Circulation* 118, 1314–1320.

Chung, C.E., Ramanathan, V. and Kiehl, J.T. (2002). Effects of the south Asian absorbing haze on the northeast monsoon and surface-air heat exchange. J. of Climate, 15(17), 2462-2476. doi, 10.1175/1520-0442(2002)015<2462,EOTSAA>2.0.CO;2.

Chung, C.E. and Ramanathan, V. (2006). Weakening of North Indian SST gradients and the monsoon rainfall in India and the Sahel. J. of Climate, 19(10), 2036-2045. doi, 10.1175/JCLI3820.1.

Chung, S. H. and Seinfeld, J. (2005). Climate response of direct radiative forcing of anthropogenic black carbon. *J. Geophys. Res.* 110, D11102, doi,10.1029/2004JD005441.

Clarke, A. and Noone, K. (1985). Soot in the Arctic, a cause for perturbation in radiative transfer. *J. Geophys. Res.* 19(12), 2045–2053.

Cohen, A. J., Anderson, H. R., Ostro, B., Pandey, K. D., Krzyzanowski, M., Kunzli, N. Gutschmidt, K., Pope, A., Romieu, I., Samet, J. M. and Smith, K. (2004). Urban air pollution. In, Ezzati, M., Lopez, A. D., Rodgers, A. and Murray, C. J. L. (eds). *Comparative Quantification of Health Risks, Global and Regional Burden of Disease Due to Selected Major Risk Factors.* World Health Organization, Geneva, 1353–1434.

Collier, J. C. and Zhang, G. J. (2009). Aerosol direct forcing of the summer Indian monsoon as simulated by the NCAR CAM3. *Climate Dynamics* 32(2–3), 313–332.

Collins, W. J., Derwent, R. G., Johnson, C. E. and Stevenson, D. S. (2002). The oxidation of organic compounds in the troposphere and their global warming potentials. *Climate Change* 52, 453–479. doi, 10.1023/A,1014221225434

Collins, W. J., Sitch, S. and Boucher O. (2010). How vegetation impacts affect climate metrics for ozone precursors. *J. Geophys. Res.*, 115, D23308, doi,10.1029/2010JD014187.

Cook, J. and Highwood E. J. (2004). Climate response to tropospheric absorbing aerosols in an intermediate general-circulation model. *Quarterly Journal of the Royal Meteorological Society* 130(596), 175–191.

Corbett, J. J., Winebrake, J. J., Green, E. H., Kasibhatla, P., Eyring, V. and Lauer, A. (2007). Mortality from ship emissions, a global assessment. *Environ. Sci. Technol.* 41, 8512–8518.

Curjuric, I., Imboden, M., Schindler, C., Downs, S. H., Hersberger, M., Liu, S. L., Matyas, G., Russi, E. W., Schwartz, J., Thun, G. A., Postma, D. S., Rochat, T., Probst-Hensch, N. M. and the SAPALDIA team (2009). HMOX1 and GST variants modify attenuation of FEF25-75-decline due to PM_{10} reduction. *Eur. Respir. J.* 35, 505–514, doi, 10.1183/09031936.000443-2009.

Dash, S. K., Kulkarni, M. A., Mohanty, U. C. and Prasad, K. (2009). Changes in the characteristics of rain events in India. *J. Geophys. Res.* 114, D10109.

Delfino, R. J., Staimer, N., Tjoa, T., Polidori, A., Arhami, M., Gillen, D. L., Kleinman, M. T., Vaziri, N. D., Longhurst, J., Zaldivar, F. and Sioutas, C. (2008). Circulating biomarkers of inflammation, antioxidant activity, and platelet activation are associated with primary combustion aerosols in subjects with coronary artery disease. *Environ. Health Perspect.* 116(7), 898–906.

Dherani, M., Pope, D., Mascarenhas, M., Smith, K. R., Weber, M. and Bruce, N. (2008). Indoor air pollution from unprocessed solid fuel use and pneumonia risk in children aged under five years, a systematic review and meta-analysis. *Bull. World Health Organ.* 86(5), 390–398C.

Ding, Y., Liu, S., Li, J. and Shangguan, D. (2006). The retreat of glaciers in response to recent climate warming in western China. *Annals of Glaciology* 43(1), 97–105.

Doherty, S. J., Warren, S. G., Grenfell, T. C., Clarke, A. D. and Brandt, R. E. (2010). Light-absorbing impurities in Arctic snow. *Atmos. Chem. Phys. Discuss.* 10(8), 18 807–18 878, doi,10.5194/acpd-10-18807-2010.

Elagöz, V. and Manning, W. J. (2005). Responses of sensitive and tolerant bush beans (*Phaseolus vulgaris L.*) to ozone in open-top chambers are influenced by phenotypic differences, morphological characteristics, and the chamber environment. *Environ. Pollut.* 136, 371–383.

Eleftheriadis, K., Vratolis, S. and Nyeki, S. (2009). Aerosol black carbon in the European Arctic, measurements at Zeppelin station, Ny-Alesund, Svalbard from 1998–2007. *Geophys. Res. Lett.* 36, L02809.doi:10.1029/2008GL035741.

Emberson, L. D., Ashmore, M. R. and Murray, F. (2003). *Air Pollution Impacts on Crops and Forests, A Global Assessment.* Imperial College Press, London.

Emberson, L. D., Buker, P., Ashmore, M. R., Mills, G., Jackson, L. S., Agrawal, M., Atikuzzaman, M. D., Cinderby, S., Engardt, M., Jamir, C., Kobayashi, K., Oanh, N. T. K., Quadir, Q. F. and Wahid A. (2009). A comparison of North American and Asian exposure-response data for ozone effects on crop yields. *Atmospheric Environment* 43(12), 1945–1953.

Ezzati, M., Lopez, A.D., Rodgers, A., Murray, C,J.L. (2004). Comparative Quantification of Health Risks, Global and Regional Burden of Disease. WHO, Geneva 2004. Chapter 18, Indoor Air Pollution from Household Use of Solid Fuels. Kirk R Smith, Sumi Mehta, Mirjam Maeusezahl-Feuz.

Feichter, J., Roeckner, E., Lohmann, U. and Liepert, B. (2004). Nonlinear aspects of the climate response to greenhouse gas and aerosol forcing. *J. Climate* 17, 2384–2398.

Ferris, B. G., Dockery, D. W., Ware, J. H., Speizer, F. E. and Spiro, R. (1983). The Six-City Study, examples of problems in analysis of the data. *Environ. Health Perspect.* 52, 115–123.

Filleul, L., Cassadou, S., Medina, S., Fabres, P., Lefranc, A., Eilstein, D., Le Tertre, A., Pascal, L., Chardon, B., Blanchard, M., Declercq, C., Jusot, J.-F., Prouvost, H. and Ledrans, M. (2006). The relation between temperature, ozone and mortality in 9 French cities during the heat wave 2003. *Environ. Health Perspect.* doi,10.1289/ehp.8328.

Fiscus, E. L., Booker, F. L. and Burkey, K. O. (2005). Crop responses to ozone, uptake, modes of action, carbon assimilation and partitioning. *Plant Cell Environment* 28, 997–1011.

Fishman, J., Creilson, J.K., Parker, P.A., Ainsworth, E.A., Vining, G.G., Szarka, J., Booker, F.L. and Xu, X. (2010). An investigation of widespread ozone damage to the soybean crop in the upper Midwest determined from ground-based and satellite measurements. *Atmospheric Environment*, 44, 2248-2256.

Flanner, M. G., Zender, C. S., Randerson, J. T. and Rasch, P. J. (2007). Present-day climate forcing and response from black carbon in snow. *J. Geophys. Res.* 112, D11202, doi,10.1029/2006JD008003, 2007.

Flanner, M. G., Zender, C. S., Hess, P. G., Mahowald, N. M., Painter, T. H., Ramanathan, V. and Rasch, P. J. (2009). Springtime warming and reduced snow cover from carbonaceous particles. *Atmos. Chem. Phys.* 9(7), 2481–2497.

Forster, P., Ramaswamy, V., Artaxo, P., Berntsen, T., Betts, R., Fahey, D. W., Haywood, J., Lean, J., Lowe, D. C., Myhre, G., Nganga, J., Prinn, R., Raga, G., Schulz, M. and Van Dorland, R. (2007). Changes in atmospheric constituents and in radiative forcing. In, Solomon, S., Qin, D., Manning, M., Chen, Z., Marquis, M., Averyt, K. B., Tignor, M. and Miller, H. L. (eds) *Climate Change 2007, The Physical Science Basis. Contribution of Working Group I to the Fourth Assessment Report of the Intergovernmental Panel on Climate Change*. Cambridge University Press, Cambridge, UK and New York, NY, USA.

Fowler, D, Pilegaard, K., Sutton, M. A., Ambus, P., Raivonen, M., Duyzer, J., Simpson, D., Fagerli, H., Fuzzi, S., Schjoerring, J. K, Granier, C., Neftel, A., Isaksen, I. S. A., Laj, P., Maione, M., Monks, P. S., Burkhardt, J., Daemmgen, U., Neirynck, J., Personne, E., Wichink-Kruit, R., Butterbach-Bahl, K., Flechard, C., Tuovinen, J. P., Coyle, M., Gerosa, G., Loubet, B., Altimir, N., Gruenhage, L., Ammann, C., Cieslik, S., Paoletti, E., Mikkelsen, T. N., Ro-Poulsen, H., Cellier, P., Cape, J. N., Horvath, L., Loreto, F., Niinemets, U., Palmer, P. I., Rinne, J., Misztal, P., Nemitz, E., Nilsson, D., Pryor, S., Gallagher, M. W., Vesala, T., Skiba, U., Brueggemann, N., Zechmeister-Boltenstern, S., Williams, J., O'Dowd, C., Facchini, M. C., de Leeuw, G., Flossman, A., Chaumerliac, N. and Erisman, J. W. (2009). Atmospheric composition change, ecosystems-atmosphere interactions. *Atmospheric Environment* 43, 5193–5267.

Franklin, M. and Schwartz, J. (2008). The impact of secondary particles on the association between ambient ozone and mortality. *Environ. Health Perspect.* 116(4), 453–458.

Frei, M., Tanaka, J. P. and Wissuwa, M. (2008). Genotypic variation in tolerance to elevated ozone in rice, dissection of distinct genetic factor linked to tolerance mechanisms. *Journal of Experimental Botany* 59, 3741–3752.

Frei, M., Tanaka, J. P., Chen, C. and Wissuwa, M. (2010). Mechanisms of ozone tolerance in rice, characterization of two QTLs affecting leaf bronzing by gene expression profiling and biochemical analysis. *Journal of Experimental Botany*, 61(5),1405-1417.

Fuglestvedt, J. S., Shine, K. P., Berntsen, T., Cook, J., Lee, D. S., Stenke, A., Skeie, R. B., Velders, G. J. M. and Waitz, I. A. (2009). Transport impacts on atmosphere and climate, metrics. *Atmospheric Environment* 44, 4648–4677.

Fuhrer, J. and Booker, F. (2003). Ecological issues related to ozone, agricultural issues. *Environment International* 29, 141–154.

Fuhrer, J. (2009). Ozone risk for crops and pastures in present and future climates. *Naturwissenschaften* 96, 173–194.

Garrett, T. J. and Zhao, C. (2006). Increased Arctic cloud longwave emissivity associated with pollution from mid-latitudes. *Nature* 440, 787–789, doi,10.1038/nature04636.

Gautam, R., Hsu, N. C., Lau, K.-M., Tsay, S.-C. and Kafatos, M. (2009). Enhanced pre-monsoon warming over the Himalayan-Gangetic region from 1979 to 2007. *Geophys. Res. Lett.* 36, L07704.

Gimeno, B. S., Bermejo, V., Sanz, J., de la Torre, D. and Gil, J. M. (2004). Assessment of the effects of ozone exposure and plant competition on the reproductive ability of three therophytic clover species from Iberian pastures. *Atmospheric Environment* 38, 2295–2303.

Gold, D. R., Litonjua, A. A., Zanobetti, A., Coull, B. A., Schwartz, J., MacCallum, G. Verrier, R. L., Nearing, B. D., Canner, M. J., Suh, H. and Stone, P. H. (2005). Air pollution and ST-segment depression in elderly subjects. *Environ. Health Perspect.* 113(7), 883–887.

Gong, S., Zhao, T., Sharma, S., Toom-Sauntry, D., Lavoue, D., Zhang, X., Leaitch, W. and Barrie L. (2010). Identification of trends and interannual variability of sulfate and black carbon in the Canadian High Arctic, 1981–2007. *J. Geophys. Res.* 115(D7), D07,305.

Goswami, B. N., Venugopal, V., Sengupta, D., Madhusoodanan, M. S. and Xavier, P. K. (2006). Increasing Trend of extreme rain events over India in a warming environment. *Science* 314(5804), 1442–1445.

Graf, H.-F., Shirsat, S. V., Oppenheimer, C., Jarvis, M. J., Podzun, R. and Jacob, D. (2010). Continental scale Antarctic deposition of sulphur and black carbon from anthropogenic and volcanic sources. *Atmos. Chem. Phys.* 10, 2457–2465.

Gu, L. H., Baldocchi, D., Verma, S. B., Black, T. A., Vesala, T, Falge, E. M. and Dowty, P. R. (2002). Advantages of diffuse radiation for terrestrial ecosystem productivity. *J. Geophys. Res.* 107, D5-6, 4050.

Hammitt, J. K. (2000). Valuing mortality risk, theory and practice. *Environ. Sci. Technol.* 34(8), 1396–1400.

Hansen, J. E., Sato, M. and Reudy, R. (1997). Radiative forcing and climate response. *J. Geophys. Res.* 102, 6831–6864.

Hansen, J. and Nazarenko L. (2004). Soot climate forcing via snow and ice albedos. *PNAS* 101(2), 423–428.

Hansen, J., Sato, M., Ruedy, R., Nazarenko, L., Lacis, A., Schmidt, G. A., Russell, G., Aleinov, I., Bauer, M., Bauer, S., Bell, N., Cairns, B., Canuto, V., Chandler, M., Cheng, Y., Del Genio, A., Faluvegi, G., Fleming, E., Friend, A., Hall, T., Jackman, C., Kelley, M., Kiang, N. Y., Koch, D., Lean, J., Lerner, J., Lo, K., Menon, S., Miller, R. L., Minnis, P., Novakov, T., Oinas, V., Perlwitz, J., Perlwitz, J., Rind, D., Romanou, A., Shindell, D., Stone, P., Sun, S., Tausnev, N., Thresher, D., Wielicki, B., Wong, T., Yao, M. and Zhang, S. (2005). Efficacy of climate forcings. *J. Geophys. Res.* 110, D18104, doi,10.1029/2005JD005776.

Hansen, C. S., Sheykhzade, M., Moller, P., Folkmann, J. K., Amtorp, O., Jonassen, T. and Loft, S. (2007). Diesel exhaust particles induce endothelial dysfunction in apoE-/- mice. *Toxicol. Appl. Pharmacol.* 219(1), 24–32.

Hayes, F., Jones, M. L. M., Mills, G. and Ashmore, M. R. (2007). Meta-analysis of the relative sensitivity of semi-natural vegetation species to ozone. *Environ. Pollut.* 136, 9.

Heck, W. W., Adams, R. M., Cure, W. W., Heagle, A. S., Heggestad, H. E., Kohut, R. J., Kress, L. W., Rawlings, J. O. and Taylor, O. C. (1983). A reassessment of crop loss from ozone. *Env. Sci. Tech.* 17(12), 572–581.

Hegerl, G. C., Zwiers, F. W., Braconnot, P., Gillett, N. P., Luo, Y., Marengo-Orsini, J. A., Nicholls, N., Penner, J. E. and Stott, P. A. (2007). Understanding and attributing climate change. In, Solomon, S., Qin, D., Manning, M., Chen, Z., Marquis, M., Averyt, K. B., Tignor, M. and Miller, H. L. (eds) *Climate Change 2007, The Physical Science Basis. Contribution of Working Group I to the Fourth Assessment Report of the Intergovernmental Panel on Climate Change.* Cambridge University Press, Cambridge, UK and New York, NY, USA.

Hegg, D. A., Warren, S. G., Grenfell, T. C., Doherty, S. J., Larson, T. V. and Clarke, A. D. (2009). Source attribution of black carbon in Arctic snow. *Environ. Sci. Technol.* 43, 4016–4021.

Hegg, D. A., Warren, S. G., Grenfell, T. C., Doherty, S. J. and Clarke, A. D. (2010). Sources of light-absorbing aerosol in arctic snow and their seasonal variation. *Atmos. Chem. Phys. Discuss.* 10(6), 13 755–13 796, doi,10.5194/acpd-10-13755-2010.

Held, I. M. and Soden, B. J. (2006). Robust responses of the hydrological cycle to global warming. *Journal of Climate* 19(21), 5686–5699.

Hoek, G., Brunekreef, B., Goldbohm, S., Fischer, P. and van den Brandt, P. A. (2002). Association between mortality and indicators of traffic-related air pollution in the Netherlands, a cohort study. *The Lancet* 360(9341), 1203–1209.

Holland, M., Kinghorn, S., Emberson, L., Cinderby, S., Ashmore, M. R., Mills, G. and Harmens, H. (2006). *Development of a Framework for Probabilistic Assessment of the Economic Losses caused by Ozone Damage to Crops in Europe.* Centre for Ecology and Hydrology, Bangor, UK.

Holland, D., Thomas, R., De Young, B., Ribergaard, M. and Lyberth, B. (2008). Acceleration of Jakobshavn Isbrae triggered by warm subsurface ocean waters. *Nature Geoscience* 1(10), 659–664.

ICIMOD (2011). Glacial lakes and glacial lake outburst floods in Nepal; ICIMOD Publication; ICIMOD, Kathamndu, Nepal. Available at, http,//books.icimod.org/index.php/search/publication/750.

Ito, K., De Leon, S. F. and Lippmann, M. (2005). Associations between ozone and daily mortality, analysis and meta-analysis. *Epidemiology* 16(4), 446–457.

IPCC (2007). *Climate Change 2007, Synthesis Report. Contribution of Working Groups I, II and III to the Fourth Assessment Report of the Intergovernmental Panel on Climate Change.* Geneva, Switzerland.

Isaksen, I. S. A., Granier, C., Myhre, G., Berntsen, T. K., Dalsøren, S. B., Gauss, M., Klimont, Z., Benestad, R., Bousquet, P., Collins, W., Cox, T., Eyring, V., Fowler, D., Fuzzi, S., Jockel, P., Laj, P., Lohmann, U., Maione, M., Monks, P., Prevot, A. S. H., Raes, F. R., A. , Rognerud, B., Schulz, M., Shindell, D., Stevenson, D. S., Storelvmo, T., Wang, W.-C., vanWeele, M., Wild, M. and Wuebbles, D. (2009). Atmospheric composition change, climate-chemistry interactions. *Atmos. Env.* 43, 5138-5192.

Ives, J.D.; Shrestha, R.B.; Mool, P.K. (2010). Formation of glacial lakes in the Hindu Kush-Himalayas and GLOF risk assessment. ICIMOD Publication; ICIMOD, Kathamndu, Nepal. http,//www.unisdr.org/preventionweb/files/14048_ICIMODGLOF.pdf.

Jacobson, M. Z. (2002). Control of fossil-fuel particulate black carbon and organic matter, possibly the most effective method of slowing global warming. *J. Geophys. Res.* 107, 4410, doi,10.1029/2001JD001376.

Jacobson, M. Z. (2004). Climate response of fossil fuel and biofuel soot, accounting for soot's feedback to snow and sea ice albedo and emissivity. *J. Geophys. Res.* 109, D21201, doi,10.1029/2004JD004945.

158

Jacobson, M. Z. (2010). Short-term effects of controlling fossil-fuel soot, biofuel soot and gases, and methane on climate, arctic ice, and air pollution health. *J. Geophys. Res.* 115, D14209, doi,10.1029/2009JD013795.

Jäger, H. J., Unsworth, M., De Temmerman, L. and Mathy, P. *(eds) (*1992*). Effects of Air Pollution on Agricultural Crops in Europe. The Air Pollution Research Report 46.* Results of the European Open-Top Chambers Project. *Commission of The European Communities, Tervuren, Belgium.*

Janke, K., Propper, C. and Henderson, J. (2009). Do current levels of air pollution kill? The impact of air pollution on population mortality in England. *Health Economics* 18(9), 1031–1055.

Jerrett, M., Burnett, R. T., Pope, C. A. III, Ito, K., Thurston, G., Krewski, D., Shi, Y., Calle, E. and Thun, M. (2009). Long-term ozone exposure and mortality. *N. Engl. J. Med.* 360, 1085–1095.

Johnson, B. T., Shine, K. P. and Forster, P. M. (2004). The semi-direct aerosol effect, impact of absorbing aerosols on marine stratocumulus. *Quarterly Journal of the Royal Meteorological Society* 130(599), 1407–1422.

Jones, G. S, Christidis, N. and Stott, P. A. (2010). Detecting the influence of fossil fuel and bio-fuel black carbon aerosols on near surface temperature changes. *Chem. Phys. Discuss*. 10, 20921–20974.

Jones-Lee, M. (1974). The value of changes in the probability of death or injury. *J. of Pol. Econ.* 82(4), 835–849.

Kaliakatsou, E., Bell, J. N. B., Thirtle, C., Rose, D. and Power, S. A. (2010). The impact of tropospheric ozone pollution on trial plot winter wheat yields in Great Britain, an economic perspective. *Environ. Pollut.* 158(5), 1948–1954.

Kang, S. M., Held, I. M., Frierson, D. M. W. and Zhao, M. (2008). The response of the ITCZ to extratropical thermal forcing, idealized slab-ocean experiments with a GCM. *J. Climate* 21, 3521–3532, doi,10.1175/2007JCLI2146.1.

Karlsson, P. E., Pleijel, H., Belhaj, M., Danielsson, H., Dahlin. B., Andersson, M., Hansson, M., Munthe, J., and Grennfelt, P. (2005). Economic assessment of the negative impacts of ozone on crop yields and forest production, a case study of the estate Ostads Sateri in southwestern Sweden. *Ambio* 34(1), 32–40.

Karnosky, D. F. and Steiner, K. C. (1981). Provenance variation in response of *Fraxinus americana* and *Fraxinus pennsylvanica* to sulfur dioxide and ozone. *Phytopathology* 71, 804–807.

Karnosky, D. F., Skelly, J. M., Percy, K. E. and Chappelka, A. H. (2007). Perspectives regarding 50 years of research on effects of tropospheric ozone air pollution on US forests. *Environ. Pollut.* 147, 489–506.

Kaser, G., Cogley, J., Dyurgerov, M., Meier, M. and Ohmura, A. (2006). Mass balance of glaciers and ice caps, consensus estimates for 1961–2004. *Geophys. Res. Lett.* 33(19), L19, 501.

Katsouyanni, K., Schwartz, J., Spix, C., Touloumi, G., Zmirou, D., Zanobetti, A., Wojtyniak, B., Vonk, J. M., Tobias, A., Ponka, A., Medina, S., Bacharova, L. and Anderson, H. R. (1996). Short-term effects of air pollution on health, a European approach using epidemiologic time series data, the APHEA protocol. *Journal of Epidemiology and Community Health* 50(suppl), S12–18.

Kehrwald, N., Thompson, L., Tandong, Y., Mosley-Thompson, E., Schotterer, U., Alfimov, V., Beer, J., Eikenberg, J. and Davis, M. (2008). Mass loss on Himalayan glacier endangers water resources. *Geophys. Res. Lett.* 35(22), L22, 503.

Kleinman, M. T., Araujo, J. A., Nel, A., Sioutas, C., Campbell, A., Cong, P. Q., Li, H. and Bondya, S. C. (2008). Inhaled ultrafine particulate matter affects CNS inflammatory processes and may act via MAP kinase signaling pathways. *Toxicol. Lett.* 178(2), 127–130.

159

Klingberg, J., Engardt, M., Uddling, J., Karlsson, P.E., and Pleijel, H. (2011) Ozone risk for vegetation in the future climate of Europe based on stomatal ozone uptake calculation. *Tellus*, 63A, 174–187.

Kloster, S., Dentener, F., Feichter, J., Raes, F., Lohmann, U., Roeckner, E. and Fischer-Bruns, I. (2009). A GCM study of future climate response to aerosol pollution reductions. *Climate Dynamics* 34, 1177–1194, doi,10.1007/s00382-009-0573-0.

Knohl, A. and Baldocchi. D. D. (2008). Effects of diffuse radiation on canopy gas exchange processes in a forest ecosystem. *J. Geophys. Res. – Biogeosciences* 13, G02023.

Koch, D. and Hansen, J. (2005). Distant origins of Arctic black carbon, a Goddard Institute for Space Studies ModelE experiment, *J. Geophys. Res.* 110, D04204, doi,10.1029/2004JD005296.

Koch, D., Menon, S., Del Genio, A., Ruedy, R., Aleinov, I. and Schmidt, G.A. (2009). Distinguishing aerosol impacts on climate over the past century. *J. Climate* 22, 2659–2677.

Kolb, T. E. and Matyssek, R. (2001). Limitations and perspectives about scaling ozone impact in trees. *Environ. Pollut.* 115, 373–393.

Krol, M., Houweling, S., Bregman, B., van den Broek, M., Segers, A., van Velthoven, P., Peters, W., Dentener F. and Bergamaschi P., (2005) The two-way nested global chemistry-transport zoom model TM5, algorithm and application. *Atmos. Chem. Phys.*, 4, 3975–4018

Krupa, S. V., Muntifering, R. and Chappelka, A. H. (2004). Effects of ozone on plant nutritive quality characteristics for ruminant animals. *The Botanica* 54, 1–12.

Krishnamurti, T. N., Chakraborty, A., Martin, A., Lau, W. K., Kim, K.-M., Sud, Y. and Walker G. (2009). Impact of Arabian Sea pollution on the Bay of Bengal winter monsoon rains, *J. Geophys. Res.* 114.

Kumari, B.P. Londhe, A.L. Daniel, S. and Jadhav, D.B. (2007) Observational evidence of solar dimming, Offsetting surface warming over India. *Geophys. Res. Lett.* 34, L21810.

Kumari, B. P. and Goswami, B. N. (2010). Seminal role of clouds on solar dimming over the Indian monsoon region. *Geophys. Res. Lett.* 37, L06703.

Kvalevåg, M. M. and Myhre, G. (2007). Human impact on direct and diffuse solar radiation during the industrial era. *J. Clim.* 20, 4874-4883.

Lau, K., Kim, M. and Kim, K. (2006). Asian summer monsoon anomalies induced by aerosol direct forcing, the role of the Tibetan plateau. *Climate Dynamics* 26(7), 855–864.

Lau, K.-M., Ramanathan, V., Wu, G.-X., Li, Z., Tsay, S.C., Hsu, C., Sikka, R., Holben, B., Lu, D., Tartari, G., Chin, M., Koudelova, P., Chen, H., Ma, Y., Huang, J., Taniguchi, K. and Zhang, R. (2008). The Joint Aerosol-Monsoon Experiment. *Bull. Amer. Meteor. Soc. 89*, 1–15.

Lesikhina, N., Rudaya, I., Kireeva, A., Krivonos, O. and Kobets, E. (2007). *Offshore Oil and Gas Development in Northwest Russia, Consequences and Implications.* Bellona.

Lesser, V. M., Rawlings, J. O., Spruill, S. E. and Somerville, M. C. (1990). Ozone effects on agricultural crops, statistical methodologies and estimated dose-response relationships. *Crop Science* 30, 148–155.

Levy, J. I., Chemerynski, S. M. and Sarnat, J. A. (2005). Ozone exposure and mortality, an empiric Bayes metaregression analysis. *Epidemiology* 16(4), 458–468.

Levy, H., Schwarzkopf, M. D., Horowitz, L., Ramaswamy, V. and Findell, K. L. (2008). Strong sensitivity of late 21st century climate to projected changes in short-lived air pollutants. *J. Geophys. Res.* 113, D06102, doi,10.1029/2007JD009176.

Liepert, B. and Tegen, I. (2002). Multidecadal solar radiation trends in the United States and Germany and direct tropospheric aerosol forcing. *J. Geophys. Res.* 107, 4153, 15 pp. doi,10.1029/2001JD000760.

Lipsett, M., Hurley, S. and Ostro, B. (1997). Air pollution and emergency room visits for asthma in Santa Clara County, California. *Environ. Health Perspect.* 105(2), 216–222.

Liu, Y., Sun, J. R. and Yang, B. (2009a). The effects of black carbon and sulphate aerosols in China regions on East Asia monsoons. *Tellus B-Chem. Phys. Meteorol* 61(4), 642–656.

Liu, X., Cheng, Z., Yan, L. and Yin, Z-Y. (2009b). Elevation dependency of recent and future minimum surface air temperature trends in the Tibetan Plateau and its surroundings. Global and Planetary Change, 68, 164–174.

Liu, J., Mauzerall, D. L. and Horowitz, L. W. (2009c). Evaluating inter-continental transport of fine aerosols, (2) Global health impact. *Atmospheric Environment* 43, 4339–4347.

Lobell, D. B. and Field, C. B. (2007). Global scale climate-crop yield relationships and the impacts of recent warming. *Environ. Res. Lett.* 2, 014002, doi,10.1088/1748-9326/2/1/014002.

Long, S. P., Ainsworth, E. A, Leakey, A. D. B. and Morgan, P. B. (2005). Global food insecurity, treatment of major food crops with elevated carbon dioxide or ozone under large-scale fully open-air conditions suggests recent models may have overestimated future yields. *Phil. Trans. R. Soc. B.* 360, 2001–2020.

Lubin, D. and Vogelmann, A. (2006). A climatologically significant aerosol longwave indirect effect in the Arctic. *Nature* 439(7075), 453–456.

Lundback, M., Mills, N. L., Lucking, A., Barath, S., Donaldson K., Newby, D. E. Sandström, T. and Blomberg, A. (2009). Experimental exposure to diesel exhaust increases arterial stiffness in man. *Particle and Fibre Toxicology* 6, 7.

Madrigano, J., Baccarelli, A., Wright, R., Suh, H., Sparrow, D., Vokonas, P. and Schwartz, J. (2009). Air pollution, obesity, genes, and cellular adhesion molecules. *Occupational and Environmental Medicine* 67, 312-317.

Manoj, M. G., Devera, P. C. S. and Safai, P. D. (2010). Absorbing aerosols facilitate transition of Indian monsoon breaks to active spells. *Climate Dynamics* doi,10.1007/s00382-010-0971-3, 1-18.

Marland, G., Boden, T. A. and Andres, R. J. (2008). Global, regional, and national fossil fuel CO_2 emissions. In, *Trends, A Compendium of Data on Global Change.* Carbon Dioxide Information Analysis Center, Oak Ridge National Laboratory, US Department of Energy, Oak Ridge.

Matsuo, K. and Heki, K. (2010). Time-variable ice loss in Asian high mountains from satellite gravimetry. *Earth and Planetary Science Letters* 290(1–2), 30–36.

Maynard, D., Coull, B. A., Gryparis, A. and Schwartz, J. (2007). Mortality risk associated with short-term exposure to traffic particles and sulfates. *Environ. Health Perspect.* 115(5), 751–755.

McConnell, J. R., Edwards, R., Gregory, L. K., Flanner, M. G., Zender, C. S., Saltzman, E. S., Banta, J. R., Pasteris, D. R., Carter, M. M. and Kahl, J. D. W. (2007). 20th-century industrial black carbon emissions altered Arctic climate forcing. *Science* 317(5843), 1381–1384.

McCracken, J. P., Smith, K. R., Diaz, A., Mittleman, M. A. and Schwartz, J. (2007). Chimney stove intervention to reduce long-term wood smoke exposure lowers blood pressure among Guatemalan women. *Environ. Health Perspect.* 115(7), 996–1001.

McCracken, J. P. and Schwartz, J. (2009). *Estimation of Cardiovascular Mortality Due to Elevated Blood Pressure Attributable to Household Solid Fuel.* Report to US EPA.

Medina-Ramon, M., Goldberg, R., Melly, S., Mittleman, M. A. and Schwartz, J. (2008). Residential exposure to traffic-related air pollution and survival after heart failure. *Environ. Health Perspect.* 116(4), 481–485.

Meehl, G. A., Arblaster, J. M. and Collins, W. D. (2008). Effects of black carbon aerosols on the Indian monsoon. *J. Climate* 21, 2869–2882.

Menon, S., Del Genio, A. D., Koch, D. and Tselioudis G. (2002). GCM simulations of the aerosol indirect effect, sensitivity to cloud parameterization and aerosol burden. *J. Atmos. Sci.* 59, 692–713.

Mercado, L. M., Bellouin, N., Sitch, S., Boucher, O., Huntingford, C., Wild, M. and Cox, P. M. (2009). Impact of changes in diffuse radiation on the global land carbon sink. *Nature* 458, 1014–1018.

Mills, G., Buse, A., Gimeno, B., Bermejo, V., Holland, M., Emberson, L. and Pleijel, H. (2007). A synthesis of AOT40-based response functions and critical levels for ozone for agricultural and horticultural crops. *Atmospheric Environment* 41, 2630–2643.

Mills, G., Hayes, F., Simpson, D., Emberson, L., Norris, D., Harmens, H. and Büker, P. (2010). Evidence of widespread effects of ozone on crops and (semi-)natural vegetation in Europe (1990–2006) in relation to AOT40 and flux-based risk maps. *Global Change Biology*, 17, 592–613. Doi, 10.1111/j.1365-2486.2010.02217.x.

Ming, J., Cachier, H., Xiao, C., Qin, D., Kang, S., Hou, S. and Xu, J. (2008). Black carbon record based on a shallow Himalayan ice core and its climatic implications. *Atmos. Chem. Phys.* 8, 1343–1352.

Ming, Y. and Ramaswamy, V. (2009). Nonlinear climate and hydrological responses to aerosol effects. *J. Climate* 22, 1329–1339.

Mitchell, J. F. B., Davis, R. A., Ingram, W. J. and Senior, C. A. (1995). On surface temperature, greenhouse gases, and aerosols, models and observations. *J. Climate* 8, 2364–2386.

Mool, P. K., Bajracharya, S. R. and Joshi, S. P. (2001). *Inventory of Glaciers, Glacial Lakes, and Glacial Lake Outburst Floods, Monitoring and Early Warning Systems in the Hindu Kush-Himalayan Region, Nepal.* International Centre for Integrated Mountain Development, Mountain Environment and Natural Resources' Information System.

Mordukhovich, I., Wilker, E., Suh, H., Wright, R., Sparrow, D., Vokonas, P.S. and Schwartz, J. (2009). Black carbon exposure, oxidative stress genes, and blood pressure in a repeated measures study. *Environ. Health Perspect., 117(11), 1767-1772.*

Morgan, P. B., Mies, T. A., Boller, G. A., Nelson, R. L. and Long, S. P. (2006). Season-long elevation of ozone concentration to projected 2050 levels under fully open-air conditions substantially decreases the growth and production of soybean. *New Phytologist* 170, 11.

Muller, N. Z. and Mendelsohn, R. (2007). Measuring the damages of air pollution in the United States. *Journal of Environmental Economics and Management* 54(1), 1–14.

Nagashima, T., Shiogama, H., Yokohata, T., Takemura, T., Crooks, S. and Nozawa, T. (2006). The effect of carbonaceous aerosols on surface temperature in the mid twentieth century. *Geophys. Res. Lett.* 33, L04702.

National Academy of Sciences (2008). *Estimating Mortality Risk Reduction and Economic Benefits from Controlling Ozone Air Pollution.* National Academies Press. Washington, D.C., USA.

Niyogi, D., Chang, H., Saxena, V. K., Holt, T., Alapaty, K., Booker, F., Chen, F., Davis, K. J., Holben, B., Meyers, T., Oechel, W. C., Pielke, R. A., Wells, R., Wilson, K. and Xue, Y. (2004). Direct observations of the effects of aerosol loading on net ecosystem CO_2 exchanges over different landscapes. *Geophys. Res. Lett. 31*, L20506.

O'Brien, K., Eriksen, S., Sygna, L. and Næss, L. O. (2006). Questioning complacency, climate change impacts, vulnerability, and adaptation in Norway. *Ambio* 35(2), 50–56.

Oliveira, P. H. F., Artaxo, P., Pires, C., de Lucca, S., Procopio, A., Holben, B., Schafer, J., Cardoso, L. F., Wofsy,. S. C. and Rocha, H. R. (2007). The effects of biomass burning aerosols and clouds on the CO_2 flux in Amazonia. *Tellus B-Chem. Phys. Meteorol.* 59, 338–349.

O'Neill, M. S., Zanobetti, A. and Schwartz, J. (2003). Modifiers of the temperature and mortality association in seven US cities. *Am. J. Epidemiol.* 157(12), 1074–1082.

Ostro, B., Lipsett, M., Reynolds, P., Goldberg, D., Hertz, A., Garcia, C., Henderson, K. D. and Bernstein, L. (2010). Long-term exposure to constituents of fine particulate air pollution and mortality, results from the California Teachers Study. *Environ. Health Perspect.* 118(3), 363–9.

Pang, J., Kobayashi, K. and Zhu, J. G. (2009). Yield and photosynthetic characteristics of flag leaves in Chinese rice (*Oryza sativa L.*) varieties subjected to free-air release of ozone. *Agriculture, Ecosystems and Environment* 132, 203–211.

Park, S. K., O'Neill, M. S., Vokonas, P. S., Sparrow, D., Spiro, A. III, Tucker, K. L., Suh, H., Hu, H. and Schwartz, J. (2008). Traffic-related particles are associated with elevated homocysteine, the VA Normative Aging Study. *Am. J. Respir. Crit. Care Med., 178, 283-289.*

Peters, A., von Klot, S., Heier, M., Trentinaglia, I., Hormann, A., Wichmann, H. E. and Löwel, H. (2004). Exposure to traffic and the onset of myocardial infarction. *N. Engl. J. Med.* 351(17), 1721–1730.

Podgorny, J. M. and Ramanathan, V. (2001). A modelling study of the direct effect of aerosols over the tropical Indian Ocean. *J. Geophys. Res.* 106(D20), 24 097–24 105.

Pope, C. A. III, Schwartz, J. and Ransom, M. R. (1992). Daily mortality and PM_{10} pollution in Utah Valley. *Archives of Environmental Health* 47(3), 211–217.

Pope, C. A. III, Burnett, R. T., Thun, M. J., Calle, E. E., Krewski, D., Ito, K. and Thurston,. G. D. (2002). Lung cancer, cardiopulmonary mortality, and long-term exposure to fine particulate air pollution. *JAMA* 287, 1132–1141.

Pope, C. A. III, Rodermund, D. L. and Gee, M. M. (2007). Mortality effects of a copper smelter strike and reduced ambient sulfate particulate matter air pollution. *Environ. Health Perspect.* 115(5), 679–683.

Pope, C. A. III, Ezzati, M. and Dockery, D. W. (2009). Fine-particulate air pollution and life expectancy in the United States. *N. Engl. J. Med.* 360(4), 376–386.

Prather, M., Ehhalt, D., Dentener, F., Derwent, R., Dlugokencky, E., Holland, E., Isaksen, I., Katima, J., Kirchhoff, V., Matson, P., Midgley, P., Wang, M., Berntsen, T., Bey, I., Brasseur, G., Buja, L. Collins, W.J. Daniel, J. DeMore, W.B. Derek, N. Dickerson, R. Etheridge, D. Feichter, J. Fraser, P. Friedl, R. Fuglestvedt, J. Gauss, M. Grenfell, L. Grübler, A. Harris, N., Hauglustaine, D., Horowitz, L., Jackman, C., Jacob, D., Jaeglé, L., Jain, A., Kanakidou, M., Karlsdottir, S., Ko, M., Kurylo, M., Lawrence, M., Logan, J.A., Manning, M., Mauzerall, D., McConnell, J., Mickley, L., Montzka, S., Müller, J.F., Olivier, J., Pickering, K., Pitari, G., Roelofs, G.J., Rogers, H., Rognerud, B., Smith, S., Solomon, S., Staehelin, J., Steele, P., Stevenson, D., Sundet, J.,, Thompson, A. van Weele, M.,von Kuhlmann, R., Wang, Y., Weisenstein, D., Wigley, T., Wild, O., Wuebbles, D. and Yantosca R. (2001). Atmospheric chemistry and greenhouse gases. In Climate Change 2001, The Scientific Basis. Contribution of Working Group I to the Third Assessment Report of the Intergovernmental Panel on Climate Change (eds. Houghton J.T. *et al.*) 239–287. Cambridge University Press, Cambridge, UK.

Puett, R. C., Schwartz, J., Hart, J. E., Yanosky, J. D., Speizer, F. E., Suh, H., Paciorek, C. J., Neas, L. M. and Laden, F. (2008). Chronic particulate exposure, mortality, and coronary heart disease in the Nurses' Health Study. *Am. J. Epidemiol.* 168(10), 1161–1168.

Puett, R., Hart, J.E., Yanosky, J., Paciorek, C.J., Schwartz, J., Suh, H., Speizer, F.E., Laden, F. (2009) Chronic fine and coarse particulate exposure, mortality and coronary heart disease in the Nurses' Health Study, *Environ. Health Perspect.*, 117(11),1697–701.

Qian, Y., Kaiser, D. P., Leung, L. R., & Xu, M. (2006). More frequent cloud-free sky and less surface solar radiation in China from 1955 to 2000. *Geophys. Res. Lett.*, 33(1), 2-5. doi, 10.1029/2005GL024586.

Quaas, J., Boucher, O., Bellouin, N. and Kinne, S. (2008). Satellite-based estimate of the direct and indirect aerosol climate forcing. *J. Geophys. Res.* 113, D05204, doi,10.1029/2007JD008962.

Quinn, P. K., Bates, T. S., Baum, E., Doubleday, N., Fiore, A. M., Flanner, M., Fridlind, A., Garrett, T. J., Koch, D., Menon, S., Shindell, D., Stohl, A. and Warren, S. G. (2008). Short-lived pollutants in the Arctic, Their climate impact and possible mitigation strategies. *Atmos. Chem. Phys.* 8, 1723–1735, doi,10.5194/acp-8-1723-2008.

Raes, F. and Seinfeld, J. H. (2009). New directions, Climate change and air pollution abatement, a bumpy road. *Atmospheric Environment* 43(32), 5132–5133.

Ramana, M. V., Ramanathan, V., Feng, Y., Yoon, S-C., Kim, S-W., Carmichael, G. and Schauer, J. J. (2010). Warming influenced by the ratio of black carbon to sulphate and the black-carbon source. *Nature Geoscience* 3, 542–545.

Ramanathan, V., Crutzen, P.J., Lelieveld, J., Mitra, A.P., Althausen, D., Anderson, J., Andreae, M.O., Cantrell, W., Cass, G.R., Chung, C.E., Clarke, A.D., Coakley, J.A., Collins, W.D., Conant, W.C., Dulac, F., Heintzenberg, J., Heymsfield, A.J., Holben, B., Howell, S., Hudson, J., Jayaraman, A., Kiehl, J.T, Krishnamurti, T.N., Lubin, D., McFarquhar, G., Novakov, T., Ogren, J.A., Podgorny, I.A., Prather, K., Priestley, K., Prospero, J.M., Quinn, P.K., Rajeev, K., Rasch, P., Rupert, S., Sadourny, R., Satheesh, S.K., Shaw, G.E., Sheridan, P., Valero, F.P.J. (2001). Indian Ocean Experiment, an integrated analysis of the climate forcing and effects of the great Indo-Asian haze. *J. Geophys. Res.* 106(D22), 371-398. Doi,10.1029/2001JD900133.

Ramanathan, V., Chung, C., Kim, D., Bettge, T., Buja, L., Kiehl, J. T., Washington, W. M., Fu, Q., Sikka, D. R. and Wild, M. (2005). Atmospheric brown clouds, impacts on South Asian climate and hydrological cycle. *PNAS*, 102(15), 5326–5333.

Ramanathan, V. and Balakrishnan, K. (2007). *Reduction of Air Pollution and Global Warming by Cooking with Renewable Sources, A Controlled and Practical Experiment in Rural India* (Project Surya). http,//www-ramanathan.ucsd.edu/files/SuryaWhitePaper.pdf.

Ramanathan, V., Li, F., Ramana, M. V., Praveen, P. S., Kim, D., Corrigan, C. E. and Nguyen, H. (2007). Atmospheric brown clouds, hemispherical and regional variations in long-range transport, absorption, and radiative forcing. *J. Geophys. Res.* 112, D22S21, doi,10.1029/2006JD008124.

Ramanathan, V. and Carmichael, G. (2008). Global and regional climate changes due to black carbon. *Nature Geoscience* 1, 221–227.

Ramanathan, V., Agrawal, M., Akimoto, H., Auffhammer, M., Devotta, S., Emberson, L., Hasnain, S. I., Iyngararasan, M., Jayaraman, A., Lawrence, M., Nakajima, T., Oki, T., Rodhe, H., Ruchirawat, M., Tan, S. K., Vincent, J., Wang, J. Y., Yang, D., Zhang, Y. H., Autrup, H., Barregard, L., Bonasoni, P., Brauer, M., Brunekreef, B., Carmichael, G., Chung, C. E., Dahe, J., Feng, Y., Fuzzi, S., Gordon, T., Gosain, A. K., Htun, N., Kim, J., Mourato, S., Naeher, L., Navasumrit, P., Ostro, B., Panwar, T., Rahman, M. R., Ramana, M. V., Rupakheti, M., Settachan, D., Singh, A. K., St. Helen, G., Tan, P. V., Viet, P. H.,

Yinlong, J., Yoon, S. C., Chang, W. C., Wang, X., Zelikoff, J. and Zhu, A. (2008). *Atmospheric Brown Clouds, Regional Assessment Report with Focus on Asia*. United Nations Environment Programme, Nairobi, Kenya.

Ramaswamy, V., Boucher, O., Haigh, J. D., Hauglustaine, D. A., Haywood, J., Myhre, G., Nakajima, T., Shi, G. Y. and Solomon, S. (2001). Radiative forcing of climate change. In, Houghton, J. T. (ed) *Climate Change 2001*. Cambridge University Press, Cambridge, 349-416.

Ramesh, K. V. and Goswami, P. (2007). Reduction in temporal and spatial extent of the Indian summer monsoon. *Geophys. Res. Lett.*, 34, L23704.

Randles, C. and Ramaswamy, V. (2008). Absorbing aerosols over Asia, a Geophysical Fluid Dynamics Laboratory general circulation model sensitivity study of model response to aerosol optical depth and aerosol absorption. *J. Geophys. Res.* 113.

Reich, P. B. (1987). Quantifying plant response to ozone, a unifying theory. *Tree Physiology* 3, 63–91.

Ren, C., Williams, G. M., Mengersen, K., Morawska, L. and Tong, S. (2008). Does temperature modify short-term effects of ozone on total mortality in 60 large eastern US communities? An assessment using the NMMAPS data. *Environment International* 34, 451–458.

Rignot, E., Velicogna, I., van den Broeke, M. R., Monaghan, A. and Lenaerts, J. (2011). Acceleration of the contribution of the Greenland and Antarctic ice sheets to sea level rise. Geophysical Research Letters, 38 Article Number, L05503, doi, 10.1029/2011GL046583.

Roberts, D. L. and Jones, A. (2004). Climate sensitivity to black carbon aerosol from fossil fuel combustion. *J. Geophys. Res.* 109, D16202, doi,10.1029/2004JD004676.

Rojas-Martinez, R., Perez-Padilla, R., Olaiz-Fernandez, G., Mendoza-Alvarado, L., Moreno-Macias, H., Fortoul, T., McDonnell, W., Loomis, D. and Romieu, I. (2007). Lung function growth in children with long-term exposure to air pollutants in Mexico City. *Am. J. Respir. Crit. Care Med.* 176(4), 377–384.

Roman, H. A., Walker, K. D., Walsh, T. L., Conner, L., Richmond, H. M., Hubbell B. J. and Kinney, P. L. (2008). Expert judgment assessment of the mortality impact of changes in ambient fine particulate matter in the US. *Environ. Sci. Technol.* 42, 2268–2274.

Romieu, I., Barraza-Villarreal, A., Escamilla-Nunez, C., Almstrand, A. C., Diaz-Sanchez, D., Sly, P. D. and Olin, A.-C. (2008). Exhaled breath malondialdehyde as a marker of effect of exposure to air pollution in children with asthma. *J. Allergy Clin. Immunol.* 121(4), 903–909.

Rotstayn, L. D. and Lohmann, U. (2002). Tropical rainfall trends and the indirect aerosol effect. *J. Climate* 15, 2103–2116.

Royal Society (2008). *Ground-level Ozone in the 21st Century, Future Trends, Impacts and Policy Implications*. Science Policy Report 15/08. http://royalsociety.org

Satheesh, S. K. (2002). Radiative forcing by aerosols over Bay of Bengal region. *Geophys. Res. Lett.* 29(22), 2083.

Samuelsen, M., Nygaard, U. C. and Lovik, M. (2008). Allergy adjuvant effect of particles from wood smoke and road traffic. *Toxicology* 246(2–3), 124–131.

Sanderson, M. G., Jones, C. D., Collins, W. J., Johnson, C. E. and Derwent, R. G. (2003). Effect of climate change on isoprene emissions and surface ozone levels. *Geophys. Res. Lett.* 30(18), 1936, doi,10.1029/ 2003GL017642.

165

Sanderson, M. G., Collins, W. J. and Hemming, D. L. (2007). Stomatal conductance changes due to increasing carbon dioxide levels, projected impact on surface ozone levels. *Tellus B-Chem. Phys. Meteorol.* 59, 404–411.

Sarnat, S. E., Suh, H. H., Coull, B. A., Schwartz, J., Stone, P. H. and Gold, D. R. (2006). Ambient particulate air pollution and cardiac arrhythmia in a panel of older adults in Steubenville, Ohio. *Occupational and Environmental Medicine* 63(10), 700–706.

Schindler, C., Keidel, D., Gerbase, M. W., Zemp, E., Bettschart, R., Brandli, O., Brutsche, M. H., Burdet, L., Karrer, W., Knöpfli, B., Pons, M., Rapp, R., Bayer-Oglesby, L., Künzli, N., Schwartz, J., Liu, L.-J. S., Ackermann-Liebrich, U. and Rochat, T. (2009). Improvements in PM_{10} exposure and reduced rates of respiratory symptoms in a cohort of Swiss adults (SAPALDIA). *Am. J. Respir. Crit. Care Med.* 179(7), 579–587.

Schulz, M., Textor, C., Kinne, S., Balkanski, Y., Bauer, S., Berntsen, T., Berglen, T., Boucher, O., Dentener, F., Guibert, S., Isaksen, I. S. A., Iversen, T., Koch, D., Kirkevag, A., Liu, X., Montanaro, V., Myhre, G., Penner, J. E., Pitari, G., Reddy, S., Seland, O., Stier, P. and Takemura, T. (2006). Radiative forcing by aerosols as derived from the AeroCom present-day and pre-industrial simulations. *Atmos. Chem. Phys.* 6, 5225–5246.

Schwartz, J. (2004). How sensitive is the association between ozone and daily deaths to control for temperature? *Am. J. Respir. Crit. Care Med.*, Volume 171, Number 6, March 2005, 627-631 doi,10.1164/rccm.200407-933OC.

Schwartz, J., Coull, B., Laden, F. and Ryan, L. (2008). The effect of dose and timing of dose on the association between airborne particles and survival. *Environ. Health Perspect.* 116(1), 64–69.

Serreze, M. C., Holland, M. M. and Stroeve, J. (2007). Perspectives on the Arctic's shrinking sea-ice cover. *Science* 315, 1533–1536, doi,10.1126/science.1139426.

Sharma, S., Andrews, E., Barrie, L., Ogren, J. and Lavoue, D. (2006). Variations and sources of the equivalent black carbon in the High Arctic revealed by long-term observations at Alert and Barrow, 1989–2003. *J. Geophys. Res.* 111, 1998–2007.

Shindell, D. T., Faluvegi, G., Lacis, A., Hansen, J. E., Ruedy, R. and Aguilar, E. (2006). The role of tropospheric ozone increases in 20th century climate change. *J. Geophys. Res.* 111, D08302, doi,10.1029/2005JD006348.

Shindell, D. (2007). Local and remote contributions to Arctic warming. *Geophys. Res. Lett.* 34, L14704, doi,10.1029/2007GL030221.

Shindell, D. T., Levy, H. II, Schwarzkopf, M. D., Horowitz, L. W., Lamarque, J.-F. and Faluvegi, G. (2008). Multi-model projections of climate change from short-lived emissions due to human activities. *J. Geophys. Res.* 113, D11109, doi,10.1029/2007JD009152.

Shindell, D. and Faluvegi, G. (2009). Climate response to regional radiative forcing during the 20th century. *Nature Geoscience* 2, 294–300.

Shindell, D., Faluvegi, G., Koch, D., Schmidt, G.A., Unger, N. and Bauer, S. E. (2009). Improved attribution of climate forcing to emissions. *Science* 326(5953), 716–718.

Shindell, D. and Faluvegi, G. (2010). The net climate impact of coal-fired power plant emissions. *Atmos. Chem. Phys.* 10, 3247–3260.

Shindell, D., Schulz, M., Ming, Y., Takemura, T., Faluvegi, G. and Ramaswamy, V. (2010). Spatial scales of climate response to inhomogeneous radiative forcing. Journal of Geophysical Research-atmosphere, 115, Article Number, D19110. doi, 10.1029/2010JD014108.

Shine, K. P., Fuglestvedt, J. S., Hailemariam, K. and Stuber, N. (2005). Alternatives to the global warming potential for comparing climate impacts of emissions of greenhouse gases. *Climate Change* 68, 281–302.

166

Siegenthaler, U. and Joos, F. (1992). Use of a simple model for studying oceanic tracer distributions and the global carbon cycle. *Tellus* 44, 186-207.

Singh, P. and Kumar, N. (1997). Impact assessment of climate change on the hydrological response of a snow and glacier melt runoff dominated Himalayan river. *Journal of Hydrology* 193(1–4), 316–350.

Sitch, S., Cox, P. M., Collins, W. J. and Huntingford, C. (2007). Indirect radiative forcing of climate change through ozone effect on land-carbon sink. *Nature* 448, 4.

Skarby, L., Ro-Poulsen, H., Wellburn, F. A. M. and Sheppard, L. J. (1998). Impacts of ozone on forests, a European perspective. *New Phytologist* 139, 109–122.

Smith, K. R., Samet, J. M., Romieu, I. and Bruce, N. (2000). Indoor air pollution in developing countries and acute lower respiratory infections in children. *Thorax* 55(6), 518–532.

Smith, K. R., Mehta, S. and Feuz, F. (2004). Indoor smoke from household solid fuels. In, Ezzati, M. R., Lopez, A. and Murray, C. (eds). *Comparative Quanitification of Health Risks, Global and Regional Burden of Disease Due to Selected Major Risk Factors.* World Health Organization, Geneva.

Smith, K. R., Jerrett, M., Anderson, H. R., Burnett, R. T., Stone, V., Derwent, R., Atkinson, R. W., Cohen, A., Shonkoff, S. B., Krewski, D., Pope, C. A. III, Thun, M. J. and Thurston, G. (2009). Public health benefits of strategies to reduce greenhouse-gas emissions, health implications of short-lived greenhouse pollutants. *The Lancet* 374(9707), 2091–103.

Søreide, J. E., Jørgen Berge, E. L., Graeve, M. and Falk-Petersen, S. (2010). Timing of blooms, algal food quality and *Calanus glacialis* reproduction and growth. *Global Change Biology* 16, 3154–3163.

SOU (Statens Offentliga Utredningar) (2007). *Sweden Facing Climate Change, Threats and Opportunities.* Final Report of the Swedish Commission on Climate and Vulnerability. SOU 2007,60.

Stanhill, G. and Cohen, S. (2001). Global dimming, a review of the evidence for a widespread and significant reduction in global radiation with discussion of its probable causes and possible agricultural consequences. *Agricultural and Forest Meteorology* 107, 255–278.

Stevens, G. A., Dias, R. H. and Ezzati, M. (2008). The effects of 3 environmental risks on mortality disparities across Mexican communities. *PNAS* 105(44), 16860–16865.

Stier, P., Feichter, J., Roeckner, E., Kloster, S. and Esch, M. (2006). The evolution of the global aerosol system in a transient climate simulation from 1860 to 2100. *Atmos. Chem Phys*. 6, 3059–3076.

Stohl, A. (2006). Characteristics of atmospheric transport into the Arctic troposphere. *J. Geophys. Res.* 111, D11306, doi,10.1029/2005JD006888.

Tamagawa, E., Bai, N., Morimoto, K., Gray, C., Mui, T., Yatera, K., Zhang, X., Xing, L., Li, Y., Laher, I., Sin, D. D., Man, S. F. and van Eeden, S. F. (2008). Particulate matter exposure induces persistent lung inflammation and endothelial dysfunction. *Am. J. Physiol. Lung Cell. Mol. Physiol.* 295(1), L79–85.

Taylor, K. E. and Penner, J. E. (1994). Response of the climate system to atmospheric aerosols and greenhouse gases. *Nature* 369, 734–737.

Tedesco, M., Fettweis, X., van den Broeke, M. R., van de Wal, R. S. W., Smeets, C. J. P. P., van de Berg, W. J., Serreze, M. C. and Box, J. E. (2011). The role of albedo and accumulation in the 2010 melting record in Greenland. *Environ. Res. Lett*, 6,1.doi:10.1088/1748-9326/6/1/014005.

Thompson, L. G., Mosley-Thompson, E., Davis, M. E., Lin, P., Henderson, K. A. and Mashiota, T. (2003). Tropical glacier and ice core evidence of climate change on annual to millennial time scales. *Climatic Change* 59, 137–155.

Thwaites, R. H., Ashmore, M. R. and Morton, A. J. (2006). The effects of tropospheric ozone on species dynamics of calcareous grassland. *Environ. Pollut.* 144, 500–509.

Timonen, U., Huttunen, S. and Manninen, S. (2004). Ozone sensitivity of wild field layer plant species of Northern Europe, a review. *Plant Ecology* 172, 27–39.

Tol, R. S. J. (2008). The social cost of carbon, trends, outliers and catastrophes. *Economics – the Open-Access, Open-Assessment E-Journal* 2(25), 1–24.

Tonne, C., Yanosky, J., Gryparis, A., Melly, S., Mittleman, M., Goldberg, R., von Klot, S. and Schwartz, J. (2009). Traffic particles and occurrence of acute myocardial infarction, a case-control analysis. *Occup. Environ. Med.* 66(12), 797–804, doi,10.1136/oem.2008.045047.

Touloumi, G., Katsouyanni, K., Zmirou, D., Schwartz, J., Spix, C., de Leon, A. P., Tobias, A., Quennel, P., Rabczenko, D., Bacharova, L., Bisanti, L., Vonk, J. M. and Ponka, A. (1997). Short-term effects of ambient oxidant exposure on mortality, a combined analysis within the APHEA project. *Am. J. Epidemiol.* 146(2), 177–185.

Tuovinen, J.-P., Simpson, D., Emberson, L., Ashmore, M. and Gerosa, G. (2007). Robustness of modelled ozone exposures and doses. *Environ. Pollut.* 146, 578–586.

Turner, B.L., Kasperson, R.E., Matson, P.A., McCarthy, J.J., Corell, R.W., Christensen, L., Eckley, N., Kasperson, J.X., Luers, A., Martello, M.L., Polsky, C., Pulslpher, A. and Schiller, A. (2003) A framework for vulnerability analysis in sustainability science. PNAS 100, 8074–8079.

Uddling, J., Hogg, A. J., Teclaw, R. M., Carroll, M. A. and Ellsworth, D. S. (2010). Stomatal uptake of O_3 in aspen and aspen-birch forests under free-air CO_2 and O_3 enrichment. *Environ. Pollut.*, 158, 2023–2031.

UNECE (United Nations Economic Commission for Europe) (2010). *Manual on Methodologies and Criteria for Modelling and Mapping Critical Loads and Levels and Air Pollution, Risks and Trends*. Available at http://www.icpmapping.org

US EPA (US Environmental Protection Agency) (1999). *The Benefits and Costs of the Clean Air Act, 1990 to 2010*. US EPA, Washington, D.C. EPA 410-R-99-001.

US EPA (US Environmental Protection Agency) (2006). *Air Quality Criteria for Ozone and Related Photochemical Oxidants* (final). US EPA, Washington, D.C.

USGCRP (US Global Change Research Program) (2009). *Global Climate Change Impacts in the United States*. http,//www.globalchange.gov/publications/reports/scientific-assessments/us-impacts.

Van Dingenen, R., Dentener, F., Raes, F., Krol, M. C., Emberson, L. and Cofala, J. (2009). The global impact of ozone on agricultural crop yields under current and future air quality legislation. *Atmospheric Environment* 43, 604–618.

Velicogna, I. (2009). Increasing rates of ice mass loss from the Greenland and Antarctic ice sheets revealed by GRACE. *Geophys. Res. Lett.* 36(19), L19, 503.

Viscusi, W. K. (1978). Labor market valuations of life and limb, empirical evidence and policy implications. *Public Policy* 26(3), 359–386.

Volk, M., Bungener, P. and Contat, F. (2006). Grassland yield declined by a quarter in 5 years of free-air ozone fumigation. *Global Change Biology* 12, 74–83.

168

von Klot, S., Gryparis, A., Tonne, C., Yanosky, J., Coull, B. A., Goldberg R. J., Lessard, D., Melly, S. J., Suh, H. H. and Schwartz, J. (2009). Elemental carbon exposure at residence and survival after acute myocardial infarction. *Epidemiology* 20(4), 547-554.

Wang, B., Bao, Q., Hoskins, B., Wu, G. and Liu, Y. (2008). Warming and precipitation changes in East Asia. *Geophys. Res. Lett.* 35(14), L14, 702.

Wang, C. (2004). A modeling study on the climate impacts of black carbon aerosols. *J. Geophys. Res.* 109, D03106, doi,10.1029/2003JD004084.

Wang, C. (2009). The sensitivity of tropical convective precipitation to the direct radiative forcings of black carbon aerosols emitted from major regions, *Ann. Geophys*, 27, 3705-3711.

Wang, C., Kim, D., Ekman, A. M. L., Barth, M. C. and Rasch, P. J. (2009). Impact of anthropogenic aerosols on Indian summer monsoon. *Geophys. Res. Lett.* 36, L21704, doi,10.1029/2009GL040114.

Wang, X. and Mauzerall, D. L. (2004). Characterising distributions of surface ozone and its impacts on grain production in China, Japan and South Korea. *Atmospheric Environment* 38, 20.

Warren, S. G. and Wiscombe, W. J. (1980). A model for the spectral albedo of snow II, snow containing atmospheric aerosols. *J. Atmos. Sci.* 37, 2734-2745.

West, J. J., Fiore, A. M., Horowitz, L. W. and Mauzerall, D. L. (2006). Global health benefits of mitigating ozone pollution with methane emission controls. *Proc. Natl Acad. Sci.* 103, 3988–3993.

West, J. J., Szopa, S. and Hauglustaine, D. A. (2007). Human mortality effects of future concentrations of tropospheric ozone. *C. R. Geosci.* 339, 775–783.

West, J. J., Naik, V., Horowitz, L. W. and Fiore, A. M. (2009). Effect of regional precursor emission controls on long-range ozone transport. Part 2, steady-state changes in ozone air quality and impacts on human mortality. *Atmos. Chem. Phys.* 9, 6095–6107.

WHO (2009). World Health Organization. Global health risks, mortality and burden of disease attributable to selected major risks. WHO Press, World Health Organization, 20 Avenue Appia, 1211 Geneva 27, Switzerland.

Wild, M., Gilgen, H., Roesch, A., Ohmura, A., Long, C. N., Dutton, E. G., Forgan, B., Kallis, A., Russak, V. and Tsvetkov, A. (2005). From dimming to brightening, decadal changes in solar radiation at Earth's surface. *Science* 308(5723), 847–850.

Wilkinson, S. and Davies, W. J. (2009). Ozone suppresses soil drying- and abscisic acid (ABA)-induced stomatal closure via an ethylene-dependent mechanism. *Plant, Cell and Environment* 32, 949–959.

Wilkinson, S. and Davies, W. J. (2010). Drought, ozone, ABA and ethylene, new insights from cell to plant community. *Plant, Cell and Environment* 33, 510–525.

Williams, P. J. and Wallis, M. (2009). Permafrost and climate change, geotechnical implications. *Philosophical Transactions, Physical Sciences and Engineering* 352(1699), 347–358.

Xu, B., Cao, J., Hansen, J., Yao, T., Joswia, D. R., Wang, N. Wu, G., Wang, M., Zhao, H., Yang, W., Liu, X. and He, J. (2009). Black soot and the survival of Tibetan glaciers. *Proc. Natl. Acad. Sci.*,106(52), 22114-22118. doi,10.1073/pnas.0910444106.

Yasunari, T. J., Bonasoni, P., Laj, P., Fujita, K., Vuillermoz, E., Marinoni, A., Cristofanelli, P., Duchi, R., Tartari, G. and Lau, K.-M. (2010). Estimated impact of black carbon deposition during pre-monsoon season from Nepal Climate Observatory – Pyramid data and snow albedo changes over Himalayan glaciers. *Atmos. Chem. Phys.* 10(14), 6603–6615, doi,10.5194/acp-10-6603-2010.

Zanobetti, A., Canner, M. J., Stone, P. H., Schwartz, J., Sher, D., Eagan-Bengston, E., Gates, K. A., Hartley, L. H., Suh, H., and Gold, D. R. (2004). Ambient pollution and blood pressure in cardiac rehabilitation patients. *Circulation* 110(15), 2184–2189.

Zanobetti, A. and Schwartz, J. (2007). Particulate air pollution, progression, and survival after myocardial infarction. *Environ. Health Perspect.* 115(5), 769–775.

Zanobetti, A. and Schwartz, J. (2008). Mortality displacement in the association of ozone with mortality, an analysis of 48 cities in the United States. *Am. J. Respir. Crit. Care Med.* 177(2), 184–189.

Zanobetti, A., Bind, M. A. and Schwartz, J. (2008). Particulate air pollution and survival in a COPD cohort. *Environmental Health* 7, 48.

Zanobetti, A. and Schwartz, J. (2009). The effect of fine and coarse particulate air pollution on mortality, a national analysis. *Environ. Health Perspect,* 117,898-903. http,//dx.doi.org/10.1289/ehp.0800108.

Zanobetti, A., Stone, P. H., Speizer, F. E., Schwartz, J. D., Coull, B. A., Suh, H. H., Nearing, B. D., Mittleman, M. A., Verrier, R. L. and Gold, D. R. (2009). T-wave alternans, air pollution and traffic in high-risk subjects. *Am. J. Cardiol.* 104(5), 665–670.

Zeka, A., Melly, S. J. and Schwartz, J. (2008). The effects of socioeconomic status and indices of physical environment on reduced birth weight and preterm births in eastern Massachusetts. *Environmental Health* 7, 60.

Zhang, B., Chen, L. X., He, J. H., Zhu, C. W. and Li, W. (2009). Characteristics of atmospheric heat sources over Asia in summer, Comparison of results calculated using multiple reanalysis datasets. *Acta Meteorologica Sinica* 23, 585–597.

Zwally, H. J., Abdalati, W., Herring, T., Larson, K., Saba, J. and Steffen, K. (2002). Surface melt-induced acceleration of Greenland ice-sheet flow. *Science* 297, 218–222.

Chapter 5. Options for policy responses and their impacts

Co-ordinating lead author: Martin Williams, (Kings College, London, UK).

Lead authors: Markus Amann (International Institute for Applied Systems Analysis, Austria), Susan Anenberg (US Environmental Protection Agency), Lisa Emberson (Stockholm Environment Institute, University of York, UK), Mark Flanner (University of Michigan, USA), Zbigniew Klimont (International Institute for Applied Systems Analysis, Austria), Johan Kuylenstierna (Stockholm Environment Institute, University of York, UK), Nicholas Muller (Middlebury College, USA), Erika Rosenthal (Earth Justice, USA), Joel Schwartz (Harvard University, USA), Drew Shindell (National Aeronautics and Space Administration, Goddard Institute for Space Studies, USA), Rita Van Dingenen (Joint Research Centre, European Commission, Italy), Harry Vallack (Stockholm Environment Institute, University of York, UK), Elisabetta Vignati (Joint Research Centre, European Commission, Italy).

Contributing authors: Kristin Aunan (Center for International Climate and Environmental Research, Norway), Luis Cifuentes (The Catholic University of Chile, Chile), Greg Faluvegi (National Aeronautics and Space Administration, Goddard Institute for Space Studies, USA), George Milly (National Aeronautics and Space Administration, Goddard Institute for Space Studies, USA), N. T. Kim Oanh (Asian Institute of Technology, Thailand), T. S. Panwar (The Energy and Resources Institute, India), Michael Walsh (International Council for Clean Transportation, USA), Eric Zusman (Institute for Global Environmental Studies, Japan).

Key findings

A package of 16 measures has been identified that could yield the largest reductions in radiative forcing from short-lived substances at the global scale in 2030. They are in two groups: measures that address methane (CH_4); and measures that reduce emissions of black carbon (BC) and other products of incomplete combustion. These were selected from approximately 2000 measures in the technology and emission databases of the International Institute for Applied Systems Analysis (IIASA) Greenhouse Gas and Air Pollution Interactions and Synergies (GAINS) model, which were aggregated into about 400 packages of measures. The net effect of these emission changes on radiative forcing at the global scale, integrated over a 100-year period, has been estimated for each measure and the top 16 that collectively achieve nearly 90 per cent of the overall mitigation potential have been selected.

Most of the measures targeted at CH_4 involve action by large international and national energy companies (coal mining, oil and gas production), municipalities (treatment of waste and wastewater), and the agricultural sector (rice fields). Measures to reduce emissions of BC and other products of incomplete combustion require action in the transport, domestic and agricultural sectors, and in a few industrial sectors in developing countries. In addition to the introduction of new technologies, some BC measures will also require better governance, for example, to remove high-emitting vehicles from the road or to ban the open-burning of agricultural waste, as well as providing access to cleaner forms of energy to the poor in developing countries.

Reductions in CH$_4$ emissions are virtually certain to mitigate near-term warming. The effects of BC measures have a much larger uncertainty, but are also likely to mitigate near-term warming. These measures have an especially significant influence in the northern hemisphere mid-latitudes and in the Arctic. In these areas, warming is projected to be ~1.1±0.5^{o}C in 2040 relative to 2010 for the reference scenario. The combination of CH$_4$ and BC measures is able to eliminate approximately 0.6±0.4^{o}C of this warming. These regional temperature changes, as well as the global mean, are consistent with the output of a fully-coupled ocean-atmosphere climate calculation by one climate model. Benefits may also be enhanced in glaciated areas such as the Himalayas, where deposition of BC is substantially reduced in the two climate models used in this study by the BC measures.

The effects of the measures recommended by this Assessment are complementary to those of an aggressive low-carbon dioxide (CO$_2$) scenario aimed at achieving a global concentration of 450 ppm CO$_2$ equivalent (CO$_2$e). At the end-point of 2070 used here, the impact on temperatures of the low-carbon measures is comparable to the joint air quality/climate measures analysed in this Assessment. However, the temperature paths up to 2070 are very different. While the low-carbon measures result in strong warming in the next two decades mainly due to the dominance of CO$_2$ already in the atmosphere, they show their full effect in the more distant future and lead to lower rates of warming by 2070. In contrast, the air quality/climate measures analysed for this Assessment lower the rate of temperature increase in the coming decades. Once they have unfolded their full effect in the second half of the century, however, temperature will increase at a faster rate due to the absence of CO$_2$ reduction measures.

The measures analysed substantially decrease the regional atmospheric forcing by aerosols, and are hence very likely to reduce projected regional shifts in precipitation relative to what occurs in the reference scenario. As the reductions of atmospheric forcing are greatest over South Asia, the emissions reductions may have a substantial effect on the Asian monsoon. Results from global climate models are not yet robust in the magnitude or timing of monsoon shifts due to either greenhouse gas (GHG) increases or absorbing aerosol changes, however.

The influence of the adoption of these measures during the 2010–2030 has been compared with the adoption of the same measures over 2030–2050. In effect, this addresses the question of whether, as air quality improvements involving ozone (O$_3$) precursors and BC will be made eventually anyway, there is any climate benefit in making them now. **The results show that there is clearly much less warming during the 2020–2060 period if the measures were adopted earlier.** Over the longer term, from 2070 onwards, there is still a reduction in warming in the early measures case, but the value becomes quite small. This reinforces the conclusions drawn from previous analyses that reducing emissions of O$_3$ precursors and BC can have substantial benefits in the near term, but that long-term climate change is much more dependent on emissions of long-lived GHGs such as CO$_2$.

These measures have a particularly large impact on warming in the Arctic: the CH$_4$ and Group 1 and 2 BC measures may reduce Arctic warming by 0.37^{o}C, 0.33^{o}C and 0.14^{o}C, respectively, which is 35 per cent of the overall temperature increase expectedin 2070. The CH$_4$ measures result in the largest effect on temperature, while the BC group 1 measures are of particular relevance are the widespread

Integrated Assessment of Black Carbon and Tropospheric Ozone

introduction of pellet stoves and boilers replacing the use of fuelwood in industrialized countries, and the substitution of coal by coal briquettes in the residential sector. These lead to substantial reductions in northern hemisphere high-latitude emissions of carbonaceous aerosols and O_3 precursors, and account for about a quarter of the avoided temperature increase that could be achieved through implementation of all the measures. However, as with the other BC measures, uncertainty ranges are large.

The combustion of both fossil fuels and biofuels are substantial sources of carbonaceous aerosol emissions, but the organic carbon (OC) to black carbon (OC/BC) ratio of these sources can vary substantially. In particular, emissions from biofuel combustion that are affected by the measures examined here (mainly in small and industrial combustion and in waste burning) tend to have a higher OC/BC ratio, suggesting that their control might be less likely to mitigate warming. However, **the analysis indicates that controls on these particular biofuel combustion sources are likely to provide substantial global warming mitigation due to the combined influences of BC and OC reductions, although there remains a small probability that these measures produce little or no global benefit (though they would still produce substantial regional climate change mitigation, health and agricultural benefits).** In our analysis, CH_4 measures lead to a reduction of about 0.31°C in 2070, while BC measures (including the additional pellet stoves and residential briquette measures) add another 0.26°C reduction, of which ~0.12°C is from measures on biofuel combustion and 0.14°C from all other BC measures (mainly on fossil fuel combustion). The chosen measures for biofuel combustion also have substantial health benefits, contributing about 61 per cent of the global avoided deaths due to all the measures together, mostly due to reductions in fine particulate matter ($PM_{2.5}$).

The measures have substantial benefits for global public health, resulting in large decreases in mortality related to outdoor exposure to $PM_{2.5}$ and O_3. Overall, $PM_{2.5}$ mortality impacts are an order of magnitude larger than those for O_3, owing to both changes in concentration and the stronger relationship between $PM_{2.5}$ and mortality. Implementing all measures avoids an estimated 0.6–4.4 million annual $PM_{2.5}$-related deaths, associated with 5.3–37.4 million years of life lost. More than 80 per cent of the mortality benefits from implementing all measures occur in Asia. If valued in monetary terms, these health benefits amount to about US$5 (US$1.6–10.1) trillion (in 2006 US$ dollars).

Reducing emissions of BC and CO from biomass combustion will result in reductions in exposure to those combustion products indoors, with attendant health benefits. Approximately 220 000 deaths and 6 million disability-adjusted years of life lost could be avoided each year in India due to reduced indoor air pollution if the portfolio were implemented. In China, these could lead to a reduction of 153 000 deaths per year and 1.9 million disability-adjusted years of life lost.

The combined impact of the package of measures studied here would lead to a worldwide benefit in crop yields compared to the 2030 reference scenario from a 1.3 per cent (+1.5 per cent, -1.2 per cent) yield increase for rice to a 3.2 per cent (+1.6 per cent, -1.1 per cent) increase for soybeans. These benefits arise from the reductions in tropospheric O_3 resulting from application of the measures. The largest benefits emerge in the two Asian regions studied. The total global production gains of all crops range between 30 and 140 million tonnes (model mean: 52 million tonnes). The economic gains for all four crops in all regions range between US$4 billion and US$33 billion, of which US$2–28 billion are in Asia.

Case studies from across the world, in both developed and developing countries, are presented which describe the successful implementation of the mitigation measures included in the analysis. These examples demonstrate that technologies and practices are available and currently in use in various locations around the world. The challenge that remains is facilitating their widespread implementation.

An enhanced understanding of cost-effective technical and policy options for BC and tropospheric O_3/CH_4 under different national circumstances would help to inform national air quality and climate policy-makers as well as regional agreements. Initiation of a review of BC and tropospheric O_3 reduction technologies and regulatory approaches, based on local knowledge, could contribute to advancing adoption of effective mitigation action at multiple levels.

Improved international governance, policies and finance mechanisms would accelerate the adoption of the key mitigation measures. In particular, international coordination building on existing regional air quality agreements may be the most effective approach in the near term. International financing and technology transfer would facilitate more rapid action, especially in developing countries with multiple pressing needs. Any strengthened governance regime would be most effective if it included financing targeted specifically at pollution mitigation to maximize climate and air quality benefits.

5.1 Introduction

The purpose of this chapter is to assess the potential for reductions in emissions and, where possible, identify the impact these reductions will have on public health, ecosystems and climate. It assesses the options for reducing emissions of BC and O_3 precursors. The goal of these reductions is to mitigate the impacts of these pollutants not solely on climate, but also on public health and the wider environment. An account of these effects has been given in Chapter 4.

Environmental impacts resulting from emission changes, and hence concentration changes in the atmosphere, are driven by activity in economic sectors. Technical and non-technical measures are available and can be applied to priority source categories. Emission changes resulting from these measures are expected to reduce the targeted pollutant, such as BC, but in most instances will also result in changes to emissions of other pollutants. For example, energy efficiency measures would be expected to reduce emissions of all pollutants. As a result, to understand the full climate and public health implications of each measure, it is important to look at the suite of pollutants affected by any given measure. This integrated approach is particularly relevant in this Assessment as traditional pollutants and climate forcers are often emitted from the same sources and many emitted substances affect both climate and air quality. This chapter presents a discussion and analysis by sector, which will provide a more integrated and coordinated assessment of overall impacts and efficacy of mitigation measures.

An integrated approach is also necessary because co-emissions associated with both BC and tropospheric O_3 will differ markedly from one sector and source to another, an important consideration in deriving effective mitigation strategies to reduce climate impacts. As has been noted, the behaviour of OC as a cooling aerosol can potentially offset the climate benefits of reducing BC depending on the relative amounts of the two pollutants in each source/sector emission profile, as well as the location of the emission source. Similarly, addressing O_3 by mitigating CH_4 or nitrogen oxides (NO_x) will have different climate impacts. This Assessment also identifies and quantifies the negative consequences associated with each mitigation strategy. These can be significant – examples include the potentially enhanced emissions of health-damaging particulates entailed in switching from gasoline to diesel vehicles, and the use of wood burning to replace "cleaner" fuels.

The regional nature of the impacts of short-lived climate forcers (SLCFs) is of particular relevance to identifying effective mitigation

strategies for these components. The regional nature applies to their impacts as directly acting air pollutants as well as their impacts on climate. As described elsewhere in this Assessment, the short lifetimes of SLCFs imply that their impacts on a range of climate variables depend on where and when emissions take place. For instance, impacts of BC on snow and ice albedo imply that the efficacy of the radiative forcing from BC emission reductions differs from one region to another.

The evaluation of mitigation strategies uses the existing peer-reviewed literature, but also includes some analyses carried out specifically for this report based on emission scenarios developed at the International Institute for Applied Systems Analysis (IIASA), making use of energy scenarios of the World Energy Outlook 2009 of the International Energy Agency (IEA).

The sections below present an assessment of the impacts of a selected set of measures on radiative forcing and regional and global temperature changes, and on both the physical and economic aspects of human health, agriculture, and ecosystems. Particular attention is paid to impacts on vulnerable communities. Identifying mitigation policies, measures and strategies from a dispassionate modelling analysis is but one step in the practical realization of such measures and this chapter will also examine the practicability and feasibility of implementing the identified measures and policies in the real world, including possible institutional arrangements that could facilitate implementation in different parts of the world.

5.2 Analysis of the mitigation potential of black carbon and tropospheric ozone precursors

As part of a specific analysis of possible mitigation options for reducing the impacts of BC and tropospheric O_3, a number of key measures have been chosen by taking into account the following considerations:

i   There is a need to reduce climate change in the long term – this leads to a natural focus on long-lived GHGs that must decline dramatically.

ii   Climate change also causes damage in the near term (the rate of temperature change could exceed the capacity of ecosystems to adapt – e.g. Himalayas, Arctic, biodiversity), and rainfall patterns respond rapidly to changes in regional forcing.

iii.   Climatic changes in the near future will be determined more by CO_2 already in the atmosphere than by the CO_2 emissions over next 20 years, and by SLCFs. Therefore reducing climate impacts in the near term requires an additional focus on reducing SLCFs to avoid irreversible damage in the long term.

The following section gives more detail on the selection of the measures.

5.2.1 Measures to reduce precursor emissions of SLCFs

In the reference scenario, global anthropogenic emissions of CH_4 are expected to increase by approximately a third between 2000 and 2030 as a consequence of the growing human population and higher levels of economic activity. At the same time, anthropogenic emissions of BC, OC, carbon monoxide (CO) and sulphur dioxide (SO_2) are likely to stabilize, or even decline slightly at the global level, due to changes in lifestyles and industrial structures that are implied by anticipated economic development, as well as due to progressing implementation of current air pollution emission control legislation (see Chapter 2).

In addition to what is planned under current legislation, a host of technical and non-technical measures is available that could reduce emissions of the various substances in 2030 substantially more than is expected under the current legislation reference scenario.

As discussed in Chapter 3, however, emissions of different substances have different impacts on near-term climate change, some of them heating and others cooling. At the same time, virtually all emission control measures have simultaneous impacts on a wide range of emitted substances. Only the net effect on forcing that results from these emission

175

changes will determine the overall effect of a particular measure.

As the net effect of specific emission control measures can be positive or negative, a small portfolio with the most important measures has been identified that could yield in 2030 the largest reductions in radiative forcing from SLCFs at the global scale. Measures that have only a relatively small net impact or that would even increase radiative forcing have been excluded from this portfolio.

This analysis uses the technology and emission databases of the IIASA Greenhouse gas: Air pollution Interactions and Synergies (GAINS) model, which estimates mitigation potentials for the full range of air pollutants and GHGs of approximately 2000 individual measures in 108 regions in the world that have different impacts on emissions. These can be grouped into roughly 400 broader emission control categories such as those used here (e.g. EURO VI on diesel cars, on light duty trucks, and on heavy duty trucks have distinct effects on emissions but can all be categorized as part of a diesel vehicle measure).

The analysis estimated, for each of the 400 mitigation measures included in GAINS, their impacts on the emissions of all pollutants that are affected (i.e., CH_4, CO, BC, OC, SO_2, NO_x, volatile organic compounds (VOCs) and CO_2) in each source region. In a further step, the net effect of these emission changes on global radiative forcing has been estimated using the global warming potentials (GWP_{100}) listed in Table 4.1. Finally, the measures were ranked according to their effect of reducing that global radiative forcing.

An uncertainty analysis quantified the probability distributions of the net effects of each measure on radiative forcing given the uncertainty ranges in the radiative impacts of the different substances (Figure 5.1). This was achieved through a Monte-Carlo analysis with uncertainty ranges for the radiative forcing of different substances derived from the scientific literature (Table 4.1). It should be noted here that the radiative forcings shown in Figure 5.1 were used solely to

identify the emission reduction measures, and were not used in the climate modelling carried out as part of this Assessment. The global climate modelling used the values of the forcings discussed in Chapter 3. It was found that all measures targeted at CH_4 (including the co-controls for other pollutants) result in net reductions of radiative forcing, while net effects of measures to reduce BC emissions from biomass combustion are less certain as they reduce OC and other co-emitted species at the same time. Reducing atmospheric concentrations of PM and O_3 brings concomitant reductions in adverse impacts on human health as well as vegetation and crops. The selection criterion for the measures was the reduction in radiative forcing, so no attempt has been made in this analysis to optimize the health, vegetation and crop impacts of the selected measures.

Finally, out of about 130 measures that lead to lower global average radiative forcing, the top 16 have been selected that collectively achieve nearly 90 per cent of the overall mitigation potential according to the GWP_{100} metric. Many of these measures have already been applied, at least in some parts of the world. While the benefits of the measures are assessed and valued, an assessment of the costs of all the measures was outside the scope of this report. However, the examples of implementation of the measures discussed in Section 5.4 demonstrate that costs need not be a barrier to implementation and in some cases, such as gas recovery, may even be profitable in direct monetary terms.

Three groups of measures are distinguished (see also Box 5.1, Figure 5.2 and Figure A.5.1 in Appendix A.5):

i.   Measures that affect emissions of CH_4 and that can be implemented centrally by large national and international energy companies and municipalities and through modified agricultural practices. If implemented globally, these measures could reduce the long-term impact of 2030 emissions of SLCFs by about one-third compared to the reference scenario (Figure 5.2).

176
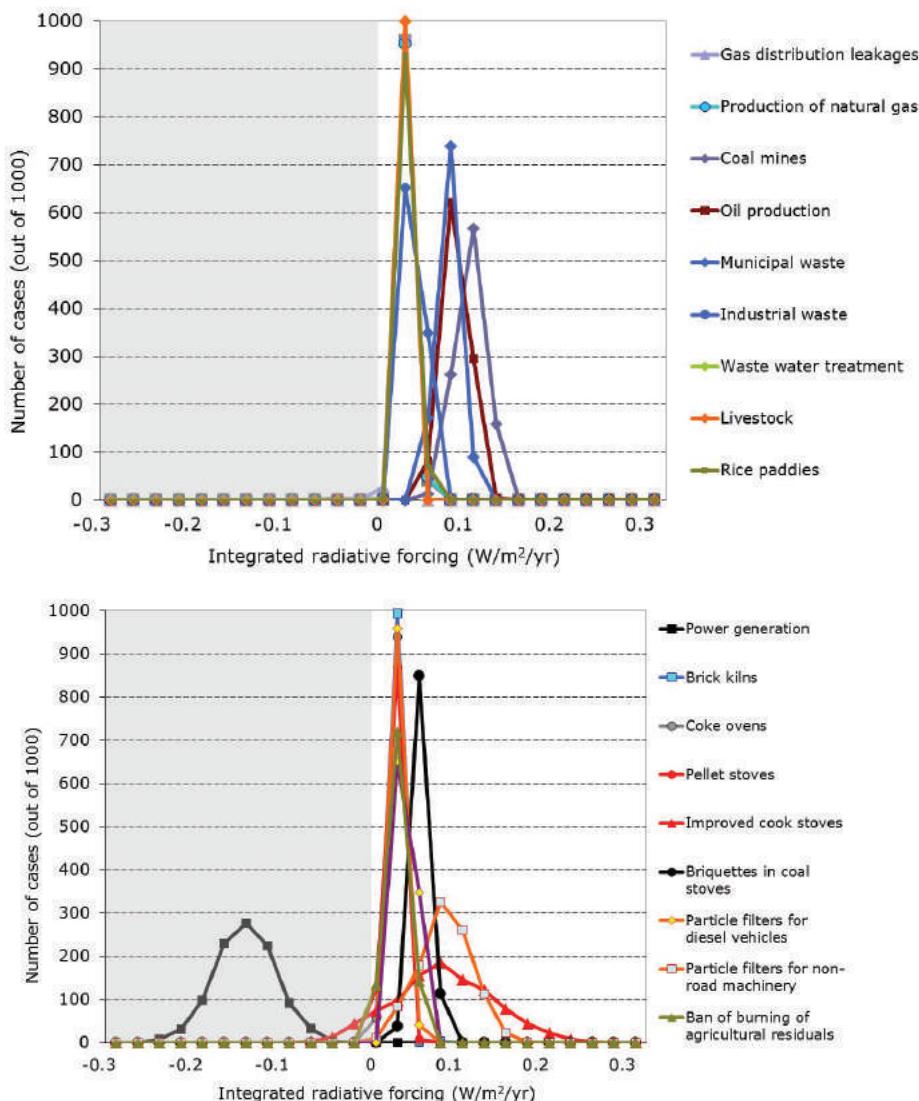
Figure 5.1. Probability distributions of the impacts of the key measures on avoidable global radiative forcing (integrated over 100 years). The top graph shows measures for CH$_4$, the bottom for BC. The analysis used the IIASA GAINS model.

ii. BC Group 1 measures are those that reduce emissions of BC and other products of incomplete combustion, mainly at small stationary and mobile sources, through the direct application of technologies. Together with the CH$_4$ measures these could reduce the long-term impact of emissions of SLCFs by about half compared to the 2030 reference scenario. (Figure 5.2)

iii. BC Group 2 measures that largely require national legislation and infrastructure development for implementation. Inclusion of these measures in the portfolio would reduce net radiative forcing from SLCF by about two-thirds compared to the 2030 reference scenario (Figure 5.2).

Since this portfolio has been chosen based on the capacity to reduce global average radiative forcing, it excludes emission control measures that would increase radiative forcing. If all 400 available measures were selected, radiative forcing would be about 50 per cent higher than from the selected subset of measures (see for example Figure A.5.1 in Appendix A.5.1), mainly due to the impact of measures removing SO$_2$ emissions (see discussion in 5.2.2 and Figure 5.3a).
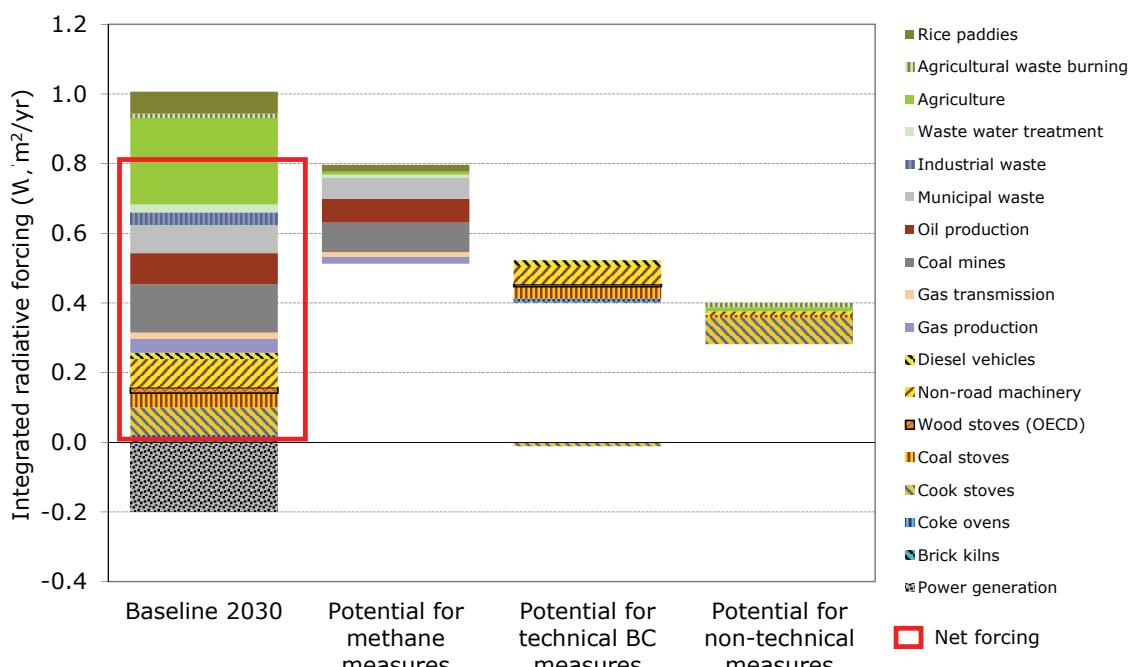
Figure 5.2. Contributions to global forcing (over 100 years) made by key activities and associated mitigation potentials. The analysis used the IIASA GAINS model.

The impacts of full application of these measures have been explored for the reference scenario described in Chapter 2, as well as for aggressive climate scenarios directed at the long-lived GHGs, referred to in this report as the GHG and CO_2 scenarios. It builds on a scenario of the IEA's World Energy Outlook 2009 that explores how global energy markets could evolve were countries to take coordinated action to restrict the global temperature increase to 2°C by stabilizing GHG concentrations at at a level equivalent to 450 ppm CO_2. Countries of the Organisation for Economic Cooperation and Development (OECD) are assumed to take on national emission reduction commitments for 2020. All other countries are assumed to adopt domestic policies and measures, and to generate and sell emission credits. In this scenario, global energy-related CO_2 emissions peak just before 2020 at 30.9 Gt and decline thereafter to 26.4 Gt in 2030 (IEA, 2009). For CH_4, the scenario assumes for 2030 a 30 per cent reduction compared to 2000, mainly through reductions in emissions from fossil fuel production and distribution (coal mines, oil and gas). (Uncertainties of emission estimates are discussed in Chapter 2).

5.2.2 Impacts of the packages of measures on emissions

The BC Group 1 and Group 2 measures have a large effect on emissions in the year 2030, as shown in Figure 5.3 in conjunction with the reference scenario and Figure 5.4 in conjunction with the GHG scenario. The reduction in total global emissions by the different measures is shown numerically in Table A.5.1 in Appendix A.5.1.

Relative to the reference scenario, these 16 measures achieve 75–80 per cent reductions of BC and OC, reduce $PM_{2.5}$ and CO by 50–60 per cent, CH_4 by 40 per cent, and NO_x by 30 per cent, but affect SO_2 and CO_2 emissions only marginally. In contrast, full application of all 400 measures – maximum feasible reduction (MFR) – would reduce all compounds by 70–90 per cent, except CH_4 (by 45 per cent) and CO_2. The high reduction of SO_2 in the MFR case (Figure 5.3a) has a strong impact on the net forcing, as indicated in Figure A.5.1 in the Appendix. The GHG scenario without further emission controls, due to its lower consumption of fossil fuels and CH_4, leads to 30 per cent lower CO_2, CH_4 and

Box 5.1: Identified measures to reduce radiative forcing from short-lived substances

Measure[1]	Sector
CH₄ measures	
Extended pre-mine degasification and recovery and oxidation of CH₄ from ventilation air from coal mines	Extraction and transport of fossil fuel
Extended recovery and utilization, rather than venting, of associated gas and improved control of unintended fugitive emissions from the production of oil and natural gas	
Reduced gas leakage from long-distance transmission pipelines	
Separation and treatment of biodegradable municipal waste through recycling, composting and anaerobic digestion as well as landfill gas collection with combustion/utilization	Waste management
Upgrading primary wastewater treatment to secondary/tertiary treatment with gas recovery and overflow control	
Control of CH₄ emissions from livestock, mainly through farm-scale anaerobic digestion of manure from cattle and pigs	Agriculture
Intermittent aeration of continuously flooded rice paddies	
BC Group 1 measures, affecting BC and other co-emitted compounds	
Diesel particle filters as part of a Euro 6/VI package for road and off-road diesel vehicles	Transport
Replacing coal by coal briquettes in cooking and heating stoves	Residential
Pellet stoves and boilers, using fuel made from recycled wood waste or sawdust, to replace current wood-burning technologies in the residential sector in industrialized countries	
Introduction of clean-burning biomass stoves for cooking and heating in developing countries[1,2].	
Replacing traditional brick kilns with vertical shaft kilns and with Hoffman kilns.	Industry
Replacing traditional coke ovens with modern recovery ovens, including the improvement of end-of-pipe abatement measures in developing countries.	
BC Group 2 measures affecting BC and other co-emitted compounds	
Elimination of high-emitting vehicles for road and off-road transport.	Transport
Ban of open field burning of agricultural waste[1]	Agriculture
Substitution of clean-burning cook stoves using modern fuels for traditional biomass cook stoves in developing countries[1,2]	Residential

[1] Motivated in part by its effect on health and regional climate, including areas of ice and snow.
[2] For cookstoves, given their importance for BC emissions, two alternative measures are included.
[3] There are other measures than those identified that could be implemented. For example, electric cars would have a similar impact on diesel particulate filters but these are not yet widely available; forest fire controls could also be important but are not included due to the difficulty in establishing the proportion of fires that are anthropogenic.

SO_2 emissions and 20 per cent lower NO_x, but does not significantly change emissions of BC, OC and CO. Thus, the 10 BC Group 1 and Group 2 measures affecting incomplete combustion would yield similar reductions as in the reference scenario, and are therefore not contingent upon the policies in the GHG scenario analysed here.

At the global level, for both scenarios, the largest potential for reductions of BC, OC and CO emissions emerges in the residential and transport sectors. However, in developing countries a sizeable potential has been identified for brick kilns, coke ovens and the open burning of agricultural waste.
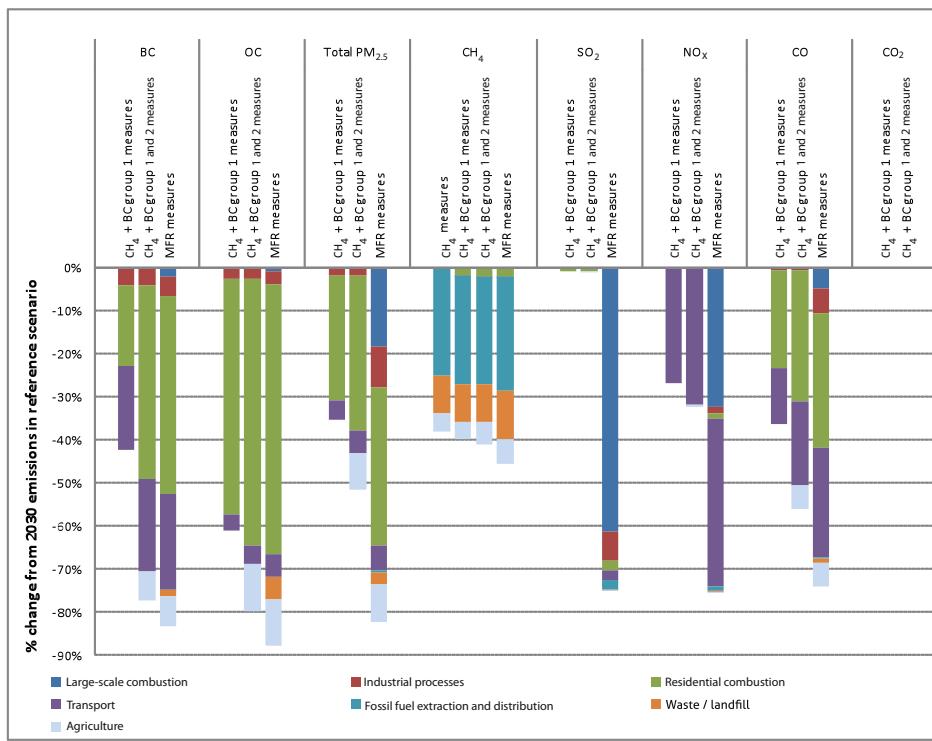
Figure 5.3a. Emission reductions in 2030 from the three packages of measures compared to the reference scenarios. The maximum feasible reduction (MFR) scenario represents the emission reductions from application of all 400 measures.
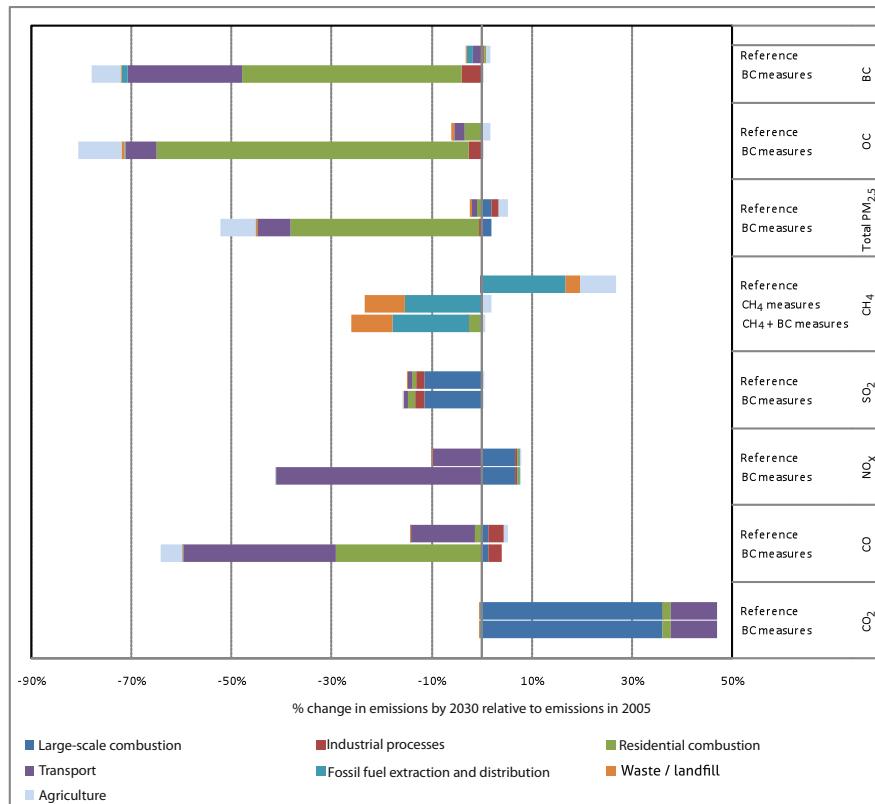
Figure 5.3b. Percentage change in anthropogenic emissions in 2030, relative to 2005 emissions, for the reference, CH$_4$ measures and CH$_4$ + BC measures (i.e. Group 1 + Group 2) scenarios. (The CH$_4$ measures have minimal effect on emissions of anything other than CH$_4$, so this scenario is omitted for the other species).

180
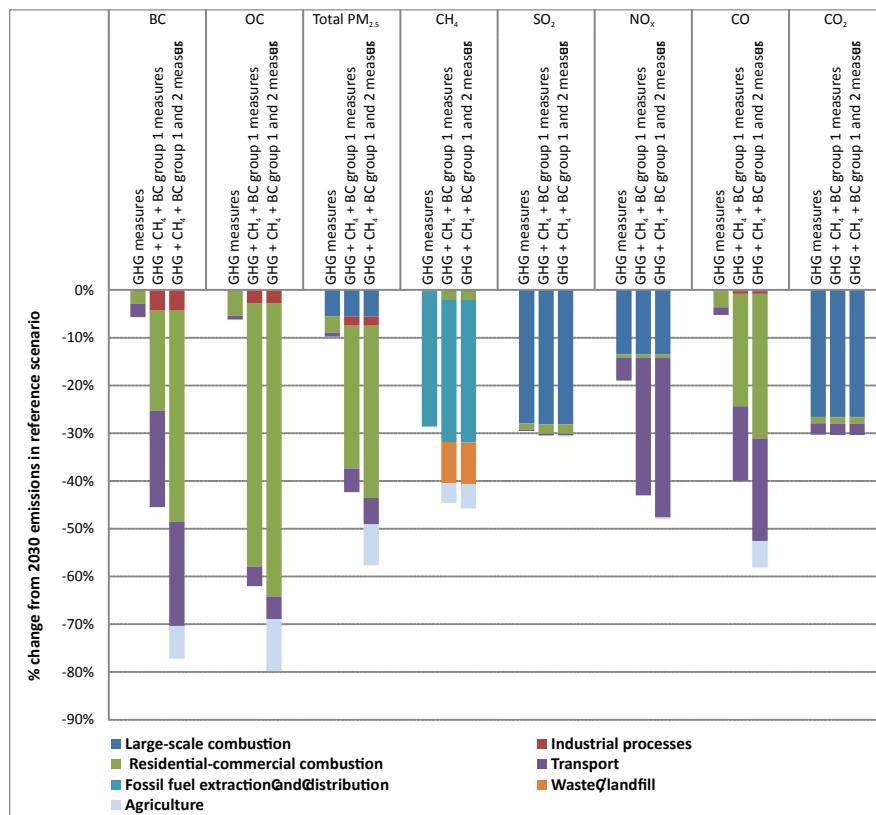
Figure 5.4. Emission reductions in 2030 from the three packages of measures under the GHG scenario, compared to the emissions of the reference scenario. All data are from IIASA GAINS for this Assessment.

For CH$_4$, the 30 per cent reduction in the GHG scenario results from the lower production of fossil fuels, and from targeted measures for coal, oil and gas production and distribution. The largest contribution from additional measures for CH$_4$ that are not included in the GHG scenario originates from waste treatment and livestock.

Impacts of additional measures in the residential sector
Two BC Group 1 emission-reduction measures were analysed separately in the calculations using full three-dimensional composition-climate models. These are the emission reductions due to a switch from currently installed fires and boiler designs to biomass pellet stoves in North America and Europe, and the substitution of raw coal chunks with honeycomb coal briquettes in the residential sector, mainly in China. The impacts of these measures are shown in Table A.5.1 in Appendix A.5.1. For North America and Europe, the

importance of the BC emission reductions, despite representing a small overall global reduction, lies in the fact that many sources lie close to the Arctic and so have a potentially larger impact there due to this proximity (see Section 5.3.1.2). Although not analysed specifically, the same is likely to be true for high-altitude regions of snow and ice near these sources.

In summary, the measures were implemented in the analysis in three packages as shown in Table 5.1.

5.3 Impacts of the measures

The impact of the measures on global temperatures, sensitive regions, human health and vegetation and crops are explored in the following sections.

Table 5.1. Policy packages used in this Assessment

Scenario	Description[1]
Reference	Includes all presently agreed policies based on the IEA *World Energy Outlook 2009.*
CH_4 measures	Reference scenario plus CH_4 measures.
CH_4 + BC measures	Reference scenario plus CH_4 and BC measures (Group 1 + Group 2; the BC measures affect many pollutants, especially BC, OC, and CO).
GHG measures	Emissions modelled using the assumptions of the IEA *World Energy Outlook 2009* 450 ppm CO_2e scenario and the IIASA GAINS database. Includes CO2 and some CH_4 measures. The CO_2 measures affect other emissions, especially SO_2.[2]
CO_2 measures	Emissions modelled using the assumptions of the IEA *World Energy Outlook 2009* 450 ppm CO_2e scenario and the IIASA GAINS database. Includes CO_2 measures only.[2]
CO_2 + CH_4 + BC measures	Climate change mitigation scenario plus the additional CH_4 and BC measures

[1] In all scenarios, trends in all pollutant emissions are included up to 2030, after which only CO_2 trends are included.
[2] Emissions of SO_2 are reduced by 35-40 per cent due to the implementation of CO_2 measures. A further reduction would be beneficial to health but would increase global warming. This is because sulphate particles act to cool the climate by reflecting sunlight back to space.

5.3.1 Impacts of the emission reduction measures on global temperatures

The impacts of the three packages of selected measures on radiative forcing have been recalculated using two state-of-the-art global climate-composition models: GISS-PUCCINI and ECHAM-HAMMOZ. The results were scaled using the ratios between the best estimate of the radiative forcing of the individual compounds, as described in Chapter 3, and the average of the radiative forcing calculated by the models. The effects on global and regional temperatures were subsequently calculated using global and regional temperature potentials (Shine et al., 2005; Shindell and Faluvegi, 2010; see Method description).

5.3.1.1 Packages of measures
As analysis of the impact of each measure individually with the full composition-climate models would have been overly demanding computationally, the measures were examined in groups or packages for CH_4, BC Group 1 and BC Group 2 as described in Box 5.1. Analysis of BC Group 1 measures was performed in two stages, with the impact of 14 measures assessed by both models and, because of potential interest in their impacts, the remaining two – pellet stoves and coal briquettes – assessed

separately by one model. The benefits analyses for BC Group 1 measures in this section were restricted to the 14 measures examined with both models (impacts of the remaining two are presented in Section 5.2.1.2).

Implemented in full, the measures would be able to reduce the rate and total magnitude of global and regional warming by about half over the next 25 years relative to the reference scenario (see Figures 5.5a and 5.5d). In fact, the measures would be able to entirely eliminate warming due to emissions changes relative to 2010 for roughly 25 years. However, the response to forcing experienced prior to 2010 is so large that despite the lack of additional positive forcing from 2010 to 2035, the Earth would continue to warm even with all measures examined here. In the reference scenario, increases in O_3 forcing and decreases in sulphate forcing cause the northern hemisphere to warm more rapidly than the southern hemisphere. In the reference scenario plus all measures case, there is strong negative forcing due to decreases in O_3 and BC in the northern hemisphere relative to the reference scenario so that the two hemispheres warm equally (Figure 5.5d).

A key point to emerge from these results is the complementarity between the measures

to counteract SLCFs and the longer-term measures addressing CO_2. The effect of the reductions in SLCFs begins to disappear after about 2040 when temperatures begin to rise more steeply; it is at this point, however, that the benefits of the GHG scenario appear, with the result that the steeper temperature rise in Figure 5.5d is slowed significantly (Figure 5.5e and 5.6c and d). What is also clear from these results is that the strategy to reduce CO_2 in the GHG scenario analysed here will do nothing to mitigate near-term temperature increases.

Reductions in CH_4 emissions are virtually certain to mitigate near-term warming (Figure 5.6). The effects of BC Group 1 and Group 2 measures have a much larger uncertainty (see also Table 5.2), but are also likely to mitigate near-term warming. These measures have an especially large influence in the northern hemisphere mid-latitudes and in the Arctic. In those areas, warming is projected to be ~1.1±0.5°C in 2040 under the reference scenario relative to 2010. The combination of CH_4, BC Group 1 and Group 2 measures is able to eliminate approximately 0.6±0.4°C of this warming. These regional temperature changes, as well as the global mean, are consistent with the output of a fully-coupled ocean-atmosphere climate calculation by one climate model (see section on methodology). Reductions in impacts may also be enhanced in glaciated areas such as the Himalayas, where deposition of BC is substantially reduced in both models by the BC Group 1 and 2 measures (Figure 5.9).

Uncertainty ranges are much smaller for CH_4 reductions (or the predominantly CO_2-driven changes under the low-carbon CO_2 measures) than for reductions in emissions of products of incomplete combustion. Variations in temperature response from one region to another are also much less for CH_4- (or CO_2-) driven changes, as these are quasi-uniform forcings, than for reductions in emissions of products of incomplete combustion. The CH_4 forcing calculated in the GISS-PUCCINI and ECHAM-HAMMOZ models are almost identical. Differences between the two models are larger for O_3 and aerosol forcing, where the GISS model

has a 44 per cent greater net negative forcing for the BC Group 1 measures or for the BC Group 1 plus Group 2 measures (primarily due to differences in the O_3 response, as the aerosol responses are within 15 per cent of one another). The spatial patterns are extremely similar, however (Figure 5.7). Likewise, the spatial pattern of changes in BC deposition is similar in the two models, which implies a similar effect on climate through BC darkening snow and ice.

The uncertainty ranges for the temperature response to BC Groups 1 and 2 measures usually encompass zero (Table 5.2). This is true even when accounting for systematic uncertainty (uncertainty in climate sensitivity is entirely systematic across scenarios; uncertainty due to forcing is partially systematic). However, over ~85 per cent of the range of the influence of the measures is cooling (e.g. the global response to all BC measures is between 0.05°C and -0.30°C). This implies that it is very likely that reduced emissions of products of incomplete combustion lead to temperature reductions, but there is also some chance that the net effect of these measures could be roughly zero, or even a small warming. Note that looking at BC alone or even BC+OC, as in many prior studies, the results would overlap much more as O_3's forcing helps make the net impact of emissions of products of incomplete combustion positive. The uncertainties for the impact of BC Groups 1 and 2 measures are skewed based on the assumption that constraints on total aerosol forcing make a very high positive value for BC unlikely (see Chapter 3), yielding an asymmetric uncertainty for BC forcing.

Since the GHG scenario CH_4 reduction measures overlap with the measures analysed here (section 5.2.2), both the full GHG scenario and also the GHG with low CO_2 measures only are presented, which avoids duplication of the near-term measures (see Figure 5.5). At the end-point of 2070 used here, the impact of the low-carbon CO_2 measures is comparable to the joint air quality/climate measures analysed in this Assessment. However, the warming rates at 2070 are extremely different, with very rapid warming in the absence of CO_2 reduction measures. The near-term impact of the

183

low-carbon measures, which reduce CO_2 and co-emitted pollutants (mainly SO_2), is a slight warming due to the more rapid response of sulphate aerosols than of CO_2 concentrations (consistent with the "bumpy road" of Raes and Seinfeld (2009)).

The measures analysed here substantially decrease the regional atmospheric forcing by aerosols and are hence very likely to reduce projected regional shifts in precipitation relative to what occurs in response to higher atmospheric aerosol loadings of the reference scenario (see Figure 5.8). As the reductions of atmospheric forcing are greatest over South and other parts of Asia, the emissions reductions may have a substantial effect on the Asian monsoon, mitigating disruption of traditional rainfall patterns. However, results from global climate models are not yet robust in the magnitude or timing of monsoon shifts due to either GHG increases or absorbing aerosol changes. Nonetheless, results from climate models provide an example of the type of change that might be expected (e.g. Section 4.2.3). Shifts in the timing and strength of precipitation can have large impacts on human well-being because of changes in water supply, drought, flooding and agricultural productivity. Figure 5.8 (c and d) shows that in Africa there could also be a considerable reduction in the disruption of traditional rainfall patterns.

While the measures analysed here can clearly have a substantial impact on climate change in the coming decades, their long-term effect is highly dependent on the reference scenario against which they are compared. For example, it is frequently assumed that over the long term, economic advancement in the developing world will lead to the eventual adoption of air quality regulations similar to those in place and projected for North America, Europe and Japan (e.g., Riahi *et al.*, 2007; Fujino *et al.*, 2006; Clarke *et al.*, 2007; van Vuuren *et al.*, 2006). This prompts the question of whether comparison with a reference case in which emissions of aerosols and O_3 precursors remain constant at 2030 levels through 2070 is appropriate. While no one can predict emissions many decades from now with confidence, the influence of the measures with respect to a less polluted future

atmosphere is examined by contrasting the influence of adoption of these measures during the 2010–2030 time frame with adoption of the same measures over 2030–2050 (using the same magnitude of forcing for a simpler comparison rather than the same percentage reduction applied to different reference 2030 emissions). In effect, this addresses the question that if air quality improvements involving O_3 precursors and BC will be made eventually anyway, is there any climate benefit in making them now rather than later. The results show that there is clearly much less warming during the 2020–2060 period if the measures are adopted earlier (Figure 5.12). From 2070 onwards, there is still a reduction in warming in the early measures case, but the value over the longer term becomes quite small. This reinforces the conclusions drawn from the previous analyses (Figures 5.5 and 5.6), that reducing emissions of O_3 precursors and BC can have substantial benefits in the near term, but that long term climate change is much more dependent on emissions of long-lived GHGs such as CO_2.

The temperature response calculations demonstrate that the time scale of climate change mitigation in response to the near-term measures is quite different from that for the GHG measures. We also find that the impact of the near-term measures is largely independent of whether the GHG measures are imposed. For example, the forcing from BC due to all near-term measures when the GHG measures have been imposed is within 3 per cent of the forcing when these measures have not been imposed. In general, forcings are all within 10 per cent in these two cases, since, as shown by the emissions changes, the GHG measures are largely independent of those identified here (other than for CH_4, where this is overlap).

5.3.1.2 The effects of widespread introduction of pellet stoves and boilers in industrialized countries and coal briquettes in the residential sector

The impact of these two BC measures was explored separately. These measures lead to substantial reductions in northern hemisphere high-latitude BC emissions and in carbonaceous aerosol and O_3 precursor emissions

184

Table 5.2. Temperature changes at 2070 relative to 2010 for the reference scenario, and relative to the reference scenario in 2070 for the measures (^{o}C).

	Global	Southern hemisphere extratropics	Tropics	Northern hemisphere mid-latitudes	Arctic
2010 baseline	1.93 (+1.06, -0.77)	1.46 (+0.80, -0.59)	2.01 (+1.11, -0.81)	2.14 (+1.20, -0.84)	2.31 (+1.27, -0.86)
Methane	-0.31 (+0.10, -0.16)	-0.21 (+0.07, -0.11)	-0.32 (+0.11, -0.16)	-0.39 (+0.13, -0.20)	-0.37 (+0.21, -0.30)
BC Group 1	-0.11 (+0.12, -0.07)	-0.02 (+0.02, -0.01)	-0.11 (+0.13, -0.06)	-0.19 (+0.20, -0.13)	-0.21 (+0.20, -0.15)
Two additional BC Group 1[1]	-0.05 (+0.06, -0.04)	-0.01 (+0.01, -0.01)	-0.05 (+0.05, -0.03)	-0.10 (+0.10, -0.07)	-0.12 (+0.12, -0.09)
BC Group 2	-0.10 (+0.13, -0.07)	-0.01 (+0.03, -0.01)	-0.11 (+0.15, -0.08)	-0.15 (+0.18, -0.11)	-0.14 (+0.16, -0.11)

Positive and negative uncertainties are given separately in parentheses.
[1]These two additional measures are those on pellet stoves and coal briquettes.
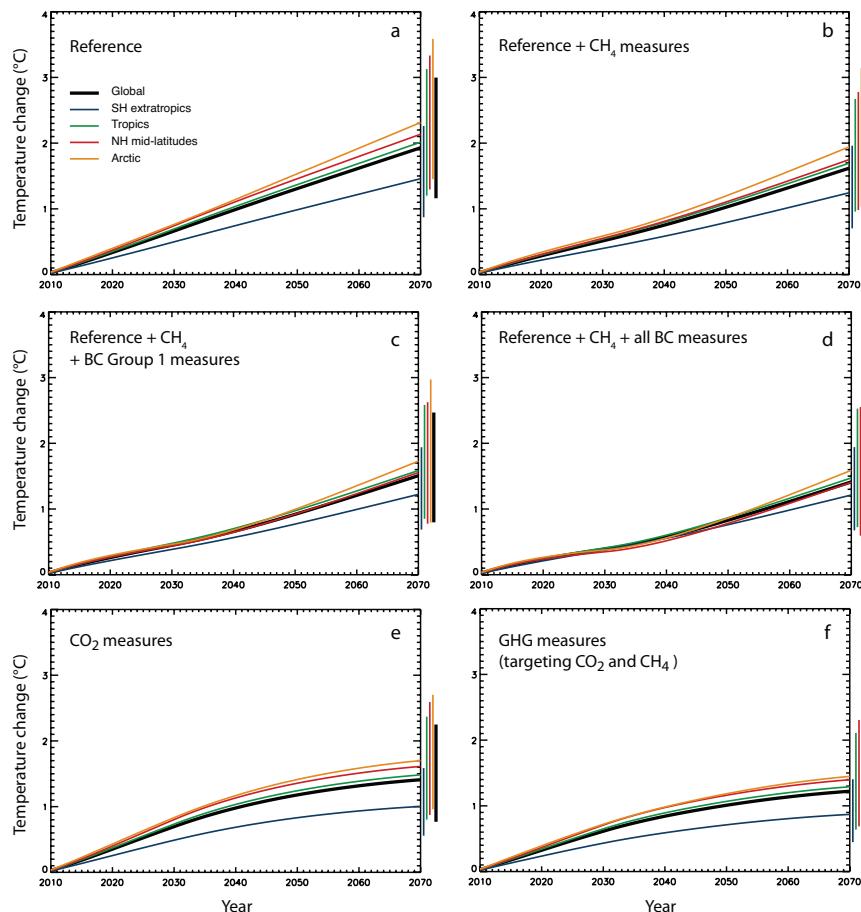
Figure 5.5a-f. Global and regional temperature changes relative to 2010 projected under the reference scenario, with the addition of emissions control measures and under the low-carbon scenarios. Values are based on O_3, aerosol and CH_4 radiative forcings and responses in the GISS and ECHAM climate models and also include forcings from both historical and projected CO_2 increases. Bars on the right side of each plot give the temperature range at 2070 based on uncertainty in radiative forcing and climate sensitivity. Uncertainties at earlier times are not shown for clarity, but have roughly the same proportion to the temperature change as the 2070 uncertainties.

Note: SH and NH mean southern hemisphere and northern hemisphere, accordingly.
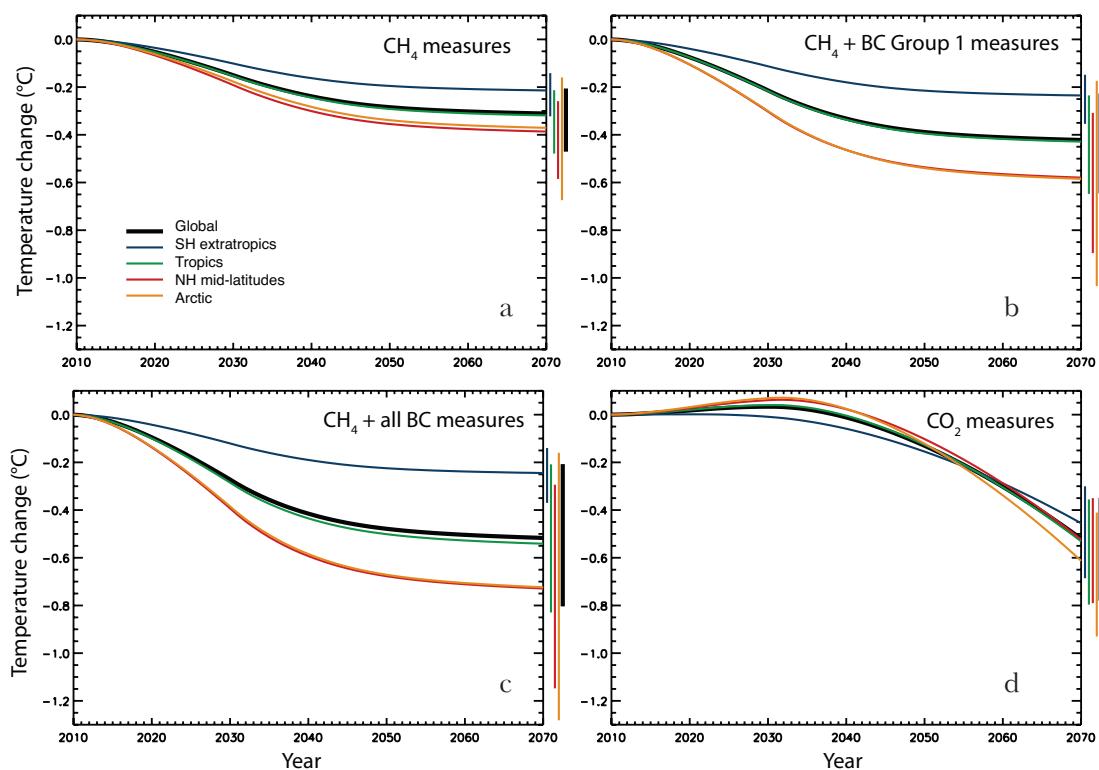
Figure 5.6. Global and regional temperature differences relative to the reference due to the various emissions control measures (a, b and c) and due to the CO_2 scenario (d). Values and uncertainties are calculated as in Figure 5.5.
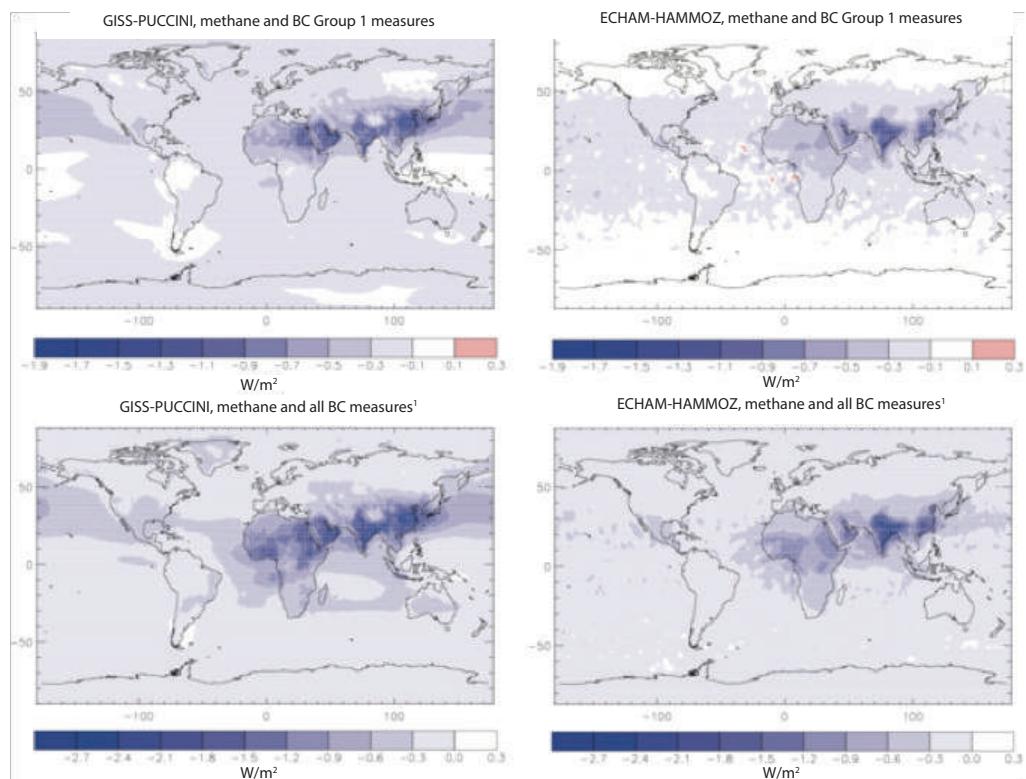
Figure 5.7. Radiative forcing at 2030 from O_3 and aerosols in the two models relative to the reference case (direct aerosol forcing only).   [1] Excluding measures on pellet stoves and coal briquettes.

Integrated Assessment of Black Carbon and Tropospheric Ozone
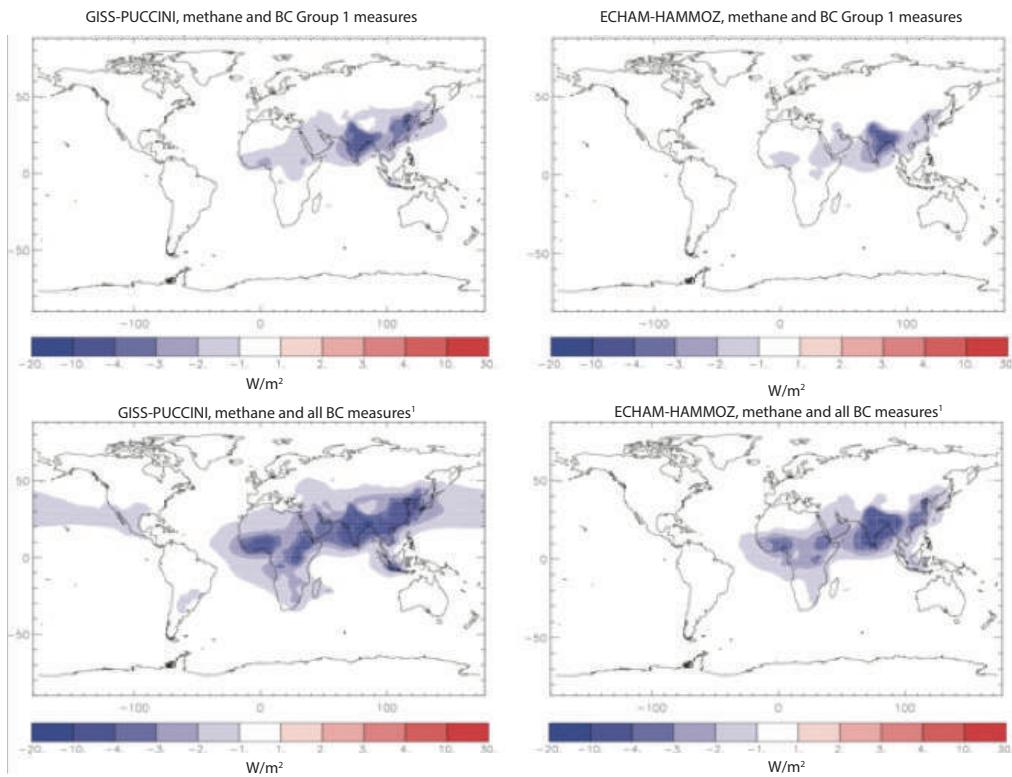
Figure 5.8. Change in atmospheric forcing at 2030 relative to the reference case in the two models.
[1]Excluding measures on pellet stoves and coal briquettes.
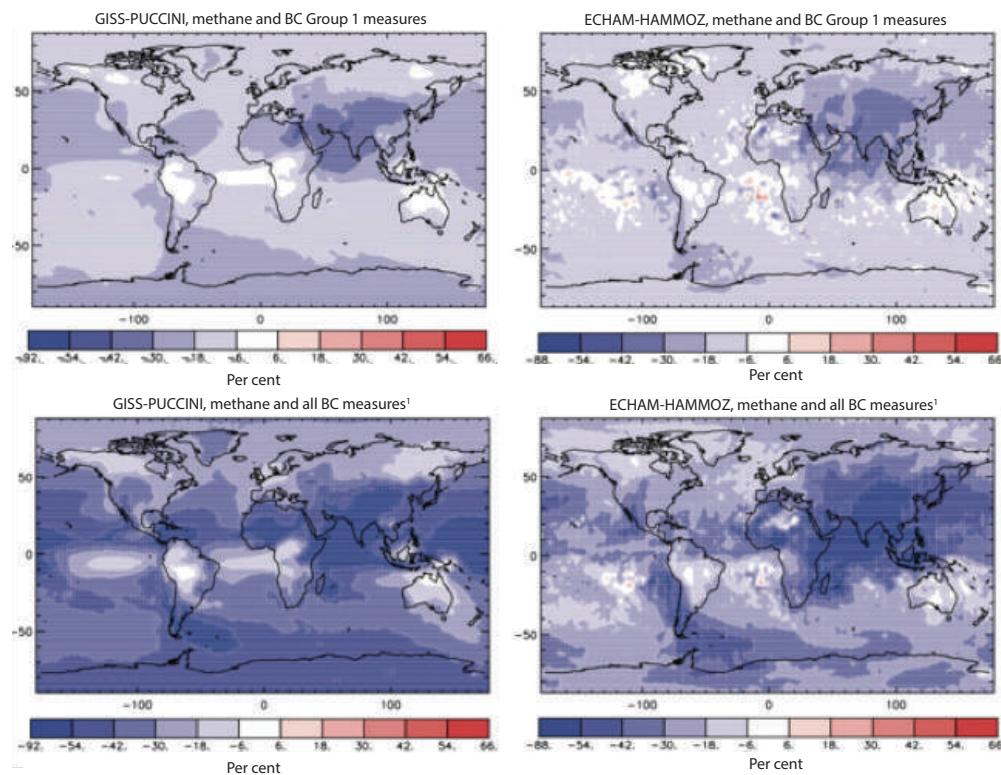
Figure 5.9. Change in BC deposition at 2030 relative to the reference case in the two models.
[1]Excluding measures on pellet stoves and coal briquettes.

Chapter 5. Options for policy responses and their impacts
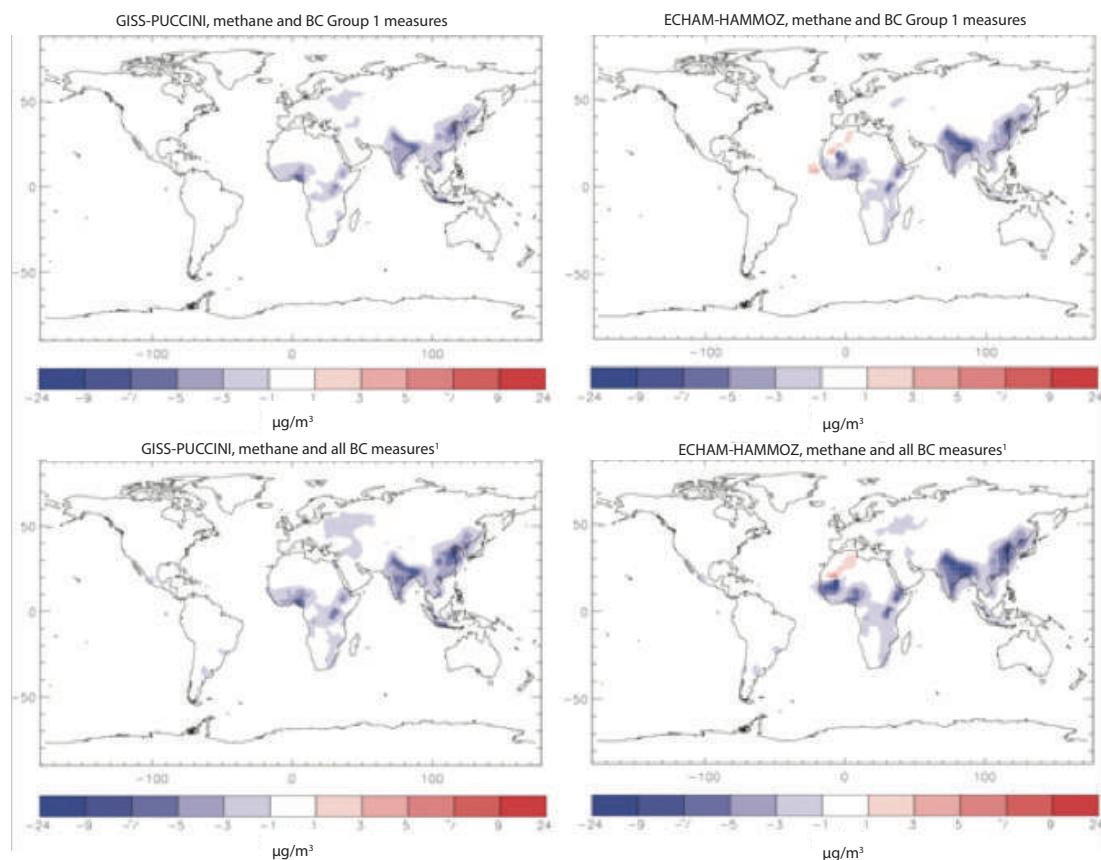
Figure 5.10. Change in surface $PM_{2.5}$ at 2030 relative to the reference case in the two models.

[1]Excluding measures on pellet stoves and coal briquettes.

from countries where coal is used in residential settings, notably China but also, among others, parts of Russia and Eastern Europe. The potential effect of these measures on global mean temperatures is fairly modest, but not insubstantial, adding about 0.05°C of avoided warming to the 0.4°C achieved by the other BC Group 1 measures (Figure 5.13 and Table 5.2). The effect on the Arctic is large, however, with an additional 0.1°C warming in the near term i.e.avoided during the next 25–30 years on top of the 0.45°C at 2035-2040 due to the CH_4 plus other BC Group 1 measures, an enhancement of 20–25 per cent (and an enhancement of ~35 per cent over the other BC Group 1 measures alone). As with the other BC Group 1 and Group 2 measures, uncertainty ranges are large (Table 5.2).

5.3.2 Benefits to polar and glaciated regions

Implementation of the measures would substantially slow, but not halt, the current rapid pace of temperature rise and other changes already occurring at the poles and high-altitude glacier regions. This is in part because particles co-emitted with BC, which are reflecting and therefore cooling over other regions, are still dark and absorb heat over ice and snow, leading to greater warming impacts.

Studies in the Arctic indicate that it is highly sensitive both to local pollutants and those transported from sources close to the Arctic, as well as to the climate impact of pollutants in the mid latitudes of the northern hemi-
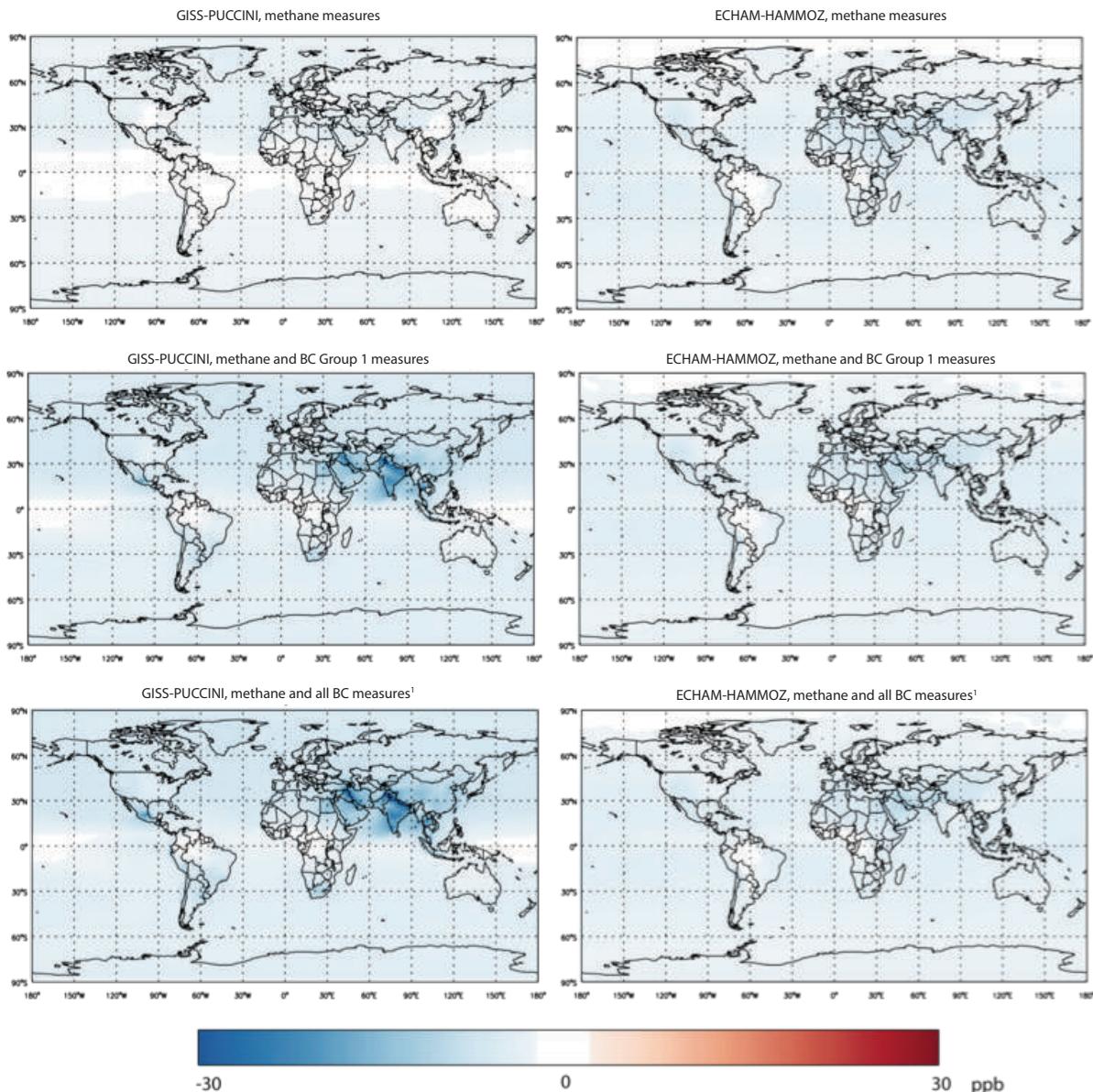
Figure 5.11. Change in surface O_3 (maximum six-month average of the one-hour daily maximum) for the different scenarios relative to the 2030 reference scenario, simulated by the two models. The scenarios are: CH_4 measures; CH_4 + BC Group 1 measures (but without the measures on pellet stoves and coal briquettes), and 'all measures' refer to CH_4+BC measures (BC Groups 1 and 2, but without the measures on pellet stoves and coal briquettes).

[1]Excluding measures on pellet stoves and coal briquettes.

sphere. Much of the needed implementation lies within Europe and North America.

In all scenarios, Arctic warming in 2070 is greater than the global-mean temperature increase because of high-latitude radiative and dynamical feedbacks. As described above (Table 5.2), however, the CH_4, BC Group 1 and Group 2 measures may reduce Arctic warming in 2070 by 0.37°C, 0.21°C and 0.14°C, respectively. The two additional Group 1 measures (pellet stoves and coal briquettes) drive the highest ratio of Arctic/global climate benefit in 2070, reducing Arctic warming by an additional 0.12°C (Table 5.2). Hence, if Arctic climate change becomes a focus of targeted mitigation action (e.g. because of threats from sea-level rise), these two technical actions may warrant deeper consideration. Moreover, co-emitted OC, which has a
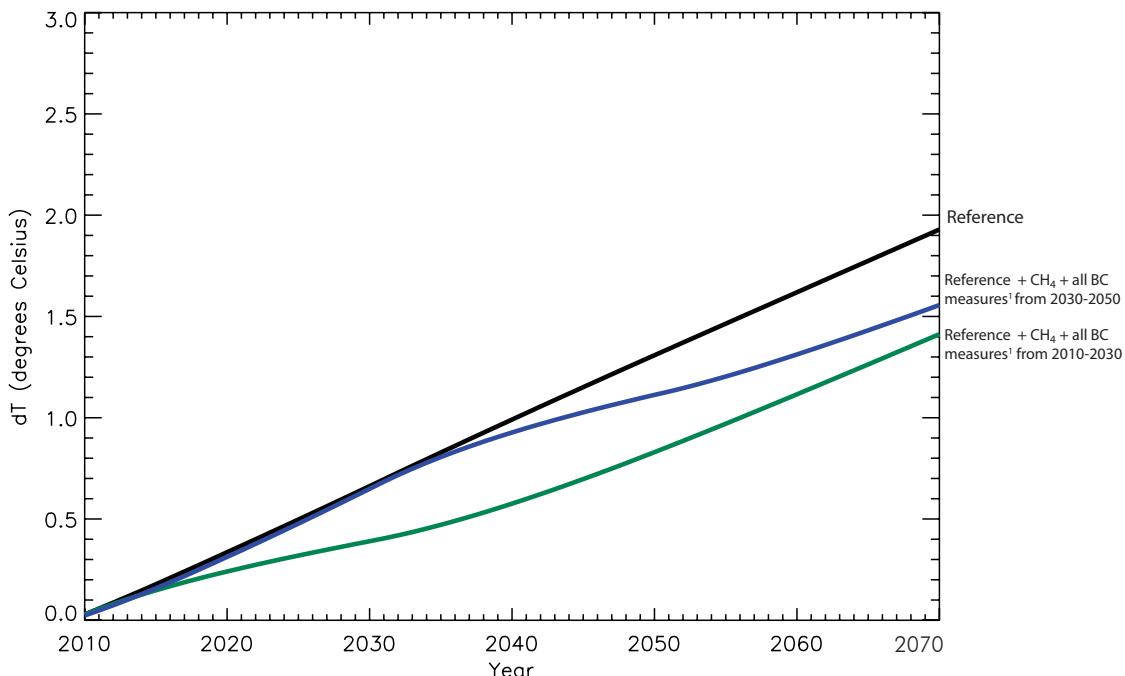
Figure 5.12. Projected global mean temperature changes for the reference scenario and for the reference plus measures to limit emissions of O_3 precursors and BC immediately or delayed by 20 years. Values calculated as in Figure 5.5.

global cooling effect, has much less influence in the Arctic because it does not brighten snow and ice and can actually increase atmospheric solar absorption over reflective Arctic surfaces (Section 4.2).

As snow and sea-ice melt in a warming world, Arctic BC forcing and the strength of the snow/ice positive feedback mechanism will both wane, even without reductions in emissions. As described in section 4.2, BC darkening of snow and ice drives a roughly
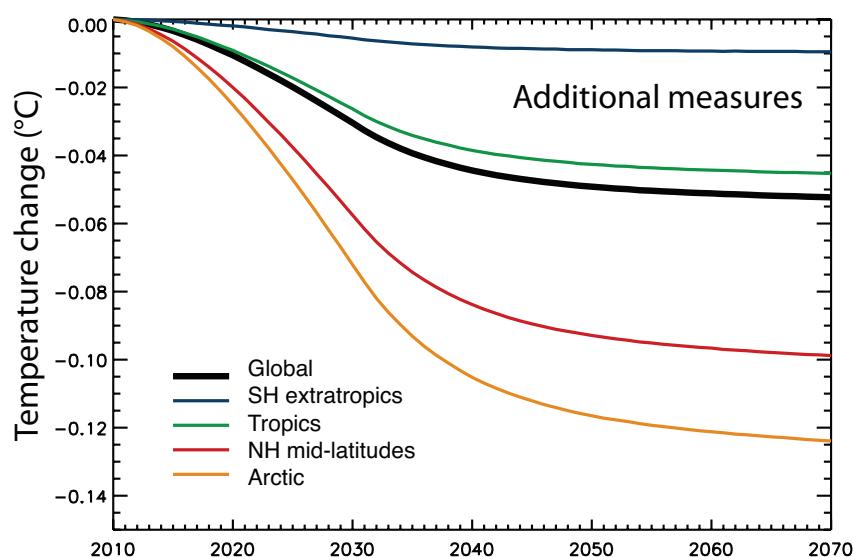
Figure 5.13. Global and regional temperature changes due to widespread use of pellet stoves and boilers in industrialized countries and coal briquettes in the residential sector in China. Values are relative to the simulations of the other BC Group 1 measures. Temperature responses are calculated using the same methodology, except that these results include only the GISS model values for the fraction of total anthropogenic impact reduced by these measures (both BC Group 1 and 2).

Box 5.2 The effect of fossil fuel versus biofuel emissions controls

As discussed in Chapter 2, combustion of both fossil fuels and biofuels are substantial sources of carbonaceous aerosol emissions, but the OC/BC ratio of these can be substantially different. In particular, emissions from biofuel combustion that are affected by the measures examined here, mainly in small and industrial combustion and in waste burning, tend to have a higher ratio, suggesting that their control is less likely to mitigate warming. Comparison of the temperature response to all measures with the response to all measures other than biofuel combustion using this Assessment's methodology indicates that controls on these particular biofuel combustion emissions are likely to provide substantial warming mitigation (Figure a). The biofuel measures examined separately here are (see Box 5.1) those on pellet stoves, the introduction of clean-burning biomass stoves in developing countries and the clean-burning cookstoves using modern fuels substituting for biomass cookstoves in developing countries. In the analysis, CH_4 measures lead to a reduction of about $0.31^{o}C$ in 2070, while BC Group 1 measures, including the additional pellet stoves and residential briquette measures, add another $0.16^{o}C$, while BC Group 2 measures add $0.10^{o}C$. The total contribution of BC measures is thus about $0.26^{o}C$, of which $\sim0.12^{o}C$ is from measures on biofuel combustion and $0.14^{o}C$ from all other BC measures (mainly fossil fuel combustion) (see Table 5.2). The greater warming influence of fossil fuel emissions over biofuel emissions is in line with other studies examining the effect of all BC/OC emissions rather than specific measures (e.g. Jacobson (2010)).

The biofuel combustion measures also have substantial health benefits, contributing about 61 per cent of the global avoided deaths due to all the measures together, mostly due to $PM_{2.5}$ reductions. As a percentage of the health response to all measures together, the contribution of biofuel combustion measures to avoided deaths is greatest in Africa (83 per cent) and South, West and Central Asia (65 per cent), more than the contribution from all other measures in East Asia, Southeast Asia and Pacific (56 per cent) and Latin America and Caribbean (53 per cent), and smallest in North America and Europe (37 per cent), as shown in Figure 5.17. Estimated changes in mortality due to these measures are for outdoor exposures only and do not account for the significant expected improvements in indoor air quality.
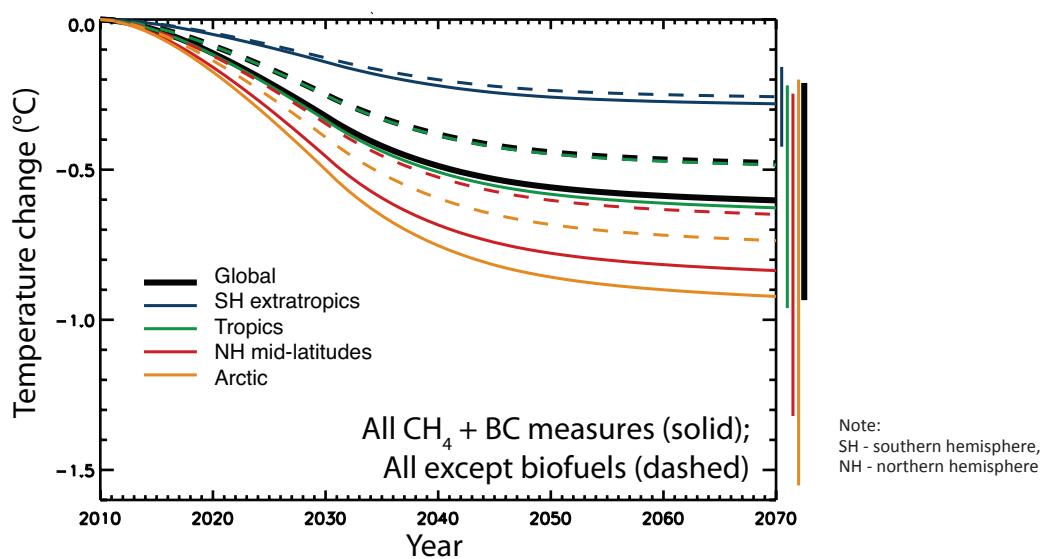
Figure a. Global and regional temperature changes due to all near-term measures (solid) and all measures except biofuels. Values are relative to the reference scenario. Temperature responses are calculated using the same methodology, except that these results include only the GISS model values for forcing relative to total anthropogenic forcing (in both reference and measures cases, where the measures are all measures including the additional pellet stoves and residential briquettes). Uncertainties are shown (bars on right) for the all-measures case at 2070, with comparable percentage values at other times or for the all except biofuels case (uncertainties for northern hemisphere mid-latitudes and the Arctic extend to values below -1ºC).

Box 5.3: Elimination of black carbon from cookstoves: a regional model study for Asia

Black carbon from cooking with biofuels (firewood, cow-dung and crop residues) contributes as much as 70 per cent to South Asian BC emissions while it is about 25 per cent in China. A regional aerosol-transport model (Adhikary *et al.*, 2007) that has been tuned and validated with satellite and ground-based data was used to simulate the impact of eliminating BC emissions from biofuel cooking (over all of Asia) on BC optical depths. Over India the BC optical depths (and hence its forcing) reduced by a factor of 2 to 3, while the reductions in East Asia were about 25 per cent to 50 per cent (Figure a).

a) With Biofuel BC from cooking	b) Without Biofuel BC from cooking
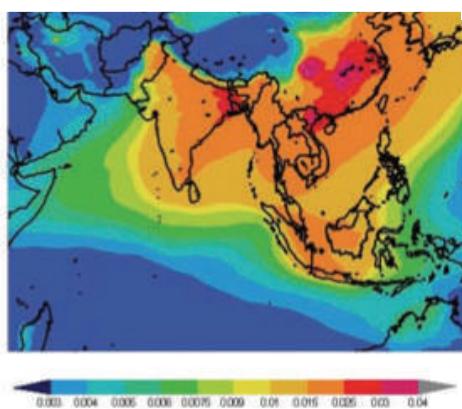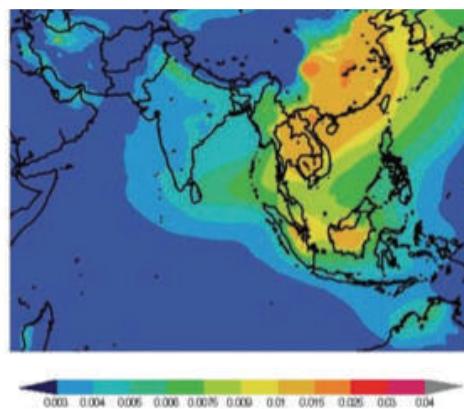
The effect of biofuel cooking on Asian BC loading. (a). The simulated annual mean optical depth of BC aerosols for 2004–2005 using the regional aerosol/chemical/ transport model. The values include BC emissions from biofuel cooking (indoor cooking with wood/dung/crop residues), fossil fuels and biomass burning (b) as for left panel, but without biofuel cooking. (Ramanathan and Carmichael, 2008).

The effect of biofuel cooking on Asian BC loading. (a) The simulated annual mean optical depth of BC aerosols for 2004–2005 using the regional aerosol/chemical/ transport model. The values include BC emissions from biofuel cooking (indoor cooking with wood/dung/crop residues), fossil fuels and biomass burning; (b) as for left panel, but without biofuel cooking. (Ramanathan and Carmichael, 2008).

Scaling the changes in optical depths with the warming trends over elevated regions of the Himalayan region shown earlier (see Chapters 3 and 4), reductions in BC could reduce the anomalously large warming trends over the Tibetan region (Liu and Chen, 2000) and the Indian Himalayas (Ramanathan *et al.*, 2005; Gautam *et al.*, 2009), by about 0.3⁰C or larger. In addition, the large reductions in BC deposition that should result from the BC reductions (Flanner *et al.*, 2009) shown above, should result in additional cooling over the Himalayas. Furthermore, reduction in the dimming, the reductions in the BC impact on the monsoons (Chapter 4.1.2) and reduction in warming trends should lead to additional benefits for agriculture productivity (Aufhammer *et al.*, 2006) and public health.

three to five-fold greater temperature response than greenhouse and atmospheric aerosol forcings of equal magnitude, highlighting the importance of how the different measures influence BC deposition to snow and ice. This depends not only on pollutant transport pathways and deposition processes, but also on the spatial and temporal patterns of snow and sea-ice cover. The forcing depends further on coincident sunlight. In the GISS and ECHAM simulations described here, Arctic-mean BC deposition is reduced by 19–20 per cent in the 2030 reference

scenario relative to 2005. The BC Group 1 measures (excluding the two additional measures) decrease Arctic BC deposition by an additional 12–13 per cent relative to 2030 while the combined Group 1 and Group 2 measures reduce it by 19–22 per cent (Figure 5.9). The additional two measures on pellet stoves and coal briquettes reduce deposition by an additional 15 per cent (GISS model only). Base case (2005) total annual Arctic BC deposition in the GISS model is 0.23Tg. This compares well (12 per cent greater) with base present-day Arctic BC deposition

simulated by Flanner *et al.* (2009), who estimated 60–90°N snow/ice direct forcing of 0.28 W/m². Because snow/ice forcing scales about linearly with BC concentration when the BC load is small, it is estimated that the combined BC measures Groups 1 and 2 can reduce efficacy-scaled Arctic forcing by about 0.21 W/m², indicating some potential to slow high-latitude climate change during the next several decades.

Extra-Arctic glaciated regions will also benefit from BC reductions. In many cases, these regions are closer to large BC emissions sources than the Arctic and are consequently more polluted, indicating greater capacity for mitigation. Measurements are sparse, however, and uncertainty in the spatial heterogeneity of aerosol deposition in mountainous regions is large. See Figure 4.8 for ice core time series of BC deposition in the Tibetan Plateau/Hindu Kush region. Flanner *et al.* (2009) estimated BC/snow forcing on the Tibetan Plateau, averaged only over the snow-covered surfaces, of 1.7 W/m², more than 4-fold greater than the snow/ice-cover averaged forcing in the Arctic. Larger snow forcing is enabled by greater surface insolation and more BC deposition on the Tibetan Plateau. This estimate may be representative of the effect on local glaciers (Box 4.5) and other non-Arctic northern latitude regions where there is winter snow cover, though large uncertainties persist in BC impacts on glaciers (Section 4.2).

The Antarctic is a far-less studied region in terms of SLCF impacts. However, there are studies demonstrating BC deposition even in central portions of the continent, and reductions in O_3 and CH_4 should slow warming in places like the Antarctic Peninsula, currently the area on the globe showing the most rapid temperature rise of all.

5.3.3 Benefits to human health

The impacts of the policy measures on human health are estimated using the methodology described in Chapter 4, and have incorporated estimates of uncertainties in the health effect outcomes. The sets of policy measures examined are increasingly stringent, beginning with CH_4 measures, then the addition

of BC Group 1, and finally the addition of the Group 2 measures. Changes in mortality relative to the 2030 reference scenario are calculated using surface $PM_{2.5}$ and O_3 concentrations simulated by the two models, GISS-PUCCINI and ECHAM-HAMMOZ (see Figures 5.10 and 5.11.)

The measures have substantial benefits for global public health, resulting in significant decreases in $PM_{2.5}$- and O_3-related mortality. Overall, $PM_{2.5}$ mortality impacts are an order of magnitude larger than O_3 mortality impacts, owing to both changes in concentration and the stronger relationship between $PM_{2.5}$ and mortality. The spatial patterns of total $PM_{2.5}$ and O_3 mortality impacts are very similar for both models (Figure 5.14). The only exception is for the CH_4 measures where ECHAM-HAMMOZ simulates a small increase in $PM_{2.5}$ concentrations in South, West and Central Asia due to oxidant chemistry that affects particle formation (see Figure 5.15). ECHAM-HAMMOZ also simulates greater O_3 decreases from the CH_4 measures in East Asia, Southeast Asia and the Pacific, which are more visible on the scale shown than the O_3 reductions simulated by GISS-PUCCINI.

For the impacts of the three sets of policy measures on $PM_{2.5}$-related mortality, both models yield similar magnitudes and regional distributions (Figure 5.15), with ECHAM-HAMMOZ slightly larger in magnitude but well within the confidence intervals. Both models also agree that BC Group 1 measures benefit $PM_{2.5}$-related mortality most, followed by the Group 2 measures. The CH_4 measures have a negligible impact on $PM_{2.5}$-related mortality, since only CH_4 emissions are affected. Implementing all measures could avoid 2.4 million premature deaths (within a range of 0.7–4.6 million) associated with reductions in $PM_{2.5}$, associated with 5.3–37.4 million years of life lost (YLL), based on the 2030 population. This range includes both models and associated 95 per cent confidence intervals. For both models, 72 per cent of these benefits are achieved by implementing BC technology measures with the rest achieved through the other measures. Both models agree that over 80 per cent of the mortality

benefits from implementing all measures would occur in Asia. For the GISS model, avoided deaths are about evenly distributed between East Asia, Southeast Asia and the Pacific (41 per cent) and South, West and Central Asia (44 per cent), while for ECHAM-HAMMOZ, 49 per cent of the total avoided mortalities occur in South, West and Central Asia and 34 per cent in East Asia, Southeast Asia and the Pacific. For both models, about 10 per cent, 5 per cent, and 1 per cent of the total avoided mortalities occur in Africa, North America and Europe, and Latin America and the Caribbean, respectively.

The measures also have substantial benefits for O_3-related mortality, but the two models yield different patterns for the impact of each set of policy measures (Figure 5.16). For GISS-PUCCINI, BC Group 1 measures in provide the greatest O_3 mortality benefit, contributing about 68 per cent of the health benefits from all measures together, followed by CH_4 measures (22 per cent), and Group 2 measures (10 per cent). The large O_3 impact from BC Group 1 measures results from substantial reductions in co-emitted O_3 precursors (NO_x, VOC, and CO). Contrastingly, the CH_4 measures produced the majority of the O_3 benefits in ECHAM-HAMMOZ, with little impact from BC Group 1 and a small disbenefit from Group 2 measures. Despite the large differences in modelled O_3 responses to the BC measures, the total impact of O_3 and $PM_{2.5}$ on health is fairly similar as it is dominated by $PM_{2.5}$-related impacts. In general, the differences between the two models are less than the uncertainty arising from the concentration-response relationship.

Incorporating the avoided deaths calculated from both models and the associated 95 per cent confidence intervals from the concentration-response relationship, all measures together avoid an estimated 0.04–0.52 million O_3-related deaths annually (0.35–4.7 million YLL), based on the 2030 population. As with $PM_{2.5}$ mortality benefits, the vast majority of O_3-related benefits occur in Asia: about 35–50 per cent of the benefits from implementing all measures together occur in South, West and Central Asia and 35–38 per cent

in East Asia, Southeast Asia and the Pacific, depending on the model. The rest are about evenly distributed between Africa, North America and Europe, and Latin America and the Caribbean.

With low-carbon CO_2 measures included in the reference scenario, the impacts of the joint air quality/climate measures are estimated to be similar but about 10 per cent smaller in East Asia, Southeast Asia and the Pacific and South, West and Central Asia. These results demonstrate that the joint air quality/climate measures have very substantial benefits for global public health regardless of whether low-carbon CO_2 measures are enacted.

The health impact of the BC measures on pellet stoves and coal briquettes have a further impact on health as they lead to reductions in $PM_{2.5}$, with the largest number of additional annually avoided premature mortalities (relative to the main package of BC Group 1 measures in each region) from both $PM_{2.5}$ and O_3 in East, Southeast Asia and the Pacific (~86 000, 13 per cent), South, West and Central Asia (~22 000, 3 per cent) and North America and Europe (~22 000, 30 per cent). As with climate impacts results in this case are based on a single global composition model.

Benefits from improved indoor air quality

The benefits to public health from improved indoor air quality have also been estimated. Reducing emissions of BC and CO from biomass combustion will result in reductions in exposure to those combustion products indoors, with attendant health benefits. Due to data limitations, these have only estimated benefits for India and China. The data are taken from the Global Burden of Disease report of 2004 for the burden of solid fuel use in the domestic sector in those countries in 2000 (WHO, 2004). This report provides a summary of the health effects and the dose-response relation. Work by IIASA for the new Global Burden of Disease report contains estimates of exposure for 2030 under the reference scenario, and under the alternative scenario. From these, estimates of the difference in health burden can be made. These are again presented as deaths avoided per year by the

strategy, and years of life lost. Again, mortality rates have been held constant in the analysis, which may be conservative.

Using the methodology outlined above, 220 000 deaths and 6 million disability-adjusted years of life lost could be avoided each year in India due to reduced indoor air pollution if the portfolio were implemented. In China, there would be a reduction of 153 000 deaths per year and 1.9 million disability-adjusted years of life lost.

Valuation of the benefits to human health

The analysis presented in this section employs the methods discussed in Chapter 4. Specifically, the results reported in Table 5.3 use country-specific values of a statistical life (VSLs) for both the GISS and ECHAM modelling results, and the health impacts are estimated from the changes in total $PM_{2.5}$ mass which result from the measures. (Results using the uniform VSLs are reported in the appendix to Chapter 5.). The results are shown in Table 5.3 which focuses on the valuation of avoided mortalities associated with the three policy scenarios: CH_4, CH_4 plus BC Group 1 measures (not including those for pellet stoves or coal briquettes), and CH_4 plus BC Groups 1 and 2 measures.

The increasing stringency of these measures is evident in Table 5.3 when looking at the global results. Beginning with the results from the GISS model (reported in column 3), in global aggregate terms the value of avoided mortalities increases from US$150 billion for the application of the CH_4 measures, to US$ 3.7 trillion for the CH_4 plus BC Group 1 measures. The application of all three packages of measures yields avoided mortalities that are valued at $US5.0 trillion. Employing the ECHAM model, the value of avoided mortalities is equal to $US145 billion, $US4.1 trillion and $US5.6 trillion for the three increasingly stringent packages of measures.

Table 5.3 also reveals that when the ECHAM model is applied to gauge the mortality impacts of these three policy scenarios, the absolute value of avoided mortalities increases for

the two most stringent scenarios. The value of avoided mortalities is nearly equal between GISS and ECHAM for the CH_4 package. The differences are well within the overlap of the uncertainty bounds for these estimates.

The fifth and sixth columns indicate the ratio of the change in mortalities in 2030 due to the three policy scenarios relative to the predicted change in the reference scenarios from 2005 to 2030. Beginning with the country-specific VSLs, Table 5.3 indicates that the CH_4 package yields additional mortality reductions that are 12 per cent of the value of reductions predicted to occur between the 2005 and 2030 reference cases. The CH_4 plus BC Group 1 measures yields mortality improvements that are nearly three times larger than the 2005–2030 change, while the three combined packages produce mortality reductions that are just under four times greater than in the reference cases.

The next three sections of Table 5.3 present the regional impacts of the policy scenarios. In all the scenarios, when using the GISS model, values are negative for all regions. This implies that the mortality burden due to exposures to $PM_{2.5}$ and O_3 declines. However, it is important to note that Africa and South, West and Central Asia experience changes in mortality that are of different signs (direction of change in mortality) than in the 2005–2030 reference scenario. Specifically, these two regions are predicted to incur a mortality improvement under each policy scenario while mortalities were predicted to increase between 2005 and 2030 in the business as usual reference case.

For Africa, the magnitude of the change due to the CH_4 package is of the order of 20 per cent of the mortality change between 2005 and 2030; however, note again that the direction of impact is different between these two cases. The results are similar for South, West and Central Asia with the principal difference being the relatively small share (approximately 3 per cent) of the mortalities avoided under the CH_4 package relative to the 2005–2030 reference comparison. East Asia, Latin America and the Caribbean,

195

Table 5.3: Valuation of premature mortalities: Three policy scenarios relative to the reference scenario. (See also Table A.5.6)

Model scenario	Region	Gross Mortality Value (2006 US$, billions)		Impact Ratio*	
		GISS	ECHAM	GISS	ECHAM
CH_4	Global	-150 (-49, -247)	-145 (-46, -236)	0.12	0.05
CH_4+BC Group 1	Global	-3 670 (-1 200, -6 460)	-4 060 (1 330, -7 200)	2.88	1.5
CH_4+ BC Groups 1+2	Global	-4 980 (-1 610, -8 870)	-5 600 (-1 820, -10 100)	3.90	2.06
CH_4	Africa	-13 (-4, -21)	-13 (-4, -21)	0.17	0.51
	East Asia, Southeast Asia and the Pacific	-53 (-17, -87)	-141 (-47, -236)	0.22	0.08
	Latin America and the Caribbean	-14 (-5, -23)	-20 (-7, -33)	4.36	0.52
	North America and Europe	-43 (-14, -71)	-29 (-9, -47)	0.02	0.01
	South, West and Central Asia	-28 (-9, -46)	58 (21, 101)	0.03	0.03
CH_4+BC Group 1	Africa	-248 (-83, -436)	-336 (-111, -598)	3.39	13.28
	East Asia, Southeast Asia and the Pacific	-1 580 (-516, -2 770)	-1 530 (-503, -2 680)	6.67	0.89
	Latin America and the Caribbean	-113 (-38, -192)	-116 (-39, -198)	35.20	3.03
	North America and Europe	-353 (-118, -601)	-410 (-137, -701)	0.17	0.14
	South, West and Central Asia	-1 380 (-450, -2 460)	-1 670 (-543, -3 020)	1.48	0.82
CH_4+BC Groups 1+2	Africa	-319 (-105, -565)	-453 (-148, -818)	4.36	17.91
	East Asia, Southeast Asia and the Pacific	-2 240 (-722, -3 990)	-2 180 (-709, -3 890)	9.45	1.27
	Latin America and the Caribbean	-154 (-51, -264)	-180 (-60, -310)	47.98	4.70
	North America and Europe	-472 (-158, -805)	-597 (-199, -1 020)	0.23	0.20
	South, West and Central Asia	-1 790 (-578, -3 250)	-2 190 (-700, -4 020)	1.92	1.08

- All values expressed in (2006 US$, billions), and represent the annual monetary benefit arising in 2030.

- Values reflect change in mortality damage; negative values imply improvement in welfare.

- 95 per cent confidence intervals in parenthesis, confidence intervals derived from reported 95 per cent confidence intervals for mortality dose-response parameter.

* Impact ratio: These columns show the ratio of the change in mortality values resulting from the policy measures relative to the change in mortality values resulting from the comparison between the 2030 reference scenario and the base 2005 impacts.

and North America and Europe experience mortality impacts that are of the same direction as the 2005–2030 change; mortalities continue to decrease under the CH_4 package. For East Asia and North America and Europe, the value of the additional mortality reduction is 22 per cent and 2 per cent of the value of reduced mortalities predicted to occur in the 2005–2030 change, respectively. Finally, Latin America and the Caribbean are predicted to incur mortality improvement under the CH_4 package that is roughly 4.4 times larger than the mortality improvement between 2005 and 2030.
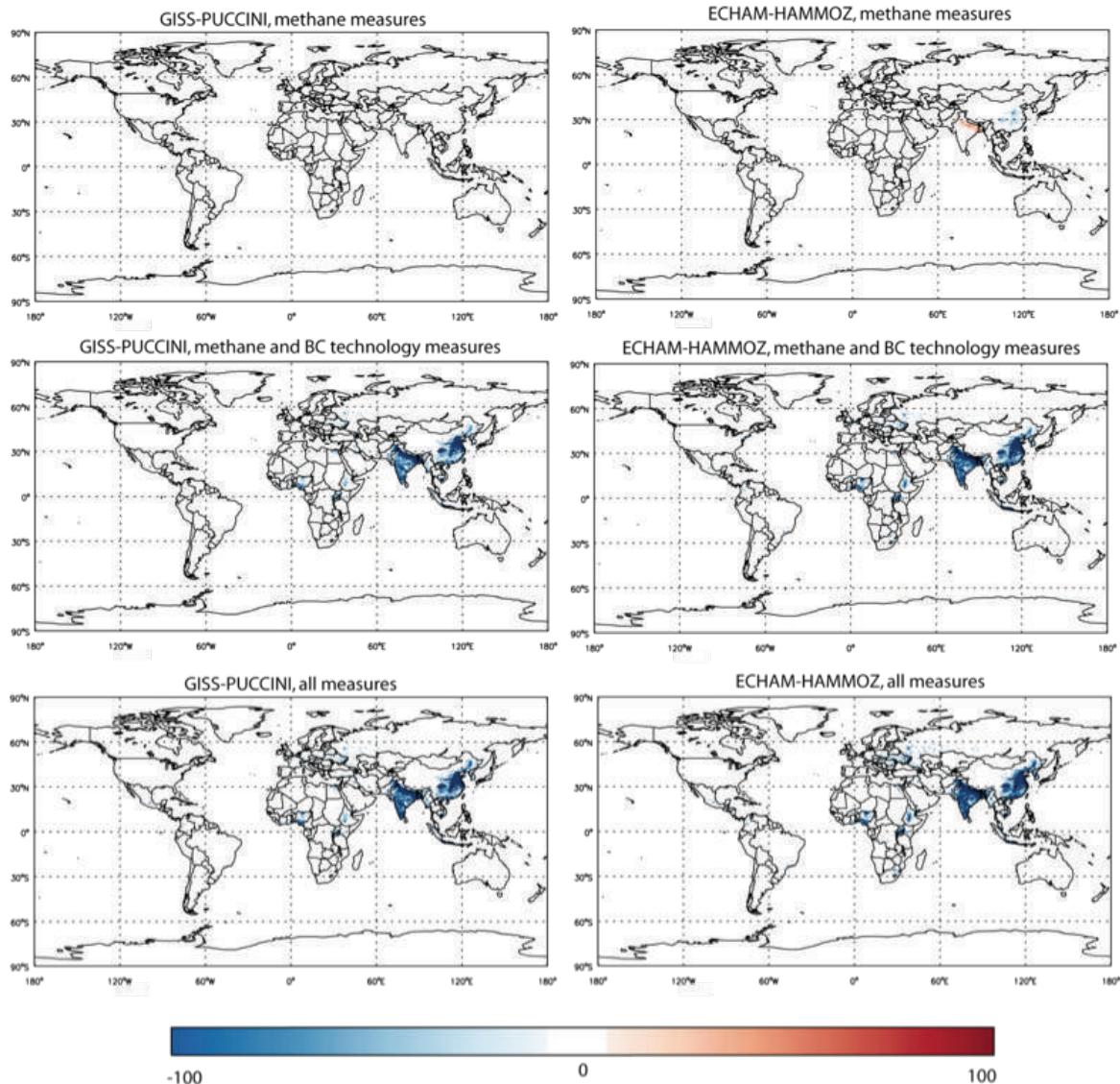
Figure 5.14. Change in annual total PM$_{2.5}$ cardiopulmonary and lung cancer and O$_3$ respiratory mortality (lives per 1 000 km²) in 2030 relative to the 2030 reference case, using concentrations simulated by both models. The scenarios are CH$_4$ measures; CH$_4$ + BC Group 1 measures (but without those on pellet stoves and coal briquettes), and all measures refers to CH$_4$+BC measures (BC Groups 1 and 2, but without the measures on pellet stoves and coal briquettes).

The results when using the ECHAM model are in broad agreement with the results derived from GISS, but there are two exceptions. First, South, West and Central Asia incur an increase in mortalities valued at US$58 billion employing ECHAM (compared to a reduction in mortalities valued at US$28 billion for GISS). Second, with ECHAM the magnitude of the reduction in mortalities in Latin America and the Caribbean under the CH$_4$ package is 50 per cent of the predicted reduction for the 2005–2030 reference case comparison. In contrast, GISS suggests that this package yields mortality improvements in Latin America and the Caribbean that are over four times greater than in the reference case comparison.

With the application of the CH$_4$ plus BC Group 1 measures, all regions experience a reduction in mortalities in both GISS and ECHAM. Perhaps most notable under this scenario is the magnitude of the difference in mortality impacts in Africa, East Asia, and Latin America and the Caribbean relative to

197
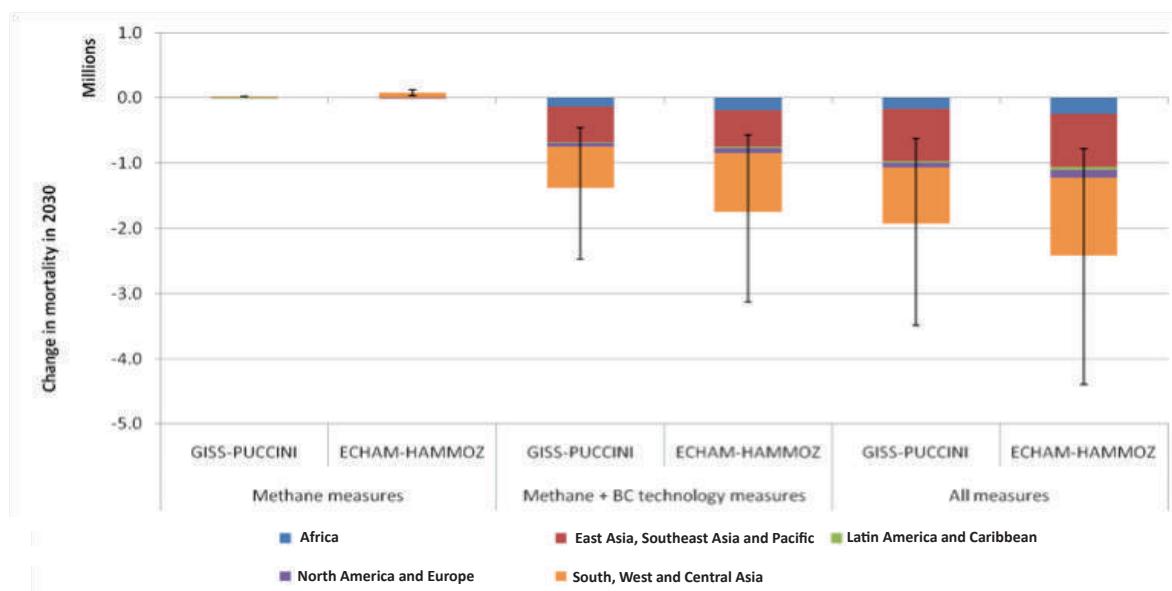
Figure 5.15. Regional change in annual PM$_{2.5}$ cardiopulmonary and lung cancer mortality in 2030 relative to the 2030 reference scenario, using simulated concentrations from the two models. Confidence intervals (95 per cent) are based on uncertainty in the concentration-response relationship only. BC technology measures refers to BC Group 1 measures. All measures refers to CH$_4$+BC Groups 1 and 2 (but without those on pellet stoves and coal briquettes).
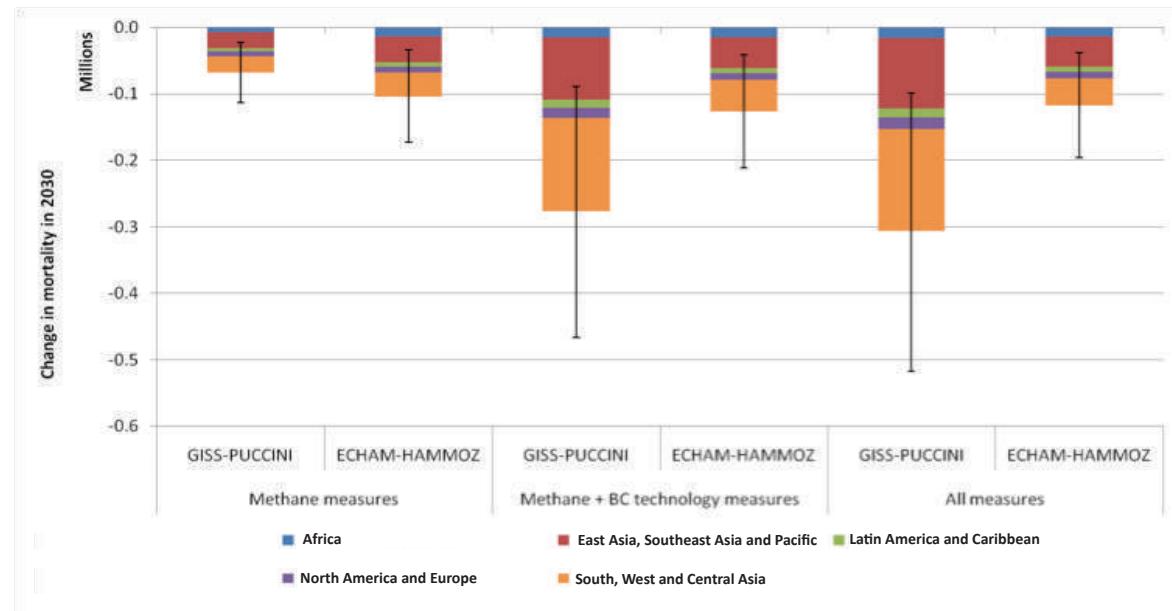
Figure 5.16. Regional change in annual O$_3$ respiratory mortality in 2030 relative to the 2030 reference scenario, using simulated concentrations from the two models. Confidence intervals (95 per cent) are based on uncertainty in the concentration-response relationship only. BC technology measures refers to BC Group 1 measures. All measures refers to CH$_4$+BC Groups 1 and 2 (but without those on pellet stoves and coal briquettes).

Integrated Assessment of Black Carbon and Tropospheric Ozone
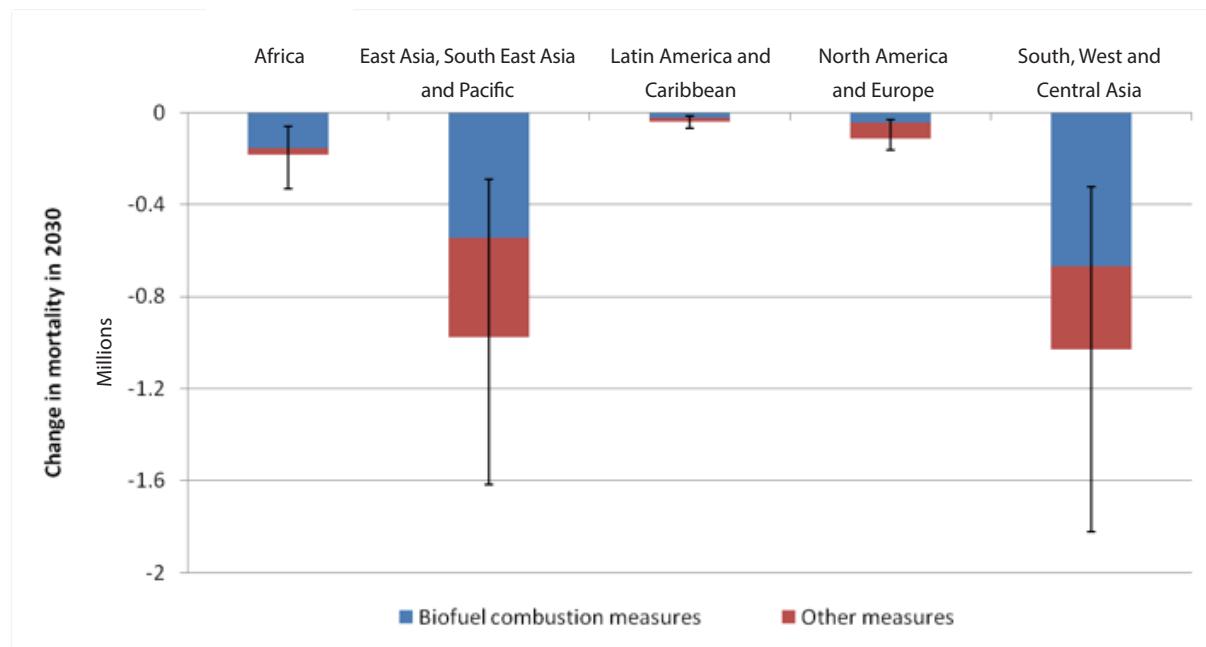
Figure 5.17. Regional change in annual $PM_{2.5}$ cardiopulmonary and lung cancer and O_3 respiratory mortality (in millions of lives) in 2030 due to biofuel combustion measures and all other measures. Confidence intervals (95 per cent) are based on uncertainty in the concentration-response factor only. Estimated changes in mortality do not account for indoor exposure.

the reference case comparison. Specifically, using GISS, in Africa, the reduction in mortality impacts is just over three times larger than the mortality reductions between 2005 and 2030. East Asia, South East Asia and the Pacific experiences mortality reductions with a value that is more than six times greater than the reduction in mortalities predicted to occur in the 2005–2030 comparison. In Latin America and the Caribbean, the mortality improvements are approximately 35 times greater than in the reference comparison.

When using ECHAM, although the value of the mortality impacts of the CH_4 plus BC Group 1 measures are quite similar to that derived from GISS, the magnitude of these impacts relative to the 2005–2030 comparison is quite different than for GISS. Specifically, Africa shows the largest increase in mortality reductions relative to the reference comparison; the magnitude of mortality reductions is 13 times greater than in the reference case. In contrast, when using GISS, the greatest increase occurs in Latin America and the Caribbean.

The policy scenario with all three packages of measures also yields mortality reductions in all

regions. Much like the CH_4 plus BC Group 1 measures package, the agreement between GISS and ECHAM in terms of the value of these mortality reductions is quite good. The value of these reductions is uniformly larger than the reductions projected to occur under the other two packages. In addition to increasing values of mortality reductions, the ratios of the mortality changes under the three combined packages relative to the 2005–2030 comparison are also larger than for the CH_4 plus BC Group 1 measures. In Africa, East Asia, Latin America and the Caribbean, when using GISS, the differences in the value of mortality reductions (relative to the 2005–2030 comparison) are substantial. In Africa, the reduction is more than four times larger than the mortality reductions between 2005 and 2030. In East Asia, the mortality improvements are approximately 10 times greater than the reference comparison. Latin America and the Caribbean show the greatest increase in the value of mortality reductions; under this policy scenario, mortality reductions are projected to be nearly 50 times greater than the change determined to occur in the 2005–2030 comparison.

Similar to the case of the CH_4 plus BC Group 1 measures policy scenario, when using

Table 5.4. Valuation of BC, CO, NO_X, and CH_4 emission changes: policy measures compared to 2030 reference.

Social cost of carbon (SCC)	Pollutant / global warming potential	Policy	BC	CH_4	CO	NO_X	OC	SO_2	CO_2	Total
US$265/tC	GWP_{100}	CH_4	0	331	0	0	0	0	0	331
		CH_4+BC Group 1	112	347	71	-264	40	2	1	309
		CH_4+BC Groups 1+2	205	357	110	-318	52	3	1	410
US$265/tC	GWP_{20}	CH_4	0	1 050	0	0	0	0	0	1 050
		CH_4+BC Group 1	401	1 110	271	-984	142	8	1	949
		CH_4+BC Groups 1+2	731	1 140	419	-1 190	186	10	1	1 297
US$21/tC	GWP_{100}	CH_4	0	26.2	0	0	0	0	0	26.2
		CH_4+BC Group 1	8.9	27.5	5.7	-20.9	3.1	0.2	0.1	24.6
		CH_4+BC Groups 1+2	16.2	28.3	8.7	-25.2	4.1	0.2	0.1	32.5
US$21/tC	GWP_{20}	CH_4	0	83.4	0	0	0	0	0	83.4
		CH_4+BC Group 1	31.8	87.6	21.5	-78.8	11.3	0.6	0.1	74.9
		CH_4+BC Groups 1+2	57.9	90.1	33.2	-94.1	14.8	0.8	0.1	103

All values expressed in (2006 US$, billions), and represent the annual monetary benefit arising in 2030.

Positive values reflect benefits of avoided climate impacts.

Estimates rely on GWP values reported in 4.1.1.

ECHAM to model the impacts of all three combined packages, Africa shows the greatest impact relative to the 2005–2030 comparison; the reduction in mortality damage in Africa is projected to be nearly 18 times greater than in the 2005–2030 reference case.

Valuation of climate benefits

As well as estimating the value of the impacts of the emission control measures on human health, the valuation of global climate impacts associated with emission changes for each of the policy scenarios have also been estimated, and these are shown in Table 5.4. (The reader is encouraged to return to 4.1.4 for a discussion both of the motivation for and analytical issues associated with this exercise). Table 5.4 reports the benefits due to emissions abatement due to each of the policy scenarios. Hence, positive values reported in Table 5.4 indicate benefits to society due to emission reductions, while negative values indicate additional (harmful) climate impacts due to emission increases.

For each pollutant, to allow for uncertainties, two values for the social cost of carbon (SCC) are used, US$265/tC and US$21/tC (Tol, 2008) and two GWP parameters are employed. GWP_{100} refers to the 100-year time scale and GWP_{20} refers to the 20-year time scale. There are no reductions of BC, CO, OC, SO_2, CO_2, or NO_x for the policy scenario dealing with CH_4 measures. Emission reductions of CH_4 generate benefits that range between US$330 billion and US$1.1 trillion in 2030. (Note that the range is associated with the different assumption regarding the timescale of GWP). For the CH_4 plus BC Group 1 measures scenario, total emission reductions generate benefits of between US$309 billion and US$949 billion. Note that reductions in NO_x emissions lead to increased climate damage (negative benefits) that nearly cancel the benefits associated with reductions in CH_4. For the policy scenario involving all three packages, the benefits range between US$410 billion and US$1.3 trillion. Employing the lower US$21/tC value for the SCC decreases (in absolute value) the value of the modelled emission changes by approximately one order of magnitude across emitted pollutants.

5.3.4 Benefits to agriculture and ecosystems

This section describes the impact of the various measures on crops, using the methodology described in Chapter 4. Results are

shown from two composition-climate models (ECHAM-HAMMOZ and GISS-PUCCINI). Where central values are shown, they are the mean of the models' outputs; the error bars show the minimum and maximum values from the model ensemble, resulting from the 95 per cent confidence interval on the crop O_3 damage function.

The combined impact of the complete control package (in the absence of the GHG controls in the GHG scenario) leads to a worldwide benefit in crop yields compared to the 2030 base case: from 1.3 per cent (+1.5 per cent, -1.2 per cent) yield increase for rice to 3.2 per cent (+1.6 per cent, - 1.1 per cent) increase for soybeans. The largest benefits emerge in the two Asian regions studies as shown in Figure 5.18.

The two models, however, assign a different weight to each of the individual measure packages: whereas ECHAM realizes virtually the complete benefit through CH_4 measures, GISS has about 60 per cent of the benefit achieved through BC Group 1 measures (labeled LGWP) and 30 per cent through CH_4 measures. The additional implementation of BC Group 2 measures (labeled LWST) has no significant effect on O_3 levels and crop yields (Figure 5.19).

The corresponding annual production gains are highest for corn, 21 million tonnes, and most beneficial in Asia with an aggregated production gain for the four crops of 32 million tonnes. Total global production gains of all crops ranges between 30 and 140 million tonnes (model mean: 52 million tonnes). The annual economic gains for all four crops in all regions ranges between US$4billion and US$33 billion, of which US$2–28 billion in Asia.

There is a clear additional benefit on O_3 levels and crop yields in all regions from CO_2 emission controls under the GHG scenario, thanks to associated NO_x emission reductions. Also under this scenario, largest benefits are expected in Asia as shown in Figure 5.20.

5.3.5 Relative importance and scientific confidence in the measures

Methane measures have a large impact on global and regional warming, which is achieved by reducing CH_4 and O_3 emissions. The climate mitigation impacts of the CH_4 measures are also the least uncertain because there is a high degree of confidence in the warming effects of this GHG. The reduced CH_4 and hence O_3 concentrations also lead to significant benefits for crop yields.

The BC measures identified here reduce concentrations of BC, OC and O_3, the latter largely through reductions in emissions of CO. The warming effect of BC and O_3 and the compensating cooling effect of OC, introduces large uncertainty into the net effect of some BC measures on global warming (reflected in Figure 5.1). This uncertainty is particularly large for the biomass cookstoves and open burning of biomass measures. Hence, with respect to global warming, there is much higher confidence in measures that mitigate diesel emissions than those that reduce biomass burning because the proportion of co-emitted cooling OC particles is much lower.

On the other hand, the BC measures have large impacts on local and regional health through reducing concentrations of inhalable PM, on crop yields through reduced O_3, and on regional climate such as the impacts on tropical rainfall, monsoons and snow and ice melt. These regional impacts are largely independent of their impact on global warming. In fact, biomass cookstoves and open biomass burning can have much larger effects than fossil fuels regionally. This is because BC directly increases atmospheric heating by intercepting sunlight, which, according to numerous published studies, affects the monsoon and tropical rainfall and this is largely separate from the effect of co-emitted OC. The same conclusion applies with respect to the impact of BC measures on snow and ice. Black carbon, because it is dark, significantly increases absorption of sunlight by snow and ice when it is deposited on these bright surfaces. Organic carbon

Change in relative yield loss for all measures compared to 2030 base

■ Soy   ■ Corn   ■ Rice   ■ Wheat

	World	Africa	East Asia, Southeast Asia, and Pacific	Latin America and Caribbean	North America and Europe	South, West, and Central Asia
■ Soy	-3.2%	-2.3%	-4.4%	-3.1%	-2.3%	-7.0%
■ Corn	-2.7%	-2.2%	-4.4%	-1.1%	-1.8%	-4.6%
■ Rice	-1.3%	-0.9%	-1.0%	-0.3%	-0.7%	-1.9%
■ Wheat	-2.3%	-2.4%	-2.4%	-1.1%	-1.5%	-4.0%
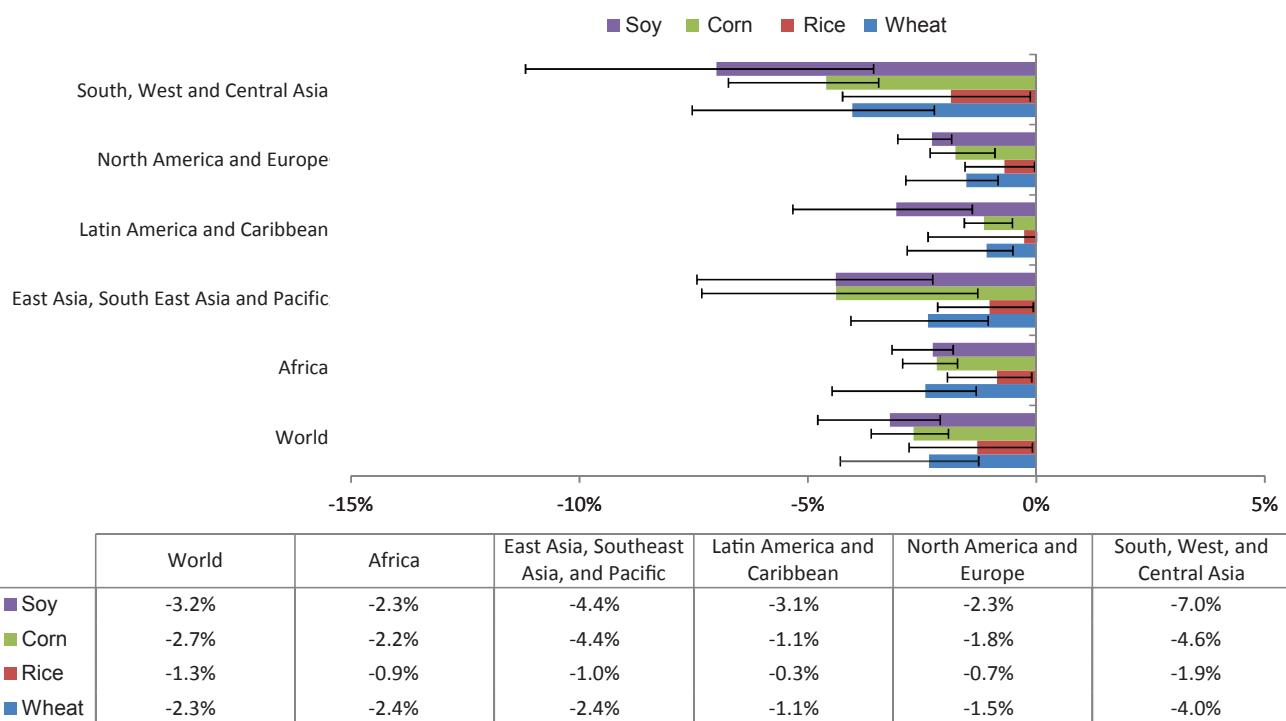
Figure 5.18. Impact of CH_4 and BC measures on regional crop yield losses (negative values correspond to a gain in crop yield compared to the reference run for 2030).

Reductions in crop yield by measure

■ CH_4 ■ LGWP   ■ LWST
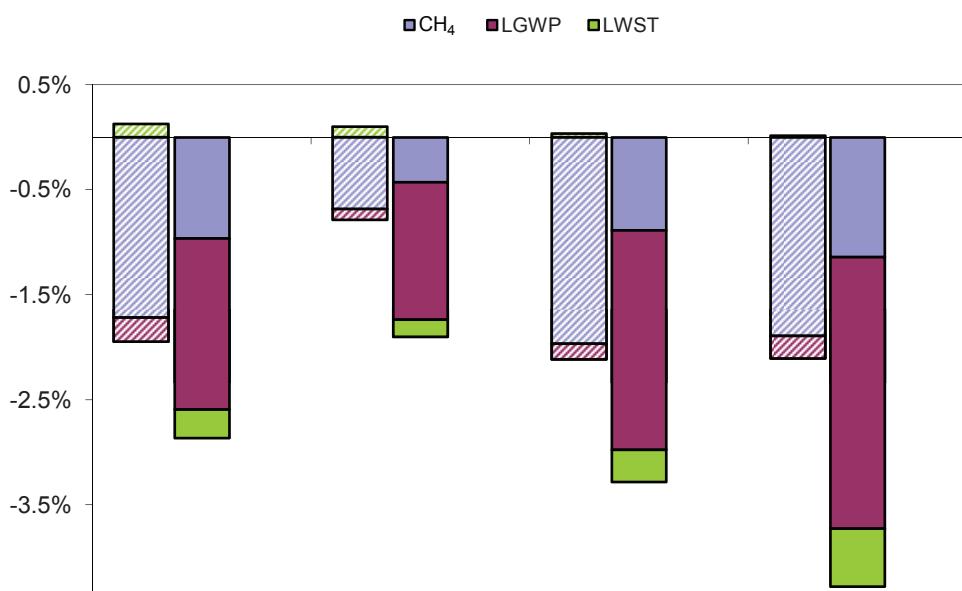
Figure 5.19. Contribution of individual measure packages to the annual reduction in global crop-yield losses from ECHAM-HAMMOZ (hatched bars) and GISS-PUCCINI (solid bars). Note LGWP = BC Group 1 measures; LWST = BC group 2 measures.

Change in relative yield loss for 450 ppm scenario compared to 2030 base

	World	Africa	East Asia, Southeast Asia, and Pacific	Latin America and Caribbean	North America and Europe	South, West, and Central Asia
■ Soy	-2.8%	-0.3%	-5.5%	-0.4%	-2.8%	-3.0%
■ Corn	-2.6%	-0.5%	-5.6%	-0.4%	-1.5%	-2.0%
■ Rice	-1.0%	-0.6%	-1.1%	-0.1%	-0.6%	-0.9%
■ Wheat	-1.4%	-1.1%	-2.1%	-0.3%	-1.1%	-1.5%
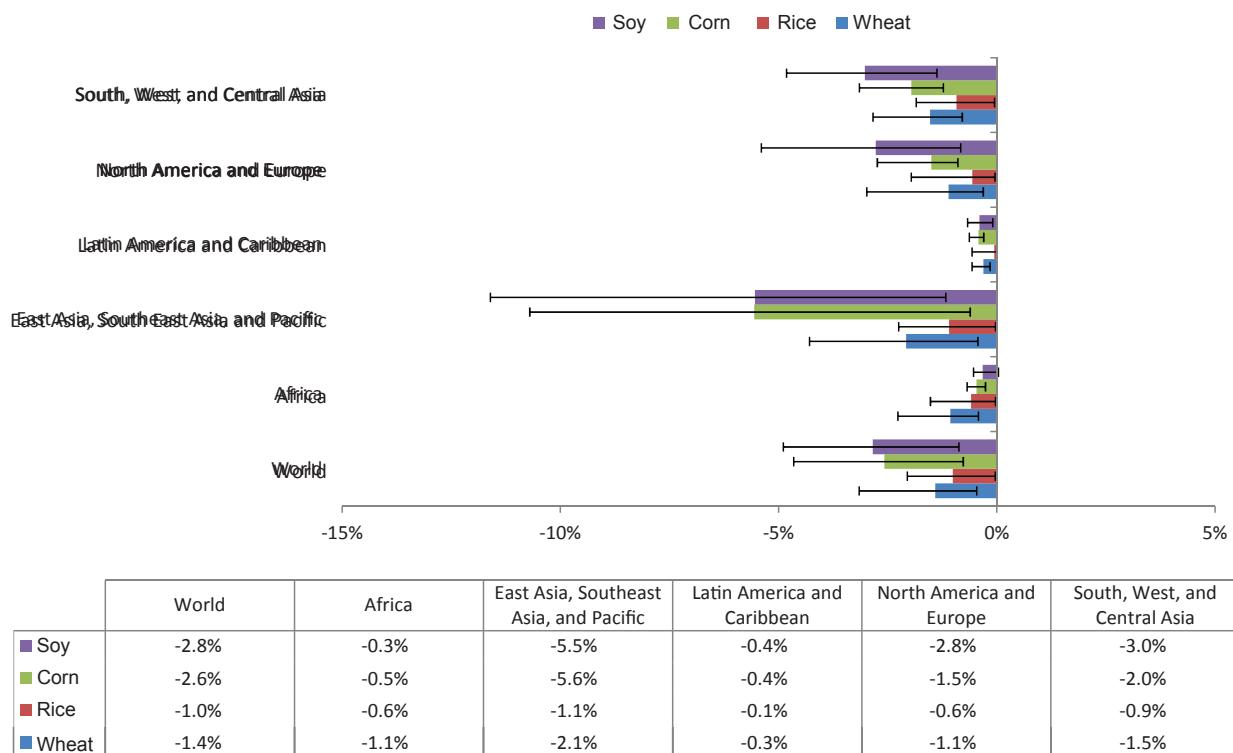
Figure 5.20. Impact of GHG reduction measures under the GHG scenario on crop yield losses.

that is deposited along with BC, has very little effect on sunlight reflected by snow and ice since these surfaces are already very white. Hence knowledge of these regional impacts is in some cases more robust than the global impacts, and with respect to regional impacts, all the BC measures are likely to be important. Confidence is high that a large proportion of the health and crop benefits would occur in Asia.

5.4 Policy approaches to promote the mitigation measures

This Assessment shows that measures to reduce short-lived climate forcers, implemented in combination with CO_2 control measures, would increase the chances of staying below the 2°C goal agreed under the United Nations Framework Convention on Climate Change (UNFCCC). The measures would also slow the rate of near-term temperature rise and lead to significant improvements in health, decreased disruption of regional precipitation patterns and water supply, and improved

food security. The impacts of the measures on temperature change would be felt over larger geographical areas, while the air quality and regional precipitation impacts would be more localized near the regions where emissions changes take place.

Therefore, areas that control their emissions will receive the greatest human health and agricultural benefits, but also many of the climate benefits will be felt close to the region taking action. Moreover, the benefits would be realized in the near term, thereby providing additional incentives to overcome financial and institutional hurdles to the adoption of these measures.

Countries in all regions of the world have successfully implemented the identified measures to differing degrees for multiple environment and development objectives. These experiences provide a considerable body of knowledge and potential models for others that wish to take action.

In most countries, responding to public concern, mechanisms, albeit at different levels of maturity, have already been put in place to address air pollution. Mechanisms to tackle GHG emissions are less well deployed, and systems to maximize the co-benefits from reducing air pollution and address climate change are virtually non-existent. Coordination across institutions to address climate, air pollution, energy and development policy is particularly important to maximize the achievement of synergistic goals across multiple sectors.

Many BC control measures require implementation by multiple actors on diffuse emission sources including diesel vehicles, field burning, cooking stoves and residential heating. Although air quality and emission standards exist for particulate matter in some regions, they may or may not reduce BC, and implementation remains a challenge. Relevance, benefits and costs of different measures vary from region to region. Many of the measures entail cost savings over time but require substantial upfront investments. Accounting for air quality, climate and development co-benefits will be key to scaling up the implementation of identified measures.

Methane is one of the six GHGs governed by the Kyoto Protocol, but there are no explicit targets for it. Health and safety have been traditional drivers of national CH_4 controls, not climate. Many CH_4 measures are cost-effective and its recovery is, in many cases, economically profitable. There have been many Clean Development Mechanism (CDM) project proposals in key CH_4 emitting sectors, though few such projects have been approved in recent years.

Case studies from both developed and developing countries show that technical solutions are available to deliver all of the measures (described below). Given appropriate policy mechanisms, the measures can be implemented. However, to achieve the benefits at the scale described much wider implementation is required.

For those regions or countries where policies are not already in place to reduce emissions of these SLCFs, there are several approaches that could be considered, including regulatory, economic, planning, informational, and voluntary ones.

Regulatory approaches include rules or standards that define allowable levels of emissions, types of pollution control technologies, quality of fuel or resource inputs, and amount of emission activity. A typical example is an emissions standard for light-duty diesel-powered vehicles. In contrast, economic, or market-driven approaches use financial incentives or disincentives in the form of taxes, fees, subsidies and markets to encourage emissions reductions. By giving sources more discretion over abatement options, this approach may bring down the costs of abatement. A typical example is an emissions trading scheme.

Planning approaches can be effective in reducing pollution. These often focus on infrastructure investments and land-use changes that can limit the amount of pollution activity, especially in the transportation sector. A typical example is transport-oriented urban planning that reduces travel activity and distances travelled. In some instances existing institutions might need their remit modifying, in other, new institutions might need to be created.

Informational approaches increase awareness of unsustainable consumption patterns and alternative production techniques. Disseminating that information to the public in easily accessible formats can change behaviour or generate pressure on pollution sources to reduce emissions. Finally, voluntary approaches typically involve setting agreements between private companies, industry associations and government agencies to reduce emissions to mutually agreed levels.

Each of these approaches are reflected in the case studies of successful BC and O_3 precursor (i.e. CH_4) reduction measures profiled in the next section of this chapter. It is important to recognize the significant governance and finance challenges to the successful implementation of pollution reduction policies that are faced in many resource-constrained countries. For example, coordination across agencies is particularly important for successful imple-

204

mentation of the mitigation measures for SL-CFs, as frequently different agencies address climate change and air pollution agendas. Additionally, successful implementation and enforcement often require adequate funding and this can be a challenge for some agencies.

Many of the identified measures require high initial investments and have long-term pay-back periods. These initial costs can act as a significant constraint on policy action. Equally importantly, in many instances there is not a full appreciation of the economic value of the myriad benefits that accrue from pollution control measures. Policymakers often lack the tools to measure and monetize benefits from policies. Dependable data and technical knowledge are especially critical for identifying, prioritizing and justifying pollution control investments, yet they are typically less available in developing countries.

Related challenges are the subsidies or price supports provided to fossil fuels. For instance, the price of diesel is frequently suppressed to make it more affordable to non-road users. This can result in the overuse of diesel in off-road sources but may also establish lower diesel prices generally, incentivising the use of on-road diesel vehicles as well, in effect, subsidizing particulate matter pollution.

The very fact that reduction in emissions of SLCFs provides multiple health, climate and development co-benefits may hold a key to overcoming implementation and financial challenges. As suggested in the next section, from the dissemination of successful experience of good practice could significantly help make this possibility a reality.

The following section presents a selection of case studies from different regions on the implementation of the 16 identified BC and CH_4 mitigation measures. In those cases where this could be identified the important enabling conditions for policy implementation is described and prospects for wider implementation are discussed. As financing mechanisms for BC and tropospheric O_3 mitigation is regarded as one key route to enhanced mitigation, particularly in developing countries, exist-

ing and potential future sources of financing are addressed in a separate section below.

5.5 Examples of successful mitigation of black carbon and tropospheric ozone precursors

This section reviews initiatives around the world that have successfully reduced emissions in major BC and CH_4 source sectors. The initiatives profiled here implement the 16 key measures identified at the beginning of this chapter, including measures that reduce CH_4, and measures which address the products of incomplete combustion including BC. The measures cover a range of sectors: coal, oil and gas production, transportation and other diesel machinery, municipal waste treatment, agriculture and residential heating and cookstoves.

Many, if not most, of the BC measures were adopted to satisfy air quality concerns, urban congestion and energy efficiency objectives. Recognition of and accounting for the climate benefits was, in most cases, not part of the original policy reasoning. When the climate co-benefits are considered, in addition to health and development benefits, cost effectiveness is even greater. Reducing BC emissions that reach the Arctic and other sensitive ecosystems will have yet greater benefit. The identified measures to reduce BC emissions also reduce some precursors of tropospheric O_3, notably CO and to a lesser extent NO_x, thus conferring further health and climate benefits.

In contrast, climate mitigation was a key driver for many of the CH_4 measures profiled here, along with health and safety (e.g. landfills) and economic drivers. Methane emission reductions through recovery should be profitable, generating energy or carbon credits.

The objective of this section is to illustrate the practical feasibility of BC and CH_4 emissions reductions in key sectors that may be replicated or scaled up in response to national circumstances and priorities. Where data were readily available a suite of key drivers and outcomes is described, such as the motivation for the initiative; emissions data; and air quality and health impact analyses.

205

Finally, several observations with respect to BC and CH_4 control measures merit note. First, the technology now exists to reduce emissions significantly (see Section 5.1) although relevance, costs and benefits vary across regions. Secondly, many BC mitigation measures require implementation by multiple individual actors on diffuse emission sources; for example, diesel vehicles, field burning, cookstoves and residential heating. Although air-quality and emissions standards exist for PM in some parts of the world, some are more effective at reducing BC than others, and, overall, implementation remains a challenge. Incentive programmes and a full accounting of the air quality, climate and development co-benefits will be key to scaling up mitigation measures, especially, but not exclusively, in poorer countries.

Methane mitigation has largely been voluntary; with limited exceptions such as coal mine safety, there are few standards *per se*. Most CH_4 mitigation projects explicitly account for the climate benefit, whereas BC mitigation projects typically do not. Methane mitigation measures, with the exception of small-scale rice cultivation and livestock husbandry, are implemented primarily by large private and public sector actors, such as oil and gas extraction and transmission companies; large-scale agribusiness; coal mine operators and municipal landfills and wastewater treatment facilities, thus regulatory approaches, as well as incentive approaches, may be appropriate.[1]

Methane is one of the six GHGs governed by the Kyoto Protocol; there have been some CDM projects in key CH_4 emitting sectors in many countries. Finally, while both the suite of BC and CH_4 measures are cost effective, CH_4 mitigation recovery in many cases is economically profitable. Natural gas used in energy and heating is composed almost entirely of CH_4, so recovery should be profitable. Moreover, mitigation projects may qualify for carbon credits as CH_4 is part of the Kyoto basket of GHG gases. A finance mechanism, such as the proposed CH_4 fund that would guarantee a minimum return or floor price (see Section 5.5.4), has the potential to significantly increase the number of CDM CH_4 mitigation initiatives.

5.5.1 Methane mitigation

Major measures for reducing CH_4 emissions include:

1. Recovery of coal mine methane (CMM);

2. Recovery and flaring (instead of venting) of associated gas in the production of oil and national gas;

3. Reducing gas leakage at compressor stations in long-distance gas transmission pipelines;

4. Separation and treatment of biodegradable municipal landfill waste;

5. Upgrading primary wastewater treatment to secondary/tertiary treatment with gas recovery and overflow control;

6. Livestock manure management;

7. Intermittent aeration of continuously flooded rice paddies.

Recovery of coal mine methane (CMM)
CMM refers to the CH_4 released from underground rock formations during mining activities. In active mines it can create an explosive hazard and must be vented; in abandoned mines CH_4 may escape through natural fissures.

Countries from India to Mexico and the United States of America are exploring approaches to reduce minimize CMM emissions.[2] China is a leader in CMM projects with 39 registered with the CDM including the world's largest at the Sihe mine in Jincheng City, Shanxi Province.[3] The Sihe mine project

1 Congressional Research Service. Methane Capture: Options for Greenhouse Gas Emission Reduction. http://fpc.state.gov/documents/organization/130799.pdf.

2 United States Environmental Protection Agency, Coalbed Methane Extra, Office of Air and Radiation, EPA-430-N-00-004, Fall 2010. Available at: www.epa.gov/cmop/docs/fall_2010.pdf. See also United States Environmental Protection Agency Coalbed Methane Outreach Program, http://www.epa.gov/cmop/.

3 http://cdm.unfccc.int/Projects/DB/DNV-CUK1214826895.32/view.

is projected to avoid 3 016 714 tonnes CO_2e of CH_4 emissions per year.[4] A description of the Sihe mine project in China is given in Appendix A.5.2. China accounts for 34 per cent of global CMM emissions; followed by the United States of America with 13 per cent, and Russia and Ukraine with 7 per cent each.

In many countries CMM recovery is lagging in large part because the policy environment does not incentivize CH_4 recovery, and in many cases acts as a disincentive. For example, in some countries occupational safety rules require venting for miner safety, but do not require CH_4 recovery.

Clarity with respect to the property rights to CMM is a key issue. In most countries a coal lease/permit holder does not automatically acquire the rights to the associated CMM; separate licensing for mine gas recovery and utilization is required. This is the case in the United States of America where a mining company wanting to utilize extracted CMM must get a second federal permit in addition to the coal permit and pay royalties on the extracted gas. In contrast, Germany adopted federal legislation transferring CMM ownership rights to the coal mining company for the duration of the coal lease, after which a separate gas lease must be renewed. By establishing a favourable policy environment Germany has become a global leader in utilizing CMM as a per cent of its total mine-related CH_4 emissions (US EPA, 2009).

Recovery and flaring of methane from oil and natural gas production

When drilling for crude oil, natural gas often comes to the surface along with the oil. This associated gas is often vented or flared to maintain safe pressure in the well. Venting is simply the release of the CH_4 directly into the atmosphere, while flaring is the burning of the vented gas. Various barriers such as lack of adequate infrastructure, markets, and regulations have slowed or stopped the development of CH_4 capture technologies, which could trans-form the gas from a waste to a commodity. As a second tier option, CH_4 may be flared rather than vented or recovered. The 100-year GWP of CH_4 is 21 times that of CO_2; flaring transforms it into CO_2 plus water thus eliminating 95 per cent of its warming potential.

In the past venting and flaring were necessary safety and waste management practices. Today however, technologies exist for the capture of CH_4 during oil drilling. However, market forces have yet to turn the tide in the industry towards a *de facto* capture and reuse regime. Data indicate that CH_4 emissions have been reduced by current efforts, but not in amounts that would signify a real shift in industry practice.[5] Without regulatory frameworks to push innovations in technology and force best practice in developed and developing countries, the pace of CH_4 release abatement from crude oil drilling operations may not correspond to the urgency of the effect of the emissions.

The Global Gas Flaring Reduction Partnership (GGFR) launched at the World Summit on Sustainable Development in 2002 aims to support national efforts to use currently flared gas by promoting effective regulatory frameworks and tackling the constraints on gas utilization, such as insufficient infrastructure and poor access to local and international energy markets, particularly in developing countries. The partnership promotes voluntary standards as there is currently no international regulation of gas flaring. The GGFR funded a multi-year global satellite-monitoring project for flare activity conducted by the United States National Oceanic and Atmospheric Administration (NOAA, 2010) but there is currently no global inventory of CH_4 venting.[6]

Short summaries of CDM and GGFR projects in Angola, India, Indonesia, Nigeria, Russia,and the United Arab Emirates are provided in Appendix A.5.2.

---

[4] Additional references:
   International Energy Agency, Coal Mine Methane in China: A Budding Asset with the Potential to Bloom. IEA Information Paper, February 2009, IEA.

[5] See Table A.5.2, Appendix A.5.2.

[6] See Table A.5.2, Appendix A.5.2.

Reducing gas leakage in long-distance transmission pipelines

Gas leakage from long-distance gas transmission pipelines compressor stations is a significant source of CH_4 emissions for which mitigation measures are readily available. A handful of nations with significant CH_4 leakage have begun to successfully implement regulations or other initiatives to reduce leakage from this sector. According to the most recent information available from the United States Environmental Protection Agency (US EPA), the world's largest emitters of CH_4 from the oil and natural gas industry are Russia, the United States of America, Ukraine, Mexico, and Iran (US EPA, 2010). International initiatives such as the Methane to Markets Partnership (M2M) focus on identifying sources of emissions and promoting cost-effective near-term CH_4 recovery and use as a clean energy source.[7] Most of the major national programmes outside the United States of America, for example in Russia, Ukraine and Mexico, are driven largely by the respective nations' largest oil and gas companies. A brief discussion of four countries, Mexico, Russia, USA and Ukraine, activities in reducing gas leakage is given in Appendix A.5.2.

Municipal landfill waste separation and treatment

Landfills are the third largest anthropogenic emissions source of CH_4 globally, accounting for about 12 per cent of emissions.[8] Factors that determine the level of landfill gas emissions include the amount of organic material deposited, the type of landfill practice, the extent of anaerobic decomposition and the extent of landfill CH_4 recovery (energy production) or combustion (flaring). Options for energy use include direct electricity production with turbines and other technologies; processing landfill gas for use as an alternative fuel for local industry and processing into pipeline-quality gas or alternative vehicle fuel. National solid-waste management poli-

cies that provide a supportive enabling environment for landfill gas energy projects by promoting alternative energy and requiring or incentivizing GHG reductions are critical. The Durban, South Africa, and Monterrey, Mexico, projects profiled here were selected from dozens of CDM Landfill Gas (LFG) energy projects around the world because they are two of the earliest projects, and have already served as a model for others in their countries.[9] Avoided CH_4 emissions from the Durban project are 68 833 tonnes CO_2e per year. The Monterrey project currently fuels a 12.7 megawatt plant and is projected to increase to fuel a 25 megawatt plant to be completed in 2016. Descriptions are given in Appendix A.5.2.

Wastewater treatment with gas recovery

Municipalities around the world are applying biogas treatment technologies to wastewater, such as anaerobic-aerobic activated sludge processes, to mitigate CH_4 emissions and generate energy. CDM wastewater CH_4 reduction projects are in train in India, Indonesia, Morocco and elsewhere around the world. For information on the India and Morocco wastewater CH_4 reduction CDM projects.[9] In China numerous biogas applications are found in the urban municipal and commercial wastewater treatment sector, helping to reduce pollution from wastewater to meet growing energy needs.[10]

Another example is Bolivia's Urban Wastewater Methane Gas Capture Project to capture CH_4 emissions at a private waterworks company (SAGUAPAC) emitted by the primary anaerobic treatment lagoons at all of the company's wastewater treatment facilities. The CH_4 gas will be captured from the lagoons using high-density polyethylene geo-membrane sheets and perforated PVC

---

[7] Methane to Markets, Methane to Markets Homepage, http://www.methanetomarkets.org/index.aspx (last visited July 19, 2010).

[8] Methane to Markets. Landfill Methane Recovery and Use Opportunities. March 28. Available at: www.methanetomarkets.org. Last visited, August 23, 2010.

[9] Project documentation available at: http://cdm.unfccc.int/Projects/projsearch.html, and brief summaries of a set of regionally representative LFG projects can be found in the Appendix.

[10] For more information on wastewater treatment methane capture projects in China, please see: http://www.worldwatch.org/node/4889, and http://www.wilsoncenter.org/topics/docs/wastewater_jan09.pdf.

tubes, and then transported to a flare system through an intercommunicating pipe system (World Bank Group 2010). In the United States of America, the Blue Lake Wastewater Treatment Plant, the third largest plant in the state of Minnesota, hosts a project to recover CH_4 from the plant's wastewater solids and use it to replace natural gas in the fuel part of the solids management process that has been under construction since 2009 and is expected to be completed by 2012. Once completed, the new facilities should lessen the plant's reliance on fossil fuels and thereby reduce its annual energy bill by approximately US$800 000–900 000. The basic idea is that the plant will add anaerobic digestion to the solid waste management process, which will break down organic matter into gas before the solids go through further dewatering on their way to the heat dryer; the captured CH_4 gas being used to directly power the heat dryer (Metropolitan Council, 2010).

Livestock manure management
Ruminant livestock industries alone are estimated to produce about 80 million tonnes of CH_4 a year and to account for approximately 22 per cent of global CH_4 emissions associated with human activity (US EPA, 2010). Moreover, all livestock facilities produce significant CH_4 emissions with poor waste management. Many CDM projects implement improved animal waste management systems (AWMS) to reduce the emissions associated with animal effluent.[11]

Projects fall broadly into two categories:

1. Livestock waste is used as a feedstock for energy and fertilize production; and,

2. Biogas projects in which CH_4 is captured and combusted for energy.

Livestock CH_4 emissions are typically controlled by the use of anaerobic digesters. Where the captured CH_4 is burned on site to produce energy, a double benefit can be achieved – the reduction of CH_4 emissions and a reduction in use of conventional fuel. Even simply covering lagoons of manure and slurry can help recover CH_4, which can then

be flared.[11] CDM project examples of AWMS in a large Brazilian pig farm, replacing open-air lagoons with anaerobic digesters, and a small Indian poultry-waste based power generation are noted in Appendix A.5.2.

Aeration of continuously flooded rice paddies

Rice is grown on more than 140 million hectares worldwide. Ninety per cent of the world's rice is produced in Asia, and 90 per cent of rice land is – at least temporarily – flooded.

Methane emissions from rice fields are determined mainly by the water regime and organic inputs, but are also influenced by soil type, weather, tillage and residue management, fertilizer use, and the rice cultivar. Flooding the soil is a prerequisite for sustained emissions of CH_4. Recent assessments of CH_4 emissions from irrigated rice cultivation estimate global emissions for the year 2000 at 625 million tonnes of CO_2e. Mid-season drainage, a fairly common irrigation practice in major rice growing regions of China and Japan, and intermittent irrigation, common in northwest India, significantly reduce CH_4 emissions. Rain-fed rice has a lower CH_4 emission potential than irrigated rice. A brief description of agricultural practices employed in China, Japan and the Philippines to reduce CH_4 emissions is given in Appendix A.5.2.

5.5.2 Black carbon mitigation

Significant BC emission mitigation opportunities include:

1. Retrofitting diesel engines in on-road vehicles, off-road mobile and stationary source with diesel particle filters;

2. Retiring high emitting on- and off-road diesel vehicles;

3. Modernizing traditional brick kilns and coke ovens;

---

[11] CDM Executive Board, Project Design Form, Granja Becker GHG Mitigation Project (Dec. 9, 2005), available at http://cdm.unfccc.int/UserManagement/FileStorage/MT3KUN-DZSEL2O5OE2M0B3DB63S2MYP.

4. Switching to liquefied petroleum gas (LPG) cookstoves or improved efficiency cookstoves in developing countries;

5. Use of more efficient pellet stoves and boilers in industrialized countries; and

6. Reducing open burning of agricultural wastes (crop residues).

The measures in general reduce particulate emissions in total rather than BC *per se*.

Black carbon emissions near sensitive ecosystems in regions such as the Arctic and the Himalayas, or that are carried by atmospheric transport to sensitive ecosystems, are particularly important mitigation targets. Where these vulnerable areas are close to areas of high pollution emissions, such as major urban areas in Asia, mitigation measures to reduce BC and O_3 would be particularly beneficial both for regional climate and air quality (see Section 5.3).

Although this assessment focuses on the sixteen measures identified on the basis of their effectiveness at reducing global radiative forcing, relatively smaller emissions sources in proximity to sensitive ecosystems, such as shipping emissions in the Arctic, are also critical. Melting Arctic sea ice is opening up new shipping routes. Based on models of likely increases in Arctic vessel traffic by 2030, projections indicate a 4.5 gigatonne increase in BC emissions over Arctic snow and ice (Corbett, 2010). A variety of control options exist to reduce BC emissions from marine diesel engines. A 2010 submission by Norway, Sweden and the U.S. to the Marine Environment Protection Committee (MEPC) of the International Maritime Organization (IMO, the intergovernmental organization with standard setting authority) describes the technologies as part of their request to the IMO to examine potential measures to significantly reduce BC emission from shipping that has an impact in the Arctic.[12]

---

[12] MEPC 60/4/24. Prevention of Air Pollution from Ships: Reduction of emissions of black carbon from shipping in the Arctic. Submitted by Norway, Sweden and the United States. 15 January 2010. Available at: http://www.rina.org.

Diesel particulate filters and other approaches for reducing diesel emissions

Diesel engines are a key mitigation target in both developed and developing countries. It estimated that in the United States of America and the European Union nearly 60 per cent of the BC emissions come from diesel engines (Bond, 2004), while in developing countries diesel engines are estimated to represent the fastest growing source of BC emissions (Streets *et al.*, 2004).

Technical measures such as the use of diesel particle filters (DPFs) and fuel switching, as well as non-technical approaches such as improved public rapid transit and the retirement of high-emitting diesel vehicles have been implemented around the world to reduce fine particle and BC emissions. Improved fuel standards, particularly the introduction of low-sulphur fuels, are a prerequisite for the fitting of after-treatment devices such as DPFs. This section reviews measures in several categories:

1. Measures requiring use of DPFs for road and off-road sources;

2. Scrappage programmes to retire or replace old, high-emission diesel vehicles;

3. Transportation planning, for example, congestion pricing and diesel low emissions zones (LEZs) and bus rapid transport (BRT systems); and

4. Fuel switching from diesel to compressed natural gas (CNG).

Successful policies incentivizing or mandating the use of DPFs have been implemented around the world. The United States of America's regulations on particulate matter (PM) emissions from new engines have been effective in reducing BC from on-road vehicles – mainly diesel trucks – and non-road diesel engines, locomotives, and commercial marine vessels. For example, since the 2007 model year, virtually all new road diesels in the United States have been equipped with DPFs.

---

uk/c2/uploads/mepc%2060_4_24.pdf.

The phase-in period for these new regulations extends to 2015, but given long life of diesel engines fleet turnover is slow. The US EPA estimates that the new standards under the Clean Air Non-road Diesel Rule will cut PM and BC emissions from non-road diesel engines by more than 90 per cent. US EPA rules covering locomotive diesel engines and commercial marine engines (categories C1/C2 but not C3 ocean-going vessels) will result in use of DPFs on these engines in the coming years, and an expected overall decrease in PM emissions of 90 per cent and similar reductions in BC emissions. It is important to note that the economic global downturn has significantly slowed the diesel fleet turnover to newer, cleaner engines, thus programmes to retrofit the existing on-road and legacy fleets with DPFs still offer important opportunities for BC mitigation.

The European Union has adopted specific PM emission standards for new on-road heavy-duty diesel engines, and others for new non-road diesel engines. Taken together, these are projected to drive similar adoption of the DPF technology in the EU as in the United States of America (EC 2009).

Successful BC initiatives requiring DPFs can also be found at the municipal level, for example in New York, London and Santiago. New York City adopted Local law 77 in 2003 requiring the early use of ultra-low-sulfur diesel (ULSD) fuel and best available technology including DPF for emissions reduction in off-road construction equipment working on construction projects.[13] Similarly, Transport for London, which has responsibility for the city's transport system, fitted DPFs to all buses over several years, beginning in 2003. In Santiago, Chile, a 2010 municipal law required all city buses to meet an EU emissions standard and be fitted with DPFs.

Appendix A.5.2 gives further examples of initiatives that can reduce emissions of BC and other pollutants from diesel vehicles. These include new bus rapid transit (BRT)

systems which, insofar as they usually result in the replacement of old, more polluting vehicles, and may also involve a change from diesel to a cleaner fuel such as CNG, can result in improved emissions. Examples are given from Bogota, Columbia, Mexico City and Jakarta, Indonesia.

Industrial facilities – traditional brick kilns and coke ovens

Brick kilns and coke ovens are two important industrial sources of BC emissions in many parts of the world. Old traditional brick kilns have been recognized in several developing countries as having major environmental and health impacts (Heierli and Maithel, 2008). In some regions, improved kiln designs that are more efficient and significantly reduce air pollution and CO_2 emissions have been widely adopted. There are numerous examples of initiatives to close highly polluting kilns, although there is very little data on how effective these have been. For example, China, India and Nepal have all banned the operation of several old, highly polluting kiln types, but there is neither reported information on the implementation of the bans nor the emissions reductions achieved (Zhang, 1996). And in 2009 it was reported that the Pakistani environmental authority ordered the closure of 12 brick kilns operating in the urban area around the Benazir Bhutto International Airport to improve visibility (Rehman, 2009).

Developing country contexts often include various obstacles or disincentives for technology upgrades including limited access to credit and other constraints to achieving the scale required to make the new technology profitable. However, initiatives to reduce air pollution from traditional kilns through a combination of health regulations and economic incentives have proven effective. For example, in Ciudad Juarez, Mexico, improved kiln designs boosted fuel efficiency by 50 per cent and reduced PM pollution by 80 per cent. Further description of brick kiln initiatives in Mexico and Vietnam are given in Appendix A.5.2.

Coke production is concentrated in a relatively small number of coke-making facilities

---

[13] New York City Local Law 77 is available at http://www.nycouncil.info. More information available at http://www.nyc.gov/html/dep/html/news/lowsulfu.shtml.

globally, primarily in China, which accounted for 60 per cent of global production in 2008 and 96 per cent of global production growth since 2000 (Polenske *et al.*, 2009). China is reportedly preparing a plan to expand the phase out of its highly polluting coke oven technology (Polenske, 2006).

Implementation of environmental regulation in the United States of America and the European Union has demonstrated that air emissions – including $PM_{2.5}$ emissions likely including BC – can be reduced to very low levels through proper maintenance practices and the installation of appropriate air emissions control technology (Polenske *et al.*, 2009). Until recently even in the United States of America though, the emissions from one coke oven facility were largely responsible for the works failing to meet national ambient air quality standards for $PM_{2.5}$ (Weitkamp *et al.*, 2005). In a memorandum of understanding in 2010, U.S. Steel, the owner of Clairton Coke Work (one of the largest in the country), agreed to cut the plant's PM emissions by at least 320 tonnes by December 2013. The company will shut down three of its oldest batteries in 2012 and replace a quenching tower with a low-emissions one. The emissions reductions are projected to be sufficient to attain the national air quality standard for fine particulate pollution the area (Napsha, 2010).

Improved cook stoves and fuel switching in developing countries
Improved cookstoves and clean cooking fuels are key to reducing indoor and outdoor air pollution, reducing climate emissions (both GHG and aerosols), reducing social impacts on women (e.g. time spent collecting fuelwood) and combatting deforestation thereby preserving biodiversity. There is considerable literature describing this (MacCarty, 2008).

A range of approaches to reduce cookstove emissions have been implemented around the world, including:

1. Switching to clean fuels such as LPG and biogas;

2. Introducing improved natural draft stoves to increase efficiency, reduce fuel use (and CO_2 emissions), and reduce traditional air pollutants including fine particulates and CO; and

3. Introducing various advanced combustion forced air stoves with low PM emissions which achieve anywhere from a factor of 10–15 $PM_{2.5}$ reductions (e.g. the Phillips, Turbococina and Oorja stoves[14]).

Fuel switching to LPG is the cleanest, globally available strategy to reduce CO_2 and BC (and other harmful pollution) emissions. This may require subsidies to offset the higher fuel and stove costs and achieve significant adoption rates. In Senegal for example, a major initiative to switch to LPG stoves to avoid deforestation was very successful thanks to public subsidies. These facilitated the adoption of LPG fuels and stoves through a combination of tax breaks including exemptions from customs duties on LPG equipment imports, and LPG fuel subsidies. LPG use grew from less than 3 000 tonnes in 1974, through 15 000 tonnes in 1987 to nearly 100 000 tonnes in 2006.

Another option is stove replacement with more efficient and cleaner burning stoves. It is important to note that many natural draft improved biomass cooking and heating stoves – stove models without fans – were not originally designed to reduce BC emissions, even though they are highly efficient in reducing CO_2, CO, OC and NMVOC. The natural draft stoves have been shown to reduce fuel use in the field, and have shown important $PM_{2.5}$ and CO emissions reductions in laboratory settings. These stoves are representative of many stove improvement programmes in developing countries; they effectively address indoor air pollution by reducing CO and fine PM concentrations. Advanced combustion, forced air stoves are able both to cut fuel use and significantly reduce BC emissions, but are significantly more expensive and require more in-country manufacturing and repair capacity.

---

[14] La Combustión a Baja Temperatura y Su Aplicación en la Turbococina. Available at www.bioenergylists.org/es/turbococina.

Stove replacement efforts often require financing mechanisms in addition to the facilitation of production or import, distribution, and repair networks, and local education. Selling certified CO_2 emissions-reduction credits via the CDM is one way to generate finance for stove replacement projects. For example a CDM project in seven villages in the Hebei province of China aims to replace 3 500 non-efficient, polluting coal fired stoves in rural households with environmentally friendly, efficient biomass briquette-burning appliances. The project will claim carbon credits from the displacement of fossil fuel and the associated CO_2 emissions in heaters, and most importantly aims to reduce indoor air pollution, including not only CO_2 but also SO_2, NO_x and particulates, to improve health conditions for rural households. Due to the high cost associated with the new efficient biomass gasification stoves and heaters, the project aims to use CDM revenues to subsidize the purchase of the stoves and heaters.[15] This has important policy implications in terms of ongoing revenue streams, making advanced stoves affordable, durability and scalability of results. Carbon financing also demands rigorous monitoring and evaluation. However, it is important to note that the metric of value is fuel use – and since advanced stoves may not all save significantly more fuel over non-advanced stoves, carbon financing alone may not result in advanced solutions that reduce BC.

One project that is taking an integrated approach to stove replacement and BC reductions is the Project Surya[16] (the Sanskrit word for sun) in India, although it should be stressed that this is still at an early stage. Launched in a rural village with 500 households and a population of 2 500 people, the pilot phase has been launched as a collaboration between the Energy Resource

Institute (TERI), the Scripps Institute of Oceanography and UNEP's Atmospheric Brown Cloud Project. Several available commercial cookstoves were tested for climate and health benefits, fuel efficiency and social acceptance. Stove types employed in the pilot phase include both force and natural draft models developed and manufactured locally that reduce BC emissions by 50–80 per cent compared to traditional mud stoves. Climate benefit monitoring included measurements of ambient BC concentrations; indoor (kitchen) BC concentrations, and assessment of the BC reduction capacity of different improved stoves models.

The Indian government's National Biomass Cookstoves Initiative has been launched to develop and deploy the next generation cleaner biomass cookstoves throughout the country, with the goal that stoves reach LPG-like emission levels (Venkataraman *et al.*, 2010).

There are several good examples of stoves that are being sold at large and increasing scales. Almost 500 000 Oorja stoves have been sold in India and the GERES/Cambodia charcoal stove sales have just reached 1 million units. The HELPS/Guatemala stove has quintupled sales in the last few years to about 50 000 per year and growing. These and other successes follow a wide range of business models – typically involving both private and NGO partners.

Finally, education initiatives on more efficient fuel burning techniques have been shown to achieve significant pollution reduction. An example of a simple but effective fuel efficiency improvement to cookstoves employed in South Africa to reduce particulate emissions is given in Appendix A.5.2.

Biomass heating in the residential sector in industrialized countries (pellet stoves and boilers)

In several European countries a significant growth in the installation of pellet stoves and boilers in residential and commercial sectors has been observed in the last decade. Annual sales growth rates of 20–30 per cent per year in Austria, France, Germany, Italy, Sweden (cur-

---

15 Hebei Baoding biomass combined stoves and heater (BCSH) Project 1. Clean Development Mechanism Project Design Document Form (CDM-SSC-PDD); 22 December 2006. Available at: http://cdm.unfccc.int/UserManagement/FileStorage/CBPXY7SMDFI6T3K1L4HA80QG9WREU2.

16 Ramanathan, V. and Balakrishnan, K. (2007). Reduction of Air Pollution and Global Warming by Cooking with Renewable Sources: A Controlled and Practical Experiment in Rural India (Project Surya, 2007); http://www-ramanathan.ucsd.edu/Surya-WhitePaper.pdf.

rently the largest market in the World), Switzerland have been reported, varying a little from year to year owing to changes in the price of fossil fuels compared to stove pellets.

In several European countries there are standards for PM emissions for new stoves and boilers. However, the economic aspects including fuel costs and additional economic incentives, including subsidies when such stoves are installed, have been the key drivers behind the recent growth in sales. For example, in Sweden a 52 per cent CO_2 tax on fossil fuels shifted a consumer choice and led to increased penetration of modern biomass boilers and pellet stoves. Additionally, there are public incentive programmes in several countries in support of modern biomass heating in households to reduce GHG emissions. For example, in France, value added tax on pellet stoves and boilers was reduced from 19.4 per cent to 5.5 per cent; additionally there is a tax refund of up to 50 per cent of the installation costs as well as public campaigns. In Germany, beginning in 2008, subsidies for the installation of pellet boilers of >150 kW were increased from €1 500 to at least €2 000 or even €2 500 when combined with solar panels.

Open burning of agricultural waste
Agricultural fires, used to remove crop residues, prepare fields for planting and clear brush for grazing, contribute to both rural and urban air pollution. Emissions from these fires, especially when they occur in the spring, can result in the transport and deposition of BC to the Arctic during the most vulnerable period for ice and snow melt (Pettus, 2009). Emissions from burning in northern latitudes are highest in areas across Eurasia – from Eastern Europe through southern and Siberian Russia, into northeastern China – and in the northern part of the North American grain belt (Pettus, 2009). In China, it is estimated that burning rice straw and other crop residues nationwide accounts for 11 per cent of China's total BC output (Guoliang Cao *et al.*, 2006). Fires in these countries present a clear target for mitigation. Moreover, field burning frequently ignites larger forest fires, which, in addition to increasing burn area and emissions, damage property and human health (Warneke *et al.*, 2009).

In Western Europe agricultural crop residue burning has been banned for some time because of air quality concerns (Garivait *et al.*, 2009). For example, in Denmark a ban on open straw burning was adopted in 1989 (Jørgen *et al.*, 1989). Restrictions on agricultural fires in the United States of America vary by state; many states require permits for open-field burning, and no-burn periods are declared during particularly dry periods. In the state of Idaho, for example, farmers have to prove that there is no viable alternative available in order to receive a permit to burn crop waste.[17] A programme in Southeast Asia, described further in Appendix A.5.2, may provide a model of an economically viable alternative to deal with crop waste for other developing countries. A Canadian provincial programme to reduce agricultural crop residue burning is also presented in Appendix A.5.2.

5.5.3 Scope for global and regional responses

Global inter-governmental responses
This Assessment shows that the measures to reduce SLCFs, implemented in combination with CO_2 control measures, would increase the chances of staying below the 2°C goal agreed by the parties to the UNFCCC in December 2010.

Given the importance of the impact of SLCFs, it may seem to make sense to incorporate the management of BC, O_3 and CH_4 either into a self-standing global climate instrument or within the UNFCCC. However, the likelihood of delivering a new global agreement on SLCFs – especially in the near future when it could have the greatest impact – is not high. Similarly, incorporating SLCFs into the UNFCCC would be difficult for both political and technical reasons.

As the current process of revising the UNFCCC and its Kyoto Protocol is itself complex and difficult, adding further complexity to the process does not currently look attractive. The SLCFs themselves pose challenges

---

[17] House Bill no. 391, section 22-4803, 2003 http://legislature.idaho.gov/legislation/2003/H0391.html).http://legislature.idaho.gov/legislation/2003/H0391.html.

in scientific, economic and policy terms. The impacts of SLCFs as their name implies, are near-term and their mitigation could be difficult to compare, in a negotiation forum, with the long-term effects of the Kyoto gases where reductions are measured using a 100-year GWP metric and, for the SLCFs, a GWP_{100} does not adequately reflect the climate benefits of mitigation action; a 20 year GWP has been proposed by some, and will be studied further in the 5th Assessment Report of the IPCC. Equally, the short lifetimes of the SLCFs mean that their impacts on climate are principally regional rather than global, again making comparisons with GHG impacts difficult.

Regional inter-governmental responses

Since the impacts on both climate and health, and to a large extent the wider environment, of SLCFs are principally regional in nature, regional approaches could prove promising for mitigation. However, this approach is at an early stage in most regions of the world, although basic framework approaches to regional air quality arrangements (CLRTAP, 2004) are already in place in some regions. These include the Malé Declaration on Control and Prevention of Air Pollution and its likely Transboundary Effects for South Asia (1998);[18] the *ASEAN Agreement* on *Transboundary Haze* Pollution (2002);[19] and the Lusaka Agreement (2008) of the Southern African Development Community (SADC) on Regional Policy Framework on Air Pollution.[20] Many of these share common elements, and with the Convention on Long Range Transboundary Air Pollution (CLRTAP), a long-standing regional air quality agreement in Europe, North America and parts of Eurasia[21] (CLRTAP, 2004). Finally, draft Elements for a Framework Agreement on Atmospheric Pollution in Latin America and the Caribbean were negotiated in April 2010,[22] and intergovernmen-

tal air quality monitoring networks such as the Acid Deposition Monitoring Network in East Asia (EANET) have and are being established in different regions around the world.[23]

With the exception of CLRTAP, these regional agreements predominantly concentrate on scientific co-operation and are not yet at the stage where emission reductions and abatement/mitigation strategies are agreed. Nevertheless, these instruments can serve as a platform from which to address the emerging challenges related to air pollution from BC and O_3 and other SLCFs, and as potential vehicles for finance, technology transfer and capacity development on SLCF mitigation in their respective regions. Moreover these are framework instruments that envisage stronger action in future and declare the member countries' intent to 'develop and/or adopt strategies to prevent and minimise air pollution' (Malé Declaration, paragraph 7); 'ensure that legislative, administrative and/or other relevant measures are taken to control open burning and to prevent land clearing using fire' (ASEAN Agreement on Transboundary Haze Pollution, Article 9(g)). Hence one strategy would be to build on existing regional agreements to encourage deeper collaboration and more rapid implementation of measures to reduce emissions. Given the global distribution of emissions and impacts, and an already strained institutional capacity in many developing countries and regions, any strengthened governance regime would be most effective if it included financing targeted specifically at pollution mitigation to maximize climate and air quality benefits.

An important action could be to build on the recent advances made by CLRTAP which has already been successful in reducing peak regional O_3 levels. Adopted in 1979, CLRTAP was the first international environmental agreement to address the air pollution threat to human health and well-being. The Parties are now reaping the benefits of the cuts in air pollution spurred

---

[18] Available at: http://www.rrcap.unep.org/male/.

[19] Available at http://www.disasterdiplomacy.org/aseanhaze.pdf.

[20] Available at: http://www.unep.org/urban_environment/PDFs/SADC-LusakaAgreement.pdf.

[21] Available at: http://www.unece.org/env/lrtap/lrtap_h1.htm.

[22] Available at: http://www.pnuma.org/forumofministers/17-

panama/FORO%20DE%20MINISTROS%202010%20VERSIONES%20FINALES/EXPERTOS/DE%20TRABAJO%20INGLES/UNEP-LAC-IGWG-XVII-%206%20Draft%20Elements%20Framework%20Agreement%20Atmospheric%20Pollution.pdf.

[23] For information on EANET please see: http://www.eanet.cc/.

by the convention's provisions, including legally binding protocols on air pollutants that have the greatest impact on environmental and public health. At its meeting in December 2010, the Executive Body (the Conference of the Parties) agreed to consider the incorporation of BC in the revision of the conventions's Gothenburg Protocol, with the aim of agreeing the revision by the end of 2011. It further agreed to analyse the impacts of reductions in CH_4 emissions on tropospheric O_3.

An important factor in developing policies on SLCFs will be the strengthening of the scientific capabilities within regional agreements around the world, so that some of the uncertainties about the links between emissions and impacts are resolved. CLRTAP's focus on the inclusion of mechanisms for reducing impact, rather than just emissions, was novel in terms of diplomacy, but relied on agreement on a scientific model for relating emissions to impact. The fact that this science model emerged and carried such weight in discussions is attributed to successful social and academic networks (Siebenhuner, 2002). CLRTAP has recently agreed to further the regional and wider international scientific co-operation on hemispheric transport of air pollution, notably on CH_4 and tropospheric O_3, building on its successful earlier work in this area.

The Lusaka Agreement (2008) – Southern African Development Community (SADC) Regional Policy Framework on Air Pollution lists fine particulate pollution first among the 'relevant indoor and outdoor air pollutants, that cause significant damage locally, nationally and in a transboundary context, in the SADC region…', notes 'the strong linkages between emissions of air pollutants and greenhouse gases and the co-benefits of reducing air pollution in all sectors for greenhouse gas emission reductions, reducing congestion etc.' as well as 'the linkages to the production of secondary pollutants, such as O_3, that can have significant impacts on health and crop yield and quality'; and agree to cooperate on a wide range of activities including to 'develop policies, laws and regulations with respect to air quality management, integrated with relevant Conventions and Treaties' (Lusaka Agreement, paragraph 6.1).

Additionally, there have been a number of initiatives in the Asia-Pacific region aimed at reducing air pollution such as progressive improvements in diesel and gasoline quality, improvements in vehicular technology, introduction of vehicular fuel-efficiency standards in selected countries and improvements in pollution control technology in the power sector. All of these should reduce emissions of BC and precursors of O_3. Regional initiatives to improve fuel quality have also been launched in Latin America and Africa, alongside some national programmes to reduce vehicle emissions.

Furthering developments within CLRTAP and an extended outreach programme to other regional instruments could provide a first step to a wider global approach to the management of BC, O_3, and other SLCFs. As a first step, a network of regional agreements and existing networks could be established involving, initially, a linking of regional instruments to facilitate technical cooperation, research and monitoring, and finance and capacity development and regional standard setting where appropriate, with possibly a longer term aim of a global instrument on air pollution. An international consultative process and/or a set of regional workshops convened by an intergovernmental organization such as UNEP, together with WMO, could serve as an important forum to explore approaches to linking and enhancing existing regional air quality frameworks and institutions. The remit of such a consultative process might include both seeking views on modalities to enhance cooperation between existing regional arrangements, agreements and processes with a view to enhancing effectiveness and achieving concrete mitigation results; and exploring options on how to draw on and strengthen existing capacity most effectively to facilitate adoption of air pollution control measures that deliver air quality and climate co-benefits. Furthermore, sharing good practices on an international scale is happening, in a coordinated way, within the Arctic Council and this too could provide a helpful way forward. The Arctic Council has already been very active in addressing SLCFs.[24]

---

[24] See, for example, http://www.amap.no/.

An enhanced understanding of cost-effective technical and policy options for BC and O_3, and its precursor CH_4, under different national circumstances would help to inform both national air quality and climate policy-makers as well as regional agreements. Initiation of a review of BC and tropospheric O_3 reduction technologies and regulatory approaches, under the imprimatur of an intergovernmental organization such as UNEP, with the aim of producing a technical and policy tool kit for national and regional bodies, could contribute to advancing adoption of effective mitigation action at multiple levels.

As discussed in the next section, there are also existing and proposed financial mechanisms which could help support implementation of the identified measures, or, if not directly appropriate, could provide models for the development of new mechanisms.

5.5.4 Financing abatement of black carbon and tropospheric ozone precursors

Financing emissions-reduction measures remains perhaps the most effective immediate tool for global action. This section gives some examples of existing funding mechanisms and sources which could be useful for delivering measures to reduce emissions from SLCFs, or could provide examples for new mechanisms should they be necessary. Because of its status as a Kyoto basket gas, the O_3 precursor CH_4 has an additional opportunity for financing, addressed separately below.

Existing sources of financing
A number of financing mechanisms already exist for environmental benefits that could be used immediately to target SLCFs.

Donors and multilateral development banks (MDBs) could add and integrate BC and O_3 precursor reduction projects into their existing overseas development assistance (ODA) portfolios, due to their strong co-benefits for health and development as well as the environment and climate. A strong example for such an approach might be found in cookstove projects, which, if properly designed, could decrease BC, O_3 and CO_2 for climate benefits; reduce indoor air pollution for health benefits especially among women and children under age 5; increase school attendance among girls freed from many hours of fuel gathering and generate economic benefits to women and communities enabling them to spend more time in other income-generating activities.

Similar suites of strong developmental co-benefits would accrue from projects that, for example, add a CH_4 capture component from wastewater or landfill projects, providing a clean energy source; or decrease BC emissions from industrial sources such as brick kilns.

New and targeted funding sources
The connection between poverty reduction and near-term climate-related funding will need to be drawn more directly than is presently the case; for example, by emphasizing the preventive nature of reducing the risk of environmental impacts such as flooding or water shortages that might otherwise occur making development activities difficult if not impossible. For this reason, new sources of funding with a specific SLCF focus are also important for governments and the United Nations system to pursue. For example, the Global Alliance on Cookstoves was launched in September 2010 with US$50 million seed money with the objective of facilitating local industry build-up.

Donors could choose to finance activities directly aimed at the abatement of SLCFs for the specific purpose of achieving near-term climate benefits in sensitive areas such as the Himalayas, the Amazon and the Arctic. This might include direct abatement and/or fiscal incentives for the reduction of SLCFs. Indeed, the benefits that would occur could have such a potentially rapid impact that the United Nations might consider the possibility of whether such activities might actually be classified as adaptation activities as well as mitigation ones, or nationally appropriate mitigation actions (NAMAs) under current negotiating texts.

Another option would be for groups of donors (both government and private actors) to pool funds for SLCF abatement, aimed at for example BC or O_3 precursors, or a mix of all SLCFs, through a targeted Forcer Fund. Alternatively,

instead of focusing on individual SLCFs, nations and organizations could focus on specific key high-emitting SLCF sectors, such as cookstoves; brick-making kilns; diesel; or agricultural burning among other possibilities.

National incentive programmes and links with international funds

National incentive programme funds already exist in a number of countries for the replacement of older vehicles, diesel retrofit programmes, or replacement of older heating stoves with less polluting ones. Similar programmes could be put into place specifically for the reduction of BC and O_3 precursors.

A number of governments have already some form of incentives – subsidies, vouchers, tax credits, etc. – for the earlier replacement of sources of air pollution, for example, accelerated vehicle-retirement programmes, renewal of older heating stoves for less polluting ones, or for the improvement of sources such as diesel retrofit programmes of particle traps installation, etc. In countries with a strong cash base, governments could choose to provide new or additional cash incentives or tax credits for the replacement of sources that generate SLCFs domestically.

For developing countries, national programmes could work together with international funds, directed at those measures that contribute the most to the reduction of SLCFs. For new programmes, an additional source of funding could be offered based on the contribution to the reductions of SLCFs. This kind of synergy could result in a greater penetration of the existing programmes and eventually in an increase of the number of programmes that aim to reduce emissions of SLCFs. Cookstove programmes could also be financed through micro-credit schemes that support the development of markets for stoves and fuels, both on the supply and demand sides. Given that these programmes reduce SLCFs, micro-credit schemes – and potentially rural infrastructure investment – could be linked to international funds as well.

Additional finance options for methane abatement – a targeted methane fund or a floor price guarantee mechanism

Methane projects featured prominently in the early years of the CDM but have a mixed record in terms of actual performance, depending on project category. Oil and gas CH_4 capture projects have one of the best performance rates of all CDM project "methodologies" (categories) – 94–100 per cent. At the same time, wastewater and landfill projects have among the lowest and highly variable rates – 40–85 per cent, according to the UNEP Risoe database. Nevertheless, CDM credits remain a potentially powerful source of CH_4 abatement funding for the coming years, given adequate investor confidence and the availability of start-up financing for project development and the expensive CDM registration process.

In connection with CDM CH_4 credits as well as the voluntary market, a Methane Blue-ribbon Panel at UNFCCC's COP-15 in 2009 recommended the creation of a financing mechanism that would provide a guaranteed certified emission reduction (CER) floor price for CH_4-generated credits. The motivation for donor support for this concept – in a best-case scenario, with minimal actual monetary investment as the mechanism would provide guarantees not direct financing – is the direct near-term climate benefit of CH_4 reductions that would occur both earlier in time, and to a greater extent, than would otherwise occur. Recent estimates by carbon market analysts point the fact that a fund that might require only US\$5–10 million annually in actual capitalization, with an additional US\$100–200 million in initial issued guarantees directly supporting US\$1 000 million in CH_4-related CERs.

It is worth noting that such a floor-price financing mechanism could also target CERs where non-CH_4 SLCF reductions, in BC and CO for example, are produced as significant and verifiable co-benefits.

Action on finance will depend on donor acceptance of the crisis and opportunity represented by near-term climate change in sensitive regions of the Earth and SLCF reductions as a highly effective means of addressing them. Costs and benefits of the identified measures are region specific, and face financial, regulatory and institutional barriers. However, widespread implementation of the measures may be effectively encouraged by recognizing that near-term strategies can slow the rate of global and regional warming, and lower the probability of major, non-linear disruptive climate events. Such influence should spur multilateral initiatives that focus on local health and development priorities while delivering a global common good.

Appendix A.5

A.5.1. Reductions in emissions from measures

The emission reductions of BC and CH_4 resulting from the choice of measures are shown disaggregated by region in Table A.5.1.

The contributions to global forcing by SLCFs (over 100 years) made by the measures and associated pollutants are shown in Figure A.5.1. It should be noted here that the forcings used to derive the measures and this figure were used solely to identify the measures and were not used in the global models, where the forcings in Chapter 3 were used.

Table A.5.1. Reductions in total anthropogenic global emissions of BC and CH_4 in 2030 by different measures relative to the reference scenario emissions in 2030.

Measure Package	Measures	Sector	Main regions of reduction	Emitted substance	Per cent reduction in global emissions (all sectors) due to measure
Group 1 BC measures	Improved stoves	Residential	Asia and Africa	BC	9
				OC	51
				Total PM$_{2.5}$	26
				CO	21
				CH$_4$	2
	Pellet stoves	Residential	North America and Europe	BC	3
				OC	2
				Total PM$_{2.5}$	1.4
				CO	0.3
	Coal briquettes	Residential	Global	BC	6.8
				OC	1.7
				Total PM$_{2.5}$	1.9
				CO	2.0
	Diesel particle filters for on- and off-road vehicles and associated emissions and fuel standards as part of a Euro 6/VI package	Transport	North America and Europe and Asia and Pacific	BC	18
				OC	3
				Total PM$_{2.5}$	4
				CO	1
				NO$_X$	24
	i. Modern recovery coke ovens; ii. Vertical shaft and Hoffman brick kilns iii. Particle control at stationary engines	Industrial Processes*	Asia and Pacific	BC	4.2
				OC	2.6
				Total PM$_{2.5}$	1.9
				CO	0.6

*Note: 'Industrial processes' includes associated fuel combustion emissions

Table A.5.1. Reductions in total global emissions of BC and CH$_4$ in 2030 by different measures relative to the reference scenario emissions in 2030. *(continued)*

Group 2 BC measures	Elimination of biomass cook stoves in developing countries	Residential	Asia and Africa	BC	35
				OC	55
				Total PM$_{2.5}$	31
				CO	28
	Elimination of high-emitting vehicles (in addition to fitting diesel particle filters)	Transport	Asia and Africa	BC	1.6
				OC	0.7
				Total PM$_{2.5}$	0.6
				CO	6.2
				NO$_X$	5
	Ban of open burning of agricultural waste	Agriculture	Asia and Africa	BC	7
				OC	11
				Total PM$_{2.5}$	9
				CH$_4$	1
				CO	6
Methane measures	i. Extended recovery of coal mine gas ii. Extended recovery and flaring for oil and gas production iii. Reduced leakage from gas pipeline compressors	Fossil fuel extraction and distribution	East, Southeast Asia and Pacific All All regions	CH$_4$	25
	i. Treatment of biodegradable municipal waste ii. Upgrading primary wastewater treatment	Waste / landfill	North America and Europe, Asia	CH$_4$	9
	i. Control of methane emissions from livestock ii. Aeration of continuously flooded rice paddies	Agriculture	All regions Asia	CH$_4$	4
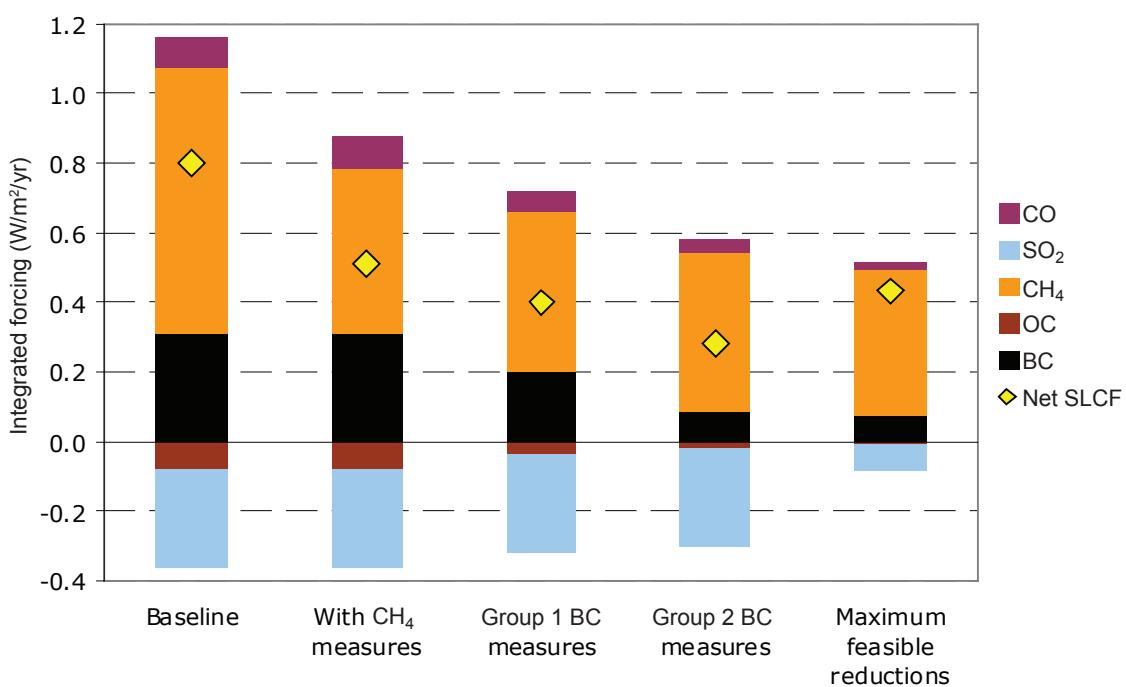
Figure A.5.1. Radiative forcing integrated over 100 years for the three groups of measures, by substance. Results are from the IIASA GAINS model and show the cumulative effect of application of the measures. Only direct radiative forcing is considered in the case of SO_2. Note that 'maximum feasible reductions' refers to applying all measures in the GAINS database, including those reducing SO_2.

A.5.2 Measures to reduce methane emissions

(i) Coal-mine methane

China: Sihe Coal Mine Methane (CMM) Project

The world's largest power generation project fuelled with CMM is in China's Shanxi Province at the Sihe mine. To develop the project, China secured technical assistance from the Methane to Markets Partnership and investments from the Japan Bank for International Cooperation, the Asian Development Bank, and the Prototype Carbon Fund of the World Bank, complementing financing by the municipal government. Methane from CMM wells has also been used to fuel a smaller, 1.6 MW, power plant near the mine since 1995.[1]

Construction began in January 2007 and by 2008 the Sihe mine had begun gener-

ating CMM power at full capacity. The facility generates 120 MW of electricity at full operation and produces an estimated 823 200 MW-hours annually. This power is sold to the North China Grid, which powers 90 000 homes and commercial and industrial facilities in Beijing, Tianjin, and other cities. The waste heat produces hot water and steam (i.e. combined heat and power) for mining operations.

The investment cost was US\$ 4 500 million (including the LNG plant) and the potential flare reduction is approximately 7 billion m³/year, with an emission reduction by the end of 2012 of 32 million tonnes of CO_2e. Over its 20-year lifetime, it is expected to avert 140 million tonnes of CO_2e by displacing electricity from the coal-dominated local power grid with electricity generated by the combustion of CMM. The Sihe mine project will also produce tradable-emission credits under the Kyoto Protocol's CDM. Finally, the CMM project reduces the risk of explosions, as CH_4 no longer needs to be

---

[1] Coal bed methane (CBM) and CMM - Project Case Study: Jincheng Anthracite Mining Group Shanxi Province, China. Available at http://www.methanetomarkets.org/successs-tories.aspx.

flared in and around the site as part of the mining process.[2]

(ii) International initiatives to reduce methane venting and flaring

The following project profiles show a snapshot of global activities to reduce venting and flaring activities (see Table A.5.2). These projects are primarily undertaken through the Kyoto Protocol's CDM carbon-crediting programmes or under the Global Gas Flaring Reduction Public-Private Partnership (GGFR). Some country programmes on flaring and venting are relatively well developed and are also included below.

Angola: LNG GGFR Project
This GGFR project gathers and ships associated gas from 20 offshore fields of GGFR-partner oil companies to a new 5 million tonne/year liquefied natural gas (LNG) plant. The investment cost is US$ 4 500 million (including the LNG plant) and the potential gas flare reduction is ~7 billion m³/year. The emissions reduction through 2012 is planned to be 32 million tonnes of CO_2e.[3]

India: Oil India Limited (OIL) – Greenhouse Gas Emission Reduction through Recovery and Utilization of Flare Gas CDM Project
OIL is a national oil company, engaged in the business of exploration, production and transportation of crude oil and natural gas. At present OIL produces about 75 000 standard m³ (SCM) of associated gas per day from its Kumchai oil field in Arunachal Pradesh in the North-East of India. At present, out of the total amount of associated gas produced from this field about 65 000 SCM per day of gas is flared due to the absence of suitable evacuation infrastructure and non-availability of consumers for this gas. The rest of the gas is consumed onsite for various purposes like fuel for gas engines or in process heaters.

The purpose of the proposed project activity is to recover gas, send it to a gas processing plant where the condensate would be separated and then transported as dry gas in a new 60 km long pipeline from Kumchai to Doomdooma in Assam. In Doomdooma this new pipeline will be connected to the Doomdooma-Tinsukia natural gas grid.

The project, which could save 53 082 tonnes CO_2e per annum[4], will contribute to increased availability of natural gas in the North-Eastern region. This project has wide replication potential due to the heavy concentration of upstream oil and gas installations in the region which in turn would help in boosting industrial growth through multiplier benefits.

Indonesia: Tambun LPG Associated Gas Recovery and Utilization CDM Project
The purpose of the project is the recovery and utilization of gases produced as a by-product of oil production at the Tambun and Pondok Tengah oil fields. Currently it is saving 390 893 tonnes CO_2e per annum[5].

The Tambun oil field is about 40 km west of Jakarta in West Java Province. This field started production in 2003 at 4 000 barrels per day. Associated gas was flared, initially at 6–7 millions of standard cubic feet per day (mmscfd); increasing to 12–15 mmscfd as oil production increased to 8 000 barrels per day in 2006. The Pondok Tengah oil field (PDT), about 10 km north of Tambun, has recently come on stream more quickly than originally planned. The technology consists of a mini LPG plant with a designed input capacity of 15 mmscfd, condensate removal facilities, a 35 km 20 cm diameter steel pipeline and associated auxiliary equipment including compressors, metering stations and safety valves.

---

[2] More information may be found at http://www.methanetomarkets.org/documents/coal_fs_eng.pdf).

[3] GGFR Project View. Available at http://siteresources.worldbank.org/EXTGGFR/Resources/ggfr.swf?resourceurlname=ggfr.swf. Last visited July 27, 2010.

[4] CDM: Oil India Limited (OIL) – Greenhouse Gas Emission Reduction through Recovery and Utilization of Flare Gas. Available at http://cdm.unfccc.int/Projects/DB/DNV-CUK1218606851.33/view. Last visited July 27, 2010.

[5] CDM: Tambun LPG Associated Gas Recovery and Utilization Project. Available at http://cdm.unfccc.int/Projects/DB/LRQA%20Ltd1180000727.07/view. Last visited July 26, 2010.

The processing plant and pipeline is constructed in full compliance with the local environmental regulations and was subject to environmental appraisals according to Indonesian environmental regulations. The processing plant is powered by the gas supply, with back-up diesel for generators and fire pumps. The supply pipeline runs 35 km to the main east-west supply line.

Indonesia: Kati-Semoga Associated Gas Utilization GGFR Project

The purpose of this project is to stripping LPG (propane/butane) and condensate from associated gas and delivering it to the domestic market. The likely investment cost is some US$21 million. It has the potential to reduce gas flaring by 1.8 bcm (billions of cubic metres) over 10 years; cutting emissions through 2012 by 0.9 million tonnes CO_2e.[6]

Russian Federation: Khanty-Mansiysk Danilovsk Gas to Power GGFR Project

Russia is by far the largest source of global gas venting and flaring. It has also made the greatest gross reductions in its emissions (see Table A.5.2). However, there is still a high volume of flaring despite the potential for more gas capture and energy production.

A 40 MW gas turbine power unit is to be built at a cost of €30.8 million. It has the potential to reduce gas flaring by 1.5 bcm over the project's lifetime and reduce emissions through 2012 by 8 million tonnes CO_2e.

Nigeria: Pan Ocean Gas Utilization CDM Project

The purpose of the project is to reduce gas flaring at the Ovade-Ogharefe oil field operated by Pan Ocean Oil Corporation (Nigeria) in a joint venture partnership with Nigerian National Petroleum Corporation (NNPC). The project activity will capture and process associated natural gas. Although the amount of flared gas will increase in the future due to the further development of the oil field, without this project, all the associated gas would continue to be flared.

Under this project, the treated gas will be injected into an existing gas transmission line for sale to an independent power plant (IPP) while the extracted natural gas liquids will be transported and sold into the national and international market. The project will reduce current flaring by approximately 98 per cent thereby contributing substantially to the reduction of GHG emissions in Nigeria and improving the local environment for the local community.

The project contributes to the sustainable development of Nigeria through the reduction of flaring, thereby reducing local air pollution and other environmental impacts associated with the combustion of natural gas. Apart from the significant reduction in CO_2, the project will also result in lower NO_x, VOCs and particulate emissions. In all reductions are estimated at 2 626 735 tonnes CO_2e per year.[7]

Given the scale of gas flaring in Nigeria, estimated by the World Bank to flare the second largest amount of gas in the world, this will serve as an important step in using CDM to address this crucial climate issue. Further as Pan Ocean is a Nigerian owned and run company, it signifies the ability of local Nigerian companies and the society to participate in CDM and the Kyoto Protocol. In addition, the gas captured in this project will be used for electrical generation in the region and thus supports the economic sustainability and growth of the country.

Nigeria: Afam Gas to Power GGFR Project

This will enable both the feeding of an existing 276 MW power plant and a new 600 MW gas run power plant with associated gas. Although no details are available for potential gas flare reductions, the investment of US$ 500 million should see emissions reductions through 2012 of 3.7 million tonnes CO_2e.[8]

---

[6] GGFR Project View. (Scroll over country to activate control) Available at http://siteresources.worldbank.org/EXTGGFR/Resources/ggfr.swf?resourceurlname=ggfr.swf. Last visited July 27, 2010.

[7] CDM: Pan Ocean Gas Utilization Project. Available at http://cdm.unfccc.int/Projects/DB/DNV-CUK1218208551.22/view. Last visited July 27, 2010.

[8] GGFR Project View. Available at http://siteresources.worldbank.org/EXTGGFR/Resources/ggfr.swf?resourceurlname=ggfr.swf. Last visited July 27, 2010.

United Arab Emirates: Masdar Initiative - Al-Shaheen Oil Field Gas Recovery CDM Project

The project aims to recover and use the associated gas produced as a by-product of oil recovery at the Al-Shaheen oil field, which is operated by Maersk Qatar Oil, in a sharing agreement with Qatar Petroleum. Oil recovery from the Al-Shaheen oil field, located about 90 km off the coast of Qatar, began in 1994.

Prior to 2004, associated gas was primarily flared, with the remaining gas used for onsite consumption (only ~3 per cent). The project will allow the capture and processing of associated gas that previously was flared, reducing emissions by about 2 500 000 tonnes of CO_2e each year[9]. Indeed, without the project, the amount of gas flared at the Al-Shaheen oil would have increased due to increased oil recovery in the field.

The project activity has three main components:

1. Recovery of associated gas;

2. Transmission of associated gas along a pipeline; and

3. Utilization of the associated gas at the gas processing plant.[10]

United States of America: Natural Gas STAR Program

Under the Natural Gas STAR Program, the United States government has taken the same course as international institutions in providing recommended standards for flaring and venting under partnerships for the mining industry and energy sector. This public/private partnership model has been extended to international companies through the Methane to Markets Partnership, providing available grant funding for non-US projects. These partnerships may be pre-empted somewhat, however, by

new regulations promulgated by the Mineral Management Service (MMS)[11] that came into effect in April 2010. These were the result of recommendations made in a report by the General Accountability Office in 2004 that cited improved monitoring and resource conservation as important goals of venting and flaring regulation.[12] However, the regulations do not set strong requirements mandating the use of capture technologies. In short, venting is still permitted and a seemingly widely used industry practice.

Vietnam: Rang Dong Oil Field Associated Gas Recovery and Utilization Project

The purpose of this project is to recover and utilize gases produced as a by-product of oil production at the Rang Dong oil field, which is about 140 km off the south-eastern coast of Vietnam. Prior to 2002, this by-product gas was flared at the platform. The project includes construction of a gas pipeline and compressor facilities to recover and transport the by-product gas. As a result of this reduction in flaring activities, CO_2 emission has been reduced by around 677 000 tonnes CO_2e per year.[13] The gas recovered is processed into dry gas (mostly CH_4), as well as LPG (butane and propane), and condensate (hydrocarbon molecules containing five or more carbons). The dry gas is supplied to nearby power plants (Phu My and Ba Ria) and will be sent to a local fertilizer plant, whereas the LPG and condensate are consumed as home-cooking fuel or used to produce gasoline.

This project contributes to the sustainable development of Vietnam in several ways. It

---

[9] CDM: Al-ShaheenOil Field Gas Recovery and Utilization Project. Available at http://cdm.unfccc.int/Projects/DB/DNV-CUK1162979371.3/view. Last visited July 26, 2010.

[10] Al-Shaheen Monitoring Report: 29 May 2007 - 31 Dec 2008. Available at http://cdm.unfccc.int/UserManagement/FileStorage/3EBYND1JFATKMGZ8PI60HL459SOQCV. Last visited July 26, 2010.

[11] "MMS to limit natural gas flaring offshore, amend production requirements." Oil and Gas Financial Journal. April 16, 2010. Available at http://www.ogfj.com/index/article-display/1178940656/articles/pennenergy/petroleum/offshore/2010/04/mms-to_limit_natural.html. Last visited July 27, 2010.

[12] Opportunities to Improve Data and Reduce Emissions. U.S. Government Accountability Office. July 2004. Available at http://www.gao.gov/new.items/d04809.pdf. Last accessed July 27, 2010.

[13] CDM: Rang Dong Oil Field Associated Gas Recovery and Utilization Project. Available at http://cdm.unfccc.int/Projects/DB/DNV-CUK1133472308.56/view. Last accessed July 26, 2010.

provides an additional source of clean-burning natural gas to support the development and contributes to a reduction of import dependency of petroleum products through provision of gas to the power plants at a significantly reduced price - about half the rate compared with other gas fields. The elimination of flaring offshore and the substitution of gas for existing fuel in domestic electricity production result in reduced atmospheric pollution. Finally, the net volume of CO_2 emissions eliminated is approximately 6.77 million tonnes over the crediting period. The CERs will be transferred to the project participants.

(iii) Reducing gas leakage from long-distance pipelines: country examples

United States of America: Natural Gas STAR Program

The Natural Gas STAR Program, facilitated by the USEPA, is a voluntary partnership that encourages oil and gas companies to adopt cost-effective technologies and practices that improve operational efficiency and thereby reduce these companies' CH_4 emissions; participating companies also document their voluntary emission reduction activities.[14]

Principal CH_4 emissions mitigation strategies for long-distance transmission include: converting gas pneumatic controls to compressed instrument air thus avoiding the releases of gas in the control systems; replacing bi-directional orifice metering with ultrasonic meters; reducing CH_4 emissions from compressor rod-packing systems; conducting directed inspections and maintenance at compressor stations; using fixed/portable compressors for pipeline pump down; installing vapour recovery units on pipeline liquid/condensate tanks; performing directed inspections and maintenance at surface facilities; identifying and replacing high-bleed pneumatic devices with low-bleed devices; and, surveying and repairing leaks.[15]

Periodic leak inspections have proved to be very cost effective by finding and remedying large process leaks that impede a system's efficiency and safety. Natural Gas STAR companies also use a range of inspections instruments and screening techniques, including a very low-cost soap solution and specialized infrared cameras that have the ability to display real-time video images of gas leaks. Moreover, Natural Gas STAR companies have found that the majority of leaks occur in a small number of components; leak inspections can thus take advantage of this finding and save time and resources by directing inspections only at problem areas.

Across the three major CH_4-emitting sectors of the oil and gas industry, including long-distance transmission, Natural Gas STAR partners reduced CH_4 emissions in 2008 by 3.25 billion m^3, which is approximately equivalent to removing 8.5 million passenger vehicles from the road for approximately one year. Since the programme first started in 1993, a domestic CH_4 emissions reduction in the oil and gas sector of almost 24 billion m^3 has been realized.

Russia: Gazprom Projects

Gazprom, Russia's state-owned and largest natural gas corporation, has implemented projects to reduce CH_4 emissions. Gazprom detects fugitive CH_4 emissions with contact sensing and distant exploration of the equipment surface. For leakage contact detection, Gazprom uses CH_4 concentration meters, gas meters and detectors, and multi-functional Infrared Data Association (IrDA) gas analysers; for remote detection and measurement, it uses helicopter distant laser gas analysers for pipelines, laser systems and IrDA sound and optical spectrometers and projectors to detect CH_4 spatial concentrations, and portable passive gas analysers.[16] Gazprom has also implemented a corporate programme aimed at modernizing compressors by using dry-seal technology. Dry seals have been proven to reduce CH_4 emissions and operating expenses,

---

[14] U.S. Environmental Protection Agency, Natural Gas STAR Program, Overview of Natural Gas STAR, http://www.epa.gov/gasstar/basic-information/index.html. Last visited July 19, 2010.

[15] U.S. Environmental Protection Agency, Natural Gas STAR Program, http://www.epa.gov/gasstar/basic-information/index.html (last visited July 19, 2010).

[16] Gazprom with the Laboratory of Environmental Protection and Resource Saving, Gazprom activities on methane emissions reduction 7 (2010). http://www.globalmethane.org/expo/docs/postexpo/oil_apokova.pdf; http://www.globalmethane.org/Data/O&G_RUS_Gazprom_poster.pdf.

Table A.5.2 Estimated flared volumes from satellite data.

Volumes in billions of cubic meters (bcm)	2005	2006	2007	2008	2009	Change 2008–2009	Change 2005–2009
Russia	55.2	48.8	50.0	40.2	46.1	5.9	-9.1
Nigeria	21.3	19.3	16.8	14.9	14.8	-0.1	-6.5
Iran	11.3	12.1	10.6	10.3	10.9	0.6	-0.4
Iraq	7.1	7.4	7.0	7.0	8.3	1.3	1.2
Kazakhstan	5.8	6.0	5.3	5.2	5	-0.2	-0.8
Algeria	5.2	6.2	5.2	5.5	4.9	-0.6	-0.3
Angola	4.6	4.0	3.5	3.1	3.6	0.5	-1.0
Libya	4.4	4.3	3.7	3.7	3.6	-0.1	-0.8
Saudi Arabia	3.0	3.3	3.4	3.5	3.5	0.0	0.5
Qatar	2.7	2.8	2.9	3.0	2.9	-0.1	0.2
Venezuela	2.1	2.0	2.1	2.6	2.8	0.2	0.7
Indonesia	2.7	3.0	2.4	2.3	2.7	0.4	0.0
China	2.8	2.8	2.5	2.3	2.4	0.1	-0.4
USA	2.0	1.9	1.9	2.3	2.0	-0.3	0.0
Mexico	0.9	1.2	1.7	2.6	2.0	-0.6	1.1
Oman	2.5	2.2	1.9	1.9	1.9	0.0	-0.6
Kuwait	2.5	2.5	2.1	1.8	1.8	0.0	-0.7
Canada	1.2	1.6	1.8	1.8	1.8	0.0	0.6
Uzbekistan	2.5	2.8	2.0	2.7	1.7	-1.0	-0.8
Egypt	1.7	1.7	1.5	1.5	1.7	0.2	0.0
Total top 20	142	136	128	118	124	6.1	-18
Rest of the world	29.0	24.0	25	20	21	1.4	-8
Global flaring level	171.0	160.0	153.0	138.0	146.0	7.5	-25
Partner countries in top 20	56.0	56.2	50.5	50.4	49.6	-0.8	-6.4

Source: NOAA (GGFR Program Manager Presentation, May 2010).

and dry-seal compressors save 90 per cent of CH_4 losses from vents.[17] Regular controls and maintenance, better equipment with gas detection devices, the development of re-sealing techniques for valves, and the use of dry seals have allowed Gazprom to reduce CH_4 emissions.

Ukraine: Cherkasytransgas Projects
Ukraine has the second largest natural gas transmission system in Europe with 171 compressor stations. In 2008 the US Agency for International Development gave Cherkasytransgas, one of Ukraine's gas system subsidiaries, an EcoLinks grant of US$50 000 to identify and repair CH_4 emissions leaks at compressor stations. The grant specifically permitted purchasing of CH_4 emissions detection equipment, training on leak measurement detection plan development and actual leak repair implementation, and measurement of leak repair success. Upon purchasing detection equipment, Cherkasytransgas discovered that 3 million m³ of CH_4 per year was

---

[17] See: http://www.gasstar.uglemetan.ru/ru/lechtenboehmer.html.

leaking from only two compressor station sites. Through identifying and repairing the leaks and measuring the leak repair success, Cherkasytransgas has been able to reduce around 2 million m³ worth of CH_4 emissions from these two compressor stations. The success of these measures has led Cherkasytransgas to roll out this CH_4 emission reduction project to all of its 23 compressor stations.[18] This project also provides a model for Byelorussian, Russian, and other Ukrainian natural gas companies.

Mexico: PEMEX Project

In 2007 Mexico's state oil company PEMEX shifted from using wet seals to dry seals on centrifugal compressors at compressor stations. As a result, Mexico has reduced 1 million m³ of CH_4 emissions per compressor per year (there are approximately 60 compressors in the PEMEX natural gas system). This reduction in CH_4 emissions is about equivalent to 438 000 tonnes of CO_2 per year.

(iv) Recovery of methane from landfill

South Africa, Durban: Landfill-gas-to-electricity Project – Marianhill and La Mercy landfills19

The project, begun in 2006, consists of an enhanced collection of landfill gas (LFG) at two sites of the municipality of Durban and the use of the recovered gas to produce electricity. Avoided CH_4 emissions from the project are 68 833 tonnes CO_2e per year.[20] This project was the first of its kind in Africa (Strachan *et al.*, 2004). Four other LFG projects in South Africa have since been initiated.[21]

The project will be implemented on the Marianhill and La Mercy landfill sites. The Marianhill landfill is an active site where waste will be deposited until 2024. It extends over 49 hectares and receives 550 to 700 tonnes of waste per day. The second landfill site, La Mercy, is an old landfill, receiving 350 tonnes of waste per day and has about one million tonnes of waste in place. The project will install 0.5 MW of electricity generation capacity at each site linked to the municipal grid. After successful installation, and depending on gas availability, electricity generation may be subsequently increased to 2 MW of combined capacity.

By displacing electricity from the grid the project will reduce emissions related to coal-fired power production that include SO_x, NO_x, and PM. It will also reduce adverse impacts related to the transportation of coal and coal mining – air pollution, acid mine drainage, etc. Near the landfill sites the project improves air quality by further reducing the amount of landfill gas released into the atmosphere, thus reducing the risk of exposure of neighbouring residents to odour.

Mexico, Monterrey: SIMEPRODE/ BENLESA Biogas Capture Plant 22

In Mexico, CH_4 emissions from landfills contribute to 10 per cent of the total human-induced GHG emissions. In 2001, Monterrey, Mexico – a city of nearly 4 million people that disposes over 4 500 tonnes of municipal solid waste a day in the SIMEPRODE landfill – explored an opportunity to capture CH_4 for energy recovery while reducing CH_4 emissions. A partnership between government and a private company turned a liability into an asset by converting LFG into electricity to help drive the public transit system by day and light city streets by night.

Bioenergía de Nuevo León, S. A. de C. V. (BENLESA) is the first renewable energy project in Mexico using the biogas from a landfill as fuel. The project is the result of a strategic alliance between Bioeléctrica de Monterrey,

---

18 Methane to Markets, Oil and Natural Gas System Methane Recovery and Use Opportunities Fact Sheet 2 (March 2008), available at http://methanetomarkets.org/documents/oil-gas_fs_eng.pdf.

19 See full project description at http://cdm.unfccc.int/Projects/DB/TUEV-SUED1154520464.04/view http://cdm.unfccc.int/UserManagement/FileStorage/XM04ZW0DZ09G-543FEOS2HIO5JU91PJ.

20 CDM project document: http://cdm.unfccc.int/Projects/DB/TUEV-SUED1154520464.04/view.

21 Detailed project documentation on the other 4 LFG projects may be found at the UNFCCC Clean Development Mechanism website: http://cdm.unfccc.int/Projects/projsearch.html.

22 SIMEPRODE http://seisa.com.mx/index.php?option=com_content&task=view&lang=en&id=54&Itemid=65 (accessed August 8, 2010).

S. A., a Mexican-owned private company, and the municipal government through SIMEPRODE (System for Ecological Waste Management and Processing), a decentralized Mexican public entity.

Funded in part by a US$ 5 million grant from the Global Environmental Facility (GEF), the BENLESA plant was opened in September, 2003, with a net capacity of 7 MW. The second phase was inaugurated five years later. With a US$ 7.5 million investment, the plant has increased its capacity by 5.3 MW, going from 7.42 to 12.72 MW.

The project generates significant environmental benefits, including abatement of GHGs. Recently, the World Bank and Bionergía de Nuevo León signed an emission reduction purchase agreement equivalent to 1 million tonnes of CO_2 for the increase in generation capacity. The first and second phase, Monterrey I and II, have an installed capacity of 12.72 MW and by February 2010 it had avoided the release of more than 81 000 tonnes of CH_4, equivalent to the reduction in emissions of 1.7 million tonnes of CO_2, generating 409 MWh of electricity for local users.

Moreover, as the SIMEPRODE landfill continues to expand, LFG generation is likely to be able to fuel a 25 MW facility, planned for completion by 2016. The expansion of Monterrey II has already been registered under the United Nations' CDM. In 2008 the estimated reductions from flaring and energy displacement totalled 36 881 tonnes CO_2e (273 372 tonnes from flaring and 33 509 tonnes from energy displacement).

A plant like Monterrey III, capable of processing enough waste to generate up to 17 MW, would require an investment of US$ 1.2–1.5 million per MW. Other Mexican cities and private companies are studying LFG potential as a cheaper and cleaner alternative to the traditional fossil fuels that generate most of Mexico's electricity.

(v) Livestock manure management

Brazil: Granja Becker GHG Mitigation Project

In Brazil, a large CDM project in the state of Mina Gerais seeks to improve animal waste management systems (AWMS) at pig confined-animal feeding operations (CAFOs) to reduce the amount of CH_4 and other GHG emissions associated with animal effluent.[23] The core activity of the project is to replace open-air lagoons, with ambient-temperature anaerobic digesters, an AWMS practice that produces far fewer GHG emissions through the capture and combustion of the resulting biogas. CDM baseline methodology AM0016, 'GHG mitigation from improved AWMS in CAFOs' (Version 2), was applied to this project.[24]

Over the course of a 10-year emissions reduction crediting period, 2004–2014, the project is predicted to reduce CH_4 and other GHG emissions by a total of 50 580 tonnes of CO_2e.

India, Hyderabad: Three MW poultry litter-based power generation project

This relatively small project, based in Andhra Pradesh, India, will use poultry litter to generate electricity that will, in turn, power the plant used to convert the CH_4 emissions to electricity and provide surplus electricity to the Andhra Pradesh state grid.[25] Two CDM baseline methodologies are applicable to this project: AMS-I.D, 'Renewable electricity generation for a grid' (Version 7), and AMS-III.E, 'Avoidance of methane production from biomass decay through controlled combustion' (Version 7).[26] During the emissions-reduction

---

[23] CDM Executive Board, Project Design Form, Granja Becker GHG Mitigation Project (December 9, 2005), available at http://cdm.unfccc.int/UserManagement/FileStorage/MT-3KUNDZSEL2O5OE2M0B3DB63S2MYP.

[24] *Id*. at 12, available at http://cdm.unfccc.int/UserManagement/FileStorage/CDMWF_AM_TJEACO7VPUASFJUDZ4W-PXHTYQPASQ3.

[25] CDM Executive Board, Project Design Form, 3 MW Poultry Litter Based Power Generation Project, Hyderabad (June 30, 2006), available at http://cdm.unfccc.int/UserManagement/FileStorage/7KJAROE2OLWKHU103LQEYUC7WMZ2ZK.

[26] *Id*. at 7, available at http://cdm.unfccc.int/UserManagement/FileStorage/SJI52M6QXGKFNOZABTHDYPU789EV3C and http://cdm.unfccc.int/UserManagement/FileStorage/HXJBK40UFD5I6WYCL3EP8S7N1OGR2Q.

crediting period, starting in 2006 and concluding in 2012, the project is estimated to reduce CH_4 and other GHG emissions by a total of 460 558 tonnes of CO_2e.

(vi) Rice paddies

Mitigating methane from Asia's rice paddies

The agriculture sector is responsible for approximately 13.5 per cent of global GHGs, a significant portion of which are CH_4 (Foster *et al.*, 2007). About 12 per cent of global CH_4 emissions or about 40 million tonnes annually come from rice production. With more than 90 per cent of the world's rice, reducing CH_4 emissions from Asia's rice paddies will be crucial in mitigating global GHGs (Wassmann *et al.*, 2009).

The most dramatic changes in these practices have been in China. At the start of the 1980s, just one per cent of Chinese farmers drained their rice paddies mid-season; two decades later nearly 80 per cent engaged in the practice. Estimates suggest that this shift reduced about five million tonnes of CH_4 emission from China's rice fields. Since a third of the world's rice and a fifth of the world's rice-paddy area is in China, the impact of these changes has been significant (Li *et al.*, 2002).

Other drainage schemes have been used elsewhere in Asia. In Japan, the term nakaboshi, referring to mid-season 10-day drainage, is a longstanding practice (Nagata, 2010). Drainage of continuously flooded paddies has also become popular elsewhere in Asia such as the Philippines and northern India. They have further gained attention with the spread of a new approach to rice cultivation known as the system of rice intensification (SRI) that incorporates intermittent drainage in a broader repertoire of resource-conserving planting, soil, and nutrient management practices (Uphoff, 2007).

There are several barriers to optimizing GHG reductions from rice cultivation. One is that while mid-season drainage brings down the release of CH_4 it can increase nitrous oxide (N_2O) emissions – N_2O is a GHG with a GWP of 198. A second challenge is that many farmers use rice straw from the previous season as fertilizer, a practice that can increase CH_4 emissions because of higher soil temperatures that typically follow intermittent draining (Nagata, 2010).

Another set of obstacles is that measuring reductions of emissions and developing baselines are difficult due to the host of factors that impact CH_4 production. Similarly, it is difficult to establish that changes in cultivation practices are additional to what would happen without support from external financing mechanisms such as the CDM. A related set of issues is that water saved is often used for other rice fields leading to further emissions (Wassman et al., 2000; Wassmann *et al.*, 2009).

Philippines: Mitigation within one irrigation system

Bohol Island, one of the largest rice-growing areas in the Visayas region of the Philippines, has experienced declining productivity from existing irrigation systems, affecting incomes. The problem has been aggravated by the practice of unequal water distribution and unnecessary water use by farmers who insist on continuous flooding to irrigate their rice crop. The construction of a new dam was accompanied by a plan to implement a water-saving technology called alternate wetting and drying (AWD), developed by the International Rice Research Institute (IRRI) in cooperation with national research institutes. Visible success of AWD in pilot farms and specific training programmes for farmers has helped to dispel the widespread misperception of possible yield losses in non-flooded rice fields. Adoption of AWD facilitated improved use of irrigation water and increased rice productivity. Using the methodology of the IPCC, modification of the water regime can reduce CH_4 emissions by almost 50 per cent as compared to rice produced under continuous flooding. The Bohol case is an example of a new technique that can increase the income of poor farmers while decreasing GHG emissions.

A.5.3 Measures to reduce emissions from incomplete combustion

(i) Measures to reduce emissions from diesel vehicles: the use of DPFs

Chile, Santiago: A new emission standard requires diesel particulate traps for public transport buses

Like many cities in developing countries, Santiago suffers from high levels of air pollution, especially of particulate matter (PM). In spite of 20 years of emission-control measures that have reduced ambient concentrations of fine PM by half, the current levels are still almost three times the WHO guideline of 10 µg/m³ annual average. Even with increasingly strict emission standards, mobile sources are responsible for 49 per cent of the primary emissions, with public transport buses contributing 22 per cent.[27]

The public transport in Santiago is privately operated, with firms bidding for the rights to operate different zones of the system. In October 2005, the Transantiago programme was introduced, which brought the opportunity to renew old buses. Although the emission standard enforced was Euro III, operators that included cleaner buses were rewarded in the bidding process. This lead indirectly to the introduction of the first buses with diesel particulate filters (DPFs) when one of the operators that had considered CNG buses, had to desist because of the lack of natural gas, and was forced to use diesel buses. To compensate the different emission rates, the authority demanded the installation of particulate filters on 110 buses that have been operating since then. Subsequently, in 2009, another operator installed filters on around 600 buses, a move that was rewarded with the extension of its concession for two additional years.

This good experience with DPFs encouraged the authority to adopt a new emission standard for buses in January 2010, consisting of Euro III with a particulate filter. Currently, from a fleet of more than 6 200 buses,

around 2 000 are equipped with a filter, and the number is expected to rise to 2 500 by the end of 2011. Due to the projected renewal of the fleet, it is expected that by 2018 the whole fleet will be equipped with DPFs. Analysis has shown high benefit-to-cost ratios and significant improvements in public health impacts.

It should be noted that the introduction of filters in Santiago was possible because low-sulphur diesel was available. The programme to reduce sulphur started in 2001, and now all diesel fuel in Chile meets 50 ppm sulphur content.

(ii) Urban bus rapid transport systems and metro systems

Responding to the twin urban priorities of improving air quality and reducing congestion, bus rapid transport systems (BRTs) are being constructed around the world, reducing air pollution from diesel buses, reducing congestion and providing high-quality, low-cost transport. BRT systems mitigate CO_2, PM and BC emissions while providing significant air-quality and climate co-benefits. BRTs are up and running in major urban areas around the world in Africa, Asia and Latin America. The BRT constructed in Johannesburg, South Africa, for the 2010 FIFA World Cup, for example, employs Euro IV diesel engines with particulate traps – significantly better than the national standard, which is Euro III.

The CDM has approved a BRT methodology. The Chongging Lines BRT in China is requesting registration while the TransMilenio BRT in Bogotá, Colombia has been certified for 246 563 tonnes CO_2e per year.[28] The Guangzhou, China, BRT, inaugurated in February 2010, is the largest in the world, daily serving more than 600 000 passengers in the first BRT corridor alone. The TrasJakarta BRT in Indonesia and the TransMilenio BRT in Bogotá, two of the first and most successful, are profiled below, along with Metrobus in Mexico City.

---

[27] See http://www.conama.cl/transparencia/transparencia2009/normativadoc/ModificaDSNo130NormaEmision-buseslocomocionStgo.pdf.

[28] See http://cdm.unfccc.int/Projects/DB/DNV-CUK1159192623.07/view.

Colombia, Bogotá: TransMilenio BRT

During the 1990s rapid population growth and an increase in automobile ownership in Bogotá resulted in extensive congestion, bringing air and noise pollution, and traffic accidents (Cohen *et al.*, 2008). In 1998 a long-term transportation strategy was launched based on bus transit improvements, restrictions on cars, and non-motorized transportation. The core element is the TransMilenio BRT system, based upon successful experiences in Brazilian cities such as Curitiba, and Quito, Ecuador.

The initial phase of TransMilenio, implemented between 1998 and 2002, consists of 41 km of exclusive busways, 61 stations, 470 articulated buses and 241 feeder buses, providing a service to around 750 000 passengers each day. Eventually the system is expected to extend to cover 388 km, but funding shortfalls have slowed the completion.

Today, TransMilenio local buses average 21 kph and express buses 32 kph – faster than many developing-world metro systems. Travel times have been reduced by 32 per cent for system users and traffic fatalities in the corridor by 88 per cent (TransMilenio, 2006) while the city consumes less energy, is less polluted and less segregated both socially and in its use of public space and transit.

Although air quality was not at the top of the agenda for the system, it has improved. Emission reductions were achieved by replacing the old transit fleet, by improving bus transit operations, and through a modal shift from less efficient modes. For example, measurements at a site in Av. Caracas in 2000 and 2001 – before and after launching the BRT – showed reductions in SO_2, NO_x and PM_{10} of 43 per cent, 18 per cent and 12 per cent respectively. Total GHGs reductions have been estimated at 134 011 tonnes CO_2e/year (GEO-LAC, 2010).

Currently the TransMilenio serves an average of 1.6 million passengers per day and has reduced the use of bus fuel and associated emissions by more than 59 per cent since 2001 by removing 7 000 small private buses from the city's roads. It has also replaced 1 500 old, polluting buses with a new fleet. In 2008, TransMilenio became the first large transportation project approved by the United Nations to generate and sell carbon credits, bringing Bogotá an estimated US$ 100 million to US$ 300 million so far.

Mexico, Mexico City: Metrobus BRT

The large and increasing size of Mexico City coupled with its geographical characteristics combine to cause intense air quality problems of both primary and secondary pollutants. Despite successful abatement action, Mexico City's levels for PM and O_3 still exceed WHO guidelines. In 1999, the Metropolitan Environmental Commission (CAM) contracted the Integrated Program on Urban, Regional and Global Air Pollution Program at the Massachusetts Institute of Technology (MIT) to help design the new air quality management programme, PROAIRE 2002–2010 (Molina and Molina, 2002). Since mobile sources are responsible for most of the air pollution, and the existing transport conditions were regarded as poor with the average daily time required for personal travel estimated at 2.5 hours, improvement of transport is an important component of the Mexico City Air Quality Program. Metrobus was officially opened to the public in June 2005, as a part of PROAIRE 2002–2010 to improve air quality and public health in the city and as part of the Climate Action Plan to reduce GHGs.

By introducing buses that operate on ultra-low sulphur diesel fuel, the Metrobus system has reduced CO_2 emissions from Mexico City traffic by an estimated 80 000 tonnes per year by removing hundreds of polluting minibuses from the road, encouraging residents to leave their cars at home and stimulating greater use of sidewalks and bicycles. It is estimated that the addition of Line 3 (17 km) will further increase the number of passengers to 600 000 and reduce GHG emissions by 20 000 t/ year CO_2e for a total reduction of 100 000 t/ year CO_2e. In late September, 2009, Metrobus was officially approved by the UNFCCC to sell carbon

reduction credits on international markets. It is only the second transportation plan to win such approval, after Bogotá's TransMilenio.

Indonesia, Jakarta: Jakarta BRT

In early 2004, the first line of Jakarta's 15-line BRT system opened for business. By December 2007, Jakarta's BRT was making 208 332 trips and carrying an average of 1 874 988 passenger-kilometres daily. About 11 per cent of the BRT's passengers came from private cars and 4 per cent came from taxis, suggesting the BRT was responsible for 7 500 avoided car trips daily.

The BRT saved passengers nearly one hour on the first line (12.9 km), reduced air pollution and improved the transport infrastructure (Ernst, 2005; ITDP 2005; Matsumoto, 2007; Sutomo et al., 2010). These benefits were generally greater on the BRT's first line than subsequent ones, though buses on these ran on CNG which has lower PM emissions.

(iii) Programmes to retire or replace old, high emission diesel vehicles

China: Vehicle emission-standards programmes

In the last decade, under the auspices of the China Air Pollution Prevention and Control Law, China has implemented a series of increasingly stringent vehicle and fuel standards, inspection and maintenance programmes, and low emissions zones to improve air quality. Nevertheless, the rapidly growing vehicle fleet poses a great challenge. With industry increasingly located away from the big cities, motorized transportation has become one of the leading contributors to $PM_{2.5}$ pollution, haze, smog, and other serious air quality problems (Fahe, 2009; Hao, 2008). Public health impacts range from increased risk of premature death to a rising incidence of respiratory and cardiovascular diseases.

Given the sheer magnitude of the growth in the number of vehicles over the past decade, the task of curbing the negative impacts of vehicle emissions has taken on increased im-

portance. The first significant policies targeting vehicle emissions were phased in with the implementation of China I standards for new light-duty vehicles[29] in Beijing and Shanghai in 1999.

Despite the massive growth in vehicle stock and activity, it is estimated that between 2000 and 2010, the cumulative emissions benefit of the current programme over a no-programme scenario has been 44.5 million tonnes for total hydrocarbon (THC), 238.7 million tonnes for CO, 38 million tonnes for of NO_x and 7 million tonnes for PM,[30] resulting in substantial public health benefits. However, as noted earlier, China is delaying the introduction of the level IV standards for diesel vehicles (see Table A.5.3 and A.5.4) because the availability of low sulphur (50 ppm) diesel cannot be guaranteed throughout the country.

China: Vehicle labelling and scrappage programmes

Consumer information and education is an important component in a transport emission-control strategy and a vehicle emission label is an increasingly popular tool for consumer education. Emission labels attached to new cars before sales inform consumers about the emission impact of a vehicle and enable them to compare similar products and make an informed purchase decision. The application of such labels can also be combined with fiscal incentives. Emissions labels applied on in-use vehicles normally facilitate the implementation of various emission-control programmes such as the introduction of low emission zones. Though such labels provide less detailed information than new car labels, they can also educate car owners and influence their use of the vehicles.

In China, the concept of vehicle-emission labels dates back to 1999, when Beijing first

---

[29] Like many countries around the world, China has chosen to mirror its vehicle and fuels programs after those set forth by the European Union. In the Euro programme, the Arabic numerals and Roman numerals denote standards for light- and heavy-duty vehicles respectively; however, in China, there is no official distinction, and Roman numerals are used to represent both light- and heavy-duty standards.

[30] International Council for Clean Transportation. See: http://www.theicct.org/.

introduced a yellow sticker for vehicles that did not meet China I emission standards (see Table A.5.3 and A.5.4). Following that, a number of provinces and major cities implemented environmental labels for motor vehicles, with a unique design for each region. Then, in 2009 the Ministry of Environmental Protection published a rule to standardize the design of vehicle emission labels across China. Table A.5.5 summarizes the new standard, and Figure A.5.2 illustrates the labels that are used. The labels are acquired at registration.

In June 2009, the Ministries of Environmental Protection and Finance, the National Development and Reform Commission and six other government agencies collaboratively initiated a one-year nationwide consumer-subsidy programme to phase out old and highly polluting vehicles. Under the programme, vehicle owners (private, governmental, or commercial) who replace and scrap their qualified old or yellow-sticker vehicles with new ones are eligible for a one-time cash rebate ranging from RMB 3 000 to RMB 6 000 (US$ 426–925), depending on vehicle class. The amount of subsidy was raised to RMB 18 000 (US$ 2 775) depending on vehicle type in January 2010. Some local governments provided additional financial incentives as well.

Beijing estimates that it has eliminated about 120 000 yellow-labelled vehicles as of July 2010, with only about 20 000 remaining. Unfortunately, anecdotal evidence indicates that only about half of these vehicles have truly been scrapped while the other half have likely been sold into other provinces. This experience shows the need for a national scrappage effort.

Of the 64 million 4- or more-wheeled motor vehicles operating in China today, 18 million are pre-China I gasoline vehicles or pre-China III diesel vehicles without particle control equipment (diesel oxidation catalysts or PM filters). These vehicles are estimated to be responsible for about 75 per cent of total exhaust emissions from all vehicles.[31]

---

[31] Ministry of Environmental Protection News, August 18, 2008, online, http://www.vecc-mep.org.cn/news/news_detail.jsp?newsid=34386.

(iv) Transportation planning: low emissions zones (LEZs)

A growing number of cities around the world have implemented low emissions zones (LEZs), often in conjunction with congestion charging schemes, to address the twin problems of air pollution and congestion.

U.K., London: low emissions zone and congestion charging

London has operated a LEZ in parallel with the congestion charging zone since 2008. The LEZ covers a broader geographic area to address the regional impacts of air pollution, levying a €220 (US$ 320) charge on vehicles heavier than 3.5 tonnes that do not meet emission standards (Pike, 2010).

The London congestion charging system was implemented in 2003 primarily to reduce congestion. It has cut congestion from the original cordon by 20 to 30 per cent (70 000 fewer cars per day). Carbon dioxide emissions dropped 15–20 per cent, and PM_{10} and NO_2 dropped 10 per cent according to the Central London Congestion Charging Impacts Monitoring Sixth Annual Report (TfL, 2008). This is important because London exceeds European standards for NO_2 and PM_{10} chiefly at roadside locations. Transportation is the largest sources of both, including tailpipe emissions and brake and tire wear (Mayor of London, 2009).

Milan has also implemented an LEZ for passenger vehicles in January 2008, resulting in emission reductions of PM_{10}, NO_x and CO_2 by 14 to 23 per cent. Both Beijing and Berlin ban passenger cars with inadequate emission controls, and Germany also charges variable truck per-kilometre tolls based on emission control levels. The Berlin LEZ is discussed below.

Germany, Berlin: Low emissions zone

EU ambient air quality limits for PM_{10} and NO_2 have been exceeded in Berlin. Thus, like many other EU cities, Berlin was required to devise an air-quality compliance plan. Two source apportionment studies indicated that vehicle traffic was the predomi-

Table A.5.3. China: emission standards for new† light-duty vehicle approval.

(ECE15 + EUDC chassis dynamometer test*)

Light-duty diesel vehicles

	New model type approval			
	China	Beijing	Shanghai	Guangzhou
China I	1 Jan 2000(T1); 1 Jan 2001(T2) [a]	1 Jan 1999		
China II	1 Jul 2004(T1); 1 Jul 2005(T2)	1 Jan 2003	1 Mar 2003	1 Jul 2005
China III [b]	1 Jul 2007		31 Dec 2007 (public buses and taxis only)	1Sep 2006
China IV	1 Jul 2010	1 Mar 2008		1 Jun 2010

Light-duty gasoline vehicles

	New model type approval			
	China	Beijing	Shanghai	Guangzhou
China I	1 Jan 2000(T1); 1 Jan 2001(T2)	1 Jan 1999		
China II	1 Jul 2004(T1); 1 Jul 2005(T2)	1 Jan 2003	1 Mar 2003	1 Jul 2005
China III [b]	1 Jul 2007	31 Dec 2005	31 Dec 2007 (public buses and taxis only)	1 Sep 2006
China IV	1 Jul 2010	1 Mar 2008	1 Nov 2009	1 Jun 2010

†   Standards for existing models typically implemented one year later than standards for new models.
*   Speed points are mostly the same as in the ECE15 test cycle (formulated by the Economic Commission for Europe) and EUDC (the extra-urban drive cycle in the EU) cycles, except for some transient speed points.
a - Type 1 M1 light-duty vehicles (LDVs) carry no more than 6 seats and weigh no more than 25 tonnes; T2-other non-type 1 LDVs.
b - The China III standard was supposed to be effective in 2007 for all new vehicle type approval, but a transition period of one year was allowed, so all approved vehicles could still be sold until 2008 (Jan for heavy-duty vehicles [HDVs] and July for LDVs).

Table A.5.4. China: emission standards for new[†] heavy-duty vehicle type approval[*]

Heavy-duty diesel vehicles

	New model type approval			
	China	**Beijing**	**Shanghai**	**Guangzhou**
China I	1 Sep 2000	1 Jan 2000		
China II	1 Sep 2003	1 Jan 2003	1 Mar 2003	1 Jul 2005
China III [b]	1 Jan 2007	30 Dec 2005	31 Dec 2007	1 Sep 2006
China IV [c]	1 Jan 2010	1 July 2008 [a]	1 Nov 2009	1 Jun 2010

Heavy-duty gasoline vehicles

	New model type approval			
	China	**Beijing**	**Shanghai**	**Guangzhou**
China I	1 Jul 2002	1 Jul 2002		
China II	1 Sep 2003	1 Sept 2003		
China III	1 Jul 2009	1 Jul 2009		
China IV	1 Jul 2012			

† Standards for existing models typically implemented one year later than standards for new models.

* China follows the same test cycle schedule as the EU but uses the Japan05 test for durability in Euro III and later models.

a – Requires on-board diagnostics for NO_x.

b – The China III standard was supposed to be effective in 2007 for all new vehicle type approval, but a transition period of one year was allowed, so all approved vehicles could still be sold until 2008 (Jan for HDV and July for LDV).

c – In Beijing, China IV covers diesel public buses and diesel trucks used for postal and public sanitary (garbage collection) services; in Shanghai, it covers those categories regulated under China IV in Beijing plus construction trucks.

nant source of PM_{10}, $PM_{2.5}$ and NO_2 pollution. Hence, a LEZ was introduced, in order to curb road traffic emissions by imposing a selective traffic ban on the most polluting vehicles, in particular Diesel. So, the LEZ was expected to reduce BC emissions drastically, creating benefits both for human health and climate protection. Equally important, the LEZ was adopted in the context of a citywide planning process for a sustainable transportation policy, which aimed to reduce vehicle traffic and reduce air pollution and CO_2 emissions.

It was determined that providing economic incentives to retrofit diesel vehicles with particle filters would not by itself be enough to accelerate the adoption rate needed to achieve the air quality and climate mitigation goals, thus the LEZ was introduced. The LEZ has not reduced traffic per se, but it has significantly increased the incentive to retrofit vehicles with after treatment technologies including particle traps.

The German government adopted a national labelling scheme that provides the basis for the control of the LEZ. The scheme, in force since March 2007, introduced four pollution classes according to the emission criteria shown in Figure A.5.3.

Vehicles not meeting any of these criteria belong to pollution class 1. They cannot be exempt from any traffic ban. Two-wheelers, vintage cars, off-road vehicles, police, fire brigade and emergency vehicles are exempt from the scheme. Diesel vehicles retrofitted with a particle trap can be upgraded into a higher pollution class depending on the filter efficiency.

Table A.5.5. Definition of China's vehicle emission labels

Vehicle type		Minimum requirement for green label otherwise a yellow label is used
4-wheelers	Petrol	Meet China I Standard
	Diesel	Meet China III Standard
Motorcycles / Scooters		Meet China III Standard

Figure A.5.2. Green and yellow vehicle labels.

The minimum filter-efficiency criterion for passenger cars and LDVs needs to be at least 30 per cent, while a particle trap for HDVs must remove between 30 and 50 per cent of the particle load for unregulated systems and at least 90 per cent for regulated Continuously Regenerating Trap systems.

In Stage I, from 1 January 2008 only red, yellow and green labelled vehicles were allowed in the LEZ. In Stage II in 2010, vehicles entering the LEZ had to have a green label. The LEZ covers the city centre area of 85 km² with more than 1.1 million residents, delimited by the local railway ring. By mid 2011 more than other 40 towns and cities in Germany introduced a LEZ.[32]

(v) Fuel switching from diesel to compressed natural gas (CNG)

Municipalities from New Delhi and Mumbai, India, to Manila, Philippines, Mexico City and Rio de Janeiro, Brazil, have switched their vehicle fleets to natural gas fuel. When diesel vehicles, especially heavy-duty vehicles are converted to CNG, PM emissions can be reduced by one or two orders of magnitude (Rabi, 2002). The New Delhi and Pakistan CNG fuel-switching experiences are profiled here.

New Delhi: Fuel-switching to compressed natural gas
Rapid increases in the number of vehicles, kilometres driven and the poor condition of many vehicles are major contributors to New Delhi's poor ambient air quality. By order of the Supreme Court of India between 2001 and 2003 all public transport vehicles in New Delhi were required to switch to CNG. The fuel switching policy was driven by air quality concerns but can also have significant climate co-benefits.

The court order mandating the fuel switching programme – made in direct response to a citizen petition – required that the entire public transportation fleet be converted to run on natural gas, including buses, taxis and rickshaws (3-wheeled motorcycles). Although the switch was scheduled to be completed by 2001, technical difficulties with retrofitting so many vehicles and the limited number of natural gas fuelling stations delayed completion until 2003 (Reynolds and Kandlikar, 2009).

---

[32] For details see www.lowemissionzones.eu.

Figure A.5.3. Berlin vehicle labelling scheme.

The entire New Delhi public transport fleet, with more than 130 000 vehicles, is now operating on CNG. There are plans to expand this policy significantly across many other cities in the country, from about 35 cities currently to 200 cities by 2015.

A 2009 analysis indicates that the New Delhi public transportation fuel switching programme resulted in a dramatic reduction in PM and BC emissions from buses. While the initial thrust was on retrofitting the diesel engines in buses with CNG engines, the new vehicles being added to the fleet are based on new CNG engines.[33] Further, a number of private cars also converted to CNG due to the price differential.

Methane emissions both from leakage from CNG vehicles and as a component of the exhaust from both liquid-fuel and CNG vehicles is an acknowledged disbenefit of the fuel switching programme, but there are technical solutions available including maintenance programmes to tune engines for low emissions, and three way catalytic converters to reduce CH_4 emissions. New CNG engines, or improved retrofits, may qualify under the CDM; these CH_4 emissions would meet addi-

tionality requirements and be verifiable CH_4 carbon credits.

A number of other cities have subsequently developed action plans for air pollution control that include fuel switching in the transport sector as a major component.

Pakistan: Compressed natural gas fuel-switching

In the 1990s, the rise in international energy prices led Pakistan to initiate a fuel substitution programme in the power and transport sectors (Farah, 1998, Government of Pakistan, 2003, Raza *et al.*, 2010). The programme resulted in a dramatic increase in CNG fuel use. CNG currently accounts for 15.2 per cent of all road transport fuels and there are more than 2 700 CNG stations across Pakistan. Rich national natural sources of CNG were clearly a driver behind its acceptance in Pakistan. Additionally, several government promotional policies contributed to the fuel's rapid introduction and spread in Pakistan's market. These included a deregulation of CNG prices, investment in CNG machinery, and targets for an increase in CNG stations/vehicles.

The increased use of CNG has had sizable effects on short-lived warming agents. A study conducted jointly by the United Nations Development Programme (UNDP) and Energy Conservation Centre's (ENERCON) and the government of Pakistan suggests that there

---

33 State of Environment report for Delhi, 2010, Department of Environment and Forests, Government of NCT of Delhi. Available at http://www.delhi.gov.in/wps/wcm/connect/environment/Environment/Home/Achievements/Ambient+Air+Quality, accessed on October 13, 2010.

have been significant reductions in PM and modest reductions in CO_2, CO, NO_x and hydrocarbons from using CNG rather than petroleum. A study conducted under the auspices of the Hydrocarbon Institute of Pakistan suggests that "large scale use of natural gas vehicles will emit less photo-chemically reactive hydrocarbons and Volatile Organic Carbons (VOCs) and lower NO_x, SO_x that will result in significant reductions in O_3 formation in urban areas.

There were initially many challenges to introducing and increasing CNG use in Pakistan. Consumers were at first hesitant to use a gaseous fuel while oil marketing companies were unwilling to let an alternative fuel challenge their hold on the market. Investor reluctance to finance new technologies for the domestic market required CNG station equipment and conversion kits to be imported. In some cases, the promotional policies discussed above helped overcome these barriers. In other cases, the public acceptance of CNG grew over time. Broad government and public support have led to plans to substitute CNG for diesel (currently accounting for 71 per cent of transport fuels).

(vi) Industrial facilities – traditional brick kilns and coke ovens

Mexico, Ciudad Juárez: brick-makers project

In Mexico, as in other developing countries around the world, small-scale traditional brick kilns are a significant informal sector source of urban air pollution. According to the Mexican Natural Resources Ministry (known by its Spanish acronym SEMARNAT), there are approximately 20 000 traditional brick kilns in Mexico – many large cities support several hundred kilns. Bricks are generally fired in small, one-chamber kilns that use various types of fuels. Firing can last for up to twenty-four hours; often kilns are fired with a mix of cheap, highly polluting fuels including plastic refuse, used tires, manure, wood scrap, and used motor oil. As a result, in some cities, they are a leading citywide source of air pollution. Moreover, they are a serious health hazard to the residents of the poor neighbourhoods that

typically host brickyards, as well as to brick makers themselves (Blackman *et al.*, 2000).

In Ciudad Juarez, there were approximately 350 brick kilns that are one of the leading contributors to air pollution in the Ciudad Juárez-El Paso area. They emit large quantities of PM, CO, VOCs, NO_x, SO_2, and heavy metals (Blackman and Bannister, 1998).

A typical traditional kiln in this region is open topped and fired with scrap wood as the dominant fuel. New kiln designs attach two kilns constructed approximately three meters apart via an underground channel (Figure A.5.4). The double-kiln design filters the toxins from the exhaust. Importantly, the kilns use the same materials and construction techniques known to the brick makers, facilitating adoption of the new kiln design (Marquez, 2002). The new design improves fuel efficiency by more than 50 per cent, emissions of pollutants are reduced by 80 per cent, firing time by 30 per cent, and the process is less labour intensive (TCEQ, 2002; Bruce *et al.*, 2007). A cost-benefit analysis by Blackman et al. (2000) shows very significant net benefits to mortality (over 80 per cent of the benefits) and to morbidity for control strategies using kilns with new design Marquez kilns or cleaner fuel (natural gas).

El Paso Electric (EPE) just across the United States' boarder in Texas paid for emissions testing and is funding the construction of many of these kilns. An important achievement of the Ciudad Juarez Brickmakers' Project has been to construct a broad base of institutional support that cuts across national and sectoral boundaries and employs low-tech solutions to fundamental health concerns in the developing world.

Vietnam: Air quality management for brick manufacturing village

The brick industry in Vietnam is growing rapidly at around 10 per cent per year (Co *et al.*, 2009), largely in the non-state, or informal, sector. It is typically small scale, virtually unregulated and mainly concentrated in rural and peri-urban areas (Singh and Asgher, 2005). Adverse environmental and health

effects from brick manufacturing are considerable, in particular significant PM air pollution (Le and Kim Oanh, 2010). Often brick kilns are located in agricultural fields near communities hence emissions affect human health and the crop yield. The emissions can also be transported over large distances, causing regional scale effects.

A wide range of brick kilns are used in Vietnam including vertical kilns, annular kilns, and tunnel kilns (Dung and Son, 2004; RERIC, 2003). The most popular is still the traditional open-topped vertical kiln that is small and low-cost. The second most popular is the traditional-improved brick kiln with a fixed chimney. Coal briquettes, made from coal particles and different types of binding materials, are commonly used as fuel. Advanced kilns such as tunnel kilns and vertical-shaft brick kilns have high initial capital investment requirements, thus their market share is still small. These advanced kilns are made available through financial support from international cooperation that aims to stimulate the development of brick production technology.

A project to monitor and reduce air pollution from brick kilns in the Song Ho village of the Bac Ninh Province in the Red River delta demonstrates how a combination of regulation, international finance, monitoring and technology transfer can improve air quality. In January 2007 the village had 45 operating kilns, an increase of 10 kilns compared to 2006, of which 90 per cent were traditional-improved kilns and the rest were traditional open-topped ones. No air pollution-emission control devices were used in any kiln in the village. Generally coal of low quality was used as there was no effective regulation for this.

High air pollution emissions from brick kilns are believed to damage the surrounding rice paddies hence brick manufacture in the Thuan Thanh district is banned during from March to September each year to protect the rice crops (AIRPET-VN, 2007).

The project designed a simple limestone scrubbing-emissions control device and a pilot scale device was applied to a kiln to demonstrate its use (Co *et al.*, 2009). The system was simple, cheap and easy to install and operate. If this simple scrubber that removes 50 per cent of the SO_2 generated is applied then the maximum number of simultaneously operated kilns in the village could be increased to 14 while keeping ambient SO_2 lower than national ambient air quality standards (AIRPET-VN, 2007).

The current ban on brick production from March to September each year certainly affects the income of brick owners and their employees. If a kiln has implemented emission-reduction measures it then it could be allowed to operate even during the rice growing period provided the total brick-kiln impact on air pollution was acceptable. This would give the kiln owners economic incentives to invest in the control-device installation and operation. Co *et al.* (2009) analysed the emission-fee scheme and showed that the total cost for the control device (operation and equipment depreciation) would be US$ 230–240 which is only 0.8 per cent of the gross income per batch. Thus, application of an appropriate fee would provide incentives to kiln owners and encourage them to use the emission control devices.

(vii) Improved cookstoves in developing countries

In South Africa, to address both the indoor and outdoor effects of air pollution from coal cookstoves the Department of Environmental Affairs and Tourism (DEAT) initiated the Clean Fires Campaign and successfully promoted the use of an alternative fire lighting methodology, known as Basa njengo Magogo (BNM), that has been demonstrated to significantly reduce emissions from traditional stoves (Figure A.5.5). In addition to demonstrating the new technology, the campaign raised awareness of the health impacts associated with smoke emissions.

The alternative methodology uses the same stove and the same fuel, just stacked differently to create a top hot-zone that burns off the smoke before it is released. In the normal bot-
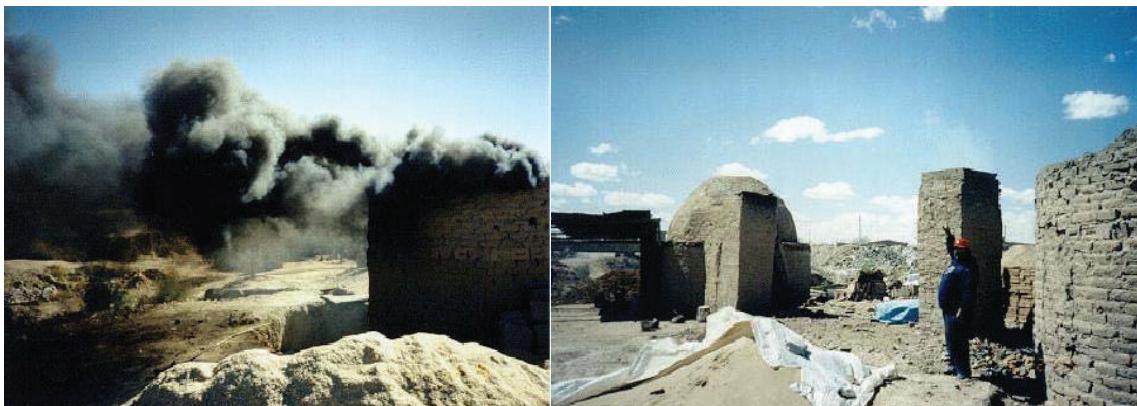
Figure A.5.4. Left: Firing of a conventional kiln in Ciudad Juarez, Chihuahua, Mexico (Photograph courtesy of Robert Marquez). Right: Firing of a Marquez kiln in Ciudad Juarez, Chihuahua, Mexico. (Photograph courtesy of Alba Corral Avitia).

tom-up coal fire ignition process, the smoke rises through the cold coals and escapes. In the top-down ignition process, the smoke rises through the hot zone and burns away.

In a controlled laboratory experiment initiated by the Department of Minerals and Energy, PM emissions (measured as total solid particulate) from coal in the BNM fires were on average 87 per cent less than in the conventional bottom-up fires. Sulphur dioxide emissions were identical and correlated with the sulphur content of the coal.

In addition to the benefits of lower emissions, the new methodology significantly improved cooking times, both reaching cooking temperature faster and boiling water more rapidly than the traditional method. The BNM top-down ignition uses approximately 1 kg less coal to reach cooking temperature than the traditional bottom–up method. This translates into a cost savings of approximately US$ 4 per month (Blackman *et al.*, 2000).

(viii) Open burning of agricultural waste

Southeast Asia: Non-burning alternatives for rice straw management
Field open burning of rice straw after harvesting is commonly practiced to clear land for faster replanting, control of weeds and pests and to return some nutrients to the soil. This field burning emits a large amount of toxic air pollutants (PM and inorganic and organic gases) and GHGs (Andreae and Merlet, 2001; Kim Oanh *et al.*, 2010) that affect local air quality and regional/global climate. The emissions from rice straw-field burning have been reported to cause high personal exposure in many parts of the world (Wu *et al.*, 2006, Torigoe *et al.*, 2000, Tipayarom and Kim Oanh, 2007). Projected increase in the rice production means air pollution from field burning could increase if no measures are taken.

Despite its potentially high contribution to air pollution in Asian cities (Kim Oanh *et al.*, 2006), this important emission source is often overlooked in air-quality management practices. In Thailand 21.9 million tonnes of rice straw are produced annually (Warneke *et al.*, 2009); almost half is burnt in the field. Thailand ratified the ASEAN Agreement on the Transboundary Haze Pollution in July 2003, which committed the country to initiate a master plan for controlling the open-burning of agricultural residues. For rice straw, a field composting solution had been introduced which aimed at ploughing the straw back into paddy soil for degradation. This requires a prolonged composting period that delays the crop replanting. Also, the appropriate plough is costly. Therefore, most farmers still prefer to burn their rice straw in the field.

Other non-burning alternatives exist that promote off site uses of rice straw. These require its collection from paddy fields and transportation to the use sites. Collection, however, is

Figure A.5.5. Basa njengo Magogo: Comparative smoke emissions from the Basa njengo Magogo fire (left) and a fire ignited with the bottom-up method (right), using traditional D-grade coal. (Source: CSIR Environmentek (2005).)

time and labour intensive due to a large volume of uncompressed straw spread over wide paddy areas. The bulky straw is also difficult to transport and store. Introduction of baler equipment which can remove most above ground biomass and produce compressed bales can overcome these difficulties; the baler operates on paddy fields 2–3 days after harvesting and hence can clear land quickly to replant the crops. Packed rice-straw bales are in demand as livestock feed, and local gardeners use it for mulching vegetables and fruit trees. Moreover rice straw is a medium for mushroom culturing that can be conducted at the household level to generate income for poor rural women. Local farmers also earn additional income from selling the straw. Other uses of collected rice straw are also being promoted in Asia, including traditional uses in handicrafts and as construction material.[34]

A.5.4 Mortality valuation using uniform VSLs

The results in Table A.5.6 calculated uniform values of a statistical life (VSLs) reflect the general patterns evident when the country-specific VSLs are employed in Chapter 5 (e.g. Table 5.3). First, the policy scenario that features abatement of methane, black carbon Group 1, and black carbon Group 2 (non-technical) measures yields the greatest reduction in mortality damage globally. The methane and black carbon Group 1 measures yield global benefits that are approximately 25 per cent smaller, while the methane policy scenario produces significantly less mortality benefit as it does not appreciably reduce components of $PM_{2.5}$.

The regional distribution of mortality benefits is somewhat different from the analysis that uses country-specific VSLs because regions with very high population densities (such as some regions in Asia) also tend to have lower per capita incomes. This implies that the country-specific VSLs are lower in these areas, which is especially important to the global damage estimates because of the large population levels in these regions. Conversely, the high income regions of Europe and North

---

[34] For more information see http://web.worldbank.org/external/projects/main?Projectid=P114893.

Table A.5.6. Mortality Valuation using uniform Value of a Statistical Life, impacts in 2030 (US$2006 billion). Reference scenario and three policy scenarios relative to the reference scenario.

Region/Scenario	Reference	Methane	Methane and BC Group 1	Methane and BC Groups 1 and 2
Africa	416 (143, 704)	-64 (-21, -106)	-1370 (-457, -2420)	-1760 (-583, -3130)
East Asia, Southeast Asia and the Pacific	-389 (-119, -876)	-191 (-62, -315)	-6080 (1990, -10700)	-8600 (-2770, -15400)
Latin America and the Caribbean	-11 (-4, -21)	-37 (-12, -61)	-282 (-94, -480)	-381 (-127, -652)
North America and Europe	-2630 (-864, -4580)	-60 (-19, -99)	-688 (-231, -1180)	-914 (-306, -1570)
South, West and Central Asia	4990 (1720, 8250)	-149 (-48, -244)	-7370 (-2400, -13100)	-9570 (3080, -17300)
Global	2380 (876, 3480)	-500 (-162, -825)	-15800 (-5170, -27900)	-21200 (-6870, -38100)

Values reflect change in mortality damage; negative values imply improvement in welfare.
95% confidence intervals in parenthesis, confidence intervals derived from reported 95% confidence intervals for mortality dose-response parameter. Values are based on concentration changes calculated with the GISS model.

America contribute less to global mortality damage when the uniform VSLs are employed. Though in agreement with the results in Chapter 5, avoided mortality damages are largest in the East Asia, Southeast Asia and the Pacific region, and in the South, West, and Central Asia region.

The global gross magnitude of the avoided mortality damages are very large and this stems from the application of the VSL calibrated to U.S. income levels to value mortality risks experienced in all regions. This method is unlikely to reflect what populations of different (especially lower) income levels are likely willing and able to pay to reduce their mortality risks.

References

Adhikary, B., Carmichael, G.R., Tang, Y., Leung, L.R., Qian, Y., Schauer, J.J., Stone, E.A., Ramanathan, V. and Ramana, M.V. (2007). Characterization of the seasonal cycle of South Asian Aerosols: a regional scale modeling analysis. J. Geophys. Res., 112, D22S22, doi:10.1029/2006JD008143.

AIRPET-VN (2007). Asian Regional Air Pollution Research Network Regional Program on Environmental and Technology (AIRPET): Improving air quality in Vietnam, Annual Report 2006, submitted by the Asian Institute of Technology, Bangkok, to the Swedish International Development Co-operation Agency.

Andreae, M.O. and Merlet, P. (2001). Emission of trace gases and aerosols from biomass burning. *Global Biogeochemical Cycles*, 15(4), 955–966.

Asian Development Bank (2001). Asian Environment Outlook. ADB, Manila, Phillipines.

Auffhammer, M., Ramanathan, V. and Vincent, J. R. (2006). Integrated model shows that atmospheric brown clouds and greenhouse gases have reduced rice harvests in India. PNAS, 10,1073/pnas.0609584104.

Aungsiri, A. (2008). Development of Assessment Method for Exposure to Open Rice Straw Burning Emission. Asian Institute of Technology, Bangkok, Thailand. Dissertation.

Balsmeyer, H. (2010). Direct communication, Verkehrsclub Deutchland e V (VC); July 23.

Blackman, A. and Bannister, G.J. (1998). Pollution Control in the Informal Sector: The Ciudad Juarez Brickmakers' Project; Discussion Paper 98-15; Resources for the Future. Washington, DC, USA, February.

Blackman, A., Newbold, S., Shih, J.-S. and Cook, J. (2000). The Benefits and Costs of Informal Sector Pollution Control: Mexican Brick Kilns; Resources for the Future. Washington, DC, USA, October.

Bond, T. (2007). Testimony for Clearing the Smoke: Black Carbon Pollution to the House Committee on Energy Independence and Global Warming, United States House of Representatives, March 16, 2010.

Bond, T.C, Streets, D.G., Yarber, K.F., Nelson, S.M., Woo, J.H. and Z. Klimont (2004). A technology-based global inventory of black and organic carbon emissions from combustion. *J. Geophys. Res.*, 109, D14203.

Bruce, C.W., Corral, A.Y. and Lara, A.S. (2007). Development of Cleaner-Burning Brick Kilns in Ciudad Juarez, Chihuahua, Mexico. *J. Air Waste Manage. Assoc.*, 57,   444-456.

Cao, G., Zhang, X. and Zheng, F. (2006). Inventory of black carbon and organic carbon emissions from China. *Atmospheric Environment*, 40, 6516–6527.

Clarke, L., Edmonds, J., Jacoby, H., Pitcher, H., Reilly, J. and Richels, R. (2007). Scenarios of Greenhouse Gas Emissions and Atmospheric Concentrations. Sub-report 2.1A of Synthesis and Assessment Product 2.1 by the U.S. Climate Change Science Program and the Subcommittee on Global Change Research. Department of Energy, Office of Biological and Environmental Research, Washington, DC, 154 pp.

CLRTAP (2004). Handbook for the 1979 Convention on Long-Range Transboundary Air Pollution and its protocols. United Nations/UNECE, New York and Geneva.

Co, H.X., Dung, N.T., Le, H.A., An, D.A., Chinh, K.V. and Kim Oanh, N.T. (2009). Integrated management strategies for brick kiln emission reduction. *International Journal of Environmental Studies*, 66 (1), 113-124.

Cohen, J. (2008). Calming Traffic on Bogota's Killing Streets. *Science*, 319, 742-743.

Corbett, J. J., Lack, D. A., Winebrake, J. J., Harder, S., Silberman, J. A. and Gold, M. (2010). Arctic shipping emissions inventories and future scenarios. *Atmos. Chem. Phys.*, 10, 9689-9704, doi:10.5194/acp-10-9689-2010.

Cresswell, A.M., Burke, G.B. and Navarete, C. (2009). Mitigating Cross-Border Air Pollution: The Power of a Network. Center for Technology in Government, State University of New York, USA. http://www.ctg.albany.edu/publications/reports/jac_mitigating.

CSIR Environmentek (2005). Laboratory Controlled Quantitative Information about Reduction in Air Pollution using the "Basa njengo Magago" Methodology and Applicability to Low-Smoke Fuels (Revised). Division of Water, Environment and Forestry Technology, CSIR, Durban, South Africa, Report No. ENV-D 2005-004.

Dung, B. T. and Son, T. T. (2004). Low cost roads working Paper No.16: Clay brick paving investigations in Vietnam. MoT, TEDI, Intech Associates.

Ernst, J. (2005). Initiating bus rapid transit in Jakarta, Indonesia. Transportation Research Records, J*ournal of the Transportation Research Board*, 1903, 20-26, http://dx.doi.org/10.3141/1903-03.

Fahe C. (2009). Air Pollution Control Law in the 12th Five Year Plan. Presentation at the 5th Regional Air Quality Management Conference, Beijing, China, 26 October 2009.

Farah N. (1998). Environmental Implications of Liquid Fossil Fuel Consumption: Case Study of Pakistan. Graduate School of Environmental Sciences, Macquarie University Sydney, Australia, thesis.

Flanner, M. G., Zender, C. S., Hess, P. G., Mahowald, N. M., Painter, T. H., Ramanathan, V. and Rasch, P. J. (2009). Springtime warming and reduced snow cover from carbonaceous particles. *Atmos. Chem. Phys.*, 9, 2481-2497.

Forster, P., Ramaswamy, V., Artaxo, P., Berntsen, T., Betts, R., Fahey, D. W., Haywood, J., Lean, J., Lowe, D. C., Myhre, G., Nganga, J., Prinn, R., Raga, G., Schulz, M. and Van Dorland, R. (2007). Changes in atmospheric constituents and in radiative forcing. In: Solomon, S., Qin, D., Manning, M., Chen, Z., Marquis, M., Averyt, K. B., Tignor, M. and Miller, H.L. (eds). Climate Change 2007: The Physical Science Basis. Contribution of Working Group I to the Fourth Assessment Report of the Intergovernmental Panel on Climate Change. Cambridge University Press, Cambridge, United Kingdom and New York, NY, USA.

Fujino, J., Nair, R., Kainuma, M., Masui, T. and Matsuoka, Y. (2006). Multigas mitigation analysis on stabilization scenarios using AIM global model. Multigas Mitigation and Climate Policy. *The Energy Journal*, Special Issue No 3, 343–354.

Gakenheimer, R., Molina, L.T., Sussman, J., Zegras, C., Howitt, A., Makler, J., Lacy, R., Slott, R.S., Villegas, A., Molina, M.J. and Sanchez, S. (2002). The MCMA transportation system: Mobility and air pollution. In: Air Quality in the Mexico Megacity: An Integrated Assessment, Molina, L.T., Molina, M.J., Eds.; Kluwer Academic Publishers: Dordrecht, The Netherlands, 213-284.

Garivait, S., Junpen, A. and Cheewapongphan, P. (2009). Agricultural Burning: Contribution to Region Air Pollution and Climate Change. Presentation to TF HTAP Workshop: Focusing on Eastern Europe, Central Asia and the Arctic in conjunction with Atmosphere. March 30 – April 3, 2009, St Petersburg, Russia. http://www.google.com/search?hl=en&q=Agricultural+Burning%3A+Contribution+to+Region+Air+Pollution+and+Climate+Change&rlz=1I7GPCK_enKE337.

Gautam, R., Liu, Z., Singh, R. P. and Hsu, N. C. (2009). Two contrasting dust-dominant periods over India observed from MODIS and CALIPSO data. *Geophys. Res. Lett.*, 36, L06813, doi:10.1029/2008GL036967.

Gene, M. G. and Krueger, A. B. (1995). Economic Growth and the Environment. *The Quarterly Journal of Economics*, 353-377.

GEO-LAC (2010). Environment Outlook for Latin America and the Caribbean: GEO LAC 3. UNEP, Panama.

Government of Pakistan (2003). Study on improving vehicle emission standards in Pakistan. Ministry of Water and Power – Government of Pakistan, UNDP/ENERCON, Pakistan.

Hao, J. (2008). Emission Control to Guarantee the Air Quality during the Olympic Games in Beijing. The 11th International Conference on Atmospheric Sciences and Applications to Air Quality. 6 November 2008. Conference Website: http://raqm08.greenresource.cn/PPTS/Presentations.htm.

Harrington, W. and Morgenstern, R.D. (2004). Economic Incentives Versus Command and Control: What's Best for Solving Environmental Problems? *Resources*, Fall/Winter 2004, 13-17.

Heierli, U. and Maithel, S. (2008). Brick by brick: the Herculean task of cleaning up the Asian brick industry. Swiss Agency for Development and Cooperation, Natural Resources and Environment Division. Available at: http://www.poverty.ch/asian-brick-industry.html.

Holloway, A., Middlebrook, L., Miller, S., Montzka, D.M., Murphy, J., Peischl, T.B., Ryerson, J.P., Gadde, B., Bonnet, S., Menke, C. and Garivait, S. (2009). Air pollutant emissions from rice straw open field burning in India, Thailand and the Philippines. Environmental Pollution, 157, 1554–1558.

INE/SEMARNAT (2008). The Benefits and Costs of a Bus Rapid Transit System in Mexico City. National Institute for Ecology (INE) Report, Mexico.

IEA (2009). Coal Mine Methane in China: A Budding Asset with the Potential to Bloom. Issues Relating to CMM in China, Based on Interviews Conducted at Coal Mines in Guizhou and Sichuan Provinces. IEA Information Paper, February 2009.

International Energy Agency World Energy Outlook (2009). IEA/OECD, Paris.

ITDP (2005). Making Trans-Jakarta a world class BRT system: Final recommendations of the Institute for Transportation and Development Policy. Institute for Transportation and Development Policy. Available at http://www.itdp.org/read/.

Jacobson, M. Z. (2010). Short-term effects of controlling fossil-fuel soot, biofuel soot and gases, and methane on climate, Arctic ice, and air pollution health. *J. Geophys. Res.*, 115, D14209, doi:10.1029/2009JD013795.

Kanabkaew, T. and Kim Oanh, N.T. (2010). Development of spatial and temporal emission inventory for crop residue field burning. Environmental Modeling and Assessment. DOI: 10.1007/s10666-010-9244-0.

Kanokkanjana, K. and Bridhikitti, A. (2009). Sustainable Rice Straw Management for Urban Air Pollution Reduction in Bangbuathong, Nonthaburi Province, Thailand. CIDA-AIT Partnership (2003-2010), SEA-UEMA Project. Asian Institute of Technology, Bangkok, Thailand.

Kim Oanh, N.T., Bich, T.L., Tipayarom, D., Manadhar, B.R., Prapat, P., Simpson, C.D., Liu, L.J. (2010). Characterization of particulate matter emission from open burning of rice straw. *Atmospheric Environment*, 45(2), 493-502.

Krupnick, A., Burtraw, B., and Markandya, A. (2000). The Ancillary Benefits and Costs of Climate Change Mitigation: A Conceptual Framework. In: Intergovernmental Panel on Climate Change (IPCC), Ancillary Benefits and Costs of Greenhouse Gas Mitigation. OECD/IPCC, Paris, France, 53-94.

Le, H. A. and Kim Oanh, N. T. (2010). Integrated Monitoring and Modeling for Air Quality Management of Brick Manufacturing Village. *Journal of Environmental Monitoring and Assessment*. 171: 381-394. DOI 10.1007/s10661-009-1285-y.

Li, C., Qiu, J., Frolking, S., Xiao, X., Salas, W., Moore III, B., Boles, S., Huang, Y. and Sass, R. (2002). Reduced methane emissions from large-scale changes in water management of China's rice paddies during 1980–2000. Geophysical Research Letters, 29(20), no. 1972. doi:10.1029/2002GL015370, 2002

Li, W. J., Shao, L. Y. and Buseck, P. R. (2010). Haze types in Beijing and the influence of agricultural biomass burning. *Atmos. Chem. Phys.*10, 8119-8130. doi:10.5194/acp-10-8119-2010.

Liu, X. D. and Chen, B. D. (2000). Climatic warming in the Tibetan plateau during recent decades. *Int. J. Climatol*. 20, 1729-1742.

Marquez, R.O. (2002). Appropriate Chemistry for the Economically Limited People of the World. Ph.D. Dissertation, New Mexico State University, Las Cruces, USA.

Matsumoto, N. (2007). Analysis of policy processes to introduce bus rapid transit systems in Asian cities from the perspective of lesson-drawing: cases of Jakarta, Seoul, and Beijing. In Air Pollution Control in the Transportation Sector: Third Phase Report of the Urban Environmental Management Project. IGES, Hayama, Japan.

Mayor of London. (2009). Clearing the Air Executive Summary. The Mayor's draft Air Quality Strategy for consultation with the London Assembly and functional bodies. October 2009. Available at: http://legacy.london.gov.uk/mayor/environment/air_quality/docs/AQS09 executive summ ary.pdf.

Miles, T. (2006). La Combustión a Baja Temperatura y Su Aplicación en la Turbococina. Available at www.bioenergylists.org/es/turbococina.

Molina, L.T. and M.J. Molina (2002). Air Quality in the Mexico Megacity: An Integrated Assessment. Kluwer Academic Publishers: Dordrecht, The Netherlands, 384 pp.

Molina, L.T., Molina, M.J., Slott, R., Kolb, C.E., Gbor, P.K., Meng, F., Singh, R., Galvez, O., Sloan, J.J., Anderson, W., Tang, X.Y., Shao, M., Zhu, T., Zhang, Y.H., Hu, M., Gurjar, B.R., Artaxo, P. Oyola, P., Gramsch, E., Hidalgo, P. and Gertler, A. (2004). Air Quality in Selected Megacities. Critical Review. Online Version ISSN 1047-3289. *J. Air and Waste Manage. Assoc*. 55:000–000. http://www.awma.org.

Nagata, A. (2010). Strategies and Policies for Mitigating Emissions from Rice Cultivation. Methane to Markets Partnership Expo, New Delhi, India, March 2-5. http://www.globalmethane.org/expo/docs/postexpo/ag_nagata.pdf

Napsha, J. (2010). U.S. Steel speeds up Clairton Coke Works pollution project. Pittsburgh Tribune-Review. Wednesday, August 18. Available at: http://www.pittsburghlive.com/x/pittsburghtrib/business/s_695321.html

Nepal Ministry of Environment, Science and Technology (2007). Ambient Air Quality of Kathmandu Valley 2007. Kathmandu, Nepal.

Nørgård, J.S. and Christensen, B.L. (1989). Shrinking Danish agriculture. *Agriculture and Human Values*, 6, 110-116.

Olson, M. (1965). The Logic of Collective Action Public Goods and the Theory of Groups. Cambridge: Harvard University Press.

Panayatou, T. (1998). The Effectiveness and Efficiency of Environmental Policy in China. In: Energizing China: Reconciling Environmental Protection and Economic Growth. McElroy, M.B., Nielsen, C.P. and Lydon, P. (Eds.), Cambridge: Harvard University Press, 431-472.

247

Pike, E. (2010). Congestion Charging: Challenges and Opportunities. The International Council on Clean Transportation. Available at: www.theicct.org.

Pettus, A. (2009). Agricultural Fires and Arctic Climate Change. Clean Air Task Force, Boston, USA. http://www.catf.us/.

Polenske, K.R. (2006). The Technology-Energy-Environment-Health (TEEH) chain in China: A case study of cokemaking. Ed. Polenske, K.R. Springer, Dordrecht, Netherlands.

Polenske, K.R., Zhang, X., Li, S., Li, J. and Liu H. (2009). Cokemaking Report to the Clean Air Task Force. Boston, USA. http://www.catf.us/.

Rabi, A. (2002). Environmental benefits of natural gas for buses. *Transport Res*. D – Tr. E., 7(6), 391-405.

Raes, F. and Seinfeld, J.H. (2009). New Directions: Climate change and air pollution abatement: a bumpy road. *Atmos. Environ.*, 2009, 43(32), 5132-5133.

Ramanathan, V., Chung, C., Kim, D., Bettge, T., Buja, L., Kiehl, J. T., Washington, W. M., Fu, Q., Sikka, D. R. and Wild, M. (2005). Atmospheric Brown Clouds: Impacts on South Asian Climate and Hydrological Cycle. *PNAS*, 102(15), 5326-5333.

Ramanathan, V. and Carmichael, G. (2008). Global and regional climate changes due to black carbon. *Nature Geosci*. 1, 221-227.

Raza, H.A., Zaheer, S.S. and Farah, N. (2010). The Co-benefits of Compressed Natural Gas (CNG): Enabling Fuel Switching in Pakistan. In: Low carbon transport in Asia: strategies for optimizing co-benefits. Zusman, E. Srinivasan A. and Dhakal, S. (Eds.) Earthscan, London, UK.

Rehman, F. (2009). 12 brick kilns directed to stop functioning. The Nation (Pakistan). March 18. 2009.

18, 2009. Available at: http://www.nation.com.pk/pakistan-news-newspaper-daily-english-online/Regional/Islamabad/18-Mar-2009/12-brick-kilns-directed-to-stop-functioning.

RERIC (2003). Regional Energy Resources Information Center. Small and medium scale industries in Asia: Energy and environment, brick and ceramic sectors. Asian Institute of Technology, Bangkok, Thailand.

Reynolds, C.C.O, and Kandlikar, M. (2008). Climate Impacts of Air Quality Policy: Switching to Natural Gas-Fueled Public Transportation in New Delhi. *Environ. Sci. Technol.*, 42, 16, 5860-5865. doi: 10.1021/es702863p.

Riahi, K., Gruebler, A. and Nakicenovic, N. (2007). Scenarios of long-term socioeconomic and environmental development under climate stabilization. Greenhouse Gases - Integrated Assessment. Special Issue of Technological Forecasting and Social Change, 74(7), 887–935. doi:10.1016/j.techfore.2006.05.026.

Schwarz, J., Spackman, R. and P. Veres (2009). Biomass burning in Siberia and Kazakhstan as an important source for haze over the Alaskan Arctic in April 2008. *Geophys. Res. Lett.*, 36, L02813.

Shine, K. P., Fuglestvedt, J. S., Hailemariam, K. and Stuber, N. (2005). Alternatives to the Global Warming Potential for Comparing Climate Impacts of Emissions of Greenhouse Gases. Clim. Change, 68, 281-302.

Shindell, D. and Faluvegi, G. (2010). The net climate impact of coal-fired power plant emissions. *Atmos. Chem. Phys.*, 10, 3247-3260.

Singh, A.L. and Asgher, M.S. (2005). Impact of brick kilns on land use/landcover changes around Aligarh city, India. *The Journal of Habitat International*, 29, 591-602.

Sodemann, J., Spackman, R. and Stohl A. (2010). An important contribution to springtime Arctic aerosol from biomass burning in Russia. *Geophys. Res. Lett.*, 37, L01801.

Strachan, L., Couth, J. and Chronowski, R. (2004). Harnessing Landfill Methane to Address Global Warming and Renewable Energy: An Overview of the Durban CDM Landfill Gas to Electricity Project. Presented to the Biennial Congress of the Institute of Waste Management of Southern Africa, WasteCon 204; October, Sun City, South Africa.

Streets, D. G., Bond, T. C., Lee, T. and Jang C. (2004). On the future of carbonaceous aerosol Emissions. *J. Geophys. Res.*, 109, D2421, doi:10.1029/2004JD004902.

Sutomo, H. Romero, J. And Zusman, E. (2010). The co-benefits of Jakarta's bus rapid transit (BRT): getting the institutions right. In: Low carbon transport in Asia: strategies for optimizing co-benefits, Zusman, E. Srinivasan, A. and Dhakal, S. (Eds.) Earthscan, London, UK.

TCEQ (2002). A Study of Brick-Making Processes along the Texas Portion of the US-Mexico Border, Senate Bill 749. SFR-081, December 2002.

Teng, F. and Gu, A. (2007). Climate Change: National and Local Policy Opportunities in China. NOTA DI LAVORO 74.2007. Global Climate Change Institute, Tsinghua University, China. http://www.feem.it/Feem/Pub/Publications/WPapers/WP2007-074.htm?WP_Page=1.

Tipayarom, D. and Kim Oanh, N.T., (2007). Effects from Open Rice Straw Burning Emission on Air Quality in the Bangkok Metropolitan Region. *Journal of Science Asia*, 33(3), 339-345.

Torigoe, K., Hasegawa, S., Numata, O., Yazaki, S., Matsunaga, M., Boku, N., Hiura, M., Ino, H. (2000). Influence of emission from rice straw burning on bronchial asthma in children. Pediatrics, 42, 143-150.

Tol, RSJ. (2008). The social cost of carbon: trends, outliers and catastrophes. *Economics*, 2, 2008-25, 1-22.

TfL (2008). Transport for London. Central London Congestion Charging Impacts Monitoring, Sixth Annual Report. July, 2008. Available at: http://www.tfl.gov.uk/assets/downloads/sixth annual impacts monitoring report 2008 07.pdf

Uphoff, W. (2007). The System of Rice Intensification and its implications for agriculture. *LEISA: Magazine on Low External Input and Sustainable Agriculture*, 22.4, 6-8.

van Vuuren, D.P., Eickhout, B., Lucas, P.L. and den Elzen, M.G.J. (2006). Long-term multi-gas scenarios to stabilise radiative forcing - Exploring costs and benefits within an integrated assessment framework. Multigas Mitigation and Climate Policy. *The Energy Journal*, Special Issue #3; December 2006.

Venkataraman, C., Sagar, A.D., Habib, G, Lam, H., and Smith, K.R. (2010). The Indian National Initiative for Advanced Biomass Cookstoves: The benefits of clean combustion. Energy for Sustainable Development, 14, 63-72.

Warneke, C., R., Bahreini, J, Brioude, C.A., Brock, J.A., de Gouw, D.W., Fahey, K.D. , Froyd, J.S., Holloway, A., Middlebrook, L., Miller, S., Montzka, D.M., Murphy, J., Peischl, T.B., Ryerson, J.P., Gadde, B., Bonnet, S., Menke, C. and Garivait, S. (2009). Air pollutant emissions from rice straw open field burning in India, Thailand and the Philippines. *Environmental Pollution*, 157, 1554–1558.

Wassmann, R., Hosen, Y. and Sumfleth, K. (2009). Reducing Methane Emissions from Irrigated Rice. 2020 Vision Briefs from International Food Policy Research Institute (IFPRI). 16(3), http://www.donorplatform.org/component/option,com_docman/task,doc_view/gid,1003, accessed August 18, 2010.

Wassmann, R., Neue, H.U., Lantin, R.S., Buendia, L.V. and Rennenberg, H. (2000). Characterization of methane emissions from rice fields in Asia. I. Comparison among field sites in five countries. *Nutrient Cycling in Agroecosystems.* 58, 1-12.

Weitkamp, E.A, Lipsky, E.M., Pancras, P.J., Ondov, J.M., Polidori, A., Turpin B.J. and Robinson, A.L. (2005). Fine particulate emission profile for a large coke production facility based on highly time-resolved fence line measurements. *Atmos. Environ*. 39, 6719-6733.

Wöhrnschimmel, H., Zuk, M., Martínez-Villa, G., Cerón, J., Cárdenas, B. Rojas-Bracho, L. and Fernández-Bremauntz, A. (2008). The Impact of a Bus Rapid Transit System on Commuters' Exposure to Benzene, CO, PM2.5 and PM10 in México City. *Atmospheric Environment*, 42, 8194-8203.

World Bank (1992). World Development Report 1992. World Bank, Washington DC, USA.

World Bank (2007). "India: Strengthening Institutions for Sustainable Growth". World Bank, Washington DC, USA. http://siteresources.worldbank.org/INDIAEXTN/Resources/295583-1176163782791/complete.pdf

WHO (2004). Comparative Quantification of Health Risks: Global and Regional Burden of Disease. WHO, Geneva 2004 (specifically Chapter 18 Indoor Air Pollution from Household Use of Solid Fuels. by Kirk R Smith, Sumi Mehta, Mirjam Maeusezahl-Feuz).

WHO (2006). Fuel for Life: Household Energy and Health. World Health Organization: http://www.who.int/indoorair/publications/fuelforlife/en/index.html

Wu, C.F., Jimenez, J., Claiborn, C., Gould,T., Simpson, C.D., Larson, T. and Sally Liu, L.J. (2006). Agricultural burning smoke in eastern Washington: Part II: Exposure Assessment. Atmospheric Environment, 40, 639–650.

Yan X., Ohara, T. and Akimoto, H. (2006). Bottom-up estimate of biomass burning in mainland China. *Atmospheric Environment*, 40, 5262–5273.

Zhang, H., Ye, X., Cheng, J., Yang, X., Wang, L. and Zhang, R. (2008). A laboratory study of agricultural crop residue combustion in China: Emission Factors and Emission Inventory. *Atmospheric Environment*, 42, 8432-8441.

Zhang, Z. (1996). Energy efficiency and environmental pollution of brickmaking in China. *Energy*, 22, 33-42.

Chapter 6. Conclusions

Authors: The Assessment team

There are multiple reasons for controlling emissions of black carbon (BC) and precursors of tropospheric ozone (O_3). These emissions affect human well-being in many ways, altering climate and degrading air quality, with consequent effects on issues such as human health, water supply, agricultural yields, and sea-level rise. The effects of emissions of these compounds up to the present day have been large, contributing a substantial fraction of the warming experienced to date, especially in the northern hemisphere. Hence, there have been many suggestions that in principle, control of these emissions could be a useful way to mitigate near-term climate change, as they are short-lived, and their control would improve human health (e.g. (Shindell *et al.*, 2008; Jacobson, 2010; Hansen *et al.*, 2000; West *et al.*, 2007)). Here, the scientific understanding of black carbon and tropospheric ozone has been assessed, and then the results of that assessment used to quantify the potential impact of specific, practical emission control measures that could be implemented with current technology or through behavioural change. As multiple compounds are usually emitted simultaneously, the impacts of the measures are examined taking into account all the co-emitted pollutants from a particular source. Hence climate impacts examined here are based on all pollutants that affect climate (gases and particles) and the health impacts considered include the effects of O_3 and of all components of fine particles ($PM_{2.5}$). Agricultural impacts include only the effects of O_3.

6.1 Assessment of the science

The Assessment finds that methane (CH_4) emissions are expected to increase in the future despite current and planned regulations. The projected increase in fossil fuel production – expanded coal mining and oil and gas production – is the primary driver of a projected increase in global anthropogenic CH_4 emissions of more than 25 per cent from 2005 to 2030. Additional contributions come from a growth in agricultural activities and municipal waste generation. In contrast, global emissions of BC, organic carbon (OC) and carbon monoxide (CO) are projected to remain relatively constant to 2030. This is in part because the expected improvements from the more efficient combustion of solid biofuels will be offset by continued economic growth. The regional trends vary, however, with decreases in North America, Europe and Northeast and Southeast Asia being balanced by increases in Africa and South, West and Central Asia.

Turning to specific sources, the emissions from residential biomass combustion are expected to become more important than they are today. Because efforts to curtail BC and OC emissions from transport and industrial sources are projected to be increasingly successful, leading to the reductions in emissions in North America, Europe and East Asia, the residential use of traditional biofuels in the developing countries of Asia and Africa will dominate global emissions of carbonaceous aerosols, contributing nearly half of anthropogenic BC emissions and about two-thirds of anthropogenic OC emissions by 2030. Another large contributor to global emissions of carbonaceous aerosols and O_3 precursors is open biomass burning. Recent estimates suggest that forest fires along with savannah and grassland burning (excluding agricultural burning) contributes about half of total global BC and two-thirds of OC emissions. It is not known how these emissions will change in the future, and for this Assessment they are assumed to remain constant at today's levels. Open biomass burning can be a key contributor if it occurs close to a sensitive area such as the Arctic or the Himalayas, so the regional emission distribution is important.

The assessment of physical science finds that substantial uncertainty exists in the climate impact of BC at the global scale. Black carbon influences climate directly through the absorption of sunlight, and indirectly both by changing cloud cover and by darkening   snow and

251

ice. The overall effective net preindustrial to present-day radiative forcing is likely to be positive and in the range of 0 to 1 W/m². Forcing from tropospheric O_3 is estimated to be about 0.35 W/m², with a much smaller uncertainty range of about 0.1 W/m².

Ozone is not an emitted pollutant and therefore it is appropriate to attribute the radiative forcing by O_3 to the precursor emissions of CH_4, CO, non-methane volatile organic compounds (VOCs) and nitrogen oxides (NO_x). Two thirds of the O_3 radiative forcing to date can be attributed to the increase in atmospheric CH_4 over this period, and hence CH_4 emissions are responsible for the increase. Carbon monoxide and non-methane volatile organic compound emissions contribute to warming through their effects on both O_3 and CH_4. Scientific understanding of the impacts of CH_4 emissions in particular is high, and therefore the uncertainty in the climate response to reductions in CH_4 emissions is relatively small.

The assessment of impacts finds that several lines of evidence suggest that increases in burdens of BC and tropospheric O_3 over the 20th Century have led to global mean warming of around 0.1 to 0.8°C due to BC and 0.2 to 0.4°C for O_3, with larger contributions in the northern extra-tropics (30° to 90° N). It is very likely that BC induces a net warming effect in the Arctic, and may have caused a warming as great as 0.5 to .1.4°C there, with another 0.2 to 0.4°C warming due to increases in O_3, over this period. The large response to BC in the Arctic comes about, in part, because snow and ice-covered regions exposed to sunlight (for example, summer Arctic sea-ice), due to their high reflectance, are uniquely prone to significant climate responses to BC both within the atmosphere and near-surface snow and ice. Any mixture of BC and co-emitted OC exerts a warming influence over pure snow even though some BC+OC mixtures may cause cooling at the global scale.

Similarly, glaciers and seasonal snowpack in the Himalaya/Tibetan Plateau/Hindu Kush/Karakoram region may be quite sensitive to BC. These frozen waters help provide fresh-water to a large number of people and are proximal to, though not always downwind of, large BC sources from South and East Asia. A small, but growing, body of peer-reviewed literature suggests that BC is driving significant warming and melt in this region.

The assessment of air quality impacts found that up to 4.4 million premature deaths in 2005 globally were caused by outdoor air pollution, with an additional ~1.6 million premature deaths due to respiratory diseases associated with indoor solid-fuel smoke exposure (biomass and coal). The latter is likely to be an underestimate since one of the largest effects, cardiovascular disease, is not included in the shown values due to a lack of epidemiologic studies. Hence, reducing emissions from indoor biomass combustion, which includes both PM and O_3 precursor gases, will produce considerable health benefits, as will controls on emissions leading to outdoor O_3 and PM pollution. Around 50 per cent of the world's population, 3.2 billion people, depends on solid fuels.

Changes in global ecosystem net primary productivity caused by O_3 damage have a substantial impact on carbon (C) sequestration in ecosystems and hence climate. Results from a large number of experimental studies to assess O_3 impacts on ecosystems strongly suggest that reductions in elevated O_3 concentrations could lead to substantial increases in the net primary productivity of sensitive global ecosystems and, thus, have a substantial impact on C sequestration. While most studies to date have been at the local or regional level, a global modelling study has shown that reduction in C sequestration caused by O_3 impacts on vegetation could double the effective climate impact of tropospheric O_3.

6.2 Identifying measures and assessing their impacts

The scientific evaluation concluded that current knowledge provided ample evidence that, in principle, reductions in emissions of BC and tropospheric O_3 precursors could be beneficial in both mitigating climate change and improving human well-being. Studies had thus far virtually all looked at the effects of

all emissions of a particular compound or all emissions from a particular source. However, policy-makers would benefit from information on the climate- and air-quality impacts of specific measures that might actually be put into effect, and these had not been adequately evaluated. Hence the Assessment team decided that new analyses were needed to fulfill the goal of providing policy-relevant information on BC and tropospheric O_3.

The approach of this Assessment has been to deliberately choose a set of measures that would deliver both climate and air-quality benefits. Sixteen measures were selected to optimize global climate change mitigation (See Box 5.1). It is important to realize that these measures are not necessarily the ones that would have the largest impact on regional climate in any particular location, nor cause the largest improvements in regional air quality.

The cost of implementing the measures was also not considered, nor was the relative difficulty of implementation – it was assumed that, in general, emissions controls were implemented everywhere in the world to the maximum extent technology allows. Finally, the measures are largely based on the application of emissions control technologies, and do not encompass the full range of emissions reductions that could be achieved by large-scale societal changes such as shifting to electric vehicles (e.g. Jazcilevich et al., 2011); or a more fundamental change from private vehicles to electrified public transportation; from trucks to electrified rail for cargo, in both cases assuming electricity is derived from clean sources; enhanced standards, for example fuel economy; or dramatically greater use of renewables rather than fossil fuels, including natural gas (e.g. Delucchi and Jacobson, 2011). Hence further work could usefully characterize the choices available to policy makers in particular regions based on these various other considerations aside from mitigation of global climate change through primarily technical measures.

The temperature response to the emissions reductions resulting from the full implementation of the control measures phased in

between 2010 and 2030 has been estimated. In all cases, the impacts of all co-emitted compounds are considered, even if reference is made to some measures as BC measures, for example. The method uses a combination of information from global climate models and from the assessment of the magnitude and uncertainty range of the influence of various physical processes on climate (see Appendix A.4.1). Hence the temperature results are based not only on the modeling performed specifically for this Assessment but also encompass the wider knowledge-base of prior modelling and observations, and thus are not the results of any individual model.

The health and crop-yield implications of the reductions in emissions have been calculated by taking the concentration projections from the atmospheric models and applying them with concentration-response relationships to estimate the impacts – again considering all co-emitted compounds and using total PM2.5 to assess health impacts as there is not enough information available to separate the impacts of BC from other types of particulate. Uncertainties include how the concentration of pollutants in the atmosphere responds to the emissions changes, how the concentration affect radiative forcing, health and crop yields, and how the climate responds to forcing, but do not include uncertainty in the emissions changes themselves.

The impacts of the measures are evaluated in comparison with a reference scenario that includes projected emissions based on current and planned regulations and are also compared with a low-carbon future scenario. The latter is based on the International Energy Agency's 2009 World Energy Outlook scenario for a world aiming for 450 parts per million (ppm) carbon dioxide equivalent (CO_2e) in the atmosphere in 2100, and includes measures to reduce both emissions of CO_2 and CH_4 (greenhouse gas (GHG) measures). As many of the CH_4 measures are also included in that scenario, though they are implemented substantially later in the GHG measures scenario, this Assessment refers to both the full GHG measures scenario and to the CO_2 measures scenario without the CH_4 measures.

253

Evaluating global mean temperature change, it was found that the targeted measures to reduce emissions of methane and BC could greatly reduce warming rates over the next few decades (Figure 6.1; Box 6.1). When all measures are fully implemented, warming during the 2030s relative to the present would be only half as much as in the reference scenario. In contrast, even a fairly aggressive strategy to reduce CO_2 emissions, as for the CO_2-measures scenario, does little to mitigate warming until after the next 20-30 years (Box 6.2). In fact, sulphur dioxide (SO_2) is co-emitted with CO_2 in some of the most highly emitting activities, coal burning in large-scale combustion such as in power plants, for example, that are obvious targets for reduced usage under a CO_2-emissions mitigation strategy. Hence such strategies can lead to additional near-term warming (Figure 6.1), in a well-known temporary effect (e.g. Raes and Seinfeld, 2009), although most of the near-term warming is driven by CO_2 emissions in the past. The CO_2-measures scenario clearly leads to long-term benefits however, with a dramatically lower warming rate at 2070 under that scenario than under the scenario with only CH_4 and BC measures (see Figure 6.1 and timescales in Box 6.2). Hence the near-term measures clearly cannot be substituted for measures to reduce emissions of long-lived GHGs.

The near-term measures largely target different source sectors for emissions than the CO_2 measures, so that the emissions reductions of the short-lived pollutants are almost identical regardless of whether the CO_2 measures are implemented or not, as shown in Chapter 5. The near-term measures and the CO_2 measures also impact climate change over different timescales owing to the different lifetimes of these substances. In essence, the near-term CH_4 and BC measures are effectively uncoupled from CO_2 measures examined here.

Adoption of the near-term emission control measures described in this Assessment along

---

Box 6.1: Climate impacts: Probabilities and regional variations

For simplicity, climate impacts are presented in Figures 6.1 and 6.2 as global mean temperature changes using the central values from the calculations performed for this Assessment. A full description of the regional results and the uncertainty ranges are presented in Chapters 4 and 5. The central values are based on the best estimates of radiative forcing from this Assessment and the central value of climate sensitivity recommended in IPCC-AR4 (Hegerl *et al.*, 2007): 3°C warming due to doubling of CO_2 at equilibrium, though these calculations account for the time lag of climate response to forcing. There is about a two- to three-fold uncertainty in the climate sensitivity. The range of temperature changes is calculated using a range for the warming for CO_2 doubling of 2–4.5°C, as the IPCC AR4 finds that this is likely to be the Earth's climate sensitivity, though substantially higher values are possible. In order to illustrate the implied meaning of the central value for climate sensitivity, this Assessment referred to Figure 6.1. The reference curve in Figure 6.1 shows a warming of about 2.7°C for 2070, which should be interpreted as follows: there is a 50 per cent probability the warming could be below 2.7°C, and there is a 50 per cent probability the warming could exceed 2.7°C, taking into account only the uncertainty in climate sensitivity. There is also uncertainty in the forcing by BC and other compounds. As discussed in Chapter 3, the direct component of pre-industrial to 2005 BC forcing is in the range of 0.2–0.9 W/m², with a central value of 0.45 W/m², in the results presented here – total pre-industrial to 2005 BC forcing is 0.0–1.0 W/m². The combined range of probable outcomes due to uncertainty in radiative forcing and in climate response is shown in Figure 6.1 and also in Figure 6.3 and Table 6.2. It deviates slightly from being symmetric around the central value due to the asymmetric range of BC forcing values derived as the best estimate in this Assessment (see Chapter 3).
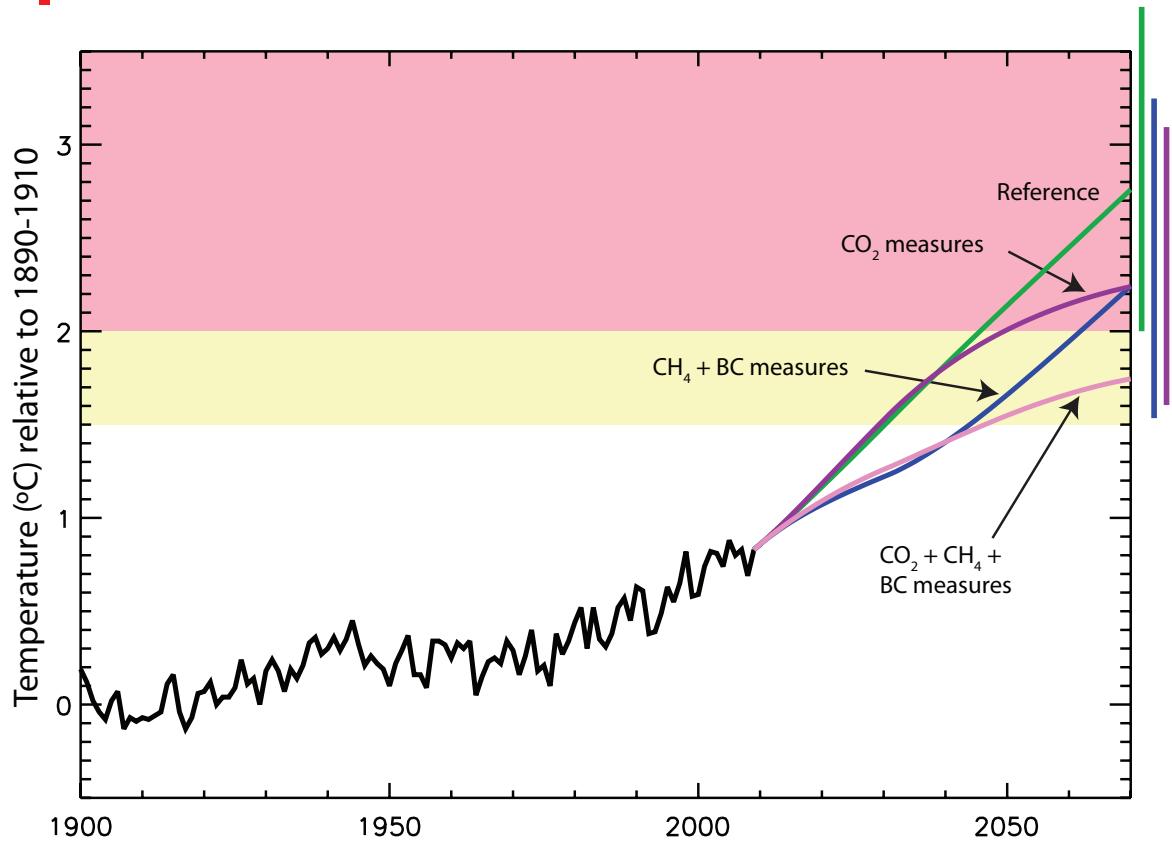
Figure 6.1. Observed temperature change through 2009 and projected temperature changes thereafter under various scenarios, all relative to the 1890-1910 mean.

Shaded backgrounds show zones beyond 1.5°C and 2°C. Observations are from (Hansen *et al.*, 2006). Results for the four future scenarios are the central values (see Box 6.1) calculated on a combination of the assessed impact of individual processes and pollutants and composition-climate modeling (see Appendix A.4.1). Uncertainty ranges for 2070 are shown in the bars on the right, and include uncertainties in radiative forcing and climate sensitivity. A portion of the uncertainties is common to all scenarios, so that overlapping ranges do not mean there is no difference (for example, if climate sensitivity is large, it is large regardless of the scenario, so temperatures in all scenarios would be towards the high end of their ranges). BC Group 1 measures include seven of the nine measures, excluding the measures on pellet stoves and coal briquettes (see Table 6.1).

with measures to reduce CO_2 emissions would greatly improve chances of keeping the Earth's temperature increase, relative to pre-industrial times, under 2°C during the next 60 years (Figure 6.1). In fact, even with the CO_2 reductions envisioned under the CO_2-measures scenario, warming would exceed 2°C around 2050, while with both the CO_2 and CH_4 reductions of the GHG-measures scenario warming exceeds 2°C in the 2060s (Figure 6.2). While emissions reductions even larger than those in the GHG-measures scenario would of course mitigate more warming, the world is not yet on a path even near the GHG-measures scenario emissions for long-lived GHGs. Actual emissions over the past decade have exceeded the most pessimistic emission scenarios.

In addition to the maximum warming, the near-term measures also greatly reduce the rate of warming over the next 30 years. The rate, rather than the magnitude, of change can be more important in determining whether plants and animals adjust to climate change. Near-term climate changes could also potentially cause changes that are irreversible in the next several generations, such as loss of land-ice or release of CH_4 or CO_2 from thawing permafrost. Thus, reducing the near-term rate of warming could decrease the risk of abrupt climate transitions.

Examining the more stringent 1.5°C threshold, the CO_2-measures scenario curve exceeds that warming by 2030, whereas the near-term measures proposed here delays the exceed-
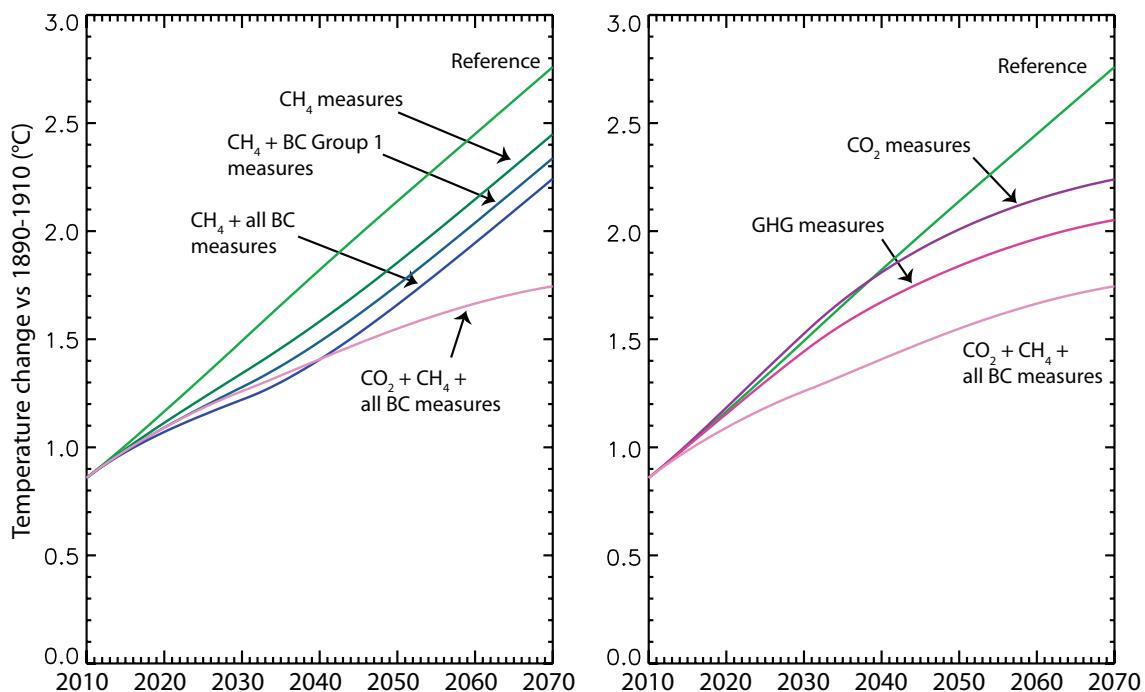
Figure 6.2. Projected changes in global mean temperatures under various scenarios relative to the 1890-1910 average.

Calculations use the same techniques as in Figure 6.1. BC Group 1 measures include seven of the nine measures, excluding the measures on pellet stoves and coal briquettes (see Table 6.1). Methane measures are the more stringent measures analyszed in this Assessment rather than those under the GHG-measures scenario, which both achieve less emission reduction and are implemented slightly later.

ance by about 15-20 years, until around 2045. Again, while substantially deeper early reductions in CO_2 emissions than those in the CO_2-measures scenarios could also delay the crossing of the 1.5°C temperature threshold, such reductions would undoubtedly be more difficult for society to achieve. Hence adoption of the near-term measures analyzed in this Assessment would increase the chances for society to keep the Earth's temperature increase below 1.5°C for the next 40 years if these measures were phased in along with CO_2 reductions. The required CO_2 reductions could be achieved over the coming decades at a relatively aggressive, but not extreme, pace.

In addition to mitigation of near-term global warming, these measures have been found to potentially increase world food supplies substantially, and reduce global premature deaths due to outdoor air pollution (Figure 6.3; Chapter 5). It is virtually certain that reductions in CH_4 emissions through technological measures would bring about

a substantial reduction in near-term warming. It is also very likely that targeted reductions in emissions of products of incomplete combustion, including BC, as a result of the measures examined here would lead to a reduction in warming as well, though the uncertainties are larger than for the CH_4 measures (Figure 6.3; Chapters 3 and 5). Most likely, the global mean climate benefits of the BC Groups 1 and 2 measures examined here are less than those of the CH_4 measures. Benefits resulting from reduced disruption of regional climate (Arctic sea ice retreat; Asian monsoon; Himalayan-Tibetan glacier/snow-pack melting) may be quite important, however. Turning to air quality, the benefits in reduced crop-yield losses due to BC measures, which occur due to reduced co-emissions of O_3 precursors, are comparable to those from the reduced CH_4, while benefits in avoided premature deaths are much larger from the BC measures. For example, considering reductions in premature deaths, mitigating CH_4 emissions contributes

256

Box 6.2: Timescales: Comparing the global mean climate impact of controls on short-lived pollutant emissions with controls on CO_2

The longer timescales of climate response to emission scenarios targeting CO_2 relative to those targeting short-lived pollutants comes about because of both socio-economic and physical factors. These include the much longer lifetime of many CO_2 emission sources, such as power plants, in comparison with many sources of short-lived pollutants, such as vehicles or cookstoves (even though these shorter-lived sources have a wide range of equipment lifetimes). Additionally, while there are few proven technologies to limit emissions of CO_2 while allowing the underlying activity to continue, such technologies are readily available for short-lived pollutants (e.g. diesel particulate filters). Hence while immediate, large reductions in CO_2 emissions would lead to substantially greater mitigation of near-term warming than in the CO_2-measures scenario examined here, such reductions are widely considered unlikely. The physical behaviour of CO_2 is also fundamentally different from the short-lived pollutants, with a very long atmospheric residence time for CO_2 leading to slower responses of atmospheric concentrations to emissions changes. Furthermore, much of the early impact of CO_2 emissions reductions is likely to be offset by reductions in cooling sulphate aerosols. While these factors lead to the failure of the plausible CO_2-reduction strategy examined here to substantially impact global mean climate change during the next few decades, they also mean that a delay in reducing emissions of CO_2 beyond that envisioned under the CO_2-measures scenario, under which global total CO_2 emissions peak during 2015-2020 and decline ~2 per cent per year thereafter (anthropogenic emissions decrease by 2.2 per cent of 2000 levels per year over 2020-2050, equivalent to 1.9 per cent of 2020 levels), would in turn delay the eventual mitigation obtained through such reductions so that they would take place largely after the time-frame examined here. For example, mitigation of 0.15°C due to CO_2 measures takes place only around 2050 (Figure 6.1) under the CO_2 measures scenario; 30 years after emissions begin to decline rapidly. The influence of the CO_2 reductions grows rapidly, however, so that they mitigate roughly 0.5°C by 2070. Hence a delay of 20 years in implementation of those CO_2 reductions would mean that only ~0.15°C of warming mitigation relative to the reference scenario would be achieved within the 2070 timeframe examined here. Thus delayed CO_2 measures plus all the near-term measures examined here would lead to warming of about 2.1°C in 2070 rather than the 1.75°C shown in Figure 6.1. Conversely, a delay in reducing emissions of short-lived species would have a large impact on near-term warming rates, but little effect on 2070 temperatures (see Figure 5.12).

about 2 per cent, BC Group 1 (see Table 6.1) measures about 72 per cent, and BC Group 2 measures about 26 per cent of the global total reduction in premature mortality from PM and O_3 concentrations. The bulk of the reduction in early deaths come about from lowering the abundance of PM rather than O_3, which is why the BC measures, which affect both, have a larger impact than the CH_4 measures, which only affect O_3. The economic valuation of the avoided damages is roughly US$4–32 billion annually from the avoided crop-yield losses using world market prices and US$2–10 trillion each year from the avoided health damages using a range of assumptions for the valuation of deaths in different countries – a uniform global value or a value tied to gross domestic product (GDP) in each country (see Chapter 4). The avoided climate damage may be substantial as well, but is difficult to quantify, especially for the large regional disruptions of climate discussed in this Assessment. The valuation of human welfare is the larger of the quantified impacts, though the value of food security for small farmers and even sometimes for nations is clearly not well-represented by an evaluation based on world market prices. Natural and managed ecosystems other than crops will also be affected by these measures, leading to additional benefits in improved ecosystem services. There will also be non-

Global Impacts of Additional Emissions Controls on Methane and Products of Incomplete Combustion
1: CH$_4$ measures, 2: CH$_4$+BC Group 1 measures, 3: CH$_4$+ all BC measures
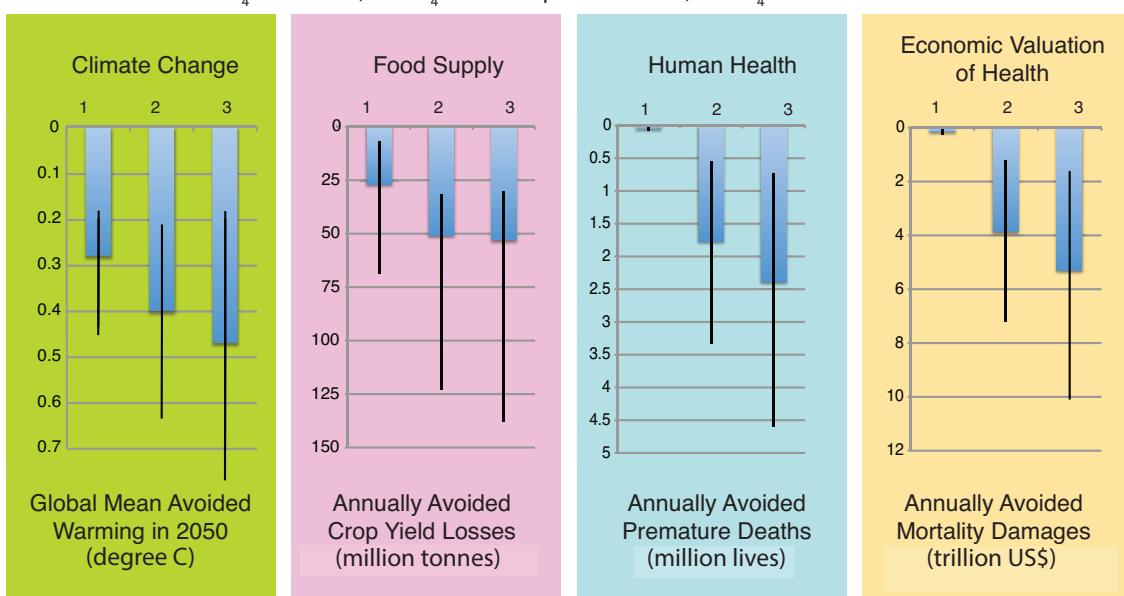
Figure 6.3. Global impacts of the additional emissions controls on methane and products of incomplete combustion (including BC, OC and CO) examined here.

Benefits are shown with increasing values moving downward to emphasize that these are reductions in damage. Crop-yield losses are summed values for wheat, rice, soybean and maize. Uncertainties include: climate change – range from uncertainty in radiative forcing and climate sensitivity, food supply – range from impacts calculated using O$_3$ changes from different models and uncertainty in exposure-response relationship, human health – uncertainty in concentration-response relationships and using results from different models, economics – range using uniform valuation of premature deaths and income-adjusted valuation and results from different models. The results for BC Group 1 measures include five of the seven measures – excluding the measures on pellet stoves and coal briquettes. See Table 6.1 and Chapter 5 for further details.

mortality health benefits (morbidity). Hence the multiple benefits of the emission-reduction measures are even broader than those analyzed here.

Examining the projected impacts by region reveals that all the land areas of the world are projected to reach temperatures at least 2°C above their 1890–1910 means by 2070 under the reference-scenario emissions trends (Figure 6.4; Table 6.2). The largest increases in surface temperature are over North America and Europe, but the amount of warming is relatively similar across the regions. In contrast, damage to agriculture and human health are projected to decrease strongly over North America and Europe due to projected reductions in air pollution precursor emissions while changing minimally over Latin America and the Caribbean and Africa. Over East Asia,

deaths are projected to decrease substantially due to reductions in PM$_{2.5}$ in some areas, but O$_3$ amounts are projected to increase, leading to significant additional crop-yield losses. Over South, West and Central Asia, health and agricultural damage due to increased O$_3$ are projected to increase dramatically through 2030, as are PM$_{2.5}$-related premature mortality due to outdoor air pollution.

Application of all of the recommended measures considered here leads to substantial reductions in all adverse impacts in all regions (Figure 6.4). The CH$_4$ and BC measures reduce warming very sharply through 2030, eliminating ~50 per cent of the 2010–2030 increase. Even at 2070, warming in all regions is substantially less than the 2010–2070 warming according to the reference scenario, but only about 25 per

258

Table 6.2. Numerical values and ranges (in brackets) for impacts shown in Figure 6.4.

	Region	Warming (°C)	Crop yield losses (million tonnes)	Premature deaths (millions)	Mortality damages (US$ trillions)
Reference					
	North America and Europe	2.6 (1.6 to 3.7)	-43 (-11 to -97)	-0.36 (-0.09 to -0.77)	-2.5 (-0.7 to -5.2)
	Latin America and the Caribbean	2.0 (1.2 to 2.9)	0.9 (0.4 to 1.7)	-0.00 (-0.00 to -0.02)	-0.0 (-0.0 to 0.1)
	Africa	2.2 (1.3 to 3.1)	0.2 (0.0 to 0.7)	0.03 (0.00 to 0.07)	0.0 (-0.0 to 0.1)
	East, Southeast Asia and the Pacific	2.2 (1.3 to 3.1)	25 (2.9 to 74)	-0.32 (-0.01 to -1.07)	-1.0 (-0.1 to -3.1)
	South, West and Central Asia	2.5 (1.5 to 3.5)	10 (4 to 42)	0.85 (0.18 to 1.86)	1.5 (0.3 to 3.2)
All measures					
	North America and Europe	-0.9 (-0.3 to -1.3)	-17 (-7.9 to -22)	-0.11 (-0.03 to -0.23)	-0.6 (-0.2 to -1.0)
	Latin America and the Caribbean	-0.5 (-0.2 to -0.7)	-3.6 (-1.4 to -4.8)	-0.04 (-0.01 to -0.08)	-0.2 (-0.1 to -0.3)
	Africa	-0.6 (-0.2 to -0.8)	-1.7 (-1.0 to -2.8)	-0.22 (-0.06 to -0.48)	-0.4 (-0.1 to -0.8)
	East, Southeast Asia and the Pacific	-0.6 (-0.3 to -0.9)	-18 (-4.1 to -23)	-0.88 (-0.28 to -1.62)	-2.2 (-0.7 to -4.0)
	South, West and Central Asia	-0.8 (-0.3 to -1.1)	-12 (-5.4 to -16)	-1.12 (-0.32 to -2.28)	-2.0 (-0.6 to -4.0)

Note: Impacts and uncertainties are the same as in Figure 6.3, but are regional. For the reference case, warming is relative to the 1890-1910 mean, while other impacts are relative to 2005. For the measures case, all impacts are relative to the reference. Negative values indicate a reduced detrimental impact, or benefit, as a result of implementing the measures.
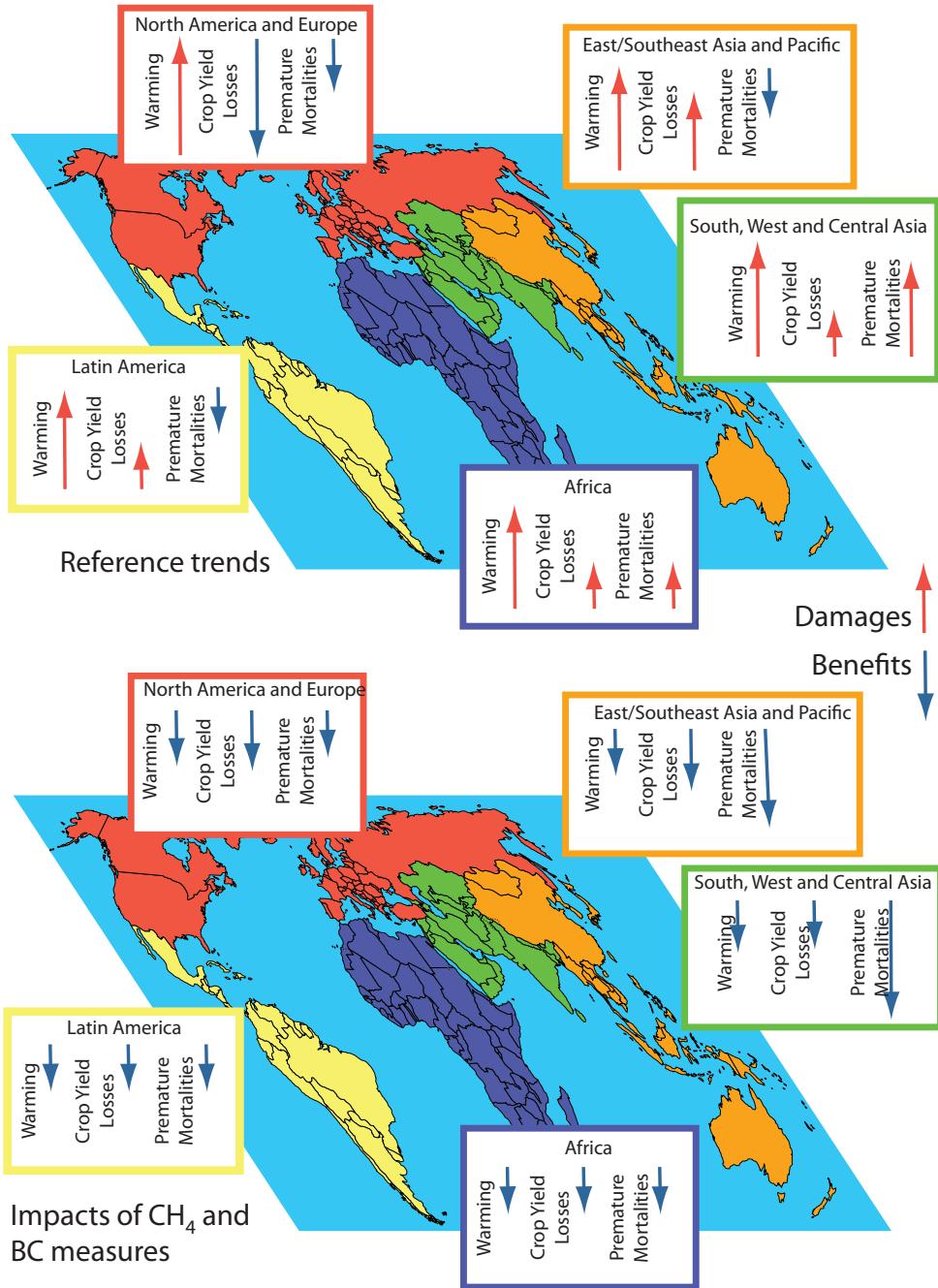
Figure 6.4. Comparison of several key impacts by region for the reference emissions trends with the effects of the CH_4 and BC measures examined here (relative to the reference).

The reference includes emissions changes in short-lived compounds from 2005 to 2030 and in CO_2 from 2005 through 2070. Emission measures are applied to CH_4 and products of incomplete combustion through 2030 only. Climate changes are the regional land-area averages and are given for 2070 to allow the climate to respond to emission changes in the early 21st century, while agricultural and mortality effects are shown for 2030 but would persist thereafter if emissions of short-lived compounds remained constant. Arrow lengths show the relative magnitude of changes in the different regions (compared with the maximum change in that impact), with the minimum length set to one-quarter of the maximum for visual clarity (see Table 6.2 for numerical values). Black carbon Group 1 measures include five of the seven measures, excluding the measures on pellet stoves and coal briquettes.

Integrated Assessment of Black Carbon and Tropospheric Ozone

cent less as long-term warming due to CO_2 is not alleviated by the measures.

The measures lead to greatly improved air quality, with substantial benefits to crop yields and decreased premature deaths, especially in Asia. The benefits of the measures are large enough that virtually all the adverse trends in impacts of outdoor air pollution on agricultural yields and human health are reversed and turned into improvements relative to 2005. The lone exception is crop yields in East and Southeast Asia and the Pacific. Even in that case, the benefits of full implementation of 14 of the 16 measures are quite large, although the reduction in yield losses of 18 million tonnes/yr does not fully overcome the baseline trend of 25 million tonnes/yr additional losses under the reference scenario.

In terms of avoided premature deaths in the all-measures case compared with the reference scenario, about 47 per cent of the avoided deaths occur in South, West, and Central Asia, 37 per cent in East Asia, Southeast Asia and Pacific, 9 per cent in Africa, 5 per cent in North America and Europe, and 2 per cent in Latin America and Caribbean. The avoided crop yield losses (in tonnage) show a different pattern, with the largest benefits again in Asia (35 per cent in East Asia, Southeast Asia and Pacific, and 28 per cent in South, West and Central Asia), but benefits that are nearly as large in North America

and Europe (26 per cent). Benefits in Latin America and Caribbean amount to 8 per cent, and are small in Africa (3 per cent).

The comparison in tonnage or valuation reflects the current production levels in each region as well as the change in O_3 exposure. Looking instead at relative-yield increases shows benefits that are typically largest in South, West and Central Asia where the average of the results from the two models are 7 per cent for soy and maize, 4 per cent for wheat and 2 per cent for rice. Yields also increase by a large amount in East Asia, Southeast Asia and the Pacific in the all-measures case, by 4 per cent for soy and maize, 3 per cent for wheat and 1 per cent for rice. Benefits are 1–2 per cent for all crops in Africa, Latin America and the Caribbean, and North America and Europe (with the exception of 3 per cent for soy and 0 per cent for rice in Latin America and the Caribbean). It is stressed that the analyses include only the direct effect of changes in atmospheric composition on health and agriculture though changes in exposure to pollutants. As such, they do not include the benefits that avoided climate change would have on human health and agriculture due to reduced disruption of precipitation patterns, reduced frequency of heatwaves, etc. Furthermore, even the
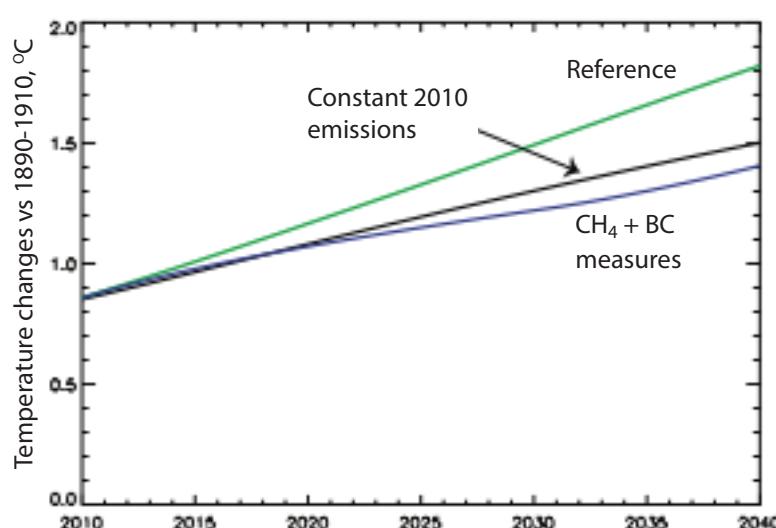
Figure 6.5. Projected temperature changes as in Figure 6.2, but also showing the warming that would occur due to constant year 2010 emissions (not constant 2010 concentrations).

direct influence on crops was only an esti-mate for four staple crops, and neither the impacts on leafy crops or grasslands nor on food quality were included, making the esti-mates conservative.

Impacts of the measures vary from region to region depending upon the local mix and size of emissions changes, the local back-ground state of the atmosphere, and particu-lar local physical processes such as rainfall rates that remove some pollutants from the atmosphere and snow cover. However, map-ping impacts reveals that the impacts of the measures on temperature change are broadly felt relative to the air quality impacts. The latter are much more localized near the re-gions where emission changes take place, indicating that those areas that control their own regional emissions will be the greatest recipients of the associated human-health and food-supply benefits. In addition, re-gional changes in precipitation are closely associated with temperature changes in the atmosphere that are caused by BC's absorp-tion of sunlight. Shifts in traditional rainfall and snowfall patterns take place under the reference scenario, and amelioration of these shifts due to BC measures will therefore be generally aligned with areas where emissions are controlled, as discussed in Chapters 4 and 5. Hence the benefits of avoided disrup-tions to regional water supplies will also be felt most strongly in those areas that control their regional emissions, although tropical areas may be affected by hemispheric-scale air-pollutant emissions. This is likely to be es-pecially true in areas where glacial meltwater is important due to both the influence of regional atmospheric forcing on precipitation patterns and the direct influence of BC dark-ening on snow and ice melting.

Large impacts of the measures examined here were also seen for the Arctic despite the minimal amount of emissions currently tak-ing place there. This occurs due to the high sensitivity of the Arctic both to pollutants that are transported there from remote sources and to radiative forcing that takes place in areas of the northern hemisphere outside the Arctic. The 16 measures examined here,

including the measures on pellet stoves and coal briquettes, reduce warming in the Arctic by 0.7°C (range 0.2 to 1.3 °C) at 2040. This is a large portion of the 1.1°C (range 0.7 to 1.7 °C) warming projected under the reference scenario for the Arctic, and hence implemen-tation of the measures would be virtually certain to substantially slow, but not halt, the pace of Arctic climate change.

We recognize that complete implementation of all the measures analyzed here is improb-able. Indeed, the reductions achieved under these measures were remarkable, with ap-plication of all near-term measures examined essentially eliminating additional warming due to emissions changes between 2010 and 2030 in the reference scenario, leaving slightly less warming than the residual warming that would be experienced were emissions to re-main perpetually at 2010 levels (a different scenario than what IPCC-AR4 referred to as 'committed', which was a constant present-day concentration scenario; Figure 6.5). In other words, the application of these emis-sions reductions slightly more than offsets the impact of economic and population growth on all emissions, including CO_2, that leads to the increased warming in the reference case relative to constant 2010 emissions. However, unlike some of the proposed technological measures to control emissions of CO_2, carbon capture and storage, for example, the mea-sures examined here draw on already mature technologies with demonstrable results at scale in the real world. Hence the results provide a target that society could decide to aim for with a reasonable chance of success on the technological side. Many of the structural changes examined here present formidable hurdles to implementation, however. These include costs for measures such as the diesel particle filters (DPFs) or CH_4 capture tech-nologies, enforcement for measures such as the ban of the open burning of agricultural waste or the elimination of high-emitting ve-hicles, and the challenge of providing modern fuels to hundreds of millions of people using traditional cookstoves. As such, achieving the benefits of the suggested measures would not be an easy task. Nonetheless, the magnitude of those benefits in terms of avoiding danger-

262

ous climate change, saving millions of lives each year and increasing worldwide supply of staple crops by millions of tonnes each year are powerful incentives for their adoption. There are substantial economic benefits as well, with US$ trillions in annually avoided mortality damage, and large reductions in economic losses from O_3 exposure to crops and from avoided climate change.

This Assessment has specifically analyzed the impacts of 16 measures that were found to provide benefits for both climate and air quality. These include seven measures to reduce CH_4 emissions and nine BC measures that reduce the emissions of products of incomplete combustion, including OC and CO, as well as BC (see Table 6.1). As noted above, the climate benefits of the CH_4 measures are virtually certain, while the BC measures are quite likely to be beneficial in terms of global mean climate but have larger impacts on regional scales. The Assessment also makes the point that while all these measures have a net effect of mitigating global warming, the relative impacts of individual BC measures on climate, health and ecosystems can vary considerably as these are strongly influenced by the mixture of co-emitted compounds.

In particular, the warming effect of BC and O_3 and the compensating cooling effect of OC, introduces large uncertainty in the net effect of some BC measures on global warming (Figure 6.3). Uncertainty in the impact of BC measures is also larger than that for CH_4 because BC and OC can influence clouds, leading to multiple effects on climate that are not fully understood. This uncertainly in global impacts is particularly large for the measures concerning biomass cookstoves and open burning of biomass as these have a low BC/OC ratio in comparison with fossil fuel BC sources such as diesel vehicles or brick kilns. A large portion of the BC reductions in the Group 1 measures come from diesel vehicles, while the largest BC reductions in the Group 2 measures come from the cookstoves measure (see Table 6.1). Additionally, there is a larger ozone response to the Group 1 than the Group 2 measures, and the ozone forcing has less uncertainty than aerosol forcings. Hence there

is greater uncertainty in the Group 2 impacts on global warming (Figure 6.2). There is even a small possibility that the Group 2 measures lead to global warming rather than cooling, though the best estimate and indeed most of the estimated range is that these lead to substantial cooling.

On the other hand, there is higher confidence that BC measures have large impacts on human health through reducing concentrations of inhalable particles, on crop yields through reduced O_3, and on climate phenomena such as tropical rainfall, monsoons and snow-ice melt. These regional impacts are largely independent of the measures' impact on global warming. In fact, biomass cookstoves and open biomass burning can have much larger effects than fossil fuels regionally. With respect to reducing regional impacts, all of the BC measures are likely to be significant.

The near-term measures presented here, which provide the large benefits to human health and agricultural productivity, rely on tested technologies and many of their impacts have been evaluated against observations. In combination with CO_2 control measures, they are likely to keep warming below 2°C for the next 60 years, though not below the more ambitious 1.5°C (Figure 6.1). In contrast, keeping below the 2°C level of warming is extremely unlikely without both measures to control emissions of short-lived pollutants and near-term measures to control emissions of long-lived pollutants, primarily CO_2. Even with the CO_2 emissions controls and the near-term measures, global mean temperatures would still have a substantial chance of passing 2°C towards the end of the century, indicating that further reductions could be required if that target, or the more stringent 1.5°C target, are not to be exceeded (e.g. Ramanathan and Xu, 2010).

The global climate benefits of the measures examined in this Assessment would be felt by all people, while the benefits to human development would be felt most strongly in the regions where emissions controls were adopted. Hence there are a variety of incentives for surmounting the hurdles to adoption of these measures.

263

A large number of case studies have been presented which describe the successful implementation of the mitigation measures included in the analysis (Chapter 5). Examples are given from across the world, in both developed and developing countries. Efforts to scale up, replicate and expand the implementation of the selected measures could include capacity building, public-private financing, technology support, regional cooperation and agreements and community empowerment, with different efforts undertaken in various regions or forums depending on the goals foremost in those areas. Such efforts could help overcome the various barriers such as lack of adequate infrastructure and technical capacity, markets and financing, and regulations that have impeded the more widespread adoption of CH_4 and BC emissions control technologies.

In most countries, mechanisms are already in place, albeit at different levels of maturity, to address air-pollution problems, responding to public concern. Improved international governance and finance mechanisms could accelerate the adoption of the key mitigation measures at multiple scales, from sub-national through national to regional. In particular international co-ordination building on existing regional agreements such as the Convention on Long-Range Transboundary Air Pollution or the Malé Declaration on Control and Prevention of Air Pollution and its Likely Transboundary Effects may be an effective approach in the near-term. Black carbon and O_3 may also be considered as part of other environment, development and energy initiatives such as bilateral assistance, the World Bank Energy Strategy, the United Nations Environment Programme and United Nations Development Programme Poverty and Environment Initiative, the Global Cookstove Alliance, and the Global Methane Fund. International financing and technology transfer would facilitate more rapid action especially in developing countries with multiple pressing needs. Any strengthened governance regime would be most effective if it included financing or increased cooperation across parts of government that was targeted specifically at pollution mitigation to simultaneously maximize climate and air quality benefits.

References

Delucchi, M. A., and Jacobson, M. Z. (2011). Providing all Global Energy with Wind, Water, and Solar Power, Part II: Reliability, System and Transmission Costs, and Policies. Energy Policy 39, 1170–1190.

Hansen, J., Sato, M., Ruedy, R., Lacis, A., and Oinas, V. (2000). Global warming in the twenty-first century: An alternative scenario. Proc. Natl. Acad. Sci. 97, 9875-9880.

Hansen, J., Sato, M., Ruedy, R., Lo, K., Lea, D. W., and Medina-Elizade, M. (2006). Global temperature change. Proc. Natl. Acad. Sci. 103, 14288-14293.

Hegerl, G. C., Zwiers, F. W., Braconnot, P., Gillett, N. P., Luo, Y., Marengo-Orsini, J. A., Nicholls, N., Penner, J. E., and Stott, P. A. (2007). Understanding and Attributing Climate Change in: Intergovernmental Panel on Climate Change Fourth Assessment Report. Edited by: Solomon, S. Cambridge, New York.

Jacobson, M. Z. (2010). Short-term effects of controlling fossil-fuel soot, biofuel soot and gases, and methane on climate, Arctic ice, and air pollution health. J. Geophys. Res. 115, D14209, doi:10.1029/2009JD013795.

Jazcilevich, A. D., Reynoso, A. G., Grutter, M., Delgado, J., Ayala, U. D., Lastra, M. S., Zuk, M., Oropeza, R. G., Lents, J. and Davis, N. (2011). An evaluation of the hybrid car technology for the Mexico Mega City. Journal of Power Sources, 196, 5704-5718.

Raes, F., and Seinfeld, J. H. (2009). New Directions: Climate change and air pollution abatement: A bumpy road. Atmos. Env. 43, 5132–5133.

Ramanathan, V., and Xu, Y. (2010). The Copenhagen Accord for limiting global warming: Criteria, constraints, and available avenues. Proc. Natl. Acad. Sci. 107, 8055–8062.

Shindell, D. T., Levy II, H., Schwarzkopf, M. D., Horowitz, L. W., Lamarque, J.-F., and Faluvegi, G. (2008). Multi-model Projections of Climate Change From Short-lived Emissions Due To Human Activities. J. Geophys. Res. 113, D11109, doi:10.1029/2007JD009152.

West, J. J., Fiore, A. M., Naik, V., Horowitz, L. W., Schwarzkopf, M. D., and Mauzerall, D. L. (2007). Ozone air quality and radiative forcing consequences of changes in ozone precursor emissions. Geophys. Res. Lett. 34, L06806, doi:10.1029/2006GL029173.
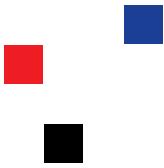
Acronyms and abbreviations

AAOD	Absorbing aerosol optical depth
ABC	Atmospheric Brown Cloud
ACS	American Cancer Society
ADB	Asian Development Bank
AERONET	Aerosol Robotic Network
AIDS	Acquired Immunodeficiency Syndrome
AIRPET	Asian Regional Air Pollution Research Network
ALOS	Advanced Land Observation Satellite
ALRI	Acute Lower Respiratory Infections
AM0016	Clean Development Mechanism methodology: Greenhouse gas mitigation from improved animal waste management systems in confined animal feeding operations
AMS-I.D	Clean Development Mechanism methodology: Grid connected renewable electricity generation
AMS-III.E	Clean Development Mechanism methodology: Avoidance of methane production from biomass decay through controlled combustion
AOD	aerosol optical depth
AOT40	Atmospheric exposure over a threshold of 40 ppm
ARTEMIS	Assessment and Reliability of Transport Emission Models and Inventory Systems
ASEAN	Association of Southeast Asian Nations
AVNIR-2	Advanced Visible and Near Infrared Radiometer type 2
AWD	alternate wetting and drying
AWMS	animal waste management system
BC	black carbon
Bcf	billion cubic feet
BENLESA	Bioenergía de Nuevo León, S. A. de C. V.
BNM	Basa njengo Magogo
BrC	brown carbon
BRT	bus rapid transport
C	carbon
CAFO	confined animal feeding operation
CAGR	compound annual growth rates
CAI	Clean Air Initiative
CALIPSO	Cloud-Aerosol Lidar and Infrared Pathfinder Satellite Observations
CAM	Metropolitan Environmental Commission
CBM	coal bed methane
CC	climatic changes
CCN	cloud condensation nuclei
CDM	Clean Development Mechanism
CER	Certified Emissions Reduction
CERES	Clouds and the Earth's Radiant Energy System
CH_4	methane
CHIMERE	Chemistry transport model maintained by the Laboratory of Dynamic Meteorology at the École Polytechnique (France)
China I/II/III/IV	China emission standard I, II, III and IV
CLRTAP	Convention on Long-Range Transboundary Air Pollution
CMM	coal mine methane
CNG	compressed natural gas

CO	carbon monoxide
CO_2	carbon dioxide
CO_2e	carbon dioxide equivalent
COP7	Seventh Conference of the Parties to the UNFCCC
COP15	Fifteenth Conference of the Parties to the UNFCCC
COPERT	Computer Programme to Calculate Emissions from Road Transport
CP	crop production
CPL	crop production loss
CRF	concentration-response function
CRT	Continuously Regenerating Trap
CRU	Climate Research Unit at the University of East Anglia (UK)
CTM	chemistry-transport model
CVD	cardiovascular disease
DEAT	Department of Environmental Affairs and Tourism (South Africa)
DEDE	Department of Alternative Energy Development and Efficiency (Thailand)
DMS	dimethylsulphide
DNA	deoxyribonucleic acid
DPF	diesel particle filter
EANET	Acid Deposition Monitoring Network in East Asia
ECE_{15}	The United Nations Economic Commission for Europe specification for urban driving cycle simulation
ECHAM	European Centre Hamburg Model
ECHAM-HAMMOZ	A fully coupled photochemistry-aerosol-climate model, composed of the general circulation model (GCM) ECHAM5, the tropospheric chemistry module MOZ, and the aerosol module HAM
ECHAM5-HAMMOZ	See ECHAM-HAMMOZ
EC-JRC	European Commission Joint Research Centre
ECMWF	European Centre for Medium-range Weather Forecast
EDGAR	Emissions Database for Global Atmospheric Research
EFMA	European Fertilizer Manufacturers Association
EL	economic loss
EMEP	European Monitoring and Evaluation Programme
ENERCON	National Energy Conservation Centre (Pakistan)
EPA	see US EPA
EPE	El Paso Electric
ERA40	ECMWF Re-analysis
EU	European Union
EUDC	Extra Urban Driving Cycle
EURO III/IV/VI	European emissions standards III, IV and VI
FACE	Free Air Concentration Enrichment
FAO	Food and Agriculture Organization of the United Nations
FAOSTAT	Food and Agriculture Organization Corporate Statistical Database
FASST	Fast Scenario Screening Tool for global air quality and instantaneous radiative forcing
GAINS	Greenhouse Gas and Air Pollution Interactions and Synergies
GAW	Global Atmospheric Watch Programme of WMO
GCM	general circulation model
GDP	gross domestic product
GEF	Global Environment Facility
GEO-LAC	Global Environmental Outlook: Latin America and the Caribbean
GFED	Global Fire Emissions Database
GGFR	Global Gas Flaring Reduction

GHG	greenhouse gas
GIOVANNI	GES-DISC (Goddard Earth Sciences Data and Information Services Center) Interactive Online Visualization and Analysis Infrastructure
GIS	geographic information system
GISS	Goddard Institute for Space Studies
GLOF	glacier lake outburst flood
GOME	Global Ozone Monitoring Experiment
GPP	global primary production
GRACE	Gravity Recovery and Climate Experiment
GTP	Global Temperature Potential
GWP	Global Warming Potential. GWP_{20} is GWP over a 20 year timescale. GWP_{100} is GWP over a 100 year timescale
HBEFA	Handbook Emission Factors for Road Transport
HC	hydrocarbon
HCHO	formaldehyde
HDV	heavy duty vehicle
HIV	human immunodeficiency virus
HKH	Hindu Kush – Himalaya
HNO_3	nitric acid
HO_x	hydrogen oxides
HTAP	Hemispheric Transport of Air Pollution
HYDE	History Database of the Global Environment
IAP	indoor air pollution
IEA	International Energy Agency
IEA CCC	IEA Clean Coal Centre
IFA	International Fertilizer Industry Association
IIASA	International Institute for Applied System Analysis
IMO	International Maritime Organization
IMPROVE	Interagency Monitoring of Protected Visual Environments
INDOEX	Indian Ocean Experiment
INTEX-B	Intercontinental Chemical Transport Experiment Phase B
IPCC	Intergovernmental Panel on Climate Change
IPCC TAR	IPCC Third Assessment Report
IPCC AR4	IPCC Fourth Assessment Report
IPCC AR5	IPCC Fifth Assessment Report
IrDA	Infrared Data Association
IRRI	International Rice Research Institute
ITDP	Institute for Transportation and Development Policy
JJA	June-July-August
JRC	See *EC-JRC*
LDV	light duty vehicle
LEZ	Low Emissions Zone
LFG	landfill gas
LIDAR	Light Detection And Ranging
LLGHG	long-lived greenhouse gas
LPG	liquefied petroleum gas
LRTAP	Long-Range Transboundary Air Pollution
M7/M12	Average mean growing season indices, where 7 or 12 refers to the daylight hourly averaging period
MAM	March-April-May
MDB	multilateral development banks
MEPC	Marine Environment Protection Committee

MISR	Multi-angle Imaging Spectroradiometer
MIT	Massachusetts Institute of Technology
$MMTCO_2E$	million metric tons of carbon dioxide equivalent
MODIS	Moderate-resolution Imaging Spectroradiometer
MOPITT	Measurements of Pollution in the Troposphere
MOZART	Model for Ozone and Related Chemical Tracers
MK	Marquez Kiln
MSS	Multispectral Scanner System
MW	Megawatts
N_2O	nitrous oxide
NAAQS	National Ambient Air Quality Standards (United States)
NAMA	Nationally Appropriate Mitigation Action
NASA	National Aeronautics and Space Administration (United States)
NCAR	National Center for Atmospheric Research (United States)
NCLAN	National Crop Loss Assessment Programme
NCO-P	Nepal Climate Observatory-Pyramid
NH	northern hemisphere
NH_3	ammonia
NMHC	non-methane hydrocarbons
NMVOC	non-methane volatile organic compounds
NO	nitric oxide
NO_3^-	nitrate
NOAA	National Oceanic and Atmospheric Administration (United States)
NO_X	nitrogen oxides
O	oxygen (atom)
O_3	ozone
OBD	On-Board Diagnostic System
OC	organic carbon
ODA	overseas development assistance
OECD	Organisation for Economic Co-operation and Development
OH	hydroxyl
OM	organic matter
OMAERUV	OMI Near-UV Aerosol Extinction and Absorption Optical Depth Daily L3 Global 1x1 deg Grid
OMC	oil marketing companies
OMI	Ozone Monitoring Instrument
PBL	Netherlands Environmental Assessment Agency (Planbureau voor de Leefomgeving)
PD	present day
PDD	project design documents
PEMEX	Petroleos Mexicanos; Mexico's state oil company
PI	pre-industrial
PM	particulate matter. $PM_{2.5}$ has a diameter of 2.5µm or less. PM_{10} has a diameter of 10µm or less
PMF	positive matrix factorization
POC	primary organic carbon
POM	particulate organic matter
PP_{2005}	producer prices for the year 2005
PPP	purchasing power parity
PROAIRE	Program to Improve Air Quality in the Valley of Mexico
PUCCINI	Physical Understanding of Composition-Climate Interactions and Impacts
PVC	polyvinyl chloride

RAINS	Regional Air Pollution Information and Simulation
RAIR	Relative Annual Intercontinental Response
RCP	representative concentration pathway
REDD	Reducing Emissions from Deforestation and Degradation
RERIC	Regional Energy Resources Information Center
RETRO	Reanalysis of the Tropospheric Chemical Composition Over the Past 40 Years
RF	radiative forcing
RMB	renminbi; the official currency of China
RS	rice straw
RYL	relative yield loss
SADC	Southern African Development Community
SAGUAPAC	Bolivian waterworks company
SCC	social cost of carbon
SCIAMACHY	Scanning Imaging Absorption Spectrometer for Atmospheric Cartography
SD	standard deviation
SEMARNAT	Ministry of Environment and Natural Resources (Mexico)
SH	southern hemisphere
SIMEPRODE	System for Ecological Waste Management and Processing
SIMEPRODESO	Monterrey, Mexico: Landfill Gas Energy Project: Metropolitan Solid Waste Processing System
SLCF	short-lived climate forcers
SLE	sea-level equivalent
SO_2	sulphur dioxide
SO_4^{2-}	sulphate
SOA	secondary organic aerosols
SON	September-October-November
S-R	source-receptor
SRES	Special Report on Emissions Scenarios
SRI	System of Rice Intensification
SST	sea-surface temperature
STAR	Science to Achieve Results
STOCHEM	UK Meteorological Office Global Three-Dimensional Lagrangian Chemistry model
SUM06	a cumulative index of ozone concentrations over a threshold of 0.06 ppm
tC	tonnes of carbon
TCEQ	Texas Commission on Environmental Quality
TERI	The Energy Resource Institute
THC	total hydrocarbon
TO	tropospheric ozone
TOA	top-of-the-atmosphere
TRACE-P	Transport and Chemical Evolution over the Pacific
ULSD	ultra-low sulphur diesel
ULSFU	ultra-low sulphur fuel
UN	United Nations
UNDP	United Nations Development Programme
UNECE	United Nations Economic Commission for Europe
UNEP	United Nations Environment Programme
UNFCCC	United Nations Framework Convention on Climate Change
US	United States
USA	United States of America
US EPA	United States Environmental Protection Agency
USD	United States Dollar
USSR	Union of Soviet Socialist Republics
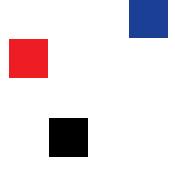
VA	value added
VAT	value-added tax
VOC	volatile organic compound
VSL	value of a statistical life
W126	a seasonal ozone exposure index developed to summarize hourly average ozone data
WHO	World Health Organization
WMO	World Meteorological Organization
WWF	World Wide Fund for Nature
YLL	years of life lost

Glossary

This glossary is compiled from citations in different chapters, and draws from glossaries and other resources available on the websites of the following organizations, networks and projects:

American Meteorological Society, California Environmental Protection Agency (United States), European Environment Agency, Eurostat, Food and Agriculture Organization of the United Nations, GreenFacts Glossary, Intergovernmental Panel on Climate Change, Met Office (United Kingdom), National Center for Biotechnology Information (United States), National Oceanic and Atmospheric Administration (United States), United Nations Economic Commission for Europe, United Nations Environment Programme, United States Environmental Protection Agency, Wikipedia and World Health Organization.

Absorption	The process in which the energy of radiation – e.g. light – is taken up by matter. In this process, the electromagnetic energy is transformed to other forms of energy, for example, to heat.
Acid rain	Rain having a pH less than 5.6. The acidity is the result of pollution caused mostly by sulphur oxides and nitrogen oxides that are discharged into the atmosphere by industry. It is also created by burning coal and oil, from the operation of smelting industries and from transportation. In the atmosphere, these gases combine with water vapour to form acids, which then fall back to Earth.
Aerosols	A collection of airborne solid or liquid particles (excluding pure water), with a typical size between 0.01 and 10 micrometers (μm) and residing in the atmosphere for at least several hours. Aerosols may be of either natural or anthropogenic origin. Aerosols may influence climate in two ways: directly through scattering and absorbing radiation, and indirectly through acting as condensation nuclei for cloud formation or modifying the optical properties and lifetime of clouds.
Albedo	The fraction of solar radiation reflected by a surface or object, often expressed as a percentage. Snow covered surfaces have a high albedo; the albedo of soils ranges from high to low; vegetation covered surfaces and oceans have a low albedo. The Earth's albedo varies mainly through varying cloudiness, snow, ice, leaf area and land cover changes.
Anaerobic digestion	A series of processes in which microorganisms break down biodegradable material in the absence of oxygen, used for industrial or domestic purposes to manage waste and/or to release energy.
Annex I countries	Parties included in Annex I to the UNFCCC. (Defined by the UNFCCC as industrialized countries.)
Anthropogenic	Made by people or resulting from human activities.
Arrythmia	Any of a large and heterogeneous group of conditions in which there is abnormal electrical activity in the heart. The heart beat may be too fast or too slow, and may be regular or irregular.
Atherosclerosis	Is a condition in which an artery wall thickens as the result of a build-up of fatty materials.
Atmosphere	The gaseous envelope surrounding the Earth.

Atmospheric forcing	The difference in the radiative forcing at the top-of-the-atmosphere or tropopause and at the surface, representing heat absorbed in the lower atmosphere. Gradients in heating from one place to another drive winds, and so regional differences in atmospheric forcing are closely connected to changes in regional circulation and precipitation. (Definition from Box 4.1.)
Baseline scenario	The baseline (or reference) is the state against which change is measured. It might be a 'current baseline', in which case it represents observable, present-day conditions. It might also be a 'future baseline', which is a projected future set of conditions excluding the driving factor of interest. Alternative interpretations of the reference conditions can give rise to multiple baselines.
Biodiversity	Shorthand for biological diversity. Variability among living organisms from all sources including terrestrial, marine and other aquatic ecosystems, and the ecological complexes of which they are part; this includes diversity within species, between species and of ecosystems.
Biofuels	Biofuels are non-fossil fuels. They are energy carriers that store the energy derived from organic materials (biomass), including plant materials and animal waste.
Biogas	Biogas typically refers to a gas produced by the biological breakdown of organic matter in the absence of oxygen. Biogas originates from biogenic material and is a type of biofuel. Biogas is produced by anaerobic digestion or fermentation of biodegradable materials such as biomass, manure, sewage, municipal waste, green waste, plant material and energy crops.
Biomass	In the context of energy, the term biomass is also often used to refer to organic materials, such as wood by-products and agricultural wastes, which can be burned to produce energy or converted into a gas and used for fuel.
Biosphere	The global ecosystem; that part of the earth and atmosphere capable of supporting living organisms.
Black carbon	Operationally defined aerosol species based on measurement of light absorption and chemical reactivity and/or thermal stability. Black carbon is formed through the incomplete combustion of fossil fuels, biofuel, and biomass, and is emitted in both anthropogenic and naturally occurring soot. It consists of pure carbon in several linked forms. Black carbon warms the Earth by absorbing heat in the atmosphere and by reducing albedo, the ability to reflect sunlight, when deposited on snow and ice.
Blue ice	Pure ice in the form of large single crystals.
Boreal forest	Forest that grows in regions of the northern hemisphere with cold temperatures. Made up mostly of cold tolerant coniferous species such as spruce and fir.
Brown clouds	High concentrations of particulate matter suspended in the atmosphere lead to light scattering, resulting in a reduction in visibility and a reddish-brown sky coloration.
'Business as usual' scenario	The scenario that examines the consequences of continuing current trends in population, economy, technology and human behaviour.
Bus rapid transport	A term applied to a variety of public transportation systems using buses to provide faster, more efficient service than an ordinary bus line. Often this is achieved by making improvements to existing infrastructure, vehicles and scheduling.
Carbonaceous aerosol	Aerosol consisting predominantly of organic substances and various forms of black carbon.

Carbon cycle	All parts (reservoirs) and fluxes of carbon. The cycle is usually thought of as four main reservoirs of carbon interconnected by pathways of exchange. The reservoirs are the atmosphere, terrestrial biosphere (usually includes freshwater systems), oceans, and sediments (includes fossil fuels). The annual movements of carbon, the carbon exchanges between reservoirs, occur because of various chemical, physical, geological, and biological processes. The ocean contains the largest pool of carbon near the surface of the Earth, but most of that pool is not involved with rapid exchange with the atmosphere.
Carbon dioxide equivalent	Carbon dioxide equivalent describes how much global warming a given type and amount of greenhouse gas may cause, using the functionally equivalent amount or concentration of carbon dioxide (CO_2) as the reference.
Carbon fertilization	Enrichment of the atmosphere surrounding a plant or crop, that is, the canopy of the crop, by increasing the concentration of carbon dioxide.
Carbon sequestration	The uptake and storage of carbon. Trees and plants, for example, absorb carbon dioxide, release the oxygen and store the carbon.
Carbon sink	A carbon sink is a natural or artificial reservoir that accumulates and stores some carbon-containing chemical compound for an indefinite period.
Cardiopulmonary	Having to do with the heart and lungs.
Cardiovascular disease	The class of diseases that involve the heart or blood vessels.
Central value	The most plausible range for a value based on the expert judgement of available evidence by the assessment authors.
Chronic (medicine)	In medicine, a chronic disease is a disease that is long-lasting or recurrent.
Clean development mechanism (CDM)	One of the three market-based mechanisms under the Kyoto Protocol to the UN Framework Convention on Climate Change (UNFCCC), whereby developed countries may finance greenhouse gas emissions-avoiding projects in developing countries, and receive certified emission reduction credits for doing so which they may apply towards meeting mandatory limits on their own emissions.
Climate 450 scenario	A scenario of the World Energy Outlook 2009 of the International Energy Agency that explores how global energy markets could evolve if countries take coordinated action to restrict the global temperature increase to 2°C by stabilizing GHG concentrations at 450 ppm.
Climate change	The long-term fluctuations in temperature, precipitation, wind, and all other aspects of the Earth's climate. It is also defined by the United Nations Convention on Climate Change as "change of climate which is attributed directly or indirectly to human activity that alters the composition of the global atmosphere and which is in addition to natural climate variability observed over comparable time periods".
Cloud condensation nuclei (CCN)	Airborne particles that serve as an initial site for the condensation of liquid water, which can lead to the formation of cloud droplets.
Coal bed methane (CBM)	The methane originating in coal seams that is drained from surface boreholes before mining takes place.
Coal mine methane (CMM)	Methane component of gases captured in a working mine by methane drainage techniques.
Coke	Coke is the solid carbonaceous material derived from destructive distillation of low-ash, low-sulfur bituminous coal. Volatile constituents of the coal—including water, coal-gas, and coal-tar—are driven off by baking in an airless furnace or oven.

Community of practice	Refers to the process of social learning that occurs when people who have a common interest in some subject or problem collaborate over an extended period to share ideas, find solutions, and build innovations.
Compound (chemical)	A material made up of two or more elements combined in a fixed ratio.
Compressed natural gas (CNG)	A fossil fuel substitute for petrol, diesel, or propane/LPG. Although its combustion does produce greenhouse gases, it is a more environmentally clean alternative to those fuels.
Concentration-response function	See *Dose-response function*.
Confidence interval	In statistics, a confidence interval is a particular kind of interval estimate of a population parameter and is used to indicate the reliability of an estimate.
Congestion pricing	A system of surcharging users of a transport network in periods of peak demand to reduce traffic congestion.
Convective precipitation	Precipitation particles forming in the active updraft of a cumulonimbus cloud, growing primarily by the collection of cloud droplets and falling out not far from their originating updraft.
Cost-effectiveness	The cost of an emission control measure assessed in terms of price per unit of air emissions reduced.
Coupled ocean-atmosphere climate models	Complex climate models which combine atmospheric global circulation models with oceanic global circulation models.
Crop residues	There are two types of agricultural crop residues. Field residues are materials left in an agricultural field or orchard after the crop has been harvested. These residues include stalks and stubble (stems), leaves, and seed pods. Process residues are those materials left after the processing of the crop into a usable resource. These residues include husks, seeds, bagasse, and roots.
Crude oil	A mixture of hydrocarbons that exist in liquid phase in underground reservoirs and remain liquid at atmospheric pressure after passing through surface separating facilities.
Cryoconite	Powdery windblown dust which is deposited and builds up on snow, glaciers, or ice-caps. It contains small amounts of soot which absorbs solar radiation melting the snow or ice beneath the deposit sometimes creating a cryoconite hole.
Cryosphere	That portion of the earth where natural materials (water, soil, etc.) occur in frozen form.
Cultivar	A cultivar is a cultivated variety of a plant that has been deliberately selected for specific desirable characteristics (such as the colour and form of the flower, yield of the crop, disease resistance, etc.).
Deep convection	Thermally driven turbulent mixing, where vertical motions take molecules from the lower to upper atmosphere.
Deforestation	The conversion of forested land to non-forested land as a direct result of human activities.
Degasification	Degasification is the removal of dissolved gases from liquids.
Deposition	The transfer of substances in air to surfaces, including soil, vegetation, surface water, or indoor surfaces, by dry or wet processes.
Diesel particle filter	A device designed to remove diesel particulate matter or soot from the exhaust gas of a diesel engine.

Dimming	Dimming is the observed widespread reduction in sunlight at the surface of the Earth. Dimming shows significant regional variations.
Discounting	Discounting is a financial mechanism in which a debtor obtains the right to delay payments to a creditor, for a defined period of time, in exchange for a charge or fee. Essentially, the party that owes money in the present purchases the right to delay the payment until some future date. The discount, or charge, is simply the difference between the original amount owed in the present and the amount that has to be paid in the future to settle the debt.
DNA methylation	Addition of a methyl group to DNA. This is a biochemical process that is important for normal development in higher organisms.
Dose-response function	Describes the change in effect on an organism caused by differing levels of exposure (or doses) to a stressor (usually a chemical) after a certain exposure time.
Ecosystem	Dynamic complex of plant, animal, microorganism communities and their non-living environment, interacting as a functional unit.
Ecosystem services	The benefits people obtain from ecosystems. These include provisioning services, such as food and water, regulating services, such as flood and disease control, cultural services, such as spiritual, recreational and cultural benefits, and supporting services, such as nutrient cycling, that maintain the conditions for life on Earth.
Efficacy	A measure of how effective a forcing species is at causing a temperature response. It is defined as the ratio of the equilibrium temperature response from a 1 Wm^{-2} increase in forcing due to a species to that of a 1 Wm^{-2} forcing from CO_2. (Definition from Box 4.1.)
Effluent	The discharge of industrial or urban waste material into the environment.
Emission inventory	Details the amounts and types of pollutants released into the environment.
Emissions factor	A unique value for scaling emissions to activity data in terms of a standard rate of emissions per unit of activity.
Emission standard	The maximum amount of discharge legally allowed from a single source, mobile or stationary.
Emissivity	The emissivity of a material is the relative ability of its surface to emit energy by radiation.
End-of-pipe technologies	Methods used to remove already formed contaminants from a stream of air, water, waste, product or similar. These techniques are called 'end-of-pipe' as they are normally implemented as a last stage of a process before the stream is disposed of or delivered.
Energy efficiency	Refers to actions to save fuels by better building design, the modification of production processes, better selection of road vehicles and transport policies, the adoption of district heating schemes in conjunction with electrical power generation, and the use of domestic insulation and double glazing in homes.
Enteric fermentation	Enteric fermentation is a digestive process by which carbohydrates are broken down by microorganisms into simple molecules for absorption into the bloodstream of an animal. It is one of the factors in increased methane emissions.
Evapotranspiration	The combined processes through which water is transferred to the atmosphere from open water and ice surfaces, bare soil, and vegetation that make up the earth's surface.
Fertilizer	Fertilizers are substances that supply plant nutrients or amend soil fertility.

Flaring	The burning of gas which cannot be contained or used productively. In some cases, when associated natural gas is released along with oil from production fields remote from energy users, the gas is burned off as it escapes, primarily for safety reasons. Some flaring may also occur in the processing of oil and gas.
Food security	The World Food Summit of 1996 defined food security as existing "when all people at all times have access to sufficient, safe, nutritious food to maintain a healthy and active life".
Force air stove	A stove where air is forced in, e.g. by a fan, in order to improve the completeness of combustion.
Fossil fuels	Coal, oil, petroleum, and natural gas and other hydrocarbons are called fossil fuels because they are made of fossilized, carbon-rich plant and animal remains. These remains were buried in sediments and compressed over geologic time, slowly being converted to fuel.
Fugitive emissions	Emissions of methane escaping from oil and gas extraction not caught by a capture system.
General circulation model (GCM)	A global, three-dimensional computer model of the climate system which can be used to simulate human-induced climate change. GCMs are highly complex and they represent the effects of such factors as reflective and absorptive properties of atmospheric water vapour, greenhouse gas concentrations, clouds, annual and daily solar heating, ocean temperatures and ice boundaries. The most recent GCMs include global representations of the atmosphere, oceans, and land surface.
Glacial mass balance	Describes the net gain or loss of snow and ice through a given year.
Global dimming	The gradual reduction in the amount of global direct irradiance at the Earth's surface that was observed for several decades after the start of systematic measurements in the 1950s. It is thought to have been caused by an increase in particulates such as sulphate aerosols in the atmosphere due to human action.
Global warming	Global warming is an average increase in the temperature of the atmosphere near the Earth's surface and in the troposphere, which can contribute to changes in global climate patterns. Global warming can occur from a variety of causes, both natural and human induced. In common usage, "global warming" often refers to the warming that can occur as a result of increased emissions of greenhouse gases from human activities.
Global temperature-change potential (GTP)	The ratio of the temperature change caused by emitting 1 kg of the species at the end of the period considered, to that caused by emitting 1 kg of CO_2.
Global warming potential (GWP)	The global warming potential of a gas or particle refers to an estimate of the total contribution to global warming over a particular time that results from the emission of one unit of that gas or particle relative to one unit of the reference gas, carbon dioxide, which is assigned a value of 1.

Greenhouse gases (GHGs)	Greenhouse gases are those gaseous constituents of the atmosphere, both natural and anthropogenic, that absorb and emit radiation at specific wavelengths within the spectrum of infrared radiation emitted by the Earth's surface, the atmosphere and clouds. This property causes the greenhouse effect. Water vapour (H_2O), carbon dioxide (CO_2), nitrous oxide (N_2O), methane (CH_4), and ozone (O_3) are the primary greenhouse gases in the Earth's atmosphere. Moreover there are a number of entirely human-made greenhouse gases in the atmosphere, such as the halocarbons and other chlorine and bromine containing substances, dealt with under the Montreal Protocol. Beside CO_2, N_2O and CH_4, the Kyoto Protocol deals with the greenhouse gases sulphur hexafluoride (SF_6), hydrofluorocarbons (HFCs) and perfluorocarbons (PFCs).
Gross domestic product	The total market value of goods and services produced within a nation during a given period (usually 1 year).
High-emitting vehicles	Poorly tuned or defective vehicles, with emissions of particulate matter many times greater than the average.
Hoffman kiln	Hoffmann kilns are the most common kiln used in production of bricks. A Hoffmann kiln consists of a main fire passage surrounded on each side by several small rooms which contain pallets of bricks. Each room is connected to the next room by a passageway carrying hot gases from the fire. This design makes for a very efficient use of heat and fuel.
Humidity	Humidity is the amount of water vapour in the air. Absolute humidity is the quantity of water vapour in a given volume of air. Specific humidity is a ratio of mass quantities of water vapour to dry air. Relative humidity is how much water vapour can possibly be held by the air, in its current condition of temperature and pressure.
Hydrocarbons	Substances containing only hydrogen and carbon. Fossil fuels are made up of hydrocarbons.
Hydrometeor	Any product of condensation or deposition of atmospheric water vapour, whether formed in the free atmosphere or at the earth's surface; also, any water particle blown by the wind from the earth's surface.
Hydrological cycle	Succession of stages undergone by water in its passage from the atmosphere to the earth and its return to the atmosphere. The stages include evaporation from land, sea or inland water, condensation to form clouds, precipitation, accumulation in the soil or in water bodies, and re-evaporation.
Hydrology	The scientific study of the waters of the earth, especially with relation to the effects of precipitation and evaporation upon the occurrence and character of water in streams, lakes, and on or below the land surface.
Hygroscopicity	The relative ability of a substance (as an aerosol) to absorb water vapour from its surroundings and ultimately dissolve.
Ice nuclei	Any particle that serves as a nucleus leading to the formation of ice crystals.
Incomplete combustion	A reaction or process which entails only partial burning of a fuel. Combustion is almost always incomplete and this may be due to a lack of oxygen or low temperature, preventing the complete chemical reaction.
Indoor air pollution	Air pollutants that occur within buildings or other enclosed spaces, as opposed to those occurring in outdoor, or ambient air. Some examples of indoor air pollutants are nitrogen oxides, smoke, formaldehyde, and carbon monoxide.

Industrial Revolution	A period of rapid industrial growth with far-reaching social and economic consequences, beginning in Britain during the second half of the eighteenth century and spreading to Europe and later to other countries including the United States. The invention of the steam engine was an important trigger of this development. The Industrial Revolution marks the beginning of a strong increase in the use of fossil fuels and emission of, in particular, anthropogenic carbon dioxide.
Insolation	A measure of solar radiation energy received on a given surface area in a given time.
Irrigation	An artificial application of water to the soil. It is used to assist in the growing of agricultural crops.
Ischemia	A restriction in blood supply, generally due to factors in the blood vessels, with resultant damage or dysfunction of tissue.
Jeepney	Jeepneys are the most popular means of public transportation in the Philippines. They were originally made from US military jeeps left over from World War II and are known for their flamboyant decoration and crowded seating. They have become a symbol of Philippine culture.
Kyoto Protocol	A protocol to the 1992 UN Framework Convention on Climate Change (UNFCCC) adopted at the Third Session of the Conference of the Parties to the UNFCCC in 1997 in Kyoto, Japan. The major distinction between the Protocol and the Convention is that while the Convention **encouraged** industrialised countries to stabilize GHG emissions, the Protocol **commits** them to do so. Parties included in Annex B of the Protocol agreed to control their national anthropogenic emissions of greenhouse gases so that the total emissions from these countries would be at least 5 per cent below 1990 levels in the commitment period, 2008 to 2012. The Protocol expires in 2012.
Landfill	A site where household and industrial waste can be disposed of. It is generally spread in thin layers which are then covered with soil.
Leapfrogging	The ability of developing countries to bypass intermediate technologies and jump straight to advanced clean technologies. Leapfrogging can enable developing countries to move to a low-emissions development trajectory.
Lofting	The phenomenon where the upper part of a smoke plume diffuses more rapidly upward than the bottom part diffuses downward.
Long range transport	Atmospheric transport of air pollutants within a moving air mass for a distance greater than 100 kilometres.
Low-emission zone (LEZ)	A geographically defined area which seeks to restrict or deter access by specific polluting vehicles or only allow low or zero emission vehicles, with the aim of improving the air quality.
Melt pond	A pond of liquid water (mostly from melted snow) on the surface of sea ice, usually occurring in the spring.
Meridional	A flow, average, or functional variation taken in a direction that is parallel to a line of longitude.
Mitigation	Structural and non-structural measures undertaken to limit the adverse impact of natural hazards, environmental degradation and technological hazards.
Moist-static energy	The moist static energy is a thermodynamic variable that describes the state of an air parcel. The moist static energy is a combination of a parcels kinetic energy due to an air parce's temperature, its potential energy due to its height above the surface, and the latent energy due to water vapour present in the air parcel.

Monsoon	Monsoon is traditionally defined as a seasonal reversing wind accompanied by corresponding changes in precipitation, but is now used to describe seasonal changes in atmospheric circulation and precipitation associated with the asymmetric heating of land and sea. Usually, the term monsoon is used to refer to the rainy phase of a seasonally-changing pattern, although technically there is also a dry phase.
Monte-Carlo analysis	A class of computational algorithms that rely on repeated random sampling to compute their results.
Moraine	Ridges or deposits of rock debris transported by a glacier.
Morbidity	Refers to a diseased state, disability, or poor health.
Moulin	A narrow, tubular chute, hole or crevasse through which water enters a glacier from the surface.
Municipality	An administrative division composed of a defined territory and population.
Municipal waste	Residential solid waste and some non-hazardous commercial, institutional, and industrial wastes.
Natural draft stove	A stove where the air needed for combustion is drawn in naturally due to the temperature difference between outside air and exhaust gases.
Negative forcing	A negative forcing (more outgoing energy) tends to cool a system.
Ocean acidification	A decrease in the pH of sea water due to the uptake of anthropogenic carbon dioxide.
Open biomass burning	Forest fires, savannah burning and outdoor cooking.
Optical depth	A measure of transparency, defined as the negative logarithm of the fraction of radiation (e.g., light) that is not scattered or absorbed on a path.
Optical thickness	See *Optical depth*.
Organic matter	Organic matter (or organic material) is matter that has come from a once-living organism; is capable of decay or the product of decay; or is composed of organic compounds.
Oxidation	The chemical reaction of a substance with oxygen or a reaction in which the atoms in an element lose electrons and its valence is correspondingly increased.
Ozone	Ozone (O_3), the triatomic form of oxygen, is a gaseous atmospheric constituent. In the troposphere, it is created both naturally and by photochemical reactions involving gases resulting from human activities (it is a primary component of photochemical smog). In high concentrations, tropospheric ozone can be harmful to a wide range of living organisms. Tropospheric ozone acts as a greenhouse gas. In the stratosphere, ozone is created by the interaction between solar ultraviolet radiation and molecular oxygen (O_2). Stratospheric ozone plays a decisive role in the stratospheric radiative balance. Depletion of stratospheric ozone results in an increased ground-level flux of ultraviolet (UV-) B radiation.
Ozone precursor	Chemical compounds, such as carbon monoxide (CO), methane (CH_4), NMVOCs and nitrogen oxide (NO_X), which in the presence of solar radiation react with other chemical compounds to form ozone, mainly in the troposphere.
Particulate matter	Very small pieces of solid or liquid matter such as particles of soot, dust, fumes, mists or aerosols. The physical characteristics of particles, and how they combine with other particles, are part of the feedback mechanisms of the atmosphere.

Particulate sulphate	Particulate matter that consists of compounds of sulphur formed by the interaction of sulphur dioxide and sulphur trioxide with other compounds in the atmosphere. Sulphate aerosols are injected into the atmosphere from the combustion of fossil fuels and the eruption of volcanoes like Mt. Pinatubo. Recent theory suggests that sulphate aerosols may lower the Earth's temperature by reflecting away solar radiation (negative radiative forcing).
Pellet stove	A stove that burns compressed wood or biomass pellets to create a source of heat for residential and sometimes industrial spaces.
Permafrost	Ground (soil or rock and included ice and organic material) that remains at or below 0°C for at least two consecutive years.
Photochemical reaction	Refers to any chemical reaction which occurs as a result of light energy from the sun.
Photolysis	A chemical reaction in which a chemical compound is broken down by photons.
Phytotoxicity	A term used to describe the degree of toxic effect by a compound on plant growth.
Pneumonia	Inflammation of lung alveoli, the tiny air sacs deep within the lungs where carbon dioxide and oxygen are exchanged.
Policy	Any form of intervention or societal response. Policy can be seen as a tool for the exercise of governance.
Pollutant	Any substance that causes harm to the environment when it mixes with soil, water or air.
Pollution	The presence of minerals, chemicals or physical properties at levels that exceed the values deemed to define a boundary between "good or acceptable" and "poor or unacceptable" quality, which is a function of the specific pollutant.
Positive feedback	A system exhibiting positive feedback, in response to perturbation, acts to increase the magnitude of the perturbation.
Positive forcing	A positive forcing (more incoming energy) tends to warm a system.
Precipitation	Any and all forms of water, whether liquid or solid, that fall from the atmosphere and reach the Earth's surface.
Precursor	A precursor is a chemical which precedes and is the source of another.
Pre-industrial	Prior to widespread industrialisation and the resultant changes in the environment. Typically taken as the period before 1750.
Premature deaths	The number of deaths occurring earlier due to a risk factor than in the absence of that risk factor. (Definition from Box 4.7.)
Primary energy	Energy embodied in natural resources (such as coal, crude oil, sunlight or uranium) that has not undergone any anthropogenic conversion or transformation.
Primary particles	Particles that are directly emitted from combustion and fugitive dust sources.
Primary productivity	The transformation of chemical or solar energy to biomass. Most primary production occurs through photosynthesis, whereby green plants convert solar energy, carbon dioxide, and water to glucose and eventually to plant tissue. In addition, some bacteria in the deep sea can convert chemical energy to biomass through chemosynthesis.
Primary waste water treatment	In the primary stage of waste water treatment, sewage flows through large tanks which are used to settle sludge while grease and oils rise to the surface and are skimmed off. Tanks are usually equipped with mechanically driven scrapers that continually drive the collected sludge towards a hopper in the base of the tank where it is pumped to sludge treatment facilities.

Provisioning services	The products obtained from ecosystems, including, for example, genetic resources, food, and fresh water.
Purchasing power parity	A currency conversion that equalises the purchasing power in different countries, usually by estimating what sum of money is required to buy the same basket of goods and services in each country.
Quenching tower	In a quenching tower water sprays are used to reduce the temperature of gas emissions and aid removal of pollutants.
Radiative forcing	Radiative forcing is the change in the net vertical irradiance (expressed in Watts per square metre) at the tropopause due to an internal change or a change in the external forcing of the climate system, such as, for example, a change in the concentration of carbon dioxide or the output of the Sun.
Recession	In economics, a recession is a business cycle contraction, a general slowdown in economic activity.
Reference scenario	See *Baseline scenario*.
Residence time	Residence time (also known as removal time) is the average amount of time that a particle spends in a particular system.
Runoff	The water flow that occurs when soil is infiltrated to full capacity and excess water from rain, meltwater, or other sources flows over the land.
Savannah	A tropical or subtropical region of grassland and other drought- resistant (xerophilous) vegetation. This type of growth occurs in regions that have a long dry season (usually "winter-dry") but a heavy rainy season, and continuously high temperatures.
Sea level equivalent	The change in global average sea level that would occur if a given amount of water or ice were added to or removed from the oceans.
Secondary particles	Particles that are formed in the atmosphere. Secondary particles are products of the chemical reactions between gases, such as nitrates, sulphur oxides, ammonia, and organic products.
Secondary pollutant	See *Secondary particles*.
Secondary waste water treatment	Secondary waste water treatment is a biological treatment process to remove biodegradable dissolved and colloidal organic matter using aerobic biological treatment processes. Secondary treatment follows primary treatment.
Skewness	In probability theory and statistics, skewness is a measure of the asymmetry of the probability distribution of a real-valued random variable. The skewness value can be positive or negative, or even undefined.
Solid fuel	Refers to various types of solid material that are used as fuel to produce energy and provide heating. Solid fuels include wood, charcoal, peat, coal, Hexamine fuel tablets, and pellets made from wood, corn, wheat, rye and other grains.
Stomata	Pores found in the leaf and stem of the plant epidermis that are used for gas exchange.
Stomatal conductance	A numerical measure of the rate of passage of either water vapour or carbon dioxide through the stomata of a plant.
Stratosphere	Region of the atmosphere between the troposphere and mesosphere, having a lower boundary of approximately 9 km at the poles to 16 km at the equator and an upper boundary of approximately 50 km. Depending upon latitude and season, the temperature in the lower stratosphere can increase, be isothermal, or even decrease with altitude, but the temperature in the upper stratosphere generally increases with height due to absorption of solar radiation by ozone.

Sublimation	The transition of a substance from the solid phase to the gas phase without passing through an intermediate liquid phase.
Subsistence farming	Subsistence farming relates to agricultural activity to produce food which is predominantly consumed by the farming household. The food produced is the main or a significant source of food for the farming household and little or none of the production is surplus and available for sale or trade. It is generally associated with a small farm holding size and family agricultural work as a part-time or supporting activity.
Supporting services	Ecosystem services that are necessary for the production of all other ecosystem services. Some examples include biomass production, production of atmospheric oxygen, soil formation and retention, nutrient cycling, water cycling, and provisioning of habitat.
Systematic uncertainty	A systematic uncertainty (an estimate of which is known as a measurement bias) is associated with the fact that a measured value contains an offset. In general, a systematic uncertainty, regarded as a quantity, is a component of error that remains constant or depends in a specific manner on some other quantity.
Temperature potentials	Estimates of temperature response to forcing as a function of time that characterize the relative rapid response of the land and upper ocean to forcing as well as the much slower response of the deep ocean.
Temperature response	Estimates of temperature response to radiative forcing based on observational and modelling constraints on climate sensitivity. Peer-reviewed literature has established methods for such estimates at the global scale and over large latitude bands, but not at more localized scales. (Definition from Box 4.1.)
Tertiary waste water treatment	The purpose of tertiary waste water treatment is to provide a final treatment stage to raise the effluent quality before it is discharged to the receiving environment (sea, river, lake, ground, etc.).
Therophyte	Annual plants which survive the unfavourable season in the form of seeds and complete their life-cycle during favourable seasons. Annual species are therophytes. Many desert plants are by necessity therophytes.
Tillage	Tillage is the agricultural preparation of the soil by mechanical agitation of various types, such as digging, stirring, and overturning.
Transboundary movement	Movement from an area under the national jurisdiction of one State to or through an area under the national jurisdiction of another State or to or through an area not under the national jurisdiction of any State.
Transport (atmospheric)	The movement of chemical species through the atmosphere as a result of large-scale atmospheric motions.
Troposphere	The lowest part of the atmosphere from the surface to about 10 km in altitude in mid-latitudes (ranging from 9 km in high latitudes to 16 km in the tropics on average) where clouds and "weather" phenomena occur. In the troposphere temperatures generally decrease with height.
Tundra	A type of ecosystem dominated by lichens, mosses, grasses, and woody plants. Tundra is found at high latitudes (arctic tundra) and high altitudes (alpine tundra). Arctic tundra is underlain by permafrost and is usually [water] saturated.
Ultra-low sulphur diesel (ULSD)	Ultra-low sulphur diesel is a term used to describe a standard for defining diesel fuel with substantially lowered sulphur contents. Almost all of the petroleum-based diesel fuel available in Europe and North America is of an ultra-low sulphur type.
Updraft	An updraft is the upward vertical movement of air.

Value added	An economics term referring to the difference between the sale price of a commodity and its production cost. It is a measure of the industrial contribution to GDP.
Value of a Statistical Life (VSL)	The maximum amount an individual would be willing to pay to reduce his or her chance of dying by a small amount in a specified time period. (Definition from Box 4.7.)
Vapour pressure deficit	The difference (deficit) between the amount of moisture in the air and how much moisture the air can hold when it is saturated.
Venting	The release of gas to the atmosphere which cannot be contained or used productively. In some cases, when associated natural gas is released along with oil from production fields remote from energy users, the gas is allowed to escape into the atmosphere.
Volatile organic compounds (VOCs)	Organic chemical compounds that under normal conditions are gaseous or can vaporise and enter the atmosphere. VOCs include such compounds as methane, benzene, xylene, propane and butane. Methane is primarily emitted from agriculture (from ruminants and cultivation), whereas non-methane VOCs (or NMVOCs) are mainly emitted from transportation, industrial processes and use of organic solvents.
Vulnerability assessment	The process of identifying, quantifying, and prioritizing the vulnerabilities in a system.
Water cycle	See *Hydrological cycle*.
Wetlands	Lands where water saturation is the dominant factor that determines the nature of soil development and the types of plant and animal communities living in the surrounding environment.
Wet scavenging	Removal of pollutants from the air by either rain or snow.
Years of life lost	The average number of additional years a person would have lived if he or she would not have died prematurely. (Definition from Box 4.7.)

The Integrated Assessment of Black Carbon and Tropospheric Ozone looks into all aspects of anthropogenic emissions of black carbon and tropospheric ozone precursors, such as methane. It analyses the trends in emissions of these substances and the drivers of these emissions; summarizes the science of atmospheric processes where these substances are involved; discusses related impacts on the climatic system, human health, crops in vulnerable regions and ecosystems; and societal responses to the environmental changes caused by those impacts. The Assessment examines a large number of potential measures to reduce harmful emissions, identifying a small set of specific measures that would likely produce the greatest benefits, and which could be implemented with currently available technology. An outlook up to 2070 is developed illustrating the benefits of those emission mitigation policies and measures for human well-being and climate. The Assessment concludes that rapid mitigation of anthropogenic black carbon and tropospheric ozone precursor emissions would complement carbon dioxide reduction measures and would have immediate benefits for human well-being. The Assessment is intended to support informed decision making at all levels as a guide for assessment, planning and management for the future.